# SUPERCRITICAL FLUID EXTRACTION AND MODELING OF ARGEMONE MEXICANA AND PONGAMIA PINNATA SEED OILS AND THEIR ANALYSIS

**Ph.D. THESIS**

*by*

**BHUPENDRA SURYAWANSI**

**DEPARTMENT OF CHEMICAL ENGINEERING**
**INDIAN INSTITUTE OF TECHNOLOGY ROORKEE**
**ROORKEE - 247667 (INDIA)**
**APRIL, 2019**

# SUPERCRITICAL FLUID EXTRACTION AND MODELING OF ARGEMONE MEXICANA AND PONGAMIA PINNATA SEED OILS AND THEIR ANALYSIS

**A THESIS**

***Submitted in partial fulfilment of the requirements for the award of the degree***

*of*

**DOCTOR OF PHILOSOPHY**

*in*

**CHEMICAL ENGINEERING**

*by*

**BHUPENDRA SURYAWANSI**

**DEPARTMENT OF CHEMICAL ENGINEERING**
**INDIAN INSTITUTE OF TECHNOLOGY ROORKEE**
**ROORKEE - 247667 (INDIA)**
**APRIL, 2019**

# INDIAN INSTITUTE OF TECHNOLOGY ROORKEE

## STUDENT'S DECLARATION

I hereby certify that the work presented in this thesis entitled **SUPERCRITICAL FLUID EXTRACTION AND MODELING OF ARGEMONE MEXICANA AND PONGAMIA PINNATA SEED OILS AND THEIR ANALYSIS** is my own work carried out during a period from July, 2013 to April, 2019 under the supervision of Dr. Bikash Mohanty, Professor, Department of Chemical Engineering, Indian Institute of Technology Roorkee.

The matter presented in the thesis has not been submitted for the award of any other degree of this or any other institution.

**Dated:** **Signature of the Student**

## SUPERVISOR'S DECLARATION

This is to certify that the above mentioned work is carried out under my supervision.

**Dated:** **Signature of Supervisor(s)**

The Ph.D. viva voice Examination of **Mr. BHUPENDRA SURYAWANSI,** Research Scholar, has been held on ……..

**Signature of External Examiner** **Chairman, SRC/DRC**

This is to certify that the student has made all the corrections in the thesis.

**Signature of Supervisor(s)** **Head of the Department**

## ABSTRACT

Some natural seeds contain valuable chemical components, which are used for medicinal purposes to cure various chronic diseases. However, extracting these chemicals in pure natural form is a challenge. This problem can be somewhat resolved by supercritical fluid extraction (SFE) technique. In the present work, two seeds, namely Argemone mexicana (L.) (AM) and Pongamia pinnata (L.) (PP) are selected for extraction. This selection is purely based on the properties and applications of these two seed oils found in literature. A thorough literature review indicates that AM and PP seeds contains good percentage of oil, which contain some valuable chemical components such as fatty acids and alkaloids that can be used as medicine to cure various chronic deceases. Besides, the medicinal requirements, these oils also have a potential to produce biofuel.

For commercial purposes, oils from these two seeds, are generally extracted by means of conventional extraction techniques such as soxhlet extraction, mechanical pressing, percolation methods, etc. However, due to the lower yield, loss of valuable components, refining hurdles and safety aspects make these conventional methods cost intensive and environmentally incompatible. Furthermore, the oil obtained through these methods, needs to be processed for cleaning and removal of organic solvents (e.g. n-hexane, methanol, isopropanol etc.) which are used during conventional extraction techniques (e.g. soxhlet extraction, percolation method). Even the added processing of the oils, do not remove organic solvents completely from the final product (oil). Therefore, the use of supercritical fluids (SFs), as an alternative solvent, during the extraction of seed oils has been attracting widespread attention due to their advantageous properties such as liquid-like density, gas-like viscosity and negligible surface tension.

This new method (e.g. SFE) also meets environmental regulations and promotes its utilization as green method. The SFE, using supercritical carbon dioxide (SC-$CO_2$) has also been recognized as the latest emerging eco-friendly and clean separation technology for various valuable food ingredients from natural products, pharmaceutical products, etc., with high yield and better quality products under a wide range of operating conditions. Among various SFs, SC-$CO_2$ has achieved the unique popularity due to its non-flammability, -non-toxicity, -non-explosive behavior, -low cost, -availability in plenty amount and -easy to separate out from the extracted product.

In the present experimental investigation, oils are extracted from AM and PP seeds by means of SC-$CO_2$. The SFE experiments have been performed using SFE 1000F apparatus, supplied by

Thar Technologies Inc., Pittsburgh. The software, 'Design Expert 10.0' has been used to design the number of experiments in a methodological way that actually help to develop a statistical analysis based correlation between input and output variables. The ANOVA (analysis of variance) has been performed to establish the relative significance of the individual input parameters (e.g. temperature, pressure, particle size, flow rate-$CO_2$ and the % of co-solvent) and their interaction effects.

For the present SFE process, the above five input parameters of significance have been screened out from thirteen influencing input parameters from the available published literature (as listed in section 2.3), and finally the effect of these input parameters on the cumulative extraction yield (CEY) of oil have been identified. Final five selected SFE operating parameters were optimized for maximum yield via response surface methodology (RSM) with a 'five-factors-three-levels' Box-Behnken design (BBD).

The regression analysis of the experimental data of SFE process for AM and PP seed oils, has confirmed that the quadratic model (second-order polynomial equation) is the best for the prediction of CEY. This quadratic model offers the $R^2$ values as 0.9737 and 0.9944 respectively for AM and PP seeds. Further, the statistical analysis has also shown that the interactions amongst all the five input parameters exist. Further, for both seeds, % of co-solvent and pressure have been observed to be the most influencing parameters followed by each one. The prediction of CEY values, through quadratic model, have been found within error range of '+14.4 to -11.28 %', and '+18.39 to -16.32 %' of experimental values for AM and PP seed oils respectively.

Furthermore, an artificial neural network (ANN) model has been developed, using experimental data and for this, a trainable, feed-forward-back-propagation (FFBP) network has been used to predict the CEY of both seed oils with an acceptable level of accuracy. From a number of performing ANN models, an optimized model 'FFBPN [5-6-1]' has been selected for prediction of the CEY. The 'FFBPN [5-6-1]' shows average absolute relative deviation percentage (AARD %), mean square error (MSE)) and best regression coefficient ($R^2$) for the SFE of AM and PP seed oils as '3.33 %, 0.0038, 0.9835' and '4.39 %, 0.00051, 0.9874' respectively.

The present SFE process has been modeled by applying two mass transfer phenomenon based models (MTPBMs) (e.g. Sovova, 1994 and Reverchon, 1996). The fitting parameters (e.g. $Z$, $W$ and $x_k$) of the Sovova model (Sovova, 1994) have been optimized using the global optimization technique (genetic algorithm (GA) approach) by running a written program in MATLAB to minimize the

AARD % between the CEY's, obtained from the Sovova model and from the experiments during the SFE of AM and PP seed oils. On the other hand, the Reverchon model (Reverchon, 1996) is also solved and fitted with the present SFE experimental data using the COMSOL Multiphysics 5.3a.

It is found that the Sovova model (SM) has produced excellent fitting with the experimental CEY data within an error band of '1.436 to 14.198 %' and '0.7706 to 14.17 %' for AM and PP seed oils respectively. From the results of SM, it has also been observed that the mass transfer coefficients in solvent phase ($k_{ya}$) are larger than the mass transfer coefficients in the solid phase ($k_{xa}$) for all parametric conditions. In comparison to SM, Reverchon model (RM) has produced partially good fittings with experimental data within an error band of '5.52 to 96.3 %' and '2.64 to 19.74 %' for AM and PP seed oils respectively. It is noted that RM is good for predicting the final value of CEY and not the intermediate CEY value with time.

After the extraction of oils from AM and PP seeds, the physico-chemical properties (e.g. calorific value (MJ/kg), flash point (ºC), fire point (ºC), cloud point (ºC), pour point (ºC), acid value (mg KOH/g), peroxide value (meq/kg sample), and saponification value (mg KOH/g)) of oil samples have been determined. The chemical compositions of seed oils, obtained through both extraction methods (soxhlet and SFE methods), were analyzed and quantified using gas chromatography (GC). In addition to these, the characterization of feed (seeds) are also performed by scanning electron microscopy (SEM), Thermo-gravimetric (TG) analysis and Fourier transform infrared (FTIR) spectroscopy.

The characterizations (e.g. total oil content (%), moisture (%), ash (%), SEM, TG analysis and FTIR analyses) were also performed on the seed particles of AM and PP seeds. The total oil content, moisture content and ash content are found as '42%, 9.6% & 3.5%' and '36%, 5.4% & 1.8%' for AM and PP seed particles respectively. The FTIR analyses of both seed particles have confirmed the presence of fatty acids, alkaloids, and protein. TG analyses has also confirmed the moisture and ash content. The morphological changes at the surfaces of AM and PP seeds have also been studied during the SFE process through SEM analysis. On the other hand, GC analysis of the product (oil) shows that AM seed oil is rich in linoleic acid (C18:2n6c), oleic acid (C18:1n9c), palmitic acid (C16:0), and stearic acid (C18:0), with the range of concentrations (weight %) as '22.54 - 59.07 %', '25.01 - 41.46%', '11.40 - 23.58 %', and '2.98 – 5.97 %' respectively. Whereas, the PP seed oil is found rich in oleic acid (C18:1n9c), arachidic acid (C20:0), cis-10-pentadecanoic acid

(C15:1), stearic acid (C18:0), cis-8,11,14-Eicosatrienoic acid (C20:3n6), linolenic acid (C18:3n3), gamma(ϒ)-linolenic acid (C18:3n6) and cis-11-Eicosenoic acid (C20:1) and are found in the range of concentrations (weight %) as '45.42 - 58.62%', '15.34 - 18.02%', '8.64 - 11.95%', '5.74 - 7.04%', '2.62 - 4.45%', '1.24 - 4.01%', '0.34 - 1.53%', and '0.0 - 3.93%' respectively.

Further, the physicochemical properties (e.g. heating value (MJ/kg), flash point, (°C), fire point (°C), cloud point (°C), pour point (°C), saponification value (mg KOH/g), peroxide value (meq/kg sample) and acid value (mg KOH/g)) of the extracted AM and PP seed oils during SFE, suggest that the oils could also be used for bio-fuel.

Finally, the economic analysis of the SFE process at industrial scale (for 1000 liters capacity of extraction vessel) has confirmed the economic feasibility, based on the obtained payback periods as '1.63' and '1.84' years for the envisaged plant of SFE process of AM and PP seed oils respectively.

## ACKNOWLEDGEMENT

The work presented in this thesis would not have been possible without my close association with many people. I take this opportunity to extend my sincere gratitude and appreciation to the following persons for their support during my Ph.D. at Indian Institute of Technology, Roorkee.

First, and foremost, I would like to express my deep and sincere gratitude to my supervisor Prof. Bikash Mohanty, Department of Chemical Engineering, Indian Institute of Technology Roorkee, for his blessings, patient guidance, enthusiastic encouragement and useful critiques of this thesis work.

Besides my supervisor, I would like to thank the rest of my thesis committee members: Prof. Shishir Sinha, Head, Department of Chemical Engineering, Prof. Basheshwer Prasad, DRC/SRC, Department of Chemical Engineering, Prof. Shabina Khanam, Internal Expert, Department of Chemical Engineering and Prof. Akhilesh Gupta, External Expert, Department of Mechanical and Industrial Engineering, for their insightful comments and encouragement, but also for the hard questions, which incented me to widen my research from various perspectives.

I owe thanks to a very special person, my wife, Mrs Sarita Banwari for her continued and unfailing love, support and understanding during my pursuit of Ph.D. work that made the completion of thesis possible. You were always around at times I thought that it is impossible to continue, you helped me to keep things in perspective. I greatly value her contribution and deeply appreciate her belief in me.

I also extend my thanks to departmental staff Mr. Vipin Ekka, Mr. Satpal Singh, Mr. Arvind Kumar, Mr. Rajkumar, Mr. Nirmal, Mr. Mohit and Mr. Bhagwan Pal for providing help at various stages of my work and for carrying out analysis and characterization of samples.

I am also thankful to my seniors, Dr. Amit Rai, Dr. Venkata Ramanaiah, and Dr. Somesh Bhambi and friends, Aniruddha Sanyal, Brajesh Kumar, Lovejeet Singh, Prashant Shrivastava, Umesh Kumar, Deepak Dwivedi, Praveen Kumar Toni, Abhishek Kumar Lal, Vibha Porwal, Smita Mondal, Bhogadi Bhaskar Rao, Baljinder Kaur Riyar, Vikrant Sharma, Priti Kumari, Ajay Sharma, Priyanka Dogra, and Shelly Garg whose communication and mental support, through from near and far places, have been great source of inspiration.

On top of that, I am deeply and thoroughly indebted to my parents and in-laws to all the freedom they have given to my choice of career and lifestyle. A special thanks to my brother 'Omprakash Suryawanshi for his support, motivation and trust in me, which helped me aim higher from time to

time. I would also like to thank my brothers, Dharmendra Suryawanshi, Hemant Malviya, and Narendra Malviya for being a constant source of inspiration and support for all possible help during all stages of this Ph.D.

I am especially grateful to my uncles Mr. H. P. Malviya (ret. Teacher) and Mr. G. R. Malviya (ret. ADEO Officer) for their support and encouragement during this work.

I offer my regards and blessings to all of those who supported me in any respect during the completion of this thesis.

And last but not the least; I am always thankful to the omnipresent, GOD, without whose elegance even this world does not exist.

September, 2019 (BHUPENDRA SURYAWANSI)

## PUBLICATIONS

The following research articles have been published from this Ph.D. thesis.

- **International journals**

1. **Bhupendra Suryawanshi**, Bikash Mohanty, **2018**. Modeling and optimization: Supercritical $CO_2$ extraction of Pongamia pinnata (L.) seed oil. **Journal of Environmental Chemical Engineering**; 6:2660-2673.
2. **Bhupendra Suryawanshi**, Bikash Mohanty, **2018**. Application of an artificial neural network model for the supercritical fluid extraction of seed oil from Argemone mexicana (L.) seeds. **Industrial Crops & Products**; 123: 64-74.
3. **Bhupendra Suryawanshi**, Bikash Mohanty, **2018**. Modeling and optimization of process parameters for supercritical $CO_2$ extraction of Argemone mexicana (L.) seed oil. **Chemical Engineering Communications;** https://doi.org/10.1080/00986445.2018.1547712.

- **International conferences**

1. **Bhupendra Suryawanshi**, Bikash Mohanty, Solution of a mass transfer based mathematical model of SCFE process using COMSOL Multiphysics 5.2. In excerpt from the Proceedings of the 2016 COMSOL conference in Bangalore , 2016.
2. **Bhupendra Suryawanshi**, Bikash Mohanty, Application of Artificial neural network approach for supercritical $CO_2$ extraction of *Pongamia pinnata* (L.) seed oil: A comparison between optimized feed forward and cascade forward back propagation networks. ICACSE-2018 (NIT Tiruchirappalli), 6-8$^{th}$ December 2018, Tiruchirappalli, India.

# CONTENTS

## LIST OF FIGURES

## LIST OF TABLES

## NOMENCLATURE

### Abbreviations

| | |
|---|---|
| AARD | Average absolute relative deviation |
| ABPR | Automated back pressure regulator |
| ACCR | Annual cost of capital recovery |
| AM | Argemone mexicana |
| ANN | Artificial neural network |
| ANOVA | Analysis of variance |
| BBD | Box-behnken design |
| BIS | Bureau of Indian standard |
| CCD | Central composite design |
| CE | Cost of electricity |
| CER | Constant extraction rate |
| CEY | Cumulative extraction yield |
| CL | Cost of labor |
| CLC | $CO_2$ liquefaction cost |
| CRM | Cost of the raw materials |
| DDD | Desorption-dissolution-diffusion |
| DM | Doehlert matrix |
| DoE | Design of experiments |
| EA | Economic analysis |
| EBP | Error back propagation |
| FAME | Fatty acids methyl esters |
| FC | Fixed cost |
| FD | Factorial design |
| FER | Falling extraction rate |
| FFA | Free fatty acids |
| FFBP | Feed forward back propagation |
| FID | Flame ionization detector |
| FIR | Far infrared |

| | |
|---|---|
| FTIR | Fourier transform infrared |
| GA | Genetic algorithm |
| GC | Gas chromatography |
| GPAD | Gross profit after depreciation |
| GPBD | Gross profit before depreciation |
| HPLC | High-performance liquid chromatography |
| HV | Heating value |
| IBFact | Incomplete block factorial |
| IS | Indian standard |
| MC | Manufacturing cost |
| MJ | Mega joule |
| MPL | Multilayer perceptron |
| MSE | Mean square error |
| MTPBM | Mass transfer phenomenon based mathematical |
| NIR | Near infrared |
| NR | Not reported |
| NSEC | Nash-Sutcliffe efficiency coefficient |
| OAD | Orthogonal array design |
| OC | Operating cost |
| OEC | Overall extraction curve |
| OVAT | One variable at a time |
| PFD | Process flow diagram |
| PID | Proportional integral derivative |
| PP | Pongamia pinnata |
| PRESS | Predicted residual sum of squares |
| psi | Pound per square inch |
| PV | Peroxide value |
| RM | Reverchon model |
| RPM | Revolution per minute |
| RSD | Relative standard deviation |

| | |
|---|---|
| RSM | Response surface methodology |
| RT | Retention time |
| SA | Sensitivity analysis |
| SC | Selling cost |
| SC-$CO_2$ | Supercritical $CO_2$ |
| SEM | Scanning electron microscopy |
| SF | Supercritical fluid |
| SFA | Saturated fatty acids |
| SFE | Supercritical fluid extraction |
| SM | Sovova model |
| TAC | Total annual cost |
| TG | Thermo-gravimetric |
| TR | Transition rate |
| USFA | Unsaturated fatty acids |
| VAC | Voltage alternating current |
| VOC | Volatile organic compounds |
| WHO | World health organization |

**Symbols**

| | |
|---|---|
| $a_0$ | Specific interfacial area ($m^{-1}$) |
| $C_o$ | Solute concentration at the entrance of the bed |
| $D_i$ | Internal diffusion coefficient ($m^2$/min) |
| $D_p$ | Distribution coefficient |
| $\varepsilon/e_p$ | Bed void fraction |
| $G$ | Grinding efficiency |
| $H$ | Height of bed (m) |
| $h$ | Axial distance along the bed (m) |
| $k_p$ | Partition coefficient |
| $k_f$ / $k_{xa}$ | Mass transfer coefficient in solvent phase (m/s) |
| $k_s$ / $k_{ya}$ | Mass transfer coefficient in solid phase (m/s) |
| $K$ | Mass of inaccessible solute (kg) |

| | |
|---|---|
| $l$ | A characteristic dimension (m) |
| $N/msi$ | Mass of solute free solid phase |
| $O$ | Initial total mass of solute (oil) in the solid (kg) |
| $P$ | Mass of easily accessible solute (kg) |
| $P_c$ | Critical pressure, bar |
| $Q_{CO_2}$ | $CO_2$ flow rate, kg/min |
| $q$ | Mass flow rate of solvent related to N ($s^{-1}$) |
| $\rho_s$ | Density of solid, $kg/m^3$ |
| $\rho$ | Density of solvent, kg/m3 |
| $t_i$ | Internal diffusion time (min) |
| $t$ | Time (min) |
| $t_{CER}$ | Constant extraction rate period (min) |
| $t_{FER}$ | Falling extraction rate period (min) |
| $T_c$ | Critical temperature, °C |
| $U$ | Superficial velocity (m/min) |
| $V$ | Volume of extraction cell ($m^3$) |
| $W$ | Parameter of slow extraction period |
| $x$ | Solute concentration in the solid phase |
| $x_o$ | Initial oil fraction |
| $X_p$ | Easily accessible solute |
| $X_k$ | Inaccessible solute |
| $y$ | Solute concentration in the solvent phase |
| $y_r$ | Solubility |
| $Z$ | Parameter of fast extraction period |
| $\Delta Z$ | Height of elemental bed (m) |
| $z_w$ | Coordinate of the boundary between fast and slow extraction |
| $\mu$ | Coefficient depending on particle geometry |

# INTRODUCTION

Supercritical fluid (SF) is defined as the state of a fluid at or above its critical pressure ($P_c$) and temperature ($T_c$) in which the fluid neither behaves like a pure liquid nor like a pure gas but achieves a combined state of gas–liquid region. This new state has the best properties of a liquid (e.g. density) and a gas (e.g. viscosity) that is required for extraction and makes this fluid (e.g. supercritical fluid) superior than the other conventional fluids (e.g. liquids and gases) (Wen et al., 2009). The history of SFs can be linked to the identification of critical points of pressure and temperature by Charles Cagniard de La Tour in 1821 (Stahl et al., 1980). Hannay and Hogarth exhibited the dissolving properties of a SF by dissolving low vapor pressure solid material in SF in 1879. Later, Buchner reported the solubilities of certain non-volatile organic materials in $CO_2$ under supercritical conditions which were higher by order of magnitude than that expected from conventional fluid alone (Mukhopadhyay, 2000; Clifford, 1993).

A thorough literature review on SFs revealed that the SF has been the subject of research, since the date of discovery of critical points, regarding its behavior and application. The first commercial applications of SFs (e.g. supercritical $CO_2$ (SC-$CO_2$)) came into existence in the late 1970s for the decaffeination of coffee and tea, refining of cooking oils, recovering of flavors and pungencies from spices and other natural products. Bruno et al., 1993 and Phelps et al., 1996 have shown some known industrial applications of SC-$CO_2$ in food industries and waste treatment industries respectively.

In addition to extracting desired compounds from natural products, another very interesting application of the supercritical fluid extraction (SFE) technique has been found for the extraction or clean-up of pesticides from natural products including herbal medicines (Lang et al., 2000). Catalytic reactions such as polymerization, hydrogenation, catalytic hydrothermal gasification and enzymatic reactions in SC-$CO_2$ have also been receiving an increased attention during the last decade (Sarkari et al., 1999; Khosravi-Darani and Vasheghani-Farahani, 2005). Pharmaceutical and cosmetic industries are also using SFs for extracting the herbal medicines and active ingredients for cosmeceutical applications and fragrances (Naik et al., 2010a). Hong and Pyun, 2001; Khosravi-

Darani and Vasheghani-Farahani, 2005 have shown SC-$CO_2$ application in material processing (e.g. coating, dyeing, crystallization, impregnation etc.) and in cleaning (e.g. dry cleaning, cleaning of metallic parts, soil reclamation, removal of undesired substance). Other special applications such as membrane-based separation, microwave-induced SFE, sterilization, powder technology, thin film extraction have also been reported in literature (Dalvi and Mukhopadhyay, 2009a; Perrut, 2012; Hrncic et al., 2018).

SC-$CO_2$ can be considered as one of the most prominent solvents in SFE processes for several reasons. Carbon dioxide has a technically convenient critical pressure and temperature as 73.8 bar and 31.1 °C respectively. It is non-toxic, non-flammable, non-reactive, non-corrosive and its solvent power may be enhanced by the addition of modifiers (liquid compounds of different polarities (Zaragoza et al., 1998). Furthermore, it is the second least expensive solvent after water and it does not leave any solvent residue after extraction. Carbon dioxide is a relatively good solvent for hydrocarbons and non-polar solutes. However, owing to the unique properties of supercritical solvents and to the rather large quadrupole moment of carbon dioxide in particular, SC-$CO_2$ dissolve many relatively volatile polar compounds. Adding small amounts of polar co-solvents (e.g. methanol, ethanol, propanol etc.), called entrainers to the bulk liquid carbon dioxide can enhance the solubility of polar, non-volatile solutes in SC-$CO_2$ (Bartle et al., 1991).

Medicines from natural products (e.g. herbal medicines) are considered of great importance amongst different urban or rural communities in many countries (Gosh, 2003). The people across the world prefers herbal medicines rather than the conventional medicines. According to World Health Organization (WHO) as many as 80% of the world's population depends on traditional medicines and in India 60% of the people in rural areas use herbal medicines. Thus, SFE based extraction of natural products for medicinal purpose can play a decisive role in Indian health sector. A preliminary search shows that two natural products (e.g. Argemone mexicana (L.) (AM) and Pongamia pinnata (L.) (PP) seeds) which are available in plenty amount in India, can be selected for the SFE using SC-$CO_2$ to extract the seed oil. The products (oils) also have excellent medicinal properties, which can be used to cure various chronic diseases.

In addition to this, health, environment and safety aspects have become the main challenges for the new upcoming technologies, which could not be fulfilled by older technologies that uses toxic

solvents. In this aspect, SFE using SC-$CO_2$ can be a good alternative green technology. The suggested SFE method has already proved its superiority over the other conventional methods (e.g. soxhlet, mechanical pressing, etc.) in terms of time consumption and quality & quantity of the products.

Although, the conventional soxhlet extraction of AM and PP seeds has only been investigated earlier (Dey et al., 2008; Mishra et al., 2009; Rao et al., 2012; Shameel et al., 1996; Prabhu et al., 2002; Meher et al., 2006; Kesari et al., 2010; Pavithra et al., 2012; Razal et al., 2012), but hardly any researcher has performed SFE of these two natural seeds. Apart from this, it appears that no investigator has studied the simultaneous effect of five most significant operating parameters namely temperature (°C), pressure (bar), particle size (mm), flow rate of $CO_2$ and the % of co-solvent (% of $CO_2$ flow rate) which mainly influence the cumulative extraction yield (CEY) of AM and PP seed oils. During experimentation response surface methodology (RSM) has been used to design the experiments and to get robust statistical correlations between input and output variables. Further, artificial neural network (ANN) methodology has been applied to develop a non-linear correlation between the inputs and output variables.

Additionally, the literature review shows that the mass transfer phenomenon based mathematical models (MTPBMs) such as Sovova's model (Sovova, 1994) and Reverchon's model (Reverchon, 1996) fits the experimental data fairly well for the SFE process of natural products (e.g. seeds, leaves, fruits, etc.). Hence, Sovova's model (Sovova, 1994) has been used to fit the present experimental data of SFE process. In addition to this, Reverchon's model (Reverchon, 1996), which is based on the integration of differential mass balances along the extraction bed, has also been used to fit the same experimental data.

Further, the physio-chemical properties of the extracted seed oils have also been determined to illustrate their applications accordingly. At the last, the economic analysis (EA) of the SFE process for large scale industrial plant has also been performed to evaluate its viability.

The main objective of the work is to extract the oils from the natural products (e.g. AM and PP seeds) through SC-$CO_2$. The experimental data obtained through the experiments, will be validated by mathematical models proposed by Sovova, 1994 and Reverchon, 1996 for the SFE process. The models will help to understand the mechanisms involved in SFE process in a fixed bed

using SC-$CO_2$ solvent, and can be utilized in the design and development of industrial scale processes.

Based on the above backdrops following objectives are framed;

1. Identification of influencing operating parameters for the SFE of seed oils from literature. Screening of important parameters from above identified parameters from literature reviews. To design the number of experiments for the extraction of Argemone mexicana and Pongamia pinnata seed oils using SFE.
2. To develop the relationship between input parameters and one output parameter (e.g. CEY of oil) based on the results obtained from experiments for the SFE of Argemone mexicana and Pongamia pinnata seed oils.
3. To develop an artificial neural network (ANN) model to relate input parameters to output parameter for the SFE of oils from Argemone mexicana and Pongamia pinnata seeds.
4. To explain the matrix effect of seed in extraction of oil from different seed matrices by performing SEM (scanning electron microscope) of extractable and extracted material.
5. To compare the experimental results with the results of mathematical models (Sovova, 1994) and (Reverchon, 1996) obtained for SFE process.
6. To characterize the extracted oil samples by the means of gas chromatography and to find out the physico-chemical properties of extracted oils.
7. To check the economic feasibility of the present SFE process by performing the economic analysis of a large scale envisaged SFE plant.

# LITERATURE REVIEW

A thorough literature review was conducted based on the objectives of the present investigation formulated in Chapter 1. As the central objective of the present work is to extract the oil from the natural seeds of Argemone mexicana (AM) and Pongamia pinnata (PP), using the carbon dioxide at its supercritical condition, a literature review was carried out related to supercritical fluids (SFs) especially supercritical carbon dioxide (SC-$CO_2$) and technology (e.g. supercritical fluid extraction (SFE)) based on it. The extraction of oils using SFE is found to be affected by many parameters; thus, a literature review was carried out to know the effect of various parameters on the SFE process. In addition to $CO_2$, some amount of organic solvent (e.g. Ethanol) was also used as a co-solvent to improve its polarity, therefore a short literature review, showing the advantages and disadvantages of it, was also conducted. Consequently, the present literature review also includes the review on the extent of wok done on selected extractable materials (e.g. AM and PP seeds).

Besides the above, the present review also includes a review on different design of experiment (DoE) techniques used and the criteria of selecting a particular DoE technique. The selected method (e.g. BBD technique), used for optimization of operating parameters during the SFE process was also reviewed based on its performance parameters.

The characterization of the extractable materials (e.g. AM and PP seeds) as well as its products (e.g. oils) were performed, thus a review, on the instruments used, physico-chemical properties of oils and their application, was presented here. In the present work, some mass transfer based mathematical models (e.g. Sovova model (Sovova, 1994) and Reverchon model (Reverchon, 1996) were used to validate the present data. Therefore, an extensive literature review on the mathematical modeling of SFE process was carried out, which also includes the chronological development of mathematical models and illustrating the selected models.

## 2.1 Supercritical fluids

A supercritical fluid (SF) is defined as the fluid that is at temperature and pressure above its critical temperature ($T_c$) and critical pressure ($P_c$), where distinct liquid and gas phases do not exist (Mukhopadhyay, 2000). The condition of critical temperature ($T_c$) and critical pressure ($P_c$) can be understood with the help of following statements: when a gas is compressed to a sufficiently high pressure, it becomes liquid. If, on the other hand, the gas is heated up beyond a specific temperature, no amount of compression of the hot gas will cause it to become a liquid. This temperature is called the critical temperature ($T_c$) and the corresponding vapor pressure is called the critical pressure ($P_c$). The state of the fluid is called the supercritical fluid (SF) state as shown in Fig. 2.1.

The supercritical state of a fluid can be illustrated with the help of a phase diagram (as shown in Fig. 2.1) of a pure substance. As shown in Fig. 2.1, three phases (e.g. solid, liquid and gas) of a pure substance coexist at the triple point but as the temperature goes high, only two phases (e.g. gas and liquid) remain exist. Further increment in the temperature and pressure brings the substance at a critical point. At the critical point and in the nearby region the temperature and the pressure are above the critical temperature ($T_c$) and pressure ($P_c$), the substance exists in a single gaseous phase that is identified as 'Supercritical Region' as shown in Fig. 2.1 (Clifford, 1993).

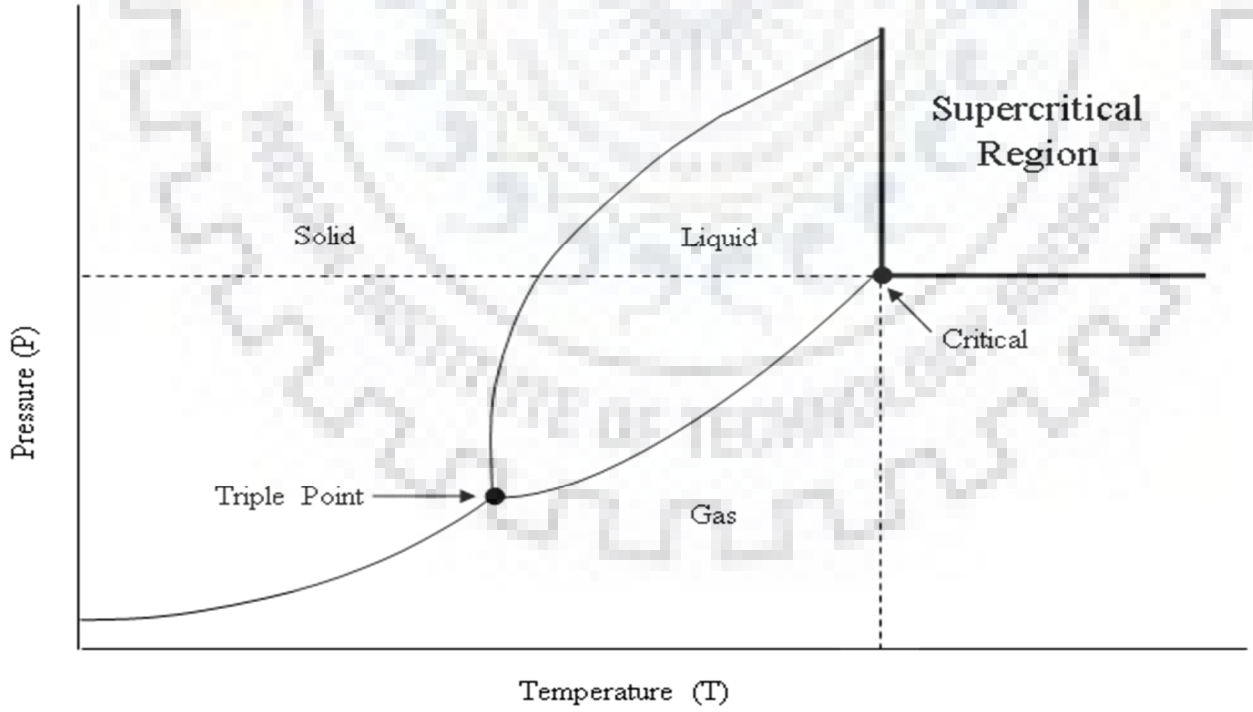


Fig. 2.1: Phase diagram for a pure component.

In the supercritical state, a solvent displays properties, which are intermediate to those of liquid and gaseous states (Mukhopadhyay, 2000). The order of magnitudes of some common physical properties of SF solvents (including the carbon dioxide) with those corresponding to the liquid and gaseous states have been given in Table 2.1. From the Table 2.1, it could be concluded that the SFs pertains the best properties of a liquid and gas means liquid-like density of a SF provides its high solvent power, whereas the gas-like viscosity and diffusivity together with zero surface tension, impart excellent transport properties (del Valle et al., 2008) to SF solvent.

Table 2.1 Orders of magnitude of physical properties of solvents in different states.

| Physical property | State of solvent | | |
|---|---|---|---|
| | Liquid | SF | Gas |
| Density (g/ml) | 1 | 0.2 - 0.9 | $10^{-3}$ |
| Diffusivity ($cm^2/s$) | $10^{-6}$ | $10^{-3}$ | $10^{-1}$ |
| Viscosity (g/cm.s) | $10^{-2}$ | $10^{-4}$ | $10^{-4}$ |

2.1.1 Discovery and historical background of supercritical fluids

The history of SFs can be linked to the discovery of critical points of temperature and pressure by Charles Cagniard de La Tour in 1821 (Stahl et al., 1980). Hannay and Hogarth described the dissolving properties of a SF by dissolving the low vapor pressure solid material in SF in 1879 (Hannay and Hogarth, 1879). Later, Buchner reported the solubilities of certain non-volatile organic materials in $CO_2$ under supercritical conditions, which were higher by order of magnitude than the expected from conventional fluid alone (Mukhopadhyay, 2000). Even though, the dissolving capacity of a SF was known to be determined by its density (e.g. pressure-temperature) to a first approximation, extraction and separation of mixtures with SFs aroused little interest during the first half of the twentieth century. A significant development in SFE was the Zosel's patent (Zosel, 1978), which provided incentives for extensive future work thereafter the first commercial applications of SFs (e.g. SC-$CO_2$) came into existence in the late 1970s for the decaffeination of coffee and tea, refining of cooking oils, recovering of flavors and pungencies from spices and other natural products.

Since 1980, there has been a rapid development of SFE, for the extraction of hops, cholesterol from butter, perfumes, flavors, oils from natural products (e.g. seeds, leaves, stems, roots, flowers etc.), residual solvents and monomers from polymers, and fatty acids from fish oils.

2.1.2 Selection of $CO_2$ as supercritical fluid for the present process

The selection of $CO_2$ gas as solvent for the present SFE process is based on some main aspects such as critical values of temperature and pressure, solubility in ethanol, health and environmental effects (e.g. toxicity), cost and availability. Table 2.2 has shown a comparison of $CO_2$ gas with the other used solvents, which have also been used as SFs. The carbon dioxide ($CO_2$) gas has the most convenient critical values of temperature ($T_c$ = 32.1 °C) and pressure (Pc = 73.8 bar) compare to other listed solvents as shown in Table 2.2 (Mukhopadhyay, 2000; Al-Darmaki et al., 2011). However, some other solvents (e.g. chlorotrifluoromethane, ethane, ethylene, nitrous oxide etc.) have also shown lower critical values of temperature and pressure but these are toxic, costly, non-availability in plenty amount.

The selected liquid $CO_2$ gas has been modified with ethanol, which acts as co-solvent for the present process. In addition to the above arguments, $CO_2$ is the second cheapest solvent after water costing Rs 18 per kg among all the listed solvents and in handling and disposal issues, other organic solvents can pose a number of environmental and health problems at atmospheric and toxicity levels. In many cases, conventional organic solvents (as shown in Table 2.2, excepting $CO_2$) are regulated as volatile organic compounds (VOCs) while certain other organic solvents (e.g. chlorotrifluoromethane) are under restriction due to their ozone-layer-depletion potential. Therefore, carbon dioxide ($CO_2$) could be an attractive alternative in place of traditional organic solvents. The further necessary qualities as reported in literature have also been discussed in the next section 2.1.3.

Table 2.2 Comparison of $CO_2$ gas with other available solvents for the SFE process.

| Solvents | Critical Temp. (Tc) (°C) | Critical Pre. ($P_c$) (bar) | Solubility in Ethanol | Health and environmental effect | Cost (Rs/kg) |
|---|---|---|---|---|---|
| Ammonia | 132.5 | 112.8 | Highly soluble | Toxic if inhaled | 60 |
| Benzene | 289 | 48.9 | Slightly soluble | Highly toxic | 10000 |
| **Carbon dioxide** | **32.1** | **73.8** | **Soluble** | **Toxic if inhaled in excess** | **18** |
| Cyclohexane | 280 | 40.7 | Soluble | Toxic | 220 |
| Chlorotrifluoromethane | 28.9 | 39.2 | NA | Toxic | 400 |
| Ethane | 32.2 | 48.8 | Insoluble | Toxic | 5240 |
| Ethylene | 9.3 | 50.4 | Soluble | Toxic | 1400 |
| Isopropanol | 235.2 | 47.2 | Soluble | Toxic | 150 |
| Nitrous oxide | 36.5 | 71.0 | Soluble | Non toxic | 500 |
| Propane | 96.7 | 42.5 | Soluble | Toxic | 7000 |
| Propylene | 91.9 | 46.2 | Soluble | Toxic | 2500 |
| Toluene | 318.6 | 41.1 | Soluble | Toxic | 85 |
| Water | 374.2 | 220.5 | Soluble | Non toxic | 10 |

### 2.1.3 Supercritical properties of carbon dioxide

Carbon dioxide can be considered as the most valuable solvent for the SFE processes for several reasons. The high selectivity is one of the most important properties of SC-$CO_2$ extraction. The selectivity of this extraction process can be adjusted by tuning the process pressure and temperature. Carbon dioxide has a technically convenient critical pressure and temperature of 73.8 bar and 32.1 °C respectively as shown in Table 2.2, specially, the critical temperature ($T_c$ = 32.1°C) of $CO_2$, is near ambient, making it an attractive solvent for temperature-sensitive materials (Kumar et al., 2005). It is non-toxic, non-flammable, non-reactive, non-corrosive, and its solvent power may be enhanced by the addition of modifiers (e.g. liquid compounds) of different polarities (del Valle and Aguilera, 1999; Lang and Wai, 2001; Alzate et al., 2013). Furthermore, it is the second least expensive solvent after water and it does not leave any solvent residue after extraction (Madras et al., 2004). Further, carbon dioxide is a relatively good solvent for hydrocarbons and non-polar solids. However, owing to the unique properties of supercritical solvents and to the rather large quadra pole moment of carbon dioxide in particular, SC-$CO_2$ will dissolve many relatively volatile polar compounds. Adding small amounts of polar co-solvents (e.g. methanol, ethanol, propanol, etc.), called as entrainers to the bulk carbon dioxide can enhance the solubility of polar, non-volatile solutes in SC-$CO_2$ (Bartle et al., 1990).

### 2.1.4 Advantages and disadvantages of SC-$CO_2$ as a solvent

The advantages of using SC-$CO_2$ as a solvent are largely associated with environmental, health, safety, and related to increased uneasiness about the presence of conventional organic solvents (e.g. as listed in Table 2.2 excepting the water) residues material for human consumption (Marr and Gamse, 2000). However, some researchers (e.g. Reverchon and Senatore, 1992; Moyler, 1993; Kerrola and Kallio, 1993; Vilegas et al., 1994; Belayneh et al., 2015) have established certain applications that the extracts obtained are more acceptable to taste panels than extracts obtained in other solvents. This, in turn, probably relates to the closeness to which the extracted flavor resembles that in the original plant. The point wise advantages and disadvantages of SC-$CO_2$ are given bellow for a better comparison of both sides of SC-$CO_2$ application.

*Advantages:*

- The SC-$CO_2$ can be recycled easily.
- Probability to form side products is negligible due to its chemical inertness.
- Accident chances (e.g. spillage, fire and explosion) reduced drastically due to its non-flammable nature.
- SC-$CO_2$ has good solvent characteristics for non-polar and slightly polar solutes.
- Carbon dioxide is a 'natural' substance, present in mineral waters and part of the life cycle.
- SC-$CO_2$ can be easily removed from the final product.
- The solvation power of SC-$CO_2$ can be controlled by the selection of a suitable combination of pressure and temperature.
- Carbon dioxide has a convenient critical temperature (32.1 $^oC$). This enables extractions to be carried out at comparatively low temperature, which decreases the risk of damage of thermo-labile compounds.
- Extraction of natural raw material with SC-$CO_2$, allows the obtained extracts with flavor and taste, which are perfectly respected and reproducible.
- SC-$CO_2$ has also proved its great solubility toward polar compounds with the addition of small quantities of other solvents (e.g. ethanol, methanol etc.) named as co-solvent or modifier.

*Disadvantages:*

Despite the large number of advantages, as mentioned above, the SC-$CO_2$ also has some disadvantages as summarized below;

- The use of high purity SFE-grade $CO_2$ is not required but impurity and moisture in industrial grade $CO_2$ can accumulate and may interfere with further analytical operations (gas or liquid chromatography).

- Online cleanup system is required to maintain the purity of $CO_2$ by removing the dust and moisture contaminants, which resulted into high capital cost.

- SC-$CO_2$ being a non-polar solvent is not capable to extract the polar compounds unless a polar solvent (e.g. ethanol, methanol etc.) as a modifier is added. Therefore, this process can be named as less green technology.

## 2.2 Supercritical fluid extraction (SFE) technology using SC-$CO_2$ in modern research scenario

Supercritical fluid extraction (SFE) is today a growing and a popular technology for rapid, contamination-free extraction in the food and pharmaceutical industries. In subsequent sections, the applications of the SFE is shown, which actually reveals its importance in modern research.

### 2.2.1 Application of SFE technology using SC-$CO_2$

The SFE using $CO_2$ is undoubtedly a good technology for the extraction of natural products such as seeds, roots, leaves, flowers, fruits, stems as reported by Suryawanshi and Mohanty, 2018a; Rodrigues et al., 2018; Kueh et al., 2018; Grijo et al., 2018; Cunha et al., 2019 and Zachova et al., 2018 respectively. SFE of chemical components from various chemical compounds such as steroids, anthracene, benzamide, ergosterol, piperine, acetaminophen, and activated carbon have been reported by Kane et al., 1993; Bakhbakhi, 2011; Li et al., 2011; Cheng et al., 2013; Kumoro et al., 2009; Sabet et al., 2012 and Ushiki et al., 2017 respectively. In addition to these, essential oils from different algae (Patil et al., 2018), components from different liquids (Asep et al., 2013), meat (Rahman et al., 2018), polymers (Viguera et al., 2018), and polluted soil (Khanpour et al., 2014) have also been extracted using SFE technique. After reviewing more than 350 research articles from the year of 1980 to 2018, based on the SFE using SC-$CO_2$ through the science direct web portal, it has been seen that the SFE technology has been used extensively as shown in Fig. 2.2. From the figure (Fig. 2.2), it can be concluded that the application of SFE technology using SC-$CO_2$ for the extraction of natural products (as mentioned above) has shown a positive increment in terms of number of publications. As evident from Fig. 2.2, the SFE of natural seeds have attracted researcher's attention significantly. These applications of SFE technology for other natural products such as algae, chemical compounds, meat, liquids, polluted soil, and polymer have also been progressed as shown in Fig. 2.2. After successful application of this technology at laboratory scale during the extraction of various materials (as mentioned above), the SFE technology has been

commercialized at large scale processes as shown in Table 2.3. Large scale production using SC-$CO_2$ has been in commercial operation since the late 1970s for the decaffeination of coffee and tea, refining of cooking oils and recovering flavors and pungencies from spices, and other plant materials (Mukhopadhyay, 2000). Bruno et al., 1993 have shown some known industrial applications of SC-$CO_2$ in food industries which includes, extraction of coffee, tea, herbs, spices, flavors and antioxidants, extraction of special oils, de-oiling of press cakes and cleaning of rice.

In addition to extracting desired compounds from plants, another very interesting application of the SFE technique is the extraction or cleanup of pesticides from natural products including herbal medicines (Lang and Wai, 2001). Catalytic reactions such as polymerization, hydrogenation, catalytic hydrothermal gasification and enzymatic reactions in SC-$CO_2$ have been receiving an increased attention during the last decade (Sarkari et al., 1999; Kumar et al., 2004; Khosravi-Darani and Vasheghani-Farahani, 2005). Pharmaceutical and cosmetic industries are also using SFs for extracting the herbal medicines and active ingredients for cosmeceutical applications and fragrances. Some researchers (e.g. Hong and Pyun, 2001; Khosravi-Darani and Vasheghani-Farahani, 2005; Dalvi and Mukhopadhyay, 2009b; Kumar et al., 2013) have shown the application of SFE technique in material processing (e.g. coating, dyeing, crystallization, impregnation etc.) and in cleaning (e.g. dry cleaning, cleaning of metallic parts, soil reclamation, removal of undesired substance). Other special applications such as membrane-based separation, microwave-induced SFE, sterilization, thin film extraction have also been reported in literature.

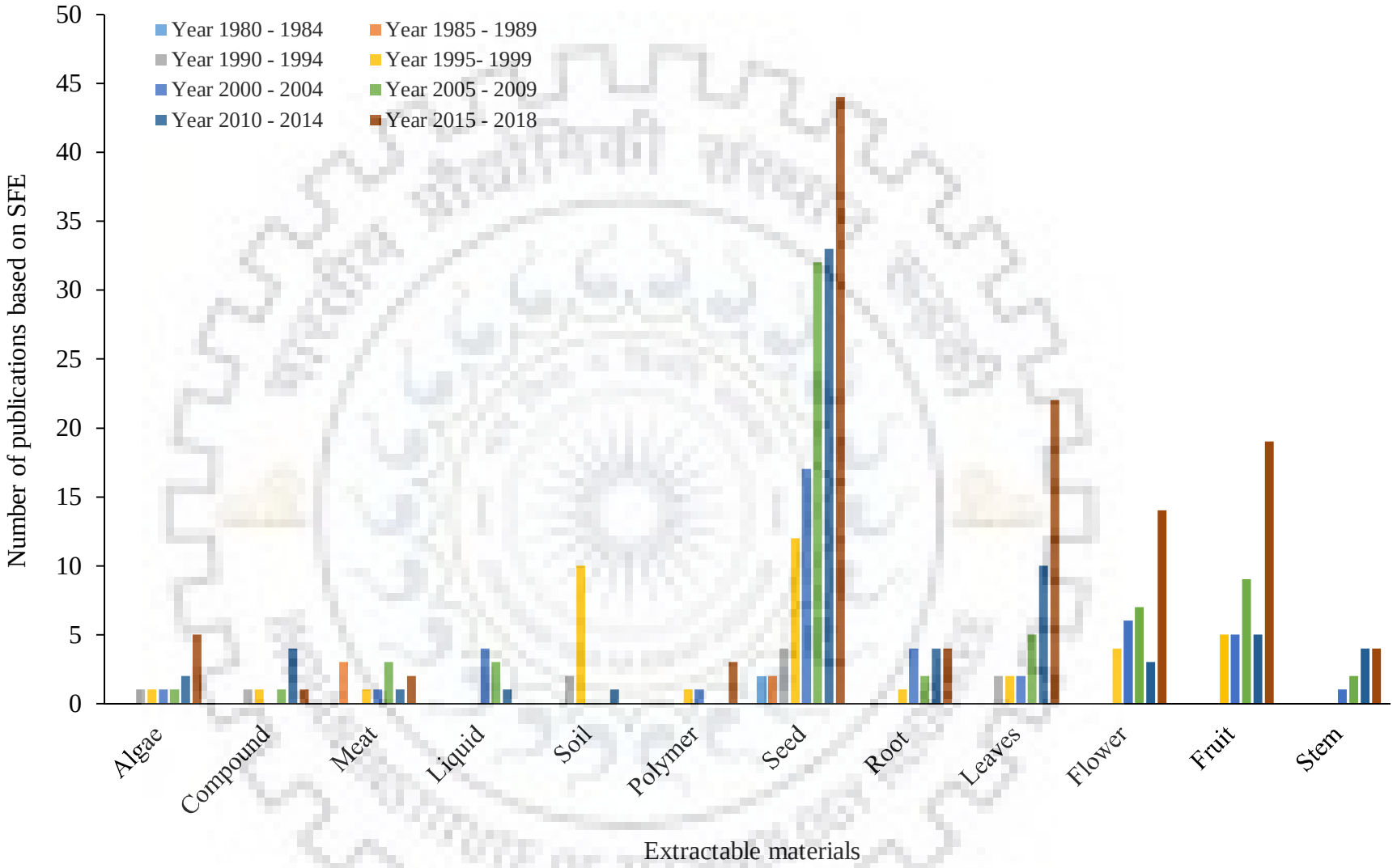


Fig. 2.2: Publications of different types of extractable materials used during SFE using SC-$CO_2$ as solvent.

Table 2.3. Commercial scaled SFE plants and processes based on $CO_2$.

| Process | Location | Manufacturer |
|---|---|---|
| Coffee decaffeination | Houston, Tex., U.S. | Maximus Coffee Group LP (formerly General Foods) |
| | Bremen, Germany | Kaffe HAG AG |
| | Bremen, Germany | Hermsen |
| | Poszillo, Italy | SKW-Trostberg AG |
| Tea decaffeination | Munchmuenster, Germany | SKW-Trostberg AG |
| Fatty acids from spent barley | Dusseldorf, Germany | Marbery, GmbH |
| Vitamin E oil, phytosterol, fatty acid methyl ester, ginger oil | Wuhan, Hubei, China | Wuhan Kaidi Fine Chemical Industrial Co. |
| Nicotine extraction | Hopewell, Va., U.S. | Philip Morris |
| Natural insecticide/pesticide (Pyrethrum extract) | High Wycombe, U.K. | Agropharm |
| Hops extraction | Wolnzach, Germany | Hopfenextraktion, HVG |
| | Yakina, Washington, U.S. | Hops Extraction Corp. of America |
| | Melbourne, Australia | Carlton & United Beverages Ltd. |
| | West Midlands, U.K. | Botanix |
| Spices/flavors/aromas/ natural products/colors | Munchmuenster, Germany | SKW-Trostberg AG |
| | Rehlingen, Germany | Flavex Gmbh |
| | Edmonton, Canada | Norac Technologies |
| | Tsukaba, Japan | Ogawa Flavours and Fragrances |
| | Milwaukee, Wisc., U.S. | Sensient Technologies |
| | Japan | Kirin Food-Tech Co. |
| Essential oils/Herbal extract/oleoresins/Organic products | India | Vidya Herbs Pvt Ltd, Bangalore, India<br>Pioneer Enterprise, Mumbai, India |
| Essential oils from plants and herbs | Holland | Proderna Biotech Pvt. Ltd., Holland |

### 2.2.2 Progress of the extraction phenomena during SFE process

The success of a SFE process also depends on the extraction step itself (e.g. nature of the extraction phenomenon and the choice/selection of SF solvent and solute). Therefore, it is necessary to understand the basic mechanism of extraction phenomenon of solute from porous structure of the seeds to the solvent at supercritical condition, which undergoes following steps:

1. SF solvent molecule transported from the bulk SF solvent phase (e.g. SC-$CO_2$) to the seed particle surface through the boundary layer adjacent to the particle surface through convection mass transfer and then from particle surface to the interior of seed particle by diffusion in solute filled pores.
2. Solutes dissolved into the SF solvent at the pore particle surface.
3. Step (1) occurs but in reverse direction means desorption of the solute molecules from the interior of solid matrix of seed particle with subsequent diffusion into the pore of solid matrix of seed particle and then solubilization of solute to the bulk SF solvent through stagnant film.
4. Sweeping out of the extraction bed of extractable by the SF.

From the above steps, it is clear that there are four types of physical mass transfer phenomenon (e.g. convection, diffusion, desorption and solubilization) played a crucial role in it.

### 2.2.3 Advantages and disadvantages of SFE technology

The SFs have the greatest dissolving power, which can be regulated by pressure and/or temperature. Since a SF solvent is highly volatile in nature, so it can be recovered easily from the extract. This process does not leave any harmful residue. Heat sensitive materials can be extracted at relatively low temperature range (Micic et al., 2011). In addition to these, the advantages of SC-$CO_2$ as a solvent (as listed in section 2.1.4) are also a value added thing for the SFE technology. On the other hand, this technology also has some disadvantages such as; compression and heating of solvent is required to meet critical conditions, which directly affects the operating cost of the process. Recycling and reuse of energy is not easy. High capital investment is required for equipment. Polar analytes are comparatively difficult to separate than non-polar analytes unless a modifier is used, making the process less 'green' (Senyay-Oncel et al., 2011). The carbon dioxide is the only practical SF solvent for this technology based on its temperature, pressure, and green requirement criteria.

## 2.3 Effect of various operating parameters on supercritical fluid extraction (SFE)

As per the published literature, SFE process is influenced by various operating parameters (e.g. temperature, pressure, particle size, flow rate of $CO_2$, type of co-solvent, % of co-solvent, extraction time, solubility parameters, solid matrix, packing of extraction bed, bed void fraction, moisture content, initial oil content and pretreatment of raw materials etc.). Therefore, the selection and optimization of these parameters have played a crucial role in determination of product yield, hence the effect of above parameters are discussed in the subsequent sections.

### 2.3.1 Effect of temperature

Some researchers (e.g. Mukhopadhyay, 2000; Nei et al., 2008; Suryawanshi and Mohanty, 2018b), have observed the duel effect of temperature during the SFE of natural materials. According to this, at constant pressure, an increase in temperature will reduce the density of SC-$CO_2$ and thus the solubility of the solute while on the other hand the same increase in temperature will increase the volatility of the solute component to be extracted. These two phenomenon are named as; density and volatility effects. However, these effects are counter acting in nature as far as the solubility of solutes in SC-$CO_2$ is concerned. This phenomenon has also been reported as 'retrograde solubility' behavior, which is mainly influenced by pressure, temperature and co-solvent effect. Hence, the effect of temperature on extraction is difficult to predict and depend on the nature of the sample too.

Ixtaina et al., 2010 have observed during the SFE of Mexican chia seed oil that at low pressures (e.g. 250 bar), the oil yield decreased with the rise of temperature, which may be attributed to reduced density of the SF with increase in temperature. However, in experiments with high pressures (e.g. 450 bar), the oil yield increased with the rise of temperature, which may be attributed to the enhanced solubility of the oil in SC-$CO_2$. On the other hand, some researchers (e.g. Pederssetti et al., 2011; Kagliwal et al., 2011) have observed during the SFE of canola seed oil and bio-actives respectively that the increase in temperature at constant pressure induces a decrease in the extraction yield of seed oil as well as bio-actives. This could be due to lower density of SC-$CO_2$ at higher temperature (Westerman et al., 2006), which decreases the solvency and solubility of solute in SC-$CO_2$.

The retrograde solubility interference phenomenon as explained by Mukhopadhyay, 2000, has also been observed during the SFE of Nigella sativa, Nitraria tangutorum, grape, and Dracocephalum

kotschyi seed oils by Solati et al., 2012; Liu et al., 2014; Duba and Fiori, 2015 and Sodeifian et al., 2016c respectively.

### 2.3.2 Effect of pressure

The extraction pressure also plays an important role during the SFE processes because it affects the density of supercritical solvent hence the, solvation power (Mukhopadhyay, 2000). This could be explained by the fact that the solvation power of solvent at the supercritical state is density dependent indicating that a rise in the extraction pressure, at constant temperature, leads to a higher fluid density, which increases the solubility of the solvent (Kagliwal et al., 2011). On the other hand, an increase in the extraction pressure leads to decrease in the diffusivity, which ultimately results in a reduction in the interaction between the SF and the solute contained within the matrix, and this makes the yield of the extraction process decrease (Khajeh et al., 2010). In addition to this, it has also been observed that the excessive extraction pressure may reduce the extraction selectivity. Further, the presence of undesired co-extracted solutes can change the solubility level of the solute of interest (Pourmortazavi and Hajimirsadeghi, 2007). Therefore, high-pressure operation is not recommended for selective extraction.

A linear increment in extraction yield during the SFE of seeds (e.g. grape, watermelon, pongamia pinnata seeds) has been observed by Duba and Fiori, 2015; Rai et al., 2015 and Suryawanshi and Mohanty, 2018a that actually supports the fact that at constant temperature the density of SF increases with pressure and thus yield. Whereas, many researchers (e.g. Celik and Guru, 2015; Maran and Priya, 2015; Wang et al., 2016; Koubaa et al., 2016; Haloui and Meniai, 2017) during the SFE of various natural seeds (e.g. milk thisle, muskmelon, gynostemma pentaphyllum, canola, argania spinose) have shown the positive as well as negative effect of pressure. The negative/negligible effect of excessive pressure on the extraction yield of various seed oils is due to the decrement in the diffusivity and selectivity of the solvent (Pilavtepe et al., 2012). For example, Koubaa et al., 2016 have shown that the extraction yield of canola seed oil increased from 21.68% to 33.19% during the pressure range 150 to 300 bar thereafter, a little decrement was observed at 350 bar.

### 2.3.3 Effect of particle size

The particle size of the raw feed materials also plays an influential role in the SFE process because the rate of removal of a solute from a solid matrix during SFE is also depend on the rate of mass transport of the solute out of the sample matrix (Tan et al., 2008). In addition to this, the particle size also influences the physical morphology of the sample matrix that can have a profound effect on the extraction yield obtained by SFE using SC-$CO_2$. From the available literature (e.g. Nguyen et al., 2011; Liu et al., 2014; Ozkal and Yener, 2016; Sodeifian et al., 2017; Suryawanshi and Mohanty, 2018a; Suryawanshi and Mohanty, 2018c)), it is readily evident that the particle size may impose a dual (positive or negative) effect on the extraction yield. As the particle size of the feed decreases, surface area per unit mass increases, hence the extraction yield increases. Further, during grinding of the seed kernel to create small particles, the cell walls are disrupted and this increases the ratio of broken to intact cells and subsequently offers more accessible oil to the SC-$CO_2$. Furthermore, small particle size might shorten the diffusion path into the plant matrices, through which the extract has to return, decreasing intra-particle mass transfer resistance hence enhancing the extraction yield. On the other hand, from the mass transfer point of view, further decreasing the particle size may inhibit the extraction, so that the oil may be conveniently re-adsorbed on matrix surfaces, leading to a reduction in solute transportation. In addition, small particle sizes may trigger bed caking formation (particles sticking together) leading to formation of channels along the bed in which supercritical fluid can superiorly flow, resulting in an inadequate contact between SC-$CO_2$ and the sample, eventually leading to insufficient extraction.

Many researchers (e.g. Reverchon et al., 2000; Doker et al., 2004; Tan et al., 2008; Rai et al., 2015; Rai et al., 2016a) have reported the single (negative) effect of particle size on the extraction yield during the SFE of various seeds (e.g. hiprose, apricot bagasse, cocoa butter, watermelon, sunflower) using SC-$CO_2$ as solvent. Whereas, some researchers (e.g. Nguyen et al., 2011; Liu et al., 2014; Ozkal and Yener, 2016; Sodeifian et al., 2017; Suryawanshi and Mohanty, 2018a; Suryawanshi and Mohanty, 2018c) have shown the dual effect of particle size on the extraction yield during the SFE of various natural seeds (e.g. moringa oleifera, nitraria tangutorum, flaxseed, dracocepthalum kotschyi, pongamia pinnata, and argemone mexicana respectively). In addition to the above arguments, suggested by various researchers, Suryawanshi and Mohanty, 2018a have also introduced another conceptual reason behind the lower yield achievement for the lowest particle size

that is the occurrence of compaction due to initial high pressure across the extraction bed of smallest particles, which ultimately leads to the channeling inside the bed. However, Reverchon, 1996 has shown that the shape of the particles can also influence the speed and completeness with which an SFE can be conducted.

### 2.3.4 Effect of flow rate-$CO_2$

The flow rate of $CO_2$ is an important parameter for the SFE that to be optimized, since it influences the contact time between the solvent (SC-$CO_2$) and the material in the extractor and it affects the extraction efficiency (Koubaa et al., 2016; Lu et al., 2007). It also controls the extraction rate, especially if the external mass transfer resistance controls the extraction process (Reverchon, 1996). The extraction yield increases significantly with flow rate of $CO_2$ due to the fact that at increasing the flow rate of $CO_2$, the thickness of the film layer around the solid particles reduced and mass transfer resistance surrounding the solid particle becomes smaller while at higher flow rate of $CO_2$, the solvent may move too quickly through the extraction bed and exit the extractor unsaturated causing a declination in extraction yield (Suryawanshi and Mohanty, 2018a).

Some researchers (e.g. Celik and Guru, 2015; Maran and Priya, 2015; Koubaa et al., 2016; Zekovic et al., 2017, Suryawanshi and Mohanty, 2018a; Suryawanshi and Mohanty, 2018c) have shown the duel effect of flow rate of $CO_2$ on the extraction yield of seed oils (e.g. milk thistle; muskmelon; canola; coriander; pongamia pinnata and argemone mexicana), during the SFE using SC-$CO_2$. On the other hand, some researchers (e.g. Rai et al., 2015; Ni et al., 2015; Duba and Fiori, 2015; Rai et al., 2016a; Ozkal and Yener, 2016; Da Porto and Natolino, 2017) have observed the increasing effect of extraction yield with increase in the flow rate of $CO_2$ during the SFE of various seeds (e.g. watermelon; torreya grandis; grape; sunflower, flaxseed; grape). However, the effect of flow rate of $CO_2$ on the extraction yield has also been explained on the basis of mass transfer coefficients (e.g. solvent and solid phase mass transfer coefficients). The external mass transfer is purely controlled by solvent phase mass transfer coefficient while the internal mass transfer is controlled by the solid phase mass transfer coefficient that has been observed by (Duba and Fiori, 2015).

2.3.5 Effect of the % of co-solvent

The amount of co-solvent (modifier) also plays an important role during the SFE using SC-$CO_2$ because being a non-polar solvent, carbon dioxide could only be suitable for dissolving the non-polar compounds such as hydrocarbons. However, some studies (e.g. Lang and Wai, 2001; Brondz et al., 2017) show that the quadrupole moment of carbon dioxide also helps in the dissolution of some moderately polar compounds such as ketones, esters, aldehydes and alcohols. However, the extraction of polar compounds have been done at large by adding the co-solvent, which improves the SC-$CO_2$ extractability by increasing the polarity of the carbon dioxide. The addition of a co-solvent to a SF, generally, increases the polarity, solute–solvent interaction and bulk density of the fluid mixture, which would contribute to solubility enhancement thus increasing the extraction yield (Rai et al., 2015; Suryawanshi and Mohanty, 2018a).

Various researchers (e.g. Cocero and Calvo, 1996; Lin et al., 1999; Illes et al., 1997; Tong and Imagawa, 1995; Abaroudi et al., 1999; Demirbas, 2000; Sheibani and Ghaziaskar, 2008) have studied the effects of several co-solvents such as ethanol, methanol, propane, dichloromethane, toluene, n-hexane and acetone during the SFE of sunflower seeds, scutellariac herbs, hiprose fruit, polluted soil, β-naphthol, pistachio seeds, olive seeds respectively. Most of the researchers have used 'Ethanol' as a co-solvent for the SFE of various materials, however, the selection of co-solvent (in our case it is 'Ethanol') has already been explained in section 2.5., of this Chapter. Recently, the researchers (e.g. Rai et al., 2015; Rai et al., 2016a; Da Porto and Natolino, 2017; Suryawanshi and Mohanty, 2018a and Suryawanshi and Mohanty, 2018c) have used 'Ethanol' as co-solvent during the SFE of different seeds such as watermelon, sunflower, grape, argemone mexicana, and pongamia pinnata respectively and found that the addition of co-solvent enhances the extraction yield of the respective seed oil.

2.3.6 Effect of extraction time

The extraction time plays a significant role during the SFE process. Extraction time strongly depends on two factors (a) structure of solid matrix and (b) the position of solute in it. If the solute is situated at the surface of the extractable then it could be extracted in shorter time while if it is available inside the core of the solid matrix then $CO_2$ has to diffuse through the core wall to reach the solute that results in a longer extraction time (Maran and Priya, 2015). As the extraction time is

increased, longer is the contact time for solvent to reach solute, which results in an increased extraction yield. In addition to this, as the extraction time is increased, the ratio of SC-$CO_2$ to the extractable is also increased which ultimately enhances the extraction rate (Sodeifian et al., 2017). However, it has also been observed that the beyond a certain extraction time (which differs according to different extractable), the extraction rate starts falling because with time the solute volume gradually disappears from the solid matrix leading to an increased mass transfer resistance as well as reduction of mass transfer driving force and thus the extraction yield decreases.

Various researchers (e.g. Belayneh et al., 2015; Przygoda and Wejnerowska, 2015; Maran and Priya, 2015; Wang et al., 2016; Goleroudbary and Ghoreishi, 2016; Belbaki et al., 2017; and Sodeifian et al., 2017) have shown an increasing behavior of extraction rate with increase in the extraction time during the SFE of camelina seeds, quinoa seeds, muskmelon seeds, gynostemma pentaphyllum seeds, safron leaves, algerian olives, and dracocephalum kotschyi seeds respectively.

### 2.3.7 Effect of solubility parameters

Solubility parameters (SPs) play an important role in the indication of the solubility of various solutes in SF solvent. King, 1989 has shown that solubility parameter estimation is very effective to gain an insight into solute solubility in SFs. The solubility parameter of a solvent can be obtained through experimental measuring, estimated using empirical equations, or calculated via molecular simulation methods. However, there are few empirical equations (given by Koenhen and Smolders, 1975; Aliada, 1984; Panayiotou, 1997) that can be used to estimate the solubility parameter (SP) of a SF. These empirical equations so far can't reveal the effect of temperature, pressure, density and co-solvents on the solubility parameter of SC-$CO_2$. Therefore, Zhang et al., 2017 carried out molecular dynamic simulation to show the effects of pressure, temperature on solubility parameter and found that the solubility parameter (SP) of $CO_2$ at the supercritical state, enhances with the raising of pressure at the fixed temperature, and reduces with the raising of temperature at the fixed pressure. These observations are in good agreement with the reports by Luo and Rui, 2015. The solubility parameter of $CO_2$ solvent were reported as $10(MPa)^{1/2}$ and $5(MPa)^{1/2}$ at pressures 75 bar and 73 bar respectively. The reason for the huge change of SP of $CO_2$ solvent around its critical point is that the physical properties of $CO_2$ at the supercritical state are considerably different from the conventional gas state. This huge difference of the SPs of $CO_2$ at its supercritical and conventional

gas state make $CO_2$ a promising solvent for a lot of nonpolar and weak polar solute thus the extraction of solute from the feed using SC-$CO_2$ at supercritical state and then desorb from the solvent at the conventional gas state is easily possible. The solubility parameter of SC-$CO_2$ solvent boosts linearly with the raising of its density, which is consistent with the findings in previous work by Kiran et al., 2012. In addition to this, the solubility parameters of 'SC-$CO_2$ - co-solvent' (e.g. ethanol, acetone, cyclohexane) enhance with the raising of pressure, reduces with the raising of temperature, and increase linearly with the raising of system density, which are similar to the behaviors of pure SC-$CO_2$ solvent and SC-$CO_2$-methanol solvent. However, the solubility parameter of 'SC-$CO_2$-ethanol' is higher than that of 'SC-$CO_2$- acetone' and 'SC-$CO_2$-cyclohexane' at the same conditions. The co-solvent effect on the solubility parameter of SC-$CO_2$ reduces in the order of co-solvents as: ethanol > acetone > cyclohexane.

### 2.3.8 Effect of solid matrix

Along with the effects of parameters discussed above, the interactions between solutes and the active sites of the matrix (means the matrix effect) can also influence the SFE process. Therefore, the success of a SFE process not only depends on the extraction step itself (e.g. operating parameters and choice of SFs) but also on the matrix considered. The physical structure of the matrix is of critical importance, as the extraction efficiency, which is related to the ability of the SF to diffuse within the matrix (Pourmortazavi and Hajimirsadeghi, 2007) plays a role. For that reason, the extraction conditions of the same group of oils may differ from one matrix to another.

As a general observation, decreasing the particle size of solid matrices leads to a higher surface area and exposure to solute imbedded into the matrix, making SFE more effective and efficient. However, the excessive grinding (to reduce the particle size) may hinder the extraction due to re-adsorption of the solutes onto matrix surfaces and pressure drop inside the extraction bed. Ling and Liao, 1996 assessed the influence of two different spiking methods (e.g. spot and slurry methods) during the SFE of organochlorine pesticides (OCPs) from sulfur containing soils. This study reveals that spot-spiking method significantly influences the SFE extraction efficiency of OCPs from soils. On the other hand, Sun et al., 2001 have shown that the chemical/physical properties of the sample matrix and the polarity of the extractant are the critical factors that affects the efficiency of '$CH_3Hg+$' from the chosen matrices and found it to be in the order as; cellulose > silica gel > starch > aluminium

oxide during a study on SFE of polar mercury species from solid samples. Librando et al., 2004 have studied the matrix effect of marine sediments during the SFE of polycyclic aromatic hydrocarbons from it. Further, progress in this direction, Araus et al., 2009 have introduced the concept of single parameter (e.g. microstructural factor) that can describe the effect of a substrate and its pretreatment on the SFE of plant essential oils. This single parameter appears to be independent of process conditions (e.g. pressure and temperature), interstitial solvent velocity, and substrate particle size, but depends on the location of the solute within the plant material, as affected by its pretreatment.

### 2.3.9 Effect of packing of bed

The effect of packing of extraction bed has also been the matter of research in present time because of its contribution to enhance the effective area for mass transfer. Various types of packings (e.g. pall rings, berl saddles, rasching rings, glass beads etc.) of inert materials have been used. However, the glass beads have been used extensively as packing material during the SFE process.

It has been seen that the glass beads mixed with the ground extractable materials to disperse the matrix and thus increases the contact surface of the sample with the solvent, and it improves the homogeneity of the sample packed into the extraction solvent (Nguyen et al., 2011). Sheibani and Ghaziaskar, 2008 have demonstrated that the use the glass beads as packing material increased the extraction yield by more than 15%, and decreased the solvent consumption during the SFE of pistachio seed oil using SC-$CO_2$. This is because the glass beads have prevented the formation of preferential channels thus allowing the SC-$CO_2$ to be distributed uniformly in the extractor. It allowed the solvent to penetrate covering wide surface areas of the ground kernels thus promoting better extraction of the oil.

### 2.3.10 Effect of bed void fraction

The bed void fraction (or equivalently, bed porosity) has also shown an influence on the extraction kinetics (extraction rate). Nei et al., 2008; Duba and Fiori, 2015 have studied the effects of bed void fraction on the extraction yield during the SFE of trout powder and grape seed respectively and concluded that the extraction yield decreases with decreasing the bed void fraction. The reduction in extraction yield with the bed void fraction is due to the fact that the flow inhomogeneity (channeling) occurred at degree of high compaction. Another potential cause is the reduction in residence time of the solvent into the extractor at the reduced bed void fraction. On the

other hand, greater bed void fraction can enlarge the contact area between solvent and extractable; hence, it can improve the mass transfer of oil to the SC-$CO_2$, although from the economic point of view, the fewer void bed is more suitable.

### 2.3.11 Effect of moisture content

Moisture content of the raw feed material is also one of the key factors in determining the quality and quantity of the output of a SFE process. Water is considered to be soluble at approximately 0.3% v/v in SC-$CO_2$ (Pourmortazavi and Hajimirsadeghi, 2007). The presence of water, however, may either assist in or be an impediment to the diffusion of SC-$CO_2$; what is necessary for effective SFE depends on the type of compounds targeted (Khaw et al., 2017). For example, Nagy and Simandi, 2008 reported extremely low extraction yield of paprika seed oil due to 85% of moisture content in it while Balasubramanian et al., 2013 have shown a negligible effect of 5% of moisture content on the extraction yield of lipid during the SFE of marine microalgae (Nannochloropsis sp.).

The water can be an aid in the SFE process or be detrimental, depending on water can, open pores or swell the solid matrix, thereby allowing the SF better access to solutes, and aid in flow through the matrix. Also, even though water is only 0.3% soluble in SC-$CO_2$ (as mentioned above), it serves to increase the polarity of the SF and enable higher recoveries of relatively polar species. However, if excess water remains in the vessel, a highly water soluble solute will prefer to partition into the aqueous phase and its SFE recovery will be low. For solutes that are insoluble in water, the solutes precipitate onto matrix surfaces, and even though the solute may be highly soluble in the SF, the excess moisture in the sample acts as a barrier in transfer of the solute to the SF. On the other hand, the semi polar solutes will dissolve in the aqueous phase, but readily partition into the SC-$CO_2$ and yield high recoveries. In addition to this, Ivanovic et al., 2011 have verified the effects of moisture content on the extraction of essential oils from the flowers of helichrysum italicum. They observed that pre-soaking of the samples in water (moisture content: 28.4% w/w) led to an increase in the extraction yield of 40% and reduced $CO_2$ consumption (decreased by 25%) with the operating parameters of pressure at 100 bar; temperature at 40 °C; $CO_2$ density 630 kg/$m^3$.

### 2.3.12 Effect of initial oil content

The effects of initial oil content of any natural material has not been studied in detail in the available literature. However, Nagy and Simandi, 2008 have shown the effect of initial oil content on the extraction yield during the SFE of the mixtures of the different parts of paprika plant and observed that the extraction yield increases with increase in the initial oil content. Initially, the oil content in small range (5-10 %) has a self-entraining effect, so increasing the oil content, an increase in extraction yield is observed. The reason is that the oil may act as co-solvent for the compounds, which have slight solubility in $CO_2$ while this effect seems to be disappeared significantly for higher oil content range (10-27 %).

### 2.3.13 Effect of pretreatment of seeds

The pretreatment of feed raw materials has become an essential part, which needs to be performed carefully during SFE of natural products. The basic pretreatment methods such as cleaning, drying, grinding, sizing, and the storage for raw feed stock of various natural materials (e.g. seeds, leaves, fruits, stems, roots etc.) have been adopted by most of the researchers during the SFE process (Lang and Wai, 2001; Pourmortazavi and Hajimirsadeghi, 2007). The grinding of the feed material is not done only for sizing purpose but also to reduce the diffusional mass transfer resistance, which leads to enhance the extraction rate. For example, Guoliang et al., 2011 have performed the grinding of the lycium barbarum seeds to break the cell of whole seed. The cell wall breakage pretreatment of lycium barbarum seeds could significantly speed up the extraction yield and achieved the maximum value in shorter extraction time. Similarly, the drying procedures for a raw feedstock could affect the yield and quality of the extracts. Ivanovic et al., 2014 have shown the effects of different mechanical pretreatment methods (e.g. grinding, flaking, shearing, and impact) during the SFE of different natural products (e.g. amaranth seeds, milk thistle and oat seeds). They concluded that the flaked material extracted out 50% more seed oil from the seeds during the SFE process compare to other methods (e.g. coarse grinding, impact, or combination of both). In addition to this, pretreatment of raw feed material by using advanced techniques such as pressing, ultra-sonication, microwave irradiation, enzyme-assistance and a hydrothermal approach has been performed by various researchers (e.g. Aladic et al., 2014; Barrales et al., 2015; Da Porto et al., 2016; Lenucci et al., 2015 and Kawamura et al., 2016).

2.4 Operating parameters studied- a review

A rigorous review on the operating parameters studied during the year of 2000 – 2018, revealed that the pressure, temperature, extraction time, co-solvent amount, flow rate-$CO_2$ and particle size have been selected for the SFE study at most as shown in Fig. 2.3. From the figure (Fig. 2.3) it is clear that the pressure and temperature have been chosen in 98.14% and 95.03% of the works, respectively. The third most chosen parameter is the extraction time, which was present in 47.83% of the works. The co-solvent amount, flow rate of $CO_2$, particle size follow the later with 31.06%, 28.57 % and 11.8 % respectively. In addition to these, a very few studies have been reported, using the types of co-solvents, superficial velocity of the solvent, types of packing, solid/solvent ratio, density and the solvent flow direction with 2.48 %, 2.48 %, 1.86%, 1.86 %, 0.62 % and 0.62 % respectively.

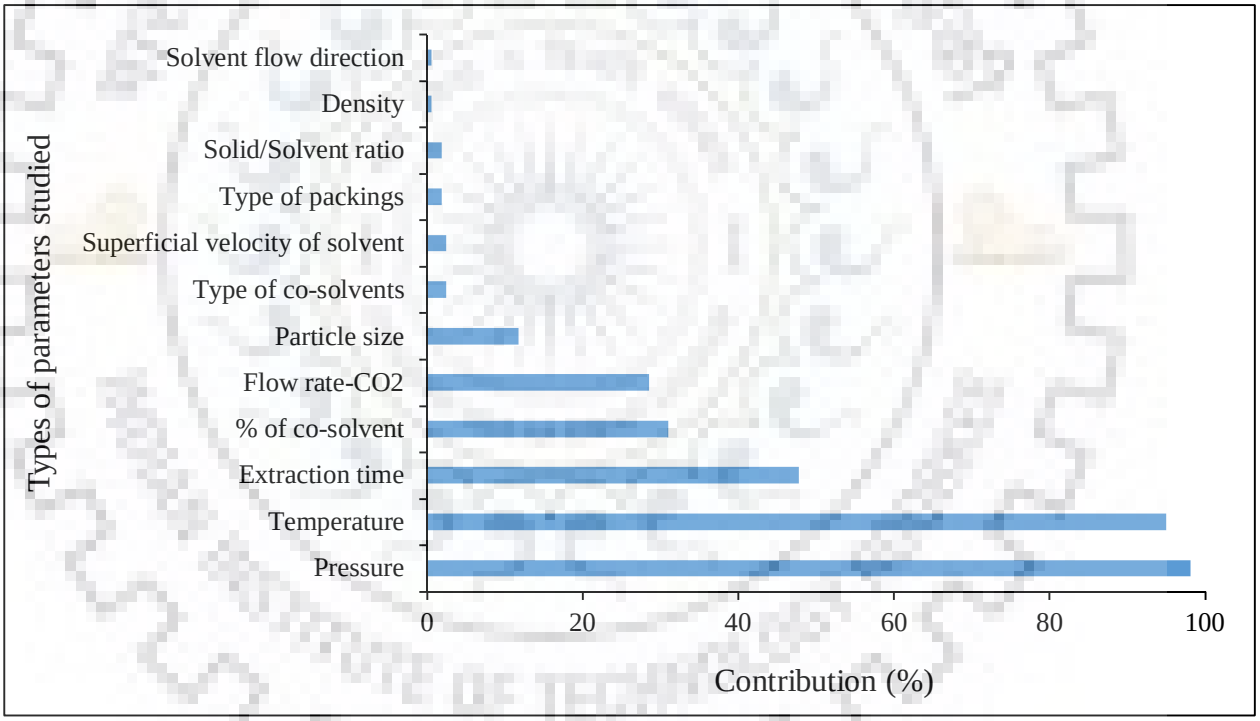


Fig. 2.3: The percentage of works found on each parameter studied during the year of 2000-2018.

## 2.5 Selection of modifier (co-solvent) for the SFE process

The selection of a co-solvent for the SFE process is purely depend on some aspects such as the purpose of co-solvent and nature of co-solvent. The main reason for adding a co-solvent to the SF solvent relies on the tunable affinity to polar solutes that modified SC-$CO_2$ allows. As discussed in the previous section 2.3.5 that a small amount of a co-solvent increases the ability of SC-$CO_2$ to dissolve polar compounds. Neat SC-$CO_2$ has very limited dissolving properties means that, by itself, carbon dioxide is very good for dissolving relatively non-polar solutes only (de Melo et al., 2014), while it is not recommendable for polar solutes. Therefore, the addition of just a small quantity of co-solvent (e.g. ethanol, methanol, acetone, propanol, n-hexane etc.) enhances the solubilizing power of the SC-$CO_2$, making it possible to extract much more polar molecules.

On the other hand, the second aspect 'nature of co-solvent' means toxic or non-toxic also play an important role for selecting the specific co-solvent for the SFE process. The added organic co-solvent should be non-toxic/less toxic to human, animal and environment as well to maintain the dignity of SC-$CO_2$ solvent, which has also been named as 'green solvent' (Beckman, 2004). In addition, of course, some other factors such as cost, availability, ease to separate it out from the solute, and recycling also influences the selection criteria of a co-solvent for the SFE process. The selection of ethanol as a co-solvent for the present study, has been chosen by keeping in though the above criteria and found that the ethanol could only fulfill them to a large extent. In addition to this, ethanol has also been used by 53% of researchers during the SFE of vegetable matrices while the rest 47% researchers have used other solvents (e.g. methanol (21%), water (5%), vegetable oil (2%), dichloromethane (3%), n-hexane (2%), mixtures of co-solvents (7%) and other co-solvents (7%)) (de Melo et al., 2014). The selection of ethanol as a co-solvent can also be justified through the advantages and disadvantages associate with it (as listed in section 2.5.1).

### 2.5.1 Advantages and disadvantages of Ethanol as co-solvent

The advantages and disadvantages of ethanol as a co-solvent are as follows;

*Advantages*:

- Ethanol is the second most popular SFE co-solvent (after water).
- It is nontoxic solvent.

- Ethanol is an innocuous solvent both at human health and environmental levels (like SC-$CO_2$) and this is a strong advantage comparing to other solvents (excepting water, particularly when SFE is devoted to applications in food, cosmetic or pharmaceutical industries (Radzali et al., 2014).
- Ethanol is substantially polar (1.69 d (Poling et al., 2001)) which means that the addition of small amounts may increase expressively the polarity of the SC-$CO_2$.
- Ethanol falls at 5$^{th}$ place in terms of polarity (Wypych, 2001) while first fours are water, acetic acid, ethylene glycol and methanol in which excluding water, each one is toxic to human, animal and environment that discourages an extended use of them.
- Ethanol has convenient critical points as shown in Table 2.4 (given below).

Table 2.4. Comparison of critical points of first five high polarity co-solvents.

| Solvent | Critical temperature (°C) | Critical pressure (bar) |
|---|---|---|
| Water | 374 | 220.8 |
| Acetic acid | 320 | 57.8 |
| Ethylene glycol | 447 | 82 |
| Methanol | 240 | 79.58 |
| **Ethanol** | **241** | **63** |

*Disadvantages:*

- It may be little costlier than methanol and water that would add extract-operating cost of SFE process.
- Polarity is lower than the water, acetic acid, ethylene glycol, and methanol.

2.6 Extent of work done on extractable material used in the present study

The SFE technique has been used extensively for various materials as shown in Fig. 2.2. From the figure (Fig. 2.2), it is clear that the most of the SFE processes were performed on the natural plant products (e.g. seeds, roots, leaves, flowers, fruits, stems etc.) in which, seeds have only been targeted at most. Fig. 2.4, shows the number of research articles published on the SFE of different types of natural seeds (92 nos.) in which the three seeds (e.g. sunflower, grape and canola) have been studied maximum time during the SFE process. The extent and type of investigation that is generally done on the above three seeds is explained below by taking the example of sunflower seed. Cocero

and Calvo, 1996 studied the SFE of sunflower seed oil at the parametric conditions (e.g. temperature (42 – 80 °C) and pressure (150 – 350 bar)) to shows the effects of ethanol (used as co-solvent) on the solubility of sunflower seed oil through a non-recirculating home-made bench-scale SFE system. Further, just after one year, Perrut et al., 1997 have shown the influence of the solid seed matrix on the extraction rate through a pilot scale apparatus at reduced parametric conditions (40 °C and 280 bar) through a mass transfer based mathematical model. The further, progress on the SFE of this seed (sunflower) was shown by Cocero and Garcia, 2001. They performed the SFE of sunflower seed oil in a pilot plant at 40 °C and 300 bar to shown the effects of different amounts of co-solvents (e.g. methanol, ethanol, butanol and hexanol) through a desorption phenomenon based mathematical model. Kiriamiti et al., 2001 added two more parameters (e.g. particle size and flow direction of $CO_2$) in the investigation to figure out influencing parameters for sunflower seed oil and applied different existing mathematical models available in the area of SFE. This time, the extraction temperature was increased up to 60 °C while the pressure was decreased up to 250 bar. Roy et al., 2006 extracted the sunflower seed oil using a semi-continues flow extractor with the temperature range 40 °C and pressure range 200 - 400 bar and shown the effect on the composition of the seed oil in addition to extraction yield. Further, Salgin et al., 2006 explained the SFE of sunflower seed through shrinking core model in which the core of the seed particle shrinks as the extraction progress. This time four parameters (e.g. pressure (200 – 600 bar), temperature (40 - 80 °C), flow rate- $CO_2$ (1 - 6 $cm^3$/min) and the mean particle size (0.23 – 2.18 mm)) were investigated.

First time, Nimet et al., 2011 used propane and SC-$CO_2$ both solvents for SFE and studied the effects of temperature (30 – 60 °C), and pressure (80 – 250 bar) on the extraction yield. And finally, the latest one, Rai et al., 2016a investigated the effects of five parameters (e.g. pressure, temperature, flow rate- $CO_2$, mean particle size and the amount of co-solvent) on the extraction yield of sunflower seed oil obtained through SFE and compared the results with the conventional extraction method (e.g. soxhlet extraction). For the selection of operating parameters, they used design of experiment technique. Hence, it is clear that the research work on the extraction of natural seeds propagated from simple conventional techniques (e.g. mechanical pressing, soxhlet extraction etc.) to SFE process using different kind of co-solvents and the operating parameters are mainly temperature, pressure, particle size of seed, flow rate of SC-$CO_2$ and amount of co-solvent added to SC-$CO_2$.

### 2.6.1 Argemone mexicana (L.) – a review

The Argemone mexicana (L.) (AM) belongs to the Papaveraceae family which is also known as Prickly poppy (-in English), Bharband (-in Hindi) and Satiyanashi (-in Sanskrit) (Rahman and Ilyas, 1962). It has been found in large quantity in tropical America, but now, it is being cultivated in all over India (Bhalke and Gosavi, 2009; Rajvaidhya et al., 2012). The AM seeds are spherical (1.5 to 2.5 mm diameter) in shape with the color of dark brown and pitted (Rajvaidhya et al., 2012; Brahmachari et al., 2013). A non-edible oil (22-40%) with pale yellow color, nauseous, bitterness has been reported (Dey et al., 2008; Mishra et al., 2009; Rao et al., 2012) from the AM seeds in literature, which is also called Argemone oil or Katkar oil and is rich in unsaturated fatty acids (e.g. linoleic, oleic, ricinoleic, palmitoleic acids etc.). This oil plays an important role in the regulation of a variety of physiological and biological functions in living organisms (Shahidi, 2005). It also contains some toxic alkaloid contents (e.g. sanguinarine, dihydrosanguinarine, berberine, protopine, coptisine etc.) which have been used to cure various chronic diseases (Dey et al., 2008; Singh et al., 2010; Liu et al., 2014). Various researchers (e.g. Azam et al., 2005; Singh et al., 2010; Singh and Singh, 2010; Bankovi-Ilic et al., 2012) have also shown that this oil is suitable for the production of esters which are main ingredients during the production of biodiesel. Generally, various traditional methods such as mechanical pressing and conventional organic solvent extraction methods etc., are used for the extraction of oil from AM seeds. But due to the lower yield, the loss of valuable components and the refining hurdles made these methods obsoleted (Sodeifian et al., 2016a; Sodeifian et al., 2017). The use of SFs as an alternative solvent during the SFE of seed oil has been attracting widespread attention due to their advantageous properties (as mentioned in section 2.1.4).

A literature review reveals that SFE of oils from various seeds has been extensively studied. However, no studies (excepting this study) have been reported for the SFE of total oil from AM seeds, as shown in Fig. 2.4. Therefore, in the present work, AM seeds have been used as the material of study for the developed SFE method.

### 2.6.2 Pongamia pinnata (L.) – a review

The Pongamia pinnata (L.) (PP) belongs to the ‘Fabaceae’ family which is also known as Indian beech in English, Karanj in Hindi and Karanja, Maktamala or Gaura in Sanskrit (Mukta and Sreevalli, 2010; Vismaya et al., 2010). It is a medium sized glabrous tree that grows on the moist

environment along rivers or sea coast all over India and further distributed eastwards mainly in the littoral regions of south eastern Asia, Philippines, Malaysia, Indonesia and the United States of America (Arote et al., 2009; Pavithra et al., 2012). A PP seed having 10-20 mm long and light brown in color is obtained from a fruit of the Pongamia pinnata tree which is ovoid in shape with dimensions 3–6 cm long and 2–3 cm wide thick walled (Sangwan et al., 2010). A red-brown, bitter, thick, non-edible, non-drying oil (27-39% of seed) has been reported from the PP seeds in literature (Borugadda and Goud, 2012), which is also called Pongamia oil or Karanja oil, used -in tanning leather, -in soap, -as a liniment to treat scabies, herpes, and rheumatism and -as an illuminating oil (Bala et al., 2011; Rao et al., 2011; Shadangi and Mohanty, 2013). The seed oil has also been used for treating various inflammatory and infectious diseases such as leukoderma, leprosy, lumbago, and rheumatism (Bala et al., 2011; Prabha et al., 2009). Various fatty acids (e.g. palmitic, stearic, oleic, linoleic, eicosenoic, arachidic, and behenic acids) have been reported in literature which play an important role in the regulation of a variety of physiological and biological functions in living organisms and for the development of new source for bio-fuel (Kumar et al., 2011; Dwivedi and Sharma, 2014). Some researchers (e.g. Vismaya et al., 2010; Prabhu et al., 2002; Pradhan et al., 2008) also reported non-fatty components of the oil, which includes karanjin, furanoflavonoid, furanoflavones, furanoflavonols, chromenoflavones, flavones and furanodiketones that make the oil non-edible and hence further encourages its application for medicinal purposes along with the bio-fuel production. PP seed oil is eco-friendly, biodegradable and has been identified as one of the best alternatives to petrochemicals. However, the PP seed oil has also been extracted using various traditional techniques such as mechanical pressing and organic solvent extraction methods, by various researchers (e.g. Shameel et al., 1996; Prabhu et al., 2002; Meher et al., 2006; Kesari et al., 2010; Pavithra et al., 2012; Razal et al., 2012). But due to lower yield, refining hurdles, loss of valuable components and major health concerns, a new extraction methods SFE is being advised in this work for extracting the oil from PP seeds.

A thorough literature review reveals that SFE of oils from various seeds using SC-$CO_2$ has been extensively studied. However, no studies (excepting the present one) have been reported for the SFE of total oil from PP seeds, as shown in Fig. 2.4. Therefore, in the present work, a suitable SFE method was developed for the SFE of oil from PP seeds to meet the objectives of this study.

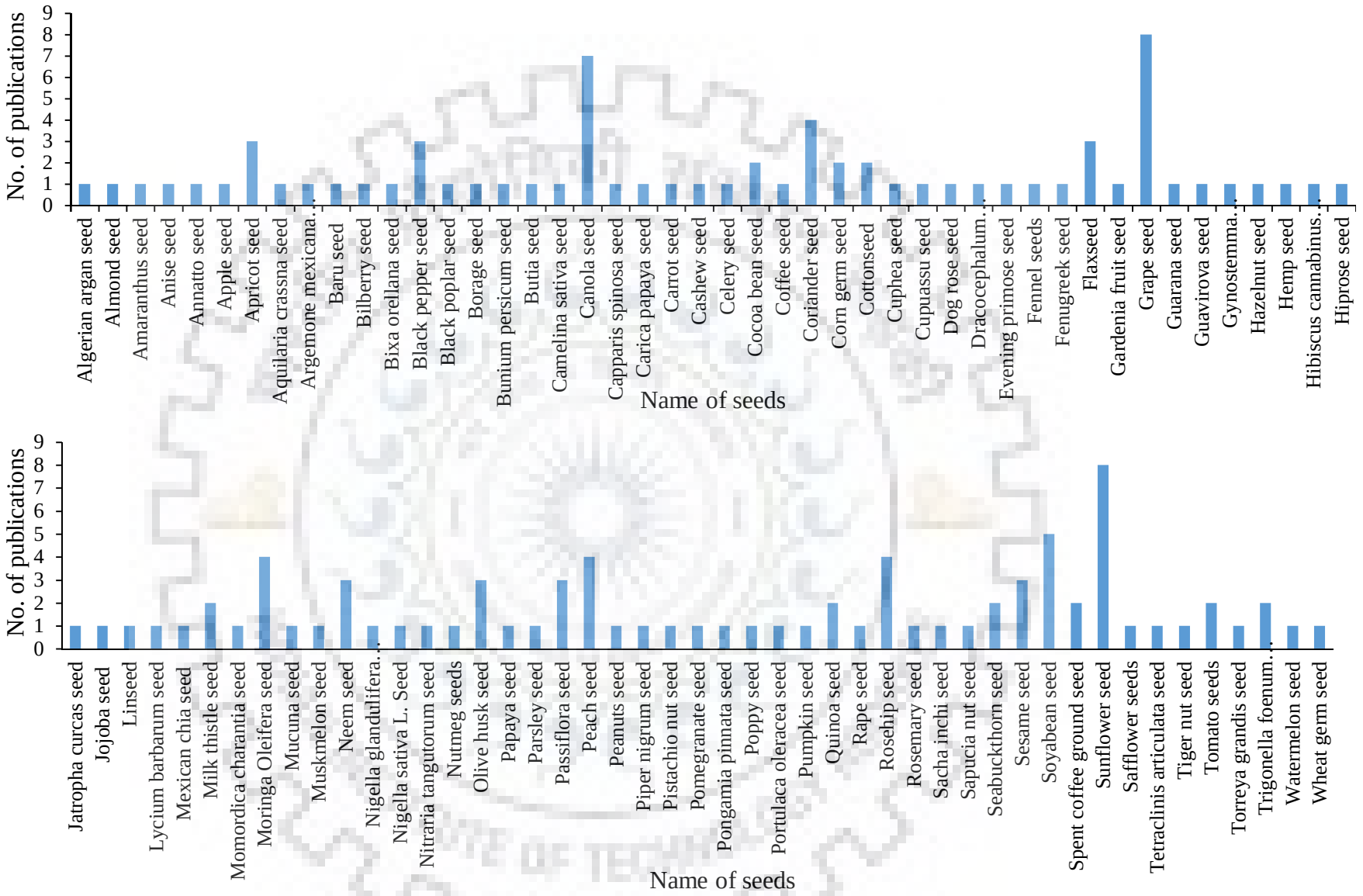


Fig. 2.4: Types natural seeds which have been extracted during the period (1980 – 2018) through SFE technique using SC-$CO_2$.

## 2.7 Design of experiments (DoE) techniques and selection of suitable one for present SFE process

The quantitative SC-$CO_2$ extraction of extractable materials involves three steps: (a) partitioning of the solute from the sample to the extraction fluid (b) removal of solute from the extraction vessel and (c) collection of the extracted solute (Fernandez et al., 1996). All of them must be optimized to obtain the highest extraction efficiency. Experimental designs are being frequently used for the optimization of different operating conditions of various processes for achieving high extraction efficiency (Sharif et al., 2014). Therefore, the experimental design is an approach to solve the problem systematically and it is applied to get optimum and valid results with a minimum effort, time and resources (Gooding, 2004; Montgomery, 2004). The choice of experimental design for SFE depends on the objectives of the study, investigator's intention, feasibility of experiment, cost-effectiveness, time consumption and many other important factors (Sharif et al., 2014; Erkucuk et al., 2009). Once, these parameters are decided, the DoE can be performed using various software like Minitab, Matlab, Design Expert, Quantum XL etc.

Sharif et al., 2014 categorized all available designs into two broad categories: (i) Screening designs and (ii) Optimization designs. Factorial design and Plackett–Burman design are used for screening purpose in which the most important factors and their interactions with all potential factors are determined. Various authors (e.g. Notar and Leskovsek, 1997; Zaragoza et al., 1998; Santos et al., 1998; Ha et al., 2007; Sheibani and Ghaziaskar, 2008; Saikaew and Kajorncheappunngam, 2008) have used factorial design (FD) to determine the optimum conditions of operating parameters. Lundstedt et al., 1998 showed that factorial design is mainly used for experimental designs of the first-degree models. From the Fig. 2.5, it can be seen that such designs have been used extensively by the 20% researchers to dealing with large number of variables than one variable at a time (OVAT) design. On the other hand, optimization is another aspect of experimental design. The optimization designs such as; central composite design (CCD), box–behnken design (BBD), orthogonal array design (OAD) and Taguchi design have also been adopted by various researchers. These designs are used mostly because both linear and quadric models can be determined by these designs. Fig. 2.5, shows that that CCD has been applied by 30% of researchers while 32% researchers have used the BBD during the optimization process of an extraction step to determine the optimum conditions of different experimental parameters.

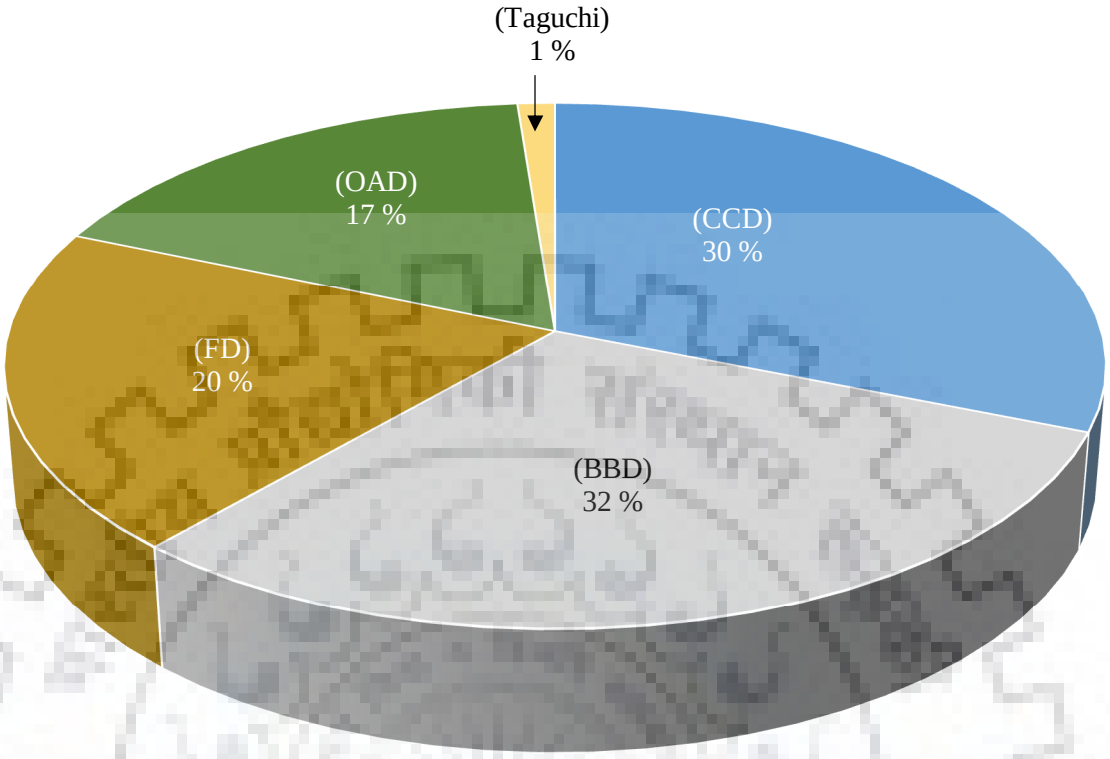


Fig. 2.5: Pie diagram showing the % of publications found on different DoE techniques.

However, a comparison between BBD and CCD with respect of the number of experiments (n) and number of coefficients (c) is shown in Table 2.5. From the Table 2.5, it is clear that BBD is more efficient than the CCD, where efficiency of one experimental design was calculated as the number of coefficients (c) involved in estimated model divided by the number of experiments (n) suggested by the respective design. The efficiency (0.60) is same for both the designs (e.g. BBD and CCD) for the set of 4 factors and 15 numbers of coefficients, which require 25 numbers of experiments for both BBD and CCD but with the increased numbers of factors, the number of experiments in the case of BBD is slightly less than CCD. For example, for 5 factors, BBD requires 41 numbers of experiments while CCD requires 43 numbers of experiments as shown in Table 2.5.

Another advantage of BBD is that it avoids the experiments with the extreme conditions (combination of highest and lowest level for every factor) which may cause unsatisfactory results. Conversely, it is not indicated for situations in which we would like to know the responses at the extremes, that is, at the vertices of the cube. In addition to this, a BBD (with 4 and 5 factors) can

also be arranged in orthogonal block which is a desirable property when the experiments have to be arranged in blocks and the block effects are likely to be large. Due to this block orthogonality, an estimated second-order model can be augmented to include block effects without affecting the parameters estimated. Ferreira et al., 2007 have shown a comparison of BBD with other available response surface designs such as CCD, DM (Doehlert matrix), and three-level full factorial design (FFD) which proved that the BBD and DM are slightly more efficient than the CCD but much more efficient than the three-level FD.

Table 2.5. Comparison between BBD and CCD based on calculated efficiency.

| Factors (*k*) | Number of coefficients (c) | Number of experiments (n) (without center points) | | Efficiency (c/n) | |
|---|---|---|---|---|---|
| | | BBD | CCD | BBD | CCD |
| 2 | 6 | 5 | 9 | 1.2 | 0.67 |
| 3 | 10 | 13 | 15 | 0.77 | 0.67 |
| 4 | 15 | 25 | 25 | 0.60 | 0.60 |
| **5** | **21** | **41** | **43** | **0.51** | **0.49** |
| 6 | 28 | 61 | 77 | 0.46 | 0.36 |
| 7 | 36 | 85 | 143 | 0.42 | 0.25 |
| 8 | 45 | 113 | 273 | 0.40 | 0.16 |

2.8 Method used for optimization of operating parameters based on BBD technique

The concept of BBD was first, developed by Box and Behnken in 1960 (Box and Behnken, 1960). A BBD come under the category of rotatable/nearly rotatable, second-order designs, which is based on incomplete factorial design with three levels of factors (Sharif et al., 2014). A 'five-factors-three-levels', BBD (using software Design-Expert 10.0, Stat-Ease, Inc, Minneapolis, U.S.) was applied for the experimental design, data analysis, model building and also to determine optimal extraction conditions in terms of temperature, pressure, particle size, flow rate-$CO_2$ and the % of co-solvent for SC-$CO_2$ extraction of AM and PP seed oils. The number of experiments (n) as predicated by BBD is given by Eq. 2.1 (Ferreira et al., 2007).

$$n = 2k(k-1) + C_0 \quad \text{… Eq. 2.1}$$

Where, $k$ is the number of factors (independent variables) and $C_o$ is the number of central points. The temperature (°C, $X_1$), pressure (bar, $X_2$), particle size (mm, $X_3$), flow rate-$CO_2$ (g/min, $X_4$) and the % of co-solvent (% of flow rate-$CO_2$, $X_5$) were chosen as independent variables to optimize the

CEY of oil from AM and PP seeds. Here, each independent variable is coded at levels of -1, 0 and +1. The experimental design, of coded and un-coded (actual) levels of variables, is shown in Table 2.6.

Table 2.6. Coded and un-coded levels of the independent variables used for BBD.

| Independent variable | Symbol | Level | | |
|---|---|---|---|---|
| | | Low (-1) | Middle (0) | High (+1) |
| Temperature ($^oC$) | $X_1$ | 60 | 80 | 100 |
| Pressure (bar) | $X_2$ | 200 | 275 | 350 |
| Particle size (mm) | $X_3$ | 0.50 | 0.75 | 1.0 |
| Flow rate (g/min) | $X_4$ | 5 | 10 | 15 |
| % of co-solvent (%) | $X_5$ | 0 | 5 | 10 |

The independent variables chosen in this study were codified according to the following expression:

$$X_i = \frac{(x_i - x_0)}{\Delta x_i}, \quad (i = 1, 2, 3, .....k) \qquad \text{… Eq. 2.2}$$

where $X_i$ is the codified value of the independent variable, $x_i$ is the real value of the independent variable, $x_0$ is the real value of an independent variable at the center point and $\Delta x_i$ is a step change in the value.

Experimental data (as shown in section 5.1 of Chapter 5) employed for response surface analysis is in general described accurately by a second order polynomial function which is also called regression or statistical quadratic models as expressed by Eq. (2.3):

$$Y = \beta_0 + \sum_{i=1}^{5} \beta_i X_i + \sum_{i=1}^{5} \beta_{ii} X_i^2 + \sum_{i=1}^{5} \sum_{j=1}^{5} \beta_{ij} X_i X_j \qquad \text{… Eq. 2.3}$$

Where, Y is the predicted response (predicted CEY), $\beta_0$ is a constant coefficient of intercept, $\beta_i$ are the model coefficients linked to linear effects, $\beta_{ii}$ are the coefficients related to quadratic effects, $\beta_{ij}$ are coefficients for interaction effects, and $X_i, X_j$ are codified independent variables. The detail solution and explanation of the above model for both seeds (e.g. AM and PP) is given in section 5.1 of the Chapter 5.

2.9 Method used for optimization of operating parameters based on ANN technique

The artificial neural network (ANN) modeling is based on the working of the natural neural networks of the human brains (Hu and Hwang, 2002). In an ANN model, each neuron added the weighted inputs from different paths and then applies a transfer function to the addition. The resulting value is then directed through outgoing paths to other neurons. A series of layers was formed with neurons that are called multilayer perceptron (MLP) (Ghoreishi and Heidari, 2013). A multilayer perceptron (MLP) model is shown in Fig. 2.6, which can be developed in MATLAB (Mathworks, Inc., 2013a). It consists of an input layer, which represents the number of input parameters (e.g. temperature, pressure, particle size, flow rate-$CO_2$ and co-solvent % as in our case), one hidden layer with 'n' number of neurons, which is to be decided by hit and trial approach and one output layer, denoting CEY as the response. Each neuron of the input layer, is connected to one or more neurons of the hidden layer that represents the nonlinear activation function and these neurons are then connected to neurons of output layer through a learning algorithm function (Pilkington et al., 2014).

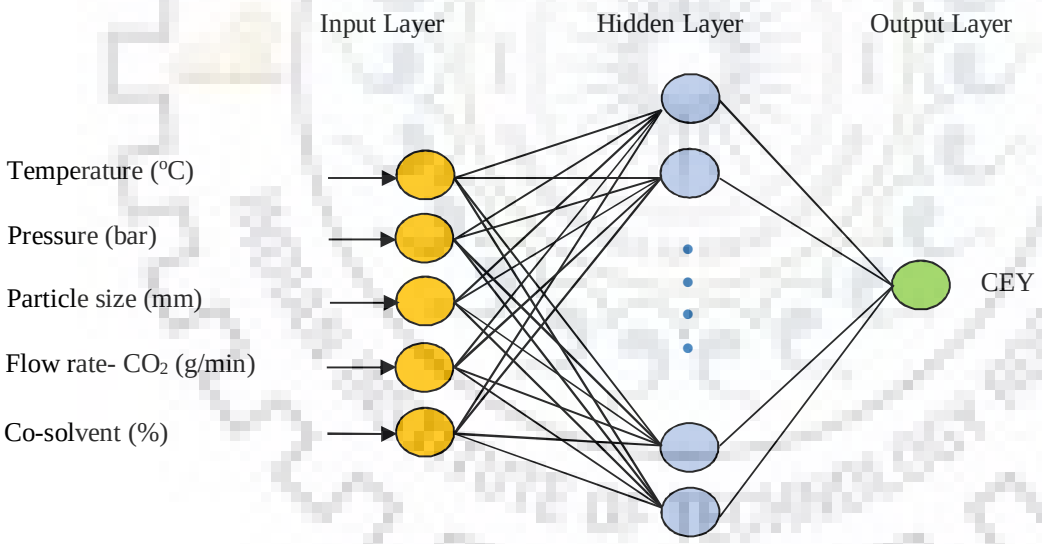


Fig. 2.6: Structure of the developed ANN with five inputs and one output.

A neuron's output was evaluated by applying a transfer function to a weighted summation of its input and resulted an output, which will be used as input for other neurons, as indicated in Eq. (2.4).

$$\gamma_{jk} = F_k\left(\sum_{i=1}^{N_{k-1}} W_{ijk}\gamma_{i(k-1)} + \beta_{jk}\right) \quad \ldots \text{Eq. 2.4}$$

Where, $\gamma_{jk}$ is the neuron $j's$ output from $k's$ layer and $\beta_{jk}$ is the bias weight from neuron *j* in layer *k*, $W_{ijk}$ is the weight connection and $F_k$ is the nonlinear activation transfer functions.

The following steps were followed during ANN modeling of the system;

***Step 1***: Firstly, the available experimental data were partitioned into training, validation and testing subsets. The ANN model was developed using 'training subset' data while its validation and examination of performance was done using 'testing subset' data.

***Step 2***: During, the training of the subset data, randomly selected weight matrices were adjusted to minimize the back propagation error.

***Step 3***: Now, based on hit and trial approach, the number of hidden layers and the number of neurons in each hidden layer were determined to form suitable network architecture.

***Step 4***: The five input parameters (e.g. temperature, pressure, particle size, flow rate-$CO_2$ and the % of co-solvent) and one output parameter (e.g. CEY) were selected to establish the ANN system. Initially, the number of neurons in the hidden layer would be equal to one and then it is increased by one each trial run until optimum condition (least error) is achieved.

***Step 5***: Now, the types of 'in-build transfer function' for each stage must be defined, using hit and trial approach. Different types of 'in-built transfers functions' (e.g. radial, linear, hyperbolic tangent sigmoid, logarithmic sigmoid etc.) are available in the 'nntool' of MATLAB.

***Step 6***: The number of hidden layers were optimized. In our case, only one hidden layer was considered since Cybenko, 1989 has reported that an ANN with only one hidden layer could approximate almost any type of nonlinear relation. The selection of number of neurons in the hidden layer is totally based on hit and trial basis. A few number of neurons can produce a network with low precision while a higher number of neurons can lead to over fitting and bad quality of interpolation (Lashkarbolooki et al., 2013).

***Step 7***: In step 6, the number of, hidden layers and neurons in the hidden layers were optimized based on some of the statistical parameters (as mentioned in section 2.10).

The development procedure of an ANN-based equation requires the experimental data (input and output). The steps are given below;

***Step 1***: Normalization of the input experimental data

The normalization of input experimental data (input layer) for ANN was done using Eq. 2.5 (given below) to scale-up the inputs and output so that they fall in the range of '+1' to '-1', corresponding to the highest and lowest values respectively.

$$Y_{norm} = \frac{(Y_{\max} - Y_{\min}) * (X_{actual} - X_{\min})}{(X_{\max} - X_{\min})} + Y_{\min} \quad \text{…Eq. 2.5}$$

Where, $Y_{norm}$ is the normalized value of $X_{actual.}$ The values of $Y_{max}$ and $Y_{min}$ are '+1' and '-1' respectively. $X_{actual}$, $X_{min}$ and $X_{max}$ are the actual, minimum and maximum values of the independent parameters of interest.

***Step 2***: Weight assignments at the hidden layer

After normalizing the all input parameters, the assignments of weights and biases to the normalized parameters were performed as shown in Fig. 2.6. These weights ($w$) and biases ($b$) were generated automatically by the network. The linear relationship (Eq. (2.6)) was developed for the above phenomenon.

$$A_{l,i,n} = \sum_{i=1}^{j} (w_{l,i,T} * (T_{norm})_n + w_{l,i,P} * (P_{norm})_n + w_{l,i,PS} * (PS_{norm})_n + w_{l,i,FR} * (FR_{norm})_n + w_{l,i,CoS} * (CoS_{norm})_n + b_{l,i}) \quad \text{… Eq. 2.6}$$

Where, '$w_{l,i,T}$' '$w_{l,i,P}$' '$w_{l,i,PS}$' '$w_{l,i,FR}$' and '$w_{l,i,CoS}$' represent the weights assigned to the operating parameters. The operating parameters (e.g. temperature, pressure, particle size, flow rate-$CO_2$, and % of co-solvent) were denoted as 'T', 'P', 'PS', 'FR' and 'CoS' respectively. The number of neurons varies from '*i*' to '*j*' while the number of hidden layer was denoted by '*l*'. $(T_{norm})_n$, $(P_{norm})_n$, $(PS_{norm})_n$, $(FR_{norm})_n$ and $(CoS_{norm})_n$ are the n$^{th}$ values of the normalized *T, P, PS, FR,* and *CoS* respectively. $A_{l,i,n}$ represents the $n^{th}$ sum of the weighted normalized variables.

***Step 3***: Transfer function for the hidden layer

Following the Fig. 2.6, the third step in developing the ANN-based model equation requires the mathematical expression of the TANSIG transfer function, which was used in hidden layer. The expression for the TANSIG function is given as:

$$TANSIG(A_{l,i,n}) = B_{l,i,n} = \frac{2}{(1+\exp(-2*A_{l,i,n})} - 1 \quad \ldots \text{Eq. 2.7}$$

Eq. (2.7) is only applicable for the single hidden layer network.

***Step 4***: Transfer function for the output layer

Still following the Fig. 2.6, at the output layer, the PURELIN transfer function was applied with the weight and biases, which were also generated by the network. They are then assigned to the previous variable ($B_{l,i,n}$) as shown in Eq. (2.8).

$$a_0 = \sum_{i=1}^{j} (w_{o,i} * B_{l,i,n}) + b_o \quad \ldots \text{Eq. 2.8}$$

Where, '$w_{o,i}$' refers to the weight at the output layer (o) attributed to each neuron (i); '$B_{l.i,n}$' is the previously defined value of the TANSIG transformed variable, associated with the sum of the $n^{th}$ normalized input variable at the last hidden layer ($l$); '$b_o$' is the bias at the output layer. '$a_o$' is the normalized final output.

***Step 5***: De-normalization of the normalized output

To obtain the actual value of the output, there is a need to de-normalize the output obtained in Eq. (2.8). At this step, the normalized output ($a_n$) was de-normalized, using Eq. (2.5).

## 2.10 Performance evaluation of optimal FFBP-ANN models

The performances of feed forward back propagation artificial neural network (FFBP-ANN) models were evaluated with some statistical parameters. These statistical parameters are expressed below:

***Average-absolute-relative-deviation-percentage (AARD %):***

This is the average of the relative deviation in the prediction of a particular variable and it is expressed as a percentage. Lower values of AARD indicate better model performance. It can be computed as follows:

$$AARD\ (\%) = \frac{1}{n}\sum_{i=1}^{n}\left[\frac{(Y_i^{Exp} - Y_i^{Model})}{Y_i^{Exp}}\right] \times 100 \quad \ldots \text{Eq. 2.9}$$

***Mean-square-error (MSE):***

The mean square-error (MSE) measures the average of the squares of the errors between the experimental value ($Y^{Exp}$) and the model predicted value ($Y^{Model}$).

$$MSE = \frac{1}{n}\sum_{i=1}^{n}(Y_i^{Exp} - Y_i^{Model})^2 \quad \text{… Eq.2.10}$$

***Coefficient of determination ($R^2$):***

The coefficient of determination ($R^2$) is defined as the ratio of explained variation to the total variation, which actually ensures the performance of a fit between the experimental data and the model predicted data as given below:

$$R^2 = \frac{\sum_{i=1}^{n}(Y_i^{Exp} - \overline{Y})^2 - \sum_{i=1}^{Exp}(Y_i^{Exp} - Y_i^{Model})^2}{\sum_{i=1}^{n}(Y_i^{Exp} - \overline{Y})^2} \quad \text{… Eq. 2.11}$$

***Nash-Sutcliffe efficiency coefficient (NSEC):***

The NSEC is used to explain the accuracy of the model outputs in relation to the experimental data. A value of NSEC equal to unity ('1') depicts a perfect match between experimental data and model data. Therefore, the closer the model efficiency is to unity, the more accurate the model. The NSEC is computed using the Eq. (2.12).

$$NSEC = 1 - \frac{\sum\left(Y_i^{Model} - Y_i^{Exp}\right)^2}{\sum\left(Y_i^{Exp} - \bar{Y}\right)^2} \quad \text{… Eq. 2.12}$$

In the statistical parameters listed above, the notations; $N$, $Y_i^{Model}$, $Y_i^{Exp}$ and $\bar{Y}$ are the number of data points, $i^{th}$ predicted CEY through ANN models, $i^{th}$ experimental CEY, and the average value of the experimental data of CEY respectively.

2.11 Characterization of the feeds and products

A thorough literature review on the characterization of the feed raw materials (e.g. AM and PP seeds) as well as the products (extracted oils from the seeds) is performed in this section. However, a short review on the selected materials of study (e.g. AM and PP seeds) has already been done in section 2.6 of this chapter. As it has also been mentioned in previous write up that none of the researchers has selected these two seeds for the SFE process. Some researchers have only performed the conventional extraction techniques such as mechanical pressing, soxhlet extraction etc., to extract the oils from these seeds.

2.11.1 Feed raw materials (e.g. AM and PP seed particles)

A thorough literature review has been performed on the characterization of feeds (AM and PP seed particles) as shown in Table 2.7. Various researchers (as listed in Table 2.7) have reported the oil content (%), moisture content (%), ash content (%), solvents used, methods used and the geographical location of AM and PP seeds. From the Table 2.7, it can be seen that the only Suryawanshi and Mohanty, 2018a have used two methods (e.g. soxhlet and SFE methods) unlike other researchers. A wide range of oil content (22 - 42%), moisture content (3.19 – 25%) and ash content (3.6 – 9.33 %) have been observed for AM seeds. Similarly, a wide range of oil content (24 – 40 %), moisture content (5.9 – 19 %) and ash content (0.07 – 2.4 %) have been reported for PP seeds, as shown in Table 2.7. This wide range of variation in above mentioned findings are due to the change in geographical locations, methods of pretreatment, solvent used, etc.

Excluding the present study (e.g. Suryawanshi and Mohanty, 2018a; Suryawanshi and Mohanty, 2018b) each one has used only conventional soxhlet extraction method. Based on data reported in Table 2.7, it can be concluded that the SFE process has been used first time for both of the seeds (e.g. AM and PP seeds) and comparatively better yield of oil has been observed. Furthermore, the analysis such as structure analysis of solid matrix of both seeds, thermal decomposition of seed particles, and the component identification inside the seeds particles were also performed, using scanning electron microscopy (SEM), thermos-gravimetric (TG), and Fourier transform infrared (FTIR) spectroscopy instruments, as described in subsequent sections. In the present study, characterization of feeds (seed particles of AM and PP) of before and after extraction has also been performed and explained in details in sections 5.7 and 5.8 of Chapter 5.

Table 2.7. Analysis of AM and PP seed particles reported in literature.

| **AM seed particles** | | | | | | |
|---|---|---|---|---|---|---|
| Author | Oil (%) | Moisture (%) | Ash (%) | Solvents used | Method used | Location of Seeds |
| Azam et al., 2005 | 35 | NR | NR | n-hexane | Soxhlet | NR |
| Dey et al., 2008 | 22 - 36 | NR | NR | NR | NR | Mexico, USA |
| Mishra et al., 2009 | 35 | NR | NR | n-hexane | Soxhlet | Lucknow, India |
| Singh et al., 2010 | 30 | 3.19 | 9.33 | petroleum ether | Soxhlet | Indore, India |
| Rao et al., 2012 | 40 | 25 | NR | n-hexane | Soxhlet | Koraput, India |
| Suryawanshi and Mohanty, 2018b | 42 | 4.48 | 3.6 | n-hexane/$CO_2$ | Soxhlet and SFE | Haridwar, India |

| **PP seed particles** | | | | | | |
|---|---|---|---|---|---|---|
| Author | Oil (%) | Moisture (%) | Ash (%) | Solvents used | Methods used | Location of Seeds |
| Meher et al., 2004 | 32 | NR | NR | n-hexane | Soxhlet | Rajasthan, India |
| Arote et al., 2009 | NR | NR | NR | petroleum ether | Soxhlet | Ahmednagar, India. |
| Kesari et al., 2010 | 33 | NR | NR | n-hexane | Soxhlet | Guwahati, India |
| Kumar et al., 2011 | NR | NR | NR | NR | NR | Bangalore, India |
| Bala et al., 2011 | 29 | NR | 3.8 | n-hexane | Soxhlet | Jodhpur, India |
| Pavithra et al., 2012 | 27-40 | NR | NR | NR | NR | Bengaluru, India |
| Bobade and Khyade, 2012 | 31 | NR | 0.07 | n-hexane | Soxhlet | Baramati, India |
| Dwivedi and Sharma, 2014 | 34 | 19 | 2.4 | NR | NR | NR |
| Goembira and Saka, 2015 | 24 | NR | NR | n-hexane | Soxhlet | Bogor, Indonesia |
| Suryawanshi and Mohanty, 2018a | 35-36 | 5.9 | 1.8 | n-hexane, $CO_2$ | Soxhlet and SFE | Haridwar, India |

NR: Not reported

2.11.1.1 Scanning electron microscopy (SEM) analysis

The scanning electron microscopy (SEM) instrument is a type of electron microscope that images a sample by scanning it with a high-energy beam of electrons in a raster scan pattern. The electrons interact with the atoms that make up the sample producing signals that contain information about the sample's surface topography, composition, and other properties such as electrical conductivity. Rai et al., 2015 and Rai et al., 2016a have shown the morphological changes in the surface of the particle (0.75 mm) of the seeds at before and after SFE of watermelon and sunflower respectively, at 500-magnification using the LEO-1550 SEM instrument and found that oil and non-extracted solid phase are closely interpenetrating in each other. In addition to these, many researchers (e.g. Barrales et al., 2015; Wang et al., 2016; Koubaa et al., 2016; Salgın et al., 2016; Montanes et al., 2018; Sodeifian et al., 2018) have also shown the morphological changes in the surface of particle of different seeds using SEM instrument during the SFE process, as shown in Table 2.8. In the present study, SEM of both seed particles (e.g. AM and PP seeds) of before and after extraction has also been performed and explained in details in the section 5.7 of Chapter 5.

Table 2.8. SEM analysis of various seeds reported in literature.

| Author | Seed particles | Particle size /Magnification |
|---|---|---|
| Rai et al., 2015 | Watermelon | 0.75 mm / 500 |
| Barrales et al., 2015 | Passiflora | 2000 |
| Wang et al., 2016 | Gynostemma pentaphyllum | NR/2000 |
| Koubaa et al., 2016 | Canola | 0.63 mm/2500 |
| Salgın et al., 2016 | Rosehip | NR |
| Rai et al., 2016a | Sunflower | 0.75 mm / 500 |
| Montanes et al., 2018 | Apple | 0.5 mm/ 800 |
| Suryawanshi and Mohanty,2018a | Pongamia pinnata | 0.75 mm / 500 |
| Suryawanshi and Mohanty,2018b | Argemone mexicana | 0.5 mm / 500 |
| Sodeifian et al., 2018 | Portulaca oleracea | 0.6 mm / 10000 |

2.11.1.2 Thermo-gravimetric (TG) analysis

Thermo-gravimetric (TG) analysis is a technique in which the mass of a substance is monitored either as a function of increasing temperature, or isothermally as a function of time, in an atmosphere of nitrogen, helium, air, other gas, or in vacuum (Khraisha and Shabib, 2002). This is an essential test for the study of physical properties of materials throughout their life cycle (failure analysis, production control) (Jain and Sharma, 2012). As a non-isothermal pyrolysis process, TG analysis is used to determine volatile contents, thermal stability, profile analysis, separation,

sintering behavior, and reaction kinetics for a wide range of materials including polymers and oils. Recently, various researchers (e.g. Rai et al., 2015; Sodeifian et al., 2017; Fetzer et al., 2018; Sodeifian et al., 2018; Suryawanshi and Mohanty, 2018a) have performed the TG analysis of watermelon, dracocephalum kotschyi, Baru, portulaca oleracea and pongamia pinnata seeds respectively as shown in Table 2.9. In the present study, TG analysis has also been performed for AM and PP seed particles as explained in detail in the section 5.8.1.1 of Chapter 5.

Table 2.9. TG analysis of various seeds reported in literature.

| Author | Seed | Atmosphere | Temperature (°C) | State of material |
|---|---|---|---|---|
| Rai et al., 2015 | Watermelon | Air | 22 – 1015 | particles |
| Sodeifian et al., 2017 | Dracocephalum kotschyi | Nitrogen | 10 - 700 | oil |
| Fetzer et al., 2018 | Baru | Oxygen | 20 - 400 | oil |
| Suryawanshi and Mohanty, 2018a | Pongamia pinnata | Air | 31 - 1200 | particles |
| Suryawanshi and Mohanty, 2018b | Argemone mexicana | Air | 31 - 1200 | particles |
| Sodeifian et al., 2018 | Portulaca oleracea | Nitrogen | 35 - 600 | oil |

2.11.1.3 Fourier transform infrared (FTIR) spectroscopy analysis

A Fourier transform infrared (FTIR) spectrometer is an instrument which acquires broadband near infrared (NIR) to far infrared (FIR) spectra based on the vibrations of the atoms of a molecule. Various researchers, as shown in Table 2.10 have already used FTIR technique. For example, Rai et al., 2015; Rai et al., 2016a; Sodeifian et al., 2017 and Sodeifian et al., 2018 have performed the FTIR for the identification of the various functional groups (bonds) present in the various seed particles such as watermelon, sunflower, dracocephalum kotschyi, and portulaca oleracea respectively. On the other hand, Liu et al., 2014 and Basaar et al., 2017 have performed the FTIR for the seed oils such as jatropha curcas and triognella foenum graecum respectively. In the present study, FTIR has also been performed for AM and PP seed particles as explained in detail in the section 5.8.1.2 Chapter 5.

Table 2.10. FTIR analysis of various seeds reported in literature.

| Author | Seed material | Analysis of solid/liquid | Wavenumber ($cm^{-1}$) |
|---|---|---|---|
| Liu et al., 2014 | Jatropha curcas | Seed oil | 500 - 4000 |
| Rai et al., 2015 | Watermelon | Seed particles | 400 - 4000 |
| Rai et al., 2016a | Sunflower | Seed particles | 400 - 4000 |
| Basaar et al., 2017 | Triognella foenum graecum | Seed oil | 500 - 4000 |
| Sodeifian et al., 2017 | Dracocephalum kotschyi | Seed particles | 400 - 4000 |
| Suryawanshi and Mohanty, 2018a | Pongamia pinnata | Seed particles | 500 - 4000 |
| Suryawanshi and Mohanty, 2018b | Argemone mexicana | Seed particles | 500 – 4000 |
| Sodeifian et al., 2018 | Portulaca oleracea | Seed particles | 400 - 4000 |

2.11.2 Extracted products (e.g. AM and PP seed oils)

The extracted products (AM and PP seed oils) have been characterized by determining the physico-chemical properties of the extracted seed oils and their fatty acids compositions. A thorough literature review has been conducted on the physico-chemical properties reported by various researchers for the AM and PP seed oils as shown in Table 2.11. However, a detailed analysis of the physico-chemical properties of AM and PP seed oils extracted in the present study has been given in the sections 5.8.1.3 and 5.8.2.3 of Chapter 5.

2.11.2.1 Physico-chemical properties of extracted AM and PP seed oils

The physico-chemical properties (e.g. heating value (MJ/kg), flash point, (°C), fire point (°C), cloud point (°C), pour point (°C), saponification value (mg KOH/g), peroxide value (milli eq./kg sample) and acid value (mg KOH/g)) of the conventionally extracted (soxhlet method) AM and PP seed oils (excepting the present study) have been reported by various researchers, as shown in Table 2.11. Based on available literature, it can be seen easily that a very limited research work has been conducted for the AM seed oil. For example, Azam et al., 2005 has shown the different prospects and potential of AM seed oil as a biofuel based on its high oil content (35%), saponification value (202.5), iodine value (128) and cetane number (44.45). However, they calculated the saponification and iodine values using empirical equations and then later found good agreement with experimentally obtained values. Further, Singh et al., 2010 produced both esters and biogas from the AM seeds and its waste through anaerobic digestion method. They also compared some fuel

properties such as heating value (35.4 MJ/kg), flash point (235 °C), fire point (260 °C), cloud point (12 °C) and pour point (1 °C) of crude AM seed oil with the fuel properties of fatty acids methyl esters (FAME) which was obtained from it. Singh and Singh, 2010 also supported the above argument and performed the cost analysis of diesel produced from the AM seed oil. On the other hand, some researchers have also studied the physico-chemical properties of PP seed oil, extracted using soxhlet method of extraction, as shown in Table 2.11.

Meher et al., 2004 determined the properties like viscosity, flash point, cloud point, and pour point for accessing the fuel quality of methyl esters of PP seed oil. Thereafter, Das et al., 2009 specifically investigated the storage stability of methyl ester of PP seed oil over storage time of 180 days under different conditions peroxide value (PV) and viscosity. Kesari et al., 2010; Bobade and Khyade, 2012 performed the PP seed oil analysis and antimicrobial activity of it and based on its physico-chemical properties they suggested, PP seeds as a potential biofuel crop. Kumar et al., 2011 studied the microwave-assisted transesterification of PP seed oil and suggested that 0.5% sodium hydroxide and 1.0% potassium hydroxide catalyst concentration were optimum for biodiesel production from PP seed oil under microwave heating. Dwivedi and Sharma, 2014 have explored the scope of PP seed oil and concluded that pongamia seeds have a great potential for the production of biodiesel, needs minimum input and management, have low moisture demand, productive life is more than 40 years and seeds have 28–34% oil content.

Table 2.11. Physio-chemical properties of AM and PP seed oils reported in literature.

| Authors | Heating value (MJ/kg) | Flash point (°C) | Fire Point (°C) | Cloud Point (°C) | Pour Point (°C) | Saponification value (mg KOH/g) | Peroxide value (meq/kg sample) | Acid value (mg KOH/g) |
|---|---|---|---|---|---|---|---|---|
| **AM seed oil** | | | | | | | | |
| Azam et al., 2005 | NR | NR | NR | NR | NR | 202.5 | NR | NR |
| Singh and Singh, 2010 | 35.4 | 235 | 260 | 12 | 1 | 202.5 | 150 | 76.2 |
| Singh et al., 2010 | 35.1 | 235 | 260 | NR | NR | NR | NR | NR |
| Rao et al., 2012 | NR | 235 | NR | 12 | -12 | 202.5 | 150 | 76.2 |
| Pramanik et al., 2012 | NR | NR | NR | 7 | NR | NR | NR | 19.517 |
| Suryawanshi and Mohanty, 2018b | 37.2 | 236 | 263 | 13 | 1 | 198.5 | 148 | 62.7 |
| **PP seed oil** | | | | | | | | |
| Meher et al., 2004 | NR | 116 | NR | 22 | 15.8 | 187 | NR | 5.06 |
| Das et al., 2009 | NR | 145 | NR | 4 | 0 | 187 | 7.2 | 5.06 |
| Kesari et al., 2010 | 44.34 | 205 | NR | 4.1 | 3.36 | NR | NR | NR |
| Kumar et al., 2011 | 38.8 | 186 | NR | NR | NR | NR | NR | 2.0 |
| Bobade and Khyade, 2012 | 36.57 | 225 | 230 | 3.5 | -3 | 184 | NR | 5.40 |
| Dwivedi and Sharma, 2014 | 34-38.5 | 205 - 270 | NR | NR | NR | 185-195 | NR | 3.8-5.06 |
| Goembira and Saka, 2015 | NR | NR | NR | NR | NR | NR | NR | 4.40 |
| Suryawanshi and Mohanty, 2018a | 32 | 216 | 231 | 13 | 3 | 192 | 6.9 | 5.4 |

NR: Not reported

2.11.2.2 Gas chromatography (GC) analysis

A thorough literature review was performed for the fatty acids composition of AM and PP seed oils, as shown in Table 2.12 and Table 2.13 respectively. A very limited study on the fatty acids of AM seed oil is found in literature as shown in Table 2.12. Azam et al., 2005; Rao et al., 2012 have reported the four major fatty acids such as palmitic acid (C16:0), stearic acid (C18:0), oleic acid (C18:1n9c) and linoleic acid (C18:2n6c) in the range of '14.5 to 14.7%', '3.8 to 6.75%', '18.5 to 40%' and '36.6 to 61%', respectively. From the Table 2.13, it can be seen that the most of researchers (as listed in Table 2.13) have confirmed the presence of palmitic acid (C16:0), stearic acid (C18:0), oleic acid (C18:1n9c) and linoleic acid (C18:2n6c) in PP seed oil.

However, a wide range of variation in percentage of these components is observed. Meher et al., 2004 performed the transesterification process for PP seed oil by means of methanol and reported the fatty acids composition as palmitic acid (11.65%), stearic acid (7.5%), oleic acid (51.59%), arachidic acid (1.35%), and behenic acid (4.45%). But, Sarin et al., 2010 did not find the arachidic and behenic acids during the investigation of the influence of the presence of metals, doped as metal naphthenates, on the oxidation stability of methyl esters of PP seed oil. Sangwan et al., 2010 reported the arachidic acid (0.8%) and linolenic acid (6.3%) which were not reported by the previous researchers. Kesari et al., 2010 performed the PP seed oil analysis and antimicrobial activity of it and based on its fatty acid composition they suggested the PP seeds as a potential biofuel crop. Bala et al., 2011 reported a wide range of fatty acid composition as reported in Table 2.13 and this time they found erucic acid (C22:1n9) (15.29 - 16.51%) which was not reported by any previous study. First time, Pavithra et al., 2012 investigated the effect of pod and seed morphological characteristics on the oil accumulation and fatty acid composition at different developmental stages of pongamia seeds. This helps in predicting the ideal time of pod harvesting to enable the presence of high oil with good quality and quantity.

In addition to above studies, some researchers (e.g. Bobade and Khyade, 2012; Dwivedi and Sharma, 2014; Dwivedi and Sharma, 2014; Goembira and Saka, 2015) have also reported the fatty acid composition with wide range of variation in the concentration of the components. Pavithra et al., 2012 have shown in their study that the variation in the composition of fatty acids might be because of variation in species or different ecological conditions, because local edaphic and

environmental factors are of crucial importance to the growth and characteristics of a particular plant, including the richness and uniqueness of the germplasm. Therefore, the concentration of palmitic and linoleic acids has been observed decreasing at the later stage of the PP seeds (at maturity stage) (Pavithra et al., 2012). In our study (SFE of PP seed oil), these components have not been found because the PP seeds used, were collected at their matured stages.

Table 2.12. Fatty acid composition of the AM seed oil reported in literature.

| Author | Fatty acid composition | | | | | | | | | | | | |
|---|---|---|---|---|---|---|---|---|---|---|---|---|---|
| | C14:0 | C16:0 | C16:1 | C17:0 | C17:1 | C18:0 | C18:1n9c | C18:2n6t | C18:2n6c | C20:0 | C18:3n3 | C22:0 | C20:5n3 |
| Azam et al., 2005 | 0.8 | 14.5 | | NR | NR | 3.8 | 18.5 | NR | 61.4 | 1.0 | NR | NR | NR |
| Rao et al., 2012 | 0.1 | 14.7 | 1.3 | NR | NR | 6.75 | 40.0 | NR | 36.6 | 0.3 | 0.3 | 0.2 | |
| Suryawanshi and Mohanty, 2018b | NR | 17.84 | 1.4 | 0.13 | 1.32 | 4.6 | 31.08 | 0.25 | 39.44 | 0.12 | 0.22 | 0.97 | 1.08 |

NR: Not reported

Table 2.13. Fatty acid composition of the PP seed oil reported in literature.

| Author | Fatty acid compositions (%) | | | | | | | | | | | | |
|---|---|---|---|---|---|---|---|---|---|---|---|---|---|
| | C15:1 | C16:0 | C18:0 | C18:1n9c | C18:2n6c | C20:0 | C18:3n6 | C18:3n3 | C20:1 | C22:0 | C20:3n6 | C22:1n9 | C20:5n3 |
| Meher et al., 2004 | NR | 11.65 | 7.5 | 51.59 | 16.64 | 1.35 | NR | NR | NR | 4.45 | NR | NR | NR |
| Sarin et al., 2010 | NR | 9.8 | 6.2 | 72.2 | 11.8 | NR | NR | NR | NR | NR | NR | NR | NR |
| Sangwan et al., 2010 | NR | 10.8 | 8.7 | 46.0 | 27.1 | 0.8 | NR | 6.3 | NR | 3.20 | NR | NR | NR |
| Kesari et al., 2010 | NR | 10.8 | 8.7 | 46.0 | 27.1 | 0.8 | NR | 6.3 | NR | NR | NR | NR | NR |
| Bala et al., 2011 | | 7.05 to | 3.18 to | 43.07 to | 17.19 to | 0.71 to | | 5.45 to | 3.28 to | 2.45 to | | 15.29 to | |
| | NR | 7.31 | 3.46 | 44.91 | 17.57 | 0.85 | NR | 5.57 | 3.58 | 2.51 | NR | 16.51 | NR |
| Pavithra et al., 2012 | | 10.01 to | 4.42 to | 48.43 to | 18.31 to | | | 5.07 to | | NR | | NR | |
| | NR | 10.35 | 5.88 | 49.79 | 19.39 | NR | NR | 6.01 | NR | | NR | | NR |
| Bobade and Khyade, 2012 | NR | 11.65 | 7.50 | 51.59 | 16.64 | NR | NR | | 1.35 | 4.45 | NR | NR | NR |
| Dwivedi and Sharma, 2014 | | 3.7 to | 2.4 to | 44.5 to | 10.8 to | 0.8 to | | 3.6 to | | 0.1 to | | NR | |
| | NR | 14.1 | 10.9 | 71.3 | 27.1 | 4.7 | NR | 6.3 | NR | 5.3 | NR | | NR |
| Goembira and Saka, 2015 | NR | 7.4 | 3.8 | 65.6 | 15.4 | NR | NR | 4.4 | NR | NR | NR | NR | NR |
| Suryawanshi and Mohanty, 2018a | 8.64 to 11.95 | 0.0 | 5.74 to 7.04 | 45.42 to 58.62 | 0.0 | 15.34 to 17.07 | 0.25 to 1.69 | 1.24 to 4.01 | 0.0 to 3.82 | 0.0 | 2.62 to 4.45 | 0.0 | 0.45 to 1.11 |

NR: Not reported

## 2.12 Mathematical modeling of SFE processes

The main aim of mathematical modeling of a SFE process is to predict the extraction curve as the function of the experimental parameters such as temperature, pressure, solvent flow rate, particle size, co-solvent amount and other parameters such as bed height, matrix of seed particles and solubility parameters. As the actual experiments at large scale are extremely expensive therefore, the mathematical models are being used to overcome this problem. In other words, mathematical models also help in scaling up.

A fundamentally sound and sufficiently detailed mathematical model may be used to project and extend the scope of the available experimental findings to obtain a better understanding of the systems and the phenomena involved for the design, scale-up and operation of the related equipment and the complex systems having such equipment (Hortacsu, 2000). It is evident that various models differ not only in the form of mathematical representation but also due to mass transfer mechanisms, which control the SFE of different matrices. Thus, a single model may not be fitted to all type of experimental data. Since, the strength of a model is measured by the number of different systems it can accurately predict, and the spans of it's applicability within acceptable limits of accuracy and precision. Therefore, it has become crucial to review all available mathematical models (used only for SFE processes) for the selection of the best one or to develop a new one if required.

### 2.12.1 Chronological development of mathematical models used for SFE processes

Table 2.14 shows that more than 35 models have been proposed by various authors based on different assumptions, nature of model equation, tuning parameters, % error and method of solution. From Table 2.14, it can be seen that various authors due to its analytical solution, which incorporates different extraction periods, have used Sovova's model (Sovova, 1994) extensively. The propagation of mathematical models for SFE process is shown in Fig. 2.7, from where it can be concluded that most of the work has been done on DDDM (desorption-dissolution-diffusion models). Based on this mechanism (e.g. DDDM), various models (e.g. ADSM, WADSM, DLM, LDFM, SSM and BICM) have been developed which are differ from each other due to different simplifications and assumptions made during modeling. A thorough literature review has been present in Table 2.14.

Table 2.14. Model variations based on different assumptions.

| Sl. no. | Author & Process | Model | Tuning parameter | Error (%) | Method of solution | Findings | Part of extraction curve | Assumptions |
|---|---|---|---|---|---|---|---|---|
| 1. | (Lee et al., 1986) (SFE of canola oil from canola seeds) | MTBM (DDDM) | NR | 0.09 | - Method of characteristics - Computer program to solve partial differential equations. | - Oil concentration profiles in both solvent and solid phases. - The overall volumetric mass transfer coefficients. | The overall volumetric mass transfer coefficient gave the best agreement with the experimental in the constant rate period. | [1], [2], [3], [4] [5], [6], [7] |
| 2. | (Schaeffer et al., 1989) (SFE of monocrotaline from crotalaria spectabilis) | MTBM (DDDM) | Overall mass transfer coefficient. | 4- 5.8 | -Method of characteristics. -Computer program to solve partial differential equations. | - Explained the dependence of the concentration. | NR | [4], [8], [9], [10], [5], [2] |
| 3. | (Hong et al., 1990) (SFE of soybean oil from dry-milled soybeans) | MTBM (DDDM) | Diffusivity in the solid phase. | 0.47 | NR | - External mass transfer coefficient | Combined mass transfer models for CER & FER but best agreement in constant rate period. | [7],[11], [12] |
| 4. | (Bartle et al., 1990) (SCFE of PAH's from railroad soil) | MTBM (DDDM) (Hot ball model) | Diffusivity in the solid phase. | NR | NR | - Concentration profile with respect to extraction time was predicted. | It gives little information about the early stage of extraction (CER) in which the majority of the material is extracted. | [13], [14],[15], [16], |
| 5. | (Cygnarowicz-Provost et al., 1992) (SFE lipids from fungal mycelia) | MTBM (DDDM) | Overall mass transfer coefficient. | 15 | - Method of characteristics. - Modified Euler's method to integrate the equations. - Computer program to solve partial differential equations. | - Lipids concentration profiles in both solvent and solid phases. - The overall volumetric mass transfer coefficients. | Overall, volumetric mass transfer coefficient gave the best agreement with the experimental in the constant rate period. | [1], [2], [3], [4], [14], [5], [6], [7] |
| 6. | (Reverchon et al., 1993) (SFE of oil and cuticular waxes from herbaceous matrices) | MTBM (DDDM) | Solid diffusivity | 8.77 - 11.75 | -Computer program to solve partial differential equations. | - Oils yield prediction. - The overall volumetric mass transfer coefficients. | Five steps describe the extraction process (extraction from single spherical particle). | [17], [13],[18] [19], [20],[21] [22], [7] |

Cont…

| Sl. no. | Author & Process | Model | Tuning parameter | Error (%) | Method of solution | Findings | Part of extraction curve | Assumptions |
|---|---|---|---|---|---|---|---|---|
| 7. | (Sovova, 1994) | MTBM (DDDM) (BICM) | - Parameters of slow and fast extraction periods | NR | Method of characteristics. | - Mass transfer coefficient in the solid phase.<br>- Oil yield prediction.<br>- Concentration profiles in solid and solvent phases. | Model has the best suitability for fast extraction period and slow extraction period. Also considered Transition period. | [3], [23], [24], [7] |
| 8. | (Roy et al., 1994) (SFE of oil from tomato seeds) | MTBM (DDDM (BICM) | NR | 0.66 - 3.17 | Runge-kutta method of solution. | - Mass transfer coefficient in the solid phase.<br>- Oil yield prediction. | Model has the best suitability for FER period. | [3], [23], [5], [2], [21], [25], [13] |
| 9. | (Sovova et al., 1994) (SFE of grape oil from grape seeds) | MTBM (DDDM) (BICM) | - Parameters of mass transfer in solvent and solid phases. | NR | Method of characteristics. | -The effects of milling, amount of solid material, solvent velocity and flow direction on the extraction curves.<br>- Mass transfer coefficients in SCF and solid phases | -Best suitability for fast extraction period and slow extraction period. Also considered transition period. | [5], [26],[29], [7] |
| 10. | (Reverchon et al., 1994) (SFE of basil oil from basil leaves) | MTBM (DDDM) | - Internal diffusion coefficient. | 10.39 - 19.08 | Numerical methods. | -External mass transfer coefficient.<br>- Oil yield prediction.<br>- Concentration profile. | NR | [13], [17], [27], [24] |
| 11. | (Roy et al., 1996) (SFE of ginger oil from ginger) | MTBM (SCM) | - Intra-particle diffusivity.<br>-Solubility | 0.83 - 2.10 | Numerical solution by Crank Nicholson method. | -External mass transfer coefficient.<br>-Binary diffusivity. | NR | [25], [29], [28], [3], [23] [30], [13] |
| 12. | (Reverchon and Poletto, 1996) (SFE of oil from flower concretes) | MTBM (DDDM) | - Constant mass transfer coefficient between the phases.<br>- Shock wave velocity. | 2.24-3.65 | - Numerical solution.<br>- Fourth order Runge-Kutta method. | -Oil yield prediction.<br>-External mass transfer coefficient.<br>-Resistance behavior during the mass transfer from the oily phase to solvent.<br>-Concentration profile between the regions. | -Two stages of the extraction process were modeled in a best way. | [1], [33],[31], [32], [23],[2], [14], [21], [4] |

Cont…

| Sr. no. | Author & Process | Model | Tuning parameter | Error (%) | Method of solution | Findings | Part of extraction curve | Assumptions |
|---|---|---|---|---|---|---|---|---|
| 13. | (Goto et al., 1996) (SFE of solute from solid matrix) | MTBM (SCM) | -Intra-particle Effective diffusivity. | NR | -Numerical solution by Crank Nicholson's method | -Oil yield prediction. -Effect of dimensionless numbers (Peclet and Biot no.) on extracted concentration. | NR | [28], [3], [30], [23], [39] |
| 14. | (Perrut et al., 1997) (SFE of sunflower oil from sunflower seeds) | MTBM (DDDM) | -Mass transfer coefficients | 1.12-6.89 | -Method of characteristics. -Fourth order Runge-Kutta method. | -Oil yield prediction. -Effect of solid matrix. | -Best description/suitable for the linear parts of the extraction curve. | [21], [35], [32], [23], [36], [37], [2], [4] |
| 15. | (Goodarznia and Eikani, 1998) (SFE of oil from herbs and spices) | MTBM (DDDM) | NR | NR | -Numerical solution by Crank Nicholson's implicit method | -Mass transfer coefficient. -Axial dispersion coefficient in the SC phase. -Diffusion coefficient in the solid phase. -Oil yield prediction. | -Two stages of the extraction process were modeled in a best way. | [38], [13],[23] [6], [40], [30], [21], [22] |
| 16. | (de França et al., 1999) (SFE of carotenoids & lipids from Buriti) | MTBM (EDM) | -Parameters of slow and fast extraction periods. | 4.50 | -Method of characteristics. | -Mass transfer coefficient in the solid phase. -Oil yield prediction | -Constant extraction rate and diffusion controlled rate periods were considered. | [3], [23], [24], [7] |
| 17. | (Abaroudi et al., 1999) (SFE of β-naphthol from impregnated porous pellets) | MTBM (SCM) | NR | NR | -The numerical solution of the model equations was performed using a MOLCH a computer program based on the method of lines. | -External and internal mass transfer coefficients. -Axial dispersion coefficient. -Intra-particle diffusivity. | NR | [34], [28],[23] [29], [40] |
| 18. | (Reis-Vasco et al., 2000) (SFE of oil from pennyroyal ) | MTBM (DDDM) | -Internal mass transfer coefficient. | 3.90-7.89 | NR | -Internal mass transfer coefficient -Oil yield prediction | NR | [41], [23], [4], [21], [30] |
| 19. | (Reverchon et al., 2000) (SFE of oil from hiprose seeds) | MTBM (DDDM) | -Internal mass transfer coefficient | 7.40 | -Finite difference method (Explicit numerical cell) | -Internal mass transfer coefficient. -Oil yield prediction. | -Suitable for linear part of the curve. | [21], [35], [48], [32], [23], [2], [37] |

Cont…

| Sr. no. | Author & Process | Model | Tuning parameter | Error (%) | Method of solution | Findings | Part of extraction curve | Assumptions |
|---|---|---|---|---|---|---|---|---|
| 20. | (Cocero and Garcia, 2001) (SFE of oil from sunflower seeds) | MTBM (EDM) | -Equilibrium coefficient. -Mass transfer parameter. | 5.94 | -(Numerical & Analytical solution) -Fourth order Runge-Kutta method. -Laplace transform. | -External mass transfer coefficient | -Best description/suitable for the linear parts of the extraction curve. | [21], [7], [32], [6], [23], [41], [46], [40] |
| 21. | (Skerget and Knez, 2001) (SFE of active ingredients from plant material) | MTBM | -Adsorption equilibrium constant | 3.8 - 13 | -Laplace transformations | -External mass transfer coefficient. -Adsorption equilibrium constant. | -Best description/suitable for the linear parts of the extraction curve. | [42], [43],[44] |
| 22. | (Ruetsch et al., 2003) (SFE of clove bud oil from clove buds) | MTBM (DDDM) | -Equilibrium coefficient. -Mass transfer parameter. | 6.67 | - Fourth order Runge-Kutta method. | -External mass transfer coefficient | -Best description of CER and FER period. | [45], [21], [6], [30], [24],[23] [4], [46] |
| 23. | (Mongkholkhajornsilp et al., 2005) (SFE of nimbin from neem seeds) | MTBM (DM) | | NR | NR | -External mass transfer coefficient. - Effective intra-particle diffusion coefficient. | -Best description/suitable for the linear parts of the extraction curve. | [2], [40], [23], [47], [4], [6], [7], [1] |
| 24. | (Kumoro and Hasan, 2006) (SFE of Andrographolide from Andrographis paniculata leaves) | MTBM (PKM) | - Desorption rate constant. | 1.89 | NR | -Fluid-soild phase mass transfer coefficient. -Effective diffusivity of solute in SC-$CO_2$. | -Suitable for linear part of the curve | [23], [21], [7], [6], [46], [2], [40] |
| 25. | (Nei et al., 2008) (SFE of fatty acids from Trout powder) | MTBM (DDDM) | NR | NR | -Implicit finite difference method. | -Mass transfer coefficients. -Axial dispersion coefficient in the bulk phase. -Effective diffusivity. | -Best description of CER and FER period. | [23], [6], [21], [14], [48], [29], [41], [4] |
| 26. | (Jia et al., 2009) SFE of oil from Plumula nelumbinis. | MTBM (DDDM) BIC | -Parameter of the fast extraction and slow extraction period. | 2.34 - 10.9 | NR | -Mass transfer coefficient of fluid phase. -Diffusion coefficient. | NR | [3], [23], [24], [7], [21] |

Cont…

| Sr. no. | Author & Process | Model | Tuning parameter | Error (%) | Method of solution | Findings | Part of extraction curve | Assumptions |
|---|---|---|---|---|---|---|---|---|
| 27. | (Ghoreishi et al., 2009) (SFE of mannitol from Olive leaves) | MTBM (DDDM) | -Adsorption equilibrium constant. -Transfer parameter. -Fraction of internal sites. | 3.40 | -Modified 4th-order Runge-Kutta finite difference method. | -Distribution coefficient and extraction yield. | NR | [49], [13], [14], [4], [50] |
| 28. | (Perakis et al., 2010) (SCFE of oil from dittany) | MTBM (DDDM) | -Partition coefficient of solute between the fluid and the solid phase. -Solid phase mass Transfer coefficien | 7 -10 | NR | -Oil yield prediction. | NR | [24], [23], [6], [29], [2], [51], [52] |
| 29. | (Patel et al., 2011) (SFE of oil from cashew nut shells and black pepper) | MTBM (DDDM) | NR | 0.74 - 2.97 | -Analytical solution | -Yield prediction at different operating parameters for the CNS and black pepper. | -Best description of CER and FER period. | [29], [41], [7], [3], [23], [24], [21], [5] |
| 30. | (Kumhom et al., 2011) (SFE of Isoflavone from soyabean meal) | MTBM (SC) | NR | 6.54 | NR | -Solubility. -Film mass transfer coefficient. -Effective diffusivity. -Axial dispersion coefficient. | NR | [23], [46], [30], [40], [21] |
| 31. | (Maksimovic et al., 2012) (SFE of oil from mentha) | MTBM (PKM) | NR | 6.21 | -Simulation of SCFE of Mentha was done by using Polymath Educational, Matlab and origin Pro Software | -External mass transfer coefficient. -Apparent internal mass transfer coefficient | -Described SFE process in two steps as fast and slow extraction periods. (best suitable) | [53], [54], [55], [56] |
| 32. | (Ahmed et al., 2012) (SFE of oil from Algerian rosemary leaves) | MTBM (SC) | -Effective diffusivity | 4.23 - 5.68 | -Finite difference method. | -Fluid mass transfer coefficient. -Diffusion coefficient of the solid phase. | NR | [2], [7], [57], [14], [6], [23] |

Cont…

| Sr. no. | Author & Process | Model | Tuning parameter | Error (%) | Method of solution | Findings | Part of extraction curve | Assumptions |
|---|---|---|---|---|---|---|---|---|
| 33. | (Honarvar et al., 2013) (SFE of oil from canola and sesame seeds) | MTBM (DDDM) | -Effective diffusivity. -Mass transfer coefficient. -Axial dispersion coefficient | 4.58 - 9.84 | -Solved numerically by the Method of lines available in MATLAB 7.1 | -Yield prediction at different operating parameters for the canola and Sesame seeds oil. | -Described SFE process in two phases as Fast & Slow extraction periods. (best suitable) | [23], [6], [30], [29], [7], [40] |
| 34. | (Scopel et al., 2013) (SFE of oil from schinus molle L. leaves) | MTBM (DDDM) | -Effective diffusivity. -The convective mass transfer coefficient. | NR | NR | -Effective diffusivity. -The convective mass transfer coefficient. | -Described SFE process in two periods as CER & FER extraction periods. (best suitable) | [21], [6], [4] |
| 35. | (Ayas and Yilmaz, 2014) (SFE of safflower seed oil) | MTBM (SCM) | -Effective diffusivity | NR | -Solved numerically by MAPLE 17 software. | -Axial dispersion coefficient. -Effective diffusivity. | -Best fitted with the linear part of the extraction curve means CER. | [6], [14], [21], [23], [24], [40] |
| 36. | (Taher et al., 2014) (SFE of Scenedesmus sp. Lipids) | MTBM DDDM (BICM) | Parameters of slow and fast extraction periods | NR | NR | -Oil concentration profiles in both solvent and solid phases. -The overall volumetric mass transfer coefficients. | Model has the best suitability for fast extraction period and slow extraction period. Also considered Transition period. | [3], [23], [24], [7], [21] |
| 37. | (Adeoti and Hawboldt, 2015) (SFE of oil from salmon processing waste) | MTBM (DDDM) | Effective intra-particle diffusion coefficient | 3.0 – 10.6 | NR | -Adsorption equilibrium constant. -Mass transfer coefficient of solvent phase. | Best fitted with the linear part of the extraction curve means CER. | [2], [6], [23], [27], [40], [58], [59] |

Table 2.15. Assumptions used in Table 2.14.

| | | | |
|---|---|---|---|
| [1] | One-dimensional steady state. | [20] | Particle radius does not affect the diffusivity of both oils in the matrix. |
| [2] | Axial dispersion is negligible in the bed. | [21] | Essential oil is treated as a single component (solute) means extraction can be described as a single pseudo-compound. |
| [3] | Solvent is oil-free at the entrance. | [22] | Solute concentration does not depend on spherical coordinates. |
| [4] | The concentration of solute (oil) in the solvent phase in equilibrium with seeds (solid) having a solute concentration. | [23] | Isothermal and isobar system |
| [5] | Plug flow exists in the bed. | [24] | Solid bed is homogeneous with respect to particle size and initial distribution of solute. |
| [6] | Physical properties are constant. | [25] | Intra-particle mass transfer is dominated. |
| [7] | Fixed extraction bed. | [26] | Down flow of $CO_2$ through the bed. |
| [8] | The solute concentration is radially uniform throughout the seed material. | [27] | Particle is porous and formed by a non-soluble matrix. |
| [9] | Solubility of the solute in the fluid phase is low. | [28] | Solvent flows axially. |
| [10] | Intra-particle diffusion is neglected. | [29] | Solvent flow rate is constant. |
| [11] | Constant extraction rate (CER) region controlled by a film controlling mass transfer and falling extraction rate (FER) region by a diffusional mass transfer. | [30] | Axial dispersion is considered. |
| [12] | Un-steady state mass transfer. | [31] | Volume fraction of the glass beads (packing) is constant. |
| [13] | Spherical particles of uniform size. | [32] | Uniformly distribution of solvent flow rate. |
| [14] | Solute is uniformly distributed within the particle at the beginning of the extraction. | [33] | Uniformly distribution of concretes on the surface of the glass beads packing |
| [15] | The rate of flow of SF past the particles is fast enough that the concentration of the extracted in the fluid is always close to zero. | [34] | Isotropic system about diffusion. |
| [16] | Extractable are to move through the matrix by a process of diffusion. | [35] | Implicit hypothesis has been adopted (relevant conc. gradients in the fluid phase develop at larger scales than the particle size). |
| [17] | Single particle approach and an internal diffusivity consideration. | [36] | The value of solute concentration in solid is an average value within the particle and depends on time and height. Means concentration gradients within the particles were not resolved. |
| [18] | The particle diameter is the weight mean diameter of the measured size distribution. | [37] | Volume fraction of the fluid is not affected by the reduction of the solid mass during the extraction. |
| [19] | Extraction of essential oils and of cuticular waxes are parallel and non -interacting processes. | [38] | Two- phase unsteady-state mass balance. |

Cont…

| | |
|---|---|
| [39] Intra-particle diffusion consideration | [50] There is no mass transfer resistance for the exterior sites on the particle surface. |
| [40] Radial concentration gradients neglected/ Radial dispersion neglected | [51] The mass transfer rate is controlled by the phase equilibrium and the oil diffusion in the solid. |
| [41] Superficial velocity of SF is constant along the extractor. | [52] Model takes into account the accumulation of the solute in the fluid phase ($\partial y/\partial t = 0$) and that the extraction is not uniform along the bed ($\partial y/\partial h = $ constant. |
| [42] Adsorption –desorption equilibrium of extractable component from solid tissue. | [53] Supercritical extraction was considered as chemical reaction, although it is a physical Phenomenon. |
| [43] Mass transfer through the external film into the bulk. | [54] They assumed that supercritical extraction consists of two main steps as Fast (disrupted cells) & Slow (intact cells) extraction periods. |
| [44] Semi-batch extraction. | [55] The rate of extraction from disrupted cells of plant material depends on resistance to the external mass transfer which is governed mainly by hydrodynamic conditions inside extractor and particle size. |
| [45] Extraction bed is made of spherical, isotropic micro porous particles arranged in a cylindrical geometry. | [56] The rate of extraction from intact cells depends mainly on resistance to diffusion through the cells membrane and it is time dependent process. |
| [46] Particle porosity, particle size, void fraction in the bed, solute diffusivity inside solid particles and dispersion coefficient are constant and uniform along the bed. | [57] The extraction is an irreversible desorption process. |
| [47] No interaction among solutes in the fluid phase or solid phase. | [58] Local equilibrium adsorption exists between solute and solid in pores of fish particle. |
| [48] Solute concentration in the particle pores was a function of radius and time as well as the bed length. | [59] Solute interaction in the fluid or solid phase is negligible. |
| [49] System is assimilated into a batch extraction column (the possible extraction during discharge period may be the cause of small deviations between the modeling predictions compared to experimental measurements). | |

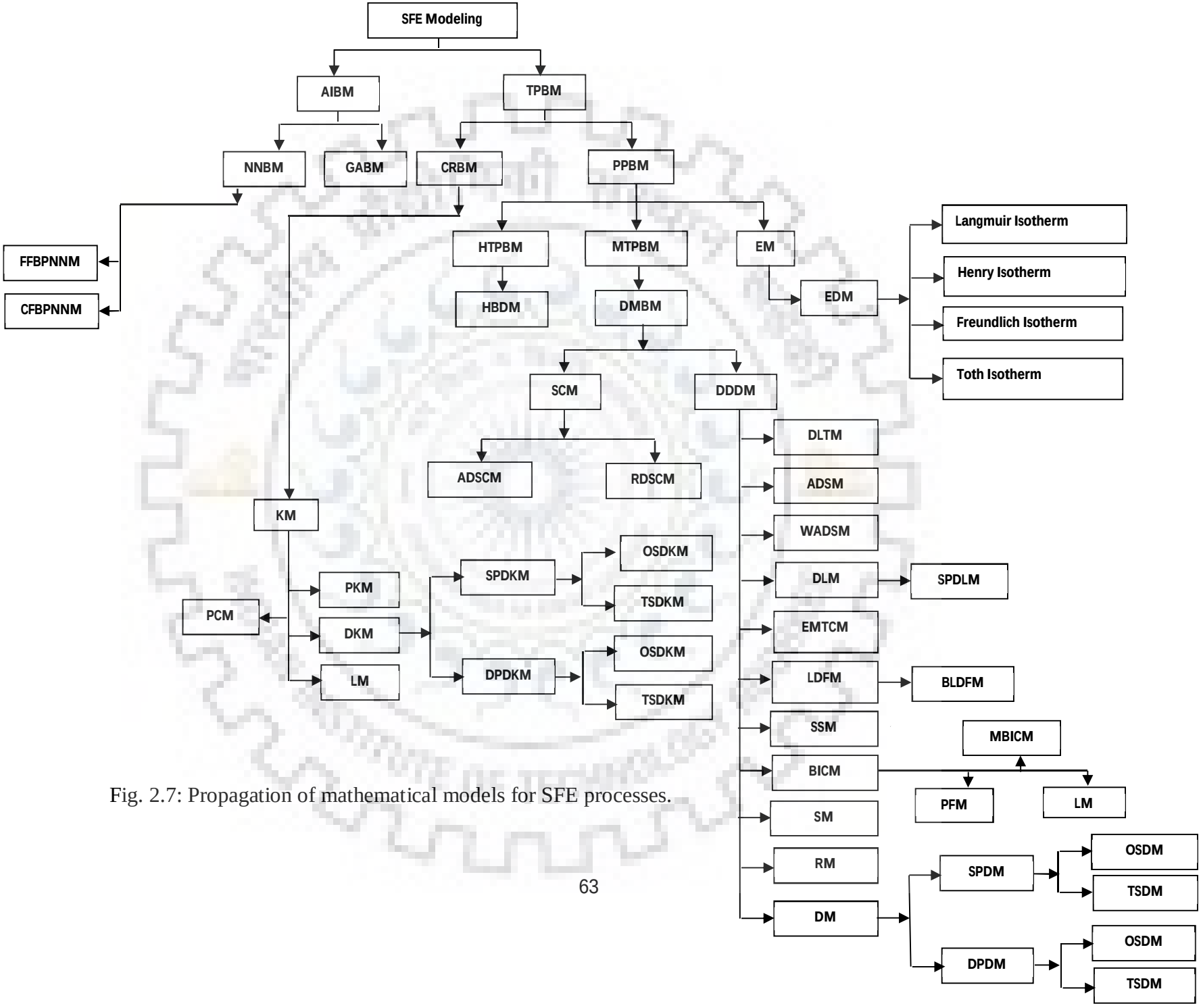


Fig. 2.7: Propagation of mathematical models for SFE processes.

Table 2.16. Different types of models shown in Fig. 2.7.

| | | | | | |
|---|---|---|---|---|---|
| **TPBM** | Transport Phenomena Based Models | **ADSM** | Axial Dispersion of Solute Model | **SPDKM** | Single Parameter Desorption Kinetic Model |
| **SSM** | Single Sphere Model | **WASDM** | Without Axial Dispersion of Solute Model | **DPDKM** | Double Parameter Desorption Kinetic Model |
| **CRBM** | Chemical Reaction Based Models | **DLM** | Differential Layer Models | **OSDM** | One Site Desorption Model |
| **PPBM** | Physical Phenomena Based Model | **EMTCM** | External Mass Transfer Control Model | **TSDM** | Two Site Desorption Model |
| **DMBM** | Differential Mass Balance Models | **LDFM** | Linear Driving Force Model | **OSDKM** | One Site Desorption Kinetic Model |
| **HTPBM** | Heat Transfer Phenomena Based Models | **BICM** | Broken and Intact Cells Model | **TSDKM** | Two Site Desorption Kinetic Model |
| **MTPBM** | Mass Transfer Phenomena Based Model | **SM** | Sovova Model | **HBDM** | Hot Ball Diffusion Model |
| **EM** | Empirical Models | **RM** | Reverchon Model | **BLDFM** | Bi-Linear Driving Force Model |
| **SCM** | Shrinking Core Model | **SPDLM** | Single parameter Differential Layer Model | **DLTM** | Diffusion Layer Theory Model |
| **DDDM** | Desorption-Dissolution-Diffusion Models | **DKM** | Desorption Kinetic Model | **PCM** | Partitioning coefficient model |
| **KM** | Kinetic Models | **EDM** | Empirical Desorption Models | **MBICM** | Modified Broken and Intact Cell Model |
| **PKM** | Pseudo kinetic model | **BICM** | Broken and Intact Cell Model | **PFM** | Plug Flow Model |
| **LM** | The Logistic Model | **ADSCM** | Axial Dispersion Shrinking Core Model | **RDSCM** | Radial Dispersion Shrinking Core Model |
| **AIBM** | Artificial Intelligence Based Models | **NNBM** | Neural Network Based Models | **GABM** | Genetic Algorithm Based Models |
| **CFBPNNM** | Cascade Forward Back Propagation Neural Network Model | **FFBPNNM** | Feed Forward Back Propagation Neural Network Model | | |

2.12.2 Sovova model (Sovova, 1994) for SFE process

From the literature, it is found that the model proposed by Sovova, 1994 has been used widely for modeling the SFE process for all types of solutes and is discussed hereunder. This model assumes that part of the extractable material is easily accessible ($X_p$) to the solvent, due to the breaking of the cell structures, which contain the solute, during the milling of the raw material. The other fraction of the solute ($X_k$) remains inside the cell structures that were not broken up by milling, so its contact with the solvent is more difficult. The following important assumptions were taken into consideration during the extraction process:

- Temperature and pressure are constant during extraction.
- Solid bed is homogeneous with respect to particle size and initial distribution of the oil.
- SC-$CO_2$ is oil-free at the extractor entrance.
- Mass transfer phenomena for all extracts are similar.
- Pseudo steady state and plug flow.
- The extraction bed is fixed.

The development of Sovova model (Sovova, 1994) is based on the model proposed by Lack, 1985 during his thesis work. In this work, he established a mass balance for a bed element where the height of the bed of particles is H and its void fraction is $\varepsilon$ is shown in Fig. 2.8 where axial distance along the bed is h.

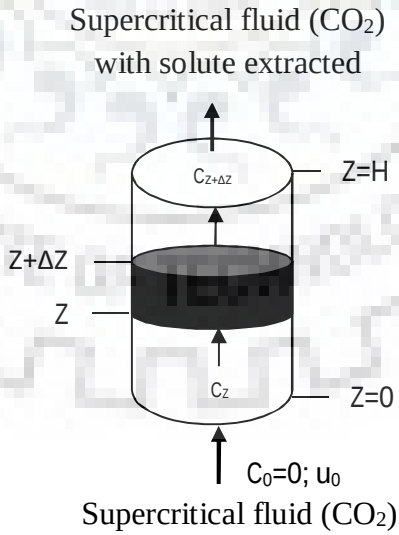


Fig. 2.8: Schematic representation of extracting bed considered during the modeling.

The material balances for an element of bed as given by Sovova, 1994 are almost similar to that has been derived by Lack, 1985.

*Solid phase:*

$$-\rho_s(1-\varepsilon)\frac{\partial x}{\partial t} = J(x,y) \quad \text{… Eq. 2.13}$$

*Solvent phase:*

$$\rho\varepsilon\frac{\partial y}{\partial t} + \rho U\frac{\partial y}{\partial h} = J(x,y) \quad \text{… Eq. 2.14}$$

It was assumed that the solvent is solute free at the entrance of the extractor so for the fluid phase the first term of Eq. (2.14) was neglected and reduced to Eq. (2.15).

$$\rho U\frac{\partial y}{\partial h} = J(x,y) \quad \text{… Eq. 2.15}$$

The initial and boundary conditions are as follows:

$$x = x_0 \; at \; t = 0 \;\; for \;\; 0 \le h \le H \quad \text{… Eq. 2.16}$$

$$y = 0 \; at \; h = 0 \;\; for \;\; t \ge 0 \quad \text{… Eq. 2.17}$$

Lack, 1985 described the two zones namely (i) diffusion resistance in the solvent phase zone and (ii) diffusion resistance in the solid phase zone during the extraction process. The easily accessible solute was extracted in the first zone, which is governed by the diffusional resistance in the solvent phase while the inaccessible solute was extracted in the second zone, which is governed by the diffusional resistance in the solid phase where concentration decreases to $x_k$. Since the mass transfer resistance in the first zone, (e.g. solvent phase) is lower than the mass transfer resistance in the second zone (e.g. solid phase). Therefore, the mass transfer rate in first zone was faster than that in second zone.

$$J(x > x_k, y) \; > J(x \le x_k, y) \quad \text{… Eq. 2.18}$$

If the easily accessible solute crosses the interfacial boundary fast enough to keep the solvent saturated at the boundary, the mass transfer rate in first zone (also named a fast period) is written as;

$$J(x > x_k, y) = \; k_f a_0 \rho (y_r - y) \quad \text{… Eq. 2.19}$$

The mass transfer rate in second zone (slow period) is written as;

$$J(x \leq x_k, y) = k_f a_0 \rho (y_r - y)\, {}^{x}/_{x_k} \quad \text{… Eq. 2.20}$$

The Eq. (2.13) and Eq. (2.15) were integrated after substituting for the rate of mass transfer $J(x, y)$ for computing the concentration profiles in the solid and solvent phases. A general equation that could be used to determine the extraction curve for different periods was obtained as given below;

$$e(t) = e(q - qt) = x_0 - \left(\frac{1}{H}\right) \int_0^H x(h, t)\, dh \quad \text{… Eq. 2.21}$$

Lack, 1985 proposed following dimensionless parameters:

$$c = \frac{x}{x_k},\ Y = \frac{(1-y)}{y_r},\ z = \frac{k_f a_0}{U} h, \tau = \frac{k_f a_0 \rho y_r}{(1-\varepsilon)\rho_s x_k} t \quad \text{… Eq. 2.22}$$

By using the above dimensionless parameters into the equations Eq. (2.13), Eq. (2.15), Eq. (2.16), Eq. (2.18), and Eq. (2.19), the dimensionless equations were obtained as follows:

$$\frac{\partial c}{\partial \tau} = \frac{\partial Y}{\partial z} = -J^*(c, Y) \quad \text{… Eq. 2.23}$$

$$c(z, \tau = 0) = r_0$$

$$Y(z = 0, \tau) = 1 \quad \text{… Eq. 2.24}$$

Where, $J^*(c, Y) = \frac{J(x,y)}{(k_f a_0 \rho y_r)}$

$$J^*(c > 1, Y) = Y \quad \text{… Eq. 2.25}$$

$$J^*(c, Y) = f(c)Y,\ f(c > 1) = 1,\ f(c \leq 1) \leq 1 \quad \text{… Eq. 2.26}$$

Solving equations Eq. (2.23) and Eq. (2.24) after eliminating '*Y*' by substituting the value of $J^*$ from the Eq. (2.25). After performing the integration, the equation (Eq. (2.27)) was obtained as follows;

$$\frac{1}{f(c)} \frac{\partial c}{\partial z} + r = r_0 \quad \text{… Eq. 2.27}$$

With the boundary condition,

$$\frac{\partial c(z=0,\tau)}{\partial \tau} = -f(c) \quad \text{… Eq. 2.28}$$

Lack, 1985 integrated the Eq. (2.26) with various forms of function *f(c)* numerically for the slow extraction period.

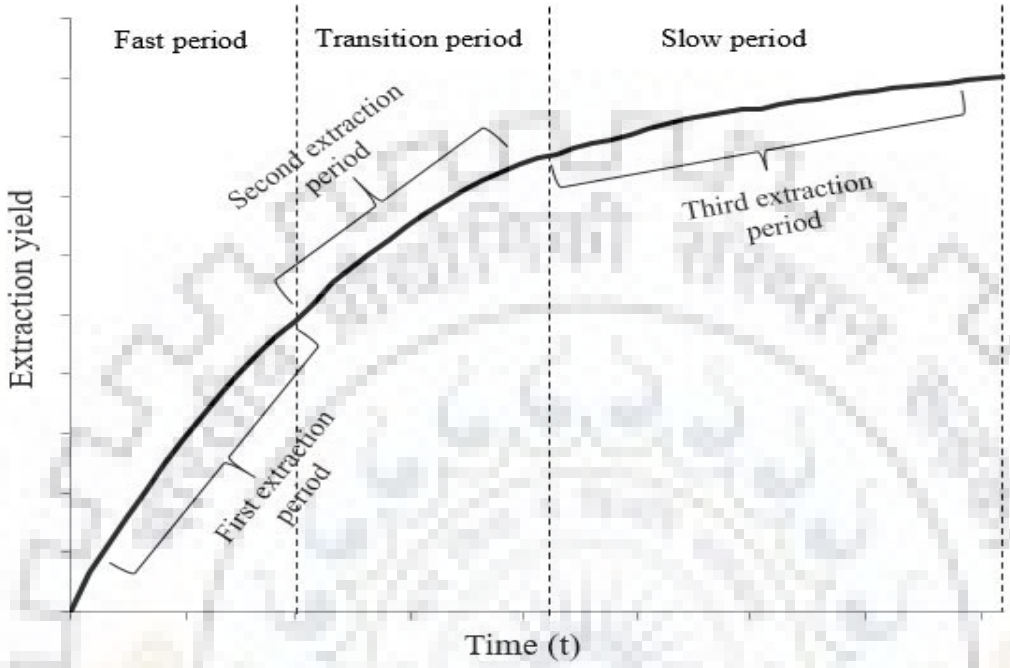


Fig. 2.9: Extraction periods during extraction process.

From this point, Sovova, 1994 extended the Lack, 1985 model by considering three zones (e.g. first, second and third period) of extraction as shown in Fig. 2.9. These three periods were also named as fast, transition and slow period based on rate of mass transfer (e.g. fast or slow) in each period. This additional zone (e.g. Transition period) is described by fact that, easily accessible solute exhausted at the solvent entrance to the solvent phase at the time when the fast extraction period end, and a transition period between the fast and slow extraction begin as shown in Fig. 2.9.

Sovova, 1994 extended the value of *f(c)*, function defining the extraction retardation by diffusion from inside of particles, by a constant $k \leq 1$ as written below;

$$f(c > 1) = 1, \quad f(c \leq 1) = kc \qquad \ldots \text{Eq. 2.29}$$

Sovova, 1994 introduced the solid-phase mass transfer coefficient ($k_s$) into the model because the extraction in the second period was controlled by diffusion in the solid phase as follows;

$$k = \frac{k_s \rho_s x_k}{k_f \rho y_r} \quad \text{… Eq. 2.30}$$

After substituting the $f(c)$ from the Eq. (2.29) into the Eq. (2.19) and using the Eq. (2.30), the mass transfer rate in the transition period is given as follows;

$$J(x \le x_k, y) = k_s a_0 \rho_s x Y \quad \text{… Eq. 2.31}$$

Now, Sovova, 1994 reported that the concentration profiles in the solid and solvent phases, which were computed analytically through Eq. (2.20), Eq. (2.21) and Eq. (2.29), and concentration profiles in solid phase were proposed as:

$$c = \begin{cases} c_0 - \tau \exp(-z) & \text{for } \tau < \tau_m \\ c_0 - \tau_m \exp[-(z - z_w)] & \text{for } \tau_m \le \tau < \tau_n, z > z_w \\ \dfrac{c_0}{(1 + \{c_0 \exp[k(\tau - \tau_m)] - 1\}\exp(-c_0 kz))} & \text{for } \tau_m \le \tau < \tau_n, z \le z_w \text{ and for } \tau \ge \tau_n \end{cases} \quad \text{… Eq. 2.32}$$

Where,

$$\tau_m = c_0 - 1,\ \tau_n = \tau_m + \frac{1}{k} ln \frac{1 + \tau_m \exp(c_0 kZ)}{1 + \tau_m},\ z = k_f a_0 H/U \quad \text{… Eq. 2.33}$$

The coordinate of the boundary between both fast and slow extraction sections was given as below;

$$z_w = \frac{1}{k c_0} ln \frac{c_0 \exp(k(\tau - \tau_m)) - 1}{c_0 - 1} \quad for \quad \tau_m \le \tau \le \tau_n \quad \text{… Eq. 2.34}$$

Similarly, the profile of the normalized concentration in the solvent phase was given as:

$$Y = \begin{cases} \exp(-z) & \text{for } \tau < \tau_m \\ \dfrac{\tau_m \exp(z_w - z)}{\{c_0 - \exp[k(\tau_m - \tau)]\}} & \text{for } \tau_m \le \tau < \tau_n, z > z_w \\ \dfrac{c_0 \exp[k(\tau - \tau_m)]}{\{\exp(c_0 kz) + c_0 \exp[k(\tau - \tau_m)] - 1\}} & \text{for } \tau_m \le \tau < \tau_n, z \le z_w \text{ and for } \tau \ge \tau_n \end{cases} \quad \text{… Eq. 2.35}$$

The extraction curve was proposed through following relations:

$$e = \begin{cases} \left(x_k \tau / Z\right)\left[1 - \exp(-Z)\right] & \text{for } \tau < \tau_m \\ \left(x_k / Z\right)\left[\tau - \tau_m \exp(z_w - Z)\right] & \text{for } \tau_m \le \tau < \tau_n \\ x_0 - \left(x_k / kZ\right)\ln\left\{1 + \left[\exp(c_0 kZ) - 1\right]\exp\left[k(\tau_m - \tau)\right] / c_0\right\} & \text{for } \tau \ge \tau_n \end{cases}$$ … Eq. 2.36

Sovova, 1994 rearranged the Eq. (2.36) to yield the amount of extract as a function of the specific amount of solvent ($q$), concentrations $x_0$, $x_k$ and $y_r$ and the parameters Z and W as given below;

$$e = \begin{cases} q\, y_r\left[1 - \exp(-Z)\right] & \text{for } q < q_m \\ y_r\left[q - q_m \exp(z_w - Z)\right] & \text{for } q_m \le q < q_n \\ x_0 - \frac{y_r}{W}\ln\left\{1 + \left[\exp\left(Wx_0 / y_r\right) - 1\right]\exp\left[W(q_m - q)\right]^{x_k / x_0}\right\} & \text{for } q \ge q_n \end{cases}$$ … Eq. 2.37

Where, the expressions for the $q_m$, $q_n$ and $z_w$ are given below;l

$$q_m = \frac{(x_0 - x_k)}{y_r Z}$$ … Eq. 2.38

$$q_n = q_m + \frac{1}{W} ln \frac{x_k + (x_0 - x_k)\exp(W x_0 / y_r)}{x_0}$$ … Eq. 2.39

$$z_w = Z\left\{\frac{y_r}{W x_0} ln \frac{x_0 \exp(W(q - q_m)) - x_k}{x_0 - x_k}\right\}$$ … Eq. 2.40

The parameter 'Z' is directly proportional to the solvent phase mass transfer coefficient ($k_f$) and inversely proportional to the specific solvent flow rate ($\dot{q}$).

$$Z = k_f a_0 \rho / [\dot{q}(1 - \varepsilon)\rho_s]$$ … Eq. 2.41

Similarly, the parameter $W$ is directly proportional to the solid-phase mass transfer coefficient ($k_s$) and inversely proportional to the specific solvent flow rate as:

$$W = k_s a_0 / [\dot{q}(1 - \varepsilon)] = kZ y_r / x_k$$ … Eq. 2.42

The final modified form of the equations were presented in Chapter 4.

2.12.2.1 Application of Sovova model (Sovova, 1994).

The mathematical model developed by Sovova, 1994, as discussed in section 2.12.2, has been used extensively by various researchers during the SFE of oil from different seeds as shown in Table 2.17. Roy et al., 1994 has found out the solid phase mass transfer coefficient ($k_{xa}$) and predicted the tomato seed oil during SFE while fitting the experimental data very well in the falling extraction rate (FER) period only. Similarly, other researchers (e.g. Marrone et al., 1998; Aleksovski et al., 1998; Papamichail et al., 2000; Kiriamiti et al., 2001; Ferreira et al., 2002; Perakis et al., 2005; Nagy and Simandi, 2008; Han et al., 2009; Mezzomo et al., 2009, Pederssetti et al., 2011; Jokic et al., 2012; Rai et al., 2016b) have applied this model successfully, during the SFE of natural seeds such as almond, grape, celery, sunflower, black pepper, black pepper, paprika, safflower, almond, canola, soybean and sunflower seeds respectively. From the Table 2.17, it can be seen clearly, that the Sovova model (SM) has been applied successfully under the wide range of operating parameters such as temperature (20 – 100 ºC), pressure (10 – 500 bar), particle size (0.08 – 10 mm), $CO_2$ flow rate (0.5 – 62 g/min), and the % of co-solvent (0 – 10 %) during the SFE process. The application of this model under the wide range of these operating parameters has proved its robustness and feasibility. From the Table 2.17, it is also clearly visible that this model has covered most of the influencing parameters such as mass transfer coefficients for solid and solvent phases, grinding efficiency, parameters for slow (FER) and fast (CER) periods of extraction which, which actually makes this model more realistic in the domain of desorption-dissolution-diffusion (DDD) mechanism modeling.

A thorough literature survey, on the effects of selected parameters involved in the SFE process, based on the Sovova model (SM) used in these process, has been given in Table 2.18. From Table 2.18, it can be seen that the increase in pressure results in an increase in the extraction yield and the reason behind this has already been explained in section 2.3.2. Similarly, an increase in the extraction yield has also been reported, as shown in Table 2.18, when the co-solvent amount is increased. This phenomena has also been explained in section 2.3.5. The other remaining parameters (temperature, particle size and $CO_2$ flow rate) have shown both negative and positive contributions on the extraction yield of oils. For example, the negative effect of temperature on the extraction yield has been reported while using the SM by various researchers (e.g. Papamichail et al., 2000; Perakis et al., 2005; Han et al., 2009; Pederssetti et al., 2011 and Sodeifian et al., 2016b) during the SFE

process of various natural products such as celery seeds, black pepper seeds, safflower seeds, canola seeds, and pistacia khinjuk. Whereas, most of the researchers (as shown in Table 2.18) have reported the positive influence of temperature on yield. A detailed explanation of this behavior of temperature has already been included in section 2.3.1. In case of particle size, most of the researchers (as shown in Table 2.18) have shown an negative effect of particle size on the extraction yield of oil, however, two researchers (e.g. Jia et al., 2009 and Huang et al., 2011b) have also reported positive effect of it. A positive effect of $CO_2$ flow rate on the extraction yield has been reported by most of the researchers (as shown in Table 2.18) while the negative of it has only been reported by Mira et al., 1999 and Taher et al., 2014 during their study of SFE of orange peel and microalgae respectively. However, the reason of this duel behavior of parameters (e.g. particle size and the $CO_2$ flow rate) has already been explained in detail in sections 2.3.3 and 2.3.4 respectively.

Table 2.17. Applications of Sovova model for different materials used during SFE.

| **Author** | **Operation** | **Process Parameter** | **Parametric conditions** | **Tuning parameter** | **Findings** | **Part of OEC** |
|---|---|---|---|---|---|---|
| Sovova, 1994 | | Pressure, Temperature, Flow rate, Particle size | NR | Parameters of slow and fast extraction periods | $k_{xa}$, $k_{ya.}$ Oil yield prediction. Concentration profiles in solid and solvent phases. | Model introduced three periods of extraction as: CER period, FER period, TR period. |
| Sovova et al., 1994 | SFE of oil from grape seeds | Pressure Temperature Flow rate Particle size | 280 bar, 40ºC 0.5 - 1 Std L/min 0.08 - 1 mm | Parameters of mass transfer in solvent and solid phases. | The effects of grinding. $k_{xa}$, $k_{ya}$ | CER period, FER period, TR period. |
| Roy et al., 1996 | SFE of oil from tomato seeds | Pressure Temperature Flow rate Particle size | 245 bar, 40 ºC (3.33 - 26.64)*$10^{-8}$ $m^3/s$ 0.25 - 1.02 mm | NR | $k_{xa}$, Oil yield prediction. | Model has the best suitability for FER period. |
| Mira et al., 1996 | SFE of oil from Orange peel | Pressure Flow rate Particle size | 40 - 50 ºC, 1 - 250 bar, 8.33 – 58.33 g/min 0.1 - 10 mm | Z, W | $y_r$, Influences of process parameters on the extraction yield of oil. | Model has the best suitability for CER period. |
| Marrone et al., 1998 | SFE of oil from almond seeds | Bed height Bed mass Flow rate Particle size | 115 - 160 mm, 0.072 - 0.16 kg, 2.38 - 12 g/min, 0.3 - 1.9 mm | NR | $k_{xa}$, $k_{ya}$ Oil yield prediction. Influences of process parameters on the extraction yield of oil. | FER period, TR period. |

Cont…

| Author | Operation | Process Parameter | Parametric conditions | Tuning parameter | Findings | Part of OEC |
|---|---|---|---|---|---|---|
| Kiriamiti et al., 2001 | SFE of oil from sunflower seeds | Pressure<br>Temperature,<br>Flow rate,<br>Particle size | 250 bar,<br>60 ºC,<br>23 – 50 g/min,<br>0.25 - 1.25 mm | $k_{xa}$, $k_{ya}$ , $x_k$ | $k_{xa}$, $k_{ya}$<br>Influences of process parameters on the extraction yield of oil. | CER period,<br>FER period,<br>TR period. |
| Ferreira et al., 2002 | SFE of oil from Black pepper seeds | Pressure<br>Temperature, | 150 - 300 bar,<br>30 - 50 ºC | k, | $k_{ya}$, $t_{CER}$ | CER period, |
| Martínez et al., 2003 | SFE of Oleoresin from Ginger | Pressure<br>Temperature, | 150 - 250 bar,<br>20 - 40 ºC, | NR | Influence of process parameters on the extraction yield of oil. | CER period,<br>FER period,<br>TR period. |
| Campos et al., 2005 | SFE of oil from Marigold flower | Pressure<br>Temperature | 120 - 200 bar,<br>20 - 40 ºC, | Z, W | $k_{xa}$, $k_{ya}$ ,<br>Influence of process parameters on the extraction yield of oil. | CER period,<br>FER period,<br>TR period. |
| Perakis et al., 2005 | SFE of oil from Black pepper seeds | Pressure<br>Temperature<br>Flow rate | 90 - 150 bar,<br>40 - 50 ºC,<br>18 - 50 g/min | Z, W, Grinding efficiency | Influence of process parameters on the extraction yield of oil. | CER period,<br>FER period,<br>TR period. |
| Vargas et al., 2006 | SFE of essential oil Baccharis trimera leaves | Temperature | 40 - 70 ºC, | Z, W, $x_k$, $y_r$ | Influence of process parameters on the extraction yield of oil. | CER period,<br>FER period,<br>TR Period. |

| Author | Operation | Process Parameter | Parametric conditions | Tuning parameter | Findings | Part of OEC |
|---|---|---|---|---|---|---|
| Aleksovski et al., 1998 | SFE of oil from grape seeds | Pressure<br>Temperature<br>Flow rate<br>Extraction time | 280 bar,<br>40 ºC,<br>0.5 Std $dm^3$/min,<br>3 hrs | NR | $k_{xa}$, $k_{ya}$ | CER period,<br>FER period,<br>TR Period. |
| de França et al., 1999 | SFE of carotenoids and lipids from buriti fruit | Pressure<br>Flow rate | 200 - 300 bar<br>18.42 – 25.8 g/min | $k_{xa}$, | $k_{xa}$, | CER period,<br>FER period,<br>TR Period. |
| Mira et al., 1999 | SFE of oil from Orange peel | Pressure<br>Temperature<br>Flow rate,<br>Particle size | 80 – 280 bar,<br>20 – 50 ºC<br>8.33 – 58.33 g/min<br>0.1 - 10 mm | Z, W | $k_{xa}$, $k_{ya}$<br>Influence of process parameters on the extraction yield of oil. | CER period, |
| Berna et al., 2000 | (SFE of oil from Orange peel | NR | NR | Z, W | NR | CER period,<br>FER period,<br>TR Period. |
| Papamichail et al., 2000 | SFE of oil from Celery seeds | Pressure<br>Temperature<br>Flow rate,<br>Particle size | 100 - 250 bar,<br>45 - 55 ºC,<br>18.33 – 50 g/min,<br>210 µm | Z, W, $x_k$ | Influence of process parameters on the extraction yield of oil. | CER period,<br>TR Period. |
| Povh et al., 2001 | SFE of oil from Chamomile flowers | Pressure<br>Temperature,<br>Flow rate, | 100 - 200 bar,<br>30 - 40 ºC,<br>1 – 4 g/min | Z, W, $t_{CER}$ | The mass ratio of solute in the supercritical phase ($Y_{CER}$) as a function of pressure behaves in a fashion similar to the retro gradation region. | CER period,<br>FER period, |

Cont…

| Author | Operation | Process Parameter | Parametric conditions | Tuning parameter | Findings | Part of OEC |
|---|---|---|---|---|---|---|
| Martinez et al., 2007 | SFE of oil from Clove and Vetiver | Pressure<br>Temperature | 100 - 200 bar,<br>35 - 40 ºC | Z, W | $k_{xa}$, $k_{ya}$ | CER period,<br>FER period,<br>TR period. |
| Bernardo-Gill and Casquilho, 2007 | SFE of oils from Hazelnut and Walnut | Pressure<br>Temperature | 180 - 234 bar,<br>35 - 48 ºC | $k_{xa}$, $k_{ya}$, $f_k$, ε | Influence of process parameters on the extraction yield of oil. | CER period,<br>FER period,<br>TR period. |
| Nagy and Simandi, 2008 | SFE of oil from Paprika seeds | Particle size<br>Moisture %,<br>Initial oil % | NR | NR | Influence of process parameters on the extraction yield of oil. | CER period,<br>FER period,<br>TR period. |
| Han et al., 2009 | SFE of oil from Safflower seeds | Pressure<br>Temperature<br>Flow rate<br>Particle size | 220 - 280 bar,<br>35 - 60 C,<br>16 – 62 g/min<br>0.35 - 0.85 mm | Z, W, $x_k$ | Influence of process parameters on the extraction yield of oil. | CER period,<br>FER period,<br>TR period. |
| Jia et al., 2009 | SFE of oil from Plumula nelumbinis | Pressure<br>Temperature<br>Particle size | 150 - 450 bar,<br>35 - 65 ºC<br>0.16 - 0.22 mm | Z, W, G | $k_{ya}$,<br>Influence of process parameters on the extraction yield of oil. | CER period,<br>FER period,<br>TR period. |
| Silva et al., 2009 | SFE of oil from Carqueja | Pressure<br>Temperature | 100 - 300 bar,<br>30 - 40 ºC, | NR | Influence of process parameters on the extraction yield of oil. | CER period,<br>FER period,<br>TR period. |

Cont…

| **Author** | **Operation** | **Process Parameter** | **Parametric conditions** | **Tuning parameter** | **Findings** | **Part of OEC** |
|---|---|---|---|---|---|---|
| Mezzomo et al., 2009 | SFE of oil from Almond seeds | NR | NR | NR | NR | FER period, |
| Bensebia et al., 2009 | SFE of oil from Rosemary leaves | Pressure<br>Temperature<br>Flow rate<br>Particle size<br>Co-solvent % | 100 - 180 bar,<br>40 - 60 ºC,<br>1 - 5 g/min,<br>150 - 436.8 µm<br>3 % | $k_{xa}$, $k_{ya}$, $x_k$ | Influence of process parameters on the extraction yield of oil. | CER period, |
| Kitzberger et al., 2009 | SFE of oil from Shiitake | Pressure<br>Temperature<br>Flow rate | 150 - 350 bar,<br>30 - 50 ºC,<br>3.33 - 6.67 g/min | $k_{xa}$, $k_{ya}$, $x_k$ | Influence of process parameters on the extraction yield of oil. | CER period,<br>FER period,<br>TR period. |
| Bernardo-Gil et al., 2009 | SFE of oils from fig leaf gourd | Pressure<br>Temper | 180 - 200 bar,<br>35 - 45 ºC | $k_{xa}$, $k_{ya}$, $x_p$ | Extraction efficiency.<br>Influence of process parameters on the extraction yield of oil. | CER period,<br>FER period,<br>TR period. |
| Pederssetti et al., 2011 | SFE of oil from Canola seeds | Pressure<br>Temperature | 200 - 250 bar,<br>40 - 60 ºC | Z, W, $x_p$ | Z, W, $x_p$,<br>Influence of process parameters on the extraction yield and composition of the oil. | CER period,<br>FER period,<br>TR period. |
| Hegel et al., 2011 | SFE of lipids from yeast | Pressure<br>Temperature<br>Co-solvent % | 200 bar,<br>40 ºC,<br>9 % | $k_{xa}$ | $k_{xa}$ | CER period,<br>FER period,<br>TR period. |

Cont…

| Author | Operation | Process Parameter | Parametric conditions | Tuning parameter | Findings | Part of OEC |
|---|---|---|---|---|---|---|
| Huang et al., 2011b | SFE of oil from Baizhu | Pressure<br>Temperature<br>Flow rate<br>Extraction time | 150 - 450 bar,<br>40 - 60 ºC<br>0.167 - 0.675 mm,<br>180 min | $k_{xa}$, $k_{ya}$, | Influence of process parameters on the extraction yield and composition of the oil. | CER period,<br>FER period,<br>TR period. |
| Martin et al., 2011 | SFE of oil from Persea indica | Pressure,<br>Plant material<br>Particle size,<br>Temperature,<br>Flow rate | 100 - 200 bar,<br>40 - 50 ºC<br>0.56 mm,<br>13 - 24 g/min | $k_{xa}$, $k_{ya}$, | Influence of process parameters on the extraction yield and composition of the oil. | CER period,<br>FER period, |
| Jokic et al., 2012 | SFE of oil from Soybean | Pressure<br>Temperature<br>Flow rate<br>Particle size | 300 - 500 bar,<br>40 - 60 ºC,<br>3.23 – 7.26 g/min,<br>0.238 - 1.059 mm | $k_{xa}$, $k_{ya}$, | Influence of process parameters on the extraction yield of oil. | CER period,<br>FER period,<br>TR period. |
| Rebolleda et al., 2012 | SFE of oil from Corn germ | Pressure<br>Temperature<br>Flow rate | 210 - 450 bar,<br>35 - 86 ºC,<br>67 – 183 g/min | | Influence of process parameters on the extraction rate. | CER period,<br>FER period,<br>TR period. |
| Wagner et al., 2013 | SFE of oil from Potato chips | Pressure<br>Temperature<br>Flow rate | 276 - 414 bar,<br>35 - 80 C,<br>0.5 - 5 g/min | Z,<br>W | Influence of process parameters on the extraction yield of oil.<br>Kinetic parameters were determined. | CER period,<br>FER period,<br>TR period. |
| Taher et al., 2014 | SFE of lipids from Scenedesmus sp. Microalgae | Pressure<br>Temperature<br>Flow rate | 200- 500 bar ,<br>35 - 65 ºC,<br>2 - 4 ml/min | Z,<br>W,<br>$x_k$ | $k_{xa}$, $k_{ya}$,<br>Influence of process parameters on the MTC and extraction rate. | CER period,<br>FER period,<br>TR period. |

Cont…

| Author | Operation | Process Parameter | Parametric conditions | Tuning parameter | Findings | Part of OEC |
|---|---|---|---|---|---|---|
| Fiori et al., 2014 | SFE of oil from grape cultivers | Six grape cultivars | NR | G, $k_{sap}$ | $k_{xa}$, Predicted extraction yield in six grape cultivars. | CER period, FER period, TR period. |
| Sodeifian et al., 2016b | SFE of oil from Pistacia khinjuk | Pressure<br>Temperature<br>Flow rate<br>Extraction time | 120 - 240 bar,<br>35 - 55 ºC,<br>2 - 6 g/min,<br>0 - 300 min | $k_{xa}$, $k_{ya}$, $x_k$ | Studied the SC-$CO_2$ extraction behavior. Oil yield predicted. | CER period, FER period, TR period. |
| Rai et al., 2016b | SFE of oil from Sunflower seeds | Pressure<br>Temperature<br>Flow rate<br>Particle size<br>Co-solvent % | 200 - 400 bar,<br>60 - 100 ºC,<br>5 - 15 g/min,<br>0.5 - 1.0 mm,<br>0 - 10 % | Z, W, $x_k$ | $k_{xa}$, $k_{ya}$ Influence of process parameters on the extraction yield of oil. | CER period, FER period, TR period. |

Table 2.18. Effects of selected parameters on the extraction yield based on Sovova model.

| Author | Operation | Process Parameter | | | | |
|---|---|---|---|---|---|---|
| | | T | P | PS | FR | CoS % |
| Roy et al., 1994 | SFE of tomato seeds | | | ↓ | ↑ | |
| Mira et al., 1996 | SFE of orange peel | | ↑ | ↓ | ↑ | |
| Marrone et al., 1998 | SFE of almond seeds | | | ↓ | ↑ | |
| de França et al., 1999 | SFE of buriti fruit | | ↑ | | ↑ | |
| Mira et al., 1999 | SFE of orange peel | ↓↑ | ↑ | ↓ | ↓ | |
| Papamichail et al., 2000 | SFE of celery seeds | ↓ | ↑ | ↓ | ↑ | |
| Povh et al., 2001 | SFE of chamomile flowers | ↑ | ↑ | | ↑ | |
| Kiriamiti et al., 2001 | SFE of sunflower seeds | ↑ | | ↓ | ↑ | |
| Ferreira et al., 2002 | SFE of Black pepper seeds | ↑ | ↑ | | | |
| Martínez et al., 2003 | SFE of Ginger | ↑↓ | ↑ | | | |
| Campos et al., 2005 | SFE of Marigold flower | ↑ | ↑ | | | |
| Perakis et al., 2005 | SFE of Black pepper seeds | ↓ | ↑ | | ↑ | |
| Vargas et al., 2006 | SFE of Baccharis trimera leaves | ↑ | | | | |
| Bernardo-Gill and Casquilho, 2007 | SFE of Hazelnut and Walnut | ↑ | ↑ | | | |
| Nagy and Simandi, 2008 | SFE of Paprika | | | ↓ | | |
| Han et al., 2009 | SFE of Safflower seeds | ↓ | ↑ | ↓ | ↑ | |
| Jia et al., 2009 | SFE of Plumula nelumbinis | ↑ | ↑ | ↑ | | |
| Silva et al., 2009 | SFE of Carqueja | ↑ | ↑ | | | |
| Bensebia et al., 2009 | SFE of Rosemary leaves | ↑ | ↑ | ↓ | ↑ | ↑ |
| Kitzberger et al., 2009 | SFE of Shiitake | ↑ | ↑ | | ↑ | |
| Bernardo-Gil et al., 2009 | SFE of fig leaf gourd | ↑ | ↑ | | | |
| Pederssetti et al., 2011 | SFE of Canola seeds | ↓ | ↑ | | | |
| Huang et al., 2011b | SFE of Baizhu | ↑ | ↑ | ↓↑ | | |
| Jokic et al., 2012 | SFE of Soybean | ↑ | ↑ | ↓ | ↑ | |
| Rebolleda et al., 2012 | SFE of Corn germ | ↑ | ↑ | | ↑ | |
| Wagner et al., 2013 | SFE of Potato chips | ↑ | ↑ | | ↑ | |
| Taher et al., 2014 | SFE of microalgae | ↑ | ↑ | | ↓ | |
| Sodeifian et al., 2016b | SFE of Pistacia khinjuk | ↓ | ↑ | | ↑ | |
| Rai et al., 2016b | SFE of Sunflower seeds | ↑ | ↑ | ↓ | ↑ | ↑ |

### 2.12.2 Reverchon model (Reverchon, 1996) for SFE process

The differential mass balance for the solute in the solvent and solid phases has already been established by assuming different approaches as described by Bulley et al., 1984 and Schaeffer et al., 1989 in their work. These mass balances are coupled with an equilibrium relationship to evaluate the mass transfer coefficients of the extraction process. However, this approach can be adopted when solubility equilibria or external diffusion are the limiting stages. Reverchon, 1996 incorporated the influence of geometrical parameter during the solution of the mass balances equation, which were

established for the SFE of sage leaves. However, the detail explanation of the model (Reverchon, 1996) is shown in section 4.2 of Chapter 4. Some researchers (e.g. Pfaf-Sovljanski et al., 2005; Vargas et al., 2006; and Rai et al., 2014) have applied this model during the SFE of Hop, Baccharis trimera and Sage leaves respectively as shown in Table 2.19. A final comparison, based on the findings from the literature on Sovova and Reverchon model has also been incorporated in the form of Table 2.20.

Table 2.19. Applications of Reverchon model for different materials used during SFE.

| Author | SFE process | Process parameters | Finding |
|---|---|---|---|
| Pfaf-Sovljanski et al., 2005 | SFE of Hop of magnum cultivar | 150 – 300 bar, 40 °C | Compared the behavior of OEC with empirical model |
| Vargas et al., 2006 | SFE of Baccharis trimera leaves | 90 bar, 40 – 70 °C | Compared the behavior of OEC with Sovova model |
| Rai et al., 2014 | SFE of Sage leaves | 90 bar, 50 °C | Validated the Reverchon model and solved it using FAMLAB software. |

Table 2.20. A comparison between Sovova and Reverchon model based on the findings from the literature.

| Sovova model | Reverchon model |
|---|---|
| 1. Three differential equations represents the three sections of the whole extraction curve during the SFE of natural seed oils. Therefore, it represents the physical phenomena in a better way. | 1. Single partial differential equation represents the whole extraction curve during the SFE natural seed oils. |
| 2. Three phenomena of extraction (e.g. convection, convection plus diffusion and diffusion only) have been taken in to account during the formulation of SFE of seed oils. | 2. Single phenomenon of extraction (e.g. diffusion only) has been taken into account during the SFE of natural seed oils. |
| 3. Division of whole extraction curve is purely based on the time duration that is taken by each extraction phenomenon (as mentioned in point 2). | 3. No division of extraction curve because an average diffusivity has been used during the each experimental run. |
| 4. Since, the SFE of seed oil is purely described by three phenomenon (as mentioned in point 2) therefore solid and solvent phases mass transfer coefficients play a crucial role in it. | 4. Since, the SFE of seed oil is purely described by a single phenomenon (as mentioned in point 2) therefore only solid phases mass transfer resistance plays a crucial role in extraction. |
| 5. More realistic based on the formulation of the model. | 5. Not realistic because of the model formulation. |
| 6. Spherical geometry of particles has been considered. | 6. Spherical geometry of particles has been considered but best fitting with slab geometry has been reported in literature. |
| 7. High possibility for predicting the maximum extraction yield of seed oils due to the involvement of multiple mass transfer phenomenon that actually takes place in reality. | 7. Low possibility of predicting the maximum extraction yield of seed oils due to the involvement of only single mass transfer phenomenon. |

# EXPERIMENTAL SETUP AND EXPERIMENTAL PROGRAM

## 3.1 Process flow diagram of the SFE unit

A schematic process flow diagram (PFD) of the experimental setup of the supercritical fluid extraction (SFE) unit is shown in Fig 3.1. Liquid $CO_2$ is stored in a long-standing cylinder (a) and is passed through a micro filter (b) which filters the $CO_2$ by entrapping the dust or other particles before getting into the piping system and maintains its purity. Then the filtered $CO_2$ is chilled down below 5 °C by passing it through cooling heat exchanger (c) in which chilled water is supplied by a chiller (d), which uses water from a water bath (e). A high pressure reciprocating feed pump (h) is used to attain the critical pressure of the chilled $CO_2$ and then transfers it to a mixer (i) where, there is provision to add organic co-solvent (in our case it is 'Ethanol') through a co-solvent pump (j) from a co-solvent bottle (k). Then this co-solvent added $CO_2$ passes through a heat exchanger (l), which preheats the fluid mixture ($CO_2$ + Ethanol) to attain the critical temperature, before entering into the extractor (m). The critical temperature was maintained by supplying heat through electrically heated jacket attached to the extractor (m). The pressure gauge and temperature sensor attached to the extractor (m) display online readings of temperature and pressure. The extractor's pressure is controlled by an automated back-pressure-regulator (ABPR) (o). Separation of oil from the SC-$CO_2$ occurs in cyclone separators (p1 and p2) and then oil is collected from the bottom to sampler flasks (u1 and u2) by operating drain valves (s1 and s2) while venting out the $CO_2$ in the atmosphere. The most of the quantity of the extracted oil is obtained from the cyclone separator (p1) only due to its higher operating pressure, which is brought down to atmospheric pressure during separation of oil. This causes rapid decrease in solubility of oil and maximum separation of oil takes place.

The co-solvent (Ethanol) is removed from the extracted oil by vacuum effect-rotary evaporator and then after bringing the oil to room temperature, the weight of oil is measured gravimetrically. The total, cumulative extraction yield (CEY) was then determined from the sum of all oil samples extracted. The same procedure was adopted for all experiments. A photographic view of experimental setup of the SFE unit is shown in Fig. E.1.

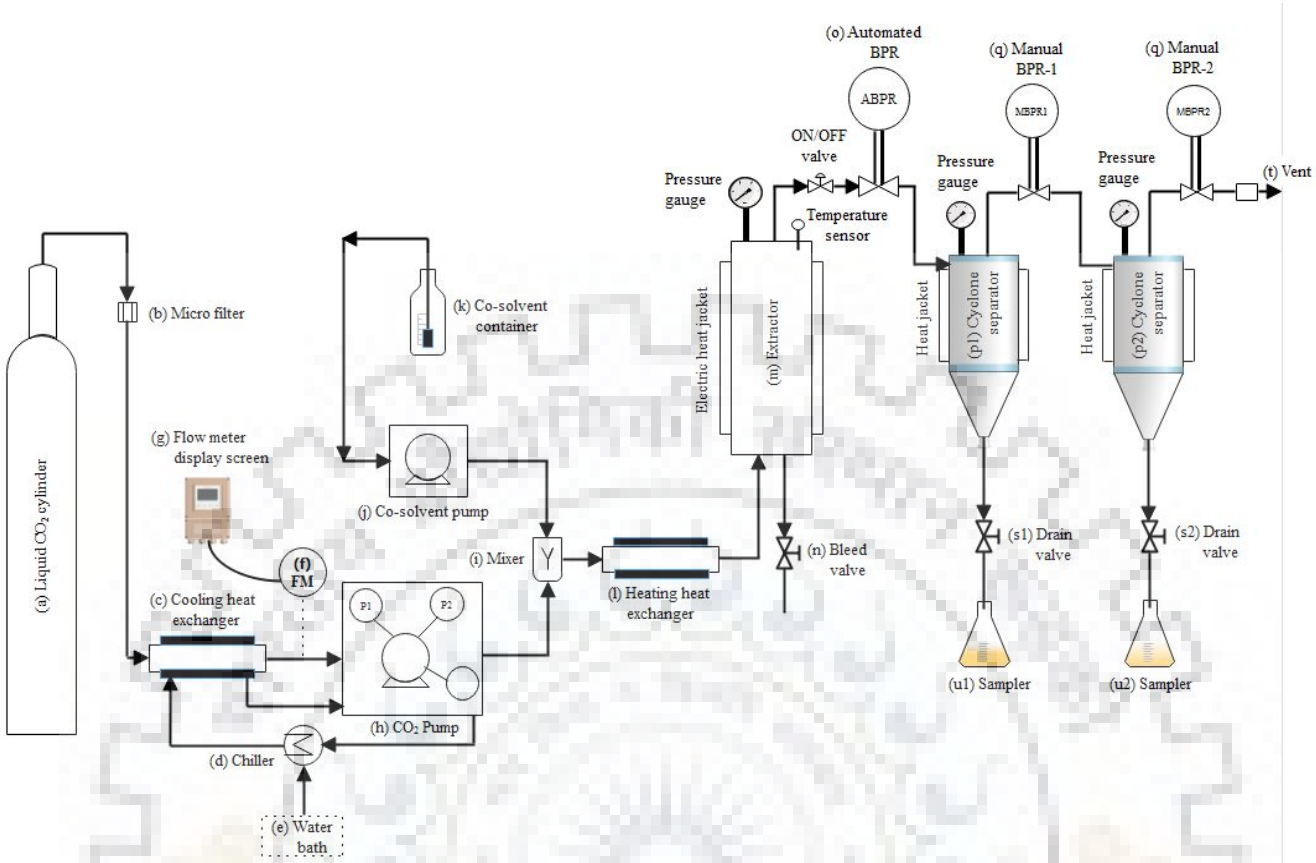


Fig. 3.1: A schematic PFD of the experimental setup of the SFE unit.

## 3.2 Software based control of the SFE unit

The operation of SFE unit, is performed using a software, called Process Suit which has already been installed in the computer system (as shown in Fig. E.1). Fig 3.2, demonstrates the first time screen shot after the start of the Process-Suit through which the setting of operating parameters (e.g. temperature, pressure, flow rate-$CO_2$ and co-solvent flow rate) is done either by direct clicking on the respective equipment or by selecting the respective component from the view list of the window screen. Four parameters (e.g. temperature, pressure, flow rate-$CO_2$ and flow rate of co-solvent) out of five parameters (excepting particle size) were set through Process-Suit software. The settings of these four components are done as follows:

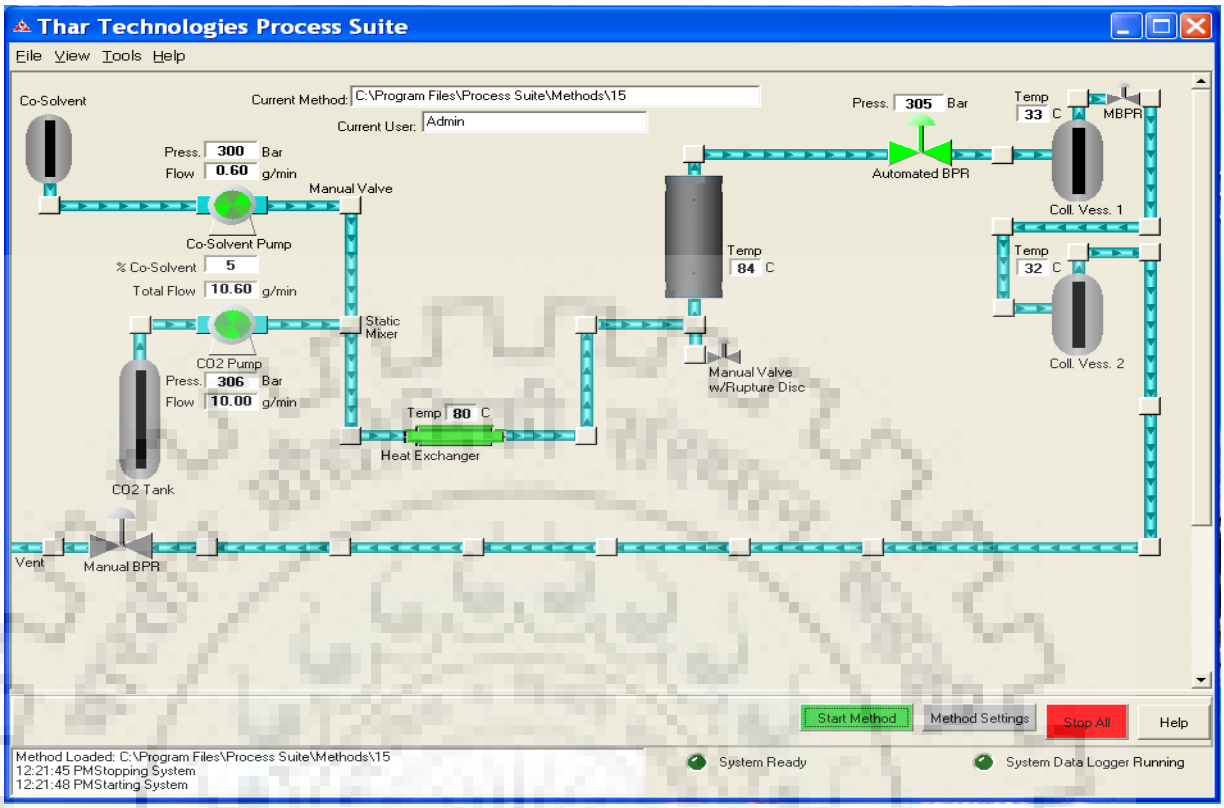


Fig. 3.2: First window appearance of the software 'Process-Suit'.

***Temperature settings:***

The setting of temperature for all zones as shown in Fig 3.3, is done as per the requirement of the experimental run. Zone 1 contains the 'Electrically Heated Heat Exchanger (HE2)' (shown in PFD as 'heating heat exchanger') which is used to increase the temperature of modified $CO_2$ up to its critical temperature. Zone 2 contains the 'Vessel 1 Heater (V1-TS2)' (shown in PFD as 'electric heat jacket'), used to maintain the operating temperature of the solvent (in our case it is SC-$CO_2$). Zone 3 contains the 'Vessel 1 Internal Temperature Sensor (V1-TS2)' (shown in PFD as a 'temperature sensor'), used to report the online temperature inside the extractor. Zone 4 contains the 'Collection Vessel 1 Heater (CS1-TS1)' (shown in PFD as 'heat jacket'), used to maintain the desired temperature of the sample which is coming out the cyclone separator (p1) while the zone 4 contains the 'Collection Vessel 2 Heater (CS2-TS1)' (shown in PFD as 'heat jacket'), used for the same purpose as 'Collection Vessel 1 Heater (CS1-TS1)'. Finally, the zone 5, which shows the status as 'None' in the software, meaning that there is no provision in the experimental set-up for Zone-5.

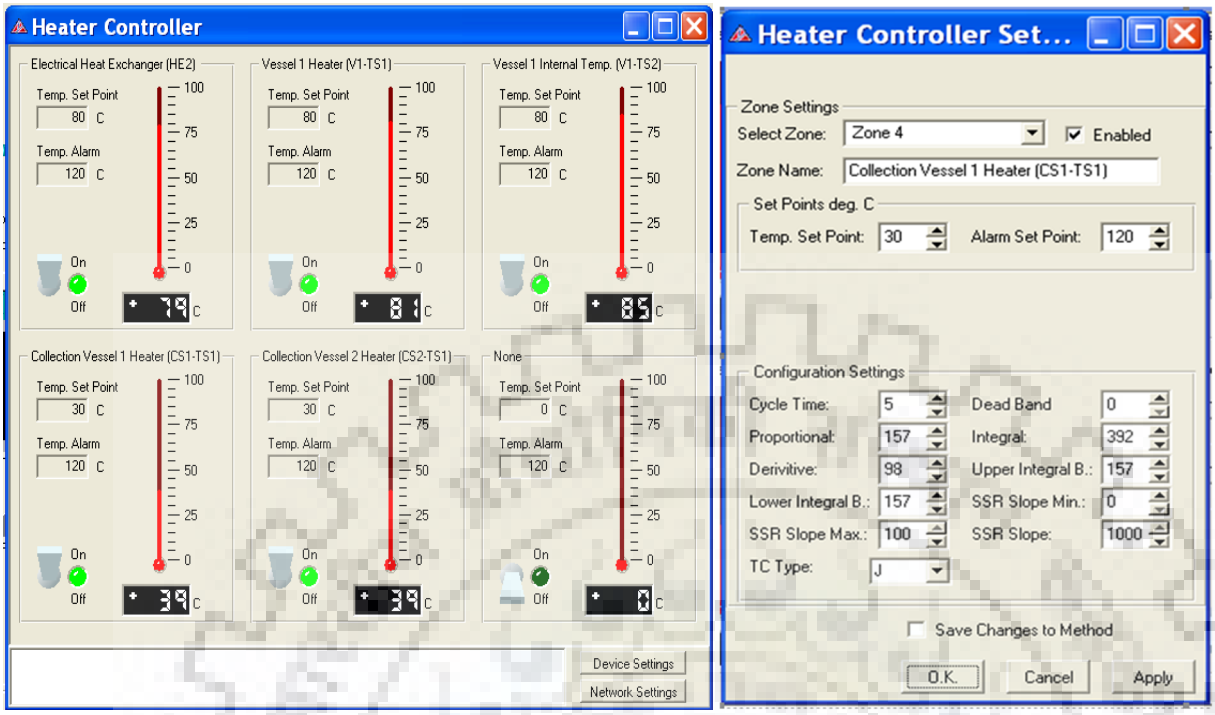


Fig. 3.3: Temperature setting window through the software 'Process-Suit'.

***Pressure settings:***

The pressure requirement (e.g. operating pressure of the solvent) for the extraction is achieved by a high pressure reciprocating pump (as shown in Fig. 3.1). The pressure setting window (as shown in Fig. 3.4) is used to set the pressure according to the requirement of the SFE process. This pressure-setting window is actually for the automated back-pressure regulator (ABPR), installed in the outlet line of the extractor, which controls and maintains the desired operating pressure by controlling the back pressure. The desired pressure is set as 'pressure set point' (e.g. 300 bar) which starts increasing as soon as the high pressure pump is started. The online increment in the pressure can be seen on the pressure regulator window (Fig. 3.4). By default the 'pressure alarm' has already been set at '640 bar' while the valve' needle position fluctuates automatically to adjust the pressure increment.

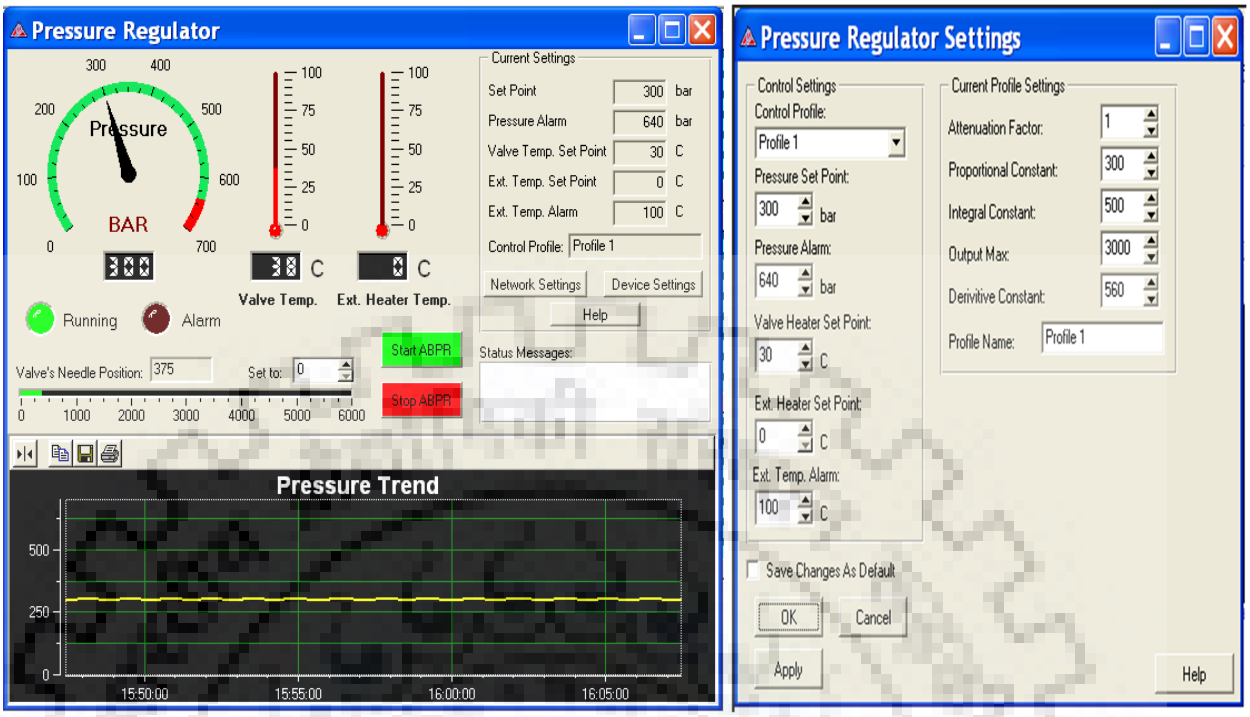


Fig. 3.4: Pressure setting window through the software 'Process-Suit'.

***Flow rate-$CO_2$ setting:***

The setting of $CO_2$- flow rate, as per the requirement, is performed using the software 'Process-Suit' as shown in Fig. 3.5. The desired value of $CO_2$- flow rate is entered as 'set point' (e.g. 10 g/min). The actual value of $CO_2$- flow rate starts increasing with starting the $CO_2$ pump, until it achieves the set value. The online trend of $CO_2$- flow rate can be seen on the pump window (as shown in Fig. 3.5). The pump's revolution per minute (RPM) is also displayed on the window for safety point of view. For example; in case of $CO_2$ shortage in the cylinders, the RPM of the $CO_2$ pump starts increasing to compensate the requirement of the $CO_2$ for the pump and these increased RPM may cause a damage to the pump. The $CO_2$ pump also stops working in case of when pressure reaches to an alarming situation.

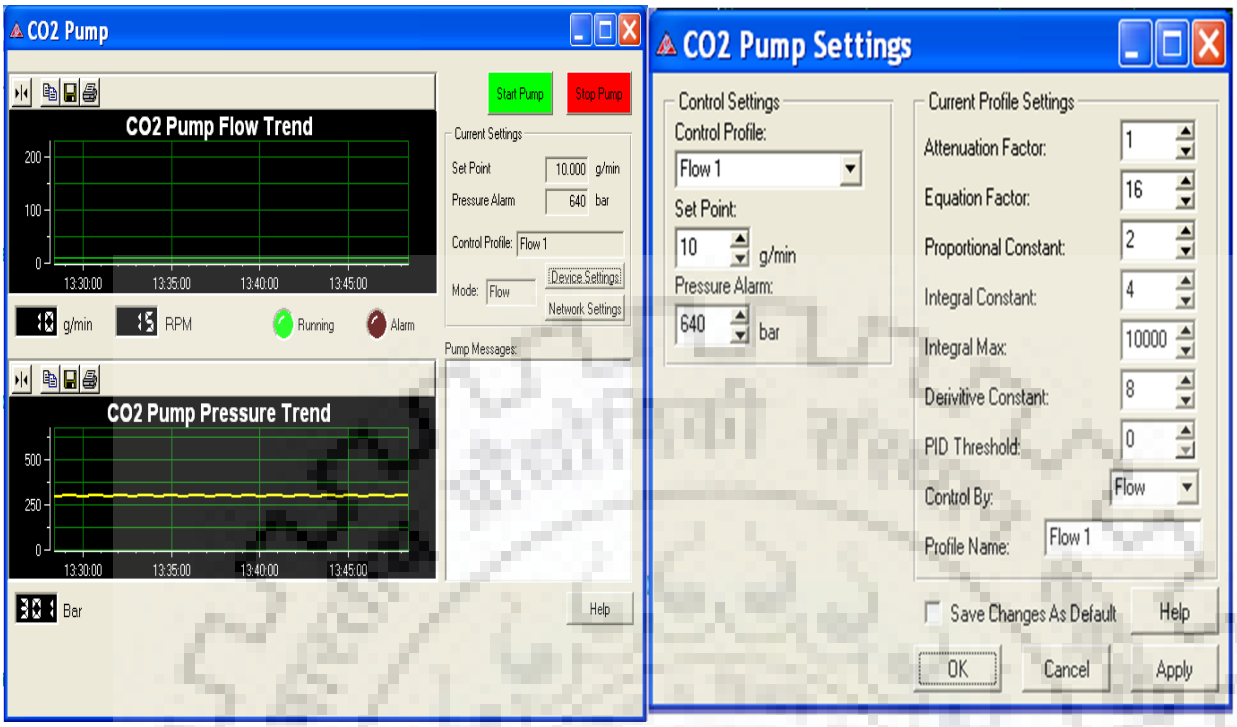


Fig. 3.5: Flow rate-$CO_2$ setting window through the software 'Process-Suit'.

***Co-solvent setting:***

The co-solvent flow rate setting window is shown in Fig. 3.6 through which the required flow rate of co-solvent (in our case it is Ethanol) is entered as a set point (e.g. 10 g/min). The 'Device setting' button is clicked to set the above-mentioned requirement. This window also displays the necessary information such as pressure high alarm and co-solvent pump pressure. The value of pressure high alarm can be set manually according to the requirement. For example, in our case the value of pressure high alarm is '371 bar' for safer side, because the maximum operating pressure in the present study is '350 bar'. The maximum pressure alarm setting value is '640 bar' (as shown in Fig. 3.4). In addition to this, the online trend of co-solvent pressure pump is also displayed so that in any break down (e.g. electrical, malfunctioning etc.) the problem could be identified easily and the corrective actions can be taken accordingly.

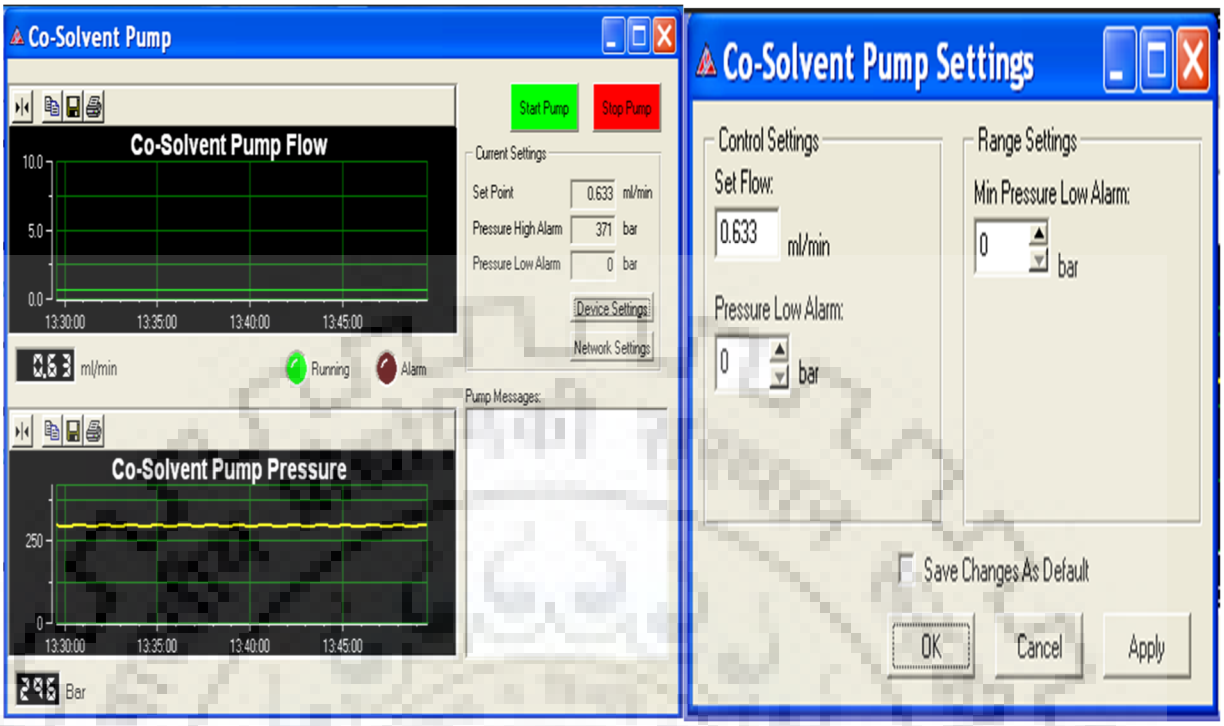


Fig. 3.6: Co-solvent flow-rate setting window through the software 'Process-Suit'.

## 3.3 Limitations of experimental set-up and trouble shootings

The experimental set-up (as shown in Fig. 3.1) consists of three main equipments (e.g. high pressure $CO_2$ pump, co-solvent pump and mass flow meter). These equipments have some technical limitations, which make them prone to experimental break down. The limitations, specifications and the trouble shootings of each above-mentioned equipment are discussed below:

***High pressure $CO_2$ pump:***

The Thar technologies Inc., P-series pump is a high pressure pump which incorporates a low dead volume head and check valves (lower and upper check valves) to provide efficient pumping of $CO_2$ and many solvents (e.g. cabon dioxide, methanol, ethanol, isopropyl alcohol, acetonitrile, methylene chloride and chloroform). This high-pressure pump consists of two pistons, which provide a pulse free delivery of solvent ($CO_2$). As the piston moves, back to refill the chamber the lower check valve opens to allow the fluid to flow into the chamber and the upper check valve closes to seal the system fluid from entering the chamber. When piston completes its fill-up cycle, it will begin to move forward causing the lower check valve to close. When the pressure in the piston

chamber exceeds the system pressure, the upper check valve opens and allows the fluid to flow into the system. Table 3.1, shows the limitations and specifications of high pressure $CO_2$ pump (as shown in Fig. 3.1) while the Table 3.2 illustrate the trouble shootings and its operation.

Table 3.1. Limitations and specifications of high-pressure $CO_2$ pump.

| **Parameters** | **Operating range** |
|---|---|
| Ambient operating temperature: | 5 - 45 °C |
| Humidity: | < 95 % non-condensing (5 – 40 °C) |
| Typical current draw (550 bar/200 RPM) | 4A@120VAC, 4A@220VAC |
| Inrush current: | <20A@120VAC, <20A@220VAC |
| Operating temperature: | 5 - 40 °C |
| Pressure rating: | 689 bar/10000 psi |
| Maximum operating pressure: | 600 bar |
| Minimum operating pressure (inlet): | 1 bar |
| Maximum flow rate: | 200 g/min |
| Minimum flow rate: | 3 g/min |

Table 3.2. Trouble shootings during the operation of high-pressure $CO_2$ pump.

| Symptom | Problem | Corrective action |
|---|---|---|
| ▪ Unable to achieve pressure.<br>▪ Unable to achieve flow rate. | a. PID values.<br>b. Low $CO_2$ supply.<br>c. Inadequate cooling.<br>d. $CO_2$ supply does not contain a dip tube.<br>e. Defective check valve.<br>f. Leaking piston seal.<br>g. Leaks in system. | a. Review /modify PID values on PC or pump.<br>b. Replace $CO_2$ supply tank.<br>c. Make sure bath temperature between -5 °C and +5 °C, check cooling lines to pump heads and heat exchanger, check fluid level.<br>d. Contact $CO_2$ supplier, replace the tank.<br>e. Replace check valve.<br>f. Replace piston seal.<br>g. Correct leaks. |
| ▪ High pressure overshoots/under | a. PID values. | a. Review/modify PID values on PC or pump. |
| ▪ Blows rupture disc. | a. Outlet valve closed.<br>b. Defective pressure transducer.<br>c. Defective/incorrect rupture disc. | a. Open outlet valve.<br>b. Replace pressure transducer, recalibrate unit.<br>c. Replace rupture disc. |
| ▪ Pressure readings on display does not match gauge. | a. Defective gauge.<br>b. Defective pressure transducer.<br>c. Mis-calibrated pressure transducer. | a. Replace gauge.<br>b. Replace pressure transducer, recalibrate unit.<br>c. Recalibrate unit. |
| ▪ Pressure reading on display does not match other system components. | a. Restriction in lines –closed valves<br>b. Defective pressure transducer<br>c. Mis-calibrated pressure transducer | a. Make sure valves are in proper position, check for proper tubing sizes and properly cut tubing, check valve alignments.<br>b. Replace pressure transducer, recalibrate unit.<br>c. Recalibrate the unit. |
| ▪ Repeated failures of check valves | a. Contamination in $CO_2$<br>b. Teflon particles in lines.<br>c. Dirt particles in lines. | a. Contact $CO_2$ supplier.<br>b. Check for proper application of Teflon tape on fittings, check seal between tank and supply line fitting, check flow meter seals<br>c. Clean the lines specially after any maintenance works in lines. |
| ▪ Erratic flow readings. | a. Flow being measured below the meters usable level. | a. Adjust the threshold level. |

***Co-solvent pump:l***

This pump comes under the category of the Series-3 high performance liquid chromatography (HPLC) pump and known as a metering pump when used for general laboratory and industrial use. The pump consists of two phases, the pumping phase and the refill phase. During the pumping phase, the pump piston moves at a constant linear speed, driven by a specially shaped cam, which is in turn driven by the motor using a toothed-belt drive. This results a constant, stable flow from the pump at high pressure. At the end of the pumping phase, the pump enters the refill phase. The cam is shaped so that the piston quickly retracts, refilling the pump head with solvent. The piston then moves forward again as the pumping phase begins. Since, the output flow completely stops during refill, a pulse damper is necessary to provide some of the lost flow. In addition, the motor speed is adjusted by the microprocessor to facilitate an efficient refill phase. This type of pumps are available with the standard 10 mL pump head and 40 mL pump head that can be set in 0.01 mL increments from 0.0 to 10 mL/min or 40 mL/min.

Table 3.3, shows the limitations and specifications of this co-solvent pump (as shown in Fig. 3.1) while the Table 3.4 illustrate the trouble shootings and its operation.

Table 3.3. Limitations and specifications of co-solvent pump.

| **Parameters** | **Operating range** |
|---|---|
| Flow rates: | 0.0 to 10 mL/min for 10 mL/min heads<br>0.0 to 40 mL/min for 40 mL/min heads |
| Pressure: | 0 to 6000 psi for 10 mL/min SS pump heads,<br>0 to 5000 psi for 10 mL/min PEEK heads,<br>0 to 1500 psi for 40 mL/min pump heads |
| Pressure accuracy: | ±1 % of full-scale pressure |
| Pressure zero offset: | ± 2 psi |
| Flow accuracy: | ±2 % for a flow rate of 0.20 mL/min and above for 10 mL/min heads<br>±2% for 0.1 to 40 mL/min for 40 mL/min head |
| Flow precision: | 0.2 % RSD |
| Power: | 100 – 240 VAC, 50-60 Hz, 45W (The main voltage supply shall not exceed ±10%) |
| Temperature: | 10 to 30 °C |
| Humidity: | 20 to 90% Relative humidity |

Table 3.4. Trouble shootings during the operation of co-solvent pump.

| Symptom | Problem | Corrective action |
|---|---|---|
| ▪ Uneven pressure trace.<br>▪ Pressure drops.<br>▪ Pump shuts OFF.<br>▪ No flow out the outlet check valve. | a. Solvent not properly degassed.<br>b. Fittings are not tight.<br>c. Mobile phase not properly filtered.<br>d. Particles from worn piston seal caught in check valve.<br>e. Plugged inlet filter. | a. Check to be certain that mobile phase is properly degassed.<br>b. Check connections for leaks by tightening fittings.<br>c. Prime the system directly from the outlet check valve.<br>d. Clean or replace the check valves.<br>e. Replace inlet filter. |
| ▪ Fluid between the pump head and the chassis | a. Long usage time since last seal change.<br>b. Salt deposits on seal. | a. Replace piston seal.<br>b. Check the piston for salt deposits and clean as necessary. |
| ▪ Pump makes a loud clanging or slapping noise (intermittent contact with cam). | a. Cap nut screws on the pump head are loose.<br>b. Seal(s) are worn.<br>c. Piston guide is worn.<br>d. Salt build-up on piston carrier from use of buffers.<br>e. Excess lubricant on piston carrier. | a. Check cap nut screws on pump head. Tighten if necessary.<br>b. Replace seals.<br>c. Replace seal backup washer and seal.<br>d. Consider changing to a self-flushing pump head if using buffers.<br>e. Clean excess lubricant and dirt off piston carrier. |
| ▪ Blue dye in mobile phase. | a. Sudden pressure drop when purging system. | a. Replace pulse damper. |
| ▪ Pump runs for 50 pump strokes and then shuts down. | a. Mobile phase is not properly filtered.<br>b. Particles from worn seal trapped in the system (e.g. tubing, filters, injection valve, column inlet). | a. Check to be certain the low-pressure limit is set to 0 psi.<br>b. Only increase the low-pressure limit after the pump attains operating pressure. |
| ▪ No power when pump turned ON. Fan does not run.<br>▪ Front panel appears OK but pump motor does not run. | a. Power surge<br>b. Internal short. | a. Replace only with the appropriate fuses 1A 250Vac.<br>b. Contact service technician if problem persists. |
| ▪ PEEK fittings or components leak. | a. Film of fluid between surfaces.<br>b. Salt crystals between surfaces.<br>c. Scratches in mating surfaces. | a. Clean and dry mating surfaces.<br>b. If scratched, replace defective part. |
| ▪ Self-flush heads leak flush solution. | a. Large (size 016) O-ring is flattened and now longer seals.<br>b. Head not sufficiently tightened.<br>c. Scratches in mating surfaces.<br>d. Leaky self-flush seal. | a. Replace O-ring.<br>b. Tightened head.<br>c. Replace leaky parts. |

***Mass flow meter:***

The mass flow meter (MASS 6000, SITRANS F C MASSFLOW), measure the flow direct in kilograms, without conversion. This instrument delivers true multi parameter measurements such as mass flow rate, total mass, density, temperature, total volume, volumetric flow rate, fraction flow etc. This instrument has inaccuracy less than ± 0.01% of the measured value, throughout a wide measuring range. Table 3.5, shows the limitations and specifications of this mass flow meter (Mass 6000) (as shown in Fig. 1) while the Table 3.6 illustrate the trouble shootings and its operation.

Table 3.5. Limitations and specifications of mass flow meter (Mass 6000).

| **Parameters** | **Operating range** |
|---|---|
| Measurement of : | Mass flow (kg/s), volume flow (l/s), fraction (%), density (kg/m$^3$), temperature (°C) |
| Current: | 0-20 mA or 4-20 mA |
| Load: | < 800 ohm |
| Time constant | : 0-30 s adjustable |
| Totalizer: | Two eight –digit counters for forward, net or reverse flow |
| Display: | Background illumination with alphanumerical text, 3x20 characters to indicate flow rate, totalized values, settings and faults. |
| Ambient temperature: | - 40 to +70 °C. |
| Power consumption: | 230 VAC |

Table 3.6. Trouble shootings during the operation of mass flow meter.

| Symptom | Problem | Corrective action |
|---|---|---|
| ▪ Empty display | a. Supply voltage<br>b. MASS 6000 defective | a. Check supply voltage.<br>b. Replace MASS 6000. |
| ▪ No flow signal | a. Current output deselected<br>b. Digital output deselected<br>c. Reverse flow direction<br>d. Measuring pipe empty<br>e. Internal error<br>f. No load on current output<br>g. MASS 6000 defective<br>h. Initializing error | a. Activate current output.<br>b. Activate digital output.<br>c. Change direction.<br>d. Ensure that the measuring pipe is full.<br>e. Replace MASS 6000.<br>f. Check cables/connections.<br>g. Replace MASS 6000.<br>h. Switch off MASS 6000 wait 5 s and switch on again. |
| ▪ Indicates flow with no flow in pipe | a. Measuring pipe empty.<br>b. Electrode cable is insufficiently screened. | a. Selected empty pipe limit and ensure that the measuring pipe is full of liquid.<br>b. Ensure that electrode cable is connected and sufficiently screened. |
| ▪ Unstable flow signal | a. Pulsating flow.<br>b. Air bubbles in medium.<br>c. Vibrations.<br>d. Pump noise. | a. Increase time constant.<br>b. Ensure medium does not contain air bubbles.<br>c. Ensure that the sensor is mounted on a rigid frame without vibrations.<br>d. Ensure that pump frequency is different from resonance frequency of sensor. |
| ▪ Measuring error | a. Faulty zero-point<br>b. Loss of internal data.<br>c. Flow exceeds 120% of maximum flow. | a. Make new zero-point adjustment.<br>b. Replace MASS 6000.<br>c. Check maximum flow (basic settings). |
| ▪ Loss of totalizer data | a. Initializing error. | a. Reset totalizer manually. |

## 3.4 Pre-treatment of feed materials

Pre-treatment of natural feed materials (AM and PP seeds) prior to their extraction can strongly influence the efficiency of the process in terms of yield and in certain cases, the content of active substances (Ivanovic et al., 2014). Therefore, proper pre-treatment of raw feed material is essential to enhance the efficiency of the SFE process. As the raw feed materials (AM and PP seeds) have been collected directly from the whole seller of natural products who collected these from the forest area as it is, the pre-treatment such as cleaning, drying, sizing of particles, storage at specific ambient temperature etc., has to be performed properly. Hence, Some specific procedures have been adopted during the pre-treatment of raw feed materials. The PP seeds having 10-20 mm long and light brown in color is obtained from fruit of the *Pongamia pinnata* tree which is ovoid in shape with dimensions 3–6 cm long and 2–3 cm and wide thick walled (Sangwan et al., 2010) while AM seeds are spherical (1.5 to 2.5 mm diameter) in shape with dark brown colour and pitted (Rajvaidhya et al., 2012; Brahmachari et al., 2013).

### 3.4.1 Procurement and cleaning of raw feed materials

The seeds of AM and PP were collected from the authorized supplier of Ayurvedic raw materials (Herbal Automation, Hanumangarhi, Kankhal (geographical coordinates: 29º 55' 48" N, 78º 9' 0" E) near the city of Haridwar located within Uttarakhand, state in India). The unwanted materials such as grass, dry mud, small stones particle etc. were removed during the cleaning of seeds. The figures of tree/plant from which these two seeds were obtained and the cleaned AM and PP seeds are shown below as Fig. 3.7(a, b) and 3.7 (c, d) respectively.

### 3.4.2 Drying of seed materials

The pre-treatment of AM and PP seeds was restricted by the physical appearance and nature of the seeds. Initially, the AM and PP seeds were dried under the sun light for 5-7 days to evaporate the external moisture and then kept in an oven (at 50 °C for 3 hours) before chopping in a domestic grinder (Bajaj, India).

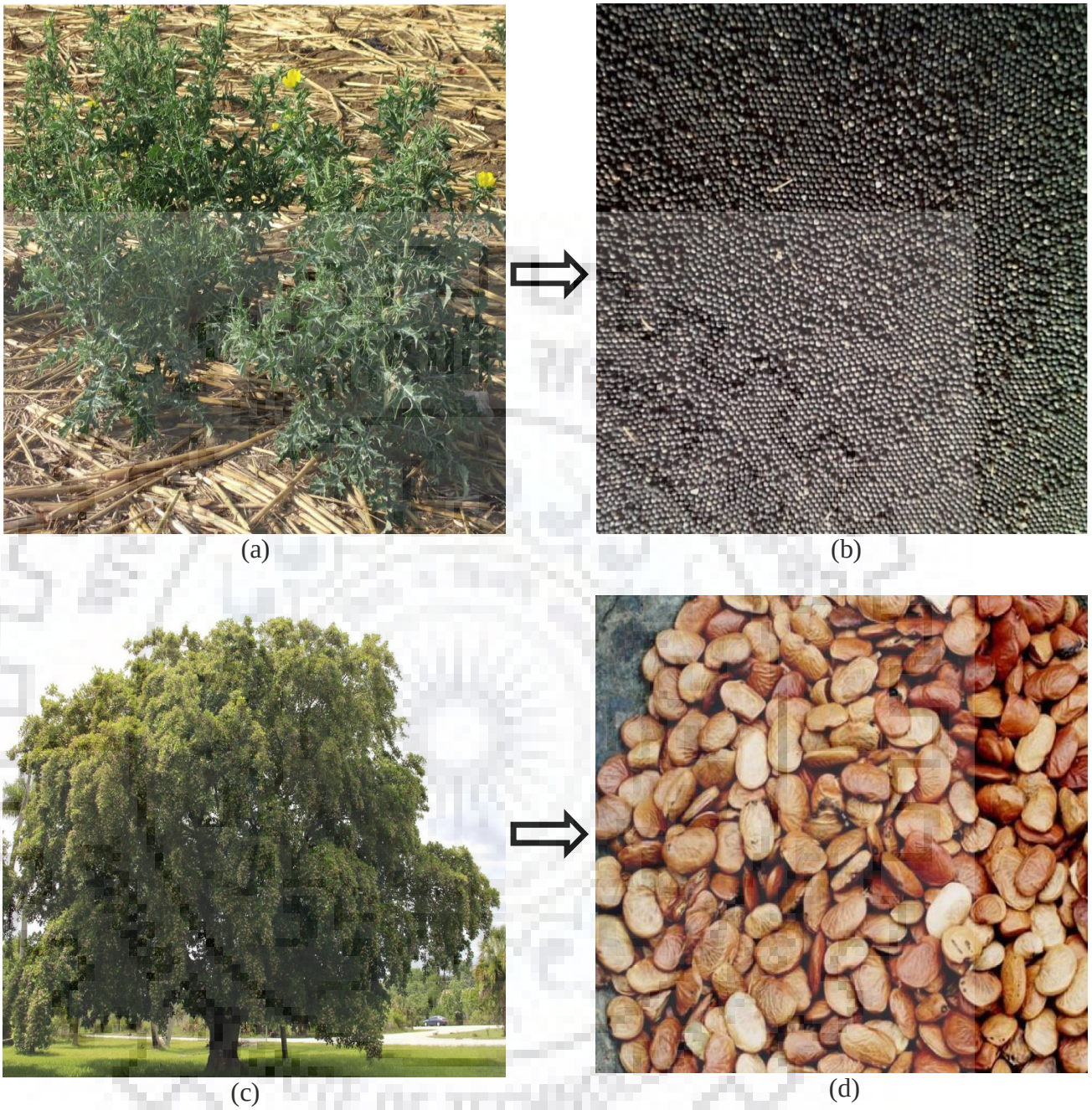

(a) (b)

(c) (d)

Fig. 3.7: Cleaned seeds of (b) AM and (d) PP seeds obtained from their respective (a) plant and (c) tree.

3.4.3 Sizing of raw feed materials

The particles of chopped seeds were screened and graded according to their respective particle sizes by certified test sieves (Endecotts Ltd., London, England) with the help of a vibratory sieve shaker (Octagon 200, Endecotts Ltd., London, England) in three ranges as shown in Table 3.7. Since an exact particle size distribution (particle diameter) is not possible during grinding, therefore, an average particle size was taken as the basis of the range of particle size (mm) as shown in Table 3.7. Three particle sizes (e.g. 1.0 mm, 0.75 mm and 0.5 mm) were obtained through sieving.

Table 3.7. Particle size distribution of seed fractions.

| No. | Range of particle size (mm) (-undersize to +oversize) | Average particle size (mm) |
|---|---|---|
| 1 | '- 1.18 to + 0.850' | ≈ 1.00 |
| 2 | '- 0.850 to + 0.710' | ≈ 0.75 |
| 3 | '- 0.600 to + 0.425' | ≈ 0.50 |

3.4.4 Storage conditions for raw feed materials

The storage conditions of raw feed materials (AM and PP seeds) could be one of the influential factors for the extraction yield of oil and its content of active substance. Therefore, before chopping and sizing of the seeds, the seeds were kept in closed container (excepting the daytime during drying the seeds) so that seeds could not absorb the moisture from the surrounding environment. After chopping and grinding, the seed particles were kept separately in the closed and dark environment at 28 °C for further uses.

3.5 Procurement and quality specification of $CO_2$ used in the process.

Liquid carbon dioxide used in experiments was of 99.9% purity. It was supplied by Sigma gases, India, in pressurized long tube cylinders. Each cylinder contained 32 kg of carbon dioxide, which could be withdrawn in liquid form through a tube within the cylinder. Approximately, 7-8 experimental runs were performed using one cylinder while the experiment time duration for each run was about 5-6 hrs.

## 3.6 Procurement and quality specification of ethanol used in the process

The purpose of adding a small amount of 'Ethanol' as co-solvent into the $CO_2$ and its selection criteria have already been discussed in sections of 2.3.5 and 2.5 under the Chapter 2. In the present study, Ethanol of absolute alcohol grade with 99% purity was purchased from Merck Ltd. (Mumbai, India).

## 3.7 Preparation of extraction bed

The schematic diagram of extraction bed used in the present SFE process as shown in Fig. 3.8. The preparation of fixed bed for extraction consists of glass beads (5 mm dia. and 4 layers of it), glass wools (0.5 cm thickness and 2 layers of it) as packing materials, one thin mesh plate (200 mesh) as a filter media and extractable material (50 g) that was to be extracted. A cylindrical basket made of stainless steel with 17 cm height and 7.5 cm in diameter was used to hold the material (50 g) to be extracted. To fill up the cylindrical basket, glass beads (5 mm dia.) and glass wool were used as an inert and packing material. Initially, the fixed bed consists of glass beads up to 3.0 cm height then a layer of glass wool having a thickness of 0.5 cm then again a layer of 3.0 cm of glass beads over the glass wool. A uniform distribution of SC-$CO_2$ could be possible through this arrangement.

Now, 50 g of seed particles were placed (x cm, height of extractable material varies according to its particle sizes) above the previous arrangement followed by glass beads and glass wool with the same pattern as previously arranged. Finally, at the top of the bed, a thin mesh plate was placed to prevent the flow of solid particles with SC-$CO_2$. It was observed that the height of the bed of particles varied marginally according to the particle size. At the start, the thickness of the layer of feed material was, little bit higher for small particles as compare to larger size particles. Further, after filling the basket with seed particles, glass beads and glass wool then remains some vacant space at the top of the basket.

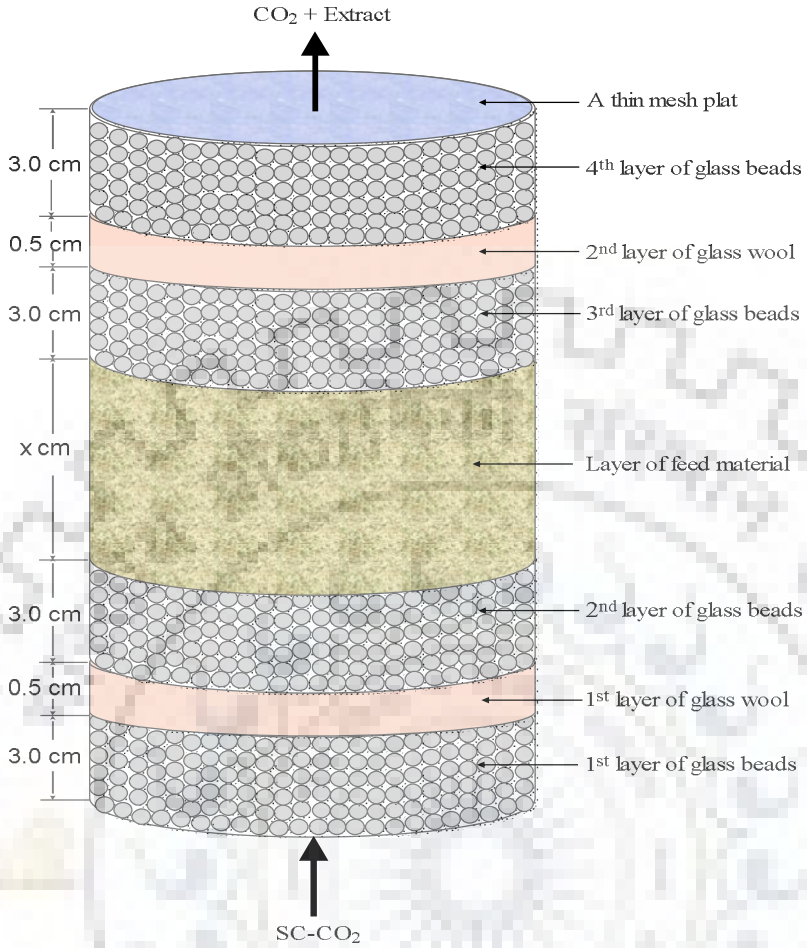


Fig. 3.8: Schematic diagram extraction bed used during SFE process.

Following the above stated procedure, the extraction basket had been prepared and subsequently put into the extraction cell/extractor (as shown in Fig. 3.1). The top of the vessel is closed with the hand-tighten lid. Further, $CO_2$ tubing to the automated backpressure regulator ('ABPR' as shown in Fig. 3.1) is then connected.

## 3.8 Operating parameters for SC-$CO_2$ based SFE and their ranges

A thorough literature review (more than 350 research articles) revealed that a wide range of operating parameters such as pressure (72.4 – 700 bar), temperature (30 – 424 °C), flow rate-$CO_2$ (0.30 - 11 kg/hr), extraction time (10 - 660 min.), particle size ( 0.001 - 2.18mm ) and the % of co-solvent (0.0 - 40%), have been used by various researchers during their SFE process with various natural seed materials. In the present study, temperature (°C), pressure (bar), particle size (mm), flow rate-$CO_2$ (g/min) and the % of co-solvent (% of flow rate-$CO_2$) have been chosen as operating

parameters for the investigation and their influence on the extraction yield. The range of the selected parameters are given in Table 3.8.

Table 3.8. Operating parameters and their range.

| Operating parameters | Temperature (°C) | Pressure (bar) | Particle size (mm) | Flow rate-$CO_2$ (g/min) | % of co-solvent (%) |
|---|---|---|---|---|---|
| Range | 60 | 200 | 0.5 | 5 | 0.0 |
| | 80 | 275 | 0.75 | 10 | 5 |
| | 100 | 350 | 1.0 | 15 | 10 |

3.9 Design of experiments (DoE) for the AM and PP seeds during the SFE process

The design of experiments (DoE), was performed by response surface methodology (RSM) using 'five-factors-three-levels' Box-Behnken design (BBD) which is the most common experimental design in RSM. The following steps were followed during the designing of experiments using the software (Design Expert 10.0).

***Step 1:*** Start the software just by double clicking the icon on desktop of the computer. The window thus appeared is shown in Fig. 3.9.

***Step 2:*** Select 'response surface methodology' under the section of 'standard designs' and then chose the 'box-behnken design' as shown in Fig. 3.10. Here, the parameters (also called as 'Factors' in software) such as temperature, pressure, particle size, flow rate-$CO_2$ and % of co-solvent are entered along with their 'Low' and 'High' values. After inserting, other desired parameters such as category factor (set as '0'), block (set as '0') and center points per block (set as '6') click the 'Next' button.

***Step 3:*** Now, select the output (also called as 'response' in software) which is the cumulative extraction yield (CEY, g oil/g seeds) in this case (as shown in Fig. 3.11). Now, click the 'Next'. This provided a table of design matrix of experiments (Table 3.9) which consist of a total 46 numbers of experimental runs (40 at IB factorial and 6 at center points) that need to be performed to get 46 experimental outputs/responses.

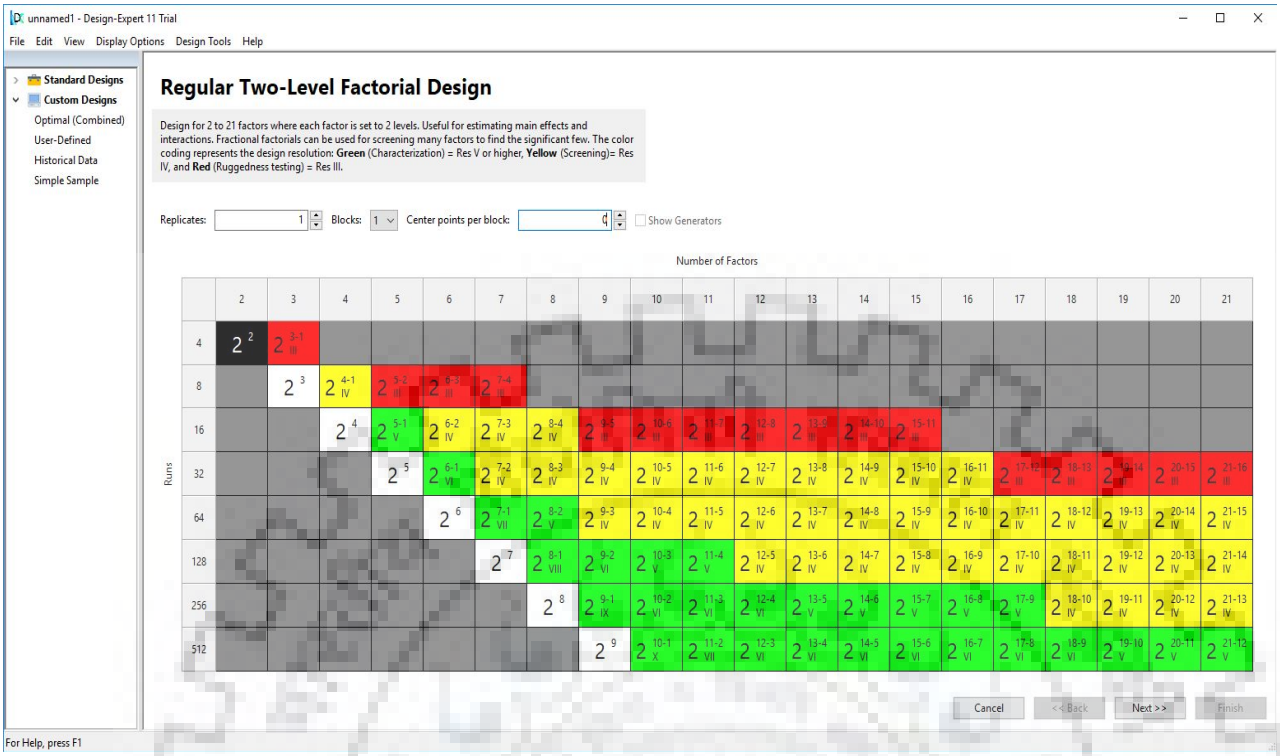


Fig. 3.9: First appearance of double click of the software 'Design Expert' during DoE.

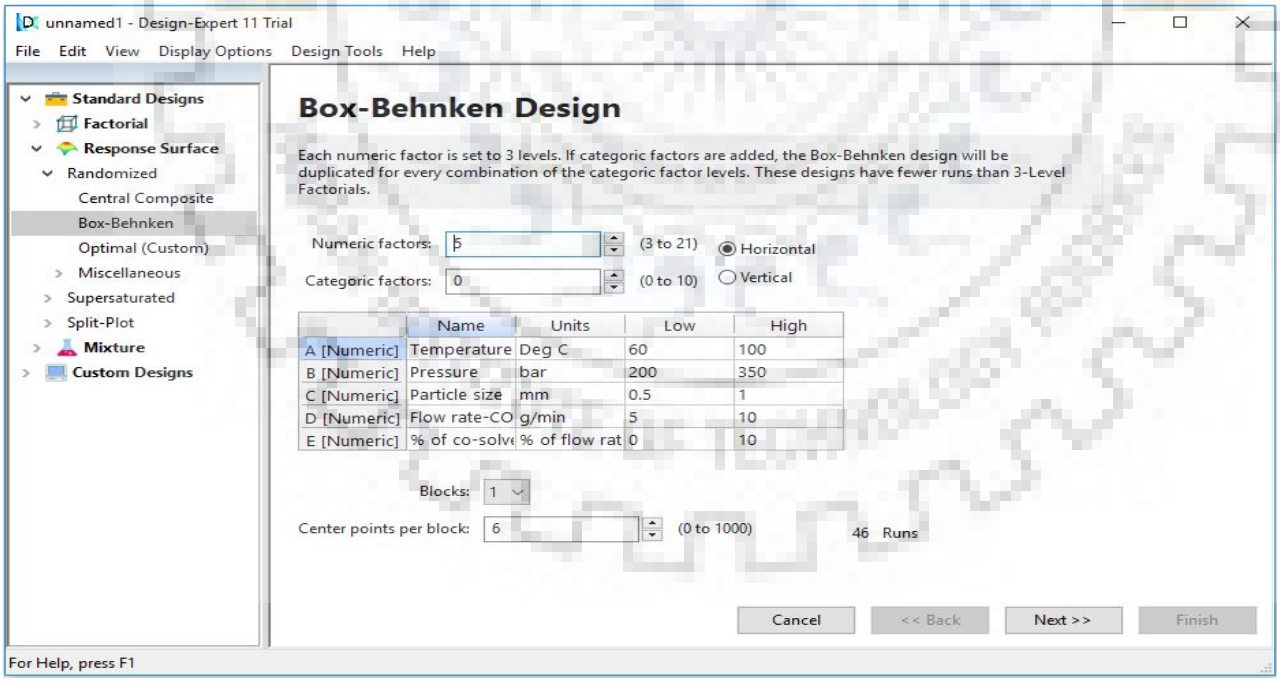


Fig. 3.10: Selection of BBD under RSM of the software 'Design Expert' during DoE.

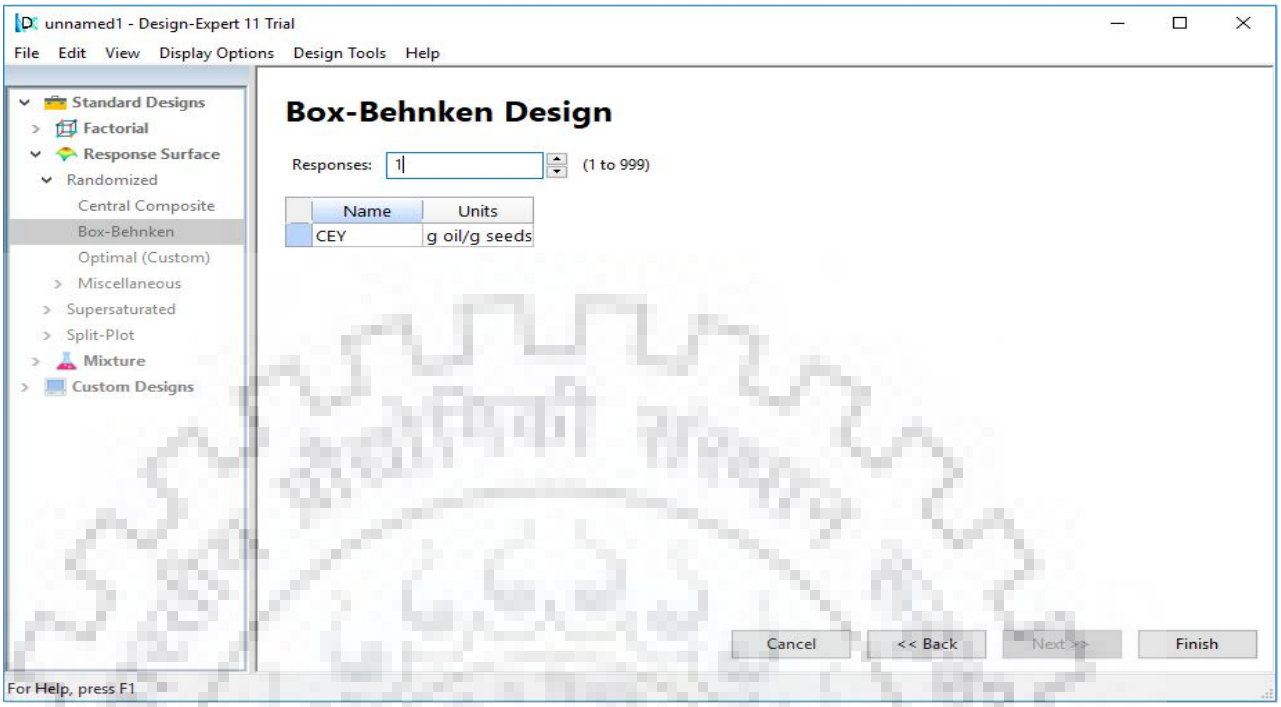


Fig. 3.11: Selection of the number of responses under the BBD of the software 'Design Expert' during DoE.

Table 3.9. Designed matrix of experiments for the SFE of AM and PP seeds.

| Run | Temperature ($X_1$, °C) | Pressure ($X_2$, Bar) | Particle size ($X_3$, mm) | Flow rate - $CO_2$ ($X_4$, g/min) | % of co-solvent ($X_5$, %) |
|---|---|---|---|---|---|
| 1 | 80 | 200 | 0.5 | 10 | 5 |
| 2 | 80 | 275 | 0.75 | 10 | 5 |
| 3 | 60 | 350 | 0.75 | 10 | 5 |
| 4 | 60 | 275 | 0.75 | 10 | 0 |
| 5 | 80 | 275 | 1 | 5 | 5 |
| 6 | 100 | 275 | 0.75 | 5 | 5 |
| 7 | 80 | 200 | 0.75 | 10 | 10 |
| 8 | 80 | 200 | 0.75 | 15 | 5 |
| 9 | 60 | 200 | 0.75 | 10 | 5 |
| 10 | 100 | 350 | 0.75 | 10 | 5 |
| 11 | 80 | 275 | 0.5 | 5 | 5 |
| 12 | 80 | 275 | 0.75 | 10 | 5 |
| 13 | 80 | 200 | 1 | 10 | 5 |
| 14 | 100 | 200 | 0.75 | 10 | 5 |
| 15 | 80 | 350 | 0.75 | 15 | 5 |
| 16 | 80 | 275 | 0.75 | 15 | 10 |
| 17 | 80 | 350 | 0.75 | 10 | 10 |
| 18 | 80 | 200 | 0.75 | 10 | 0 |
| 19 | 80 | 275 | 0.5 | 10 | 0 |
| 20 | 100 | 275 | 1 | 10 | 5 |
| 21 | 80 | 275 | 0.75 | 10 | 5 |
| 22 | 60 | 275 | 0.75 | 10 | 10 |
| 23 | 80 | 275 | 1 | 10 | 0 |
| 24 | 60 | 275 | 0.5 | 10 | 5 |
| 25 | 60 | 275 | 0.75 | 15 | 5 |
| 26 | 80 | 275 | 1 | 15 | 5 |
| 27 | 100 | 275 | 0.75 | 15 | 5 |
| 28 | 80 | 275 | 0.75 | 10 | 5 |
| 29 | 100 | 275 | 0.75 | 10 | 10 |
| 30 | 80 | 350 | 0.75 | 10 | 0 |
| 31 | 80 | 200 | 0.75 | 5 | 5 |
| 32 | 100 | 275 | 0.75 | 10 | 0 |
| 33 | 80 | 275 | 0.75 | 10 | 5 |
| 34 | 80 | 350 | 0.75 | 5 | 5 |
| 35 | 80 | 275 | 0.75 | 5 | 10 |
| 36 | 80 | 275 | 0.75 | 10 | 5 |
| 37 | 80 | 350 | 1 | 10 | 5 |
| 38 | 80 | 350 | 0.5 | 10 | 5 |
| 39 | 100 | 275 | 0.5 | 10 | 5 |
| 40 | 80 | 275 | 0.75 | 15 | 0 |
| 41 | 60 | 275 | 1 | 10 | 5 |
| 42 | 80 | 275 | 0.75 | 5 | 0 |
| 43 | 80 | 275 | 1 | 10 | 10 |
| 44 | 80 | 275 | 0.5 | 15 | 5 |
| 45 | 60 | 275 | 0.75 | 5 | 5 |
| 46 | 80 | 275 | 0.5 | 10 | 10 |

3.10 Experimental set-up's start-up procedure

First, make sure that the equipments (e.g. chiller, SFE system, computer system, rotary vacuum effect evaporator and analytical weighing balance) are connected to electric switchboard. Chiller is started first (approximately 40-50 min before the start of experiment) so that it could attain a temperature below 5 °C (minimum temperature 2 °C was the set point). During this time duration (40-50 min), the extraction vessel, cylindrical basket, separator vessels, and sample-collecting flask were cleaned using ethanol to remove any traces of impurities of previous experiment in these. Thereafter, the whole piping system was flushed with $CO_2$. The prepared extraction bed (as discussed in the section 3.7) was placed into the extraction vessel (also named as extractor), which was then tightened manually and connected to the $CO_2$ line to keep it ready for the further process. Now, the computer system was switched on and the software 'Process Suit' (as shown in Fig 3.2.) was activated. The operating parameters can be set either by clicking on the respective equipment (as shown in Fig 3.2) or by choosing the same equipment from the drop down list of 'view'.

Firstly, the operating temperature for all five zones were set using the 'Heater controller' as shown in Fig. 3.3. Electrical heat exchanger (HE2), Vessel 1 heater ( V1-TS1) and Vessel 1 internal temperature (V1-TS2) were all set at required temperature (e.g. 80 °C) while the collection vessel 1 heater (CS1-TS1) and collection vessel 2 heater (CS2-TS1) were set at room temperature (e.g. 30-35 °C). After setting the temperatures, click on the 'on/off' switch to make it ON (green light indicates ON) as shown in Fig. 3.3. The heater controller will achieve the temperature set point (set as per the requirement) within 4-5 min as indicated by the online temperature scale (red column scale as shown in Fig. 3.3). The pressure setting (e.g. 300 bar) is done using the pressure regulator window as shown in Fig. 3.4. As $CO_2$ is stored in the cylinder at 50-55 bar, initially, the pressure (60 bar) was set using the 'pressure regulator settings' window which appeared on screen after clicking on the 'device setting' option of ABPR . In this window 'pressure regulator' is kept in non-running mode until the $CO_2$ pump is started. Now, the $CO_2$ flow rate (e.g. 10 g/min) was set using the $CO_2$ pump settings window (as shown in Fig. 3.5). Further, the $CO_2$ cylinder was opened manually which would suddenly overshoot the flow rate-$CO_2$ up to 250 g/min due to the non-running mode of 'pressure regulator' but it would come down (within 1-2 min) with the start of the 'pressure regulator' (by clicking on the 'start ABPR button). Now, click the 'start pump' on the window of $CO_2$ pump. As soon as the $CO_2$ flow rate attained the set point (e.g. 10 g/min), the $CO_2$ pump started

working with showing the status 'running' on the $CO_2$ pump window. Now the pressure was increased from 50 bar up to the desired set point (e.g. 300 bar) within a time span of 15-20 min.

After ensuring that temperature, pressure regulator and $CO_2$ pump are working properly, set the co-solvent flow rate (e.g. 0.633 mL/min) using the co-solvent pump-setting window as shown in Fig. 3.6. It was advisable to keep online watch on all the windows (e.g. heater controller, pressure regulator, $CO_2$ pump and co-solvent pump) to ensure that all the components are running and working properly. Once all the operating parameters were achieved by the system, then wait for 5 min. to take out the first sample.

### 3.11 Collection and storage of the final product

Before starting the sampling, set the stopwatch at zero reading, start the heating bath (by setting the temperature 40 °C) of the vacuum effect rotary evaporator and switch on the analytical weighing balance machine. Now, at zero time reading, take the first sample of oil by opening the drain valve (as shown in Fig. 3.1) (only for 10-15 s). The sample drawn is then kept as it is for some time so that it could attain room temperature (keeping the sample for some time (4-5 mints) is necessary because sample comes out at low temperature due to de-pressurization process in the separator).

### 3.12 Required chemicals and reagents

The required standard chemicals and reagents of analytical and HPLC grade (e.g. Supelco 37 component FAME mix) were purchased from the Sigma chemicals company Co. (St Louis, MO, U.S.A). The Ethanol was purchased from Merck Ltd. (Darmstadt, Germany) while n-heptane, 2-propanol, potassium hydroxide, potassium bisulphate, pyridine, anhydrous sodium sulfate in the form of powder, were purchased from Merck Ltd., (Mumbai, India). Syringe filter of 0.25 µm were purchased from Merck Millipore Ltd, India. The other chemicals used in the process, such as sulphuric acid (98.5%), n-hexane (99%), toluene (99.8%), chloroform (99.9%), sodium chloride (99.9%), methanol (99.5%), potassium bicarbonate (99.5%) and anhydrous sodium sulphate (in powder form with 99.0%) were purchased from Merck Ltd., Mumbai, India. The water (ultrapure) used in all solutions was obtained from Milli-Q system supplied by Millipore, Bedford, MA, USA.

3.13 Characterization of the feeds

In this section, the total oil content (oil %), moisture (%), ash (%), scanning electron microscopy (SEM) analysis, Thermo-gravimetric (TG) analysis and Fourier transform infrared (FTIR) spectroscopy analysis were performed on the seed particles of AM and PP seeds as discussed in the subsequent sections.

3.13.1 Total oil content (%) of seeds

Soxhlet extraction (SE) is perhaps the oldest and reliable conventional method being used for determine the total oil content (%) of various natural products (Hawthorne et al., 2000). In this method, 50±0.1g (as in our case) of both seeds (AM and PP seed particles) loaded in a soxhlet thimble, which is connected to a 500 mL round bottom flask, is extracted with 300 mL n-hexane for 24 hours at 68 °C. Solvent (n-hexane) is removed under reduced pressure by rotary vacuum evaporator at 50 °C and the resulting amount of oil was determined gravimetrically. The soxhlet extraction of AM and PP seeds with n-hexane, following the protocol as described above gave an average oil content (%) of 42 % and 35 % respectively. However, the extraction yield (EY) (% or fractional value) is to be used in the present study in place of the '% of oil' to make it technically more convincible.

***Computation of extraction yield:***

The extraction yield ( $y_{Total}$ ) is determined by following the standard procedure given by (Kenneth Helrich, 1990) as the weight percentage which is equal to the total quantity of oil ( $q_{oil}$ ) obtained from dried seeds divided by the quantity of seed particles ( $q_{seeds}$ ) and is used as a reference for SFE process later on.

$$y_{Total}(wt.\%) = 100 * \frac{q_{oil}}{q_{seeds}} \quad \text{… Eq. 3.1}$$

In the present work, each experiment (for both seeds) is run for 250 min., during this period about 25 samples of extracted oil were collected. This means that for 10 minutes of extraction period a sample was collected. The cumulative extraction yield (CEY) is the weight of oil samples collected up to a certain time divided by the weight of seed particles. Thus CEY is dependent on extraction

time. For example CEY for 20 min. will be equal to the total weight of oil received through first two samples divided by the weight of seed particles used in the extractor.

### 3.13.2 Moisture content (%)

The moisture content (%) of AM and PP seed particles is determined, following the standard method that was recommended by guidelines of official methods of analysis (Kenneth Helrich, 1990). According to this guideline, 5 g of sample (seed particles) is taken into the dried dish (known as crucible) and placed in the oven at 105 °C. The dish is removed just after 1 hour and kept in the desiccator for cooling until room temperature is achieved. Once, the sample is cool down, it is weighed. This whole procedure is repeated until a constant weight of sample is achieved. The percentage of moisture content is then calculated using the Eq. 3.2 (Shadangi and Mohanty, 2014).

$$Moisture\ content\ (weight\ \%) = \frac{(Loss\ of\ weight,\ (g))}{(Initial\ weight\ of\ sample\ taken,\ (g))} \times 100 \quad \ldots \text{Eq. 3.2}$$

Based on above procedure, the moisture content of AM and PP seed oils has been found in the range of 9.6 % and 5.4 % respectively.

### 3.13.3 Ash content (%)

Ash is defined as the amount of inorganic residue left after burning the seed material (Sasmal et al., 2012). The ash content (%) of AM and PP seed materials is determined, following the standard method that was recommended by guidelines of official methods of analysis. According to this guideline, 2 g of sample (seed particles) is taken into the dried dish (known as crucible) and placed in the oven at 550 °C until a constant weight is achieved. The percentage of ash is calculated, following the same procedure as in the case of moisture content, using the Eq. (3.2). The ash content (%) of AM and PP seeds has been found to be as 3.5 % and 1.8 % respectively.

### 3.13.4 Scanning electron microscopy (SEM) analysis

The scanning electron microscopy (SEM) instrument is a type of electron microscope that images a sample by scanning it with a high-energy beam of electrons in a raster scan pattern. The electrons interact with the atoms that make up the sample producing signals that contain information about the sample's surface topography, composition, and other properties such as electrical conductivity. The surface morphology of AM and PP seed particle samples, before and after the SFE

were studied using LEO-1550 scanning electron microscopy (SEM) equipment. The seed particle samples (before and after extraction) were first coated with gold-palladium alloy and then placed under the microscopy for scanning. The outputs (images at various magnifications) of SEM for AM and PP seeds have been analyzed and discussed in detail in section 5.7 of Chapter 5.

### 3.13.5 Thermo-gravimetric (TG) analysis

Thermo-gravimetric (TG) analysis is performed to investigate the thermal degradation of AM and PP seeds. TG analysis was performed using EXSTAR TG/DTA 6300 for AM and PP seed particles of a size of 1.0 mm before extraction under the condition of air atmosphere (200 mL/min) at a temperature range of 30 °C - 1200 °C. The output (thermogram of both seed samples) has been explained in detail in section 5.8 of Chapter 5.

### 3.13.6 Fourier transform infrared spectroscopy (FTIR) analysis

A qualitative analysis, of organic compounds, present in AM and PP seeds, was done by using Fourier transform infrared (FTIR) spectroscopy technique. The FTIR analysis of AM and PP seeds has been done in the initial stage means before extraction to identify various functional organic groups. The FTIR spectrum of dried particles of particle sizes (1.0 mm) is recorded, in a KBr pellet, in the range of 500 – 4000 $cm^{-1}$, using FTIR instrument (Thermo Scientific -6700) as shown in section 5.8. Various peaks were observed during the FTIR of AM and PP seeds, however only sharp peaks were considered. A detailed analysis of the FTIR spectrum is given in section 5.8 of Chapter 5.

## 3.14 Characterization of the product

The characterization of extracted oils was conducted which includes the determination of physico-chemical properties of extracted AM and PP seed oils and identification and quantification of targeted chemical components (e.g. fatty acids in our case) using gas chromatography (GC) analysis as described in the further sections.

### 3.14.1 Physico-chemical properties of extracted AM and PP seed oils

The physico-chemical properties (e.g. heating value (MJ/kg), flash point, (°C), fire point (°C), cloud point (°C), pour point (°C), saponification value (mg KOH/g), peroxide value (meq/kg sample)

and acid value (mg KOH/g)) of the extracted AM and PP seed oils during SFE, were determined to highlight their different industrial applications.

3.14.1.1 Determination of heating/calorific value

Bomb calorimeter (CC01/M3, supplied by Toshniwal Technologies Pvt Ltd.)) has been used to determine the calorific/heating value of oils of both seeds. This Bomb calorimeter consists of a cylindrical stainless steel vessel, called bomb, which is capable to withstand high pressure. The bomb is provided with a lid that can be screwed firmly on the bomb. This lid contains two stainless steel electrodes and an inlet valve for oxygen. A small ring is attached to one of the electrodes, which is provided with silica crucible. The bomb is placed in a copper calorimeter containing a known mass of water with an electrically operated stirrer and Backmann's thermometer (it is sensitive enough to read up to 0.01 °C). This calorimeter is surrounded by an air-jacket, which is again followed by a water jacket to prevent heat losses due to radiation.

A known amount of seed oil is placed in the crucible. The crucible is then placed over a ring and a fine magnesium wire touching the oil sample is stretched across the electrodes. The lid is tightly screwed and the bomb is filled with oxygen at 25 atm pressure. The initial temperature is recorded. The electrodes are then connected to a 6V battery and the circuit is completed. As soon as the circuit is completed and current is switched on, the fuel in the crucible burns with the evolution of heat. Heat liberated by burning of the fuel increases the temperature of water and the maximum temperature attained is recorded. For example, the heating value of the fuel (AM seed oil) can then be determined using the heat balance. Heat given by the fuel (AM seed oil) is equal to the heat gained by the water bath.

$$Mass\ of\ fuel \times HV = Mass\ of\ water \times Specific\ heat \times Change\ in\ Temp. \quad \text{… Eq. 3.3}$$

$$HV = \frac{(5 \times 4.18 \times 9)}{(0.005)} = 37620\ \text{KJ/kg} = 37.62\ \text{MJ/kg} \quad \text{… Eq. 3.4}$$

The observed heating value (37.2 MJ/kg of the present sample) is near to the heating value reported by Singh and Singh, 2010 and Singh et al., 2010. Similarly, the HV of PP seed oil is found as 32 MJ/kg.

3.14.1.2 Determination of flash and fire point

The flash point of an oil sample is the lowest temperature at which the vapor of oil, shortly takes fire in the form of a flash only and the fire point is the lowest temperature at which the oil gets ignited and converted into a combustion. These two points (flash and fire point) were determined, using the Pensky Martin apparatus as suggested by the method, IS 1448 (P:5), of Bureau of Indian Standard. Initially, the clean and dry cup of Pensky Martin apparatus is filled up with the oil sample to be tested up to the level indicated by the filling mark. The lid is placed to close the cup in a closed system. The oil sample is then heated with stirring so that the temperature increased is about 5 to 6 $^{o}$C per min. the test flame is applied at every 5 °C rise in temperature with discontinued stirring by opening the shutter of cup. The lowest temperature at which application of the test flame causes the vapors above the liquid to ignite is noted as flash point. To determine the fire point, the heating of sample was continued until the application of the test flame causes the oil to ignite and burn at least 5 seconds. The observed flash points of AM and PP seed oil are found to be as 236 °C and 216 °C respectively while the fire points are found as 263 °C and 231 °C respectively.

3.14.1.3 Determination of cloud and pour point

The cloud point is the lowest temperature at which the oil becomes cloudy or hazy when an oil is cooled at specified rate whereas the pour point is the temperature at which the oil just ceases to flow. The cloud and pout points are related to low temperature characteristics of fuel and tells the behavior of fuel at low temperature. In this work, cloud and pour points of AM and PP seed oils were determined using the NOVA apparatus. Firstly, the oil sample is cooled up to 25 °C then the oil sample is made moisture and dirt free by filtration through a lint less filter paper until the oil is perfectly appear clear. This cleared oil sample is poured into the test jar up to the level marked. Now, this test jar is inserted in the jacket and maintained the temperature of cooling bath at 30-35 °C and put the jacket containing test jar in the cooling bath. After every 2 °C fall in temperature, the test jar is removed from the jacket and observed carefully the oil sample. If any haziness is identified at any point of time then the respective temperature is recorded as cloud point. This complete operation shall not require more than three seconds. Once the cloud point is identified, the complete process is proceeded further to identify the pour point at which the oil sample is just become ceases to flow. The observed cloud point for both seed oils is found to be the same as 13 °C. On the other hand, the pour points of AM and PP seed oils were found as 1 °C and 3 °C respectively.

3.14.1.4 Determination of saponification value

The saponification value is determined as the number of milligrams of potassium hydroxide required to neutralize the fatty acids resulting from the complete hydrolysis of 1 g of oil/fat as suggested by official method IS 1448 (P:55), Bureau of Indian Standard. 1 g of oil sample is taken in to a reaction flask and mixed with a 25 mL of alcoholic potassium hydroxide solution. On the other hand, another 25 mL of alcoholic potassium hydroxide solution is taken for blank titration. These two flasks are connected with air condensers and used water bath to heat up the solution for approximately 1 hour. The absence of any oily matter and appearance of clear solution indicates that the saponification was completed. After 1 hour, the reaction mixture is titrated with 0.5 N hydrochloric acid in the presence of 1.0 mL phenolphthalein indicator. The saponification value is calculated, using the formula as given below:

$$Saponification\ value = \frac{56.1\times(A-B)\times N}{W} \quad \ldots \text{Eq. 3.5}$$

Where, A and B are the volume quantities (mL) of standard hydrochloric acid required for blank and the sample solutions respectively. N is the normality of the standard hydrochloric acid and W is the weight (g) of oil/fat taken for the test. After, following the protocol as described above, the saponification values for AM and PP seed oils are found as 198 and 192 mg KOH/g respectively.

3.14.1.5 Determination of peroxide value

The peroxide value is defined as the amount of peroxide oxygen per 1000 g of fat or oil and is determined by the method as described below.

First of all, 5 g of oil sample is taken into a 250 mL conical flask, fitted with a ground glass stopper then a 30 ml mixture of chloroform and glacial acetic acid (with 2:3 volume ratio) is added in to this conical flask and shake to dissolve the oil sample. Now, 0.5 mL of saturated potassium iodide solution is added while shaking the solution for exactly 1 min then added 3 mL of distilled water in it. This mixture is then, titrated with 0.01N sodium thiosulphate, adding the titrant slowly with continuous shaking, until the yellow color is almost discharged. Now, 0.5 mL of starch solution is added and continues the titration, shaking vigorously, until the color is disappeared. Again, a blank test was conducted under the same conditions. The peroxide value was calculated by using the following formula as:

$$Peroxide\ value = \frac{C \times D \times 1000}{g\ of\ oil\ sample\ taken} \quad \text{… Eq. 3.6}$$

Where, *C* is the volume (mL) of $Na_2S_2O_3$ and N is the normality of $Na_2S_2O_3$ solution. Based on the above protocol, the peroxide values of AM and PP seed oils were determined as 148 and 6.9 meq/kg sample respectively.

3.14.1.6 Determination of acid value

The acid value is determined as the number of milligrams (mg) of potassium hydroxide required to neutralize the free fatty acid in 1 g of fatty oil in the presence of phenolphthalein indicator. 1 g of oil sample is taken in to a conical flask then a freshly prepared mixed solution of neutralized ethyl alcohol of 20 mL and 2 mL of phenolphthalein indicator is mixed with the oil sample. The mixture was boiled for at least 5 min. and titrated with 0.5 N KOH solutions. The solution was shaking vigorously during the titration. After titration, the acid value was calculated as;

$$Acid\ value = \frac{56.1 \times E \times F}{W} \quad \text{… Eq. 3.7}$$

Where, E and F are the volume (mL) and normality of standard potassium hydroxide solution and W is the weight (g) of sample. In the present study, the calculated acids values of AM and PP seed oils are found as 62.7 and 5.4 mg KOH/g respectively.

3.14.2 Gas chromatography (GC) analysis of fatty acids

Free fatty acids (FFA) of the oil samples (AM and PP seed oils), which exhibit high boiling point, are first converted into fatty acid methyl esters (FAME) of low boiling point, using the method suggested by (Christie, 1990), with some modifications. For example, AM seed oil (0.50±0.01 g) is added into a test tube and mixed with 1 mL toluene and then connected to a condenser. Prepared solution (2 mL) of 1% sulphuric acid in methanol is then mixed into the above mixture. This mixture is heated through a water bath at 70 °C for two hours under a total reflux condition. After two hours, this reaction mixture (converted FAME) is mixed with a freshly prepared 5% sodium chloride solution resulting into two liquid layers. Now, the upper layer (converted FAME) is extracted two times with n-hexane (2 mL) while the lower one is discarded. The collected upper layer (containing FAME in n-hexane) is then washed with freshly prepared 4 ml of 2% potassium bicarbonate solution resulting into two liquid layers. Now, the upper layer (n-hexane containing FAME) is separated out

and dried over the anhydrous sodium sulphate while the lower aqueous layer is discarded. Finally, the solvent (n-hexane) is removed through rotary vacuum effect evaporator (Buchi type). The final amount of FAME is makeup with 1 ml of n-hexane and kept in 'sample vials' for further GC analysis.

The fatty acid profiling of AM seed oil sample was carried out through GC equipment (Thermo Trace Ultra Gas chromatograph (Thermo Scientific, USA)) which is equipped with an auto-sampler (HP 7683, HP Company, Wilmington, DE), a flame ionization detector (FID) and capillary column (30 m x 0.25 mm x 0.20 µm, HP-88, Agilent Technology, USA). The injector and detector temperature were maintained constant at 250 °C while the initial oven temperature was maintained at 120 °C for 1 min. Now, the oven temperature was increased from 120 °C to 145 °C at a ramp rate of 5 °C/min and maintained constant at 145 °C for 2 min. The temperature was again increased from 145 °C to 220 °C at a ramp rate of 2 °C/min and maintained constant at 220 °C for 2 min. Auto-sampler injected 1 µl of the sample with the split ratio (50:1) into the column and a complete chromatogram is generated with a total 45.50 min. program. The obtained fatty acid peaks were identified using standard 37 FAME mixture (Supelco 37 component FAME mix, Supelco, Bellefonte, PA) and quantified by area normalization method. The same protocol was followed during the GC analysis of PP seed oil. The detail explanation of the fatty acids components found in AM and PP seed oil is reported in the sections 5.8.1.4 and 5.8.2.4 respectively.

# MATHEMATICAL MODELING

The main goal of mathematical modeling of a SFE process is to predict the extraction curve for real large-scale process as the function of the experimental parameters such as temperature, pressure, solvent flow rate, particle size, co-solvent amount and other newly introduced parameters such as bed height, matrix of seed particles and solubility parameters. As the real experiments, at large scale, are extremely expensive therefore, the mathematical models are being simulated to overcome this problem.

A fundamentally sound and sufficiently detailed mathematical model may be used to project and extend the scope of the available experimental findings to obtain a better understanding of the systems and the phenomena involved, for the design, scale-up and operation of the related equipment and the complex systems taking place with the help of such equipment (Hortacsu, 2000). It is evident that the various models differ not only from mathematical representation of the phenomena, but also, due to mass transfer mechanisms, which controls the SFE of different seed matrices. Thus, a single model may not be fitted to all type of experimental data. The strength of a model is measured by the number of different systems it can accurately predict, as well as the span of it's applicability within acceptable limits of accuracy and precision as discussed in Chapter 2. From the available literature it is clearly visible that the Sovova model (Sovova, 1994) has been applied extensively to various natural solid matrices. However, Sovova, 1994 has proved its superiority over many models for the SFE of various natural products (e.g. seeds, leaves, roots, fruits etc.) but Reverchon, 1996 has shown a best fitting for leaves only. Therefore, it would be an interesting exercise to apply these two models for the present materials (e.g. AM and PP seeds) of study for the SFE.

4.1 Sovova model (SM) used for the present SFE process.

The kinetic study of the SFE process can be linked to the extraction curve, which are obtained as the function of time of extraction. If we study the overall extraction curve (OEC), which is a function of time, we will find that the extraction phenomena changes in different segments of the curve. This is clearly shown by segmenting the extraction curve into three different time zone as given below:

1. Constant extraction rate (CER): In this period, the extraction behavior is linear with time. This takes place at the initial period of extraction when the external surface of the particles are covered with solute (easily accessible solute). For this period, the mass transfer resistance is in the solvent phase only.

2. Falling extraction rate (FER): In this period, the extraction behavior is non-linear with time. The magnitude of the slope of the curve decreases with time and thus a non-linear behavior is observed. In this period the easily accessible solute that was present earlier hardly exists. Thus, the solvent has to diffuse through solid matrix to extract solute and thus the diffusion mechanism sets in. The easily accessible solute is completely depleted at the extractor's entrance – the diffusion mechanism starts.

3. Diffusion-controlled: In this period solvent diffuses to the inner core of the solid matrix to extract the solute mass and thus the phenomena converts itself to diffusion controlled mass transfer phenomena.

Various models for SFE process have been proposed in the literature, such as artificial intelligence based models (e.g. FFBPNNM, CFBPNNM) (Lashkarbolooki et al., 2013; Suryawanshi and Mohanty, 2018b), chemical reaction based models (e.g. PKM, PCM, DKM, LM) (Savage et al., 1995; Zhao et al., 2018), heat transfer phenomenon based models (e.g. HBDM) (Bartle et al., 1990; Reverchon et al., 1993; Esquivel et al., 1999; Campos et al., 2005; Rochova et al., 2008; Huang et al., 2011a), mass transfer phenomenon based models (e.g. SCM, DDDM) (Sovova, 1994; Goto et al., 1996; Reverchon, 1996; Abaroudi et al., 1999; Ayas and Yilmaz, 2014), and empirical models (e.g. EDM) (Naik et al., 1989; Esquivel et al., 1999; Silva et al., 2008; Zhao and Zhang, 2014; Tomita et al., 2014). The solutions of these models were obtained using various analytical (Sovova, 1994), numerical (Goodarznia and Eikani, 1998) and evolutionary algorithms (Martinez and Martinez, 2008). In the present study, a concept of mass transfer phenomenon based model (e.g. DDDM)

proposed by Sovova, 1994 has been used to examine the extraction of oil from AM and PP seeds for scaling up a lab scale production to an industrial scale production. The fitting parameters of the above model have been optimized by a global optimization technique (e.g. genetic algorithm (GA)).

As mentioned in the Section 2.12, several models have already been proposed to describe the SFE from solid materials. Nevertheless, the model initially proposed by Lack, 1985 and then extended by Sovova, 1994, has the advantage of providing a reasonably simple analytical solution to the mass balance equation and a good physical description of the process.

As discussed previously (in the section 2.12), these authors proposed a similar physical representation of the seed particles as being composed of cell broken up during grinding and of cells which are still intact. Sovova, 1994, hypothesized the existence of two mass transfer resistance during the SFE. The first is located in the solvent phase (e.g. supercritical mixture of solvent and solute) and controls the extraction process until all the solute (e.g. oil) in the broken cells is exhausted. The second is in the walls of the undestroyed cells and controls the remaining part of the process. These hypotheses were translated to the mathematic model by introducing two mass balances on an elemental bed height for solvent and solid phases respectively as already discussed in the previous section 2.12.2. As mentioned in the section 2.12.2, the Sovova, 1994 model has classified the extraction curve into three zones (e.g. based on periods of extraction) which have also been named as constant extraction rate (CER) period ($t_{CER}$) (as first period), falling extraction rate period ($t_{FER}$) (as second period) and purely diffusion controlled extraction rate period ($t \geq t_{FER}$). These three periods of extraction curve has also been named as fast, transition and slow extraction periods in section 2.12 (as shown in Fig. 2.9). The above hypotheses were transferred to the final mathematical form as given below;

For CER period: $t < t_{CER}$

$$y(t) = Q_{CO_2} y_r [1 - \exp(-Z)]t \quad \text{… Eq. 4.1}$$

For FER period: $t_{CER} \leq t < t_{FER}$

$$y(t) = Q_{CO_2} y_r [t - t_{CER} \exp(z_w - Z)] \quad \text{… Eq. 4.2}$$

For the diffusion controlled period: $t \geq t_{FER}$

$$y(t) = msi\left[x_0 - \frac{y_r}{W} ln\left\{1 + \left[exp\left(\frac{Wx_0}{y_r}\right) - 1\right] exp\left[\left(\frac{WQ_{CO_2}}{msi}\right)(t_{CER} - t)\right]\frac{x_k}{x_0}\right\}\right] \quad \text{… Eq. 4.3}$$

With the following restrictions:

$$z_w = \frac{Zy_r}{Wx_0} ln\left\{\frac{x_0\, exp[WQ_{CO_2}(t-t_{CER})/msi]-x_k}{x_0-x_k}\right\} \quad \text{… Eq. 4.4}$$

$$t_{CER} = \frac{(x_0-x_k)msi}{y_r\, Z\, Q_{CO_2}} \quad \text{… Eq. 4.5}$$

$$t_{FER} = t_{CER} + \frac{msi}{WQ_{CO_2}} ln\left[\frac{x_k+(x_0-x_k)\,\exp(Wx_0/y_r}{x_0}\right] \quad \text{… Eq. 4.6}$$

$$Z = \frac{k_f a_0 \rho}{\left[\frac{Q_{CO_2}}{msi}(1-\varepsilon)\rho_s\right]} = \frac{F\, msi}{Q_{CO_2}} \quad \text{… Eq. 4.7}$$

$$W = \frac{k_s a_0}{\left[\frac{Q_{CO_2}}{msi}(1-\varepsilon)\right]} = \frac{S\, msi}{Q_{CO_2}} \quad \text{… Eq. 4.8}$$

The mathematical equations (Eq. (4.1) – Eq. (4.8)) represents the Sovova model (SM) which actually describes the extraction curve as a function of time. These model equations (Eqs. (4.1-4.8)) are used to fit the SFE's experimental extraction data of AM and PP seed oils. Martinez and Martinez, 2008 have used the global optimization method, together with the Nelder-Mead method, to find the optimal fit with three parameters viz. $t_{CER}$, Z and $t_{FER}$. Similarly, Hrncic et al., 2010 have used the genetic algorithm (GA) method to estimate the optimized fitting parameters (Z, W and $x_k$). However, GA method has proved its superiority over the global optimization technique. In the present work, GA method was used to optimize the model parameters Z, W and $x_k$ by minimizing the average absolute relative deviation percentage (AARD %) as objective function.

### 4.1.1 Optimization of model parameters by Genetic algorithm (GA) method

Genetic algorithms (GAs) refer to a procedure of search and optimization motivated by the Darwin's principles of evolution through natural selection and genetics (Goldberg, 1989; Holland, 1992; Back et al., 2000). GAs apply the evolutionary concept of 'survival of the fittest' to optimize mathematical problems, which are not easily optimized by traditional numeric methods (e.g. Fmincon, Nelder-Mead, Box complex method etc.) therefore, it can also be said that the GAs belongs to 'evolutionary algorithms'. The GAs were invented by John Holland in the 1960s and were

developed by Holland and his students and colleagues at the University of Michigan in the 1960s and the 1970s (Melanie, 1999). A genetic algorithm is generally consists of two processes (Sahu et al., 2015). The first process is the selection of the individual for the production of next generation and the second process is the manipulation of the selected individual to form the next generation by crossover and mutation techniques.

In order to perform the optimization of the decided objective function, the search process of the 'evolutionary algorithms' is leveraged by two important aspects: exploration and exploitation. Exploration visits entirely new regions of a search space to discover a promising offspring while exploitation utilizes the information from previously visited regions to determine potentially profitable regions to be visited next. To be successful, any search algorithm needs to find a good balance between exploration and exploitation.

Many researchers believe that 'evolutionary algorithms' are effective due to a good ratio between the exploration and exploitation. However, how and when to control and balance exploration and exploitation in the search process to obtain even better fitness results, and/or convergence faster, are still an on-going research in 'evolutionary algorithms' (Brest et al., 2006).

The Fig. 4.1 shows the basic steps of the GA. In the beginning, the initial population is often generated randomly. The size of the population means the number of individuals, is defined by the user before the run, with parameter pop_size, that might change during the evolution process. In the parameter estimation technique, each individual represents a set of model parameters, which need to be estimated. The model equation(s) can therefore be computed for every individual and the result represents its fitness.

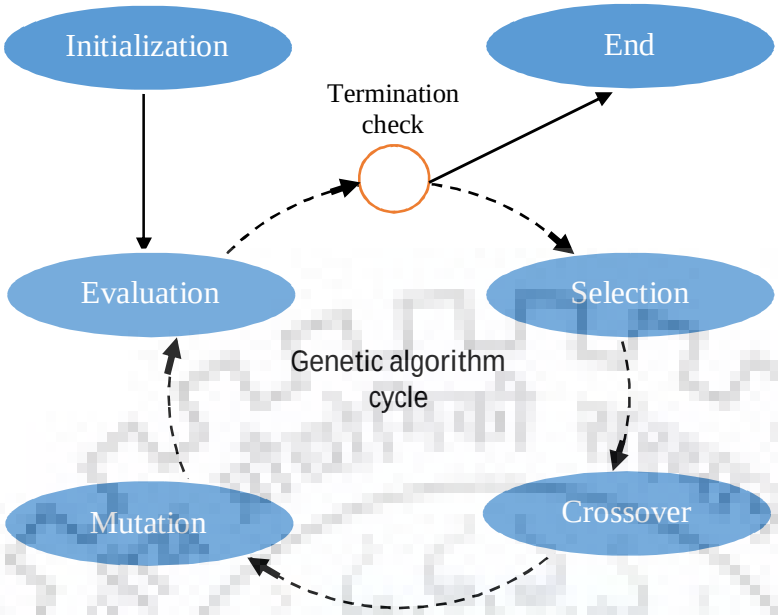


Fig. 4.1: Steps of genetic algorithm.

There are four basic steps: selection, crossover, mutation and evaluation, which are to be followed during the optimization under the GA. These steps are often problem specific and hence explained in more details later. Each iteration in the evolutionary cycle of GA (as shown in Fig. 4.1) is also called a generation. The user, with a max_gen parameter, defines the number of generations. The stopping criteria of GA is checked in the termination check step. There are many possibilities for how long to iterate the GA steps. The algorithm can stop after a certain number of fitness evaluations, after a certain number of generations (e.g. max_gen) or as in our case when the result is good enough (with minimum error range).

The representation of the individual parameter is also one of the parts of GAs because the performance and goodness of the fit is often based on the representation. Therefore, the coding of the individual, in this work is same as reported by Hrncic et al., 2010. Each model parameter, which is to be optimized is represented by a float value. Because the parameters $Z$, $W$ and $x_k$ were chosen to be estimated, the individual is represented with a vector [$Z$, $W$, $x_k$].

4.1.1.1 Selection

Through the selection step, it is decided that which individuals will survive and make up the population in the next generation. Various techniques (e.g. proportional, ranking, tournament etc.)

do exist to make the selection of the individuals (Michalewicz, 1992). The tournament selection was used in this study. In tournament selection, the algorithm randomly selects *k* individuals from the population and the best one (with the best fitness value) is selected into the next population. Because the population size is changing, it is important that this process is repeated pop_size times to reduce the size of population to one that was defined by the user. Both parameters, *k* and pop_size, are algorithm parameters defined by the user.

4.1.1.2 Evaluation

The fitness value, for every individual in the population, is calculated with the evaluation method and it is used in the selection process. In this study, for every individual, the evaluation process calculates how good Sovova model (SM) fits the experimental data with given parameter values. To calculate the fitting of the model to the experimental data, the merit function (Eq. (4.9)) was used. The value ($Y_i^{Exp}$) represents the experimentally obtained yield while '$Y_i^{Model}$' is the calculated (using the model equations Eqs. (4.1-4.3)) yield of the extract.

$$AARD\ (\%) = \frac{1}{n}\sum_{i=1}^{n}\left[\frac{|(Y_i^{Exp} - Y_i^{Model})|}{Y_i^{Exp}}\right] \times 100 \quad \ldots \text{Eq. 4.9}$$

4.1.1.3 Crossover

The crossover operator is often used to explore the search space. This operator is used to mix the 'genetic' material between two or more individuals. Generally, the crossover uses two individuals as parents and generates two new individuals or offspring. The two basic crossover mechanisms are the n-point crossover and uniform crossover. The n-point crossover cuts the parents of length L into n + 1 segments, based on randomly selected crossover points. The first offspring is created with the use of odd segments from the first parent and even segments from the second parent and vice versa for the second offspring. In the uniform crossover the decision for every element for the first offspring is made randomly, if it will be taken from first or the second parent. The second offspring is then generated using opposite decisions. Mostly the 1- or 2- point crossover is used. Because the individuals in this study are of the short length, the 1-point crossover has been used. For every individual in the population a random number between 0 and 1 is generated. If the number is lower than the crossover probability (PC), defined by the user, then this individual is selected for crossover as the first parent. The second parent is then randomly selected from the population. After both parents are known, the crossover position needs to be determined. The crossover position in 1-

point crossover is randomly chosen value between 1 and -1. After the position is selected, the new individuals are generated based on as written earlier in this subsection. Fig. 4.2 depicts this process graphically. As a result, two new individuals are made and inserted into the population.

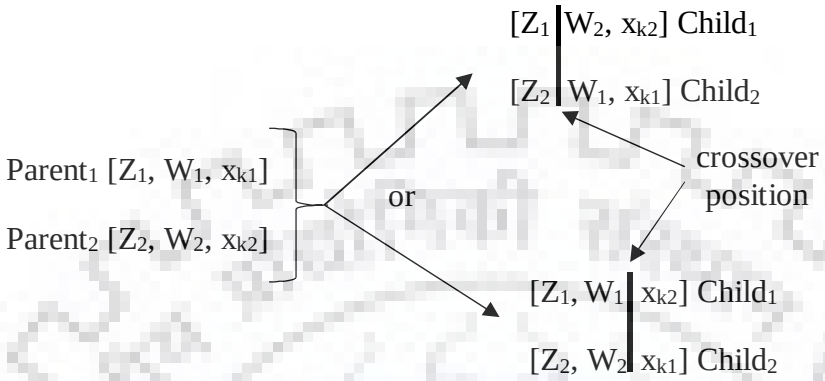


Fig. 4.2: Possible crossover for vectors [$Z_1$, $W_1$, $x_{k1}$] and [$Z_2$, $W_2$, $x_{k2}$].

4.1.1.4 Mutation

The mutation operator is used to change a part of the 'genetic' material of the individual. In the real valued representation, the basic element or gene is a floating number. Mutation is therefore implemented as it changes the value (gene) of the individual. For every gene, in the individual, the random number between 0 and 1 is generated. If this number is lower than the probability of mutation defined by the user, the gene is mutated. In this study, GA methods uses equations (Eqs. 4.10 and 4.11).

$$v_n = v + r^3 (v_{max} - v) \quad \text{… Eq. 4.10}$$

$$v_n = v - r^3 (v - v_{max}) \quad \text{… Eq. 4.11}$$

Where, $v_n$ represents value that replaces the old value $v$, $r$ is the random value between 0 and 1, $v_{max}$ is the maximum value and $v_{min}$ is the minimum value.

The boundaries of the model parameters estimated ($t_{CER}$ and $t_{FER}$) are applied as follows:

$$t_{CER}^{min} \leq t_{CER} \leq t_m \quad \text{… Eq. 4.12}$$

$$t_{CER} (1 + Z) \leq t_{FER} \leq t_{CER} + \frac{msi * x_0}{Q_{CO_2} y_r} \quad \text{… Eq. 4.13}$$

The minimum and maximum values of parameters (*Z*, *W* and $x_k$) that to be optimized using GA method were chosen as '$10^{-2}$ and 30', '$10^{-4}$ and 10' and '$10^{-3}$ and (any value < $x_0$)'.

4.2 Reverchon model (RM) used for the present SFE process

Reverchon, 1996 has developed a mathematical model for the SFE process of natural plant leaves unlike the other proposed models (e.g. Goto et al., 1993; Sovova et al., 1994) which actually were based on the hypothesis that the fraction of oil is freely available on the particle surface as result of grinding. However, the above general hypothesis could not be significant in the case of SFE of oils from natural plant leaves because of some valid reasons such as structure of seeds is completely different from the leaves; seeds have high content of oil. Therefore, it is clear that the only internal mass transfer resistance controls the extraction of oil from leaves. Hence, the external mass-transfer coefficient was neglected in the development of the model.

Reverchon, 1996 model is basically, based on the integration of differential mass balances along the extraction bed (as shown in Fig. 2.10) with the assumptions (as mentioned in section 2.12). Based on those assumptions (as mentioned in section 2.12), the mass balances (for solid and solvent phases) over an element of the extractor of height '$dh$' are shown in Eqs. (4.14) and (4.15).

$$uV\frac{\partial c}{\partial h} + \epsilon V\frac{\partial c}{\partial t} + (1-\epsilon)V\frac{\partial \bar{c}}{\partial t} = 0 \quad \text{… Eq. 4.14}$$

$$(1-\epsilon)V\frac{\partial \bar{c}}{\partial t} = -A_p K(\bar{c} - \bar{c}^*) \quad \text{… Eq. 4.15}$$

Initial condition: $c = 0,\ \bar{c} = \bar{c}_0$ at $t = 0$ … Eq. 4.16

Boundary condition: $c(0, t) = 0$ at $h = 0$ … Eq. 4.17

Assuming a linear relationship for SFE process between $c$ and $\bar{c}^*$ due to lack of experimental phase equilibrium data as given in Eq. (4.18).

$$c = k_p \bar{c}^* \quad \text{… Eq. 4.18}$$

In Eq. (4.15) the group, $A_p K/(1-\epsilon)V$ depends on the geometry of particles which is taken care by $A_p K$, and $\epsilon$ is supposed to be constant within the extraction bed. This fraction is

dimensionally equal to $1/s$. Therefore, the internal diffusion time ($t_i$) which is also the characteristic according to the hypothesis of the extraction process and is defined as:

$$t_i = \frac{(1-\epsilon)V}{A_p K} \quad \text{… Eq. 4.19}$$

Therefore, the Eq. (4.15), was written as:

$$\frac{\partial \bar{c}}{\partial t} = -\frac{1}{t_i}(\bar{c} - \bar{c}^*) \quad \text{… Eq. 4.20}$$

Where, internal diffusion time ($t_i$) is correlated with the internal diffusion coefficient ($D_i$) for different particle geometries as given in Eq. (4.21).

$$t_i = \mu \frac{l^2}{D_i} \quad \text{… Eq. 4.21}$$

where, $\mu$ is a coefficient depending on particle geometry. In the case of spherical particles ($\mu = 3/5$). For cylinders and slabs it is equal to 1/2 and to 1/3, respectively. The above Eqs. (4.14 and 4.20) were solved and fitted with the present experimental data using the COMSOL Multiphysics 5.3a. A value of partition coefficient ($k_p$) of solute (oil) between phases is required to solve the system simplified mass balance equations (Eqs. (4.14 and 4.20)). Therefore, the partition coefficient ($k_p$) is calculated using the Eq. (4.22) as given below:

$$Partition\ coefficient\ (k_p) = \frac{Distribution\ coefficient\ (D_p)}{Solid\ density\ (p_d)} \quad \text{… Eq. 4.22}$$

$$Distribution\ coefficient\ (D_p) = \frac{(kg\ oil/m^3\ of\ CO_2)}{(kg\ remaining\ oil/kg\ solid)} \quad \text{… Eq. 4.23}$$

A basis of 100 g of seed material (e.g. AM and PP seeds) is taken for the calculation. An average density of $CO_2$ (kg/m$^3$) was assumed despite of variation in temperature and pressure during the SFE. The calculated values of $k_p$, with other parameters are reported in Chapter 5. The only single parameter (e.g. diffusion coefficient ($D_i$)) was tuned to fit the experimental data. By performing the hit and trial, approach the best-tuned value of $D_i$, was suggested to fit the experimental data of each experimental run (1-46 nos).

# RESULT AND DISCUSION

The objectives of the present study are mentioned in Chapter 1. A systematic and thorough literature review has been carried out based on these objectives and has been presented in Chapter 2. To meet the objectives (as mentioned in Chapter 1), designed set of experiments (as described in section 3.9 of Chapter 3) were conducted for the extraction of oils from Argemone mexicana (AM) and Pongamia pinnata (PP) seeds using SC-$CO_2$ and SC-$CO_2$ + co-solvent (Ethanol) through the SFE technique as described in Chapter 3. Statistical optimization of parameters, using Box-Behnken design (described in section 2.8) as well as artificial neural network (described in section 2.9) were conducted. Development and optimization of correlations based on RSM and ANN (described in section 2.8 and 2.9 respectively) for the prediction of cumulative extraction yield (CEY) for the AM and PP seeds, have been carried out. The individual and interactive effects of selected operating parameters (discussed in section 2.3) on the CEY, have been discussed. The mathematical models (Sovova and Reverchon models) (discussed in sections 4.1 and 4.2 respectively) have been validated for the SFE of AM and PP seeds.

A comparison, of outcomes observed from Sovova and Reverchon models for both the above seeds, has also been performed. The characterization of feeds (AM and PP seeds) and the products (oils of both seeds), have also been carried out using available standard methods and equipments as described under the sections 3.13 and 3.14 of Chapter 3. Finally, the economic analysis of the developed SFE process at industrial scale has been presented.

5.1 Analysis of data obtained from experiments carried out using DoE technique

In this study, two types of feed materials (AM and PP seeds) were selected for the SFE process. The selection of feed materials is primarily based on the literature review about their availability and importance of the extracted product (oils). Further, it was found that there is hardly any investigation reported in open literature for the extraction of oil samples of above two seed materials using SFE process. This fact has been reported and concluded in section 2.6. As mentioned in section 2.3, a total number of 13 parameters influence the extraction process. These have been discussed in the previous sections and concluded in section 2.4 that five parameters such as temperature, pressure, particle size, flow rate-$CO_2$ and % of co-solvent are the most influencing parameters which influence the CEY of the oil during the SFE process. Thus, for the present work, the above five parameters were considered as input parameters while the CEY as output parameter. Table 5.1 shows the selected I/O (input-output) parameters with their ranges of operation.

Table 5.1. Input and output parameters with their range.

| Input parameters/variables | Unit | Low value | Mid value | High value | Output parameter |
|---|---|---|---|---|---|
| Temperature ($X_1$) | °C | 60 | 80 | 100 | CEY(g oil/g seed) |
| Pressure ($X_2$) | bar | 200 | 275 | 350 | |
| Particle size ($X_3$) | mm | 0.5 | 0.75 | 1.0 | |
| Flow rate-$CO_2$ ($X_4$) | g/min | 5 | 10 | 15 | |
| % of co-solvent ($X_5$) | % of flow rate-$CO_2$ | 0 | 5 | 10 | |

The design of experiment (DoE) technique has been adopted to develop a second-order polynomial model equation, which co-relates the input and output parameters. A box-behnken design (BBD) under the response surface methodology (RSM) suggested a total number of 46 experimental runs which consists of six runs at the center point while 40 runs at incomplete block factorial point (IBFact) (it also includes 8 runs at without co-solvent condition). The details of experiments are shown in Table 5.2. Based on the I/O parameters presented in Table 5.2, the input-output (I/O) relationship (a second order polynomial regression model equation) has been developed. The general form of the regression model equation (Eq. 5.1) is given below (Montgomery, 2004):

$$Y = \beta_0 + \sum_{i=1}^{k} \beta_i X_i + \sum_{i=1}^{k} \beta_{ii} X_i^2 + \sum_{i=1}^{k} \sum_{j=1}^{k} \beta_{ij} X_i X_j + \varepsilon \quad \text{… Eq. 5.1}$$

Where, Y is the output variable (as CEY in our case). $\beta_0$ is constant, $k$ is the number of input variables (five in our case), $\beta_i$ is the coefficient of the linear parameters terms, $X_i$ represents the variables, $\beta_{ii}$ is the coefficient of the quadratic parameters terms, $\beta_{ij}$ represents the coefficient of the interaction parameters terms and $\varepsilon$ is the residual associated with the experiments.

Table 5.2. BBD matrix and responses for the PP and AM seed oils.

| Run | Type | Temp. ($X_1$, °C) | Pressure ($X_2$, Bar) | Particle size ($X_3$, mm) | Flow rate - $CO_2$ ($X_4$, g/min) | % of co-solvent ($X_5$, %) | CEY (g oil/g seeds) PP Seed oil | CEY (g oil/g seeds) AM seed oil |
|---|---|---|---|---|---|---|---|---|
| 1 | IBFact | 80 | 200 | 0.5 | 10 | 5 | 0.07133 | 0.1289 |
| 2 | Center | 80 | 275 | 0.75 | 10 | 5 | 0.19341 | 0.3470 |
| 3 | IBFact | 60 | 350 | 0.75 | 10 | 5 | 0.31139 | 0.3430 |
| 4 | IBFact | 60 | 275 | 0.75 | 10 | 0 | 0.11257 | 0.2500 |
| 5 | IBFact | 80 | 275 | 1 | 5 | 5 | 0.14531 | 0.3000 |
| 6 | IBFact | 100 | 275 | 0.75 | 5 | 5 | 0.07756 | 0.2620 |
| 7 | IBFact | 80 | 200 | 0.75 | 10 | 10 | 0.11955 | 0.3025 |
| 8 | IBFact | 80 | 200 | 0.75 | 15 | 5 | 0.06115 | 0.2225 |
| 9 | IBFact | 60 | 200 | 0.75 | 10 | 5 | 0.13179 | 0.2800 |
| 10 | IBFact | 100 | 350 | 0.75 | 10 | 5 | 0.21887 | 0.3700 |
| 11 | IBFact | 80 | 275 | 0.5 | 5 | 5 | 0.13763 | 0.1899 |
| 12 | Center | 80 | 275 | 0.75 | 10 | 5 | 0.18141 | 0.3743 |
| 13 | IBFact | 80 | 200 | 1 | 10 | 5 | 0.10209 | 0.2060 |
| 14 | IBFact | 100 | 200 | 0.75 | 10 | 5 | 0.03699 | 0.1474 |
| 15 | IBFact | 80 | 350 | 0.75 | 15 | 5 | 0.29272 | 0.3120 |
| 16 | IBFact | 80 | 275 | 0.75 | 15 | 10 | 0.25000 | 0.3598 |
| 17 | IBFact | 80 | 350 | 0.75 | 10 | 10 | 0.35560 | 0.3986 |
| 18 | IBFact | 80 | 200 | 0.75 | 10 | 0 | 0.03600 | 0.0660 |
| 19 | IBFact | 80 | 275 | 0.5 | 10 | 0 | 0.10350 | 0.1450 |
| 20 | IBFact | 100 | 275 | 1 | 10 | 5 | 0.14487 | 0.2575 |
| 21 | Center | 80 | 275 | 0.75 | 10 | 5 | 0.18960 | 0.3610 |
| 22 | IBFact | 60 | 275 | 0.75 | 10 | 10 | 0.30337 | 0.3295 |
| 23 | IBFact | 80 | 275 | 1 | 10 | 0 | 0.08917 | 0.2000 |
| 24 | IBFact | 60 | 275 | 0.5 | 10 | 5 | 0.21000 | 0.1845 |
| 25 | IBFact | 60 | 275 | 0.75 | 15 | 5 | 0.22342 | 0.3200 |
| 26 | IBFact | 80 | 275 | 1 | 15 | 5 | 0.21827 | 0.3385 |
| 27 | IBFact | 100 | 275 | 0.75 | 15 | 5 | 0.10554 | 0.3620 |
| 28 | Center | 80 | 275 | 0.75 | 10 | 5 | 0.18810 | 0.3664 |
| 29 | IBFact | 100 | 275 | 0.75 | 10 | 10 | 0.16122 | 0.4240 |
| 30 | IBFact | 80 | 350 | 0.75 | 10 | 0 | 0.15367 | 0.2800 |
| 31 | IBFact | 80 | 200 | 0.75 | 5 | 5 | 0.04635 | 0.1695 |
| 32 | IBFact | 100 | 275 | 0.75 | 10 | 0 | 0.05278 | 0.1710 |
| 33 | Center | 80 | 275 | 0.75 | 10 | 5 | 0.18980 | 0.3720 |
| 34 | IBFact | 80 | 350 | 0.75 | 5 | 5 | 0.19586 | 0.3800 |
| 35 | IBFact | 80 | 275 | 0.75 | 5 | 10 | 0.15887 | 0.4031 |
| 36 | IBFact | 80 | 275 | 0.75 | 10 | 5 | 0.18900 | 0.3756 |
| 37 | IBFact | 80 | 350 | 1 | 10 | 5 | 0.28208 | 0.4050 |
| 38 | IBFact | 80 | 350 | 0.5 | 10 | 5 | 0.28708 | 0.2250 |
| 39 | IBFact | 100 | 275 | 0.5 | 10 | 5 | 0.12015 | 0.2626 |
| 40 | IBFact | 80 | 275 | 0.75 | 15 | 0 | 0.05695 | 0.2450 |
| 41 | IBFact | 60 | 275 | 1 | 10 | 5 | 0.23777 | 0.3425 |
| 42 | IBFact | 80 | 275 | 0.75 | 5 | 0 | 0.05892 | 0.1595 |
| 43 | IBFact | 80 | 275 | 1 | 10 | 10 | 0.29451 | 0.3800 |
| 44 | IBFact | 80 | 275 | 0.5 | 15 | 5 | 0.16000 | 0.2025 |
| 45 | IBFact | 60 | 275 | 0.75 | 5 | 5 | 0.14014 | 0.2900 |
| 46 | IBFact | 80 | 275 | 0.5 | 10 | 10 | 0.23000 | 0.2377 |

5.1.1 Development of RSM based correlation for the prediction of CEY for AM seed oil

In order to investigate the effect of chosen independent variables (e.g. $X_1$, $X_2$, $X_3$, $X_4$, and $X_5$), a box-behnken design (BBD) consisting of 46 experimental runs is planned as shown in Table 5.2. In this table, values of response (CEY of AM seed oil) at different experimental conditions are also shown wherein a considerable variation in the CEY of AM seed oil can be observed for different sets of independent variables. A regression analysis (as shown in Table F.1) was performed, using the above experimental data (Table 5.2) based on a quadratic model (Eq. 5.1) representing the CEY of AM seed oil as a function of independent variables. The predicted CEY of seed oil is represented by a second-order polynomial (quadratic model) as given below in Eq. 5.2.

$$\begin{aligned} Yield\ (CEY) = {} & 0.366 - 0.0052X_1 + 0.0744X_2 + 0.0533X_3 + 0.013X_4 + 0.0824X_5 \\ & + 0.0399X_1X_2 - 0.0408X_1X_3 + 0.0175X_1X_4 + 0.0434X_1X_5 + 0.0257X_2X_3 \\ & - 0.0302X_2X_4 - 0.0295X_2X_5 + 0.0065X_3X_4 + 0.0218X_3X_5 - 0.0322X_4X_5 \\ & - 0.0261X_1^2 - 0.0561X_2^2 - 0.0753X_3^2 - 0.0328X_4^2 - 0.0465X_5^2 \end{aligned}$$

… Eq. 5.2

The developed model (Eq. 5.2), can be improved by removing the insignificant interactive term (e.g. $X_3X_4$). However, the improved model as given in Eq. 5.3 does not make any significant difference in performance point of view only the complexity of the second order polynomial (quadratic model) could be reduced just by removing the extra insignificant interactive term ('$X_3X_4$').

$$\begin{aligned} Yield\ (CEY) = {} & 0.3661 - 0.0052X_1 + 0.0744X_2 + 0.0533X_3 + 0.013X_4 + 0.0824X_5 \\ & + 0.0399X_1X_2 - 0.0408X_1X_3 + 0.0175X_1X_4 + 0.0434X_1X_5 + 0.0257X_2X_3 \\ & - 0.0302X_2X_4 - 0.0295X_2X_5 + 0.0218X_3X_5 - 0.0322X_4X_5 - 0.0262X_1^2 \\ & - 0.0561X_2^2 - 0.0753X_3^2 - 0.0328X_4^2 - 0.0465X_5^2 \end{aligned}$$

…Eq. 5.3

The significance of the developed improved quadratic model (Eq. 5.3) is justified by ANOVA (analysis of variance). The results of ANOVA (as shown in Table 5.3) indicates that the improved quadratic model is highly significant as proved by highly significant 'p-values' and 'F-values'.

The obtained 'p-values' and 'F-values' of the model suggested that, the individual (excepting $X_1$), interaction terms (excepting $X_3X_4$) and all other terms are significant. The p-value (<0.0001) of the model shows an excellent fitting with experimental data. The p-value (0.0796) of the 'lack of fit' suggests that insignificant lack of fit, which is good for fitting the data to the model. The values of estimated correlation coefficients, $R^2$, Adjusted $R^2$, Predicted $R^2$ and Adequate precision for the Eq. 5.3 are 0.9737, 0.9545, 0.9017 and 26.845 respectively. The value of $R^2$ (0.9737) which is defined as the ratio of explained variation to the total variation ensures an excellent fit to the experimental data in the present study. The difference between Adjusted $R^2$ (0.9545) and Predicted $R^2$ (0.9017) is 0.0528 (this should be less than 0.2 for reasonable agreement), which confirms a reasonable agreement of Predicted $R^2$ with the Adjusted $R^2$. The value of Adequate precision (26.845) confirms the adequacy of the signal to noise ratio. Additionally, an excellent agreement (within +14.4% to -11.28% error band) between the observed and predicted CEY of AM seed oil, can also be seen from the parity plot for the improved model equation (Eq. 5.3) as shown in Fig. 5.1 (b). However, it has already been discussed previously that the improved/reduced model (Eq. 5.3) could not make any significant difference in the error band (+14.4 to -11.28) as it clear from the Fig. 5.1 (a & b). The percentage of error (% error) was calculated using the formula given below:

$$Error\ (\%) = \frac{\left\{Y_i^{Pre} - Y_i^{Exp}\right\}}{Y_i^{Pre}} \times 100 \quad \ldots \text{Eq. 5.4}$$

Where; $Y_i^{Pre}$ and $Y_i^{Exp}$ are the $i^{th}$ predicted and experimental CEY's respectively.

In short, the ANOVA of the improved quadratic model demonstrated that the model is significant, which is further confirmed by the Fisher's F-test (a high model F-value (50.66) and a very low P-value (P<0.0001)). The BBD showed that the quadratic model matched with the experimental results well. So, this model, can be used to navigate the design space.

A comparison between experimental and predicted CEY versus experimental runs was shown in Fig. 5.2 (a & b). This plot explains the uniform distribution of predicted CEY values around the experimental CEY values, which is a representative of a close fit. Therefore, a correlation between response (CEY) and independent operating parameters (e.g. $X_1$, $X_2$, $X_3$, $X_4$, and $X_5$), a multiple regression is possible and an equation (second-order polynomial model) can be applied to interpreting the correlation between the chosen parameters.

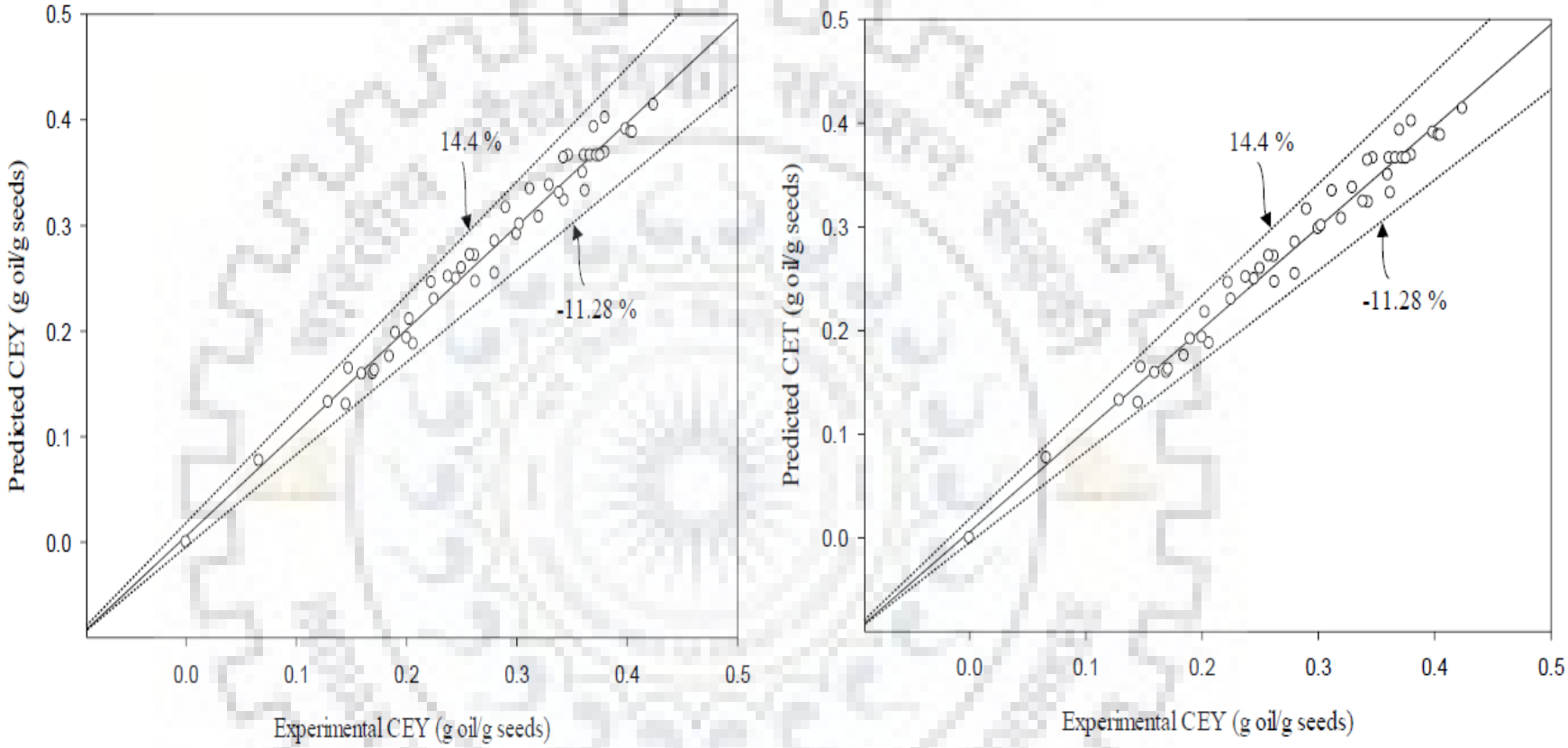


Fig. 5.1: Predicted vs. Experimental values for CEY of AM seed oil for (a) Eq. 5.2 and (b) Eq. 5.3.

Table 5.3. ANOVA analysis and regression coefficients of predicted second-order polynomial model (Eq.5.3) for AM seed oil yield.

| Source | Df | Effect | Coefficient | SE coefficient | Adj SS | Adj MS | t-value | F-value | p-value | |
|---|---|---|---|---|---|---|---|---|---|---|
| **Model** | 19 | | 0.3661 | 0.0078 | 0.3487 | 0.0184 | 46.9359 | 50.66 | < 0.0001 | Significant |
| **Linear Terms** | 5 | | | | | | | | | |
| Temperature: $X_1$ | 1 | -0.01040 | -0.0052 | 0.0048 | 0.0004 | 0.0004 | -1.0833 | 1.19 | 0.2856 | Less significant |
| Pressure: $X_2$ | 1 | 0.14880 | 0.0744 | 0.0048 | 0.0886 | 0.0886 | 15.500 | 244.66 | <0.0001 | Significant |
| Particle size: $X_3$ | 1 | 0.10660 | 0.0533 | 0.0048 | 0.0455 | 0.0455 | 11.1042 | 125.66 | <0.0001 | Significant |
| Flow rate - $CO_2$: $X_4$ | 1 | 0.02600 | 0.0130 | 0.0048 | 0.0027 | 0.0027 | 2.7083 | 7.49 | 0.0111 | Significant |
| % of co-solvent: $X_5$ | 1 | 0.16480 | 0.0824 | 0.0048 | 0.1087 | 0.1087 | 17.1667 | 300.04 | <0.0001 | Significant |
| **2- way interactions** | 09 | | | | | | | | | |
| $X_1X_2$ | 1 | 0.00010 | 0.0399 | 0.0095 | 0.0064 | 0.0064 | 4.2000 | 17.58 | 0.0003 | Significant |
| $X_1X_3$ | 1 | -0.03262 | -0.0408 | 0.0095 | 0.0067 | 0.0067 | -4.2947 | 18.36 | 0.0002 | Significant |
| $X_1X_4$ | 1 | 0.00070 | 0.0175 | 0.0095 | 0.0012 | 0.0012 | 1.8421 | 3.38 | 0.0774 | Significant |
| $X_1X_5$ | 1 | 0.00174 | 0.0434 | 0.0095 | 0.0075 | 0.0075 | 4.5684 | 20.78 | 0.0001 | Significant |
| $X_2X_3$ | 1 | 0.00548 | 0.0257 | 0.0095 | 0.0026 | 0.0026 | 2.7053 | 7.31 | 0.0119 | Significant |
| $X_2X_4$ | 1 | -0.00032 | -0.0302 | 0.0095 | 0.0037 | 0.0037 | -3.1789 | 10.10 | 0.0038 | Significant |
| $X_2X_5$ | 1 | -0.00032 | -0.0295 | 0.0095 | 0.0035 | 0.0035 | -3.1053 | 9.59 | 0.0046 | Significant |
| $X_3X_5$ | 1 | 0.06984 | 0.0218 | 0.0095 | 0.0019 | 0.0019 | 2.2947 | 5.26 | 0.0302 | Significant |
| $X_4X_5$ | 1 | -0.00516 | -0.0322 | 0.0095 | 0.0041 | 0.0041 | -3.3895 | 11.45 | 0.0023 | Significant |
| **Square** | 5 | | | | | | | | | |
| $X_1^2$ | 1 | -0.00026 | -0.0261 | 0.0064 | 0.0060 | 0.0060 | -4.0781 | 16.45 | 0.0004 | Significant |
| $X_2^2$ | 1 | -0.00004 | -0.0561 | 0.0064 | 0.0275 | 0.0275 | -8.7656 | 75.81 | <0.0001 | Significant |
| $X_3^2$ | 1 | -4.82108 | -0.0753 | 0.0064 | 0.0495 | 0.0495 | -11.7656 | 136.71 | <0.0001 | Significant |
| $X_4^2$ | 1 | -0.00524 | -0.0328 | 0.0064 | 0.0094 | 0.0094 | -5.1250 | 25.87 | <0.0001 | Significant |
| $X_5^2$ | 1 | -0.00744 | -0.0465 | 0.0064 | 0.0189 | 0.0189 | -7.2656 | 52.07 | <0.0001 | Significant |
| Residual | 26 | | | | 0.0094 | 0.0004 | | | | |
| Lack of Fit | 21 | | | | 0.0088 | 0.0004 | | 3.61 | 0.0796 | Insignificant |
| Pure Error | 5 | | | | 0.0006 | 0.0001 | | | | |
| Cor Total | 45 | | | | 0.3581 | | | | | |

| | | | | | |
|---|---|---|---|---|---|
| Std. Deviation | : 0.019 | $R^2$ | : 0.9737 | | |
| Mean | : 0.2837 | Adj $R^2$ | : 0.9545 | | |
| C.V. % | : 6.71 | Pred $R^2$ | : 0.9017 | | |
| PRESS | : 0.036 | Adeq Precision | : 26.845 | | |

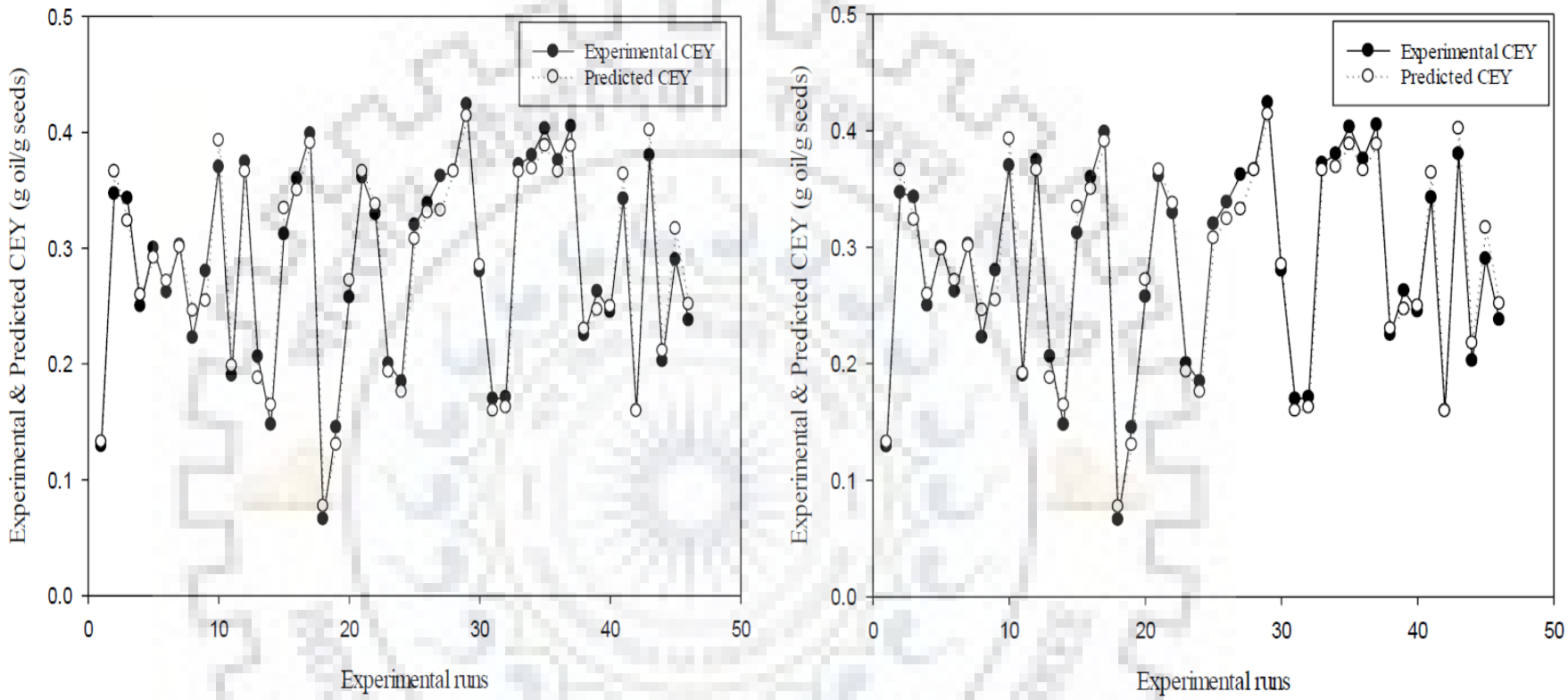


(a) (b)

Fig. 5.2. A comparison of predicted and experimental values of CEY of AM seed oil for each run (1-46) based on (a) Eq. 5.2 and (b) Eq. 5.3.

5.1.1.1 Numerical optimization: based on RSM and its experimental validation

The developed regression model (Eq. 5.3) was used to determine the optimum extraction conditions for SFE of oil from AM seeds. To obtain the optimum values, the first order derivatives of the model (Eq. 5.3), were obtained and equated to zero with respect to $X_1$, $X_2$, $X_3$, $X_4$ and $X_5$ respectively and the developed equations were solved simultaneously. This process has been carried out using Design Expert 10.0 software. For the numerical optimization, the range of input parameters were provided as 60-100 °C (for the temperature), 200-350 bar (for the pressure), 0.5-1.0 mm (for the particle size), 5-15 g/min (for the flow rate-$CO_2$) and 0-10 % (for the % of co-solvent) and under this design space the output parameter (CEY (g oil/g seeds)) has been maximized. The calculated optimal input conditions are; $X_1$ = 85.59 °C, $X_2$ = 304.91 bar, $X_3$ = 0.75 mm, $X_4$ = 11.02 g/min and $X_5$ = 9.25%. However, considering the operability of actual extraction set-up, the optimal conditions can be modified as follows; $X_1$ = 85 °C, $X_2$ = 305 bar, $X_3$ = 0.75 mm, $X_4$ = 11 g/min and $X_5$ = 9 %. After substituting these variables into the model (Eq. 5.3) produced the optimum value of CEY of oil as 0.4286 (CEY or Y = 0.4286).

To compare the experimental CEY with the predicted CEY at optimum input values, three experiments were carried out. Under the modified conditions, the average experimental CEY (0.4211) with standard deviation (0.00017) was obtained which matched well with the predicted value. As a result, the BBD was considered to be an accurate and decisive tool for predicting the maximum CEY of oil from the SFE process of AM seed using SC-$CO_2$.

5.1.2 Development of RSM based correlation for the prediction of CEY for PP seed oil

A regression analysis (as shown in Table F.2) was performed, using the experimental data of 46 runs (as shown in Table 5.2) based on a quadratic model (second order polynomial equation in coded form (Eq. 5.5)) representing the CEY of PP seed oil as a function of independent variables.

$$\begin{aligned} Yield\,(CEY) = {} & 0.1886 - 0.047X_1 + 0.0939X_2 + 0.013X_3 + 0.025X_4 + 0.076X_5 + 0.6\times10^{-3}X_1X_2 \\ & - 0.8\times10^{-3}X_1X_3 - 0.0138X_1X_4 - 0.0206X_1X_5 - 6.4\times10^{-3}X_2X_3 + 0.021X_2X_4 \\ & + 0.0296X_2X_5 + 0.0126X_3X_4 + 0.0197X_3X_5 + 0.0233X_4X_5 - 0.0141X_1^2 \\ & - 0.0038X_2^2 + 0.0072X_3^2 - 0.0357X_4^2 - 0.0184X_5^2 \end{aligned}$$

… Eq. 5.5

The developed model (Eq. 5.5) can be improved by removing the insignificant terms (e.g. $X_1X_2$, $X_1X_3$, $X_2X_3$ and $X_2^2$ ). However, the improved model as given in Eq. 5.6 does not make any significant difference in performance point of view only the complexity of the second order polynomial (quadratic model) could be reduced just by removing the extra insignificant terms.

$$Yield\ (CEY) = 0.1858 - 0.047X_1 + 0.0939X_2 + 0.013X_3 + 0.025X_4 + 0.076X_5 - 0.0138X_1X_4 - 0.0206X_1X_5 + 0.0205X_2X_4 + 0.0296X_2X_5 + 0.0126X_3X_4 + 0.0197X_3X_5 + 0.0233X_4X_5 - 0.0131X_1^2 + 0.0082X_3^2 - 0.0347X_4^2 - 0.0174X_5^2$$

… Eq. 5.6

The adequacy of the developed improved quadratic model (Eq. 5.6) is justified by the ANOVA analysis. The ANOVA results (as shown in Table 5.4) of the improved model, show that the all linear terms ($X_1$, $X_2$, $X_3$, $X_4$, and $X_5$) are highly significant. On the other hand, the quadratic terms ($X_1X_5$, $X_2X_4$, $X_2X_5$, $X_3X_5$, and $X_4X5$) are highly significant (with p-value < 0.0001) while the other quadratic terms ($X_3X_4$, and $X_1X_4$) are less significant (0.0001 < p-value < 0.05). Moreover, among all the interaction terms, three interactive terms (e.g. $X_1X_2$, $X_1X_3$, and $X_2X_3$) are insignificant with the p-value > 0.05 and that have been removed to produce the model Eq. 5.6. The ANOVA and regression analysis of the obtained improved model has also shown the values of coefficient of determination ($R^2$), Predicted $R^2$, Adjusted $R^2$, Adequate Precision, p-value and F-value as 0.9944, 0.9846, 0.9913, 72.0695, <0.0001 and 322.36 respectively.

The value of $R^2$ (0.9944) which has already been defined in section 5.1.1 ensures an excellent fit to the experimental data of the present study. The difference between Adjusted $R^2$ (0.9913) and Predicted $R^2$ (0.9846) is 0.0067 (this should be less than 0.2), which confirms a highly reasonable agreement of Predicted $R^2$ (0.9846) with the Adjusted $R^2$ (0.9913). The value of Adequate Precision (72.0695) confirms the adequacy of the signal to noise ratio. The 'p-value' of the model is less than 0.0001, which shows excellent fitting with experimental data. The 'p-value' of the 'lack of fit' is 0.0519, which suggests the insignificant lack of fit, which is good for fitting the data to the model. The ANOVA analysis of this model also demonstrated that the obtained model is significant, which is further confirmed by the Fisher's 'F-test' (a high model F-value (322.36).

The predicted residual sum of squares (PRESS = 0.0048) is a measure of how well the model fits each point in the design means the smaller the PRESS statistic, the better the model fits the data points. Additionally, an excellent agreement (within +18.39% to -16.32%) between the observed and predicted CEY of PP seed oil is obvious from the parity plot as shown in Fig. 5.3 (b). The only one data point (Run 18) show error values as -25.87%. Except for this one data point, the BBD showed that improved quadratic model matched with the experimental results well. So, this model can be used to navigate the design space. On the other hand, the model (Eq. 5.5) with all insignificant terms produced an error band (+12.98 to -5.92 %) with two data points (run 14 & 18) with the maximum error as -26.56 % and -35.79 % respectively. From the Fig. 5.3 (a & b), it is clear that the improved model (Eq. 5.6) reduced the maximum error data points from 2 to 1. A comparison between experimental and predicted CEY versus experimental runs was shown in Fig. 5.4 (a & b). This plot explains the uniform distribution of predicted CEY values around the experimental CEY values, which is a representative of a close fit. Therefore, a correlation between response (CEY) and independent operating parameters (e.g. $X_1$, $X_2$, $X_3$, $X_4$, and $X_5$), a multiple regression is possible and an improved model equation (Eq. 5.6) can be applied to interpreting the correlation between the chosen parameters.

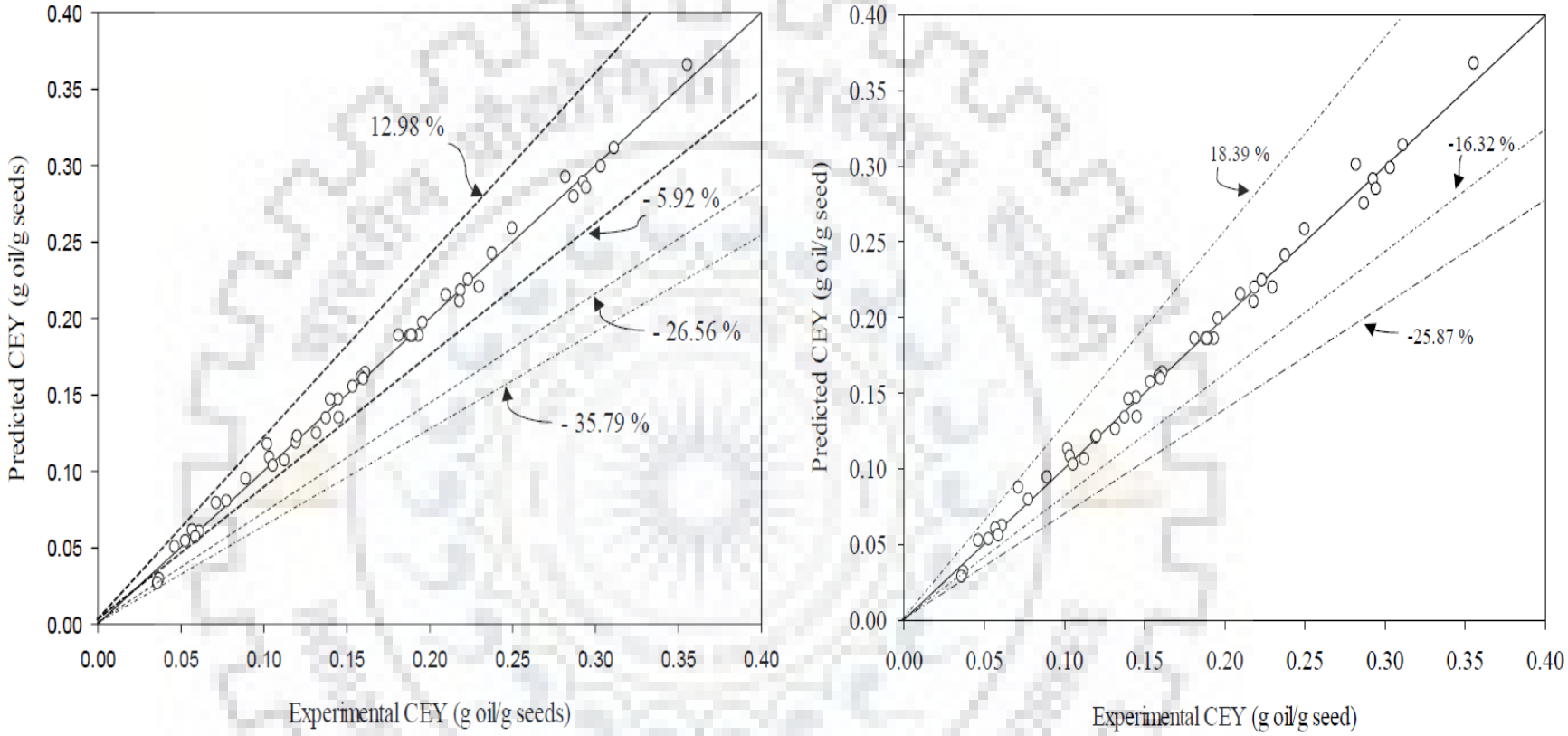


(a) (b)

Fig. 5.3: Predicted vs. Experimental CEY of PP seed oil for (a) Eq. 5.5 and (b) Eq. 5.6.

Table 5.4. ANOVA analysis and regression coefficients of predicted second-order polynomial model (Eq. 5.6) for PP seed oil yield.

| Source | Df | Effect | Coefficient | SE coefficient | Adj SS | Adj MS | t-value | F-value | p-value | |
|---|---|---|---|---|---|---|---|---|---|---|
| **Model** | 16 | | 0.1858 | 0.0025 | 0.3087 | 0.0193 | 74.32 | 322.36 | < 0.0001 | Significant |
| **Linear Terms** | 5 | | | | | | | | | |
| Temperature: $X_1$ | 1 | -0.0940 | -0.0470 | 0.0019 | 0.0354 | 0.0354 | -24.74 | 591.27 | <0.0001 | Significant |
| Pressure: $X_2$ | 1 | 0.1878 | 0.0939 | 0.0019 | 0.1410 | 0.1410 | 49.42 | 2355.92 | <0.0001 | Significant |
| Particle size: $X_3$ | 1 | 0.0256 | 0.0128 | 0.0019 | 0.0026 | 0.0026 | 6.74 | 43.62 | <0.0001 | Significant |
| Flow rate - $CO_2$: $X_4$ | 1 | 0.051 | 0.0255 | 0.0019 | 0.0104 | 0.0104 | 13.42 | 173.33 | <0.0001 | Significant |
| Co-solvent %: $X_5$ | 1 | 0.1512 | 0.0756 | 0.0019 | 0.0914 | 0.0914 | 39.79 | 1527.79 | <0.0001 | Significant |
| **2- way interactions** | 07 | | | | | | | | | |
| $X_1X_4$ | 1 | -0.0276 | -0.0138 | 0.0039 | 0.0008 | 0.0008 | -3.54 | 12.77 | 0.0013 | Significant |
| $X_1X_5$ | 1 | -0.0412 | -0.0206 | 0.0039 | 0.0017 | 0.0017 | -5.28 | 28.33 | <0.0001 | Significant |
| $X_2X_4$ | 1 | 0.0410 | 0.0205 | 0.0039 | 0.0017 | 0.0017 | 5.26 | 28.13 | <0.0001 | Significant |
| $X_2X_5$ | 1 | 0.0592 | 0.0296 | 0.0039 | 0.0035 | 0.0035 | 7.59 | 58.54 | <0.0001 | Significant |
| $X_3X_4$ | 1 | 0.0252 | 0.0126 | 0.0039 | 0.0006 | 0.0006 | 3.23 | 10.69 | 0.0028 | Significant |
| $X_3X_5$ | 1 | 0.0394 | 0.0197 | 0.0039 | 0.0016 | 0.0016 | 5.05 | 25.96 | <0.0001 | Significant |
| $X_4X_5$ | 1 | 0.0466 | 0.0233 | 0.0039 | 0.0022 | 0.0022 | 5.97 | 36.20 | <0.0001 | Significant |
| **Square** | 4 | | | | | | | | | |
| $X_1^2$ | 1 | -0.0262 | -0.0131 | 0.0025 | 0.0016 | 0.0016 | -5.24 | 26.92 | <0.0001 | Significant |
| $X_3^2$ | 1 | 0.0164 | 0.0082 | 0.0025 | 0.0006 | 0.0006 | 3.28 | 10.61 | 0.0029 | Significant |
| $X_4^2$ | 1 | -0.0694 | -0.0347 | 0.0025 | 0.0114 | 0.0114 | -13.88 | 189.87 | <0.0001 | Significant |
| $X_5^2$ | 1 | -0.0348 | -0.0174 | 0.0025 | 0.0028 | 0.0028 | -6.96 | 47.61 | <0.0001 | Significant |
| Residual | 29 | | | | 0.0017 | 0.0001 | | | | |
| Lack of Fit | 24 | | | | 0.0017 | 0.0001 | | 4.45 | 0.0519 | Insignificant |
| Pure Error | 5 | | | | 0.0001 | 0.00000 | | | | |
| Cor Total | 45 | | | | 0.3104 | | | | | |

| | | | | | |
|---|---|---|---|---|---|
| Std. Deviation | : 0.0077 | $R^2$ | : 0.9944 | | |
| Mean | : 0.1660 | Adj. $R^2$ | : 0.9913 | | |
| C.V. % | : 4.66 | Pred. $R^2$ | : 0.9846 | | |
| PRESS | : 0.0048 | Adeq. Precision | : 72.0695 | | |

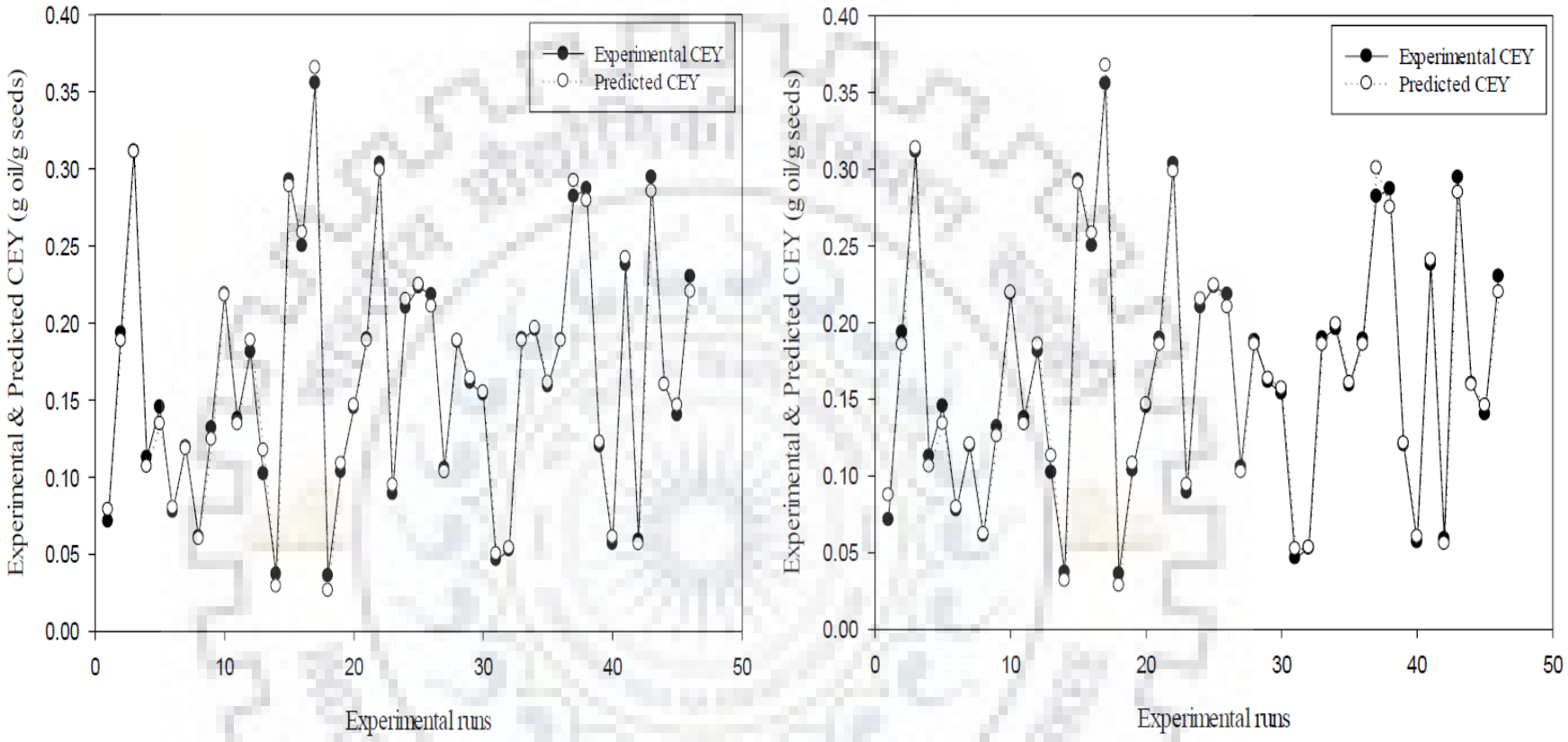


Fig. 5.4: A comparison of experimental and predicted values of CEY of PP seed oil for each run (1-46) based on (a) Eq. 5.5 and (b) Eq. 5.6.

5.1.2.1 Numerical optimization: based on RSM and its experimental validation

The developed regression improved model (Eq. 5.6) was used to determine the optimum extraction conditions for SFE of oil from PP seeds. To obtain the optimum values, the first order derivatives of the model (Eq. 5.6) were obtained and equated to zero with respect to $X_1$, $X_2$, $X_3$, $X_4$ and $X_5$ respectively and it has been carried out using Design Expert 10.0 software. For the numerical optimization of these parameters, the range of input parameters were provided as 60-100 °C (for temperature), 200-350 bar (for pressure), 0.5-1.0 mm (for the particle size), 5-15 g/min (for the flow rate-$CO_2$) and 0-10 % (for the % of co-solvent) while the output parameter (CEY (g oil/g seeds) is to be maximized. The calculated optimal parametric conditions are; $X_1$ = 60 °C, $X_2$ = 333 bar, $X_3$ = 1.0 mm, $X_4$ = 7 g/min and $X_5$ = 9 %. After substituting these variables into the model (Eq. 5.6) produced the optimum value of oil yield as 0.36 (Y = 0.36).

To compare the experimental with the predicted CEY, the experiments (triplicates) were carried out at the modified optimal extraction conditions. Under the modified conditions, the average experimental yield (0.36003) with standard deviation (0.000208) was obtained, which matched well with the predicted value. As a result, the BBD was considered to be an accurate and decisive tool for predicting the maximum CEY of oil from the SFE of PP seed using SC-$CO_2$.

5.1.3. Optimization of FFBP-ANN configuration for the SFE of AM seeds

In the present work, different discrete input operating conditions such as temperature (60, 80, 100 °C), pressure (200, 275, 350 bar), particle size (0.5, 0.75, 1.0 mm), flow rate-$CO_2$ (5, 10, 15 g/min) and the % of co-solvent (0, 5, 10 % of $CO_2$ flow rate) were used for the development of the feed-forward back-propagation artificial neural network (FFBP-ANN) model for the prediction of CEY (g oil/g seeds). Firstly, 32 data points were used for training the ANN model. The correlation-capability (CC) of the developed ANN model was evaluated based on the total 46 experimental data points. The obtained results, which are based on trial and error procedure, lead to the finding that the optimal number of neurons as 6 in the hidden layer as shown in Fig. 5.5 which depicts optimized FFBP-ANN model.

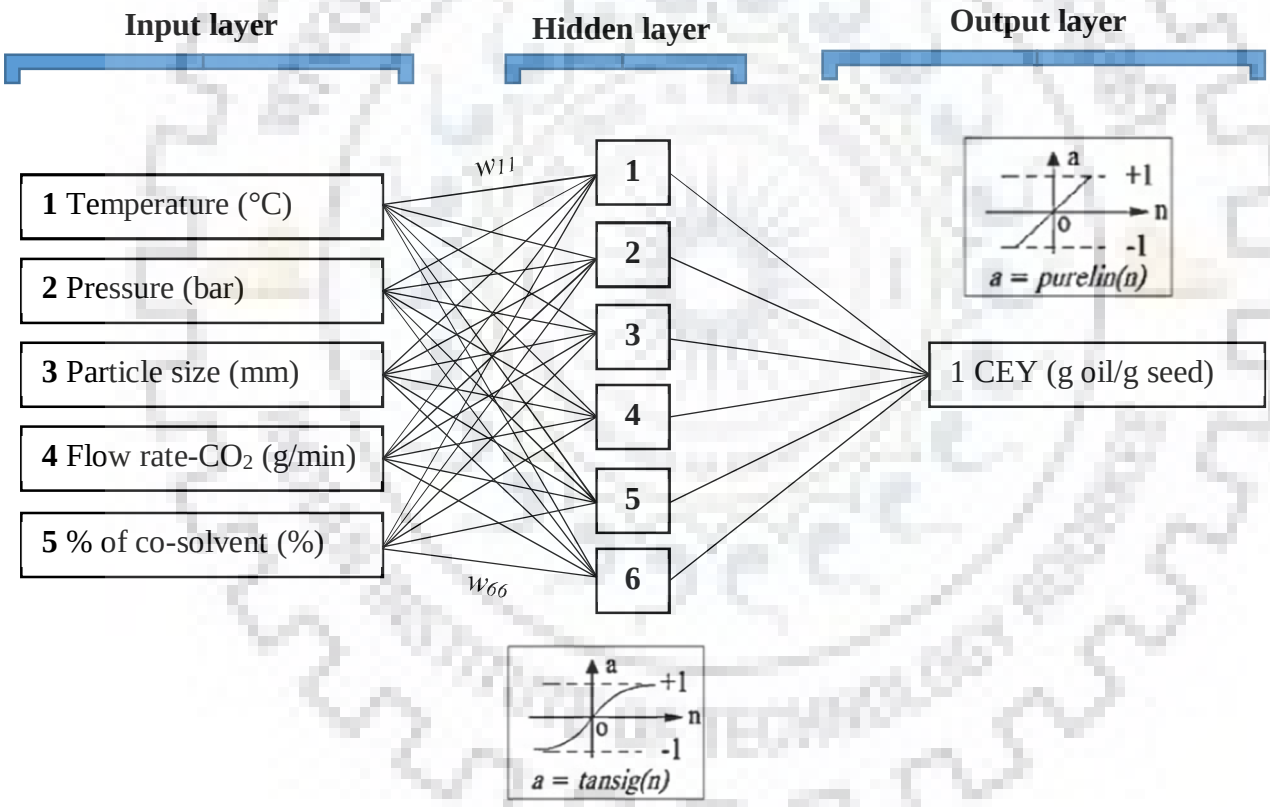


Fig. 5.5: Optimized FFBP-ANN configuration to predict the CEY of the AM seed oil during the SFE process.

The results of the obtained AARD %, MSE and $R^2$ values for the different numbers of the hidden neurons were given in Table 5.5.

Table 5.5: Results of topological studies to find the optimal FFBP-ANN configuration during the SFE of AM seed oil.

| Hidden neuron | AARD % | MSE | $R^2$ |
|---|---|---|---|
| 1 | 14.8620 | 0.0448 | 0.8500 |
| 2 | 9.6779 | 0.0350 | 0.9414 |
| 3 | 7.9362 | 0.0156 | 0.9658 |
| 4 | 10.5470 | 0.0106 | 0.9290 |
| 5 | 9.3650 | 0.0100 | 0.9218 |
| **6** | **3.3292** | **0.0038** | **0.9835** |
| 7 | 6.1287 | 0.0099 | 0.9759 |
| 8 | 7.0714 | 0.0241 | 0.9727 |
| 9 | 4.3730 | 0.0540 | 0.9728 |

Note: The bold values indicate the condition, achieved by the optimal FFBP-ANN configuration.

The network was trained several times by applying randomly generated initial values of the network parameters (e.g. weight and bias coefficients) which could affect the values of AARD % and MSE and finally resulted in the best values of AARD %, MSE and $R^2$ as shown in Table 5.5,. As mentioned earlier (in section 2.9), the network with least error measures (e.g. AARD % and MSE) and best regression coefficient ($R^2$), was selected as the optimal network configuration. Finally, it can be concluded that a FFBP-ANN model with a 5×6×1 configuration leads to the minimum level of error (e.g. AARD % and MSE) while correlating experimental data and is designated as FFBP-ANN [5-6-1]. In the present FFBP-ANN configuration, TANSIG and PURELIN were used as the activation functions in the hidden and output layer respectively as shown in Fig. 5.5. The ANN was trained through over 1000 epochs with error back propagation (EBP) training. The correlation between the experimental and ANN predicted CEY for training, validation, testing and overall data sets are shown in Fig. 5.6. The perfect fit (ANN model prediction equal to experimental data) was shown by solid line. A close proximity of the best linear fit to the perfect fit has been observed, which confirms a good correlation between the experimental CEY and the FFBP-ANN [5-6-1] model predicted CEY.

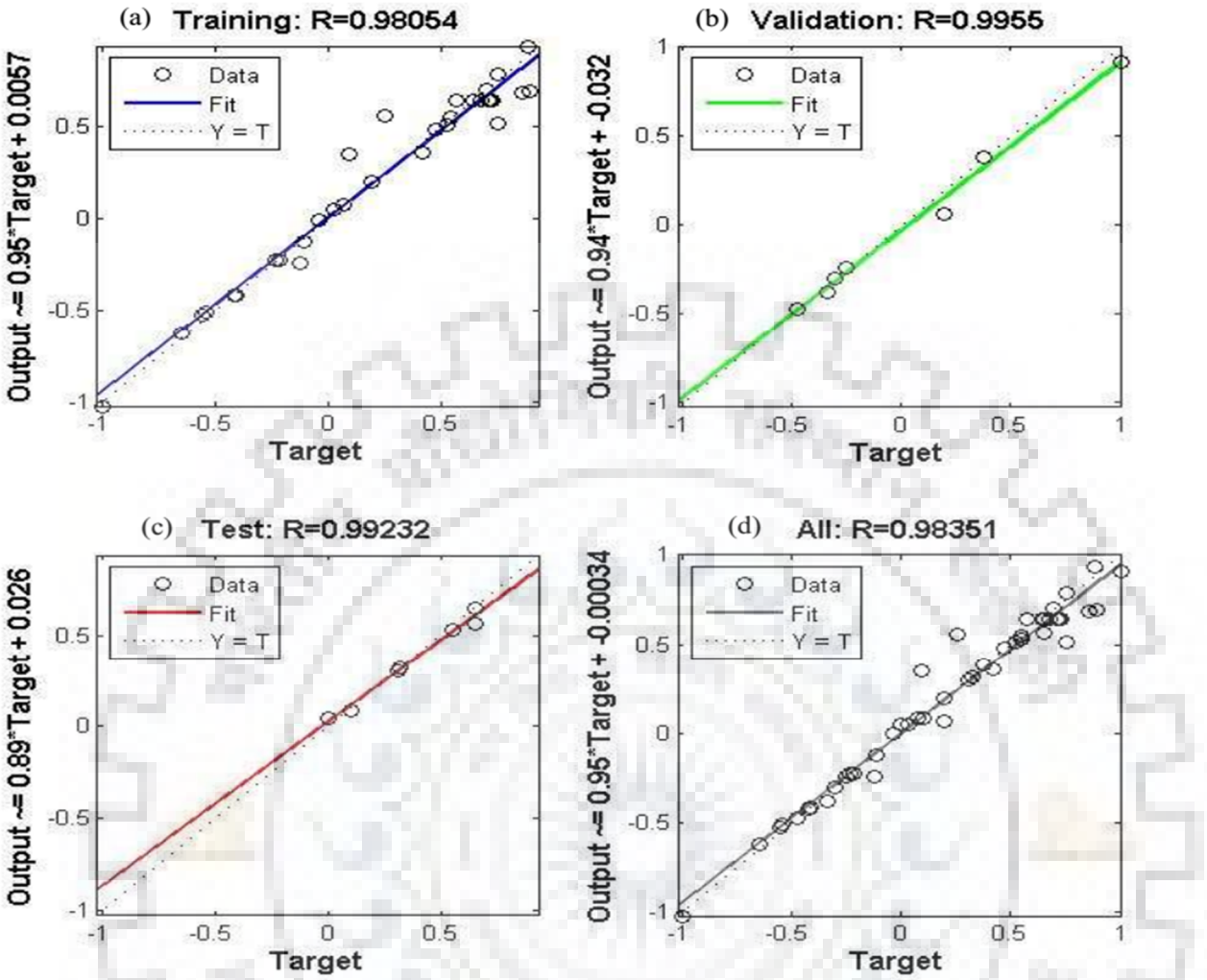


Fig. 5.6: The scatter plots of FFBP-ANN [5-6-1] for (a) training, (b) validation, (c) testing and (d) all data sets during the SFE of AM seed oil.

5.1.3.1 Development of ANN based correlation for the prediction of CEY for AM seed oil

As discussed in section 2.9, steps (1-5) were followed for developing the ANN-based equation model. For the ANN modeling, the normalization, of the independent operating parameters (e.g. temperature, pressure, particle size, flow rate-$CO_2$ and % of co-solvent), was done as follows;

$$T_{norm} = 0.05*T - 4 \quad \ldots \text{Eq. 5.7}$$

$$P_{norm} = 0.0133*P - 3.667 \quad \ldots \text{Eq. 5.8}$$

$$PS_{norm} = 4*PS - 3 \quad \ldots \text{Eq. 5.9}$$

$$FR_{norm} = 0.2*FR - 2 \quad \ldots \text{Eq. 5.10}$$

$$CoS_{norm} = 0.2*CoS - 1 \quad \ldots \text{Eq. 5.11}$$

Where, $T_{norm}$, $P_{norm}$, $PS_{norm}$, $FR_{norm}$ and $CoS_{norm}$ are the normalized values (-1 to +1) of temperature, pressure, particle size, flow rate-$CO_2$ and % of co-solvent respectively. All the five parameters (e.g. temperature, pressure, particle size, flow rate-$CO_2$ and % of co-solvent) were denoted as P, T, PS, FR and CoS% respectively during the ANN modeling of both seeds (AM and PP seeds). All the five independent operating parameters with their three levels are normalized under the values of -1 to +1 because the chosen TANSIG and PURELIN transfer functions varies in the same range (as shown in Fig. 5.5).

Weights (W) and biases (b) were assigned to the normalized parameters at the hidden layer and for the output layer the weights and biases were also generated by the network as shown in Fig. 5.5. The listed weights and biases in Table 5.6, were assigned for each of the input variables, based on the obtained optimized network (e.g. FFBP-ANN [5-6-1]) means six neurons in hidden layer of the FFBP-ANN with five neurons in input layer and one neuron in output. The values ($A_{111}$ to $A_{161}$) from a linear relationship were calculated for each experimental conditions (run 1 to run 46), using Eq. 2.6 (as given in section 2.9). Still following the lead provided in the section 2.9 and Fig. 5.5, the next step is the 'TANSIG' transfer function for '$B_{lin}$' at the hidden layer. The expression for the transfer function was expressed in Eq. 2.7 (as given in section 2.9) through which the values ($B_{111}$ to $B_{161}$) were determined for each aggregate values of ($A_{111}$ *to* $A_{161}$). Next step is to determine the output using PURELIN transfer function using Eq. 2.8 (as given in section 2.9). Now, the resulting expression was de-normalized, as described in the section 2.9. The final expression for CEY, after de-normalization, was shown in Eq. 5.12.

$$Y_{CEY} = 0.072284 * B_1 - 0.062484 * B_2 - 0.105103 * B_3 - 0.026097 * B_4 + 0.0327087 * B_5 + 0.026476 * B_6 + 0.154136$$

… Eq. 5.12

Where, $B_{lin}$ is given as $B_i$ for each of six neurons in FFBP-ANN [5-6-1], as defined in Eq. 2.7 (as given in section 2.9). Eq. 5.12, is the final expression of the ANN-based equation which was used to see the effect of individual effect of parameters on CEY of AM seed oil.

Table 5.6: Weights and biases of the trainable FFBP-ANN [5-6-1] model during the SFE of AM seed oil.

| Neuron | Hidden layer | | | | | | Output layer | |
|---|---|---|---|---|---|---|---|---|
| | Weights ($w_{ij}$)[a] | | | | | Biases | Weight | Bias |
| | T | P | PS | FR | CoS % | $b_j$ | $(W_{jk})^b$ | $b_k$ |
| 1 | -0.2913 | 0.1083 | 4.4960 | 0.4376 | 1.2266 | 0.8689 | 0.4038 | -0.5076 |
| 2 | 0.1623 | -1.1605 | -2.1718 | -1.0356 | -1.3374 | -3.4049 | -0.3491 | |
| 3 | 1.0228 | -3.1123 | 1.6703 | -0.5529 | -1.3596 | -2.1165 | -0.5872 | |
| 4 | -2.0045 | 2.3014 | -0.3659 | -0.5558 | -1.0969 | -0.3537 | -0.1458 | |
| 5 | 0.7847 | 0.8025 | -0.0588 | -1.9313 | -0.3303 | 0.2738 | 0.1827 | |
| 6 | -1.0731 | -1.5492 | 1.7209 | -0.4544 | -0.2518 | -2.8087 | 0.1479 | |

a : Weight connection from the input layer to hidden layer.
b : Weight connection from the hidden layer to output layer.

5.1.3.2. Performance of FFBP-ANN models for AM seed oil

The performance of the developed FFBP-ANN [5-6-1] model was judge by comparing its performance with some other tested FFBP-ANN configurations (models) such as FFBP-ANN [5-1-1], FFBP-ANN [5-2-1], FFBP-ANN [5-3-1] etc. These other tested configurations (models) were created by changing of the number of neurons (1 to 9) in the hidden layer during the optimization of FFBP-ANN configuration. All these tested models were compared based on some statistical parameters (e.g. AARD %, MSE, $R^2$ and NSEC) as shown in Fig. 5.7. From this figure (Fig. 5.7 (a-d)), it is clear that the FFBP-ANN [5-6-1] model, with single hidden layer performed well and resulted minimum AARD % (3.33%), minimum MSE (0.0038), maximum values of $R^2$ (0.9835) and NSEC (0.9664) among all the tested FFBP-ANN models. The AARD % shows the spreading of data from the central point which is the lowest among all the tested FFBP-ANN models for the configuration ANN-FFBP [5-6-1]. Similar pattern was also observed with MSE as shown in Fig. 5.7 (b). However, in comparison, AARD is higher than MSE for all models. This difference between AARD % and MSE is purely because of their mathematical representation as depicted in Eq. 2.9 and Eq. 2.10 respectively (as given in section 2.10). The highest value of NSEC ('0.9664' as shown in Fig. 5.7 (d)) indicates the highest efficiency of the optimum model FFBP-ANN [5-6-1] over the other tested models (e.g. FFBP-ANN [5-7-1] ('0.9461'), FFBP-ANN [5-8-1] ('0.9418'), FFBP-ANN [5-9-1] ('0.9403')). Similarly, the correlation coefficient ($R^2$), was employed to judge the

performances of the models. The closer the correlation coefficient ($R^2$) to one, the better is the performance of the model. The Fig. 5.7 (c) also shows that the FFBP-ANN [5-6-1] continues to exhibit the best performance.

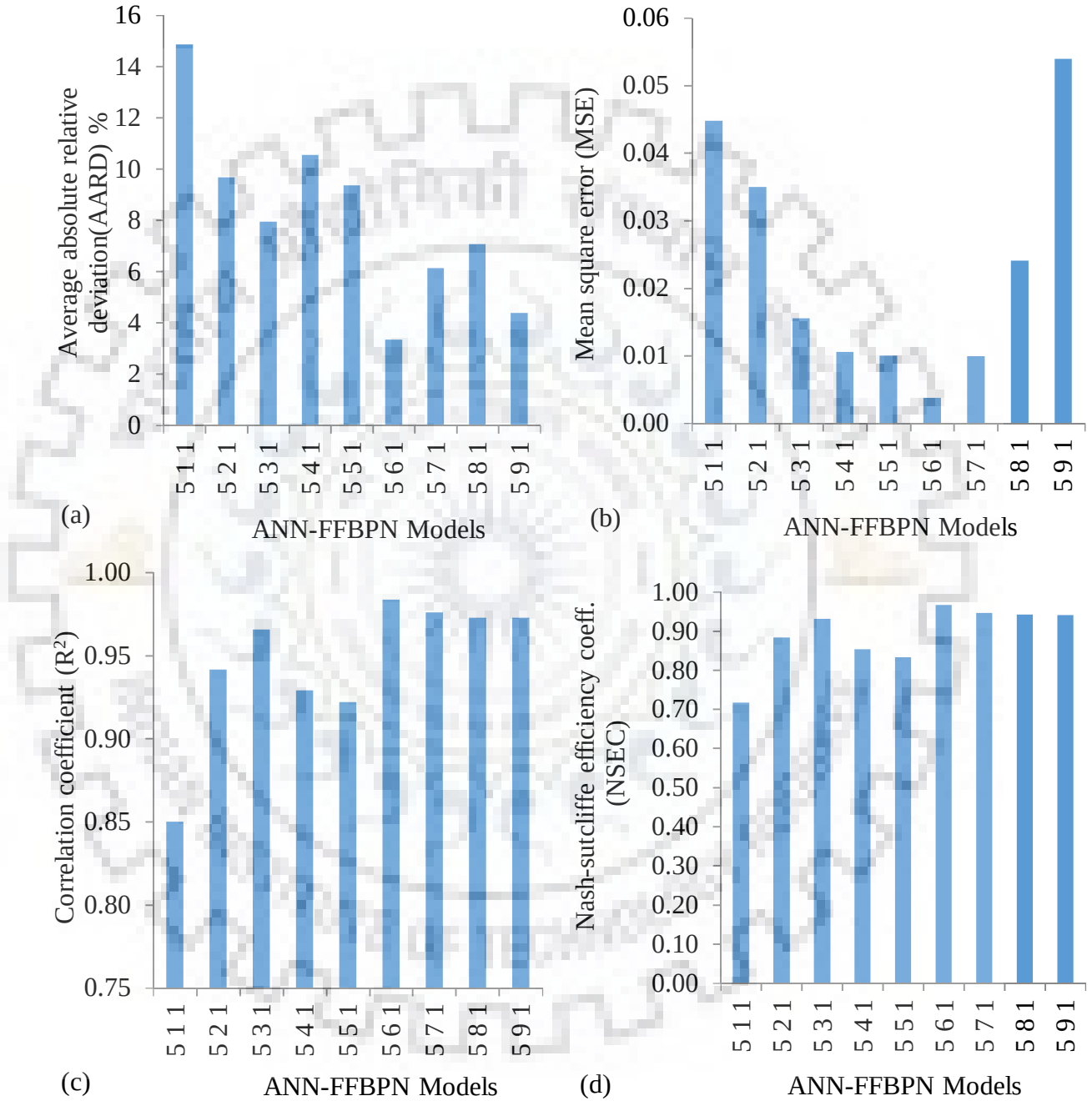


Fig. 5.7: Performances of different FFBP-ANN models based on some statistical parameters (AARD %, MSE, $R^2$ and NSEC) during the SFE of AM seed oil.

5.1.3.3 Sensitivity analysis of optimized FFBP-ANN model for AM seed oil

Sensitivity analysis (SA) was carried out to determine, how the uncertainty in the output of the developed FFBP-ANN model can be related to different sources of uncertainty in the experimental data input. In this study, the possible interaction of chosen parameters was evaluated to determine their performance with respect to each other. Therefore, five groups (e.g. one, two, three, four and five variables) were formed and investigated separately by the achieved optimal FFBP-ANN [5-6-1] model. The results of the analysis were shown in Table 5.7.

From the Table 5.7, it is clear that CoS % with mean square error (MSE) = 0.114 is the most effective parameter in the group of one variable. The other parameters (P, PS, FR, and T) have also shown the significant effect with MSE=0.121, 0.23, 0.233, and 0.263 respectively. From the findings of optimized FFBP-ANN [5-6-1] model, it can be seen that all five-extraction parameters have significant effect, in the following order: CoS % > P > PS > FR > T, on extraction yield of AM seed oil. As shown in Table 5.7, the value of MSE significantly decreased when CoS %, FR, P and PS were used in interaction with the group of two variables. The lowest values of MSE (0.071, 0.074 and 0.097) were determined during the interaction of 'PS with P', 'PS with CoS %' and 'PS with FR' respectively. Other combinations (e.g. 'T + FR', 'P + CoS %', and 'FR + CoS %') in the group of two variables have also shown a strong interactive effect with MSE's 0.185, 0.133, 0.110 respectively. The minimum value of MSE for the group of three variables was found to be '0.035' with the interaction of 'P + PS + CoS %' while the lower value of MSE's (0.054) for the group of four variables were determined with the interaction of 'T + P + PS + CoS %'. The value of MSE was decreased drastically from 0.054 to 0.0038 when FR was involved in interaction with other variables (e.g. T, P, PS, FR, and CoS %) in the group of five variables.

Table 5.7. Sensitivity analysis of the input variables for the FFBP-ANN [5-6-1] model during the SFE of AM seed oil.

| No. | Combination | MSE | $R^2$ | Equation |
|---|---|---|---|---|
| | **Group of one variables** | | | |
| 1 | T | 0.263 | 0.0372 | y = 0.0003x + 0.2903 |
| 2 | P | 0.121 | 0.5100 | y = 0.3497x + 0.1999 |
| 3 | PS | 0.230 | 0.4500 | y = 1.0373x - 0.0108 |
| 4 | FR | 0.233 | 0.0800 | y = 0.6194x + 0.1063 |
| 5 | CoS % | 0.114 | 0.5594 | y = 0.9544x + 0.0163 |
| | **Group of two variables** | | | |
| 6 | T + P | 0.379 | 0.5390 | y = 0.4228x + 0.1723 |
| 7 | T + PS | 0.387 | 0.2701 | y = 0.9345x - 0.001 |
| 8 | T + FR | 0.185 | 0.0288 | y = -0.0881x + 0.3098 |
| 9 | T + CoS % | 0.280 | 0.5345 | y = 1.0842x - 0.0173 |
| 10 | P + PS | 0.071 | 0.6860 | y = 1.2623x - 0.0697 |
| 11 | P + FR | 0.219 | 0.5288 | y = 0.7106x + 0.0747 |
| 12 | P + CoS % | 0.133 | 0.7518 | y = 1.097x - 0.0269 |
| 13 | PS + FR | 0.097 | 0.3594 | y = 0.7242x + 0.0681 |
| 14 | PS + CoS % | 0.074 | 0.7100 | y = 0.9307x + 0.0199 |
| 15 | FR + CoS % | 0.110 | 0.4860 | y = 1.0782x - 0.0205 |
| | **Group of three variables** | | | |
| 16 | T + P + PS | 0.061 | 0.7363 | y = 0.9319x + 0.0138 |
| 17 | T + P + FR | 0.055 | 0.5283 | y = 0.7272x + 0.067 |
| 18 | T + P + CoS % | 0.269 | 0.7686 | y = 0.8375x + 0.0457 |
| 19 | P + PS + FR | 0.054 | 0.6792 | y = 0.854x + 0.0339 |
| 20 | P + PS + CoS % | 0.035 | 0.8342 | y = 0.8801x + 0.0446 |
| 21 | PS + FR + CoS % | 0.142 | 0.7049 | y = 0.8185x + 0.0553 |
| | **Group of four variables** | | | |
| 22 | T + P + PS + FR | 0.086 | 0.7053 | y = 0.8968x + 0.027 |
| 23 | T + P + PS + CoS % | 0.054 | 0.9219 | y = 0.8955x + 0.0414 |
| 24 | P + PS + FR + CoS % | 0.077 | 0.9127 | y = 0.9879x + 0.0136 |
| | **Group of five variables** | | | |
| 25 | T + P + PS + FR + CoS % | 0.0038 | 0.9835 | y = 1.0193x - 0.0034 |

Note: All five parameters (temperature, pressure, particle size, flow rate-$CO_2$ and % of co-solvent) are denoted as T, P, PS, FR and CoS %.

5.1.4 Optimization of FFBP-ANN configuration for the SFE of PP seeds

In this work, different operating conditions of all five parameters (as mentioned in section 5.1.3) are also be used in feed-forward back-propagation artificial neural network (FFBP-ANN) model for the prediction of CEY (g oil/g seeds) of PP seed oil. Similar to previous case (for AM seed oil in section 5.1.3), the same approach was adopted as: firstly, 32 data points, were used for training the FFBP-ANN model. The correlation-capability (CC) of the developed FFBP-ANN model was evaluated based on the total 46 experimental data points. The obtained results, which are based on trial and error procedure lead to find out 6 neurons as the optimal number of neurons in the hidden layer as shown in Fig. 5.8 as an optimized FFBP-ANN [5-6-1] model.

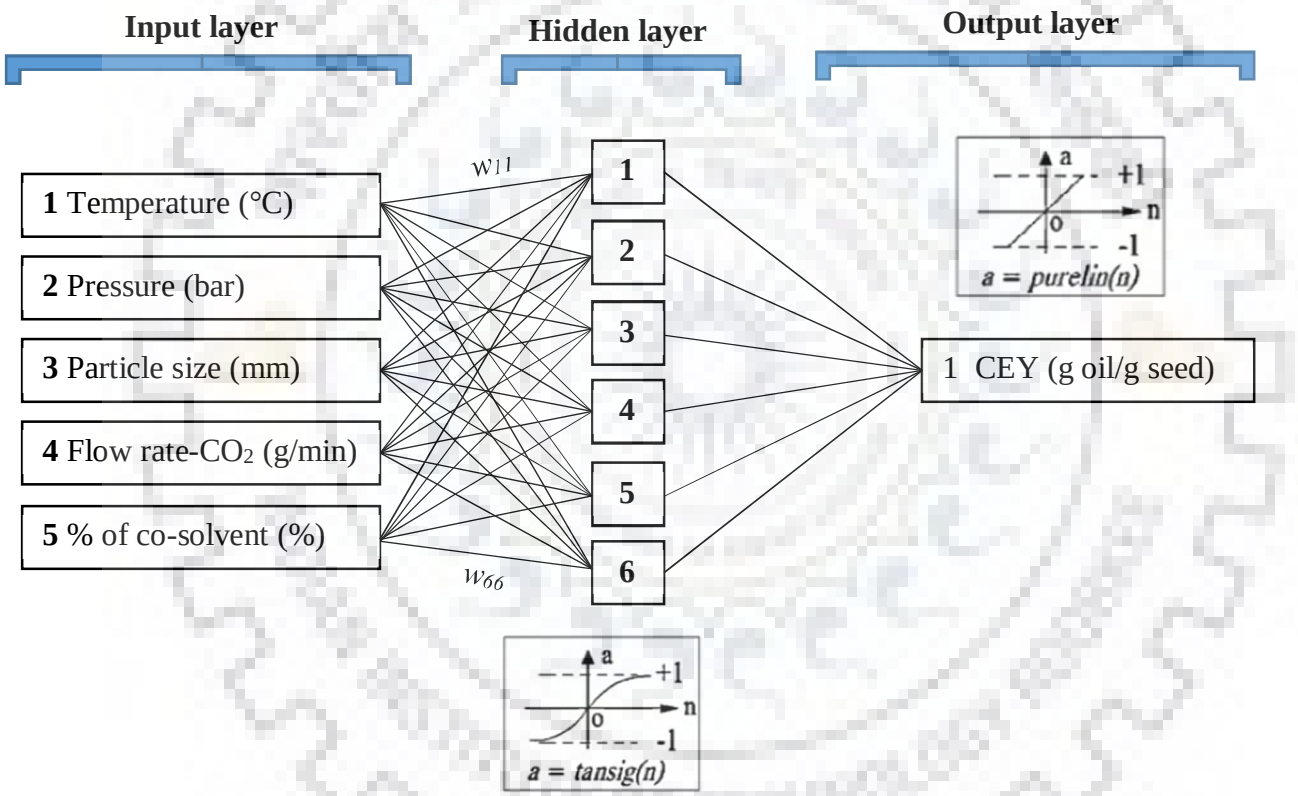


Fig. 5.8: Optimized FFBP-ANN configuration to predict the CEY of the PP seed oil during the SFE process.

The results of the obtained AARD %, MSE and $R^2$ values for the different numbers of the hidden neurons were given in Table 5.8.

Table 5.8: Results of topological studies to find the optimal FFBP-ANN configuration during the SFE of PP seed oil.

| Hidden neuron | AARD % | MSE | $R^2$ |
|---|---|---|---|
| 1 | 16.0369 | 0.06723 | 0.9555 |
| 2 | 13.6251 | 0.01390 | 0.9628 |
| 3 | 13.3677 | 0.00749 | 0.9649 |
| 4 | 11.0518 | 0.00423 | 0.9756 |
| 5 | 7.47180 | 0.00100 | 0.9795 |
| **6** | **4.39994** | **0.00051** | **0.9874** |
| 7 | 5.26161 | 0.00059 | 0.9794 |
| 8 | 7.00744 | 0.00502 | 0.9812 |
| 9 | 12.7286 | 0.00621 | 0.9705 |

Note: The bold values indicate the condition, achieved by the optimal FFBP-ANN configuration.

The network was trained several times (as it was done in the previous case) by applying randomly generated initial values of the network parameters (e.g. weight and bias coefficients) which could affect the values of AARD % and MSE and finally resulted in the best values of AARD %, MSE and $R^2$ as shown in Table 5.9. Table 5.9 make able anyone to reproduces every used data points in the present work. As mentioned earlier (section 2.9), the network with least error measures (e.g. AARD % and MSE), and suitable regression coefficient ($R^2$), was chosen as the optimal network configuration. Finally, from the study, it can be understood that a FFBP-ANN model with the configuration of 5×6×1 leads to the minimum level of error (e.g. AARD % & MSE) during the correlation of experimental data. Therefore, it can be concluded that proposed ANN model with the number of neurons, 5, 6 and 1 in the input, hidden and output layer respectively could be considered as the best ANN architecture. The obtained optimized model was named as FFBP-ANN [5-6-1].

TANSIG and PURELIN were used as the activation functions in the hidden and output layer respectively. The ANN was trained through over 1000 epochs with error back propagation (EBP) training. The correlation between the experimental and ANN predicted CEY for training, validation, testing and overall data sets are shown in Fig. 5.9. The perfect fit (ANN model prediction equal to experimental data) was shown by solid line. A close proximity of the best linear fit to the perfect fit has been observed, as shown in Fig. 5.9, which confirms a good correlation between the experimental CEY and the FFBP-ANN [5-6-1] model CEY of PP seed oil. The listed weights and biases in Table 5.9, were assigned for each of the input variables, based on the six neurons in FFBP-ANN [5-6-1].

Table 5.9. Weights and biases of the trainable FFBPN [5-6-1] model for the optimal during the SFE of PP seed oil.

| | Hidden layer | | | | | | Output layer | |
|---|---|---|---|---|---|---|---|---|
| | Weights ($w_{ij}$)[a] | | | | | Biases | Weight | Bias |
| Neuron | T | P | PS | FR | CoS % | $b_j$ | $(W_{jk})^b$ | $b_k$ |
| 1 | -2.0203 | 1.0876 | 0.79929 | 2.2282 | -0.18888 | 1.5883 | 0.30745 | -0.39531 |
| 2 | 1.2052 | -0.27448 | 1.2274 | -1.3974 | -2.3299 | -1.4943 | -0.29300 | |
| 3 | -1.4486 | 1.1717 | 0.58307 | 2.3296 | 1.3074 | -0.84494 | -0.60232 | |
| 4 | -1.0198 | -1.4234 | -0.73797 | 1.3563 | -1.0298 | 0.006677 | -0.40896 | |
| 5 | -1.7447 | 1.3904 | 0.31439 | 1.8873 | 1.4216 | -1.2132 | 0.86195 | |
| 6 | -0.4046 | -0.745 | -0.54985 | -1.458 | 1.5243 | -2.3218 | -0.10658 | |

a : Weight connection from the input layer to hidden layer.
b : Weight connection from the hidden layer to output layer.

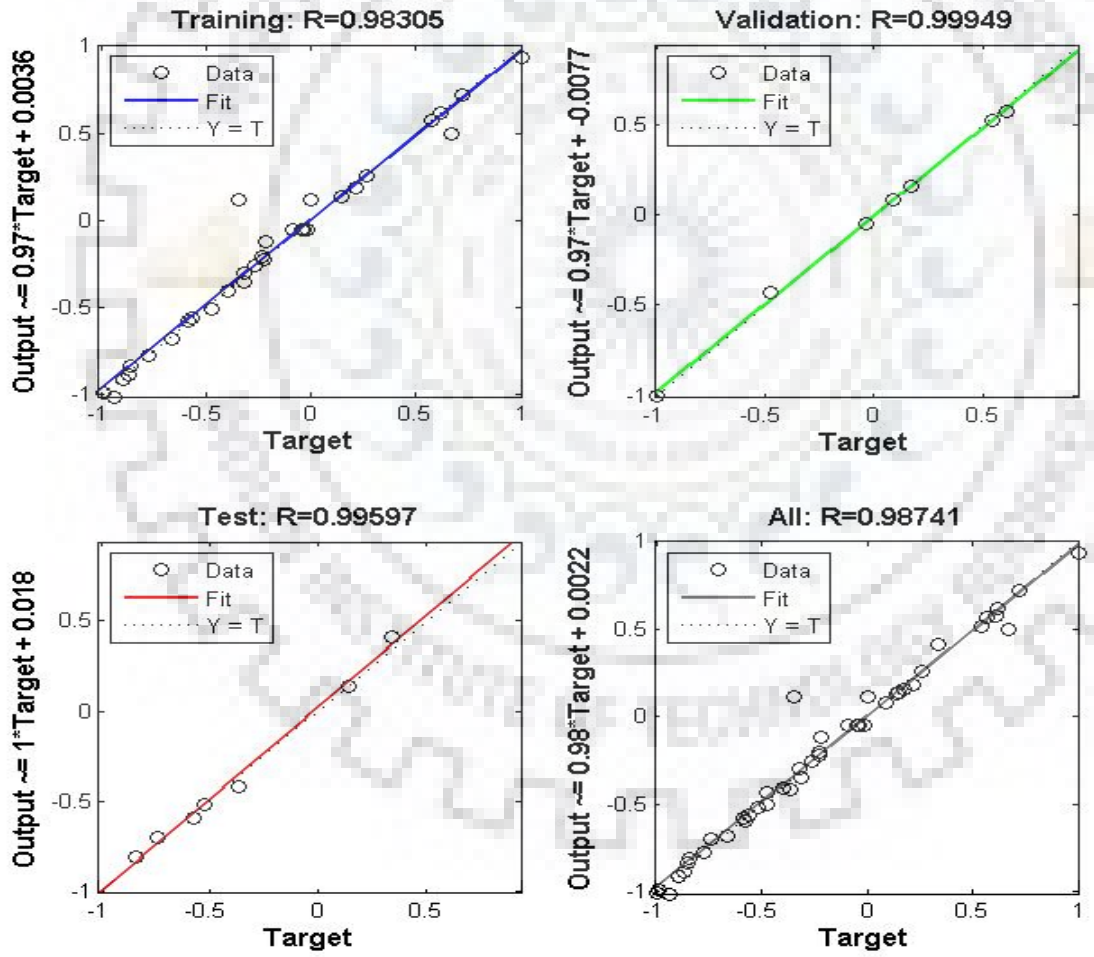


Fig. 5.9. The scatter plots of FFBP-ANN [5-6-1] for (a) training, (b) validation, (c) testing and (d) all data sets during the SFE of PP seed oil.

5.1.4.1 Development of ANN based correlation for the prediction of CEY for PP seed oil

In this direction, the normalization of the independent operating parameters (temperature, pressure, particle size, flow rate-$CO_2$ and % of co-solvent) has already been done as given in Eqs. (5.7-5.11) and by adopting the same procedure, an equation (Eq. 5.13) is derived here.

$$Y_{CEY} = 0.0491305 * B_1 - 0.0468214 * B_2 - 0.096251 * B_3 - 0.065352 * B_4 + 0.1377396 * B_5 - 0.01703148 * B_6 + 0.1326295$$

… Eq. 5.13

Eq. 5.13 is the final expression of the optimized FFBP-ANN [5-6-1] configuration, which was used to see the individual effect of parameters on CEY of PP seed oil.

5.1.4.2 Performance of ANN-FFBP models for PP seed oil

The performance of the developed FFBP-ANN [5-6-1] model was judge by comparing its performance with some other tested FFBP-ANN configurations (models) such as FFBP-ANN [5-1-1], FFBP-ANN [5-2-1], FFBP-ANN [5-3-1] etc. These other tested configurations (models) were created by changing of the number of neurons (1 to 9) in the hidden layer. All these tested models were compared based on some statistical parameters (e.g. AARD %, MSE, $R^2$ and NSEC) as shown in Fig. 5.10. From the figure (Fig. 5.10 (a-d)), it is clear that the FFBP-ANN [5-6-1] model with single hidden layer performed well and resulted minimum AARD % (4.4%), minimum MSE (0.00051), maximum value of $R^2$ (0.9874) and NSEC (0.975) among all the tested FFBP-ANN models. The AARD % shows the spreading of data from the central point which is the lowest among all the tested FFBP-ANN models for the configuration FFBP-ANN [5-6-1]. Similar pattern was also observed with MSE as shown in Fig. 5.10 (b). However, in comparison, AARD is higher than MSE for all models. The highest value of NSEC ('0.975' as shown in Fig. 5.10 (d)) indicates the highest efficiency of the developed FFBP-ANN [5-6-1] model over the other tested models (FFBP-ANN [5-7-1] (0.9794), FFBP-ANN [5-8-1] (0.9812), FFBP-ANN [5-9-1] (0.9705)). Similarly, the correlation coefficient ($R^2$) was employed to judge the performances of the models. The closer the correlation coefficient ($R^2$) to one, the better the performance of the model. The Fig. 5.10 (c) shows that the FFBP-ANN [5-6-1] continues to exhibit the best performance.

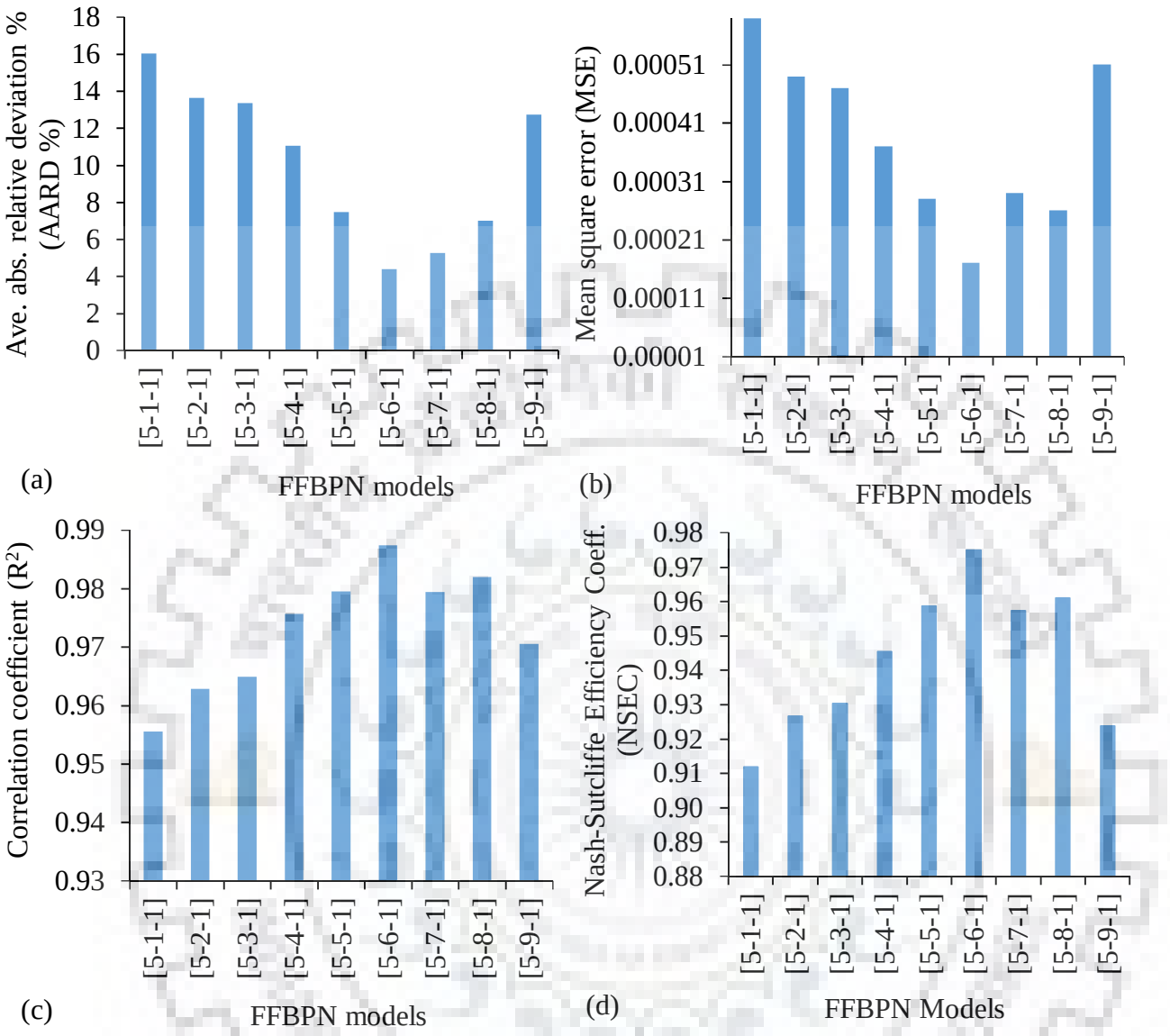


Fig. 5.10. Performances of different FFBP-ANN models based on some statistical parameters (AARD %, MSE, $R^2$ and NSEC) during the SFE of PP seed oil.

5.1.4.3 Sensitivity analysis of optimized FFBP-ANN model for PP seed oil

Similar to previous case (AM seed oil), five groups (e.g. one, two, three, four and five variables) were formed and investigated separately by the achieved optimal FFBP-ANN [5-6-1] model for the SFE of PP seed oil. The results of the analysis were shown in Table 5.10. From the Table 5.10, it is clear that P with mean square error (MSE) = 0.132 is the most effective parameter in the group of one variable. The other parameters (CoS %, T, FR and PS) have also shown the significant effect with MSE=0.155, 0.358, 0.458 and 0.492 respectively. From the findings of optimized FFBP-ANN [5-6-1] model, it can be seen that all five-extraction parameters have significant effect, in the following order: P > CoS % > T > FR > PS, on the extraction yield of PP seed oil.

As shown in Table 5.10, the value of MSE significantly decreased when T, P, PS and CoS % were used in interaction with the group of two variables. The lowest values of MSE (0.053, 0.115, and 0.129) were determined during the interaction of 'T with P', 'P with CoS %' and 'PS with CoS %' respectively. Other combinations (e.g. 'T + CoS %', 'P + FR', and 'P + PS') in the group of two variables have also shown a strong interactive effect with MSE's 0.144, 0.147, and 0.165 respectively. The minimum value of MSEs for the group of three variables were found to be 0.047, 0.059 and 0.061 with the interaction of 'T + P + CoS %', 'P + PS + CoS %' and 'PS + FR + CoS %' respectively while the lower value of MSE's (0.015) for the group of four variables were determined with the interaction of 'T + P + PS + CoS %'. The value of MSE was decreased drastically from 0.015 to 0.0005 when FR was involved in interaction with other variables (T, P, PS, FR, and CoS %) in the group of five variables.

Table 5.10. Sensitivity analysis of the input variables for the FFBP-ANN [5-6-1] model during the SFE of PP seed oil.

| No. | Combination | MSE | $R^2$ | Equation |
|---|---|---|---|---|
| | **Group of one variables** | | | |
| 1 | T | 0.358 | 0.3323 | y = 0.7069x + 0.0418 |
| 2 | P | 0.132 | 0.6703 | y = 0.9696x + 0.0041 |
| 3 | PS | 0.492 | 0.1235 | y = 1.117x + 0.0164 |
| 4 | FR | 0.458 | 0.2566 | y = 0.7018x + 0.0434 |
| 5 | CoS % | 0.155 | 0.5483 | y = 0.9955x + 0.0006 |
| | **Group of two variables** | | | |
| 6 | T + P | 0.053 | 0.7296 | y = 1.0767x – 0.0103 |
| 7 | T + PS | 0.328 | 0.2595 | y = 0.6084x + 0.0676 |
| 8 | T + FR | 0.346 | 0.2399 | y = 0.6167x + 0.0557 |
| 9 | T + CoS % | 0.144 | 0.6132 | y = 0.8815x + 0.0214 |
| 10 | P + PS | 0.165 | 0.6455 | y = 0.7573x + 0.0434 |
| 11 | P + FR | 0.147 | 0.6146 | y = 1.5023x – 0.0569 |
| 12 | P + CoS % | 0.115 | 0.8589 | y = 1.0821x – 0.0178 |
| 13 | PS + FR | 0.456 | 0.1878 | y = 0.4686x + 0.0832 |
| 14 | PS + CoS % | 0.129 | 0.5416 | y = 0.7827x + 0.0321 |
| 15 | FR + CoS % | 0.226 | 0.5235 | y = 0.6909x + 0.0473 |
| | **Group of three variables** | | | |
| 16 | T + P + PS | 0.169 | 0.5324 | y = 0.6631x + 0.0494 |
| 17 | T + P + FR | 0.180 | 0.7557 | y = 1.0721x – 0.0146 |
| 18 | T + P + CoS % | 0.047 | 0.9332 | y = 1.0039x – 0.0028 |
| 19 | P + PS + FR | 0.221 | 0.7160 | y = 1.0165x + 0.0019 |
| 20 | P + PS + CoS % | 0.059 | 0.8792 | y = 0.9388x + 0.0089 |
| 21 | PS + FR + CoS % | 0.061 | 0.5422 | y = 0.6925x + 0.0522 |
| | **Group of four variables** | | | |
| 22 | T + P + PS + FR | 0.275 | 0.6809 | y = 0.7961x + 0.0391 |
| 23 | T + P + PS + CoS % | 0.015 | 0.9505 | y = 1.007x – 0.0003 |
| 24 | P + PS + FR + CoS % | 0.102 | 0.8103 | y = 0.9589x + 0.0319 |
| | **Group of five variables** | | | |
| 25 | T + P + PS + FR + CoS % | 0.0005 | 0.9874 | Y = 0.998x – 0.0006 |

5.2 Effects of selected operating parameters on the CEY of AM and PP seed oils

The effect of selected independent input parameters such as temperature (°C), pressure (bar), particle size (mm), flow rate-$CO_2$ (g/min ) and % of co-solvent (%) on the output (CEY (g oil/g seeds)) have been discussed in this section for each of the feed raw materials (AM and PP seeds). The effects of all the operating parameters for both of the seeds at a particular point in the design space are shown through the perturbation plots (Fig. 5.11 (a & b)). The output (CEY (g oil/g seeds)) were plotted by changing only one parameter over its range at a time while holding all the other parameters at some constant values as shown in Table 5.11. By default, Design-Expert software sets the reference point as the midpoint (coded 0) of all the selected parameters, which can be changed to be any point (perhaps the optimal run conditions) by using the factors tool. The pattern of the path followed by a particular individual parameter predicts its sensitivity or insensitivity, for example, a curved or steep slope shows that response is sensitive whereas, a flat line shows that response is insensitive to that parameter (Bimakr et al., 2013).

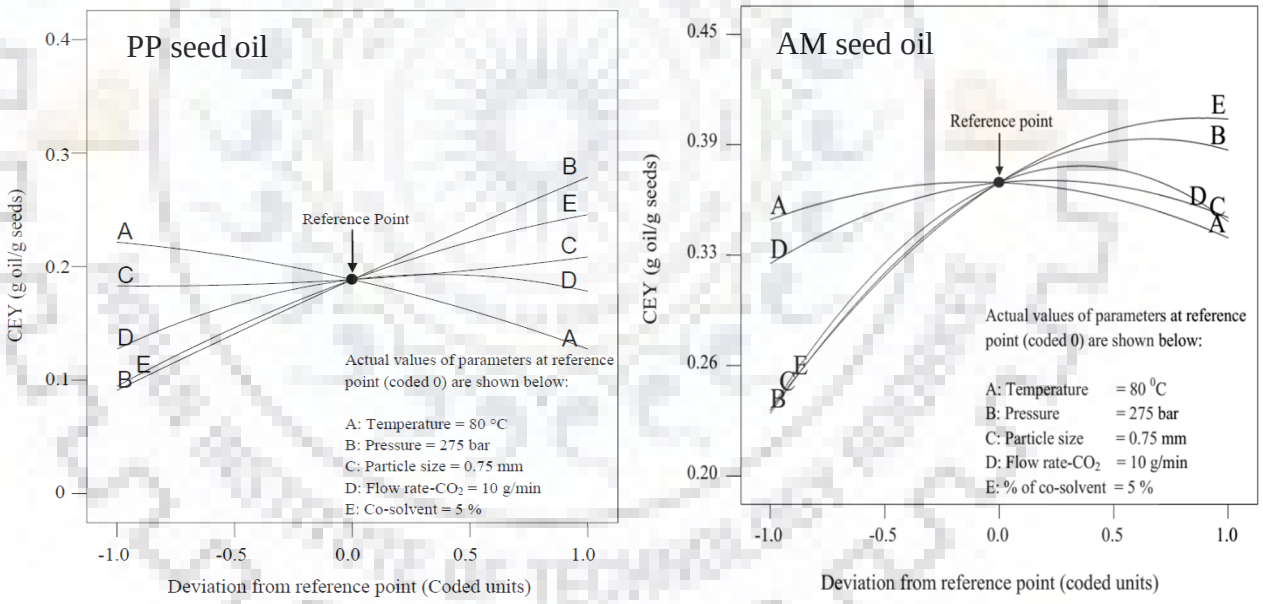


(a) (b)

Fig. 5.11: Perturbation plots for (a) PP seed oil and (b) AM seed oil.

Table 5.11. Reference point conditions for showing the effects of parameters.

| Input parameters | Coded values of parameters | | | Un-coded values of parameters | | |
|---|---|---|---|---|---|---|
| | Reference point | Range | | Reference point | Range | |
| | | Low | High | | Low | High |
| $X_1$: Temperature (°C) | 0 | -1.0 | 1.0 | 80 | 60 | 100 |
| $X_2$: Pressure (bar) | 0 | -1.0 | 1.0 | 275 | 200 | 350 |
| $X_3$: Particle size (mm) | 0 | -1.0 | 1.0 | 0.75 | 0.5 | 1.0 |
| $X_4$: Flow rate-$CO_2$ (g/min) | 0 | -1.0 | 1.0 | 10 | 5 | 15 |
| $X_5$: % of co-solvent (%) | 0 | -1.0 | 1.0 | 5 | 0 | 10 |

5.2.1 Effect of temperature on the CEY of seed oils

The effect of temperature on the CEY of PP and AM seed oils during the SFE is shown in Figs. 5.12 (a) and 5.12 (b) respectively. The effect of extraction temperature on the CEY of PP seed oil and AM seed oil were investigated at three levels of temperature 60°, 80° and 100 °C as shown in Table 5.2. Extraction temperature has exhibited negative effect (CEY decreases with increasing temperature) on CEY of PP seed oil as shown in Fig 5.12 (a). It is a known fact that an increase in temperature, decreases the solvent density but at the same time, it also increases the vapor pressure of solute. The former effect caused due to the rise in temperature decreases CEY whereas the later effect (rise in vapor pressure) increases the CEY. As the contribution of density towards extraction yield is much more prominent than the vapor pressure, the overall effect is that of decrease in CEY with increase in temperature (Doker et al., 2004).

However, the extraction temperature does not have significant effects on CEY during the SFE of AM seed oil as shown in Fig. 5.12 (b). The slight variation in CEY with temperature can be attributed to following facts. From the Fig. 5.12 (b) it is clear that CEY increases slightly up to 85 °C and then it starts to decrease due to 'retrograde solubility (Nei et al., 2008). Mukhopadhyay, 2000 has explained the retrograde solubility interference based on the relative influences of the density effect and the volatility effect on CEY. An isobaric increase in temperature decreases density of the supercritical fluid solvent (in our case it is SC-$CO_2$) and hence decreases the solubility caused due to density effect. On the other hand, the same increase in temperature increases the volatility of the solute and hence increases the solubility caused due to volatility effect. The relative supremacy of these effects in different temperature ranges creates the retrograde solubility interference. In the present case, the increase in extraction temperature from 60 to 80 °C increases the solubility due to

solute vapor pressure enhancement (over riding effect in this range) and after 80 °C reduces the solubility due to the decrease in solvent density (over riding effect in this range) (Doker et al., 2004).

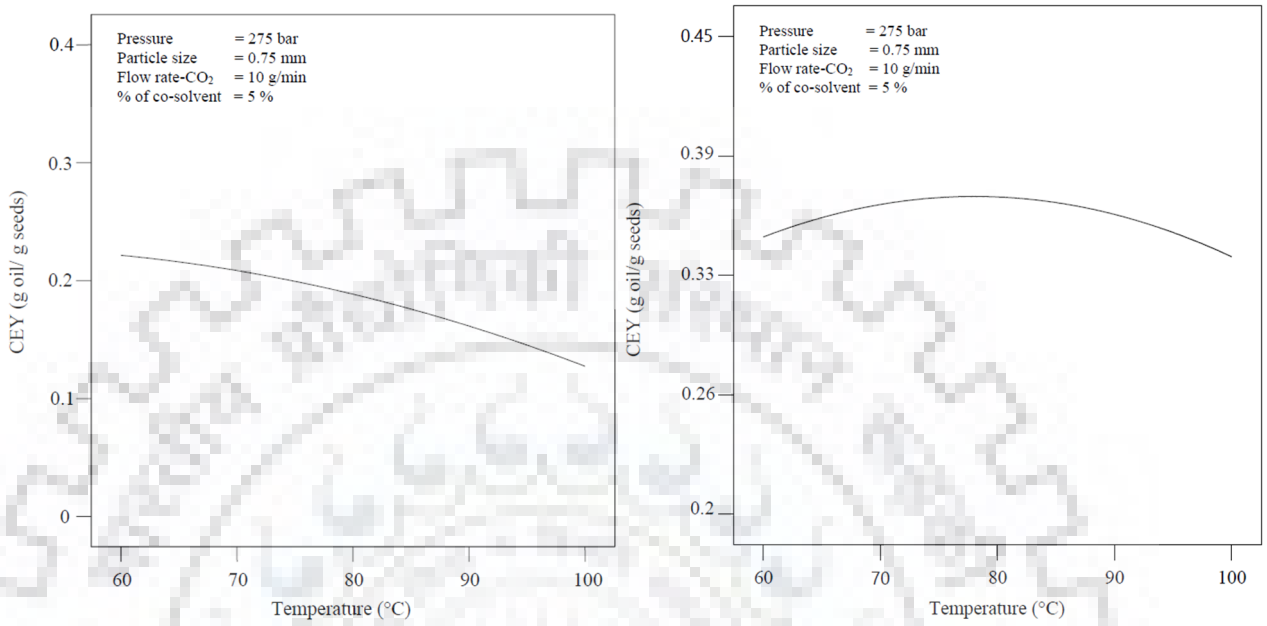


Fig. 5.12: Effect of temperature on the CEY of (a) PP seed oil and (b) AM seed oil.

5.2.2 Effect of pressure on the CEY of seed oils

The effect of extraction pressure on the CEY of PP seed oil and AM seed oil was investigated by choosing a wide range of extraction pressures (at 200, 275 and 350 bar) as presented in Table 5.2. From Fig. 5.13 (a), it is evident that the CEY of PP seed oil increases linearly with increasing pressure. This is due to an increase in solvent density with pressure, which further enhances the solvent power of SC-$CO_2$ (Nei et al., 2008; Salea et al., 2017). Thus, an increase in $CO_2$ density accelerated mass transfer between the solute and solvent during the extraction process and improved the CEY. From the Fig. 5.13 (b), it is also evident that the CEY of AM seed oil increased significantly with increasing pressure and ultimately reached a maximum value at around 312 bar and then it decreased slightly or may be assumed to attain an asymptotic value.

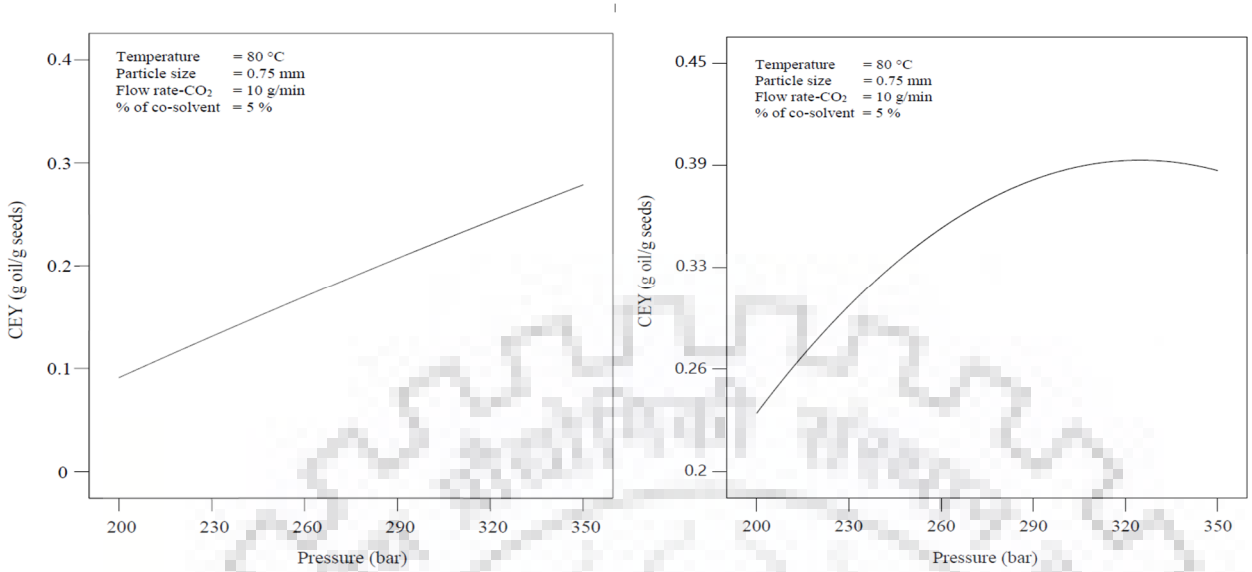


Fig. 5.13: Effect of pressure on the CEY of (a) PP seed oil and (b) AM seed oil.

5.2.3 Effect of particle size on the CEY of seed oils

The Fig. 5.14 (a) has shown only a marginal effect of particle size distributions (0.5, 0.75 & 1.0 mm) on the CEY of PP seed oil. From this figure, it appears that when particle size increases, the CEY also increases which appears to be opposite to what it should have happened. However, Sodeifian et al., 2016b; Da Porto and Natolino, 2017 during extraction using SFE, have also reported this phenomenon. An investigation to understand this phenomenon indicates that probably the interface area provided by small particles is not completely used in the process of mass transfer. This can happen due to the initial high pressure difference (~ 200 bar) across the bed, which might have forced the seed particles to stick together, as a result of it compaction might have occurred leading to reduction in the interface area significantly and might have directed the SC-$CO_2$ solvent to flow through some preferred channels (low resistance path) along the bed. This, obviously, would not have provided desired contact between complete external and intra particle surfaces and SC-$CO_2$ causing a marginal drop in CEY, in case of lower particle size. Further, it can be noted that the compaction due to initial pressure differential will be more for smaller particles than bigger particles.

From Fig. 5.14 (b) it is clear that CEY of AM seed oil increases with the particle sizes from 0.5 to 0.8 mm and thereafter decreases from 0.8 to 1.0 mm. It may be due to the initial high pressure difference (~ 200 bar) across the bed, which might have forced the small seed particles to stick

together, as a result of it compaction might have occurred leading to reduction in the available interface area (to solven) significantly and might have directed the SC-$CO_2$ solvent to flow through some channels along the bed. At particle size 0.5 mm, the compaction effect is substantial (leading to reduced surface area of solid-liquid contact) which reduces up to 0.8 mm particles and thus the extraction yield improves from particle size 0.5 to 0.8 mm. However, when particle size further increases to 1 mm, the actual surface area of solvent-particle contact area decreases due to comparatively large particle diameter and at the same time an increase in the intra particle diffusion path causes an increase in mass transfer resistance which ultimately leads to a lower CEY. Based on the physical appearance, the AM seed particles of lower sizes (e.g. 0.5 and 0.75 mm) are more softer than the particles of PP seeds of same sizes. Hence, the compression effect is more pronounced during the SFE of AM seeds than the PP seeds.

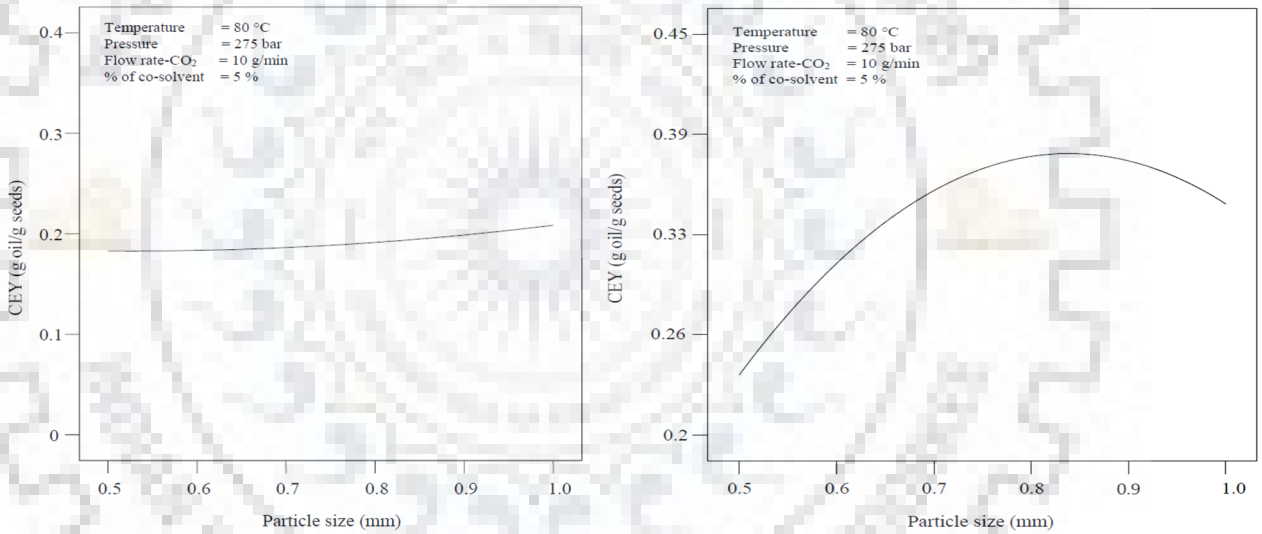


Fig. 5.14: Effect of particle size on the CEY of (a) PP seed oil and (b) AM seed oil.

5.2.4 Effect of flow rate-$CO_2$ on the CEY of seed oils

The effects of $CO_2$ flow rates on the CEY of PP and AM seed oils were investigated at 5, 10 and 15 g/min of $CO_2$ flow rates as shown in Table 5.2. From the Fig. 5.15 (a & b), it is evident that the CEY increases significantly (for both seeds oils pattern of the curve is same) with the flow rate of $CO_2$ up to 11 g/min, thereafter, it declines marginally. This behavior is attributed to the fact that the rate of mass transfer was increased with increased $CO_2$ flow rate, this is because, when higher

amount of SC-$CO_2$ passed through the extractor it decreased the stagnant solvent film thickness around the particles throughout the bed, which lowered external mass transfer resistance leading to an increase in rate of mass transfer. However, the decrement in the CEY is due to the reduction in the residence time of $CO_2$ inside the extractor at a higher flow rate of $CO_2$. And this high flow rate could not allow the solvent to achieve solute saturated state inside the extractor leading to a lower solute pickup per unit volume of solvent and thus lower CEY (Salea et al., 2017; Sodeifian et al., 2016b; Salgin and Korkmaz, 2011).

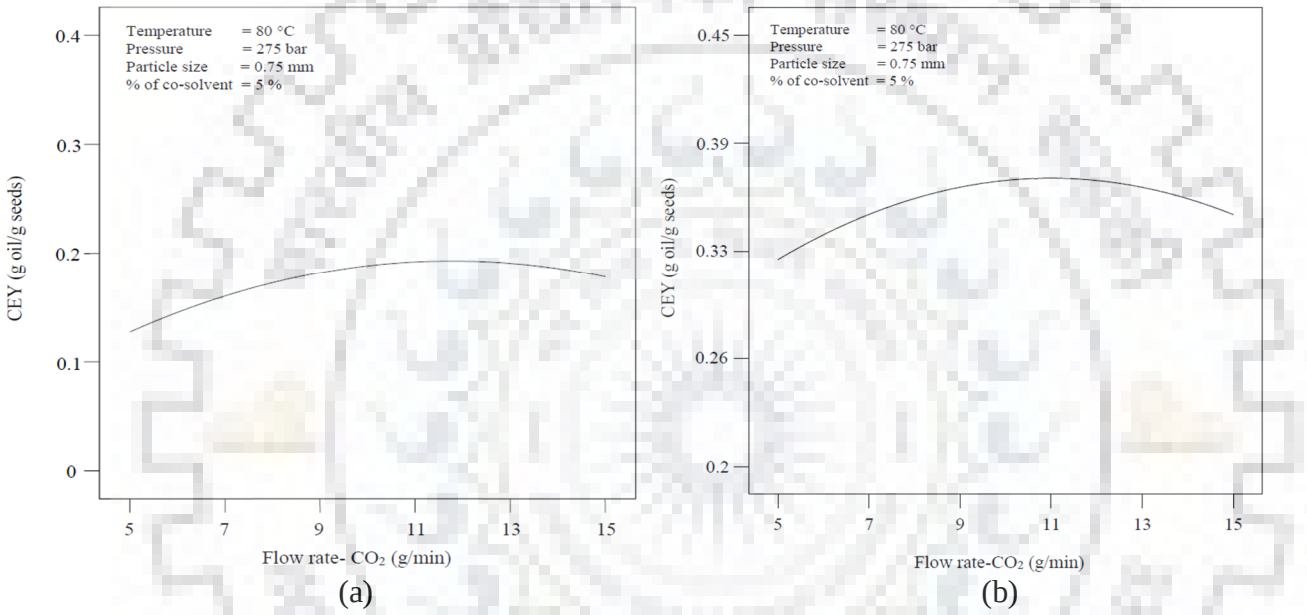


Fig. 5.15: Effect of flow rate-$CO_2$ on the CEY of (a) PP seed oil and (b) AM seed oil

5.2.5 Effect of % of co-solvent on the CEY of seed oils

The effects of three different amounts of the % of co-solvent (0, 5 and 10 % of $CO_2$ flow rate) were investigated as shown in Table 5.2. From the Figs. 5.16 (a & b), it could be seen that increment in co-solvent amount enhanced the CEY significantly during, the SFE of both seeds oils, because it increases the molar density of the solvent (SC-$CO_2$) which favors the solubilization of more polar substances from the seed particles (e.g. increases the equilibrium solubility of solute in the phase) (Chassagnez-mendez et al., 2000; Schmitt and Reid, 1986). As a matter of fact, being a non-polar solvent, carbon dioxide could only be suitable for dissolving the non-polar compounds such as hydrocarbons. However, some studies (e.g. Lang and Wai, 2001; Brondz et al., 2017) shows that the

quadrupole moment of carbon dioxide also helps in the dissolution of some moderately polar compounds such as ketones, esters, aldehydes and alcohols. However, the extraction of polar compounds have been done at large by adding the co-solvent, which improves the SC-$CO_2$ extractability by increasing the polarity of the carbon dioxide. The addition of a co-solvent to a SF, generally, increases the polarity, solute–solvent interaction and bulk density of the fluid mixture, which would contribute to solubility enhancement thus increasing the extraction yield (Rai et al., 2015; Suryawanshi and Mohanty, 2018a).

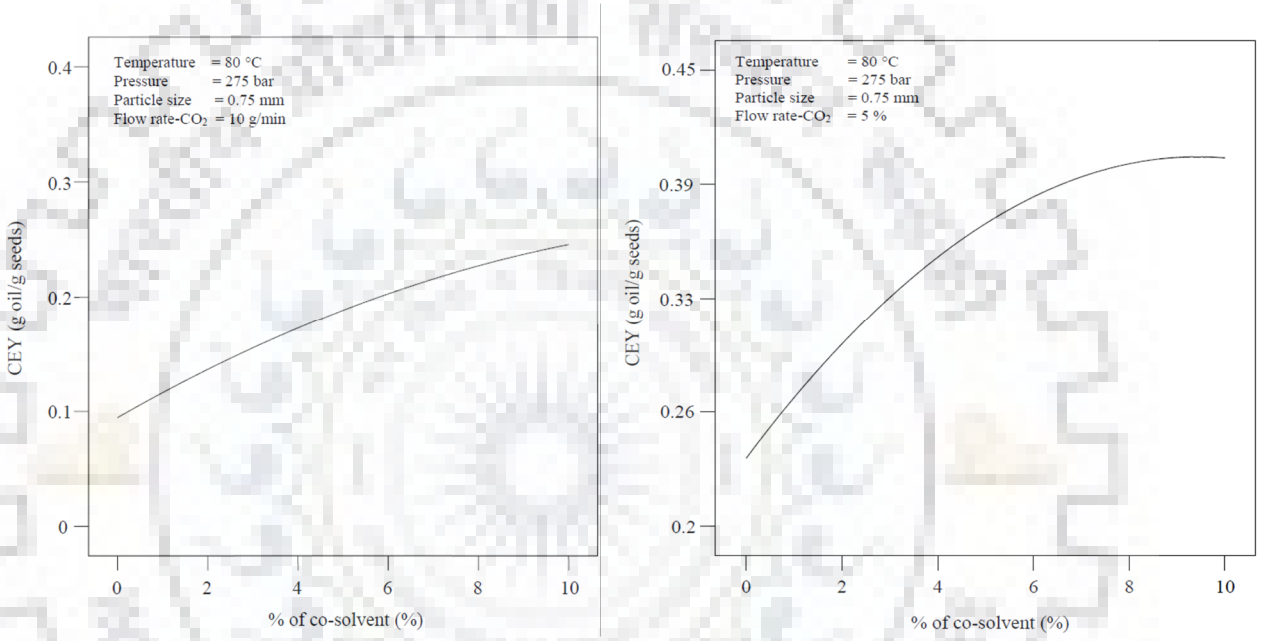


Fig. 5.16: Effect of % of co-solvent on the CEY of (a) PP seed oil and (b) AM seed oil.

5.3 Interactive effect of operating parameters on the CEY

The interactive effect of parameters on the CEY of PP and AM seed oils is explained through interaction plots (Figs. (5.17 & 5.19) created using Quantum XL software). The term 'Interaction' is used to explain the effect of different behavior of a particular input parameter on the response/output parameter (in present case it is CEY) in the presence of another parameter. As it has already been shown that the difference between the initially developed model and the improved model for the case of each seed is not significant. Therefore, all the ten interactive terms with their effects on CEY are discussed in subsequent sections for each seed.

5.3.1 Interactive effect of parameters on CEY of PP seed oil

As summarized in Fig. 5.17. & Table F.2, the interactive terms (e.g. 'pressure - % of co-solvent', 'pressure-flow rate-$CO_2$', 'particle size – % of co-solvent' and 'flow rate-$CO_2$ – % of co-solvent') have a positive and highly significant effect (p-value <0.0001) on the CEY of PP seed oil whereas, the interactive terms 'temperature- flow rate-$CO_2$', 'particle size – flow rate-$CO_2$' have less significant effect (0.0001 < p-value < 0.05). On the other hand, the interactive terms (e.g. 'temperature-pressure', 'temperature-particle size', and 'pressure-particle size') are almost insignificant (p-value > 0.05). From the Fig. 5.17, it is clear that all parameters (excepting the term 'temperature-pressure', 'temperature-particle size' and 'pressure-particle size') are involved in the interaction, though the extent of severity of interaction varies significantly. For example, for the term 'pressure-% of co-solvent' the CEY varies differently when the % of co-solvent varies from 0.0 to 10.0 % alone depending on the level of extraction pressure. Similarly, from the term 'flow rate-$CO_2$ - % of co-solvent', it can be seen that CEY varies significantly when flow rate-$CO_2$ varies from 5 to 15 g/min alone depending on the level of flow rate-$CO_2$. From the above examples, it could be clearly understood that when departing lines are different from being parallel, the degree of interaction would be more significant. Whereas, the terms 'temperature – pressure', 'temperature - particle size', 'pressure - particle size', could not show an interactive effect which is justified by the parallel lines as shown in Fig. 5.17.

5.3.2 Severity factor analysis of interactive terms for the PP seed oil

Severity factor (SF) analysis can also be used to justify the two parameters interaction. The magnitude of severity factor of two parameter interaction as given in Table 5.12, is calculated using Eq. 5.14.

$$Severity\ \ factor = \frac{(F_i - F_{\min})}{(F_{\max} - F_{\min})} \quad \text{… Eq. 5.14}$$

Where, $F_i$= $i$th F-value, $F_{min}$= minimum F-value and $F_{max}$= maximum F-value.

The magnitude of severity factor (SF) changes significantly and decides the strength of the interactive effect. For example, the magnitude of severity factors of the interactive terms (e.g. 'temperature – pressure', 'temperature - particle size', and 'pressure - particle size') are '0.0000', '0.0003'and '0.0469'respectively, this means, these interactive terms have lowest interactive effect

on the CEY of PP seed oil, which can also be seen from the box no. 1, 2 and 5 of Fig. 5.17. In these boxes, two lines are almost parallel to each other that confirms the insignificancy of these terms. On the other hand, the interactive term (e.g. 'pressure - % of co-solvent') has the highest order of SF '1.000' meaning that this interactive term has highest interactive effect on the CEY which can also be seen from the box no. 7 of Fig. 5.17 in which two lines are significantly intersecting to each other. Here, the only highest and lowest significant terms were discussed. Other intermediate interactive terms, which can be seen from the Table 5.12, can also be explained in a similar way. The order of interaction, in descending order, is given in Table 5.12. Therefore, in the present case, all seven interactive terms (excepting 'temperature – pressure', 'temperature - particle size', 'pressure - particle size') are to be considered during the SFE of PP seed oil.

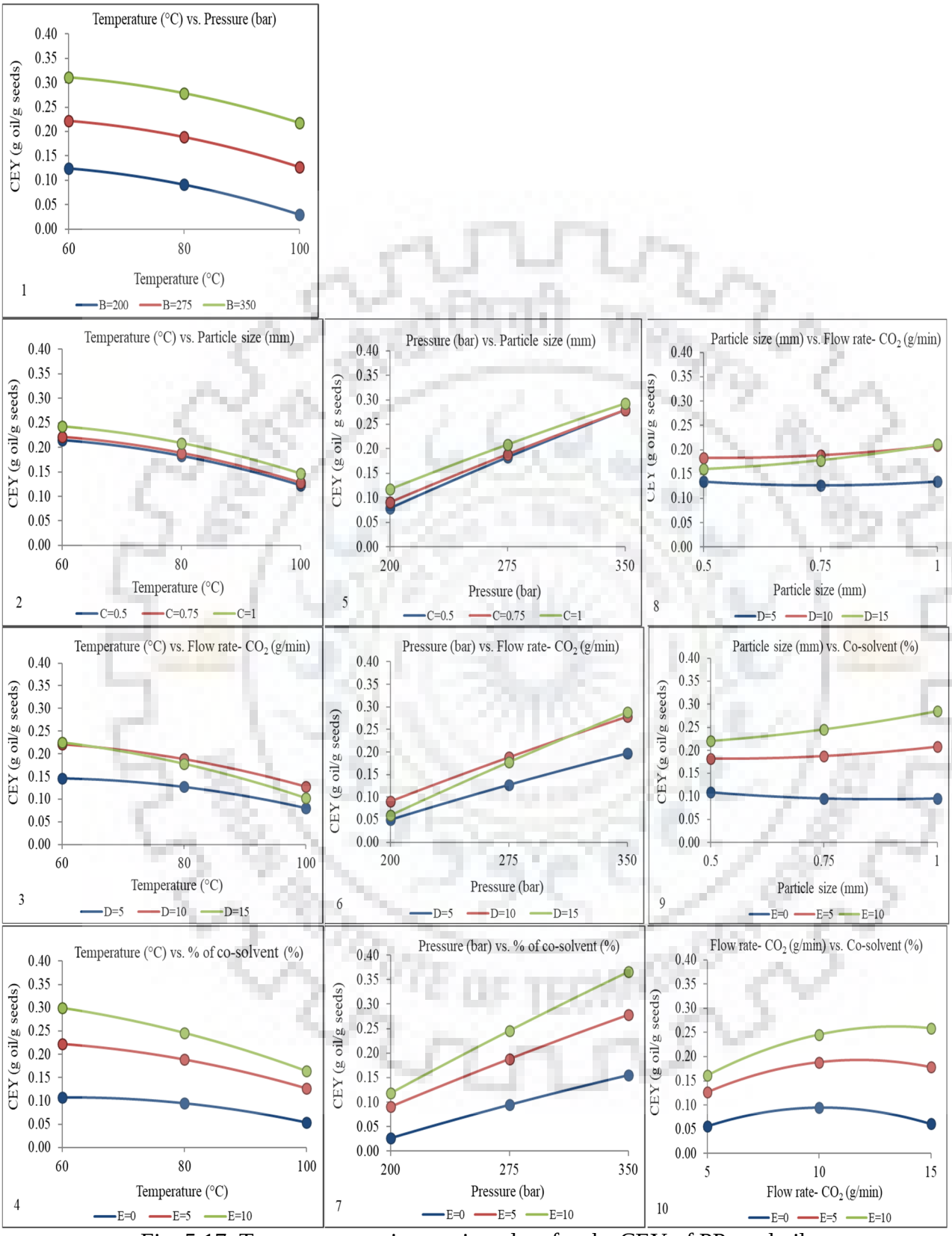


Fig. 5.17: Two parameter interaction plots for the CEY of PP seed oil.

Table 5.12. Severity factor (SF) analysis based on ANOVA analysis of Eq. 5.5.

| Two parameter interaction | Coefficient actual | Coefficient coded | p-value | F-value | Magnitude of severity |
|---|---|---|---|---|---|
| Pressure - % of co-solvent | $7.892*10^{-5}$ | 0.030 | 0.0001 | 60.69 | 1.0000 |
| Flow rate-$CO_2$ - % of co-solvent | $9.31*10^{-4}$ | 0.023 | 0.0001 | 37.54 | 0.6184 |
| Temperature - % of co-solvent | $-2.059*10^{-4}$ | -0.021 | 0.0001 | 29.38 | 0.4839 |
| Pressure - Flow rate-$CO_2$ | $5.47051*10^{-5}$ | 0.021 | 0.0001 | 29.16 | 0.4803 |
| Particle size - % of co-solvent | 0.015768 | 0.020 | 0.0001 | 26.92 | 0.4433 |
| Temperature - Flow rate-$CO_2$ | $-1.38250*10^{-4}$ | -0.014 | 0.0012 | 13.24 | 0.2179 |
| Particle size - Flow rate-$CO_2$ | 0.010118 | 0.013 | 0.0027 | 11.08 | 0.1822 |
| Pressure - Particle size | $-3.43467*10^{-4}$ | $-6.440*10^{-3}$ | 0.1024 | 2.87 | 0.0469 |
| Temperature - Particle size | $-1.52500*10^{-4}$ | $-7.625*10^{-4}$ | 0.8425 | 0.040 | 0.0003 |
| Temperature - Pressure | $3.80000*10^{-7}$ | $5.700*10^{-4}$ | 0.8819 | 0.023 | 0.0000 |

5.3.3 3D response surface analyses of CEY of PP seed oil

The three-dimensional (3D) plots with their two-dimensional (2D) projections of the RSM model according to Eq.5.1 were used to determine the interactions among different parameters and their optimum values for achieving the maximum CEY of PP seed oil as shown in Fig. 5.18. These plots were created in such a way that the z-coordinate depicts the CEY whereas, x and y coordinates represents two independent variables while the other three independent variables were kept constant at reference point (as shown in Table 5.11). The shape of the response surfaces (3D surfaces) and their 2D projections (2D contour plots) indicates that whether the two-parameter interaction was significant or not. Therefore, an outcome from these 3D plots is purely depends on the intension and accuracy of the investigator during the analysis of these plots. For example, curvy/elliptical contours indicate that interactions between corresponding parameters are significant while the circular contour plots indicate that the interactions between the corresponding parameters are less significant or insignificant. In this study, ten response surfaces with their respective contour were generated using software (Design Expert 10.0) as shown in Fig. 5.18.

Fig. 5.18 (a,b,c,d) shows the interactive effect of temperature along with other four parameters (e.g. pressure, particle size, flow rate-$CO_2$ and % of co-solvent) taken one at a time on the CEY of PP seed oil. As shown in Fig. 5.18 (a, b), increasing temperature from 60 °C to 100 °C leads to lower CEY of PP seed oil (as explained in section 5.2.1). In the aforementioned region (60-100 °C), the

negative effect of temperature which lowers SC-$CO_2$ density is more dominant than the positive effect of temperature with enhanced mass transfer coefficient and diffusivity. In addition to this, the increasing effect of pressure on the CEY of PP seed oil has already been explained in detail in section 5.2.2. It can also be seen in Table F.2, the term 'temperature-pressure' has shown a very low positive effect ('0.0012'), and the term 'temperature-particle size' has shown a small negative effect ('-0.0016') on the CEY of PP seed oil due to the effect of lower size of PP seed particles as explained in section 5.2.3. Based on the analysis of shape of 3D and their contour projection it can be concluded that these two interactive terms are 'insignificant' because of the counter effect of temperature with pressure and particle size. As shown in Fig. 5.18 (c,d), the surfaces and their contours of the terms 'temperature-flow rate-$CO_2$' and 'temperature-% of co-solvent' are seems to be more prone to shown positive effect of them on the CEY of PP seed oil then the previous terms and it can be more justified from the 2D line plots and from the Table F.2. Therefore, these terms have been remarked as 'less significant' and 'significant' respectively. The duel behavior of flow rate-$CO_2$ for the yield of PP seed oil has already been explained in section 5.2.4. The positive effect of flow rate-$CO_2$ compensated with the negative effect of temperature and resulted in to a 'less significant' of the term on the CEY of PP seed oil. Similarly, the positive effect of the % of co-solvent (as explained in section 5.2.5) might have also been neutralized up to certain extent by the negative effect of temperature and hence resulted into a 'significant' effect only.

Fig. 5.18 (e,f,g) shows the effect of pressure along with the other three parameters (e.g. particle size, flow rate-$CO_2$ and % of co-solvent) on the CEY of PP seed oil. Increasing pressure leads to higher SC-$CO_2$ density and results in enhanced solute solubility and therefore causing an increment in CEY. Whereas, at the same time, increasing pressure (excessive pressure only) also lowers the solute diffusivity and mass transfer coefficient resulting in lower CEY. From the Table F.2, it is clear that the term 'pressure-particle size' has shown a negative effect ('-0.0128'), on the other hand the terms 'pressure - flow rate- $CO_2$' and 'pressure - % of co-solvent' have shown a positive effect with the values as '0.0420' and '0.0592' respectively. Based on the visual inspection of Figs. 5.18 (e, f, g), the interactive effect of pressure with 'particle size' flow rate-$CO_2$' and % of co-solvent' were remarked as 'less significant' 'significant' and 'significant' respectively. From the Fig. 5.18 (g), it can be seen that the term 'pressure-% of co-solvent' is more significant than the other nine interactive terms.

Fig. 5.18 (h,i) shows the interactive effect of particle size along with the other two parameters (e.g. flow rate-$CO_2$ and % of co-solvent) on the CEY of PP seed oil. Based on the visual inspection of Figs. 5.18 (h,i), the interactive effect of 'particle size' with both the parameters (e.g. flow rate-$CO_2$ and % of co-solvent) can be remarked as 'significant' which is further justified by the numeric values of positive effect as '0.0252' and '0.0394' in Table F.2. Finally, the term 'flow rate-$CO_2$ - % of co-solvent' can also be seen as 'significant' term, which has shown a positive effect on the CEY of PP seed oil. Based on the analysis of 3D plots and their 2D contour plots, all the 10 interactive terms have been classified into three broad categories as 'significant' 'insignificant' and 'less significant' only.

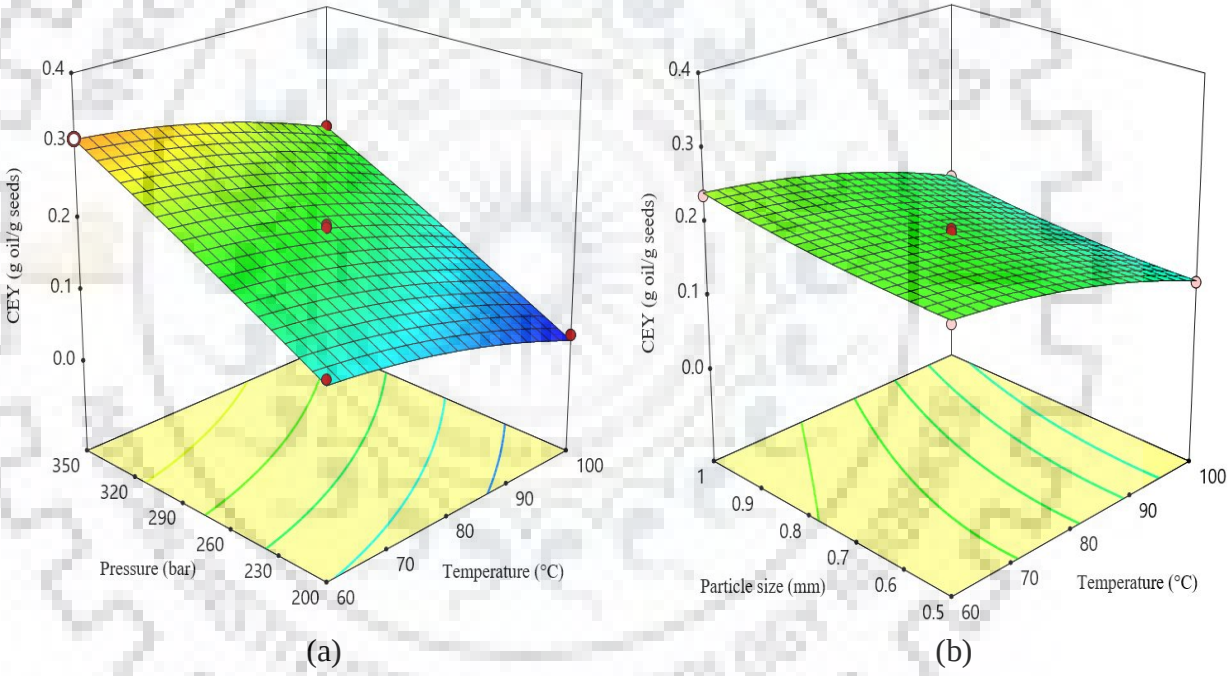


Fig. 5.18: 3D plots of response surfaces with their 2D projections for PP seed oil.

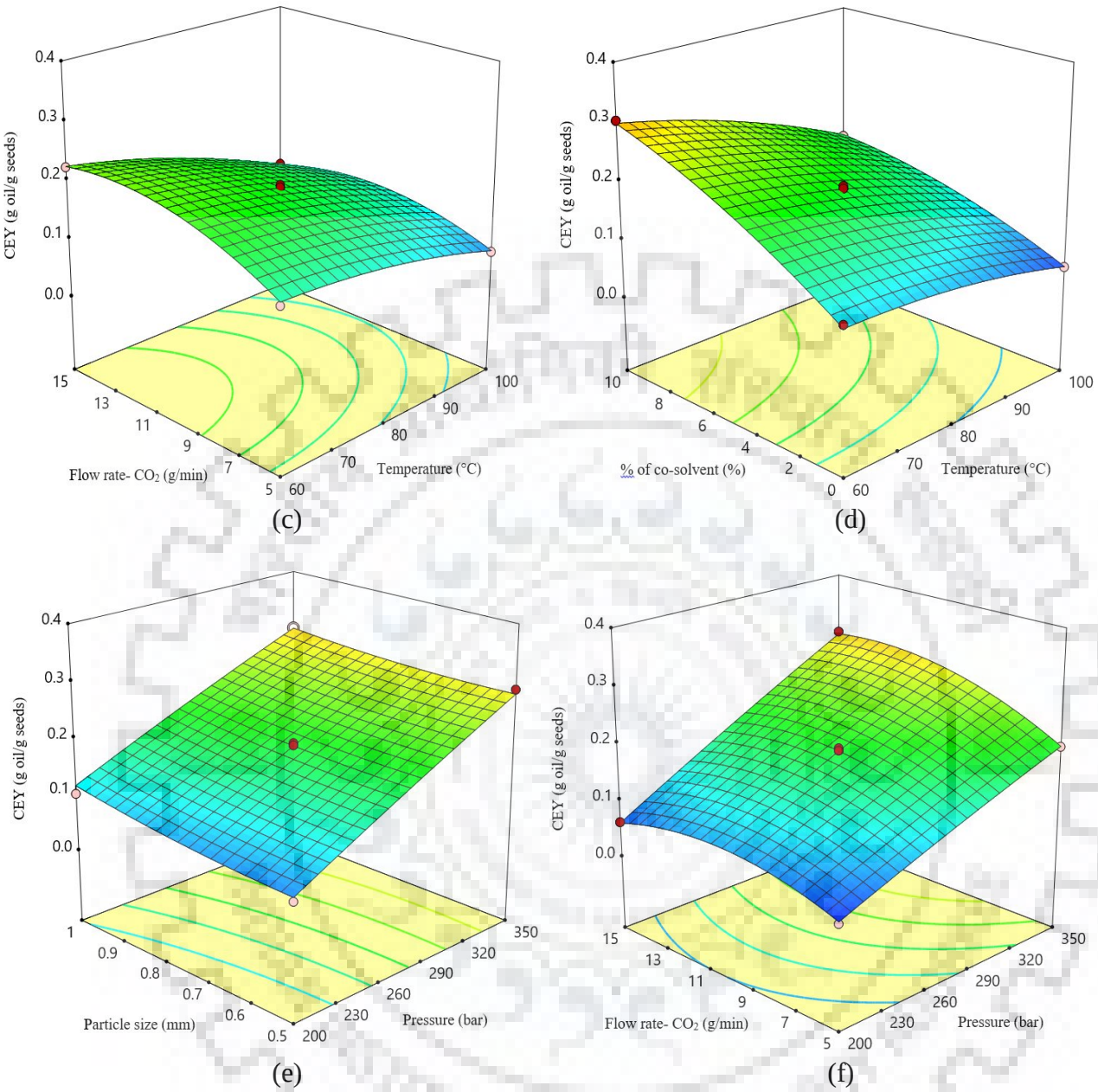
CEY (g oil/g seeds)
0.4
0.3
0.2
0.1
0.0
Flow rate- CO2 (g/min)
15
13
11
9
7
5
Temperature (°C)
60
70
80
90
100
(c)
CEY (g oil/g seeds)
% of co-solvent (%)
10
8
6
4
2
0
Temperature (°C)
60
70
80
90
100
(d)
CEY (g oil/g seeds)
Particle size (mm)
1
0.9
0.8
0.7
0.6
0.5
Pressure (bar)
200
230
260
290
320
350
(e)
CEY (g oil/g seeds)
Flow rate- CO2 (g/min)
15
13
11
9
7
5
Pressure (bar)
200
230
260
290
320
350
(f)

Fig. 5.18: (Cont…)

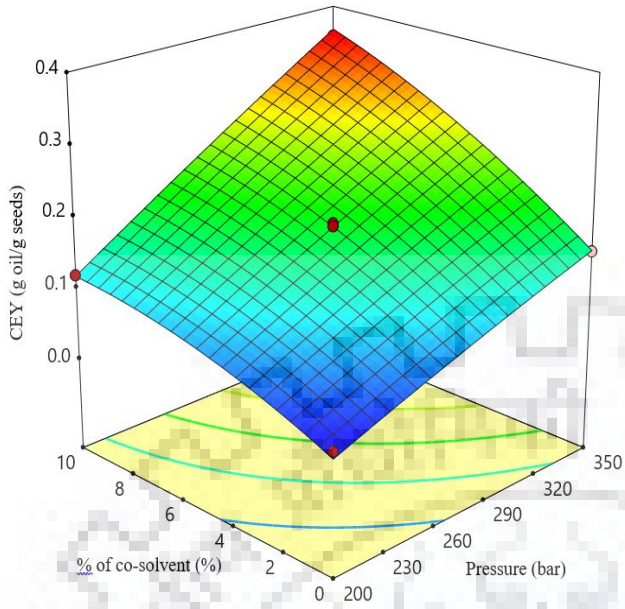


(g)

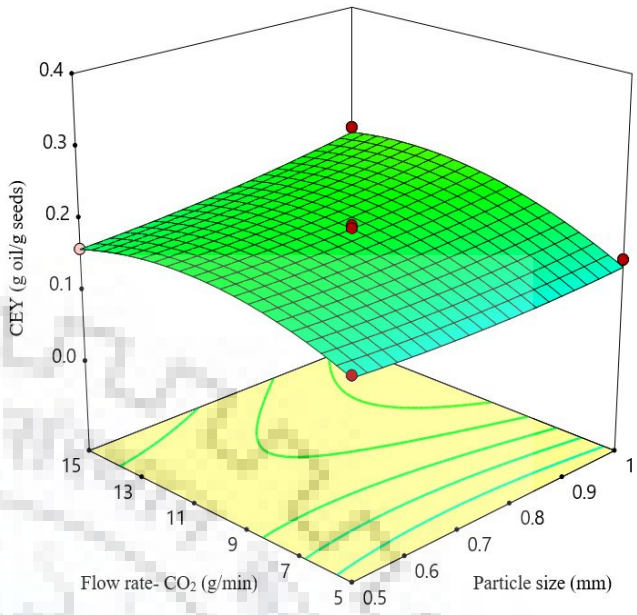


(h)

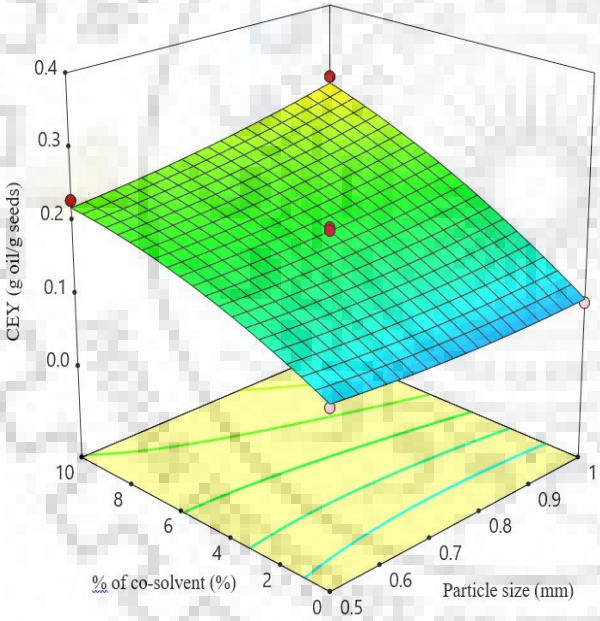


(i)

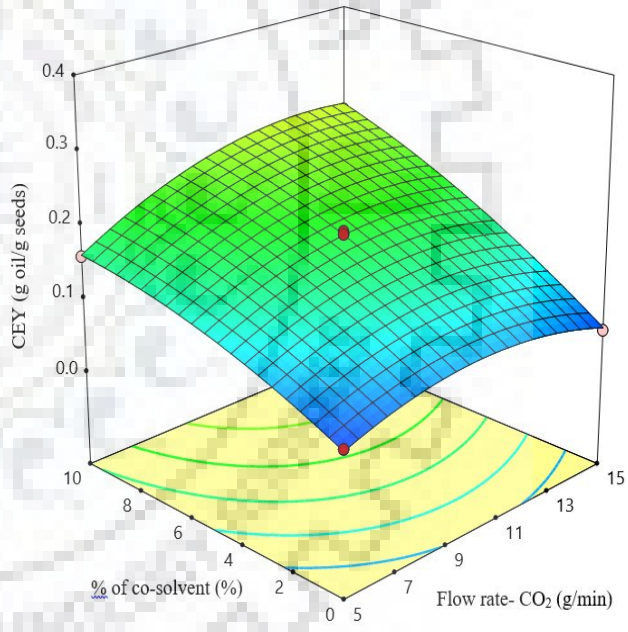


(j)

Fig. 5.18: (Cont…)

5.3.4 A final comparison among four methods of analysis of interactive terms for the SFE of PP seed

The effects of interactive terms have been discussed through qualitative and quantitative analysis in the previous sections of this chapter. The qualitative analysis consists of 2D and 3D plots, which are based on line plots (Fig. 5.17) and the response surface plots (Fig. 5.18) respectively while the quantitative analysis consists of SF (Table 5.12) and ANOVA (Table F.2) from which the magnitude of SF-value and p-value were used respectively for the classification of interactive terms accordingly. A final comparison among four methods (e.g. 2D, 3D, SF and ANOVA) of analysis of interactive terms for the SFE of AM seed oil is given in Table 5.13. The effects of interactive terms have been classified into five categories such as most significant (MS), significant (S), less significant (LS), insignificant (IS) and most insignificant (MI). The decision for the allotment of the specific category was made based on majority of the same category given by maximum number of methods (at least three) while in the case of draw situation, the quantitative analysis is given preference. For example, the term 'pressure-% of co-solvent' was categorized as 'MS' by three methods while one method says it is as 'S' therefore it can be concluded that this term is to be considered as 'MS'. Similarly, the interactive terms 'temperature-pressure' and 'temperature-particle size' were categorized as 'MI' by three methods while one method proved these as 'IS' therefore finally these terms were considered as 'MI'.

Table 5.13. A final comparison of four methods of analysis of interactive terms during the SFE of PP seed oil.

| Interactive terms | Methods of analysis | | | | |
|---|---|---|---|---|---|
| | Qualitative analysis | | Quantitative analysis | | |
| | 2D analysis (based on Line plots) | 3D analysis (based on surface and contour plots) | SF analysis (Based on the value of SF) | ANOVA analysis (Based on p-value) | Concluding remarks |
| Temperature – Pressure | IS | IS | 0.0000 (MI) | 0.8819 (MI) | Most Insignificant |
| Temperature – Particle size | IS | IS | 0.0003 (MI) | 0.8425 (MI) | Most Insignificant |
| Temperature – Flow rate-$CO_2$ | LS | LS | 0.2179 (LS) | 0.0013 (LS) | Less Significant |
| Temperature - % of co-solvent | S | S | 0.4839 (S) | < 0.0001 (MS) | Significant |
| Pressure – Particle size | IS | LS | 0.0469 (IS) | 0.1024 (IS) | Insignificant |
| Pressure - Flow rate-$CO_2$ | S | S | 0.4803 (S) | < 0.0001 (MS) | Significant |
| Pressure - % of co-solvent | MS | S | 1.000 (MS) | < 0.0001 (MS) | Most Significant |
| Particle size - Flow rate-$CO_2$ | LS | S | 0.1822 (LS) | 0.0028 (LS) | Less significant |
| Particle size - % of co-solvent | S | S | 0.4433 (S) | < 0.0001 (MS) | Significant |
| Flow rate-$CO_2$ - % of co-solvent | S | S | 0.6184 (S) | < 0.0001 (MS) | Significant |

SF value: MI ($0.0 \leq SF \leq 0.001$), IS ($0.001 \leq SF \leq 0.1$), LS ($0.1 \leq SF \leq 0.3$), S ($0.3 \leq SF \leq 0.9$), MS ($0.9 \leq SF \leq 1.0$)
p-value: MI (p-value $\geq 0.5$), IS ($0.1 \leq$ p-value $< 0.5$), LS ($0.01 \leq$ p-value $\leq 0.05$), S ($0.0001 \leq$ p-value $\leq 0.01$), MS (p-value $< 0.0001$)
Notation:
MI: Most Insignificant, LS: Less Significant, S: Significant, IS: Insignificant, MS: Most Significant, SF: Severity factor

5.3.5 Interaction effects of parameters on CEY of AM seed oil

The two-parameter interaction effect on the CEY of AM seed oil can also be explained through interaction plots (Fig. 5.19, obtained from Quantum XL software). There are 10 numbers of boxes, in Fig. 5.19, which shows the interactive effect of interactive terms (e.g. 'temperature – pressure', 'temperature - particle size', 'temperature - flow rate-$CO_2$', 'temperature - % of co-solvent', 'pressure - particle size', 'pressure - flow rate-$CO_2$', 'pressure - % of co-solvent', 'particle size - flow rate-$CO_2$', 'particle size - % of co-solvent' and 'flow rate-$CO_2$ - % of co-solvent') on CEY of AM seed oil. For example, if the interactive term 'temperature-% of co-solvent' is examined, it can be explained clearly that CEY varies differently when the % of co-solvent varies from 0.0 to 10.0 % depending on the level of extraction temperature. The above examples justify the fact that when departing lines different from being parallel, the degree of interaction would be more significant. On the other hand, in the interactive term 'particle size-flow rate-$CO_2$' does not show an interaction effect which is justified by the parallel lines. Other intermediate interactive terms, which can be seen from the box nos. 1, 2, 3, 5, 6, 7, 9 and 10 of the Fig. 5.19, can also be explained in a similar way.

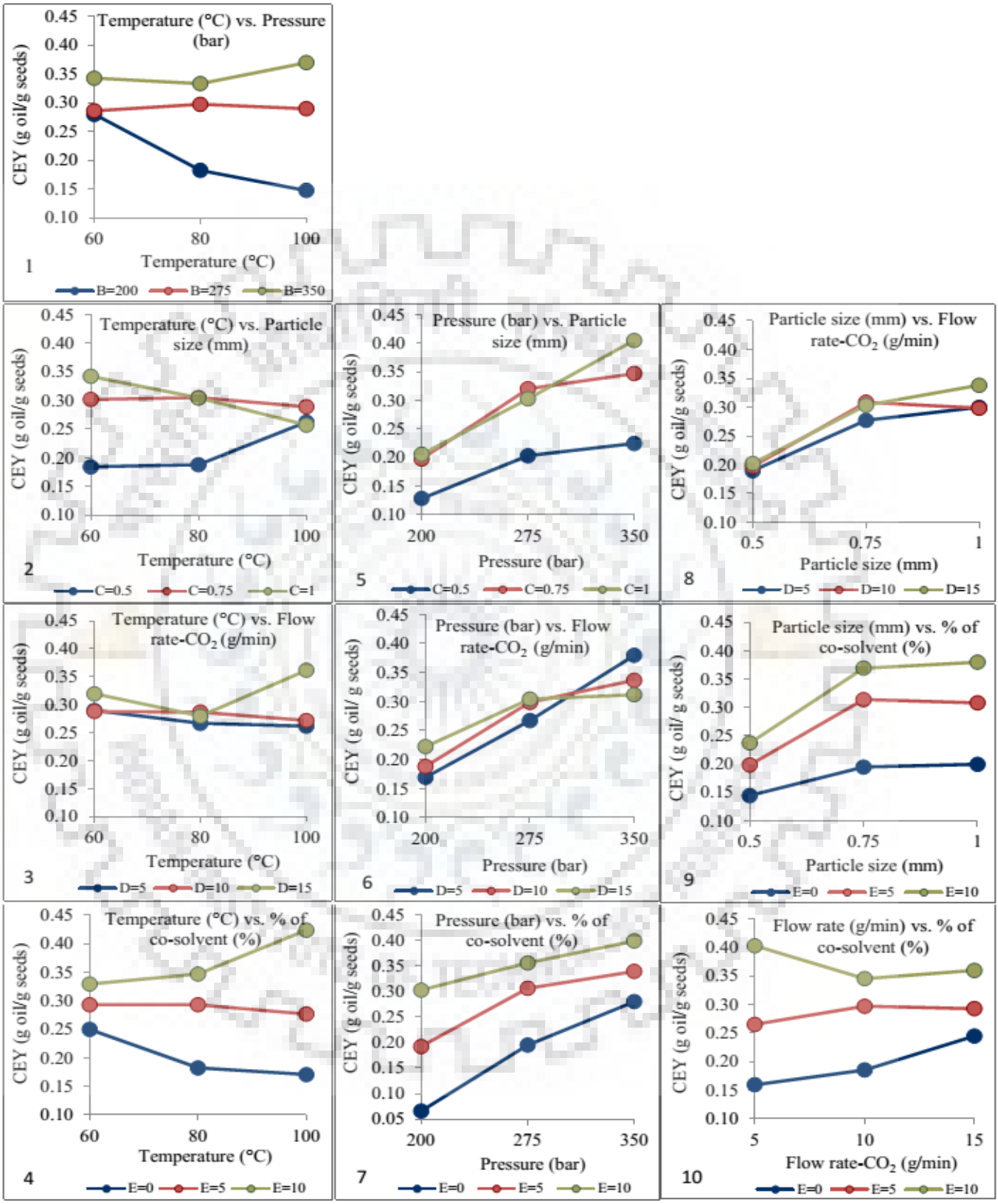


Fig. 5.19: Two-parameter interaction plots for the CEY of AM seed oil.

5.3.6 Severity factor analysis of interactive terms for the AM seed oil

The interactive effects of the operating parameters (e.g. temperature, pressure, particle size, flow rate-$CO_2$ and % of co-solvent) on the CEY of AM seed oil, can also be explained by the severity factor (SF) analysis as it was performed for the SFE of PP seed oil. The magnitude of severity factor of two parameters interaction is given in Table 5.14 which is calculated using Eq. 5.12. From the Table 5.14 and Fig. 5.19, it can be seen that all the input variables are involved in interactions within their range, though the order of severity factor (SF) changes significantly and decides the strength of the interactive effect. For example, the order of severity factor of the interactive term 'particle size - flow rate-$CO_2$' is the lowest one '0.0000' means, this interactive term has the lowest interactive effect on the extraction yield which can also be seen from the box no. 8 of the Fig. 5.19., where the two lines are almost parallel to each other. This parallel pattern confirms the insignificance of this term while the interactive term 'temperature – % of co-solvent' has the highest order of severity factor '1.000' meaning that this interactive term has the highest interactive effect on the extraction yield which can be seen from the box No. 4 of Fig. 5.19, in which two lines are significantly intersecting to each other. Here, the only highest and lowest significant terms (in box no. 4 and 8) were discussed. Other intermediate interactive terms can also be explained in a similar way. The order of interaction in descending order is given in Table 5.14. Therefore, in the present case, all ten interactive terms (excepting the term 'particle size – flow rate $CO_2$') are to be considered during the SFE of AM seed oil.

Table 5.14. Severity factor analysis (SFA) based on ANOVA analysis of Eq. 5.2.

| Two parameter interaction | Coefficient actual | Coefficient coded | p-Value | F-Value | Order of severity |
|---|---|---|---|---|---|
| Temperature - % of co-solvent | $4.33750 \times 10^{-4}$ | 0.043 | 0.0001 | 20.34 | 1.0000 |
| Temperature - Particle size | $-8.15500 \times 10^{-3}$ | -0.041 | 0.0003 | 17.97 | 0.8808 |
| Temperature - Pressure | $2.66000 \times 10^{-5}$ | 0.040 | 0.0003 | 17.21 | 0.8426 |
| Flow rate-$CO_2$ - % of co-solvent | $-1.28800 \times 10^{-3}$ | -0.032 | 0.0026 | 11.21 | 0.5410 |
| Pressure - Flow rate-$CO_2$ | $-8.06667 \times 10^{-5}$ | -0.030 | 0.0042 | 9.89 | 0.4746 |
| Pressure - % of co-solvent | $-7.86000 \times 10^{-5}$ | -0.029 | 0.0052 | 9.39 | 0.4495 |
| Pressure - Particle size | $1.37200 \times 10^{-3}$ | 0.026 | 0.0130 | 7.15 | 0.3369 |
| Particle size - % of co-solvent | 0.017460 | 0.022 | 0.0321 | 5.15 | 0.2363 |
| Temperature - Flow rate-$CO_2$ | $1.75000 \times 10^{-4}$ | 0.017 | 0.0808 | 3.31 | 0.1438 |
| Particle size - Flow rate-$CO_2$ | $5.18000 \times 10^{-3}$ | $6.475 \times 10^{-3}$ | 0.5070 | 0.45 | 0.0000 |

### 5.3.7 3D response surface analyses of CEY of AM seed oil

Three-dimensional (3D) plots with their two-dimensional (2D) projections of response surfaces are the graphical representations of regression equation obtained from RSM analysis as shown in Fig. 5.20. The constant level (80 °C, 275 bar, 0.75 mm, 10 g/min and 5 %) of each operating parameter (e.g. temperature, pressure, particle size, flow rate-$CO_2$ and % of co-solvent) was used during the interactive analysis of any two parameters through the 3D plots. For example, in the case of interactive term 'temperature – pressure', the other parameters (particle size, flow rate-$CO_2$ and % of co-solvent) were kept at constant level as mentioned above. As explained in the previous section 5.3.3, these plots provide a visual relationship between the responses and the experimental levels of each variable and their interactions as well. Fig. 5.20 involves different shapes of (2D) contour plots such as elliptical/circular and indicates that whether the two-parameter interactions were significant or not. Elliptical contours indicate that interactions between corresponding parameters are significant while the circular contours plots indicate that the interactions between the corresponding parameters are negligible. In this study, ten independent response surfaces plots (without removing the insignificant interactive terms) with their respective contours were generated using software (Design-Expert 10.0) as shown in Fig. 5.20. Based on the above criteria for analyzing the 3D plots and their 2D projections, it is clear that the terms 'particle size-flow rate-$CO_2$' is insignificant while the terms 'temperature-flow rate-$CO_2$', 'pressure - % of co-solvent' and 'particle size - % of co-solvent' have been observed comparatively less significant. The concluding remarks for other remaining terms have also been produced in Table 5.15.

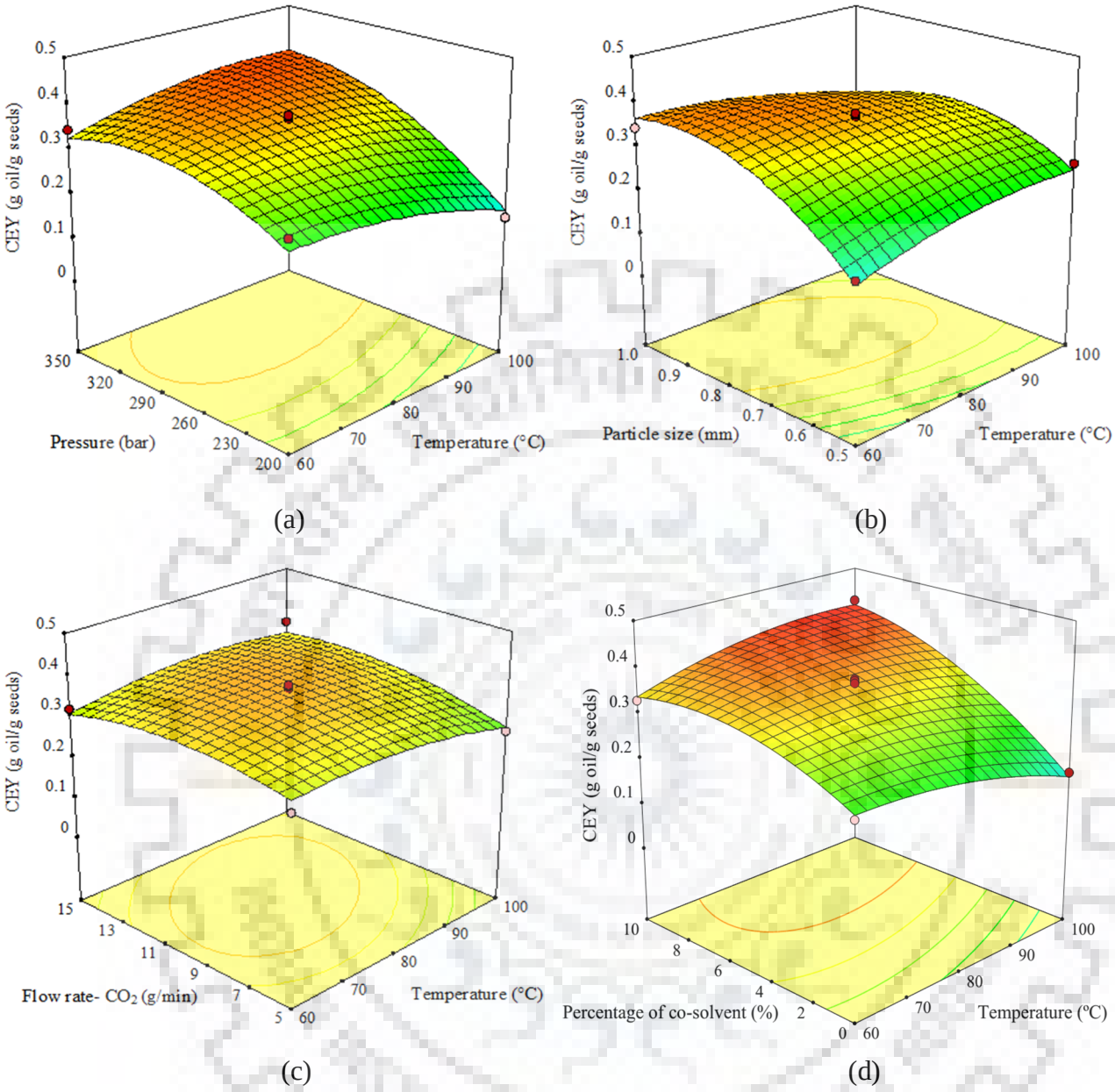


Fig. 5.20: 3D plots of response surfaces with their 2D projections for AM seed oil.

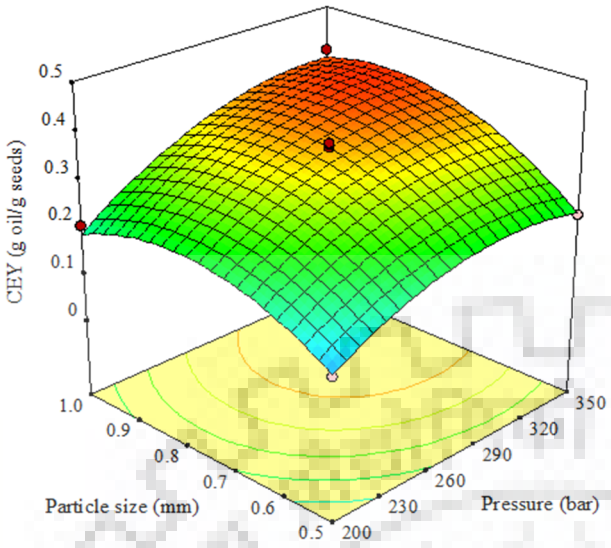


(e)

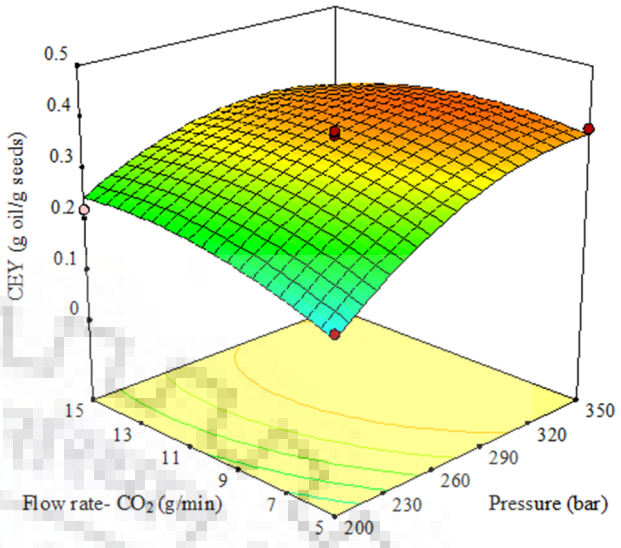


(f)

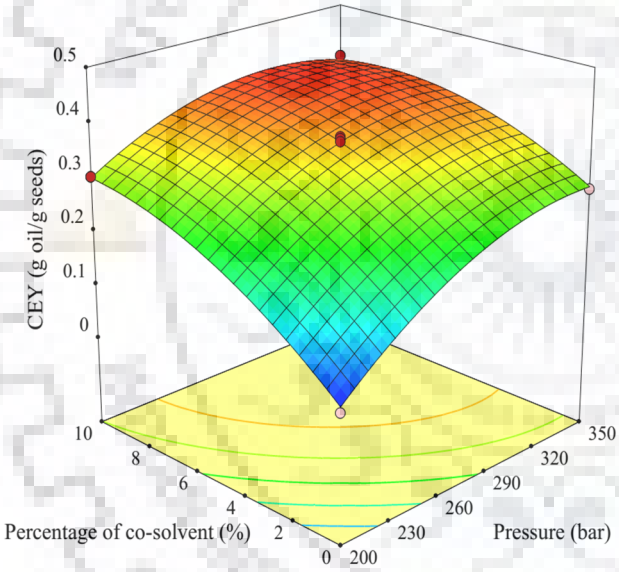


(g)

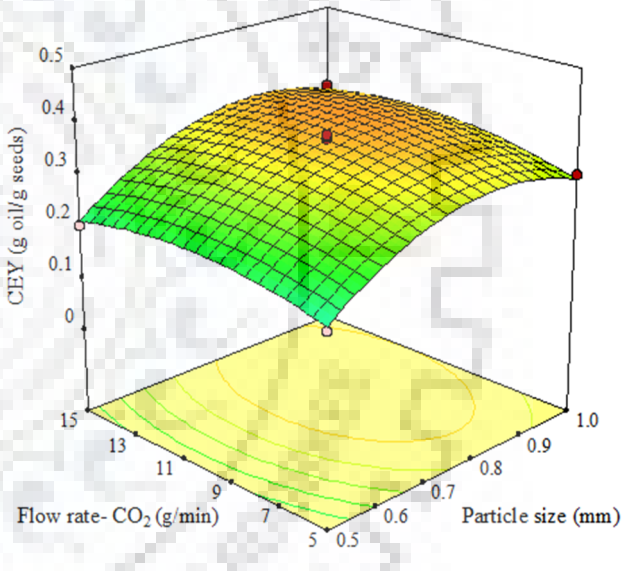


(h)

Fig. 5.20: (Cont…)

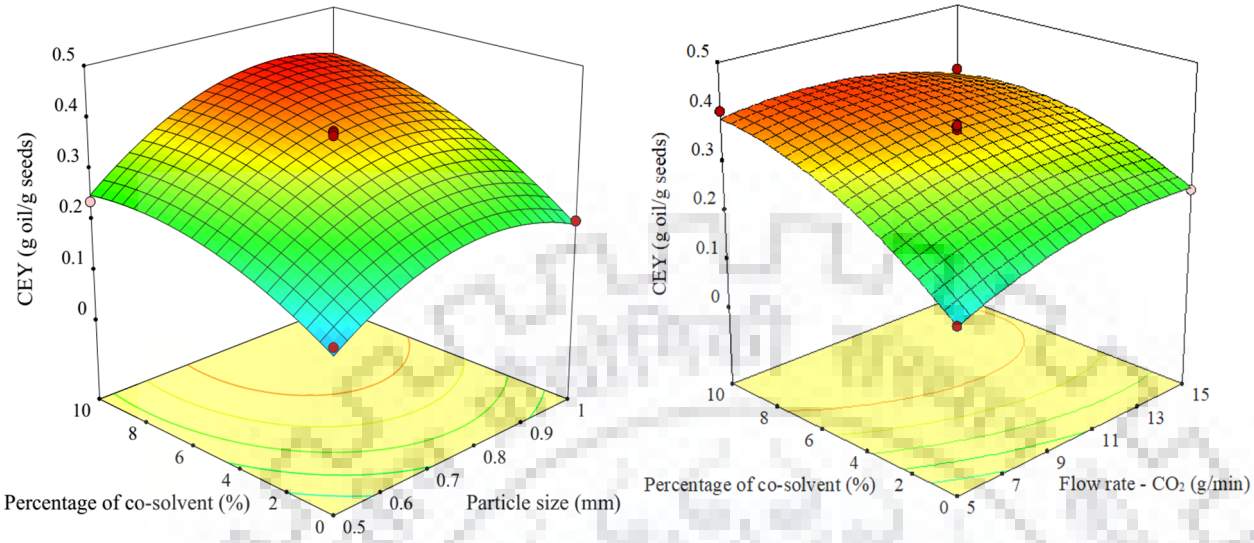


(i) (j)

Fig. 5.20: (Cont …)

### 5.3.8 A final comparison among four methods of analysis of interactive terms for the SFE of AM seed oil

The effects of interactive terms have been discussed through qualitative and quantitative analysis in the previous sections of this Chapter 5. The qualitative analysis consists of 2D and 3D plots, which are based on line plots (Fig. 5.19) and the response surface plots (Fig. 5.20) respectively while the quantitative analysis consists of SF (Table 5.14) and ANOVA (Table F.1) from which the magnitude of SF-value and p-value were used respectively for the classification of interactive terms accordingly. A final comparison among four methods (e.g. 2D, 3D, SF and ANOVA) of analysis of interactive terms for the SFE of AM seed oil is given in Table 5.15. The effects of interactive terms have been classified into five categories such as most significant (MS), significant (S), less significant (LS), insignificant (IS) and most insignificant (MI). The decision for the allotment of the specific category was made based on majority of the same category given by maximum number of methods (at least three) while in case of draw the quantitative analysis is given preference. For example, the term 'temperature-% of co-solvent' was categorized as 'MS' by three methods (e.g. 2D, SF and ANOVA) while one method (e.g. 3D) says it is as 'S' therefore it can be concluded that this term is to be considered as 'MS'. Similarly, the interactive term 'particle-flow rate-$CO_2$' was categorized as 'MI' by two methods while two methods proved it as 'IS' therefore finally these terms were considered as 'MI' based on the preference to quantitative analysis.

Table 5.15. A final comparison of four methods of analysis of interactive terms during the SFE of AM seed oil.

| Interactive terms | Methods of analysis: Qualitative analysis: 2D analysis (based on Line plots) | Qualitative analysis: 3D analysis (based on surface and contour plots | Quantitative analysis: SF analysis (Based on the value of SF) | Quantitative analysis: ANOVA analysis (Based on p-value) | Concluding remarks |
|---|---|---|---|---|---|
| Temperature – Pressure | S | S | S (0.8426) | >0.0001 (S) | Significant |
| Temperature – Particle size | S | S | S (0.8808) | >0.0001 (S) | Significant |
| Temperature – Flow rate-$CO_2$ | S | LS | LS (0.1438) | 0.0774 (LS) | Less Significant |
| Temperature - % of co-solvent | MS | S | MS (1.0000) | <0.0001 (MS) | Most Significant |
| Pressure – Particle size | S | S | S (0.3369) | 0.0119 (LS) | Significant |
| Pressure - Flow rate-$CO_2$ | S | S | S (0.4746) | 0.0038 (S) | Significant |
| Pressure - % of co-solvent | S | LS | S (0.4495) | 0.0046 (S) | Significant |
| Particle size – Flow rate-$CO_2$ | IS | IS | MI (0.0000) | 0.5070 (MI) | Most Insignificant |
| Particle size - % of co-solvent | LS | LS | LS (0.2363) | 0.0302 (LS) | Less Significant |
| Flow rate-$CO_2$ - % of co-solvent | S | S | S (0.5410) | 0.0023 (S) | Significant |

SF value: MI ($0.0 \leq SF \leq 0.001$), IS ($0.001 \leq SF \leq 0.1$), LS ($0.1 \leq SF \leq 0.3$), S ($0.3 \leq SF \leq 0.9$), MS ($0.9 \leq SF \leq 1.0$)
p-value: MI (p-value $\geq 0.5$), IS ($0.1 \leq$ p-value $< 0.5$), LS ($0.01 \leq$ p-value $\leq 0.09$), S ($0.0001 \leq$ p-value $\leq 0.01$), MS (p-value $< 0.0001$)

Notation:
MI: Most Insignificant, LS: Less Significant, S: Significant, IS: Insignificant, MS: Most Significant, SF: Severity factor

5.4 Validation of Sovova model for the SFE of AM and PP seed oils

Two types of natural feed materials (e.g. AM and PP seeds) have been used for the present study. In the present work, the SFE process has been modeled by Sovova, 1994 which also named as broken and intact cell (BIC) model. The assumptions which were taken into consideration during the development of this model have already been described in detail in section 2.12.2 of Chapter 2.

This model also assumed that the solute (oil) is contained by the seed and protected by the seed walls. However, a part of the walls has been broken up by milling (during the sizing of particles) so that the solute is directly exposed to the solvent. Further, this model considers that the initial total mass of solute (oil) in the solid (O) consists of mass of easily accessible solute (P) and the mass of inaccessible solute (K) inside the solid particle as given in Eq. 5.15.

$$O = P + K \quad \text{… Eq. 5.15}$$

The mass of solute free solid phase (N), remains constant during the SFE process and the amounts of solute are related to 'N' therefore the initial concentration can be related as follows;

$$x(t = 0) = x_0 = \frac{O}{N} = x_p + x_k = \frac{P}{N} + \frac{K}{N} \quad \text{… Eq. 5.16}$$

The quantities, $x_0$, $x_p$, and $x_k$ represent as the fraction of total initial oil, easily accessible oil and inaccessible oil respectively, present in the solid with respect to solute-free solid (N). The detailed description of the model has been given in the section 2.12.2 of Chapter 2.

The fitting parameters (e.g. Z, W and $x_k$) of the Sovova model (SM) were optimized using the global optimization technique (genetic algorithm (GA) approach) by running a written program in MATLAB. The objective of the problem is to minimize the average absolute relative deviation percentage (AARD %) between the CEY's, obtained from the SM and from the experiments during the SFE of AM and PP seed oils. The experimental parameters (e.g. initial solute fraction of seed ($x_0$), mass of non-extractable solid/solute free solid (N), solubility ($y_r$), flow rate-$CO_2$ ($Q_{CO2}$) and observed CEY ($y_{obs}$)) were used to optimize fitting parameters for the present model using a MATLAB based in-house developed program.

The solubility ($y_r$) of oil in SC-$CO_2$ and SC-$CO_2$ plus co-solvent (Ethanol) was calculated by using the starting data points that fall on the linear part of the extraction curve of each experimental run, which is a plot between mass of oil extracted and mass of solvent (SC-$CO_2$) used. The mass of non-extractable solid (means solute free solid) was calculated by subtracting the amount of solute

(oil) from the mass of material (e.g. 0.05 kg) used for the experiments while taking the maximum achieved CEY into consideration (e.g. 0.4286 for AM and 0.36 for PP seed oil during the SFE).

N = *weight of seed material – weight of solute (oil)* … Eq. 5.17

Where, the weight of seed material is '0.05 kg' and the weights of solute (oil) are 0.0215 kg and 0.018 kg for the AM and PP seed oil respectively.

The flow rates of $CO_2$ (kg/min) were taken as 0.005, 0.01 and 0.015 kg/min according to the design of experiments (as given in Table 5.2). In the MATLAB program the upper and lower values of each of the fitting parameters that are to be optimized are set as (0.01<= Z <= 30), (0.0001 <= W <= 10) and 0.001 <= $x_k$ < $x_p$) while the $x_p$, is always less than $x_0$. The mass transfer coefficients for solid phase ($k_{xa}$) and solvent phase ($k_{ya}$) were calculated, using the optimized values of Z, W and $x_k$ using the Eq. 5.18 and Eq. 5.19 (Ferreira et al., 2002).

$$Z = \frac{N\, k_{Ya} \rho_{CO_2}}{Q_{CO_2}(1-\varepsilon)\rho_s} \quad \text{… Eq. 5.18}$$

$$W = \frac{N\, k_{xa}}{Q_{CO_2}(1-\varepsilon)} \quad \text{… Eq. 5.19}$$

As described in the section 2.12.2, an extraction curve is divided into three sections as shown in Fig. 2.9. The first extraction period is named as 'constant extraction rate (CER) period' due to its linear nature of the curve, which also represents the solubility of solute (oil) in the solvent (SC-$CO_2$). This period covers the plot from $t = 0$ to $t = t_{CER}$ in which the mass transfer rate is governed by convection and mass transfer resistance mainly lies in the solvent phase side. The easily accessible solute, which is around the seed particle, is extracted first in this period. Hence, it has been observed that the extraction rate is quite high in this period, which is attributed to above phenomenon. The second extraction period which is also known as 'falling extraction rate (FER) period', covers the region from $t_{CER}$ to $t_{FER}$. In this transition period (due to the transition from CER to FER), the mass transfer of solute to solvent phase is governed by both convection as well as diffusion from solid matrix pores. The above phenomena leads to higher mass transfer resistance in the transport path and therefore, in this period, a somewhat slower mass transfer rate has been observed in comparison

to first extraction period. Until the end of the second extraction period ($t_{FER}$) it appears that most of the extractable solute (oil) is transferred to solvent extracted. After, $t = t_{FER}$, the mass transfer rate falls rapidly and is totally governed by only diffusion which is the slowest process. Hence, the extraction of oil in this period is very less.

5.4.1 Validation of Sovova model (SM) for AM seed oil

The experimental parameters required for the validation of the Sovova model (SM) were reproduced below for brevity. Table 5.16 shows the values of all input parameters for the SFE experiments. As explained earlier that 0.05 kg of AM seeds of different mean particle sizes such as 1.0, 0.75, and 0.50 mm were used as feedstock. As shown in Table 5.16, the particle sizes were of 0.5, 0.75, 1.0 mm diameter and these particle sizes offered bed densities of 550.7, 645.4, 745.4 kg/m$^3$ for AM seeds respectively with corresponding particle densities of 1101.3, 1008.3, 1007.3 kg/m$^3$. Furthermore, the values of bed porosity were 0.5, 0.36 and 0.26. The observed increment in the bed porosity (from 0.26 to 0.5) with decrease in the particle size (from 1.0 to 0.5 mm) is ascribed to the decrease in the particle sphericity with decreasing the particle size (Zhang et al., 2018). The amounts of initial oil content ($x_o$) in the AM seeds was 0.7544 kg oil/kg of oil free solid.

Table 5.16. Experimental parameters used for fitting the sovova model.

| Particle size | AM seeds | | | PP seeds | | |
|---|---|---|---|---|---|---|
| | Bed density (kg/m$^3$) | Particle density (kg/m$^3$) | Bed porosity | Bed density (kg/m$^3$) | Particle density (kg/m$^3$) | Bed porosity |
| 0.5 mm | 550.7 | 1101.3 | 0.5 | 446.7 | 899.3 | 0.5033 |
| 0.75 mm | 645.4 | 1008.5 | 0.360 | 566.7 | 944.4 | 0.4 |
| 1.0 mm | 745.4 | 1007.3 | 0.26 | 573.3 | 905.3 | 0.3667 |

| | | | |
|---|---|---|---|
| $x_0$ (kg oil/kg of oil free solid) | = | 0.7544 | 0.5625 |
| N (oil free solid kg) | = | 0.0285 | 0.032 |
| $y_r$ (kg oil/kg $CO_2$) | = | $3.22\times10^{-3}$ to $9.052\times10^{-2}$ | $9.0\times10^{-4}$ to $3.6\times10^{-2}$ |
| $Q_{CO2}$ (kg/min) | = | 0.005, 0.01, 0.015 | 0.005, 0.01, 0.015 |
| Extraction time (min) | = | 0.0 to 250 | 0.0 to 250 |
| $y_{obs}$ (kg oil/kg seeds) | = | 0.066 to 0.424 | 0.036 to 0.3556 |

Figs. (5.21-5.32), have been plotted to show a comparison between experimental and predicted (by Sovova and Reverchon models) CEY for extraction curves during the SFE of AM seed oil. However, the fitting of Reverchon model (RM) will be discussed in the upcoming sections (5.5.1 and 5.5.2) of this chapter. Table 5.17 shows the experimental conditions (for all 46 runs) and values of optimized model fitting parameters Z, W and $x_k$ obtained from experimental data for the AM seed oil by minimizing the AARD %. In the subsequent section, inherent observations from these figures (Figs. (5.21-5.32)) are presented.

From the Table 5.17, it is clear that the mass transfer coefficients in solvent phase ($k_{ya}$) are larger than the mass transfer coefficients in the solid phase ($k_{xa}$). This is due to the fact that, the solid phase mass transfer coefficient ($k_{xa}$) is related to the molecular and effective diffusion of the unreleased oil in the particles and also depends on the proprieties (e.g. particle size, bed density, particle density, bed porosity and the weight of solute free solid etc.) of the seed materials. These enhance the mass transfer resistance in the solid phase side while on the other hand, the mass transfer coefficient in solvent phase ($k_{ya}$) depends on the process parameters such as temperature, pressure, flow rate-$CO_2$ and the % of co-solvent.

The figures (Figs. (5.21-5.32)) have shown the variation of CEY (kg oil/kg seeds) of AM seed oil with time (min), for all the 46 experimental runs at the range of temperature from 60 to 100 ℃, pressure from 200 to 350 bar, particle size from 0.5 to 1.0 mm, flow rate-$CO_2$ from 5 to 15 g/min and the % of co-solvent from 0.0 to 10 %. The following observations can be drawn from the Figs. (5.21-5.32):

1. The CEY of AM seed oil increases rapidly in the early period of extraction in all the runs and then in some runs it tends towards asymptotic maxima (as shown in Figs. 5.21(b), 5.25(a), 5.26(b), 5.27(a), 5.27(c), 5.28(a), 5.29(b), 5.30(a), 5.31(a) and 5.32(b)).
2. The maximum percentage of AM seed oil has been extracted during the transition period (constant extraction period + falling extraction period) means in the first extraction period in which the mass transfer is governed by convection and in the second extraction period in which the convection as well as diffusion play a crucial role for the mass transfer.
3. From all the Figs. (5.21-5.32), it is clear that the Sovova model (SM) fits the experimental CEY data with an AARD % band of '+1.436 to +14.198 %' and an average AARD % of 5.224 % and thus it can be concluded that the model fitting is appreciably good.

4. All the plots of CEY (excepting Figs. 5.24(a), 5.25(c) and 5.32(a)) have shown an appreciably good fitting with the experimental values of CEY by SM with an average AARD % of 4.683 %.
5. For all the plots (excepting the Figs. 5.23(c), 5.25(c), and 5.31 (b)), the predicted CEY from SM and experimental values of CEY shows the same trend with an average AARD % of 5.029 %.
6. The overall average experimental CEY is found to be ~ 0.2837 kg oil/ kg seeds with a standard deviation of 0.0892 and overall average predicted values of CEY from SM is found to be ~0.2974 kg oil/kg seeds with a standard deviation of 0.0904.

The above observations during the SFE of AM seeds oil can be explained as:

Based on the computed values of time duration for the constant extraction rate ($t_{CER}$) and falling extraction rate ($t_{FER}$) as given in Table 5.17. The percentages of extracted oil (% of total oil extracted) in each period (first, second and third) are computed as shown in Table 5.18.

From the Table 5.18, it can be concluded that most of the oil (avg 77.17%) is extracted in the first and second period of extraction curve. For the Figs. 5.22(a,b,c), 5.23(c), 5.25(b,c,d), 5.26(c), 5.27(c), 5.28(c,d), 5.29(a,d), 5.30(a,d), and 5.31(b,c) the extraction rates is quite high in the third extraction period in which the mass transfer is governed by diffusion phenomena. These figures demonstrate the extraction curves of CEY of AM seed oil for middle and highest particle size (e.g. 0.75 and 1.0 mm respectively) only, which can be explained through the effect of initial high pressure difference (~200 bar) across the bed as it has already been explained in section 5.2.3. The AM seed particles (e.g. 0.5 mm) are significantly soft (based on physical appearance), which promotes the compaction for smaller particles while, for the higher particle size (0.8 to 1.0 mm) the compaction effect is comparatively low. And as the result, the solvent passes through the inter and intra pores of particles as well as bed and the effects of other parameters (e.g. pressure, flow rate-$CO_2$ and the % of co-solvent) promotes the enhancement of the CEY in the third period of extraction curve. In addition to this, it is also observable that all these runs (16 number of runs out of 46 ) were performed at higher temperature range (80 – 100 °C), and high pressure range (275 – 350 bar) for which the volatility and the density effect on the AM seed oil are high, which also improves the extraction in the third extraction period by overcoming the diffusional resistances in the particle.

Table 5.17. Parameters of Sovova model for the SFE of AM seed oil.

| | Experimental parameters | | | Tuning parameters | | | Calculated parameters from model | | | | Error |
|---|---|---|---|---|---|---|---|---|---|---|---|
| Run | Temperature (°C) | Pressure (bar) | ($y_r$) (kg oil/kg $CO_2$) | $x_k$ | Z | W | $t_{CER}$ (min) | $t_{FER}$ (min) | $k_{ya}$ ($min^{-1}$) | $k_{xa}$ ($min^{-1}$) | AARD % |
| 1 | 80 | 200 | 0.0047 | 0.6246 | 2.9540 | 0.0033 | 26.7566 | 125.4750 | 0.7672 | 0.0006 | 1.4360 |
| 2 | 80 | 275 | 0.0170 | 0.2541 | 2.0584 | 0.0117 | 40.7972 | 131.6877 | 0.6842 | 0.0026 | 2.7575 |
| 3 | 60 | 350 | 0.0214 | 0.4808 | 7.7124 | 0.0210 | 4.7212 | 50.1265 | 2.5638 | 0.0047 | 2.8548 |
| 4 | 60 | 275 | 0.0056 | 0.5004 | 24.8687 | 0.0117 | 5.1890 | 207.0155 | 8.2669 | 0.0026 | 5.8723 |
| 5 | 80 | 275 | 0.0807 | 0.7011 | 0.1017 | 0.0302 | 37.0321 | 41.3348 | 0.0196 | 0.0039 | 3.0830 |
| 6 | 100 | 275 | 0.0126 | 0.7439 | 0.6303 | 0.0702 | 7.5149 | 60.3377 | 0.1048 | 0.0079 | 4.0699 |
| 7 | 80 | 200 | 0.0552 | 0.7484 | 0.0378 | 0.0189 | 8.1466 | 8.4973 | 0.0126 | 0.0042 | 5.6105 |
| 8 | 80 | 200 | 0.0054 | 0.5337 | 7.3724 | 0.0046 | 10.5835 | 107.8268 | 3.6761 | 0.0015 | 2.1556 |
| 9 | 60 | 200 | 0.0173 | 0.3715 | 4.1802 | 0.0066 | 15.0460 | 82.3550 | 1.3896 | 0.0015 | 2.9328 |
| 10 | 100 | 350 | 0.0211 | 0.3199 | 30.000 | 0.0199 | 1.9519 | 68.8336 | 9.9726 | 0.0045 | 6.9122 |
| 11 | 80 | 275 | 0.0106 | 0.7500 | 0.2680 | 0.0385 | 8.8640 | 21.0124 | 0.0348 | 0.0034 | 6.7505 |
| 12 | 80 | 275 | 0.0178 | 0.3941 | 15.9104 | 0.0244 | 3.6259 | 76.4470 | 5.2889 | 0.0055 | 5.9327 |
| 13 | 80 | 200 | 0.0048 | 0.5647 | 30.000 | 0.0082 | 3.7656 | 180.9843 | 11.5308 | 0.0021 | 13.1753 |
| 14 | 100 | 200 | 0.0032 | 0.6269 | 30.000 | 0.0062 | 3.7601 | 206.4540 | 9.9726 | 0.0014 | 5.2731 |
| 15 | 80 | 350 | 0.0162 | 0.3440 | 2.1088 | 0.0056 | 22.8715 | 73.9387 | 1.0515 | 0.0019 | 2.4366 |
| 16 | 80 | 275 | 0.0188 | 0.2670 | 7.6612 | 0.0091 | 6.4346 | 58.7800 | 3.8201 | 0.0031 | 5.8084 |
| 17 | 80 | 350 | 0.0245 | 0.3575 | 13.438 | 0.0352 | 3.4353 | 60.7289 | 4.4671 | 0.0079 | 5.5449 |
| 18 | 80 | 200 | 0.0130 | 0.7222 | 0.1112 | 0.0022 | 63.4594 | 70.9612 | 0.0370 | 0.0005 | 4.7902 |
| 19 | 80 | 275 | 0.0053 | 0.7500 | 0.5155 | 0.0123 | 4.5712 | 10.8536 | 0.1339 | 0.0022 | 14.1982 |
| 20 | 100 | 275 | 0.0068 | 0.7500 | 0.4373 | 0.0303 | 4.2133 | 18.2971 | 0.1681 | 0.0079 | 6.7667 |
| 21 | 80 | 275 | 0.0201 | 0.4877 | 4.8137 | 0.0259 | 7.8371 | 58.1111 | 1.6002 | 0.0058 | 3.8219 |
| 22 | 60 | 275 | 0.0232 | 0.2019 | 0.8944 | 0.0037 | 75.9813 | 145.0178 | 0.2973 | 0.0008 | 9.1212 |
| 23 | 80 | 275 | 0.0318 | 0.7280 | 0.0913 | 0.0083 | 25.9111 | 28.5185 | 0.0351 | 0.0022 | 2.5467 |

Cont…

| | Experimental parameters | | | Tuning parameters | | | Calculated parameters from model | | | | Error |
|---|---|---|---|---|---|---|---|---|---|---|---|
| Run | Temperature (°C) | Pressure (bar) | ($y_r$) (kg oil/kg $CO_2$) | $x_k$ | Z | W | $t_{CER}$ (min) | $t_{FER}$ (min) | $k_{ya}$ ($min^{-1}$) | $k_{xa}$ ($min^{-1}$) | AARD % |
| 24 | 60 | 275 | 0.0082 | 0.5216 | 2.1064 | 0.0038 | 38.2496 | 129.0258 | 0.5470 | 0.0007 | 4.0079 |
| 25 | 60 | 275 | 0.0187 | 0.3399 | 2.4088 | 0.0074 | 17.5027 | 62.4475 | 1.2011 | 0.0025 | 4.2052 |
| 26 | 80 | 275 | 0.0112 | 0.4761 | 5.8373 | 0.0132 | 8.0870 | 69.1859 | 3.3655 | 0.0052 | 4.4076 |
| 27 | 100 | 275 | 0.0905 | 0.7218 | 0.0560 | 0.0222 | 12.2075 | 12.9557 | 0.0279 | 0.0075 | 7.0499 |
| 28 | 80 | 275 | 0.0178 | 0.4250 | 9.9752 | 0.0249 | 5.2877 | 73.6677 | 3.3160 | 0.0056 | 5.0204 |
| 29 | 100 | 275 | 0.0240 | 0.4555 | 27.763 | 0.0603 | 1.2812 | 56.9900 | 9.2290 | 0.0135 | 5.1053 |
| 30 | 80 | 350 | 0.0138 | 0.3548 | 1.0911 | 0.0064 | 75.7108 | 165.0534 | 0.3627 | 0.0014 | 6.3231 |
| 31 | 80 | 200 | 0.0573 | 0.6926 | 0.1099 | 0.0133 | 55.9371 | 62.6018 | 0.0183 | 0.0015 | 2.3424 |
| 32 | 100 | 275 | 0.0598 | 0.6429 | 0.1166 | 0.0054 | 45.5897 | 51.0610 | 0.0387 | 0.0012 | 3.3723 |
| 33 | 80 | 275 | 0.0229 | 0.5291 | 5.5220 | 0.0301 | 5.0740 | 43.8272 | 1.8356 | 0.0068 | 4.3873 |
| 34 | 80 | 350 | 0.0225 | 0.1671 | 30.000 | 0.0276 | 4.9609 | 166.4709 | 4.9863 | 0.0031 | 6.5399 |
| 35 | 80 | 275 | 0.0216 | 0.7310 | 0.6791 | 0.2038 | 9.1175 | 112.0952 | 0.1129 | 0.0229 | 4.2574 |
| 36 | 80 | 275 | 0.0238 | 0.6259 | 30.000 | 0.0365 | 0.5126 | 25.1525 | 9.9726 | 0.0082 | 5.1793 |
| 37 | 80 | 350 | 0.0189 | 0.7365 | 0.7508 | 0.0701 | 3.5997 | 16.2968 | 0.2886 | 0.0182 | 5.8247 |
| 38 | 80 | 350 | 0.0105 | 0.4199 | 1.5286 | 0.0035 | 59.3313 | 156.3263 | 0.3970 | 0.0006 | 6.4928 |
| 39 | 100 | 275 | 0.0107 | 0.4364 | 2.6285 | 0.0081 | 32.3088 | 131.5357 | 0.6826 | 0.0014 | 1.8841 |
| 40 | 80 | 275 | 0.0130 | 0.6946 | 9.0352 | 0.0069 | 0.9667 | 11.5026 | 4.5052 | 0.0023 | 1.5440 |
| 41 | 60 | 275 | 0.0147 | 0.2042 | 1.6148 | 0.0059 | 66.2078 | 177.3170 | 0.6207 | 0.0015 | 7.6600 |
| 42 | 80 | 275 | 0.0807 | 0.7011 | 0.1017 | 0.0302 | 36.9982 | 41.2956 | 0.0169 | 0.0034 | 3.0830 |
| 43 | 80 | 275 | 0.0108 | 0.7500 | 0.4992 | 0.0541 | 2.3278 | 14.0550 | 0.1919 | 0.0140 | 4.4205 |
| 44 | 80 | 275 | 0.0080 | 0.4830 | 7.7925 | 0.0021 | 8.2920 | 76.9975 | 3.0356 | 0.0005 | 6.5861 |
| 45 | 60 | 275 | 0.0134 | 0.4368 | 30.000 | 0.0297 | 4.5094 | 203.9101 | 4.9863 | 0.0033 | 11.5826 |
| 46 | 80 | 275 | 0.0080 | 0.4370 | 11.8038 | 0.0048 | 9.6152 | 138.2141 | 3.0655 | 0.0008 | 5.1840 |

Table 5.18. Extracted oil in each period of extraction curve for AM seed oil during each run.

| Run | Oil extracted (% of total oil extracted) | | |
|---|---|---|---|
| | Three periods of extraction curve of each run | | |
| | $t \leq t_{CER}$ | $t_{CER} \leq t \leq t_{FER}$ | $t > t_{FER}$ |
| 1 (Fig. 5.21(a)) | 16.98 | 53.64 | 29.38 |
| 2 (Fig. 5.21(b)) | 33.53 | 53.56 | 12.91 |
| 3 (Fig. 5.21(c)) | 5.83 | 47.11 | 47.06 |
| 4 (Fig. 5.21(d)) | 2.22 | 86.36 | 11.42 |
| 5(Fig. 5.22(a)) | 9.51 | 1.78 | 88.71 |
| 6 (Fig. 5.22(b)) | 2.34 | 21.17 | 76.49 |
| 7 (Fig. 5.22(c)) | 1.67 | 0.60 | 97.73 |
| 8 (Fig. 5.22(d)) | 7.15 | 62.91 | 29.95 |
| 9 (Fig. 5.23(a)) | 17.44 | 62.41 | 20.15 |
| 10(Fig. 5.23(b)) | 2.90 | 70.93 | 26.17 |
| 11(Fig. 5.23(c)) | 1.27 | 6.37 | 92.35 |
| 12(Fig. 5.23(d)) | 4.63 | 63.86 | 31.51 |
| 13(Fig. 5.24(a)) | 2.35 | 80.58 | 17.07 |
| 14(Fig. 5.24(b)) | 2.17 | 86.95 | 10.88 |
| 15(Fig. 5.24(c)) | 33.39 | 44.44 | 22.17 |
| 16(Fig. 5.24(d)) | 15.07 | 64.04 | 20.90 |
| 17(Fig. 5.25(a)) | 5.93 | 61.75 | 32.32 |
| 18(Fig. 5.25(b)) | 25.52 | 2.06 | 72.42 |
| 19(Fig. 5.25(c)) | 1.13 | 1.97 | 96.90 |
| 20(Fig. 5.25(d)) | 0.92 | 6.50 | 92.58 |
| 21(Fig. 5.26(a)) | 10.49 | 43.48 | 46.03 |
| 22(Fig. 5.26(b)) | 61.55 | 34.29 | 4.16 |
| 23(Fig. 5.26(c)) | 6.80 | 2.12 | 91.08 |
| 24(Fig. 5.26(d)) | 30.81 | 48.98 | 20.21 |
| 25(Fig. 5.27(a)) | 29.91 | 44.77 | 25.32 |
| 26(Fig. 5.27(b)) | 9.44 | 48.70 | 41.86 |
| 27(Fig. 5.27(c)) | 3.68 | 3.58 | 92.74 |
| 28(Fig. 5.27(d)) | 4.66 | 59.50 | 35.84 |
| 29(Fig. 5.28(a)) | 3.28 | 61.08 | 35.64 |
| 30(Fig. 5.28(b)) | 49.72 | 39.48 | 10.81 |
| 31(Fig. 5.28(c)) | 19.27 | 4.37 | 76.36 |
| 32(Fig. 5.288(d)) | 33.24 | 3.05 | 63.71 |
| 33(Fig. 5.29(a)) | 5.81 | 40.01 | 54.18 |
| 34(Fig. 5.29(b)) | 2.93 | 91.38 | 5.70 |
| 35(Fig. 5.29(c)) | 2.61 | 51.97 | 45.43 |
| 36(Fig. 5.29(d)) | 0.95 | 28.46 | 70.59 |
| 37(Fig. 5.30(a)) | 2.52 | 7.72 | 89.76 |
| 38(Fig. 5.30(b)) | 43.55 | 46.19 | 10.26 |
| 39(Fig. 5.30(c)) | 25.86 | 52.85 | 21.29 |
| 40(Fig. 5.30(d)) | 3.01 | 12.16 | 84.83 |
| 41(Fig. 5.31(a)) | 44.92 | 51.09 | 3.99 |
| 42(Fig. 5.31(b)) | 9.51 | 1.79 | 88.70 |
| 43(Fig. 5.31(c)) | 1.70 | 5.26 | 93.04 |
| 44(Fig. 5.31(d)) | 11.53 | 68.08 | 20.39 |
| 45(Fig. 5.32(a)) | 2.28 | 88.71 | 9.02 |
| 46(Fig. 5.32(b)) | 6.65 | 79.06 | 14.29 |

From the Figs. (5.21-5.32) it is clear that the extraction curve (simulated by SM) fits well at the initial period (first period) of extraction means the linear part of it, while it deviates little bit from the experimental data in second and third extraction period. However, the third period has shown the larger deviation (as shown in Figs. 5.21(c), 5.23(c), 5.25(c), 5.27(c), 5.30(a) and 5.31(b)) than the second period of extraction curve. The probable reason for this departure lies in the model equations for the second and third periods of extraction curve (as discussed in section 2.12.2) which is reproduced below as Eq. 5.20 and Eq. 5.21.

$$t_{CER} = \frac{(x_0 - x_k)}{(y_r * Z)} \frac{msi}{Q_{CO2}} \quad \ldots \text{Eq. 5.20}$$

$$t_{FER} = t_{CER} + \left(\frac{msi}{Q_{CO2} * W}\right) * ln\left[\frac{x_k + (x_0 - x_k) * exp(W x_0 / y_r)}{x_0}\right] \quad \ldots \text{Eq. 5.21}$$

From the above equations (Eq. 5.20 and 5.21), proposed by Sovova, 1994, it is clear that the initial oil content ($x_0$) and the solubility ($y_r$) of oil in SC-$CO_2$ strongly affect the second and third extraction periods. In the present case, the high value of initial oil content ($x_0$ = 0.7544 kg oil/kg of oil free solid) and the very low value of solubility ($y_r$ = $3.22\times10^{-3}$ to $9.052\times10^{-2}$ kg oil/kg $CO_2$) leads to high values of $t_{CER}$ and $t_{FER}$ according to the Eq. 5.20 and Eq. 5.21. Therefore, from the definitions of first, second and third extraction periods (e.g.$(t \leq t_{CER})$, $(t_{CER} \leq t \leq t_{FER})$ and $(t > t_{FER})$ respectively), it is clear that the model equation which should only cover the first extraction period actually could not cover the all data points on the extraction curve.

Additionally, an excellent agreement (within +13.27% to -4.43% error band) between the experimental and predicted values of CEY of AM seed oil, can also be found from the parity plot for the SM, shown in Fig. 5.33. The SM produces an excellent fitting with 95.45% data points excepting only two data points (runs 19 and run 42) as deviation. The percentage of error (% error) was calculated using the formula as described previously in the section 5.1.1 (Eq. 5.4). From the Fig. 5.33, it can be seen clearly that 44 number of runs means 95.65% of total runs (e.g. 46 runs) falls within the error band '-4.43 to +13.27%'. 45 number of runs (e.g. 97.82% of total runs falls within the error band of '-4.43 to +24.4%' and 100% of total runs means 46 runs falls within the error band of '-4.43 to +44.48%'.

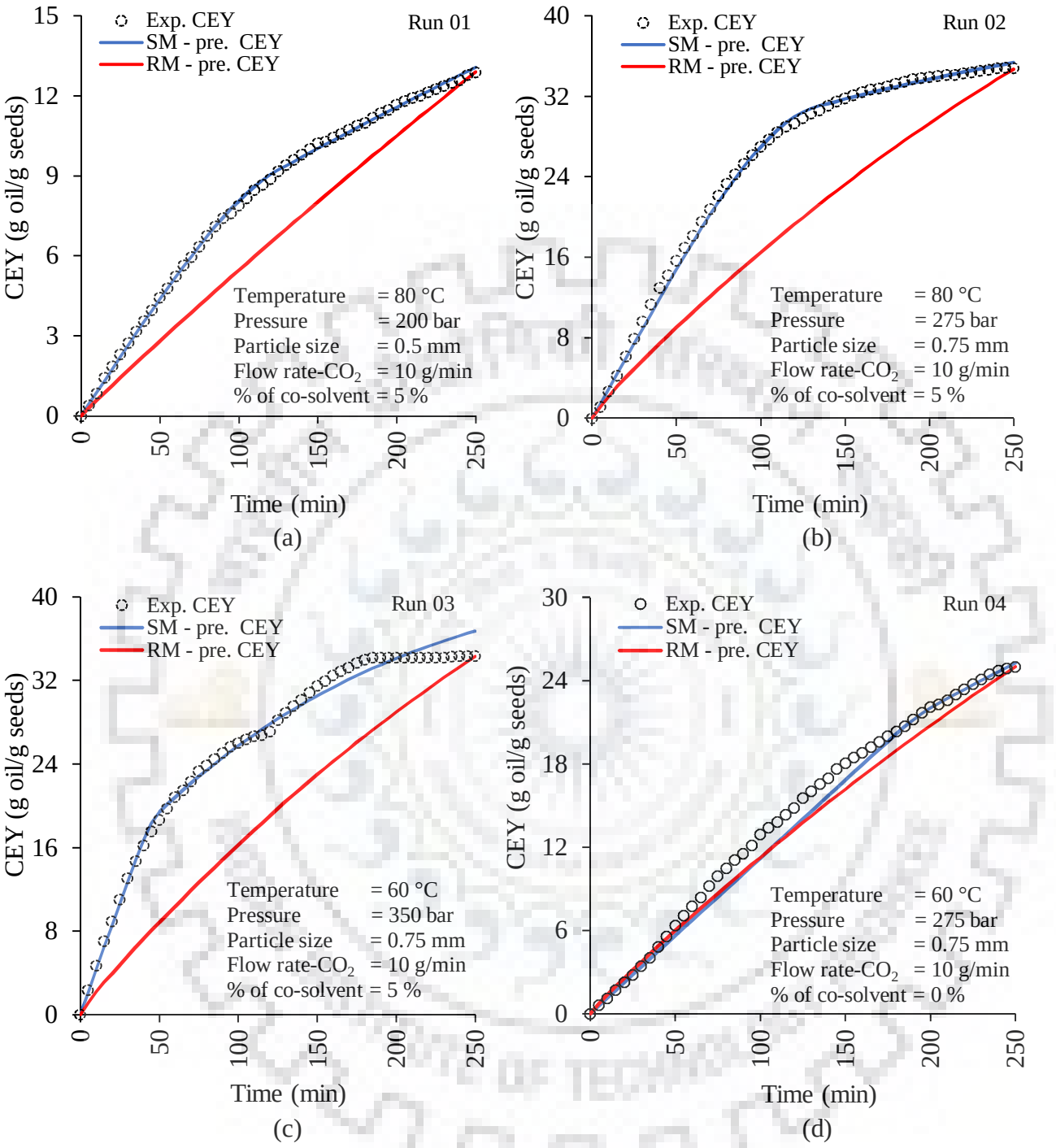


Fig. 5.21: Experimental and predicted CEY curves for AM seed oil during the SFE runs (01-04).

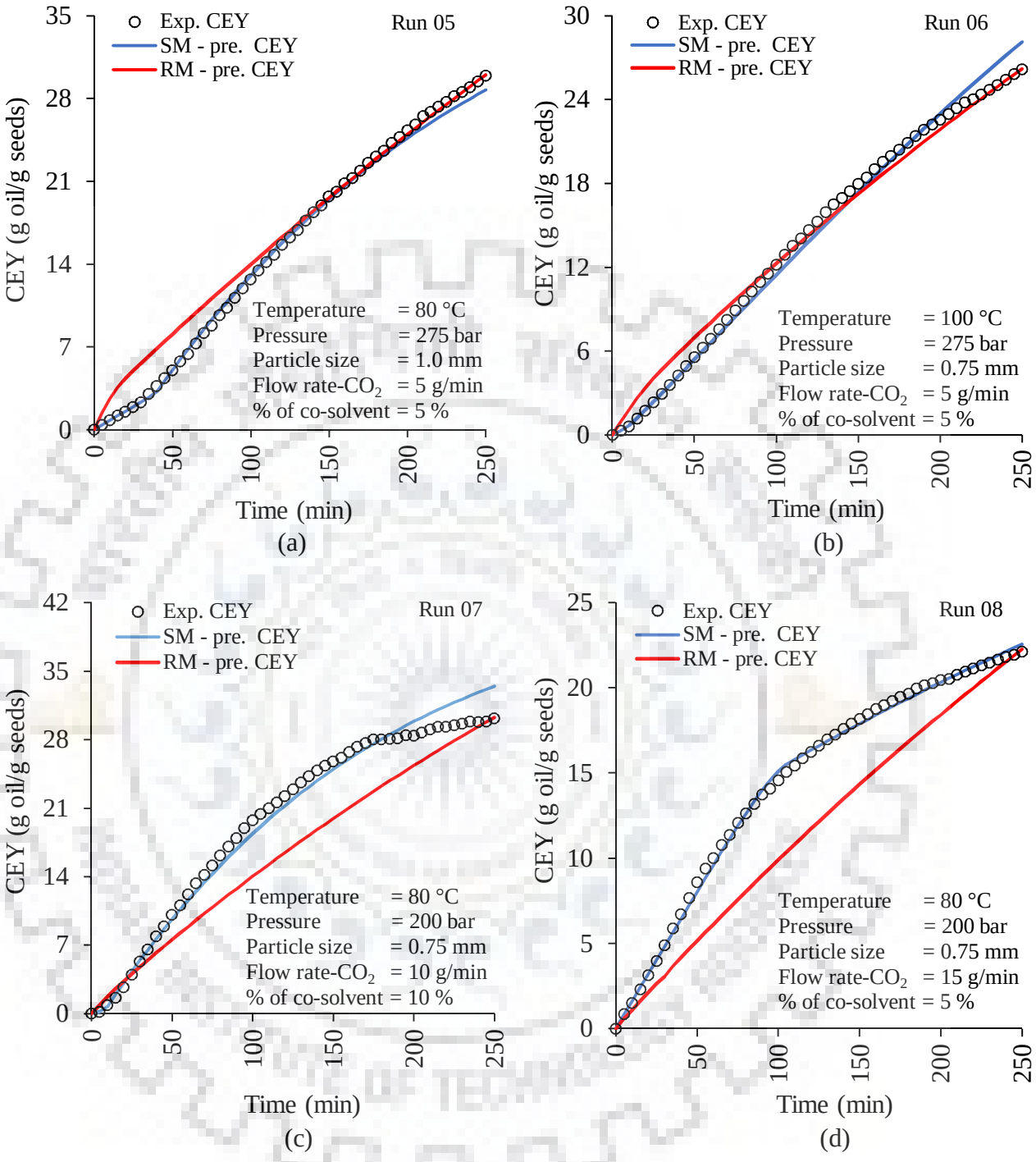


Fig. 5.22: Experimental and predicted CEY curves for AM seed oil during the SFE runs (05-08).

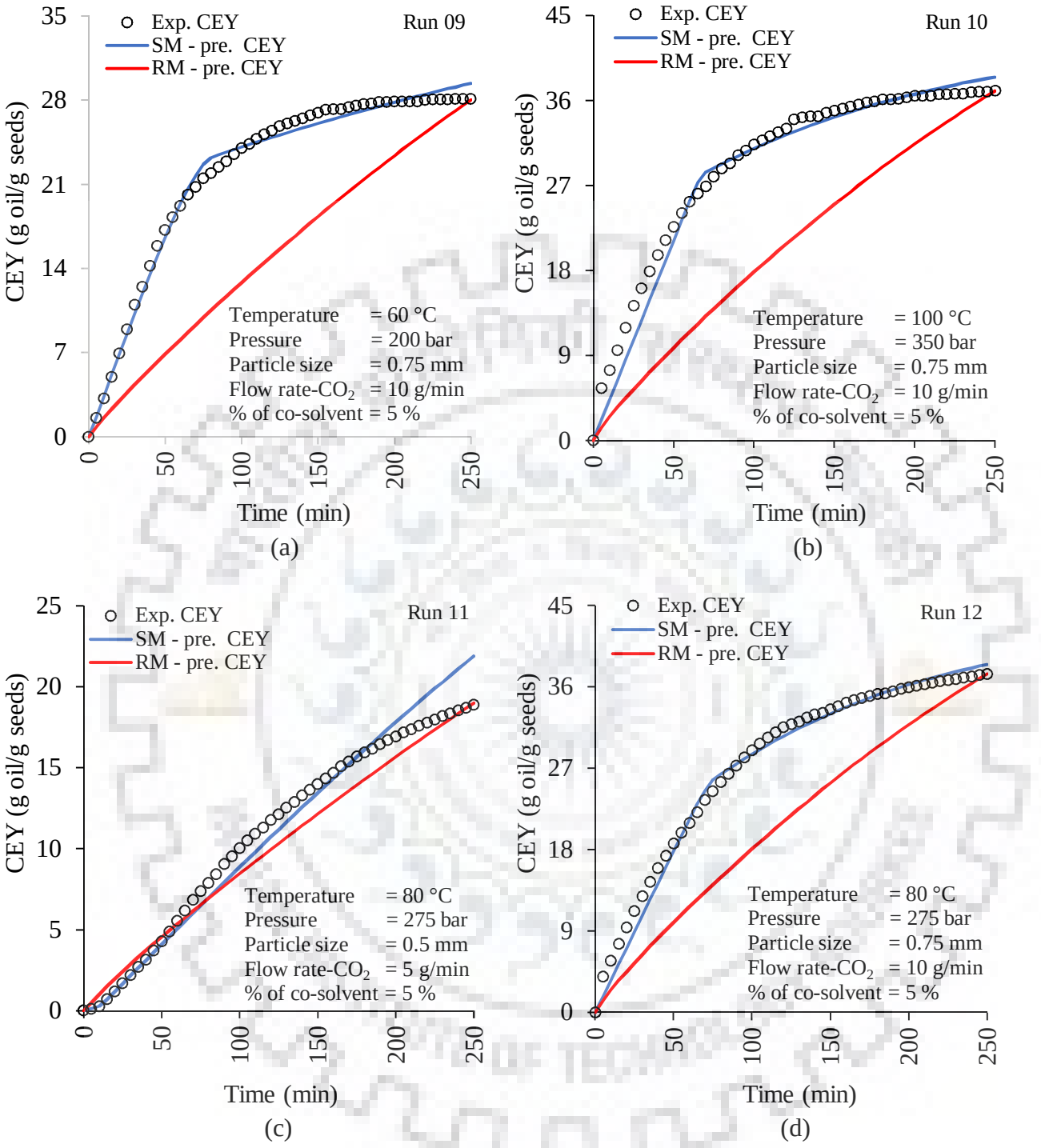


Fig. 5.23: Experimental and predicted CEY curves for AM seed oil during the SFE runs (09-12).

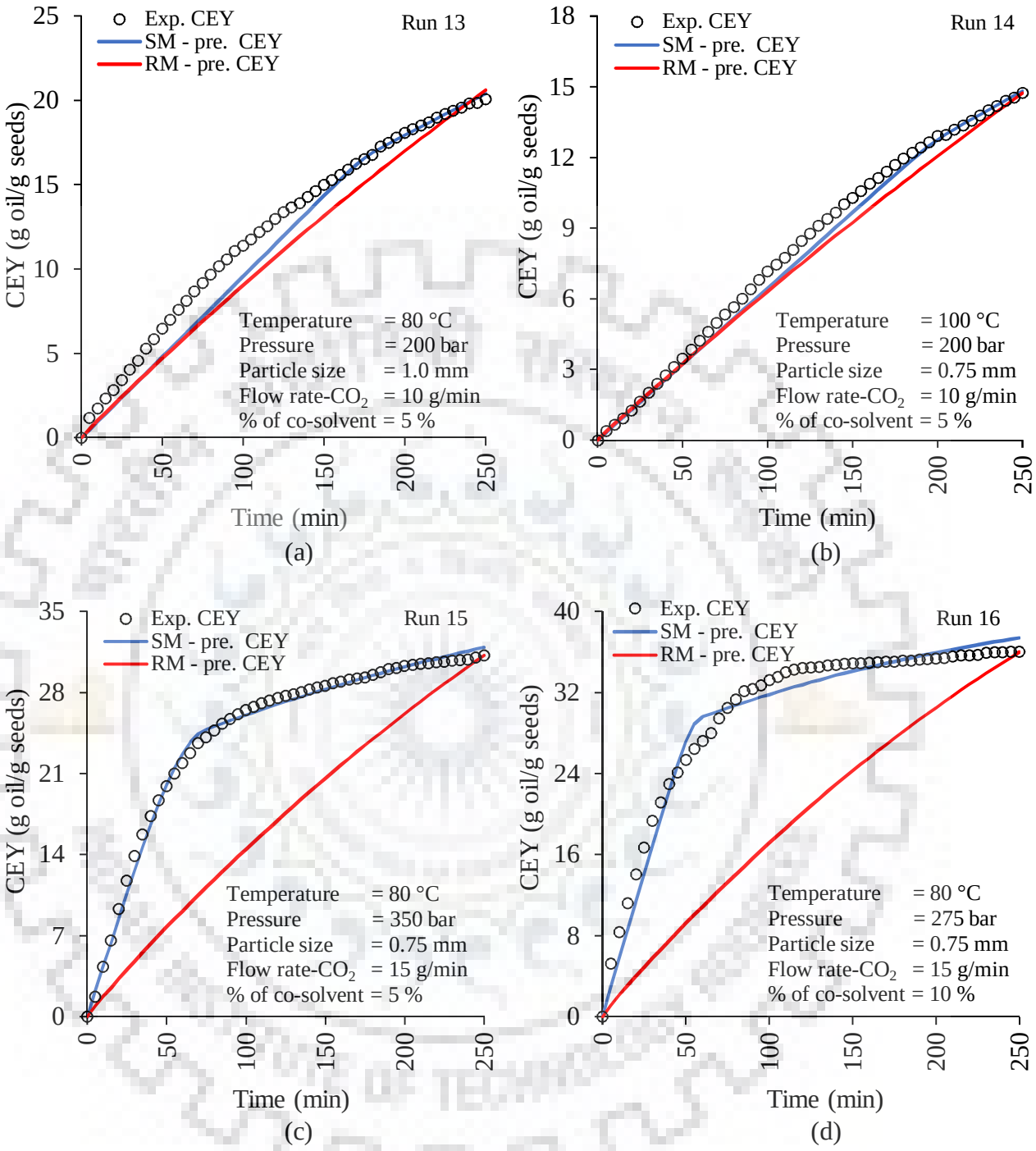


Fig. 5.24: Experimental and predicted CEY curves for AM seed oil during the SFE runs (13-16).

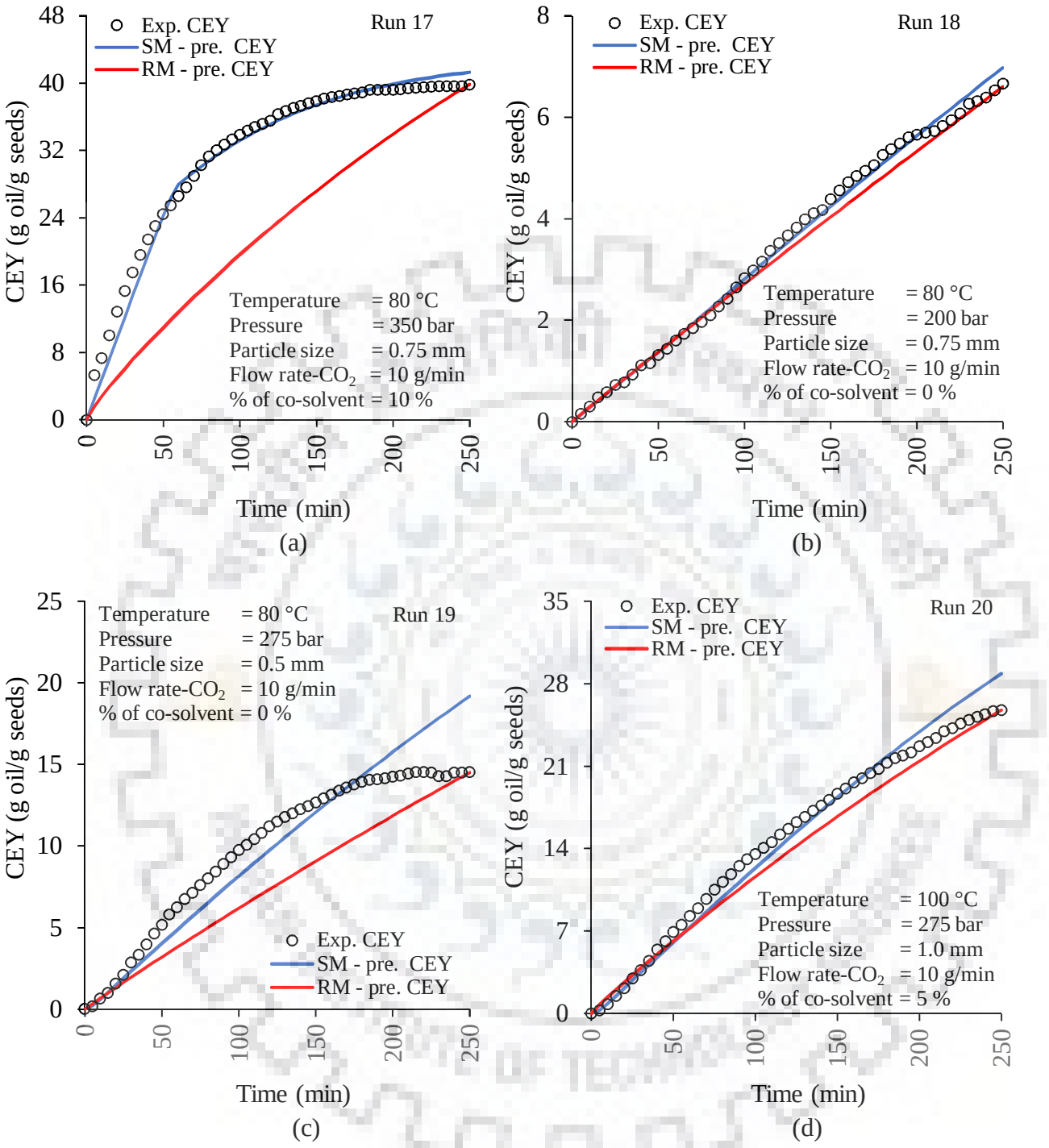


Fig. 5.25: Experimental and predicted CEY curves for AM seed oil during the SFE runs (17-20).

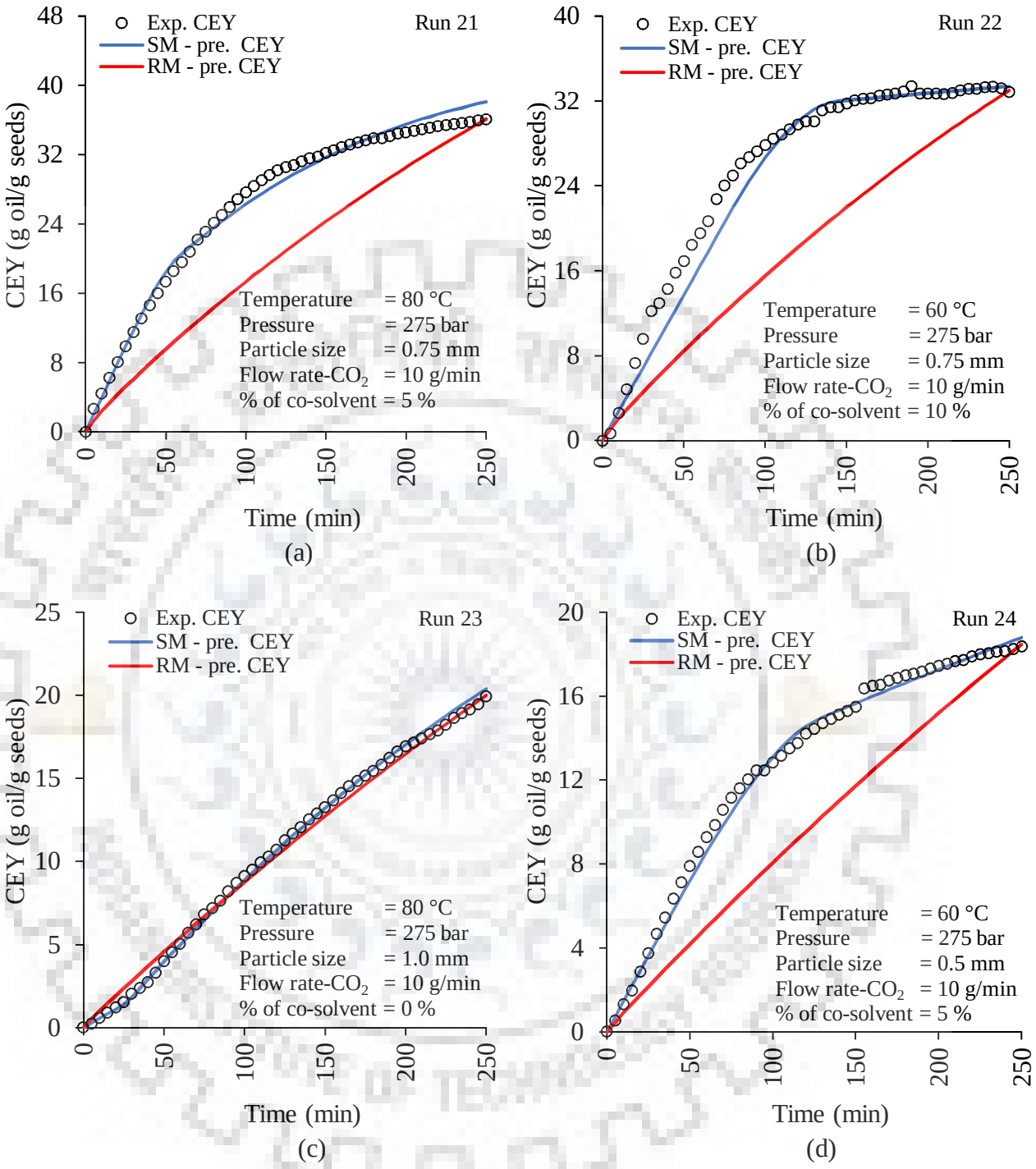


Fig. 5.26: Experimental and predicted CEY curves for AM seed oil during the SFE runs (21-24).

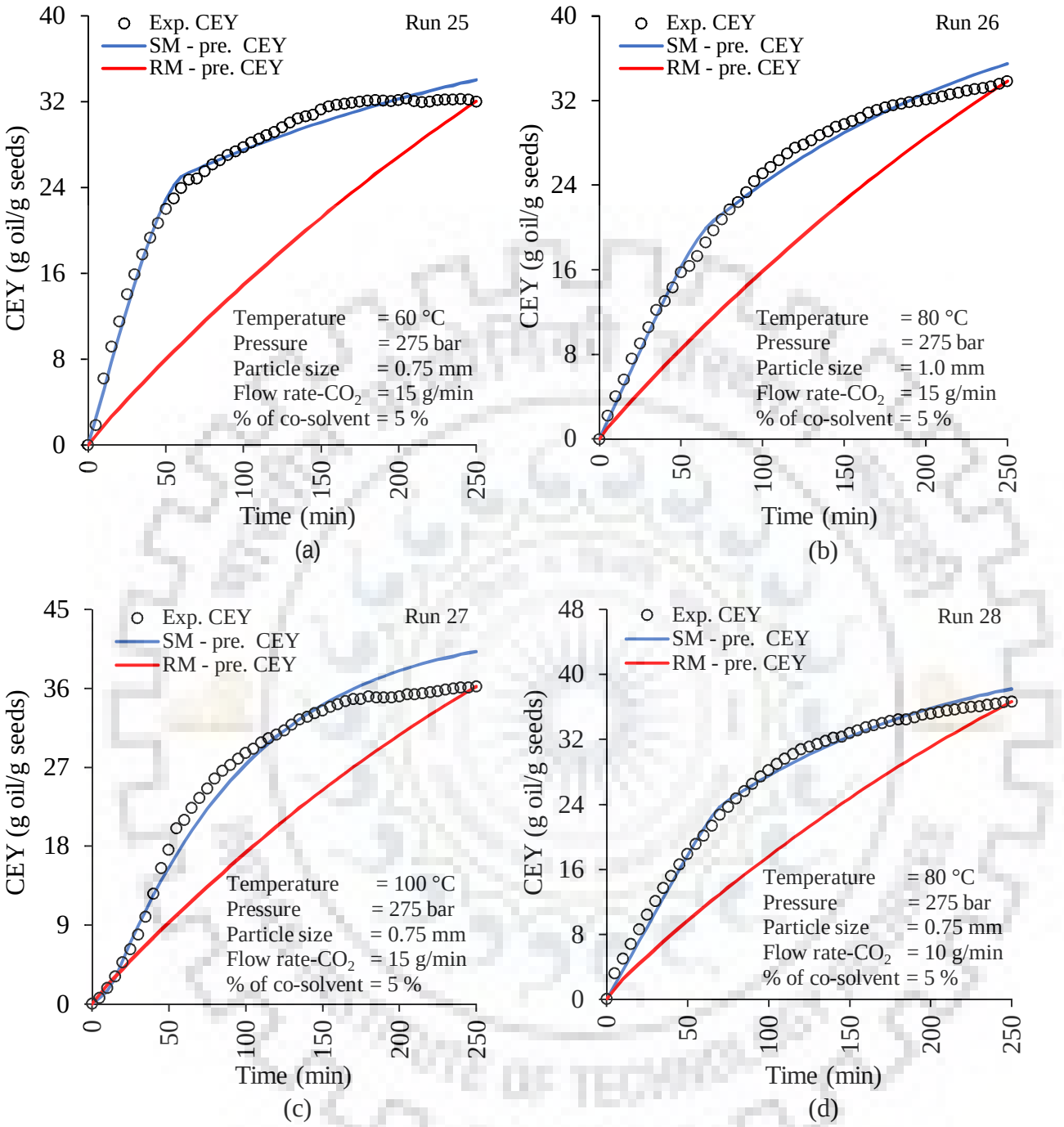


Fig. 5.27: Experimental and predicted CEY curves for AM seed oil during the SFE runs (25-28).

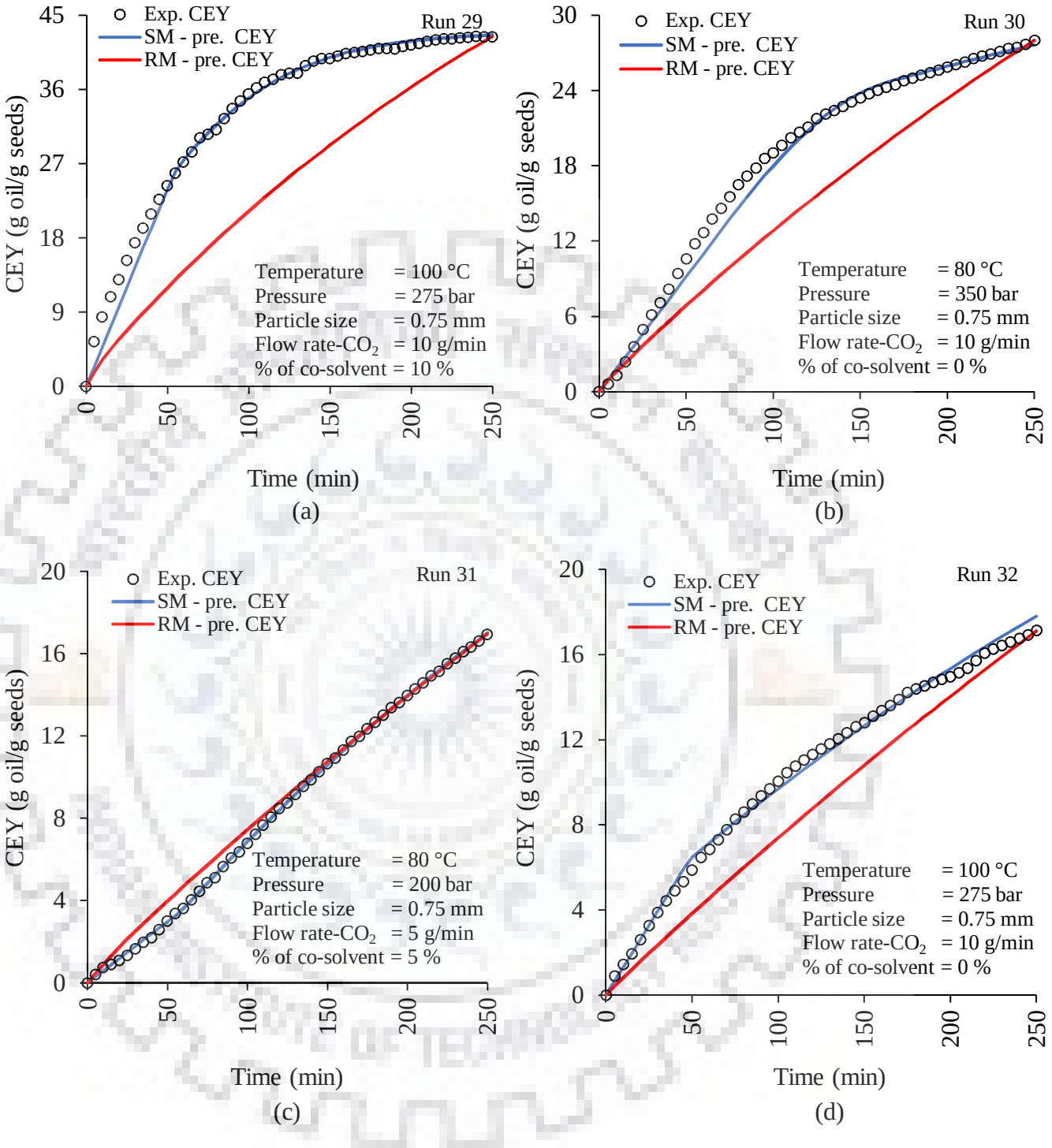


Fig. 5.28: Experimental and predicted CEY curves for AM seed oil during the SFE runs (29-32).

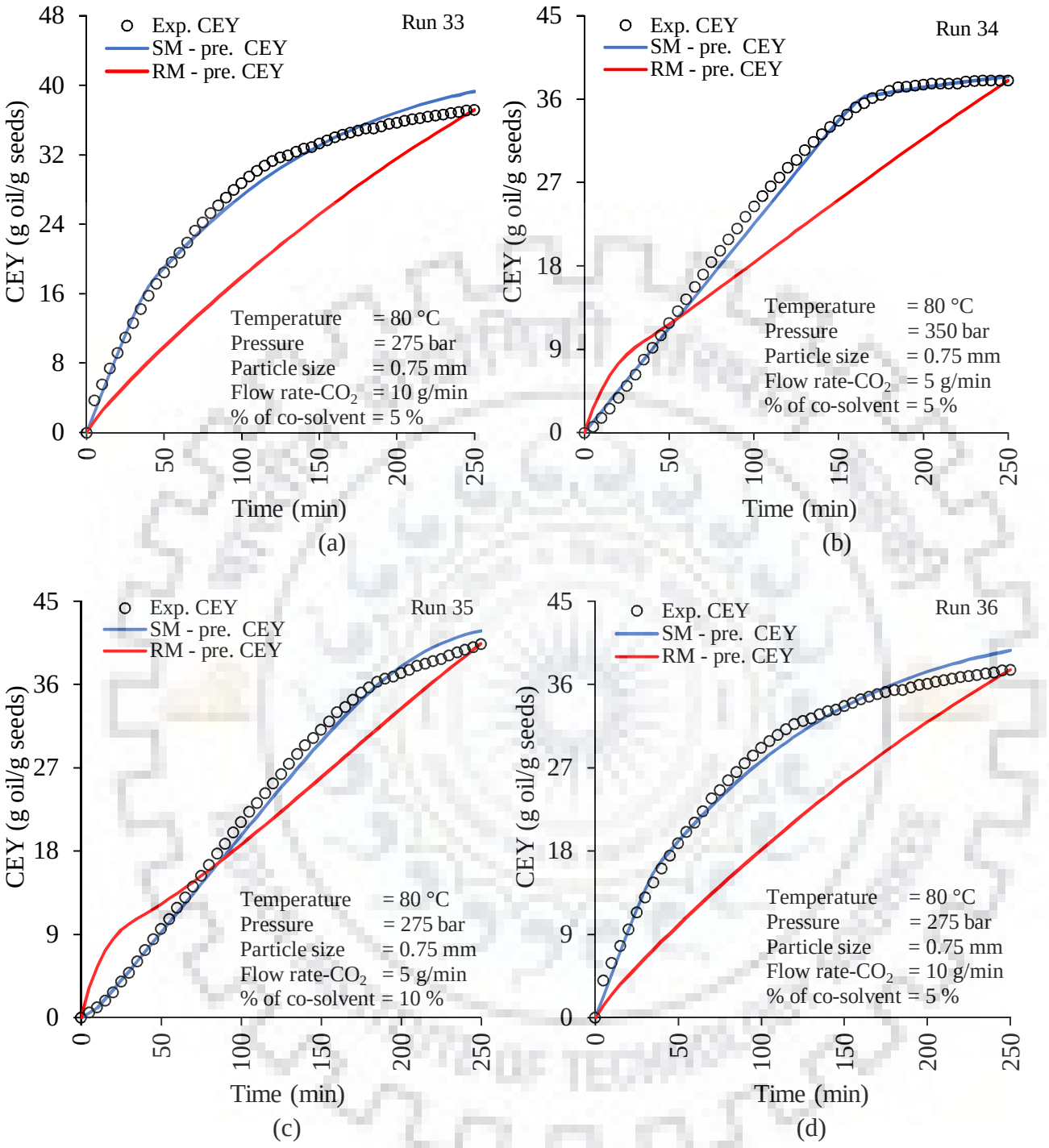


Fig. 5.29: Experimental and predicted CEY curves for AM seed oil during the SFE runs (33-36).

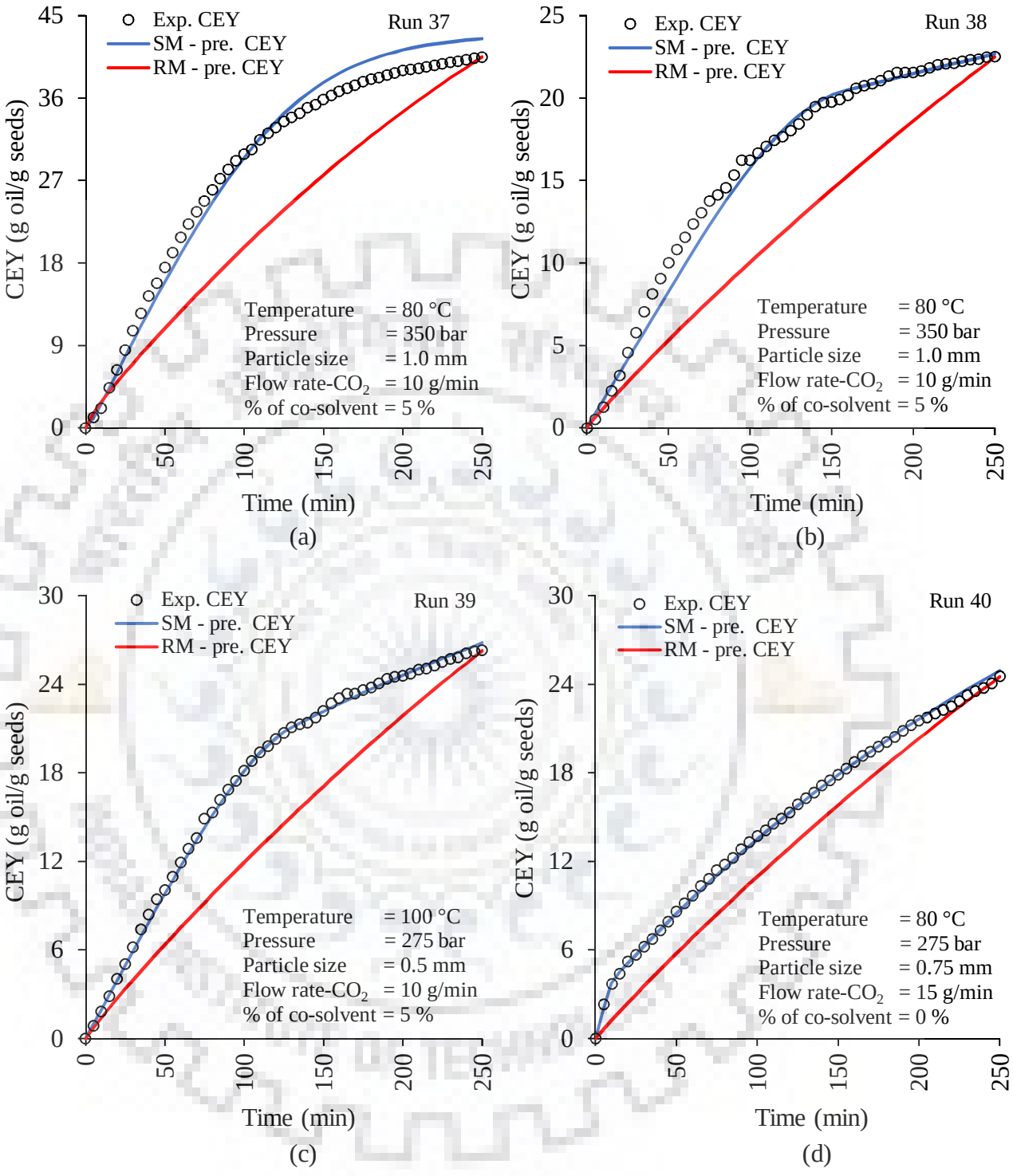


Fig. 5.30: Experimental and predicted CEY curves for AM seed oil during the SFE runs (37-40).

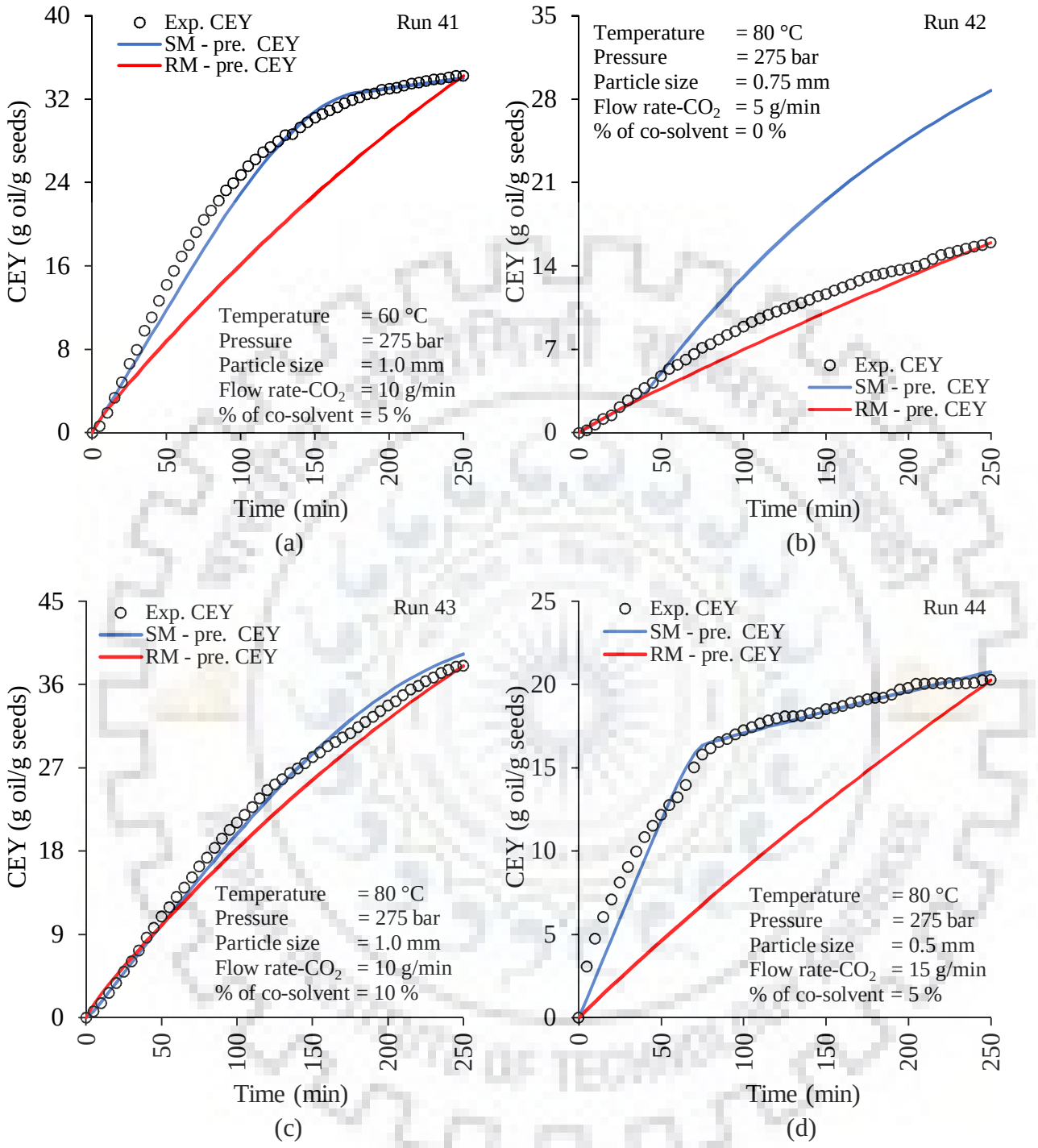


Fig. 5.31: Experimental and predicted CEY curves for AM seed oil during the SFE runs (41-44).

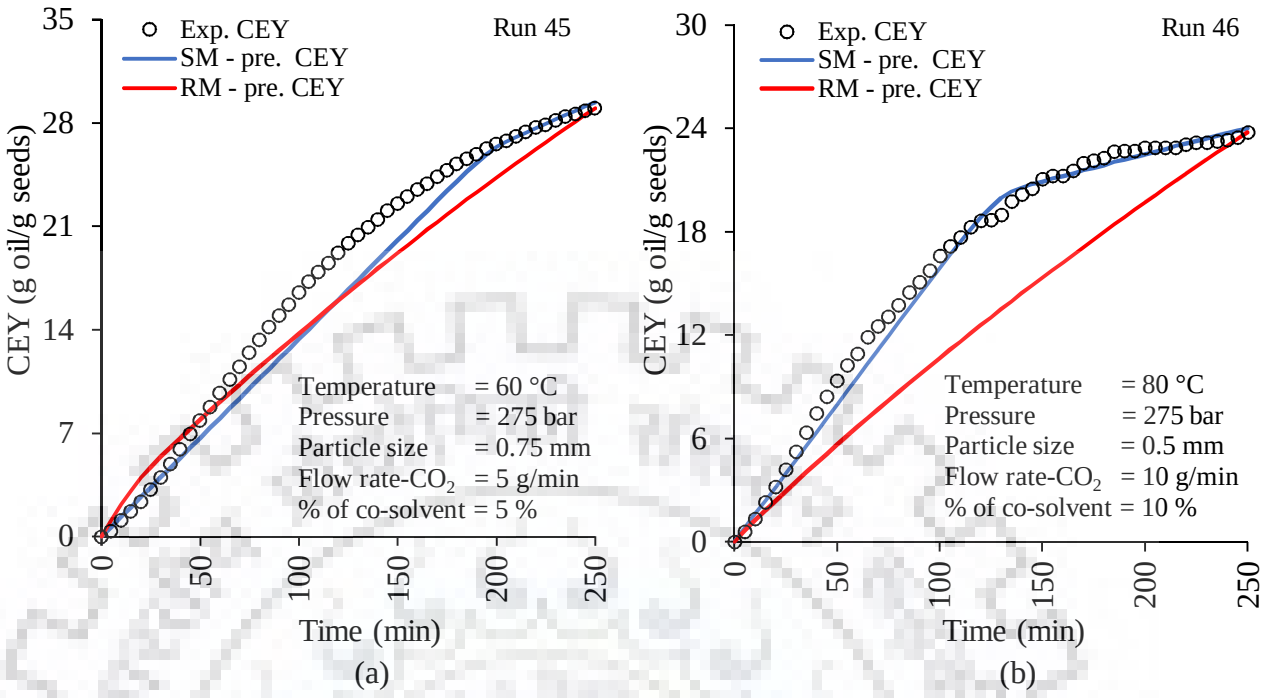


Fig. 5.32: Experimental and predicted CEY curves for AM seed oil during the SFE runs (45-46).

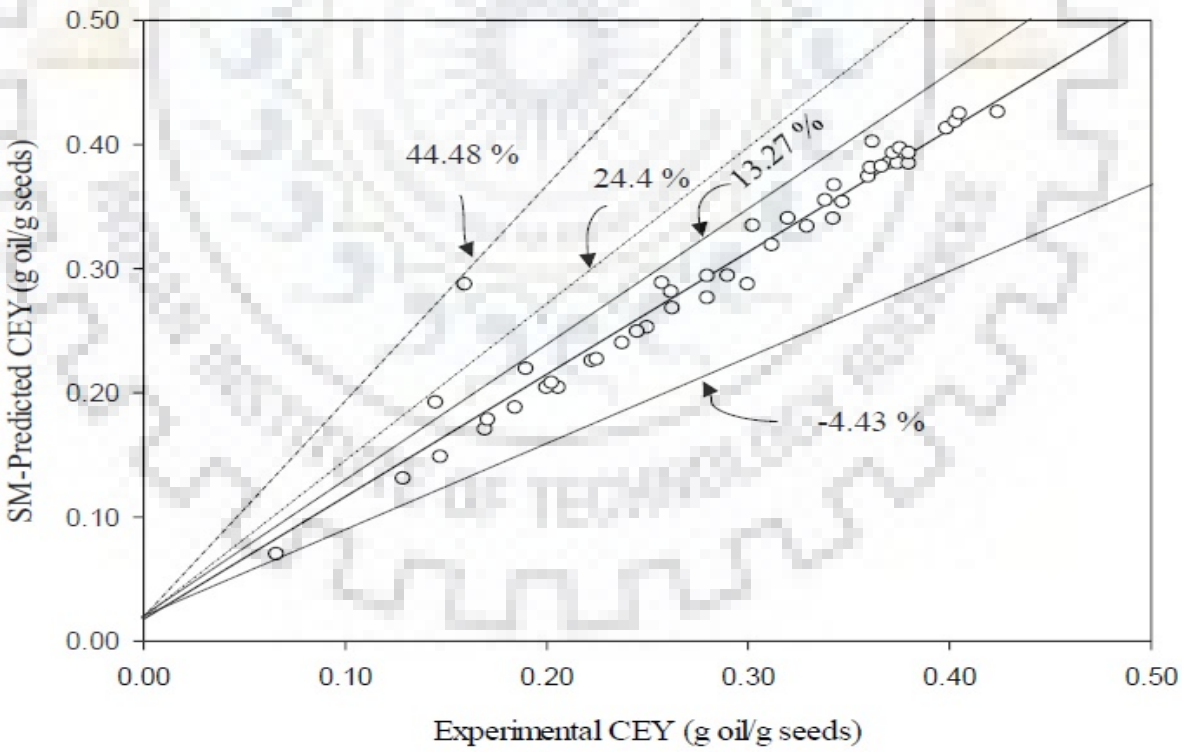


Fig. 5.33: Predicted (by SM) vs. Experimental CEY of AM seed oil.

5.4.2 Validation of Sovova model (SM) for PP seed oil

As shown in Table 5.16, the particle sizes were of 0.5, 0.75, 1.0 mm diameter and these particle sizes offered bed densities of 446.7, 566.7, 573.3 kg/m$^3$ for PP seeds respectively with corresponding particle densities of 899.3, 944.4, 905.3 kg/m$^3$. The observed increment in the bed porosity (from 0.26 to 0.5) with decreasing the particle size (from 1.0 to 0.5 mm) is ascribed to the decrease in the particle sphericity with decreasing the particle size. The amounts of initial oil content ($x_o$) in the PP seed was 0.5625 kg oil/kg of oil free solid. Figs. (5.34-5.45), have been plotted to show a comparison between experimental and predicted (by Sovova and Reverchon models) CEY for extraction curves during the SFE of PP seed oil. Table 5.19 shows the experimental conditions for all 46 runs and values of optimized model fitting parameters Z, W and $x_k$ obtained from experimental data for the PP seed oil by minimizing the AARD %. In the subsequent section, inherent observations from these figures (Figs. 5.34-5.45) are presented.

From the Table 5.19, it is clear that the mass transfer coefficients in solvent phase ($k_{ya}$) are much larger than the mass transfer coefficients ($k_{xa}$) in the solid phase. The reason behind this fact has already been discussed in section 5.4.1 of this chapter. Similar to previous case, in this case (SFE of PP seed oil), the mass transfer coefficient in solvent phase ($k_{ya}$) also depends on the process parameters as mentioned in section 5.4.1. The following observations can be drawn from the Figs. (5.34-5.45).

1. The CEY of PP seed oil increases rapidly in the early period of extraction in all the runs and then in some runs tends towards asymptotic maxima (as shown in Figs. 5.38(a), 5.43(a), and 5.44(c)).
2. All the extraction curves (Figs. (5.34-5.45) excepting the Figs. (5.37(a), 5.37(b), 5.38(a), 5.38(b) and 5.43(a)) have shown the linear trend of SFE process.
3. From all the Figs. (5.34-5.45), it is clear that the SM fits all experimental CEY data within an AARD % band of '+0.7706 to +14.17 %' and with an average AARD % of 4.254 % and thus it can be concluded that the model fitting is appreciably good.
4. All the plots of CEY (excepting the Figs. 5.36(c), 5.42(c), and 5.44(a)) have shown an appreciably excellent fitting with 94% experimental CEY data with an average AARD % of '3.59 %'.

5. The overall average experimental CEY is found to be ~ 0.1658 g oil/g seeds with a standard deviation of 0.0827 and for predicted CEY(results from SM) the overall average CEY is found to be ~0.1665 g oil/g seeds with a standard deviation of 0.0829.

The above observations are explained as:

The calculated values of $t_{CER}$, and $t_{FER}$, as given in Table 5.19, suggest that the maximum percentage of total extractable oil is extracted up to a time equal to $t_{FER}$. From the Table 5.20, it can be concluded that the range of percentage of extracted oil (% of total oil extracted) in the first period of extraction ($t \leq t_{CER}$), transition period ($t_{CER} \leq t \leq t_{FER}$) and in the third period of extraction are '0.08 – 33.52 %', '15.72 – 99.92 %' and '0.0 – 46.70 %' respectively. Hence, it can be concluded that the maximum percentage of oil (80.95 %) is extracted till the end of transition period (second period). The explanation for the above conclusion has already been discussed in the section 5.4.1. However, some experimental runs (3, 6, 14, 15, 16, 18, 20, 22, 23, 26, 27, 28, 29, 30, 31, 32, 38, 40, 43, 44) show opposite of this phenomenon meaning that the percentage of extracted oil in the third period of extraction curve is found higher than the first two periods (first and second). This phenomenon occurred due the effect of higher particle size range (0.75 – 1.0 mm) and higher pressure (275-350 bar). The larger particles contain the oil in the inner core which is not broken up during the grinding and at higher pressure (275 – 350 bar) this inner core part collapse as the extraction proceeds and facilitates the extraction of high amount of oil trapped in these broken cells in the third period ($t > t_{FER}$). The high flow rates of $CO_2$ (10 - 15 g/min) have also been observed in these runs which actually reduces contact time for interaction of solute (oil) molecules with the SC-$CO_2$ molecules (does not allow the solvent to saturate) during the first two periods hence, the higher CEY of PP seed oil is observed in the third period. In addition to this, the high temperature (80 - 100 °C) has also been observed during the above-mentioned experimental runs. This high temperature range (80-100 °C) might have increased the volatility of the PP seed oil, which resulted the better extraction in the third period. Additionally, an excellent agreement (within +15.08 % to -17.67 % error band) between the experimental and predicted CEY of PP seed oil, can also be seen from the parity plot drawn for the SM as shown in Fig. 5.46. The SM produce an excellent fitting with all 46 runs data points. The percentage of error (% error) has been calculated using the formula as described previously in the section 5.1.1 (Eq. 5.4).

Table 5.19. Parameters of Sovova model for the SFE of PP seed oil.

| | Experimental parameters | | | Tuning parameters | | | Calculated parameters from model | | | | Error |
|---|---|---|---|---|---|---|---|---|---|---|---|
| Run | Temperature (°C) | Pressure (bar) | ($y_r$) (kg oil/kg $CO_2$) | $x_k$ | Z | W | $t_{CER}$ (min) | $t_{FER}$ (min) | $k_{ya}$ ($min^{-1}$) | $k_{xa}$ ($min^{-1}$) | AARD % |
| 1 | 80 | 200 | 0.001775 | 0.5126 | 29.9575 | 0.0031 | 3.0037 | 145.9430 | 0.0208 | 0.0024 | 4.2873 |
| 2 | 80 | 275 | 0.004446 | 0.4597 | 30.0000 | 0.0163 | 2.4665 | 162.1625 | 7.3434 | 1.2348 | 4.7498 |
| 3 | 60 | 350 | 0.007497 | 0.5276 | 30.0000 | 0.0553 | 0.4962 | 92.0590 | 7.3434 | 0.0104 | 4.4325 |
| 4 | 60 | 275 | 0.002245 | 0.5604 | 30.0000 | 2.7821 | 0.1000 | 795.3827 | 7.3434 | 0.5216 | 6.4196 |
| 5 | 80 | 275 | 0.005940 | 0.5410 | 30.0000 | 0.0477 | 0.7739 | 201.7422 | 3.8757 | 0.0047 | 2.5519 |
| 6 | 100 | 275 | 0.004580 | 0.5321 | 29.6257 | 0.0073 | 1.4336 | 67.6877 | 3.6259 | 0.0007 | 2.8040 |
| 7 | 80 | 200 | 0.002986 | 0.4616 | 4.5943 | 0.0069 | 23.536 | 204.8238 | 1.1246 | 0.0013 | 1.6156 |
| 8 | 80 | 200 | 0.000902 | 0.5280 | 30.0000 | 0.0025 | 2.7165 | 179.8544 | 11.0151 | 0.0007 | 4.8047 |
| 9 | 60 | 200 | 0.003439 | 0.4765 | 6.0151 | 0.0075 | 13.306 | 146.9875 | 1.4724 | 0.0014 | 2.3517 |
| 10 | 100 | 350 | 0.005342 | 0.4407 | 30.0000 | 0.0186 | 2.4323 | 147.2639 | 7.3434 | 0.0035 | 5.3508 |
| 11 | 80 | 275 | 0.004836 | 0.5570 | 0.5979 | 4.8101 | 12.159 | 750.4170 | 0.0606 | 0.3733 | 13.3069 |
| 12 | 80 | 275 | 0.004446 | 0.5616 | 0.0629 | 5.6106 | 10.030 | 411.1657 | 0.0154 | 1.0520 | 5.4235 |
| 13 | 80 | 200 | 0.005470 | 0.4831 | 29.9999 | 0.0030 | 1.5492 | 54.6426 | 7.7513 | 0.0006 | 5.4431 |
| 14 | 100 | 200 | 0.002978 | 0.5408 | 30.0000 | 0.0011 | 0.7788 | 26.5693 | 7.3434 | 0.0002 | 2.1437 |
| 15 | 80 | 350 | 0.013376 | 0.4430 | 30.0000 | 0.0137 | 0.6350 | 24.4623 | 11.0151 | 0.0038 | 1.0831 |
| 16 | 80 | 275 | 0.008309 | 0.4973 | 30.0000 | 0.0116 | 0.5581 | 24.3554 | 11.0151 | 0.0033 | 0.9814 |
| 17 | 80 | 350 | 0.010158 | 0.5352 | 0.5932 | 9.9987 | 14.501 | 190.7364 | 0.1452 | 1.8747 | 5.4915 |
| 18 | 80 | 200 | 0.002928 | 0.5411 | 30.0000 | 0.0011 | 0.7778 | 26.5941 | 7.3434 | 0.0002 | 2.1450 |
| 19 | 80 | 275 | 0.002084 | 0.5606 | 29.7934 | 2.5899 | 0.1000 | 856.7151 | 6.0368 | 0.4020 | 3.0688 |
| 20 | 100 | 275 | 0.003519 | 0.5365 | 30.0000 | 0.0130 | 0.7887 | 69.9173 | 7.7514 | 0.0026 | 1.1734 |
| 21 | 80 | 275 | 0.004446 | 0.4819 | 30.0000 | 0.0169 | 1.9334 | 139.6688 | 7.3434 | 0.0032 | 0.7753 |
| 22 | 60 | 275 | 0.010759 | 0.5361 | 30.0000 | 0.0338 | 0.2622 | 19.7277 | 7.3434 | 0.0063 | 1.1216 |
| 23 | 80 | 275 | 0.004524 | 0.5338 | 30.0000 | 0.0038 | 0.6765 | 26.1974 | 7.7514 | 0.0007 | 2.5404 |

Cont…

| | Experimental parameters | | | Tuning parameters | | | Calculated parameters from model | | | | Error |
|---|---|---|---|---|---|---|---|---|---|---|---|
| Run | Temperature (°C) | Pressure (bar) | ($y_r$) (kg oil/kg $CO_2$) | $x_k$ | Z | W | $t_{CER}$ (min) | $t_{FER}$ (min) | $k_{ya}$ ($min^{-1}$) | $k_{xa}$ ($min^{-1}$) | AARD % |
| 24 | 60 | 275 | 0.005597 | 0.4517 | 30.0000 | 0.0157 | 2.1119 | 117.1645 | 6.0787 | 0.0024 | 5.8979 |
| 25 | 60 | 275 | 0.005382 | 0.4332 | 15.8443 | 0.0094 | 3.2357 | 76.9620 | 5.8175 | 0.0026 | 3.4559 |
| 26 | 80 | 275 | 0.010310 | 0.5509 | 0.0945 | 0.0106 | 25.4544 | 28.6815 | 0.0366 | 0.0031 | 4.6504 |
| 27 | 100 | 275 | 0.004191 | 0.5247 | 30.0000 | 0.0033 | 0.6410 | 24.3986 | 11.0151 | 0.0009 | 3.8993 |
| 28 | 80 | 275 | 0.004446 | 0.5617 | 0.4170 | 0.0282 | 1.3329 | 6.5862 | 0.1021 | 0.0053 | 3.2922 |
| 29 | 100 | 275 | 0.003550 | 0.5619 | 5.5597 | 0.0208 | 0.1003 | 4.4585 | 1.3609 | 0.0039 | 4.4996 |
| 30 | 80 | 350 | 0.003370 | 0.5609 | 0.7247 | 0.0272 | 2.0509 | 28.9591 | 0.1774 | 0.0051 | 2.7419 |
| 31 | 80 | 200 | 0.004526 | 0.5490 | 27.0866 | 0.0037 | 0.7066 | 24.8466 | 3.3151 | 0.0003 | 1.5629 |
| 32 | 100 | 275 | 0.002206 | 0.5438 | 5.8706 | 0.0025 | 4.6269 | 41.9736 | 1.4370 | 0.0005 | 2.8061 |
| 33 | 80 | 275 | 0.004446 | 0.4820 | 30.0000 | 0.0169 | 1.9312 | 139.9111 | 7.3434 | 0.0032 | 0.7707 |
| 34 | 80 | 350 | 0.011135 | 0.3533 | 1.6611 | 0.0216 | 72.398 | 235.7048 | 0.2033 | 0.0020 | 7.4927 |
| 35 | 80 | 275 | 0.006121 | 0.5596 | 30.0000 | 7.7193 | 0.1000 | 583.8823 | 3.6717 | 0.7237 | 13.6707 |
| 36 | 80 | 275 | 0.004434 | 0.4849 | 30.0000 | 0.0170 | 1.8673 | 137.5643 | 7.3434 | 0.0032 | 1.0612 |
| 37 | 80 | 350 | 0.008025 | 0.4420 | 30.0000 | 0.0318 | 1.6023 | 104.3675 | 7.7514 | 0.0063 | 5.2973 |
| 38 | 80 | 350 | 0.011522 | 0.5231 | 30.0000 | 0.0271 | 0.3644 | 21.2062 | 6.0787 | 0.0042 | 2.2654 |
| 39 | 100 | 275 | 0.002986 | 0.4924 | 17.2540 | 0.0078 | 4.3535 | 146.9235 | 3.4961 | 0.0012 | 1.4957 |
| 40 | 80 | 275 | 0.001279 | 0.5493 | 30.0000 | 0.0022 | 0.7325 | 37.0281 | 11.0151 | 0.0006 | 2.6600 |
| 41 | 60 | 275 | 0.004232 | 0.5585 | 30.0000 | 5.3397 | 0.1000 | 422.4953 | 7.7514 | 1.0568 | 14.1711 |
| 42 | 80 | 275 | 0.002029 | 0.5615 | 30.0000 | 1.9536 | 0.1000 | 1753.1736 | 3.6717 | 0.1832 | 7.7298 |
| 43 | 80 | 275 | 0.036050 | 0.5396 | 0.0797 | 0.0268 | 25.4499 | 27.9439 | 0.0206 | 0.0053 | 5.6797 |
| 44 | 80 | 275 | 0.016700 | 0.5222 | 0.1129 | 0.0063 | 45.5772 | 51.2631 | 0.0343 | 0.0015 | 3.3669 |
| 45 | 60 | 275 | 0.005223 | 0.5601 | 30.0000 | 6.5853 | 0.1000 | 684.1016 | 3.6717 | 0.6174 | 9.7012 |
| 46 | 80 | 275 | 0.031150 | 0.5208 | 0.1025 | 0.0154 | 41.7991 | 46.6794 | 0.0208 | 0.0024 | 3.4583 |

Table 5.20. Extracted oil in each period of extraction curve for PP seed oil during each run.

| Run | Oil extracted (% of total oil extracted) | | |
|---|---|---|---|
| | Three periods of extraction curve of each run | | |
| | $t \leq t_{CER}$ | $t_{CER} \leq t \leq t_{FER}$ | $t > t_{FER}$ |
| 1 | 2.38 | 69.86 | 27.76 |
| 2 | 2.11 | 73.66 | 24.23 |
| 3 | 0.61 | 47.26 | 52.14 |
| 4 | 0.25 | 99.75 | 0.00 |
| 5 | 0.51 | 80.37 | 19.12 |
| 6 | 0.76 | 40.48 | 58.76 |
| 7 | 14.29 | 71.57 | 14.14 |
| 8 | 1.09 | 76.42 | 22.48 |
| 9 | 8.11 | 62.37 | 29.53 |
| 10 | 1.21 | 69.70 | 29.10 |
| 11 | 2.72 | 97.28 | 0.00 |
| 12 | 0.25 | 99.75 | 0.00 |
| 13 | 1.32 | 56.12 | 42.56 |
| 14 | 1.95 | 39.26 | 58.78 |
| 15 | 0.87 | 35.09 | 64.03 |
| 16 | 0.62 | 25.84 | 73.54 |
| 17 | 5.83 | 93.23 | 0.94 |
| 18 | 1.93 | 38.83 | 59.25 |
| 19 | 0.12 | 99.88 | 0.00 |
| 20 | 0.44 | 32.70 | 66.87 |
| 21 | 1.06 | 63.24 | 35.69 |
| 22 | 0.22 | 13.81 | 85.97 |
| 23 | 0.63 | 26.63 | 72.74 |
| 24 | 1.32 | 60.41 | 38.27 |
| 25 | 3.54 | 49.75 | 46.70 |
| 26 | 4.34 | 0.98 | 94.67 |
| 27 | 0.69 | 27.55 | 71.76 |
| 28 | 0.52 | 1.87 | 97.61 |
| 29 | 0.08 | 2.04 | 97.88 |
| 30 | 0.87 | 10.80 | 88.33 |
| 31 | 1.23 | 24.28 | 74.49 |
| 32 | 4.26 | 24.25 | 71.49 |
| 33 | 1.16 | 63.12 | 35.71 |
| 34 | 33.52 | 64.06 | 2.42 |
| 35 | 0.12 | 99.88 | 0.00 |
| 36 | 1.16 | 62.88 | 35.95 |
| 37 | 1.04 | 58.20 | 40.76 |
| 38 | 0.25 | 15.72 | 84.03 |
| 39 | 2.39 | 66.82 | 30.79 |
| 40 | 0.39 | 23.52 | 76.09 |
| 41 | 0.08 | 99.92 | 0.00 |
| 42 | 0.12 | 99.88 | 0.00 |
| 43 | 3.72 | 3.96 | 92.32 |
| 44 | 16.27 | 5.24 | 78.49 |
| 45 | 0.12 | 99.88 | 0.00 |
| 46 | 10.75 | 4.76 | 84.50 |

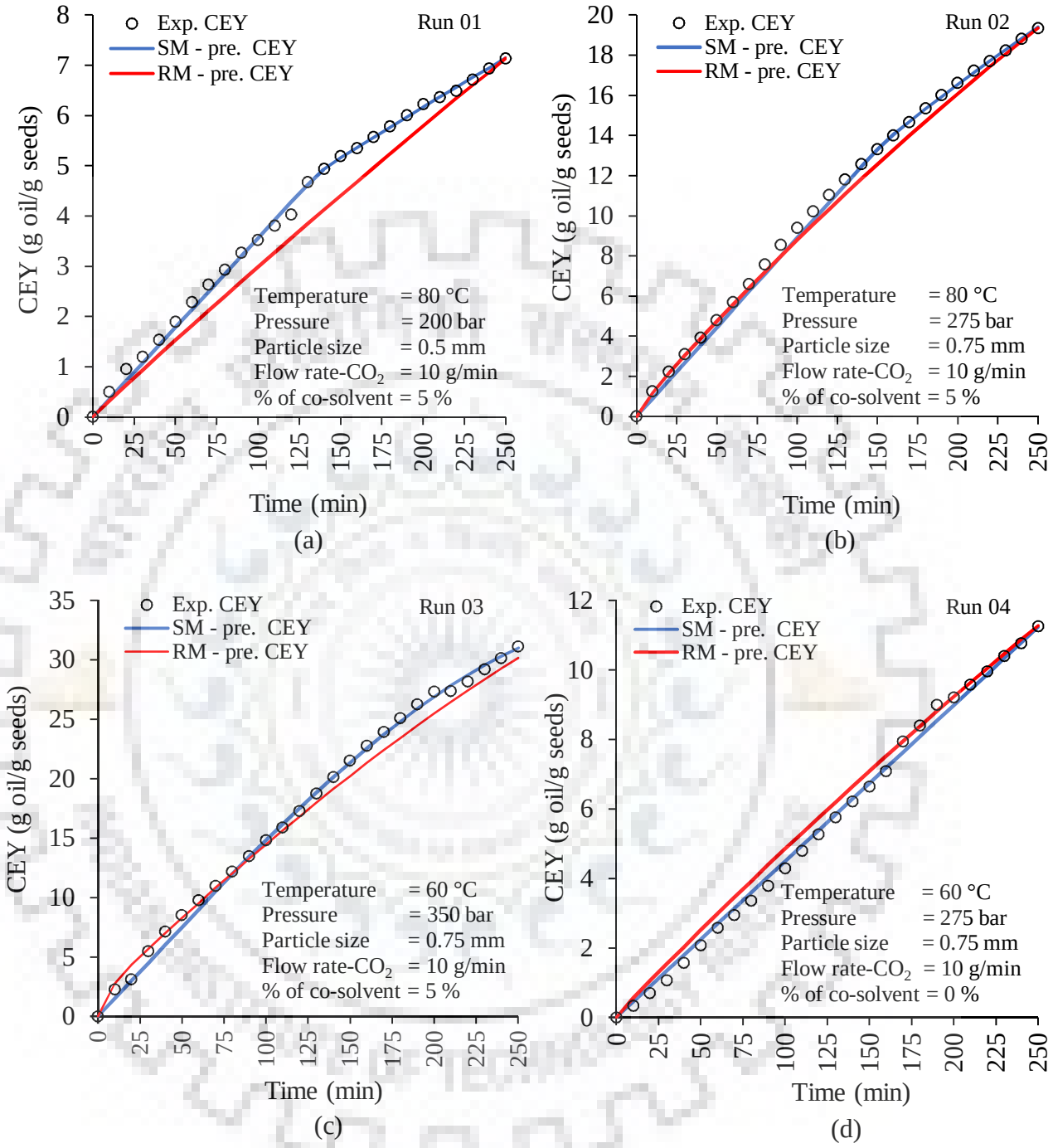


Fig. 5.34: Experimental and predicted CEY curves for PP seed oil during the SFE runs (01-04).

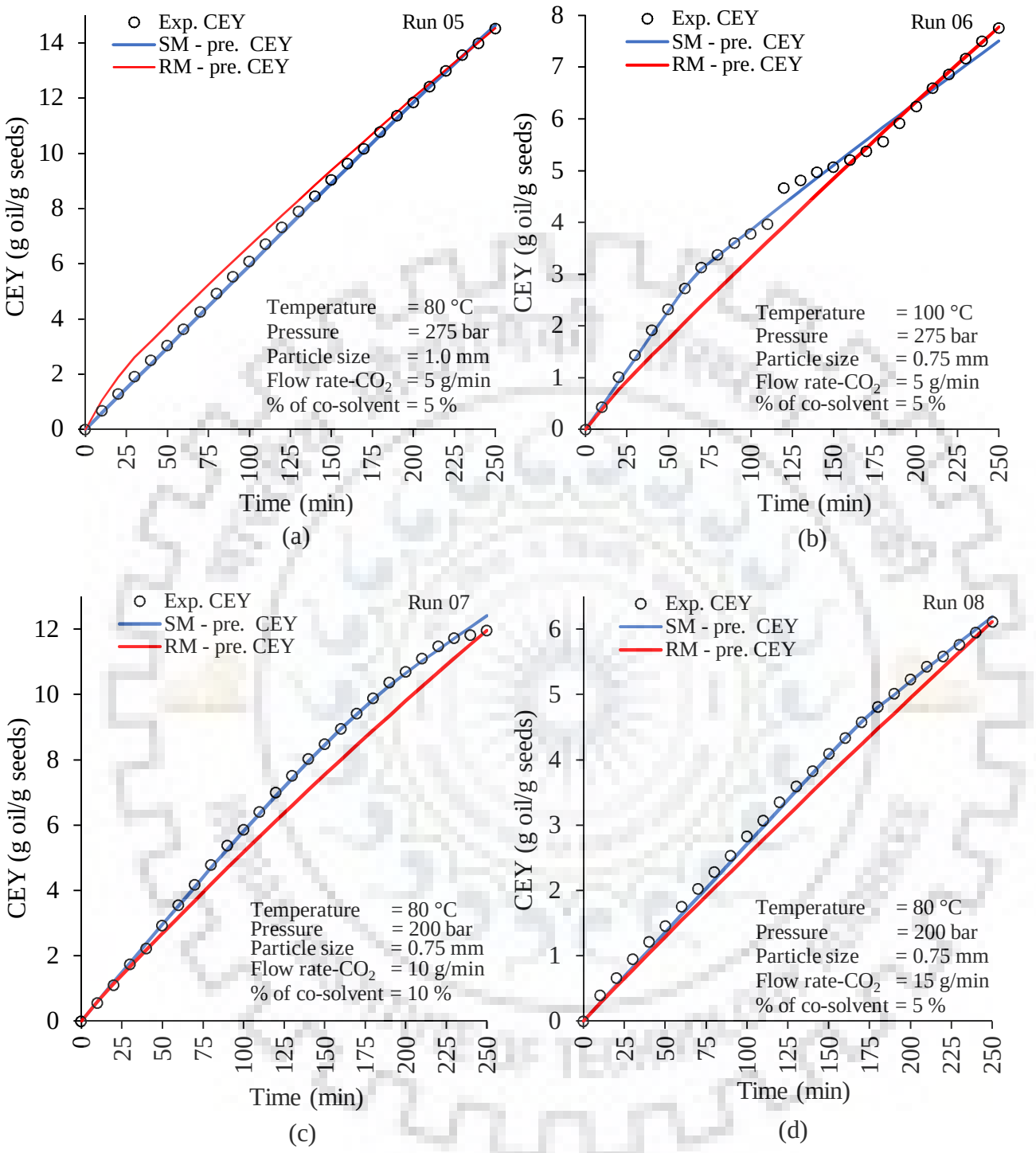


Fig. 5.35: Experimental and predicted CEY curves f or PP seed oil during the SFE runs (05-08).

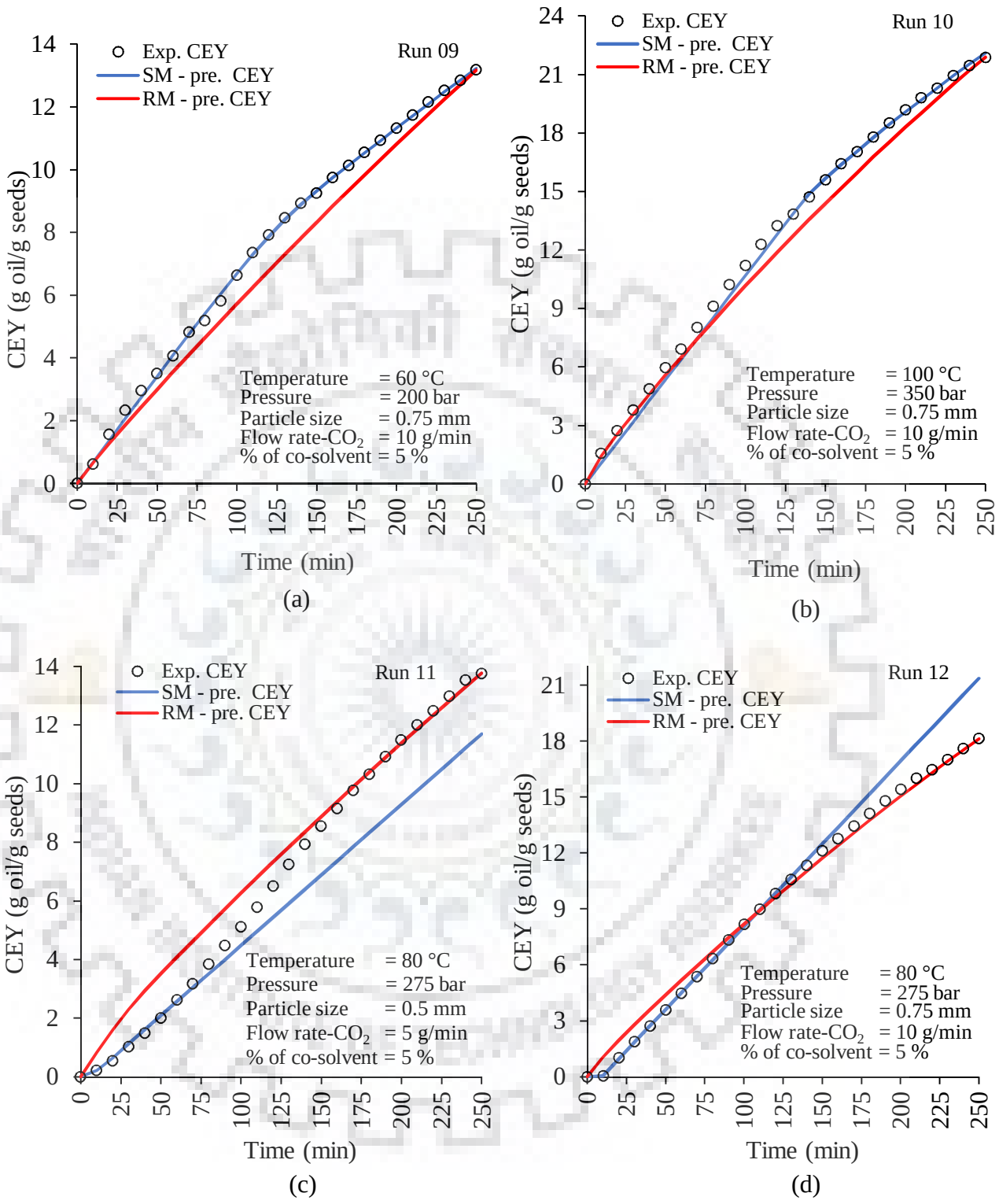


Fig. 5.36: Experimental and predicted CEY curves for PP seed oil during the SFE runs (09-12).

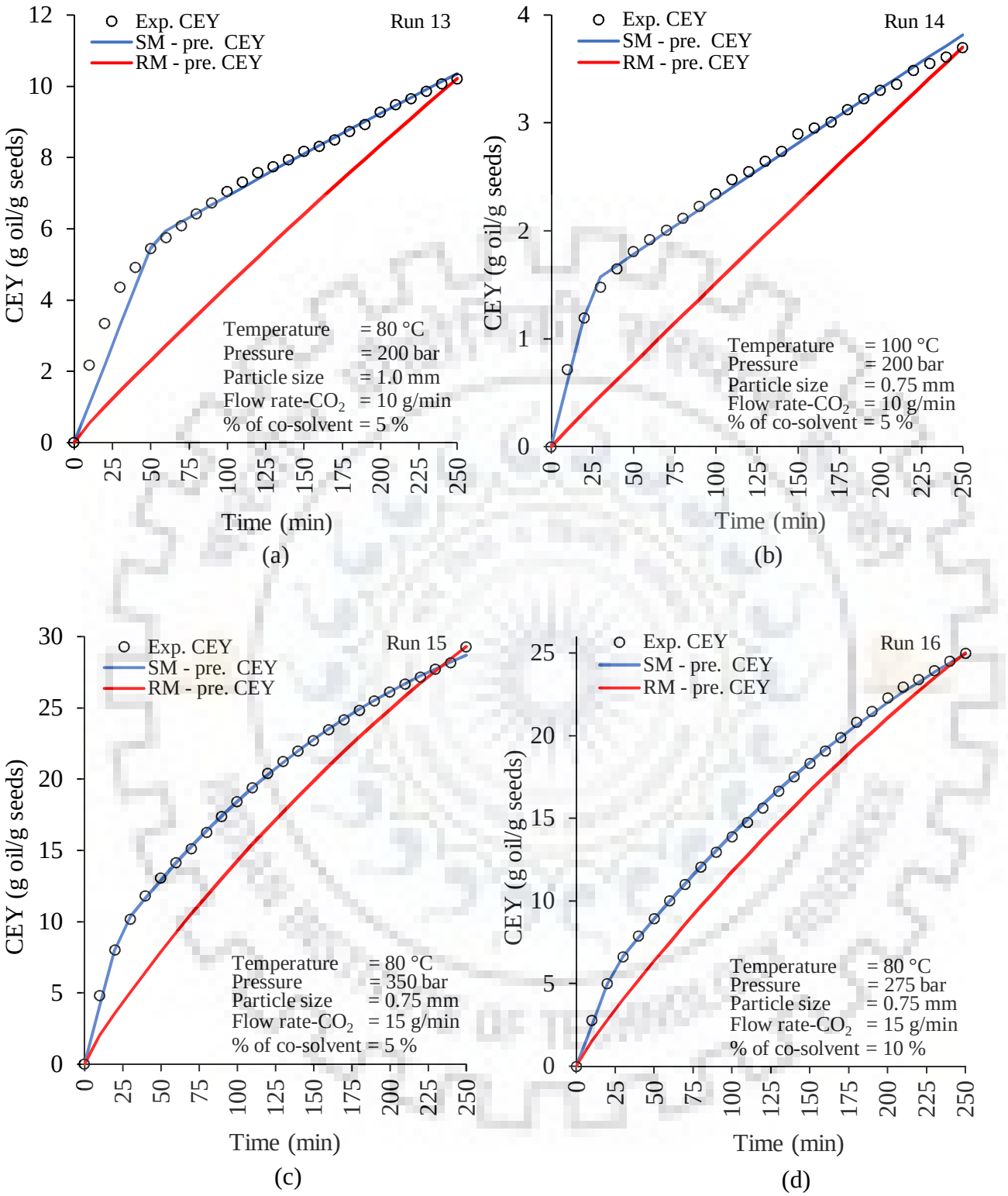


Fig. 5.37: Experimental and predicted CEY curves for PP seed oil during the SFE runs (13-16).

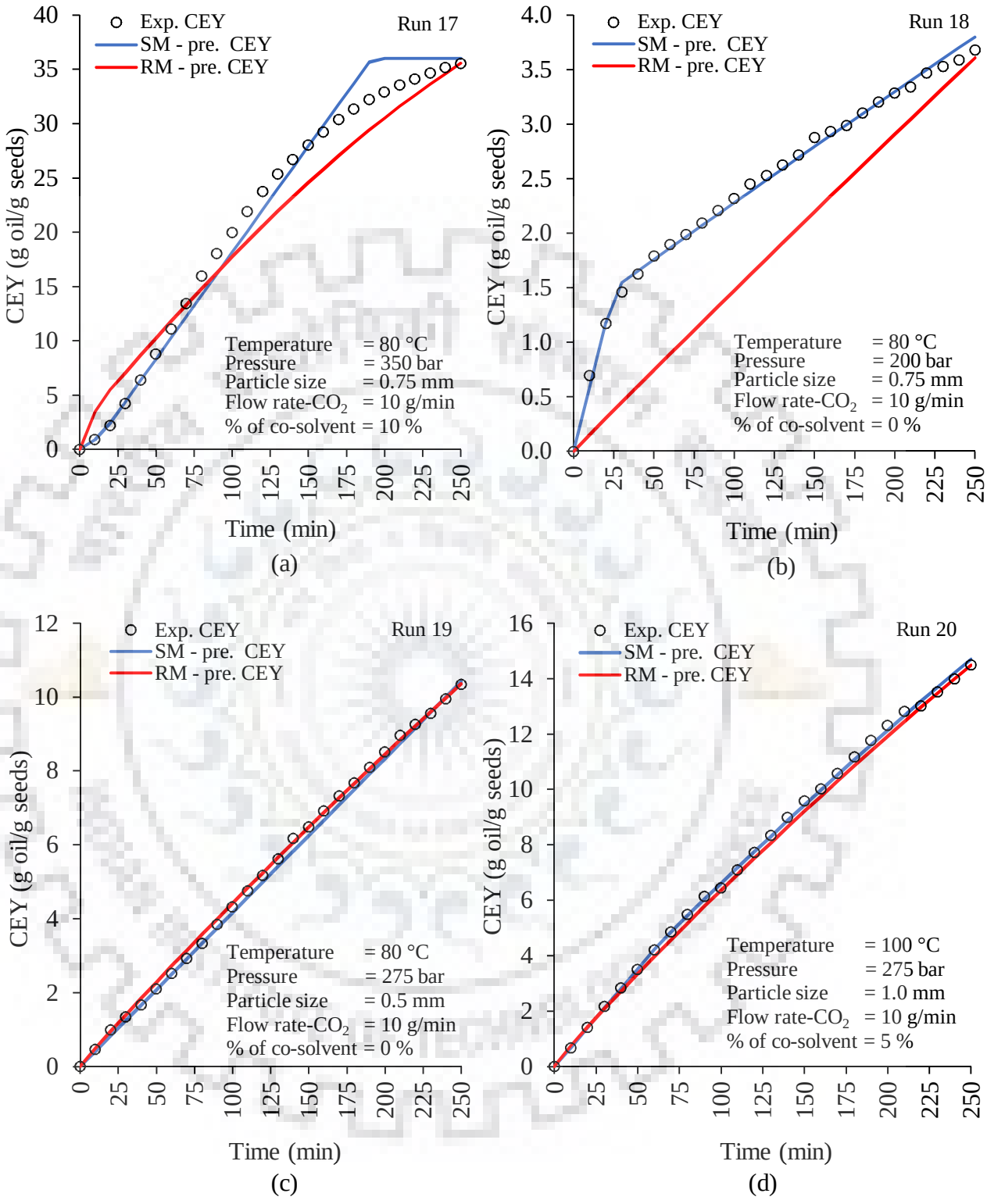


Fig. 5.38: Experimental and predicted CEY curves for PP seed oil during the SFE runs (17-20).

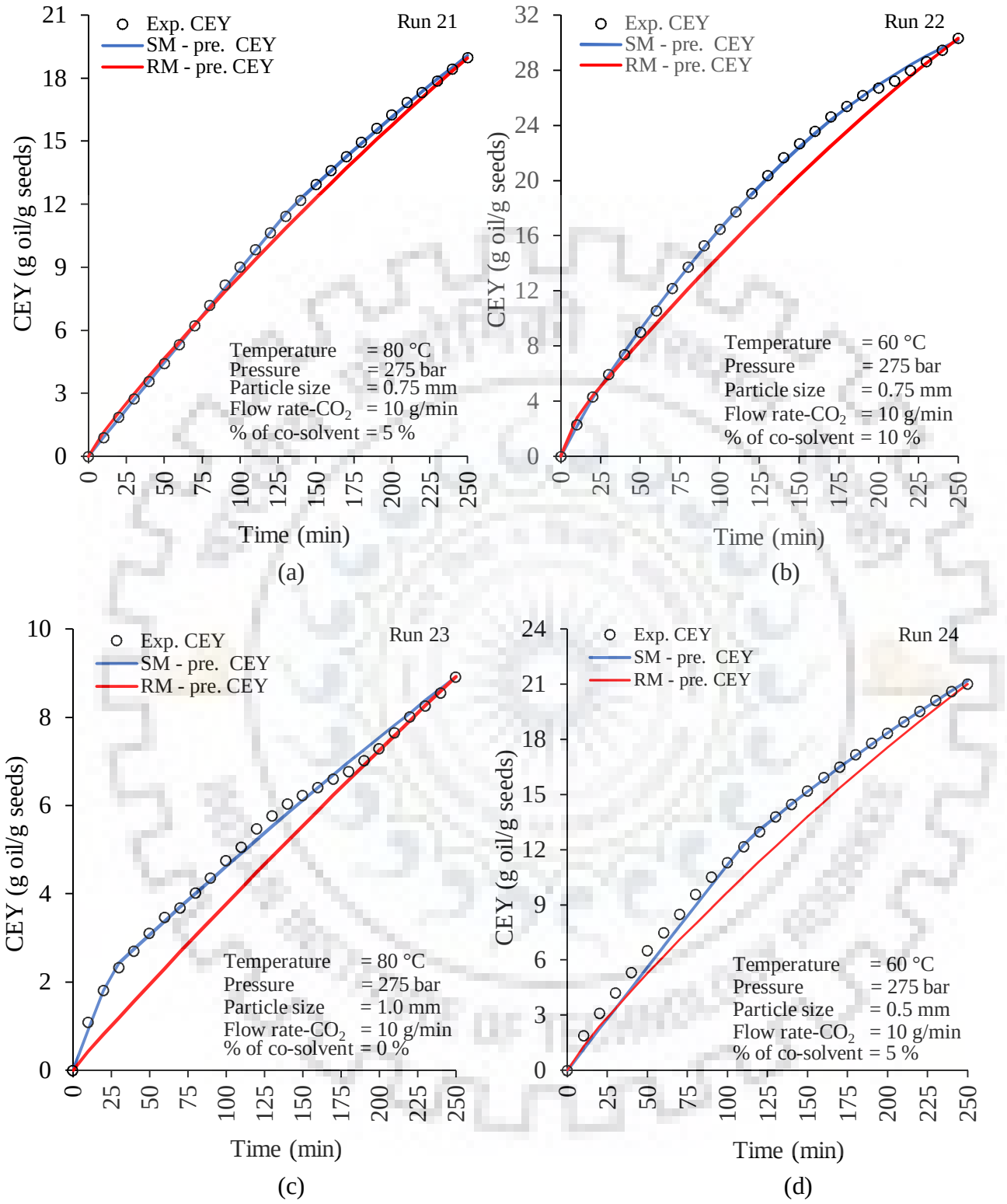


Fig. 5.39: Experimental and predicted CEY curves for PP seed oil during the SFE runs (21-24).

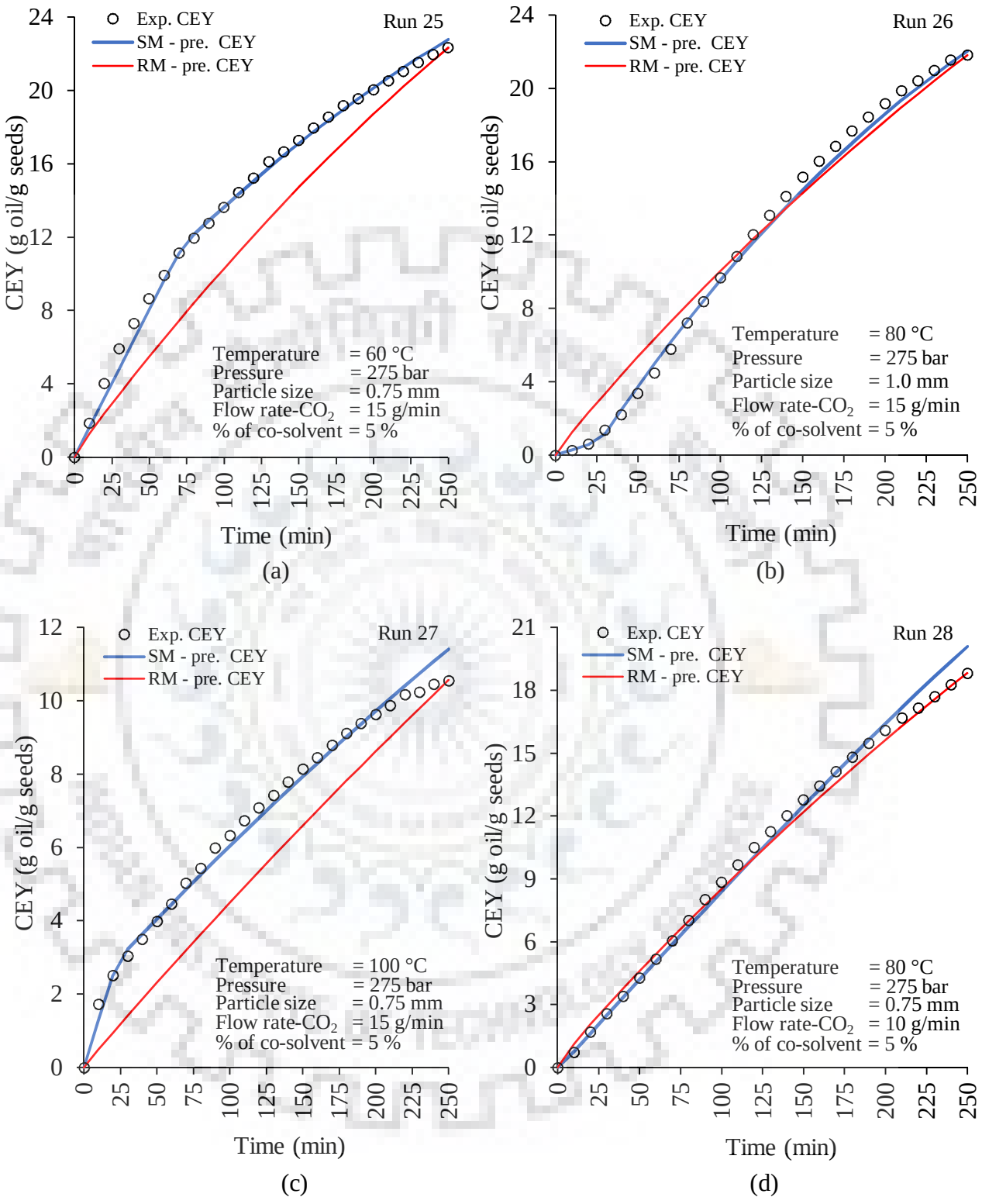


Fig. 5.40: Experimental and predicted CEY curves for PP seed oil during the SFE runs (25-28).

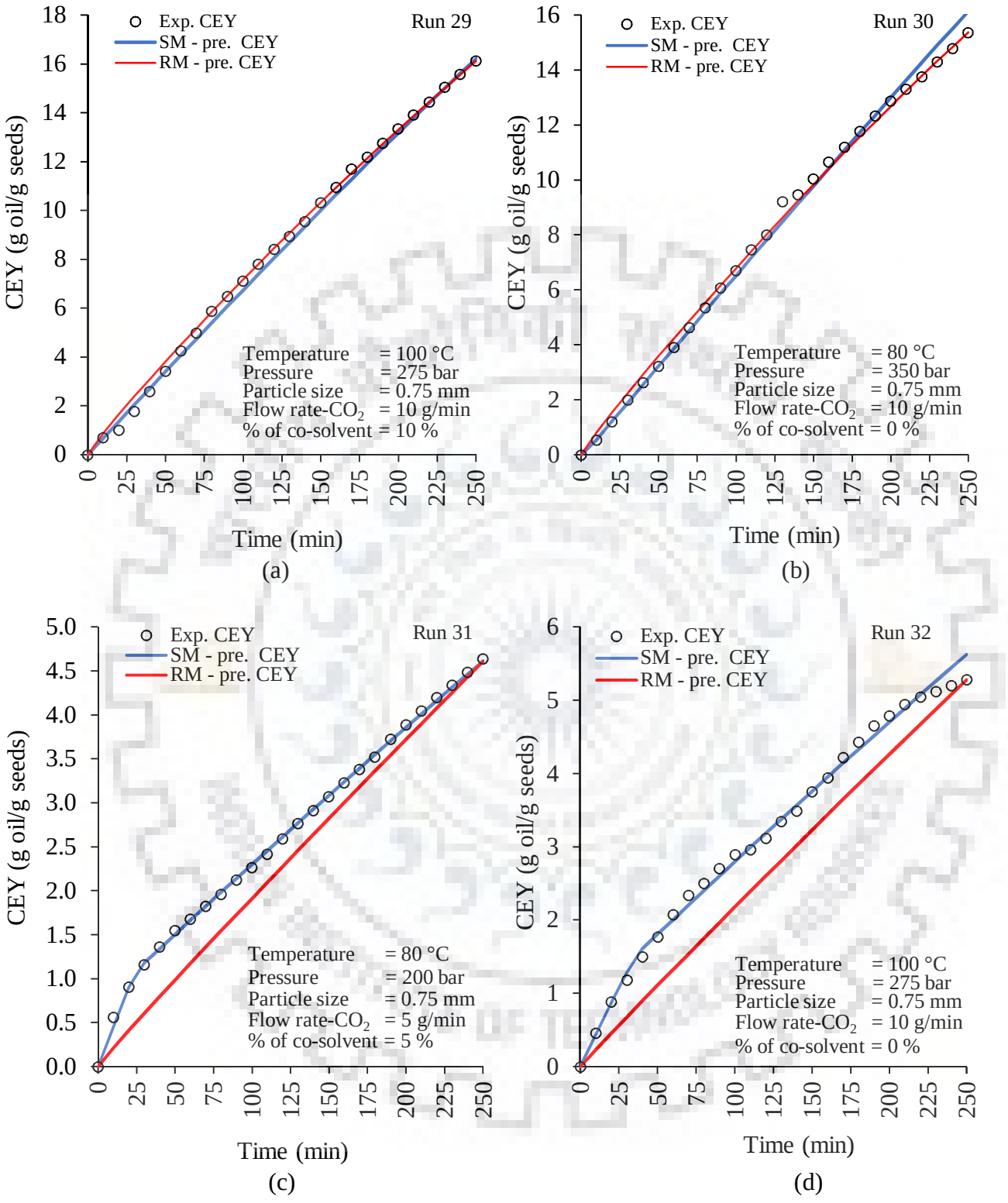


Fig. 5.41: Experimental and predicted CEY curves for PP seed oil during the SFE runs (29-32).

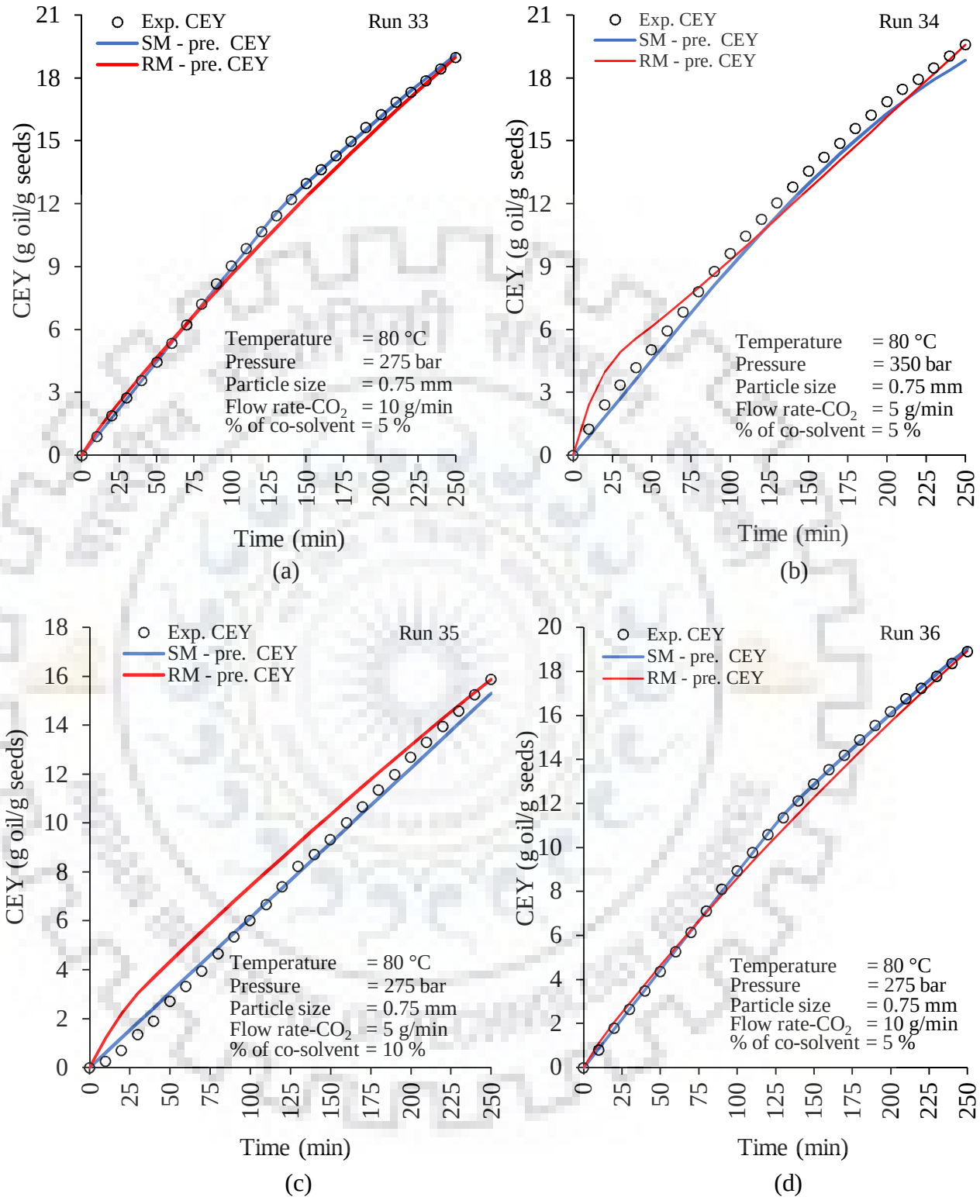


Fig. 5.42: Experimental and predicted CEY curves for PP seed oil during the SFE runs (33-36).

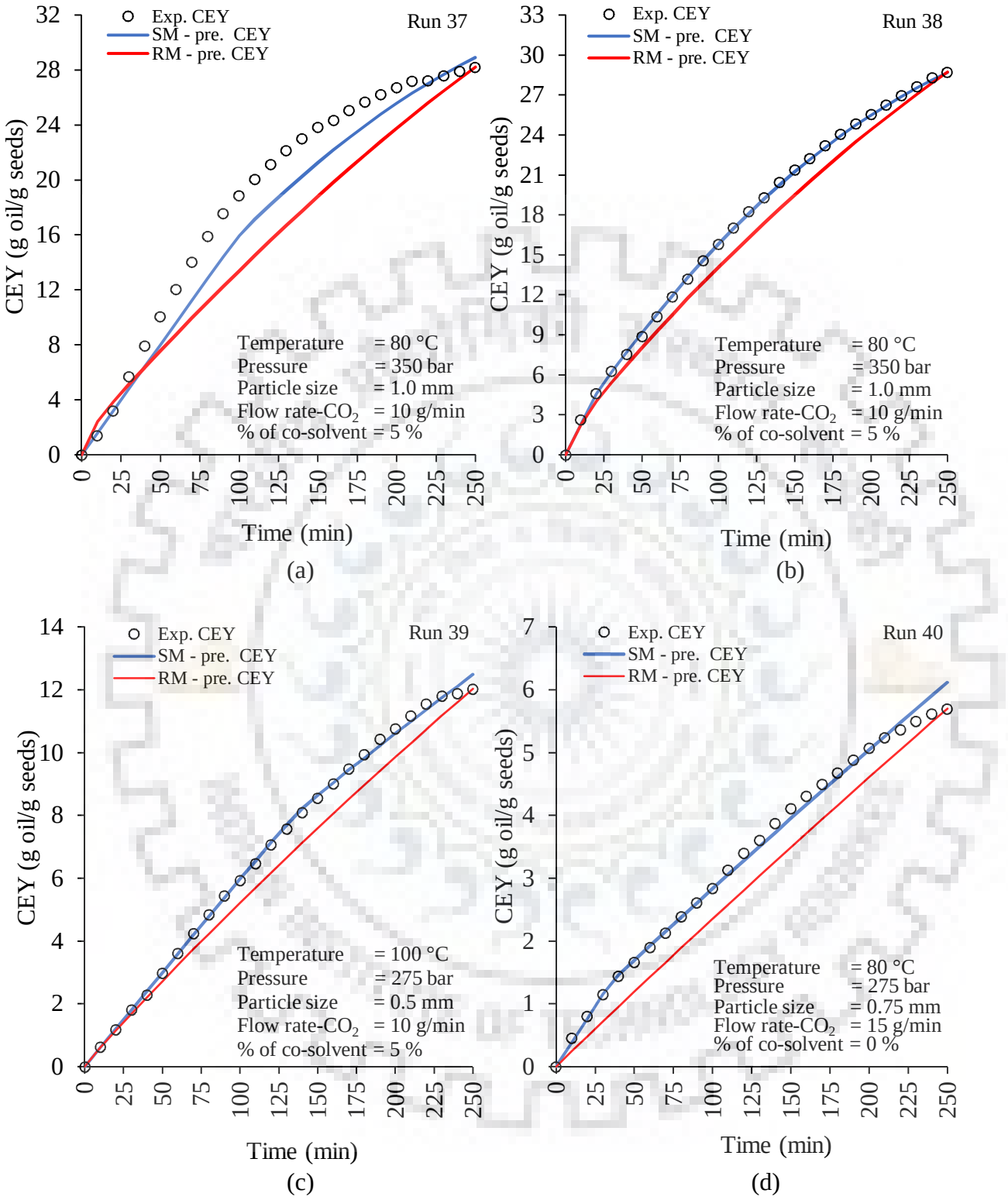


Fig. 5.43: Experimental and predicted CEY curves for PP seed oil during the SFE runs (37-40).

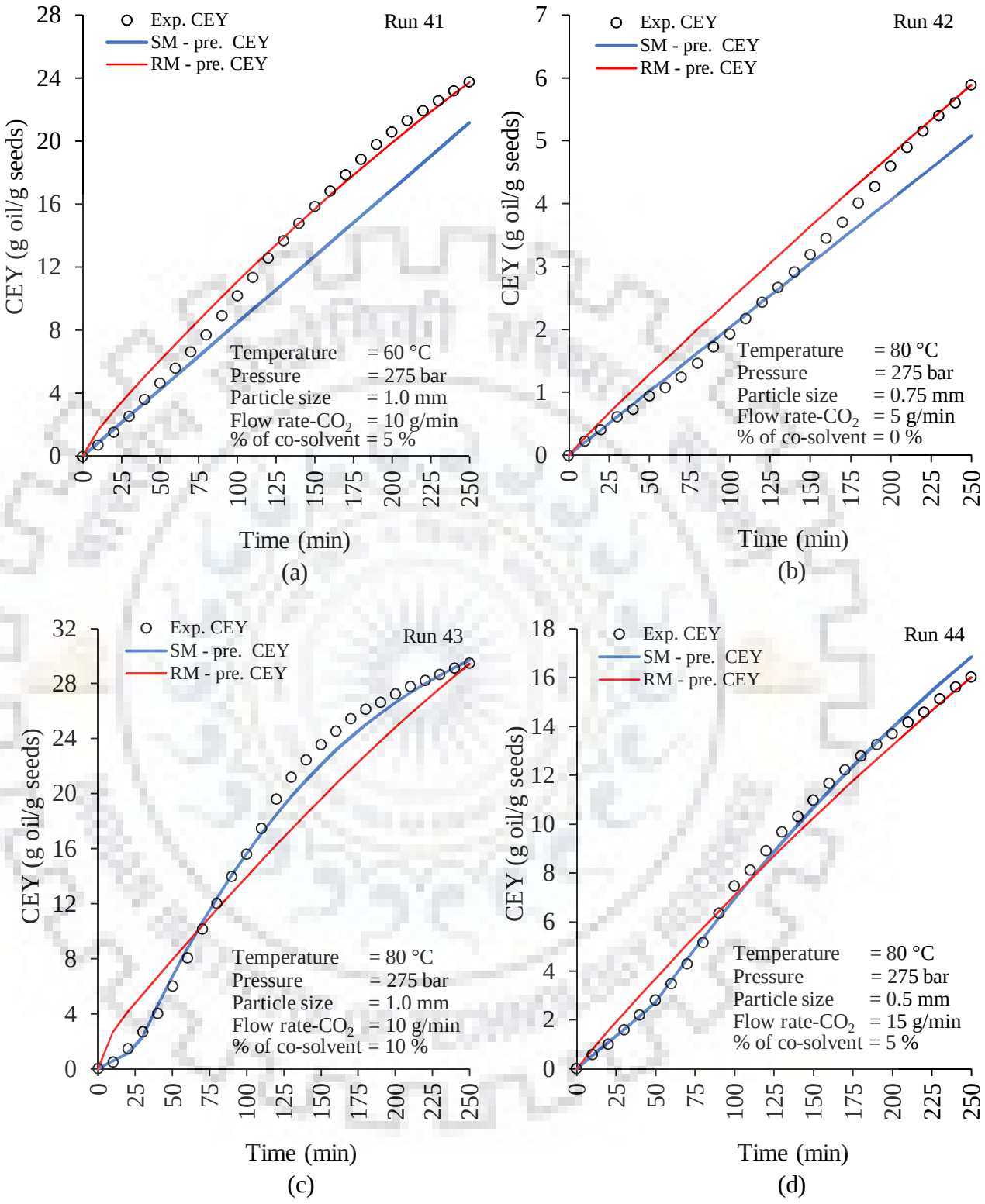


Fig. 5.44: Experimental and predicted CEY curves for PP seed oil during the SFE runs (41-44).

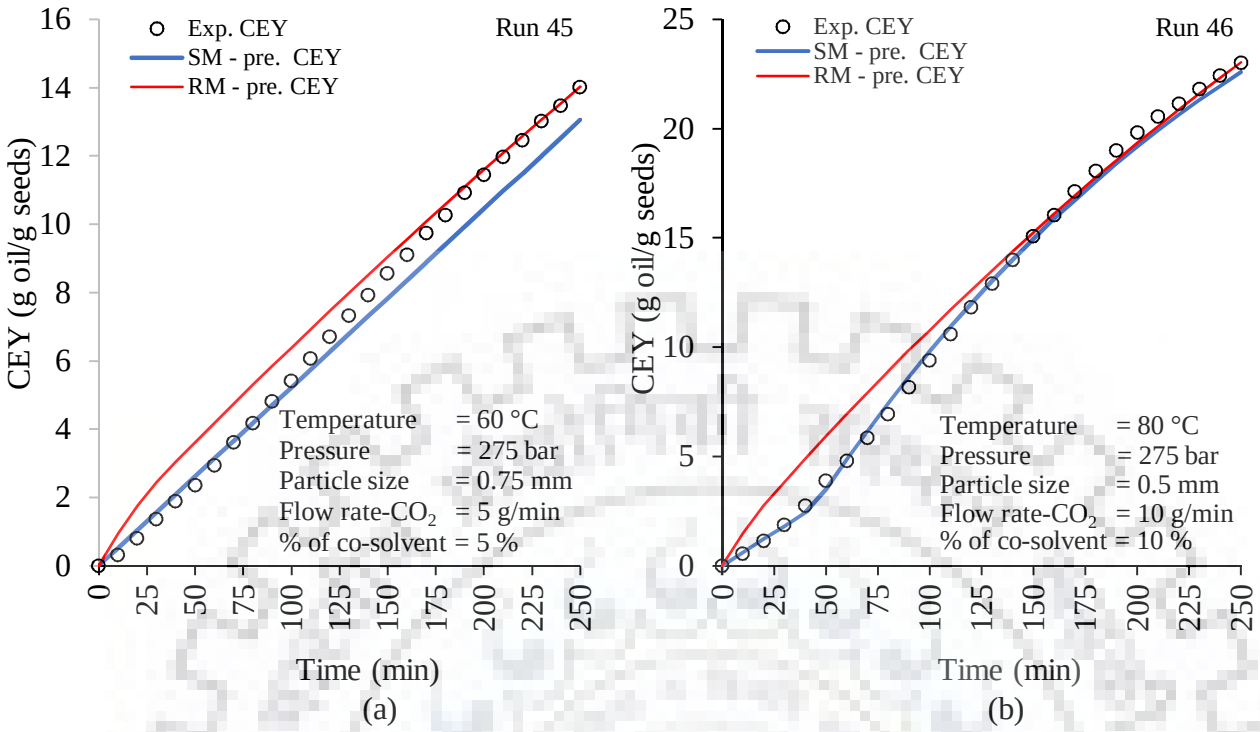


Fig. 5.45: Experimental and predicted CEY curves for PP seed oil during the SFE runs (45-46).

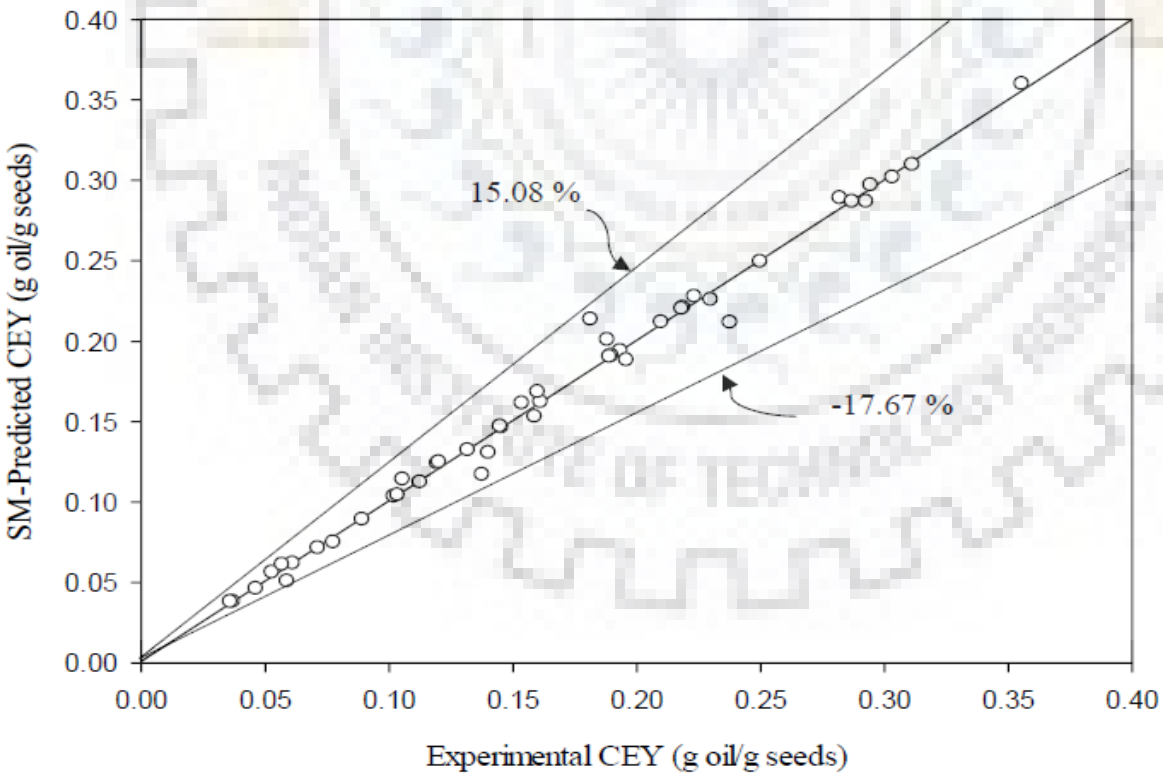


Fig. 5.46: Predicted (by SM) vs. Experimental CEY of PP seed oil.

5.5 Validation of Reverchon model for the SFE of AM and PP seed oils

The SFE process of both natural seeds (e.g. AM and PP seeds) has also been modeled by Reverchon model (Reverchon, 1996). The following assumptions were taken into consideration during the development of this model:

- Geometry of particles is taken into consideration.
- External mass transfer coefficient is neglected.
- The extracted oil is treated as a single component.
- Axial dispersion is neglected.
- Solvent (SC-$CO_2$) density and flow rate are constant along the bed.
- Extraction bed is assumed as a fixed bed.
- Plug flow exists in the bed.
- Internal diffusivity is taken into consideration.

The whole SFE process is divided in two parts based on mass-transfer resistances such as (a). External mass-transfer resistance and (b). Internal mass-transfer resistance. Since, the geometry of the particles is primarily assumed to be a slab (e.g. similar to the structure of leaves). However, later it has been corrected to include most of the shapes using a variable factor 'μ' which changes for different geometry in which the propagation of solutes (oils) is mainly controlled by the internal mass-transfer resistance therefore, the external mass-transfer coefficient is neglected in the development of this model. Thus, this model is based on the integration of differential mass balance over the fixed extraction bed as proposed. A detail description of the model has already been given in section 4.2 of Chapter 4.

As per the assumptions of the model, since the internal mass-transfer phenomenon plays a major role during the SFE of natural products, a correlation between the internal diffusion time ($t_i$) and internal diffusion coefficient ($D_i$) has been established as denoted by Eq. 5.22.

$$t_i = \mu \frac{l^2}{D_i} \quad \text{… Eq. 5.22}$$

Where, μ is a coefficient depending on the particle geometry. In the case of spherical particles μ=3/5, for cylindrical particles, μ=1/2 while for slabs, μ=1/3. The '*l*' is a characteristic dimension, which is defined by the Eq. 5.23.

$$l = \frac{(Particle\ volume,\ V_p)}{(Particle\ surface, A_p)} \quad \text{… Eq. 5.23}$$

In the case of spherical particles, $l = r/3$, where, 'r' is the mean particle radius. In the present, case (SFE of AM and PP seed oils), the geometry of both seeds is assumed 'spherical' instead of slabs.

5.5.1 Validation of Reverchon model (RM) for AM seed oil

The experimental parameters required for the validation of the Reverchon model (RM) were reproduced below for brevity. Table 5.21 shows the values of all input parameters for the SFE experiments. As explained earlier 0.05 kg of AM seeds of different mean particle sizes such as 1.0, 0.75, and 0.50 mm were used as feedstock. As shown in Table 5.21, the particle sizes were of 0.5, 0.75, 1.0 mm diameter and these particle sizes offered bed densities of 550.7, 645.4, 745.4 kg/m$^3$ for AM seeds respectively with corresponding particle densities of 1101.3, 1008.3, 1007.3 kg/m$^3$.

The solid density '1039 kg/m$^3$' was computed as the mean of all particle densities of each particle size of AM seeds. The solid volume '$4.8123\times10^{-5}$ m$^3$' was computed by dividing the weight of feedstock of each experimental run (e.g. 0.05 kg) by the solid density of AM seeds. It has already been discussed in the section 2.3 of Chapter 2 that the density of $CO_2$ is strongly influenced by temperature and pressure therefore an average density of $CO_2$ (701.88 kg/m$^3$) was taken into consideration for the model fitting. Since, the real velocity of the solvent (SC-$CO_2$) varies point to point throughout the extraction bed therefore the concept of superficial velocity was introduced hence, it was calculated by dividing the volumetric flow rate of $CO_2$ by the cross sectional area of bed as given in Table 5.21. As defined by Eq. 5.22, the geometrical parameter (μ) depends on the geometry of the seed particle (e.g. spherical, cylindrical, slab etc.) In our case, as 'spherical' geometry was considered and it's value of μ was taken as 3/5. The value of the volumetric partition coefficient ($k_p$) is required to solve the mass balance equations (as discussed in detail in section 4.2) around the extraction bed at equilibrium. Therefore, the value of volumetric partition coefficient ($k_p$) '0.34' was computed using Eq. 4.22 of Chapter 4 for AM seeds which represents the distribution of

AM seed oil between the phases (e.g. solid and solvent phases). The other necessary parameters related to extraction cell, for the development of the model are listed in Table 5.21.

Table 5.21. Experimental parameters used for fitting the Reverchon model.

| Particle size (diameter) | AM seeds | | | PP seeds | | |
|---|---|---|---|---|---|---|
| | Bed density ($kg/m^3$) | Particle density ($kg/m^3$) | Bed porosity | Bed density ($kg/m^3$) | Particle density ($kg/m^3$) | Bed porosity |
| 0.5 mm | 550.7 | 1101.3 | 0.5 | 446.7 | 899.3 | 0.5033 |
| 0.75 mm | 645.4 | 1008.5 | 0.360 | 566.7 | 944.4 | 0.4 |
| 1.0 mm | 745.4 | 1007.3 | 0.26 | 573.3 | 905.3 | 0.3667 |

| | | |
|---|---|---|
| Initial oil fraction (kg oil/kg oil free solid) | 0.7544 | 0.5625 |
| Avg. solid density ($kg/m^3$) = | 1039 | 916.3 |
| Solid volume ($m^3$) = | $4.8123\times10^{-5}$ | $5.4567\times10^{-5}$ |
| Volumetric partition coefficient ($k_p$) = | 0.34 | 0.20 |
| Avg. density of $CO_2$ ($kg/m^3$) = | 701.88 | |

| Flow rate-$CO_2$ | Volumetric flow rate-$CO_2$ ($m^3$/min) | Superficial velocity (m/min) |
|---|---|---|
| 5 g/min | $7.12372\times10^{-6}$ | 0.00185128 |
| 10 g/min | $1.42474\times10^{-5}$ | 0.00370256 |
| 15 g/min | $2.13712\times10^{-5}$ | 0.00555384 |

| **Parameters related to extraction cell** | | |
|---|---|---|
| Volume of extraction cell (bed containing) ($m^3$) | = | $6.539\times10^{-4}$ |
| Weight of feedstock (kg) | = | 0.05 |
| Cross sectional area of bed ($m^2$) | = | 0.003848 |
| Height of bed (m) | = | 0.17 |
| Diameter of bed (m) | = | 0.07 |
| Geometrical parameter (μ) (for spherical particles) | = | 0.6 |

Figs. (5.21-5.32), have been plotted to show a comparison between experimental and predicted (by RM) CEY of extraction curves during the SFE of AM seed oil. Table 5.22 shows the parameters required for validation of Reverchon model (RM) for SFE of AM seed oil. The parameter 'diffusivity ($D_i$)' of the solute (oil) was selected as the tuning parameter while the 'internal diffusion time ($t_i$)' was calculated from the model using the tuned value of diffusivity. As the tuning parameter 'diffusivity ($D_i$)' is computed for the whole extraction period, it is an average value for the whole period.

This wide range of extracted diffusivity ($D_i$) for the model is observed for different experimental runs due to the effect of operating parameters (e.g. temperature, pressure, particle size, flow rate-$CO_2$ and the % of co-solvent).

Figs. (5.21-5.32) are drawn to represent all 46 experimental runs, designed by BBD and given in Table 5.22 to show the variation of CEY (kg oil/kg seeds) of AM seed oil with time for all operating parameters (as mentioned above). Further, these figures also show the variation of CEY predictions using the RM. Following interesting facts can be observed from the prediction of RM.

1. A linear behavior of CEY of AM seed oil has been observed in all experimental runs (1-46) from the prediction of the RM though the actual experimental extraction curve is non-linear in nature.
2. The end points of CEY predicted by the model and the experimental extraction curve matched well. The maximum deviation between the experimental extraction curve and that predicted through RM is somewhere in the middle of extraction period.
3. For those experiments which exhibit linear extraction curve (e.g. Figs. 5.21(d), 5.22(a,b), 5.23(c), 5.24(b), 5.25(b,d), 5.6(c), 5.28(c), 5.29(c), 5.31(b,c) and 5.32(a)), the RM provides better fitting.
4. From all the Figs. (5.21-5.32), it is clear that the RM fits the experimental CEY data with an AARD % band of '+5.52 to +96.3 %' and an average AARD % of 37.76 %, thus it can be concluded that the RM does not fit non-liner behavior of the data.
5. All the plots of CEY (excepting Figs. 5.21(d), 5.22(a,b), 5.23(c), 5.24(b), 5.25(b,d), 5.6(c), 5.28(c), 5.29(c), 5.31(b,c) and 5.32(a)) of AM seed oil have not shown a good fitting with the experimental CEY by RM with an average AARD % ( 47.77 %).
6. Only 28 % of total number of experimental runs (46), means 13 runs (4, 5, 6, 11, 14, 18, 20, 23, 31, 35, 42, 43, and 45) have shown a better fitting with an AARD % band of '+5.52 to 20.05 %'.

The prediction from RM is not unusual. As the model uses an average diffusivity factor ($D_i$) extracted from the whole data sets of a particular extraction run, the prediction is almost linear. The little non-linearity that is being observed is due to the fact that, $\ln(c - c^*) \propto t$. Thus if the predictions from RM will be plotted on a semi log graph it will provide a perfect linear relationship between (c-c*) and t. As the mass transfer resistance (given in terms of diffusivity in this model) in the RM is not a function of time. The model predicts almost linear behavior of concentration with time and meets the final concentration at the end of the extraction period. That is, it predicts the final concentration accurately. However, it does not predict the intermediate concentrations properly.

Table 5.22. Parameters of Reverchon model for the SFE of AM seed oil.

| | | | Influencing experimental parameters | | | | Tuning parameter | Calculated Parameter | Error |
|---|---|---|---|---|---|---|---|---|---|
| Run | Temp. | Pre. | Solubility ($y_r$) | Superficial velocity ($u_s$) | Porosity ($e_p$) | Characteristic dimension ($l$) | Diffusivity ($D_i$) | Internal diffusion time ($t_i$) | AARD % |
| | (°C) | (bar) | (kg oil/kg $CO_2$) | (m/min) | | (m) | ($m^2$/min) | (min) | % |
| 1 | 80 | 200 | 0.0047 | 0.00370 | 0.5 | 8.3333E-05 | 3.2973E-12 | 1263.67 | 32.17 |
| 2 | 80 | 275 | 0.0170 | 0.00370 | 0.36 | 1.2500E-04 | 3.0181E-11 | 310.63 | 39.98 |
| 3 | 60 | 350 | 0.0214 | 0.00370 | 0.36 | 1.2500E-04 | 2.9496E-11 | 317.83 | 55.40 |
| 4 | 60 | 275 | 0.0056 | 0.00370 | 0.36 | 1.2500E-04 | 1.7832E-11 | 525.73 | 8.85 |
| 5 | 80 | 275 | 0.0807 | 0.00185 | 0.26 | 1.6667E-04 | 6.9366E-11 | 240.28 | 16.01 |
| 6 | 100 | 275 | 0.0126 | 0.00185 | 0.36 | 1.2500E-04 | 2.4348E-11 | 385.05 | 11.35 |
| 7 | 80 | 200 | 0.0552 | 0.00370 | 0.36 | 1.2500E-04 | 2.3959E-11 | 391.30 | 25.54 |
| 8 | 80 | 200 | 0.0054 | 0.00555 | 0.36 | 1.2500E-04 | 1.4334E-11 | 654.03 | 33.37 |
| 9 | 60 | 200 | 0.0173 | 0.00370 | 0.36 | 1.2500E-04 | 2.1202E-11 | 442.18 | 69.13 |
| 10 | 100 | 350 | 0.0211 | 0.00370 | 0.36 | 1.2500E-04 | 3.4200E-11 | 274.12 | 71.09 |
| 11 | 80 | 275 | 0.0106 | 0.00185 | 0.5 | 8.3333E-05 | 1.2937E-11 | 724.70 | 15.47 |
| 12 | 80 | 275 | 0.0178 | 0.00370 | 0.36 | 1.2500E-04 | 3.4907E-11 | 268.57 | 50.02 |
| 13 | 80 | 200 | 0.0048 | 0.00370 | 0.26 | 1.6667E-04 | 2.4582E-11 | 678.00 | 22.21 |
| 14 | 100 | 200 | 0.0032 | 0.00370 | 0.36 | 1.2500E-04 | 8.8200E-12 | 1062.93 | 8.11 |
| 15 | 80 | 350 | 0.0162 | 0.00555 | 0.36 | 1.2500E-04 | 2.3251E-11 | 403.20 | 71.49 |
| 16 | 80 | 275 | 0.0188 | 0.00555 | 0.36 | 1.2500E-04 | 2.8986E-11 | 323.43 | 91.57 |
| 17 | 80 | 350 | 0.0245 | 0.00370 | 0.36 | 1.2500E-04 | 4.0308E-11 | 232.58 | 65.21 |
| 18 | 80 | 200 | 0.0130 | 0.00370 | 0.36 | 1.2500E-04 | 3.5520E-12 | 2639.33 | 5.52 |
| 19 | 80 | 275 | 0.0053 | 0.00370 | 0.5 | 8.3333E-05 | 3.7800E-12 | 1102.30 | 36.16 |
| 20 | 100 | 275 | 0.0068 | 0.00370 | 0.26 | 1.6667E-04 | 3.4003E-11 | 490.15 | 12.13 |
| 21 | 80 | 275 | 0.0201 | 0.00370 | 0.36 | 1.2500E-04 | 3.2856E-11 | 285.33 | 45.06 |
| 22 | 60 | 275 | 0.0232 | 0.00370 | 0.36 | 1.2500E-04 | 2.7651E-11 | 339.05 | 54.90 |
| 23 | 80 | 275 | 0.0318 | 0.00370 | 0.26 | 1.6667E-04 | 2.3682E-11 | 703.77 | 8.66 |

Cont…

| | | | Influencing experimental parameters | | | | Tuning parameter | Calculated Parameter | Error |
|---|---|---|---|---|---|---|---|---|---|
| Run | Temp. | Pre. | Solubility ($y_r$) | Superficial velocity ($u_s$) | Porosity ($e_p$) | Characteristic dimension ($l$) | Diffusivity ($D_i$) | Internal diffusion time ($ti$) | AARD % |
| | (°C) | (bar) | (kg oil/kg $CO_2$) | (m/min) | | (m) | ($m^2$/min) | (min) | % |
| 24 | 60 | 275 | 0.0082 | 0.00370 | 0.5 | 8.3333E-05 | 5.0604E-12 | 823.38 | 43.03 |
| 25 | 60 | 275 | 0.0187 | 0.00555 | 0.36 | 1.2500E-04 | 2.4450E-11 | 383.43 | 86.01 |
| 26 | 80 | 275 | 0.0112 | 0.00555 | 0.26 | 1.6667E-04 | 4.8270E-11 | 345.28 | 46.39 |
| 27 | 100 | 275 | 0.0905 | 0.00555 | 0.36 | 1.2500E-04 | 2.9268E-11 | 320.32 | 39.93 |
| 28 | 80 | 275 | 0.0178 | 0.00370 | 0.36 | 1.2500E-04 | 3.3498E-11 | 279.87 | 49.46 |
| 29 | 100 | 275 | 0.0240 | 0.00370 | 0.36 | 1.2500E-04 | 4.6668E-11 | 200.88 | 57.53 |
| 30 | 80 | 350 | 0.0138 | 0.00370 | 0.36 | 1.2500E-04 | 2.1180E-11 | 442.63 | 29.21 |
| 31 | 80 | 200 | 0.0573 | 0.00185 | 0.36 | 1.2500E-04 | 1.1736E-11 | 798.82 | 9.25 |
| 32 | 100 | 275 | 0.0598 | 0.00370 | 0.36 | 1.2500E-04 | 1.0632E-11 | 881.77 | 30.41 |
| 33 | 80 | 275 | 0.0229 | 0.00370 | 0.36 | 1.2500E-04 | 3.4533E-11 | 271.48 | 49.54 |
| 34 | 80 | 350 | 0.0225 | 0.00185 | 0.36 | 1.2500E-04 | 7.1640E-11 | 130.86 | 25.08 |
| 35 | 80 | 275 | 0.0216 | 0.00185 | 0.36 | 1.2500E-04 | 1.6364E-10 | 101.85 | 20.05 |
| 36 | 80 | 275 | 0.0238 | 0.00370 | 0.36 | 1.2500E-04 | 3.5158E-11 | 266.65 | 50.51 |
| 37 | 80 | 350 | 0.0189 | 0.00370 | 0.26 | 1.6667E-04 | 7.9170E-11 | 210.52 | 32.63 |
| 38 | 80 | 350 | 0.0105 | 0.00370 | 0.5 | 8.3333E-05 | 6.5826E-12 | 633.00 | 41.99 |
| 39 | 100 | 275 | 0.0107 | 0.00370 | 0.5 | 8.3333E-05 | 8.1366E-12 | 512.07 | 33.44 |
| 40 | 80 | 275 | 0.0130 | 0.00555 | 0.36 | 1.2500E-04 | 1.6383E-11 | 572.23 | 33.59 |
| 41 | 60 | 275 | 0.0147 | 0.00370 | 0.26 | 1.6667E-04 | 5.5695E-11 | 299.25 | 33.47 |
| 42 | 80 | 275 | 0.0807 | 0.00185 | 0.36 | 1.2500E-04 | 1.0776E-11 | 869.98 | 17.14 |
| 43 | 80 | 275 | 0.0108 | 0.00370 | 0.26 | 1.6667E-04 | 6.8670E-11 | 242.70 | 10.33 |
| 44 | 80 | 275 | 0.0080 | 0.00555 | 0.5 | 8.3333E-05 | 5.5674E-12 | 748.40 | 96.30 |
| 45 | 60 | 275 | 0.0134 | 0.00185 | 0.36 | 1.2500E-04 | 2.9868E-11 | 313.88 | 17.74 |
| 46 | 80 | 275 | 0.0080 | 0.00370 | 0.5 | 8.3333E-05 | 7.0878E-12 | 587.87 | 34.61 |

5.5.2 Validation of Reverchon model (RM) for PP seed oil

The experimental parameters required for the validation of the Reverchon model (RM) for SFE of PP seed oil were reproduced below for brevity. Table 5.21 shows the values of all input parameters for the SFE experiments. As explained earlier 0.05 kg of PP seeds of different mean particle sizes such as 1.0, 0.75, and 0.50 mm were used as feedstock. As shown in Table 5.21, the particle sizes were of 0.5, 0.75, 1.0 mm diameter and these particle sizes offered bed densities of 446.7, 566.7, 573.3 kg/m$^3$ for PP seeds respectively with corresponding particle densities of 899.3, 944.4, 905.3 kg/m$^3$.

The solid density '916.3 kg/m$^3$' was computed as discussed in section 5.5.1. The solid volume '$5.4567\times10^{-5}$ m$^3$' was computed by dividing the mass of feedstock of each experimental run (e.g. 0.05 kg) by the solid density of PP seeds. It has already been discussed in the section 2.3 of Chapter 2 that the density of $CO_2$ is strongly influenced by temperature and pressure therefore an average density of $CO_2$ (701.88 kg/m$^3$) was taken into consideration for the modeling.

The other contributing parameters such as superficial velocity ($u_i$), geometry of the particle of PP seeds have also been given in Table 5.21. The volumetric partition coefficient ($k_p$) was computed as '0.2' which differs in value from the AM seed case due to the different values of initial oil content, solubility and the solid density used during its calculation as described in section 5.5.1. The conditions of parameters related to extraction cell are same for both the cases (SFE of AM and PP seeds).

Figs. (5.34-5.45), have been plotted to show a comparison between experimental and predicted (by RM) CEY of extraction curves during the SFE of PP seed oil. Table 5.23 shows the parameters required for validation of RM for SFE of PP seed oil. The parameter 'diffusivity ($D_i$)' of the solute (oil) was selected as the tuning parameter, while the 'internal diffusion time ($t_i$)' was computed from the model using the tuned value of diffusivity ($D_i$).

This wide range of extracted diffusivity ($Di$) for the model is observed for different experimental runs due to the effect of operating parameters (e.g. temperature, pressure, particle size, flow rate-$CO_2$ and the % of co-solvent). Figs. (5.34-5.45) are drawn to represent all 46 experimental runs, designed by BBD and given in Table 5.23 to show the variation of CEY (kg oil/kg seeds) of PP seed oil with time for all operating parameters as mentioned in the section 5.4.1. Further, these

figures also show the variation of CEY predictions using the RM. Following interesting facts can be observed from the prediction of RM.

1. A linear behavior of CEY of PP seed oil has been observed in all experimental runs (1-46) from the prediction of the RM though the actual experimental extraction curve is non-linear in nature.
2. The end points of CEY predicted by the model and the experimental extraction curve matched well. The maximum deviation between the experimental extraction curve and that predicted through RM is somewhere in the middle of extraction period.
3. From all the Figs. (5.34-5.45), it is clear that the RM fits the experimental CEY data with an AARD % band of '+2.64 to +19.74 %' for 74 % of total experimental runs (46) while 26 % of total experimental runs, with an AARD % band of '+21.18 to +73.16%. On the other hand, an average AARD % '17.93 %' was achieved from the total number of experimental runs (46), thus it can be concluded that the RM fits partially well.
4. Only 26 % of total number of experimental runs (46), means 12 runs (e.g. 13, 14, 15, 16, 18, 23, 25, 27, 31, 32, 37, and 40) have shown a worse fitting (e.g. AARD % > 20 %) with an AARD % band of '+21.18 to +73.16 %'.

The above observations during the SFE of PP seeds oil are explained on the basis, of the computed values of internal diffusion time ($t_i$), tuning parameter 'diffusivity ($D_i$)' and the 'AARD %' found between the experimental and the predicted CEY values obtained for extraction curve as given in Table 5.23.

The prediction from RM is not unusual. As the model uses an average diffusivity factor ($D_i$) extracted from the whole data sets of a particular extraction run, the prediction is almost linear. The little non-linearity that is being observed is due to the fact that, $\ln(c - c^*) \propto t$. Thus if the predictions from RM will be plotted on a semi log graph it will provide a perfect linear relationship between (c-c*) and t. As the mass transfer resistance (given in terms of diffusivity in this model) in the RM is not a function of time the model predicts almost linear behavior of concentration with time and meets the final concentration at the end of the extraction period. That is, it predicts the final concentration accurately. However, it does not predict the intermediate concentrations properly.

Table 5.23. Parameters of Reverchon model for the SFE of PP seed oil.

| | | | Influencing experimental parameters | | | | Tuning parameter | Calculated Parameter | Error |
|---|---|---|---|---|---|---|---|---|---|
| Run | Temp. | Pre. | Solubility ($y_r$) | Superficial velocity ($u_s$) | Porosity ($e_p$) | Characteristic dimension ($l$) | Diffusivity ($D_i$) | Internal diffusion time ($ti$) | AARD % |
| | (°C) | (bar) | (kg oil/kg $CO_2$) | (m/min) | | (m) | ($m^2$/min) | (min) | % |
| 1 | 80 | 200 | 0.0018 | 0.00370 | 0.503 | 8.3333E-05 | 2.416380E-12 | 1724.33 | 17.24 |
| 2 | 80 | 275 | 0.0044 | 0.00370 | 0.400 | 1.2500E-04 | 2.145000E-11 | 437.07 | 3.77 |
| 3 | 60 | 350 | 0.0075 | 0.00370 | 0.400 | 1.2500E-04 | 5.934000E-11 | 157.99 | 5.22 |
| 4 | 60 | 275 | 0.0022 | 0.00370 | 0.400 | 1.2500E-04 | 9.600000E-12 | 976.57 | 9.97 |
| 5 | 80 | 275 | 0.0059 | 0.00185 | 0.367 | 1.6667E-04 | 3.390000E-11 | 491.65 | 8.84 |
| 6 | 100 | 275 | 0.0046 | 0.00185 | 0.400 | 1.2500E-04 | 6.708000E-12 | 1397.58 | 12.73 |
| 7 | 80 | 200 | 0.0030 | 0.00370 | 0.400 | 1.2500E-04 | 1.038000E-11 | 903.18 | 9.10 |
| 8 | 80 | 200 | 0.0009 | 0.00555 | 0.400 | 1.2500E-04 | 4.512000E-12 | 2077.83 | 11.17 |
| 9 | 60 | 200 | 0.0034 | 0.00370 | 0.400 | 1.2500E-04 | 1.185600E-11 | 790.73 | 11.02 |
| 10 | 100 | 350 | 0.0053 | 0.00370 | 0.400 | 1.2500E-04 | 2.700000E-11 | 347.22 | 6.64 |
| 11 | 80 | 275 | 0.0048 | 0.00185 | 0.503 | 8.3333E-05 | 6.508200E-12 | 640.22 | 18.13 |
| 12 | 80 | 275 | 0.0044 | 0.00370 | 0.400 | 1.2500E-04 | 1.920000E-11 | 488.28 | 10.61 |
| 13 | 80 | 200 | 0.0055 | 0.00370 | 0.367 | 1.6667E-04 | 1.800000E-11 | 925.93 | 66.81 |
| 14 | 100 | 200 | 0.0030 | 0.00370 | 0.400 | 1.2500E-04 | 2.760000E-12 | 3396.67 | 69.53 |
| 15 | 80 | 350 | 0.0134 | 0.00555 | 0.400 | 1.2500E-04 | 4.020000E-11 | 233.22 | 33.00 |
| 16 | 80 | 275 | 0.0083 | 0.00555 | 0.400 | 1.2500E-04 | 2.912400E-11 | 321.90 | 21.18 |
| 17 | 80 | 350 | 0.0102 | 0.00370 | 0.400 | 1.2500E-04 | 7.620000E-11 | 123.03 | 15.23 |
| 18 | 80 | 200 | 0.0029 | 0.00370 | 0.400 | 1.2500E-04 | 2.580000E-12 | 3633.67 | 73.16 |
| 19 | 80 | 275 | 0.0021 | 0.00370 | 0.503 | 8.3333E-05 | 3.750000E-12 | 1111.12 | 2.64 |
| 20 | 100 | 275 | 0.0035 | 0.00370 | 0.367 | 1.6667E-04 | 2.448000E-11 | 680.83 | 3.38 |
| 21 | 80 | 275 | 0.0044 | 0.00370 | 0.400 | 1.2500E-04 | 2.072400E-11 | 452.37 | 4.48 |
| 22 | 60 | 275 | 0.0108 | 0.00370 | 0.400 | 1.2500E-04 | 6.030000E-11 | 155.47 | 11.71 |
| 23 | 80 | 275 | 0.0045 | 0.00370 | 0.367 | 1.6667E-04 | 1.287000E-11 | 1295.00 | 30.72 |

Cont…

| | | Most influencing experimental parameters | | | | | Tuning parameter | Calculated Parameter | Error |
|---|---|---|---|---|---|---|---|---|---|
| Run | Temp. | Pre. | Solubility ($y_r$) | Superficial velocity ($u_s$) | Porosity ($e_p$) | Characteristic dimension ($l$) | Diffusivity ($D_i$) | Internal diffusion time ($ti$) | AARD % |
| | (°C) | (bar) | (kg oil/kg $CO_2$) | (m/min) | | (m) | ($m^2$/min) | (min) | % |
| 24 | 60 | 275 | 0.0056 | 0.00370 | 0.503 | 8.3333E-05 | 1.020000E-11 | 408.50 | 13.62 |
| 25 | 60 | 275 | 0.0054 | 0.00555 | 0.400 | 1.2500E-04 | 2.379000E-11 | 394.07 | 27.10 |
| 26 | 80 | 275 | 0.0103 | 0.00555 | 0.367 | 1.6667E-04 | 4.173000E-11 | 399.40 | 16.64 |
| 27 | 100 | 275 | 0.0042 | 0.00555 | 0.400 | 1.2500E-04 | 8.490000E-12 | 1104.23 | 46.26 |
| 28 | 80 | 275 | 0.0044 | 0.00370 | 0.400 | 1.2500E-04 | 2.045400E-11 | 458.35 | 5.46 |
| 29 | 100 | 275 | 0.0035 | 0.00370 | 0.400 | 1.2500E-04 | 1.596000E-11 | 587.40 | 5.05 |
| 30 | 80 | 350 | 0.0034 | 0.00370 | 0.400 | 1.2500E-04 | 1.475400E-11 | 635.42 | 5.06 |
| 31 | 80 | 200 | 0.0045 | 0.00185 | 0.400 | 1.2500E-04 | 3.534000E-12 | 2652.83 | 29.00 |
| 32 | 100 | 275 | 0.0022 | 0.00370 | 0.400 | 1.2500E-04 | 3.912000E-12 | 2396.50 | 31.24 |
| 33 | 80 | 275 | 0.0044 | 0.00370 | 0.400 | 1.2500E-04 | 2.074200E-11 | 451.98 | 4.39 |
| 34 | 80 | 350 | 0.0111 | 0.00185 | 0.400 | 1.2500E-04 | 5.010000E-11 | 187.13 | 9.85 |
| 35 | 80 | 275 | 0.0061 | 0.00185 | 0.400 | 1.2500E-04 | 2.245800E-11 | 417.45 | 19.74 |
| 36 | 80 | 275 | 0.0044 | 0.00370 | 0.400 | 1.2500E-04 | 2.070000E-11 | 452.90 | 4.90 |
| 37 | 80 | 350 | 0.0080 | 0.00370 | 0.367 | 1.6667E-04 | 9.147000E-11 | 182.22 | 23.26 |
| 38 | 80 | 350 | 0.0115 | 0.00370 | 0.503 | 8.3333E-05 | 1.932000E-11 | 215.67 | 8.81 |
| 39 | 100 | 275 | 0.0030 | 0.00370 | 0.503 | 8.3333E-05 | 4.551000E-12 | 915.55 | 9.29 |
| 40 | 80 | 275 | 0.0013 | 0.00555 | 0.400 | 1.2500E-04 | 4.176000E-12 | 2245.00 | 23.55 |
| 41 | 60 | 275 | 0.0042 | 0.00370 | 0.367 | 1.6667E-04 | 5.778000E-11 | 288.45 | 11.55 |
| 42 | 80 | 275 | 0.0020 | 0.00185 | 0.400 | 1.2500E-04 | 4.722000E-12 | 1985.33 | 14.40 |
| 43 | 80 | 275 | 0.0360 | 0.00370 | 0.367 | 1.6667E-04 | 1.038000E-10 | 160.57 | 18.89 |
| 44 | 80 | 275 | 0.0167 | 0.00555 | 0.503 | 8.3333E-05 | 6.240000E-12 | 667.73 | 10.27 |
| 45 | 60 | 275 | 0.0052 | 0.00185 | 0.400 | 1.2500E-04 | 1.692000E-11 | 554.08 | 15.41 |
| 46 | 80 | 275 | 0.0311 | 0.00370 | 0.503 | 8.3333E-05 | 1.200000E-11 | 347.22 | 15.18 |

5.6 Comparison of results from the SM and RM for the SFE of both seeds

The validation of both models (SM and RM) has been done in the previous sections (5.4 and 5.5) using the experimental data of both seeds (e.g. AM and PP seeds). Despite the MTPBM category (as described in section 2.12.1) of both models (e.g. SM and RM), a significant difference in the outcomes of the models has been observed. A comparison of results obtained from SM and RM for the SFE of AM and PP seed oils is done in the next sections 5.6.1 and 5.6.2 respectively.

5.6.1 Comparison of outcomes from SM and RM for the SFE of AM seed oil

Table 5.24 has been created on the basis of observations and their explanations during the validation of SM and RM using the experimental data obtained from the SFE of AM seed oil. The SM has proved its superiority over the RM in terms of fitting of the experimental data in terms of observed error, extent of representation of actual physical phenomenon during the SFE of seed oil and the realistic behavior of the obtained extraction curve. However, a final comparison of findings from the validation of SM and RM has also been given in Table 5.26, which makes it amply clear that the SM has predicted the SFE phenomenon of AM seed oil in a better manner.

Table 5.24. A comparison of outcomes from SM and RM for the SFE of AM seed oil.

| Sovova model (SM) | Reverchon model (RM) |
|---|---|
| 1. This model has predicted the linear as well as curvy part of the extraction curve of AM seed oil satisfactorily (as shown in Figs. 5.21-5.32). | 1. This model has only predicted well the linear part of the extraction curve of the AM seed oil. (as shown in Figs. 5.21-5.32). |
| 2. This model quantified the extracted AM seed oil in different parts of the extraction curve (as shown in Table 5.18) due to the involvement of three parameters which represents three time zones (e.g. $t \leq t_{CER}$, $t_{CER} \leq t \leq t_{FER}$, and $t > t_{FER}$). | 2. This model could not quantify the extracted AM seed oil in different parts of the extraction curve (as shown in Figs. 5.21-5.32). |
| 3. An error (AARD %) band of '+1.44 to +14.20 %' with an average error (AARD %) of 5.22 % was obtained from the data of SFE of AM seed oil. | 3. An error (AARD %) band of '+5.52 to 96.3%' with an average error (AARD %) of 37.76 % was obtained for the data of SFE of AM seed oil. |
| 4. For '93.5%' of total number of runs (e.g. 43 runs out of 46) the model predictions were within an average error of '4.67%'. | 4. For '28.26 %' of total number of runs (e.g. 13 runs out of 46) the model predictions were within an average error of '12.36 %'. |

5.6.2 Comparison of outcomes from SM and RM for the SFE of PP seed oil

Similar to section 5.6.1, Table 5.25 has also been prepared based on the observations and their explanations during the validation of SM and RM using the experimental data obtained from the SFE of PP seed oil. The SM has again proved to be better over the RM. However, in this case (SFE of PP seed oil) RM has shown a partial improvement as compared to previous case (SFE of AM seed oil) which can be verified from the Table 5.25.

Table 5.25. A comparison of outcomes from SM and RM for the SFE of PP seed oil.

| Sovova model (SM) | Reverchon model (RM) |
|---|---|
| 1. This model has predicted the linear as well as curvy part of the extraction curve of PP seed oil satisfactorily (as shown in Figs. 5.34-5.45). | 1. This model has only predicted well the linear part of the extraction curve of the PP seed oil. (as shown in Figs. 5.34-5.45). |
| 2. This model quantified the extracted PP seed oil in different parts of the extraction curve (as shown in Table 5.20) due to the involvement of three parameters which represents three time zones (e.g. $t \leq t_{CER}$, $t_{CER} \leq t \leq t_{FER}$, and $t > t_{FER}$). | 2. This model could not quantify the extracted PP seed oil in different parts of the extraction curve (as shown in Figs. 5.34-5.45). |
| 3. An error (AARD %) band of '+0.77 to +14.17 %' with an average error (AARD %) of 4.25 % was obtained from the data of SFE of PP seed oil. | 3. An error (AARD %) band of '+2.64 to +73.16 %' with an average error (AARD %) of 17.94 % was obtained for the data of SFE of PP seed oil. |
| 4. This model provided an average error '3.59 %' with '93.5 %' of total number of runs means 43 runs out of 46. | 4. This model provided an average error '10.31 %' with '74 %' of total number of runs means 34 runs out of 46. |

Table 5.26. A final comparison of results obtained from SM and RM.

| | Based on the findings from the literature | | |
|---|---|---|---|
| | **Results obtained from SM** | | **Results obtained from RM** |
| 1. | Three analytical differential equations represents the three sections of the whole extraction curve during the SFE of AM and PP seed oils. Therefore, it represents the physical phenomena in a better way. | 1. | Single partial differential equation represents the whole extraction curve during the SFE of AM and PP seed oils. |
| 2. | Three phenomena of extraction (e.g. convection, convection plus diffusion and diffusion only) were taken in to account during the SFE of AM and PP seed oils. | 2. | Single phenomenon of extraction (e.g. diffusion only) was taken into account during the SFE of AM and PP seed oils. |
| 3. | Division of whole extraction curve is purely based on the time duration that is taken by each extraction phenomenon (as mentioned in point 2.). | 3. | No division of extraction curve because an average diffusivity was used during the each experimental run. |
| 4. | Since, the SFE of seed oil is purely described by three phenomenon (as mentioned in point 2.) therefore solid and solvent phases mass transfer coefficient play a crucial role in it. | 4. | Since, the SFE of seed oil is purely described by single phenomenon (as mentioned in point 2.) therefore only solid phases mass transfer resistance play a crucial role in extraction. |
| 5. | More realistic based on the nature of the model. | 5. | Not realistic because of the nature of the model. |
| 6. | Spherical geometry of particles was considered. | | Spherical geometry of particles was considered but best fitting with slab geometry was found as reported in literature. |
| 7. | High possibility for predicting the maximum % of CEY of seed oils due to the involvement of multiple mass transfer phenomenon that actually takes place in nature. | 7. | Low possibility of predicting the maximum % of CEY of seed oils due to the involvement of only single mass transfer phenomenon. |
| | **Based on the findings from the present study** | | |
| 1. | Since, three parameters (e.g. Z, W and $x_k$) were tuned through an optimization technique hence this model predicts more accurately than RM. | 1. | Only one parameter (e.g. diffusivity) was tuned. |
| 2. | • AARD % band is '+1.436 to +14.198%' with an average AARD % '5.224%'. (for SFE of AM seed oil).<br>• AARD % band is '0.7706 to +14.17 %' with an average AARD % '4.254%'. (for SFE of PP seed oil). | 2. | • AARD % band is '+5.52 to +96.3 %' with an average AARD % '37.6 %'.(for SFE of AM seed oil).<br>• AARD % band is '2.64 to 19.74 %' with an average AARD % '17.93 %'.(for SFE of PP seed oil). |
| 3. | Two types of mass transfer resistances one for solid and other for solvent phases (e.g. internal mass transfer resistance and external mass transfer resistance) were taken into consideration. | 3. | One type of resistance for solid phase (e.g. internal mass transfer resistance) was taken into consideration. |
| 4. | Only spherical geometry of the seed particles was assumed. | 4. | Different geometries (e.g. slab, cylindrical, spherical) have been tested by incorporating a 'coefficient depending on the particle geometry'. |
| 5. | Produced excellent fitting with the experimental data of both seeds based on error band and average error. | 5. | Produced partially good fittings with experimental data of both seeds based on error band and average error. |

## 5.7 Analysis of the structure of AM and PP seed samples using scanning electron microscope

The surface morphology of AM and PP seeds particle samples, before and after the SFE process, were studied using LEO-1550 scanning electron microscope (SEM) instrument. The seed particle samples (at before and after extraction) were first coated with gold-palladium alloy before it is used in SEM. Fig. 5.47 shows the SEM images at 200, 500 and 1000 magnification of the AM seed particle, at before extraction (Fig. 5.47 (a, b, c)) and after extraction (Fig. 5.47 (d, e, f)). From the Fig. 5.47 (a, b, c) it is clear that oil is contained in the cell/cavity of the seed particle in the form of layers which can be justified easily by the cloudy appearance of the SEM images of before extraction samples, which appear more distinctly as the magnification increases from 200 to 1000. Similarly, the Fig. 5.48 shows the SEM images of PP seed particles, at before extraction (Fig. 5.48 (a, b and c at 200, 500 and 1000 magnifications respectively)) and after extraction (Fig. 5.48 (d, e and f at 200, 500 and 1000 magnifications respectively)). Here, the cloudy appearance shows the presence of oil.

These cells/cavities were broken up by the influence of extraction parameters (e.g. temperature, pressure, particle size, flow rate-$CO_2$ and the % of co-solvent) and oil was extracted out as evident from the broken and empty portions of cell that had appeared in Fig. 5.47 (c, d, f) and Fig. 5.48 (c, d, f). It can be observed from the above images that after extraction the surface of the particle is left with a structure of broken cavities/empty cavities also called cells, which have once contained oil at before extraction. Before extraction, these oil-filled cells have been arranged in the form of layers and oil have been uniformly distributed in each layer. After extraction, the cells are found broken and cracked which confirms that at high pressure the cells are broken and ultimately the structure of solid matrix of seed particle is changed.

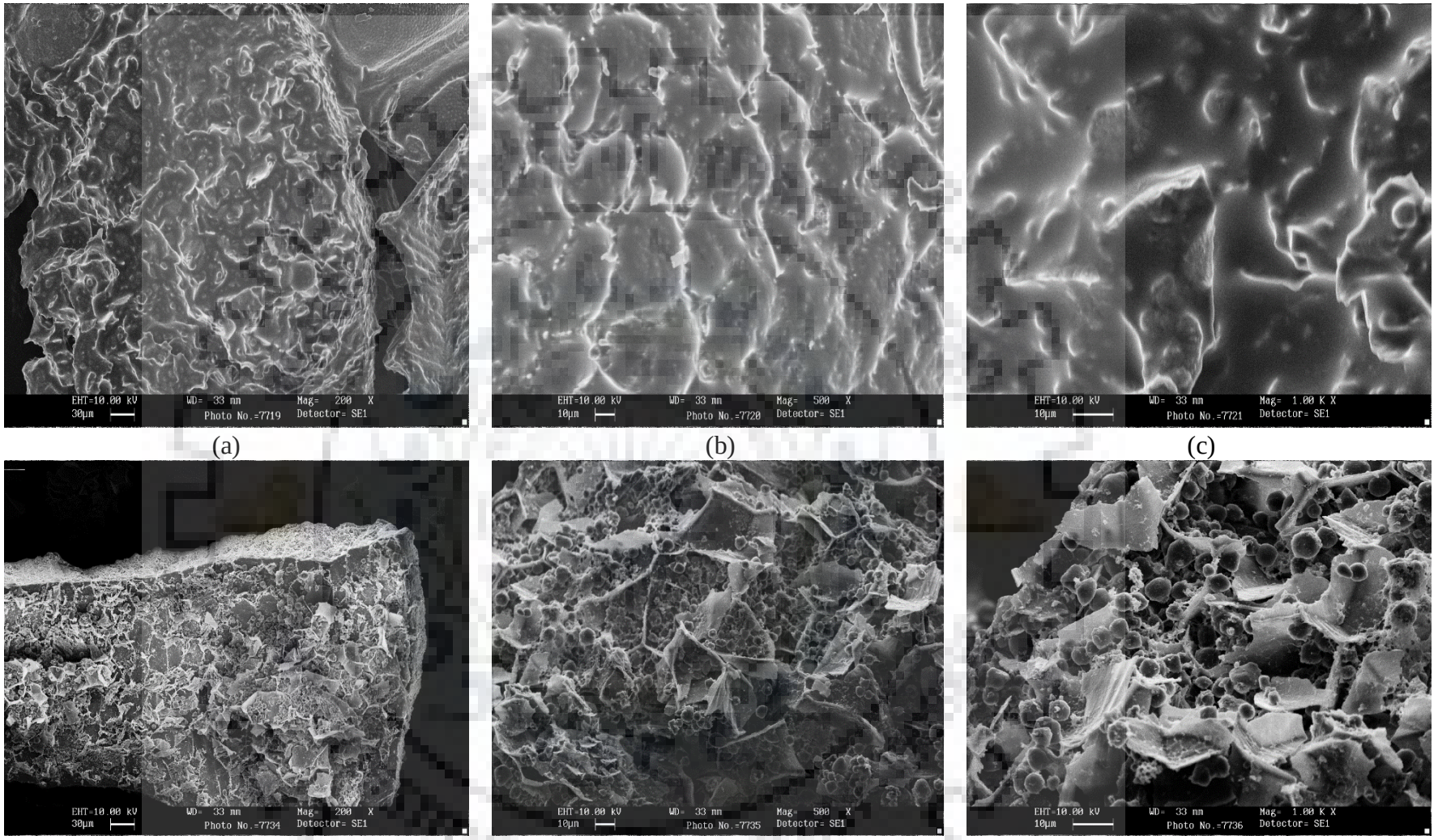


(a) (b) (c)

(d) (e) (f)

Fig. 5.47: SEM images of AM seed particles at before extraction (a, b and c at 200, 500 and 1000 magnifications respectively) and after extraction (d, e and f at 200, 500 and 1000 magnifications respectively).

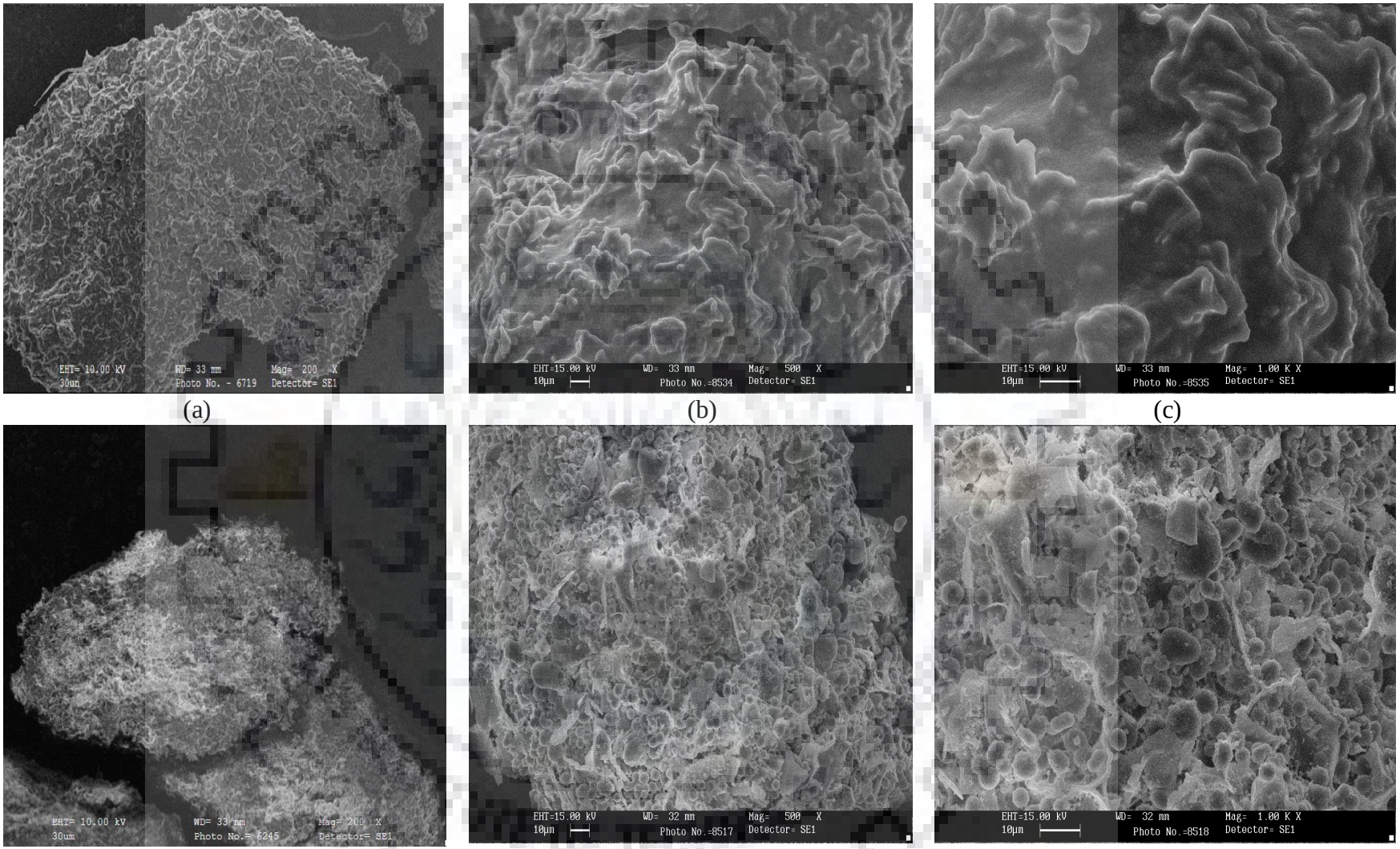


(a) (b) (c)

(d) (e) (f)

Fig. 5.48: SEM images of PP seeds, before extraction (a, b and c at 200, 500 and 1000 magnifications respectively) and after extraction (d, e and f at 200, 500 and 1000 magnifications respectively).

## 5.8 Characterization of the feeds and product oils

In this section, the characterization of the raw feed materials (e.g. AM and PP seeds) and their extracted oils are examined to determine whether these oils could also be used as a good source for bio-fuel along with its medicinal applications. Various fuel properties such as; heating value, flashpoint, fire point, cloud point and pour point and chemical properties such as; saponification value, peroxide value and acid value were determined in the laboratory and finally fatty acids compositions were determined so that the practical applications of these oils could be suggested accordingly.

### 5.8.1 Characterization of AM seed and seed oil

Some researchers (e.g. Dey et al., 2008; Mishra et al., 2009; Rao et al., 2012) have reported a pale yellow color nauseous, bitter, non-edible oil ranging from 22 to 40% which is rich in unsaturated fatty acids (e.g. linoleic, oleic, ricinoleic, palmitoleic acids etc.). Apart from the fatty acids found in oil, it also contains some toxic alkaloid contents (e.g. sanguinarine, dihydrosanguinarine, berberine, protopine, coptisine etc.) which have been used to cure various chronic diseases (Dey et al., 2008; Singh et al., 2010). AM seed oil contains palmitic acid (11.4 - 23.58%), stearic acid (2.98 - 5.97%), oleic acid (25.01 - 41.46%), linoleic acid (22.54 - 59.07%) and palmitoleic acid (0.0 - 2.48%) which confirm its suitability for the production of bio-fuel. In addition to this, some researchers (e.g. Azam et al., 2005; Singh et al., 2010; Singh and Singh, 2010; Bankovi-Ilic et al., 2012) have also shown that this oil is suitable for the production of esters which are main ingredients during the production of biodiesel. The seed oil has also been used medicinally to cure ulcers and eruptions, to cure dysentery, asthma and other intestinal infections. Further, it can be used as a mild painkiller (Rahman and Ilyas, 1962; Dey et al., 2008; Singh and Singh, 2010; Singh et al., 2010; Brahmachari et al., 2013).

The whole plant (Argemone Mexicana (L.)) has been accepted as an important medicinal plant in India. The yellow juice, which exudes when the plant is injured has long been used in India as traditional medicine for dropsy, jaundice, ophthalmia, scabies and cutaneous infections (Chopra et al., 1956; Ambasta, 1986; Sharma et al., 2012). Leaves and seeds have also been employed as a remedy for dysentery, ulcers, asthma and to maintain normal blood circulation and cholesterol level in human body (Prajapati et al., 2003; Savithramma et al., 2007; de Albuquerque et al., 2007) and also possess anti-venom property (Minu et al., 2012). Flowers are also used as an expectorant and

have been used in the treatment of coughs (Brahmachari et al., 2013). TGA and FTIR were performed for the qualitative analysis of the AM seeds while the quantitative analysis of the extracted oil is done by gas chromatography.

5.8.1.1 Thermo-gravimetric (TG) analysis of AM seeds

The thermogram obtained from thermo-gravimetric (TG) analysis of AM seed samples is shown in Fig. 5.49, which provides an approximate estimation of moisture content, total organic components and ash content. Thermo-gravimetric (TG) analysis is used to investigate the thermal degradation of AM seeds as shown in Fig. 5.49. TG analysis was performed using EXSTAR TG/DTA 6300 for AM seed particles of size of 1.0 mm before extraction under air atmosphere (200 mL/min) at a temperature range of 30 ℃ - 1200 ℃. Fig. 5.49 also shows the TG thermogram of the sample (before extraction). The TG plot (Fig. 5.49), thus obtained, could be divided into three sections. The first section of the thermogram, from 30 ℃ to 190 ℃, is associated with the dehydration of seed particle which undergoes a weight loss of approx. 10% (wt%). The second section of the thermogram, from 190 ℃ to 500 ℃, is associated with the decomposition of organic matter present in the seed particle and reports a weight loss of approx. 76% (wt%). Thereafter, the third section of the thermogram, from 500 ℃ to 1200 ℃, is related to the decomposition of most of the components of seed particles with a weight loss of approx. 10% (wt %). There is around 3.6% of residue left at the final temperature of 1200 ℃, which is most probably due to the presence of inorganic oxides in ash.

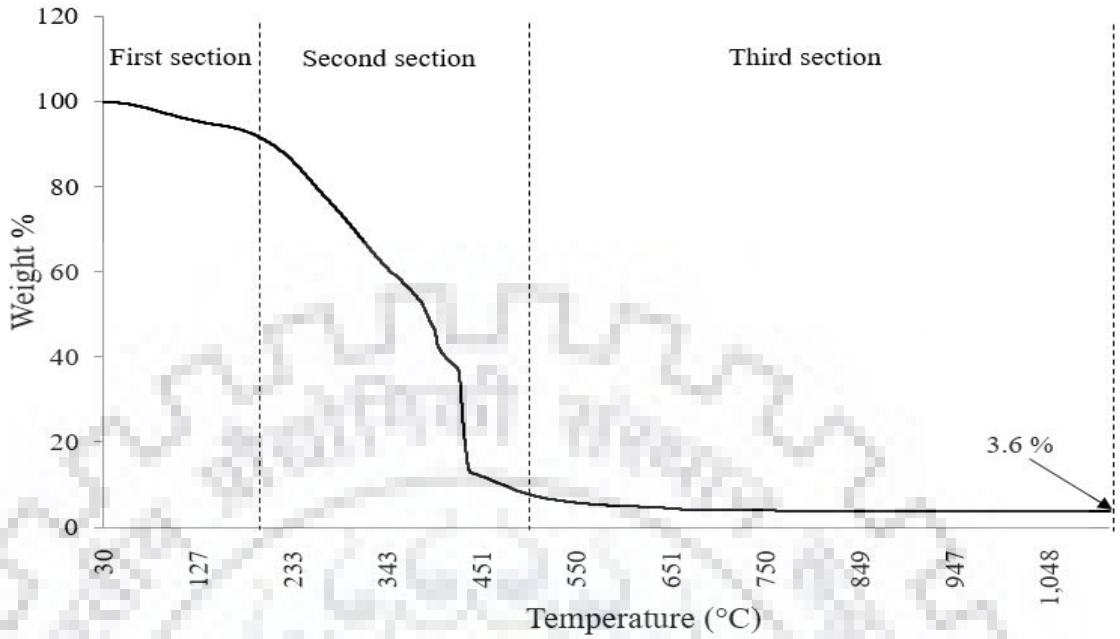


Fig. 5.49: TG thermogram of AM seed particles.

5.8.1.2 Fourier transform infrared (FTIR) spectroscopy analysis of AM seeds

A qualitative analysis, of organic compounds, present in AM seeds, was done by using Fourier transform infrared (FTIR) spectroscopy technique in the initial stage (before extraction) to identify various functional organic groups. The FTIR spectrum of dried particles (size: 1.0 mm) is recorded, in a KBr pellet, in the range of 500 – 4000 $cm^{-1}$, as shown in Fig. 5.50. Various peaks were observed during the FTIR of AM seeds, however, only sharp peaks were considered. Peaks at a wavelength range from 3700-3600 $cm^{-1}$ may be attributed to the stretching of O-H bonds which are present in carbohydrates, fatty acids and proteins (Stuart, 2005; Ibrahim et al., 2006). The peaks identified at 2925.09 $cm^{-1}$ and 2857.01 $cm^{-1}$ confirm the presence of C-H bond of the $CH_2$ present in fatty acids (Stuart, 2005). One of the peaks at 3351.12 $cm^{-1}$ confirms the presence of N-H bond of amide group, which proves the presence of protein content in the oil. Some peaks at 1742.90 $cm^{-1}$ and 1652.95 $cm^{-1}$ confirm the presence of carbonyl bonds (C=O; C-O) in AM seeds which are strongest bands in the spectrum of an ester (Kwaambwa and Maikokera, 2008). Several peaks were attributed at 1455.54 $cm^{-1}$, 1239.56 $cm^{-1}$, 1165.55 $cm^{-1}$ and 722.43 $cm^{-1}$ which confirms the presence of nitrogen-containing compounds like alkaloids (e.g. sanguinarine) (Baranska and Schulz, 2009). The presence of fatty acid components in the extract from SFE can be identified and quantified through MS and GC respectively. In the present study, fatty acids were quantified through GC.

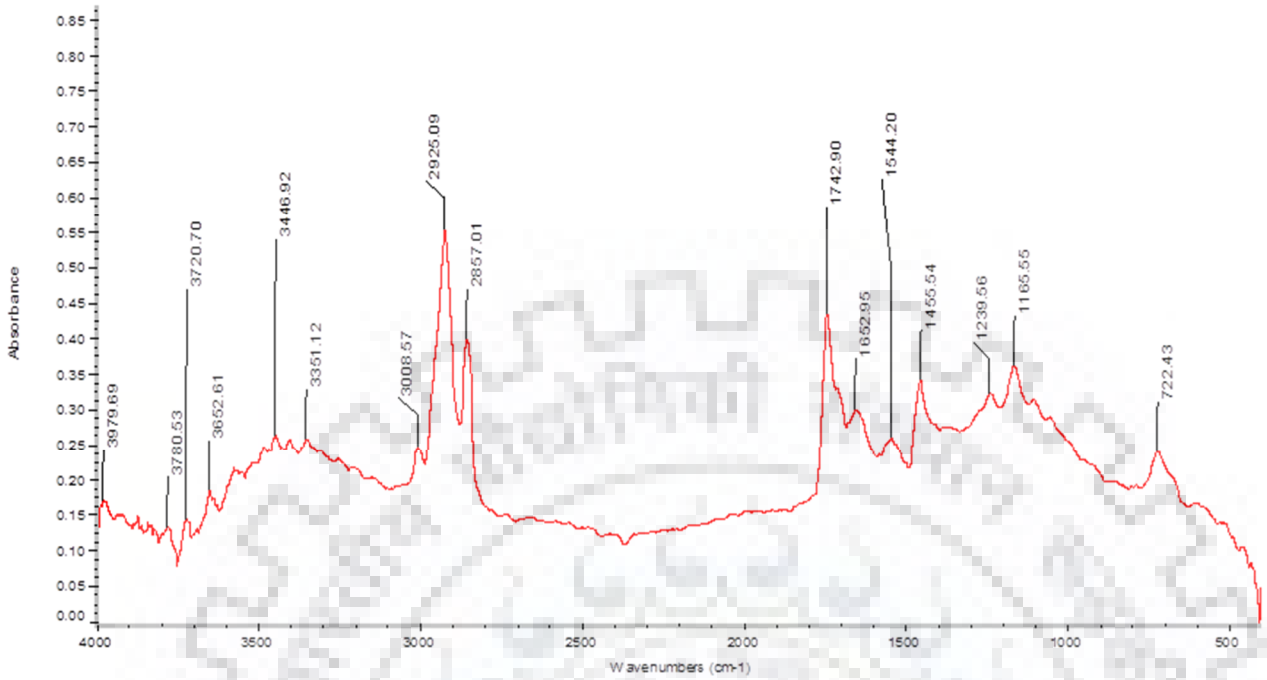


Fig.5.50: FTIR spectrum of AM seed particles.

5.8.1.3 Physico-chemical properties of extracted AM seed oil

Various fuel properties (e.g. heating value, flashpoint, fire point, cloud point and pour point) and chemical properties (e.g. saponification value, peroxide value and acid value) were determined for the extracted AM seed oil, following the methods as described in section 3.14 of Chapter 3. The determined physico-chemical properties of AM seed oil are given in Table 5.27.

According to method suggested by Williams, 1966 and Jacob, 1958, the acid value (62.7 mg KOH/g) for the present AM seed oil was determined as the percentage of free fatty acid present in oil estimated by titrating it against potassium hydroxide in presence of phenolphthalein indicator. The peroxide value (148 meq/kg sample) for the oil was determined by titrating against sodium thio-sulphate in presence of potassium iodide with starch as an indicator. The calculated acid and peroxide values suggest that AM seed oil can be stored for a longer duration. This is a desirable property especially when it is proposed to be used for biodiesel production. According to Hilditch, 1949, the saponification value of the AM seed oil of present work is 198.5 mg KOH/g and this has been determined as the amount of alkali required to saponify a definite amount (1 g) of AM seed oil. The saponification value shows the bounded and unbounded free fatty acids present in the oil.

On the other hand, some fuel physical properties such as heating value (determined by bomb calorimeter), flash point (determined by 'Pensky marten' closed type), fire point (determined by 'Pensky marten'), cloud point and pour point (determined by NOVA apparatus) were also determined as shown in Table 5.27. These properties confirm its suitability for fuel purposes.

Heating value (or energy value or calorific value) of a substance is the amount of heat released during the combustion of a specified amount of it. Heating value of the extracted AM seed oil was determined using bomb calorimeter as described in section 3.14 of Chapter 3. The observed heating value (37.2 MJ/kg of the present sample) is near to the heating value reported by Singh and Singh; Singh et al., 2010. In addition to this, the higher flash point and fire point of the seed oil fuels suggests that the fuels (AM seed oil) were less flammable than diesel and therefore safer to store and handle. The flash and fire points of fuel is not directly related to engine performance. These parameters (as shown in Table 5.27) reflects fuel's safety, the higher the flash and fire points the less likelihood that the fuel will accidentally ignite. The cloud point (13 °C) and pour point (1 °C) of the extracted AM seed oil, as shown in Table 5.27, are higher, however, the bio-diesel produced from it has shown the lower cloud point (1 to 2 °C) and pour point (-1 to -19 °C) as reported by Singh and Singh, 2010.

Table 5.27. Physico-chemical properties of AM seed oil.

| Properties | Reported in literature (Singh and Singh, 2010; Singh et al., 2010) | In the present work |
|---|---|---|
| Heating value (MJ/kg) | 35.4 | 37.2 |
| Flash point (°C) | 235 | 236 |
| Fire point (°C) | 260 | 263 |
| Cloud point (°C) | 12 | 13 |
| Pour point (°C) | 1 | 1 |
| Saponification value (mg KOH/g) | 202.5 | 198.5 |
| Peroxide value (meq/kg sample) | 150 | 148 |
| Acid value (mg KOH/g) | 76.2 | 62.7 |

5.8.1.4 Fatty acids composition of AM seed oil using gas chromatography

The fatty acid analysis was done using GC-FID of Thermo scientific, Agilent Technology and results were shown in Appendix B. In addition to this, the fatty acid analysis of Soxhlet extracted (using n-hexane) oil (as shown in Fig. A.2) and oil samples all 46 runs were reported here for better comparison. Table 5.28 shows the identified fatty acids, which is the combination of saturated fatty acids (e.g. lauric acid (C12:0), pentadecanoic acid (C15:0), palmitic acid (C16:0), heptadecanoic

acid (C17:0), stearic acid (C18:0), arachidic acid (C20:0), heneicosanoic acid (C21:0), behenic acid (C22:0) and tricosanic acid (C23:0)) and unsaturated fatty acids (e.g. cis-10-pentadecenoic acid (C15:1), palmitoleic acid (C16:1), cis-10-Heptadecenoic C17:1, oleic acid (C18:1n9c), linolelaidic acid (C18:2n6t), linoleic acid (C18:2n6c), linolenic acid (C18:3n3), cis-11-eicosenoic acid (C20:1), cis-13,16-docasadience acid (C22:2n6), cis-5,8,11,14,17-eicosapentaenoic acid (C20:5n3) and cis-4,7,10,13,16,19-docosahexaenic acid (C22:6n3)). The results show that, four leading fatty acids (e.g. C16:0 (11.40 – 23.58%), C18:0 (2.98 – 5.97%), C18:1n9c (25.01 – 41.46%) and C18:2n6c (22.54 – 59.07%) were present in the recovered oil from AM seeds with larger concentration. However, it also contains lower concentrations of C16:1 (0.0 – 2.48%), C17:0 (0.0 – 1.33%), C17:1 (0.0 – 1.33%), C22:0 (0.0 – 1.9%) and C20:5n3 (0.0 – 1.81%) while the other components (e.g. C12:0, C15:0, C15:1, C18:2n6t, C20:0, C18:3n3, C20:1, C21:0, C22:2n6, and C22:6n3 are found in traces. On the other hand, the fatty acids (only four leading components e.g. C16:0, C18:0, C18:1n9c and C18:2n6c) were found in Soxhlet extracted oil samples with C12:0, C20:0, C20:1, C23:0, C20:5n3 and C22:6n3 as traces. The variation in the concentration of all the fatty acids found in all 46 runs are due to the effects of all five independent parameters (e.g. temperature, pressure, particle size, flow rate-$CO_2$ and % of co-solvent) and their interactive nature.

These four leading fatty acids (e.g. C16:0, C18:0, C18:1n9c, and C18:2n6c) have been used for medicinal purposes. For example, some reserachers (e.g. Jaglan et al., 2019; Jandacek, 2017; de Lorgeril et al., 2001) have reported that linoleic acid (C18:2n6c) can be used -to treat the coronary heart disease, -to reduce the blood cholesterol, to be used as an antioxidant, -to control the diabetes, cancer, atherosclerosis, obesity, allergy etc. Oleic acid (C18:1n9c) can be used as an antifungal, antioxidant and to cure paracoccidioidomycosis (Pinto et al., 2017). In addition to this, saturated fatty acids (e.g. palmitic acid (C16:0) and stearic acid (C18:0)) have also been found suitable to be used as -an insecticide, -an antimicrobial by de Melo et al., 2018 and Davoodbasha et al., 2018. In addition to this, the higher concentration range of unsaturated fatty acids (USFAs = 66.53 - 85.1%) in the extracted AM seed oil is responsible for the lower viscosity of trans-esterified oil which is one of the most desirable qualities for biofuel production. In the present case, SUPELCO 37 component FAME mixture (Std. solution for 37 fatty acids) was used to calibrate the GC. A chromatogram with Std FAME mix of 37 FA components is shown in Fig. A.1.

Table 5.28. A comparison between fatty acid compositions (% w/w) of AM seed oil extracted by SFE with co-solvent (runs without '*'superscript notation), SFE without co-solvent (runs with '*' superscript notation) and Soxhlet extraction (named as 'n-hexane extracted').

| | Fatty acid composition (%) | | | | | | | | | | | | | | | | | | | | |
|---|---|---|---|---|---|---|---|---|---|---|---|---|---|---|---|---|---|---|---|---|---|
| | C12:0 | C15:0 | C15:1 | C16:0 | C16:1 | C17:0 | C17:1 | C18:0 | C18:1n9c | C18:2n6t | C18:2n6c | C20:0 | C18:3n3 | C20:1 | C21:0 | C22:0 | C23:0 | C22:2n6 | C20:5n3 | C22:6n3 | USFA | SFA |
| RT (min) | 12.75 | 16.58 | 17.42 | 17.83 | 20.08 | 21.58 | 22.42 | 22.75 | 24.08 | 25 | 25.33 | 26.33 | 28.58 | 29 | 29.58 | 32.08 | 37.08 | 37.75 | 39.92 | 44.33 | | |
| Run | | | | | | | | | | | | | | | | | | | | | | |
| 1 | 0.0 | 0.0 | 0.0 | 23.58 | 0.04 | 1.75 | 1.12 | 5.92 | 35.69 | 0.79 | 27.26 | 0.46 | 0.27 | 0.06 | 0.19 | 1.46 | 0.12 | 0.45 | 0.09 | 0.25 | 66.53 | 33.47 |
| 2 | 0.11 | 0.02 | 0.20 | 11.40 | 0.01 | 0.06 | 0.0 | 3.09 | 25.29 | 0.08 | 59.07 | 0.0 | 0.11 | 0.19 | 0.10 | 0.04 | 0.08 | 0.10 | 0.03 | 0.02 | 85.10 | 14.90 |
| 3 | 0.13 | 0.25 | 0.08 | 17.88 | 1.40 | 0.13 | 1.33 | 4.62 | 31.15 | 0.25 | 39.53 | 0.12 | 0.22 | 0.09 | 0.13 | 0.97 | 0.21 | 0.19 | 1.09 | 0.23 | 75.56 | 24.44 |
| 4* | 0.12 | 0.0 | 0.0 | 13.48 | 0.41 | 0.07 | 0.02 | 3.04 | 27.01 | 0.15 | 53.15 | 0.42 | 0.12 | 0.12 | 0.10 | 0.07 | 0.38 | 0.42 | 0.84 | 0.07 | 82.33 | 17.67 |
| 5 | 0.08 | 0.0 | 0.0 | 11.95 | 0.0 | 0.0 | 0.0 | 2.98 | 25.67 | 0.0 | 58.25 | 0.26 | 0.0 | 0.10 | 0.0 | 0.0 | 0.05 | 0.18 | 0.45 | 0.003 | 84.66 | 15.34 |
| 6 | 0.11 | 0.02 | 0.04 | 15.83 | 1.05 | 0.08 | 0.28 | 4.57 | 27.10 | 0.20 | 48.52 | 0.10 | 0.16 | 0.04 | 0.08 | 0.62 | 0.06 | 0.14 | 0.81 | 0.18 | 78.53 | 21.47 |
| 7 | 0.11 | 0.11 | 0.05 | 14.83 | 1.51 | 0.07 | 0.18 | 4.57 | 31.53 | 0.20 | 43.52 | 0.20 | 0.16 | 0.08 | 0.04 | 0.62 | 0.06 | 0.24 | 1.81 | 0.11 | 79.39 | 20.61 |
| 8 | 0.08 | 0.15 | 0.03 | 11.13 | 1.41 | 0.09 | 0.08 | 4.02 | 30.51 | 0.19 | 50.25 | 0.20 | 0.11 | 0.08 | 0.05 | 0.52 | 0.01 | 0.14 | 0.81 | 0.14 | 83.74 | 16.26 |
| 9 | 0.0 | 0.0 | 0.0 | 23.58 | 0.04 | 1.75 | 1.12 | 5.92 | 35.69 | 0.79 | 27.76 | 0.46 | 0.27 | 0.06 | 0.19 | 1.46 | 0.12 | 0.45 | 0.09 | 0.25 | 66.53 | 33.47 |
| 10 | 0.15 | 0.18 | 0.0 | 18.42 | 1.31 | 1.20 | 0.0 | 4.87 | 36.85 | 0.0 | 35.20 | 0.0 | 0.29 | 0.0 | 0.13 | 0.90 | 0.0 | 0.15 | 0.0 | 0.35 | 74.15 | 25.85 |
| 11 | 0.00 | 0.17 | 0.0 | 20.31 | 1.03 | 1.70 | 0.0 | 5.30 | 34.80 | 0.0 | 33.83 | 0.21 | 0.21 | 0.0 | 0.13 | 1.51 | 0.21 | 0.26 | 0.21 | 0.13 | 70.48 | 29.52 |
| 12 | 0.11 | 0.02 | 0.20 | 11.40 | 0.01 | 0.06 | 0.0 | 3.09 | 25.29 | 0.08 | 59.07 | 0.0 | 0.11 | 0.19 | 0.10 | 0.04 | 0.08 | 0.10 | 0.03 | 0.02 | 85.10 | 14.90 |
| 13 | 0.13 | 0.23 | 0.07 | 15.65 | 0.76 | 0.21 | 1.06 | 3.52 | 30.03 | 0.12 | 44.51 | 0.20 | 0.19 | 0.16 | 0.10 | 0.97 | 0.07 | 0.18 | 1.55 | 0.29 | 78.92 | 21.07 |
| 14 | 0.11 | 0.0 | 0.0 | 13.37 | 0.40 | 0.06 | 0.02 | 3.03 | 26.01 | 0.15 | 54.40 | 0.32 | 0.12 | 0.12 | 0.10 | 0.07 | 0.38 | 0.42 | 0.84 | 0.07 | 82.57 | 17.43 |
| 15 | 0.09 | 0.0 | 0.0 | 12.05 | 0.33 | 0.0 | 0.0 | 3.25 | 26.52 | 0.0 | 57.04 | 0.14 | 0.10 | 0.03 | 0.15 | 0.0 | 0.0 | 0.0 | 0.0 | 0.29 | 84.31 | 15.69 |
| 16 | 0.0 | 0.0 | 0.0 | 11.99 | 0.0 | 0.0 | 0.11 | 3.27 | 26.33 | 0.0 | 57.17 | 0.25 | 0.69 | 0.05 | 0.15 | 0.0 | 0.0 | 0.0 | 0.0 | 0.0 | 84.34 | 15.66 |
| 17 | 0.11 | 0.0 | 0.0 | 13.37 | 0.40 | 0.06 | 0.02 | 3.03 | 26.01 | 0.15 | 54.40 | 0.32 | 0.12 | 0.12 | 0.10 | 0.07 | 0.38 | 0.42 | 0.84 | 0.07 | 82.57 | 17.43 |
| 18* | 0.12 | 0.0 | 0.0 | 13.48 | 0.41 | 0.07 | 0.02 | 3.04 | 27.01 | 0.15 | 53.15 | 0.42 | 0.12 | 0.12 | 0.10 | 0.07 | 0.38 | 0.42 | 0.84 | 0.07 | 82.33 | 17.67 |
| 19* | 0.0 | 0.0 | 0.0 | 22.52 | 1.01 | 1.44 | 0.0 | 5.45 | 37.69 | 0.38 | 31.05 | 0.0 | 0.25 | 0.0 | 0.15 | 0.0 | 0.0 | 0.05 | 0.0 | 0.0 | 70.44 | 29.56 |
| 20 | 0.09 | 0.0 | 0.0 | 14.58 | 0.21 | 0.01 | 0.03 | 2.04 | 25.01 | 0.15 | 55.48 | 0.41 | 0.15 | 0.14 | 0.12 | 0.07 | 0.40 | 0.38 | 0.74 | 0.08 | 82.39 | 17.61 |
| 21 | 0.11 | 0.02 | 0.20 | 11.40 | 0.01 | 0.06 | 0.0 | 3.09 | 25.29 | 0.08 | 59.07 | 0.0 | 0.11 | 0.19 | 0.10 | 0.04 | 0.08 | 0.10 | 0.03 | 0.02 | 85.10 | 14.90 |
| 22 | 0.12 | 0.0 | 0.63 | 15.42 | 0.0 | 0.46 | 0.0 | 3.74 | 31.82 | 0.50 | 45.89 | 0.0 | 0.14 | 0.0 | 0.13 | 0.35 | 0.0 | 0.28 | 0.29 | 0.22 | 79.79 | 20.21 |
| 23* | 0.10 | 0.0 | 0.0 | 11.93 | 0.18 | 0.01 | 0.0 | 2.96 | 25.51 | 0.0 | 58.29 | 0.08 | 0.0 | 0.15 | 0.07 | 0.0 | 0.12 | 0.18 | 0.43 | 0.0 | 84.73 | 15.27 |
| 24 | 0.15 | 0.0 | 0.12 | 22.55 | 2..51 | 0.0 | 0.0 | 5.97 | 37.60 | 0.32 | 28.50 | 0.0 | 0.18 | 0.0 | 0.10 | 1.90 | 0.0 | 0.11 | 0.0 | 0.0 | 69.33 | 30.67 |
| 25 | 0.14 | 0.0 | 0.0 | 14.48 | 0.31 | 0.07 | 0.05 | 3.50 | 25.01 | 0.15 | 53.72 | 0.53 | 0.16 | 0.10 | 0.08 | 0.07 | 0.28 | 0.52 | 0.74 | 0.08 | 80.86 | 19.15 |

Cont…

| | Fatty acid composition (%) | | | | | | | | | | | | | | | | | | | | |
|---|---|---|---|---|---|---|---|---|---|---|---|---|---|---|---|---|---|---|---|---|---|
| | C12:0 | C15:0 | C15:1 | C16:0 | C16:1 | C17:0 | C17:1 | C18:0 | C18:1n9c | C18:2n6t | C18:2n6c | C20:0 | C18:3n3 | C20:1 | C21:0 | C22:0 | C23:0 | C22:2n6 | C20:5n3 | C22:6n3 | USFA | SFA |
| RT (min) | 12.75 | 16.58 | 17.42 | 17.83 | 20.08 | 21.58 | 22.42 | 22.75 | 24.08 | 25 | 25.33 | 26.33 | 28.58 | 29 | 29.58 | 32.08 | 37.08 | 37.75 | 39.92 | 44.33 | | |
| Run | | | | | | | | | | | | | | | | | | | | | | |
| 26 | 0.16 | 0.0 | 0.0 | 13.78 | 0.49 | 0.08 | 0.02 | 3.49 | 27.41 | 0.25 | 51.72 | 0.43 | 0.11 | 0.18 | 0.10 | 0.07 | 0.48 | 0.42 | 0.74 | 0.06 | 81.42 | 18.58 |
| 27 | 0.10 | 0.0 | 0.0 | 12.48 | 0.51 | 0.08 | 0.02 | 4.04 | 28.01 | 0.11 | 52.65 | 0.52 | 0.11 | 0.10 | 0.09 | 0.06 | 0.28 | 0.22 | 0.54 | 0.08 | 82.36 | 17.64 |
| 28 | 0.11 | 0.02 | 0.20 | 11.40 | 0.01 | 0.06 | 0.0 | 3.09 | 25.29 | 0.08 | 59.07 | 0.0 | 0.11 | 0.19 | 0.10 | 0.04 | 0.08 | 0.10 | 0.03 | 0.02 | 85.10 | 14.90 |
| 29 | 0.08 | 0.0 | 0.0 | 11.48 | 0.41 | 0.07 | 0.02 | 3.04 | 28.01 | 0.15 | 53.65 | 0.62 | 0.18 | 0.15 | 0.11 | 0.11 | 0.48 | 0.62 | 0.64 | 0.17 | 84.02 | 15.98 |
| 30* | 0.09 | 0.0 | 0.40 | 12.44 | 0.02 | 0.03 | 0.0 | 3.08 | 26.90 | 0.0 | 56.24 | 0.0 | 0.02 | 0.14 | 0.08 | 0.09 | 0.10 | 0.14 | 0.15 | 0.08 | 84.08 | 15.92 |
| 31 | 0.09 | 0.0 | 0.0 | 12.19 | 0.40 | 0.20 | 0.0 | 3.22 | 27.38 | 0.08 | 55.62 | 0.0 | 0.06 | 0.01 | 0.10 | 0.0 | 0.0 | 0.15 | 0.14 | 0.36 | 84.19 | 15.81 |
| 32* | 0.0 | 0.0 | 0.71 | 20.18 | 1.59 | 0.0 | 0.0 | 5.03 | 37.11 | 0.18 | 33.64 | 0.0 | 0.17 | 0.0 | 0.13 | 0.94 | 0.0 | 0.13 | 0.0 | 0.18 | 73.72 | 26.28 |
| 33 | 0.11 | 0.02 | 0.20 | 11.40 | 0.01 | 0.06 | 0.0 | 3.09 | 25.29 | 0.08 | 59.07 | 0.0 | 0.11 | 0.19 | 0.10 | 0.04 | 0.08 | 0.10 | 0.03 | 0.02 | 85.10 | 14.90 |
| 34 | 0.07 | 0.0 | 0.31 | 11.95 | 0.04 | 0.19 | 0.0 | 3.13 | 27.32 | 0.0 | 56.05 | 0.0 | 0.05 | 0.0 | 0.12 | 0.0 | 0.0 | 0.43 | 0.05 | 0.28 | 84.54 | 15.46 |
| 35 | 0.05 | 0.0 | 0.31 | 13.18 | 0.0 | 0.0 | 0.0 | 3.15 | 26.38 | 0.0 | 56.07 | 0.0 | 0.10 | 0.15 | 0.09 | 0.0 | 0.0 | 0.06 | 0.10 | 0.36 | 83.53 | 16.47 |
| 36 | 0.11 | 0.02 | 0.20 | 11.40 | 0.01 | 0.06 | 0.0 | 3.09 | 25.29 | 0.08 | 59.07 | 0.0 | 0.11 | 0.19 | 0.10 | 0.04 | 0.08 | 0.10 | 0.03 | 0.02 | 85.10 | 14.90 |
| 37 | 0.10 | 0.0 | 0.0 | 14.51 | 0.60 | 0.51 | 0.0 | 3.74 | 30.69 | 0.05 | 47.64 | 0.0 | 0.04 | 0.07 | 0.12 | 0.30 | 0.0 | 0.31 | 0.34 | 0.99 | 80.72 | 19.28 |
| 38 | 0.0 | 0.0 | 0.83 | 18.77 | 0.0 | 1.81 | 0.0 | 4.97 | 33.70 | 0.0 | 38.79 | 0.34 | 0.0 | 0.0 | 0.0 | 0.55 | 0.0 | 0.09 | 0.15 | 0.0 | 73.56 | 26.44 |
| 39 | 0.23 | 0.0 | 0.0 | 23.60 | 1.59 | 0.48 | 0.0 | 6.14 | 41.46 | 0.0 | 22.54 | 0.0 | 0.0 | 0.0 | 0.0 | 1.74 | 0.0 | 0.0 | 0.80 | 1.41 | 67.81 | 32.19 |
| 40* | 0.0 | 0.18 | 0.18 | 11.75 | 0.09 | 0.0 | 0.0 | 3.11 | 25.81 | 0.0 | 57.74 | 0.14 | 0.0 | 0.11 | 0.15 | 0.0 | 0.11 | 0.16 | 0.39 | 0.08 | 84.56 | 15.44 |
| 41 | 0.08 | 0.0 | 0.0 | 11.48 | 0.41 | 0.07 | 0.02 | 4.04 | 29.01 | 0.15 | 51.65 | 0.62 | 0.18 | 0.15 | 0.11 | 0.11 | 0.48 | 0.62 | 0.64 | 0.17 | 83.02 | 16.98 |
| 42* | 0.0 | 0.0 | 0.50 | 14.65 | 0.08 | 0.14 | 0.0 | 3.49 | 28.80 | 0.0 | 51.28 | 0.0 | 0.08 | 0.06 | 0.08 | 0.16 | 0.0 | 0.09 | 0.0 | 0.59 | 81.48 | 18.52 |
| 43 | 0.10 | 0.0 | 0.55 | 13.50 | 0.0 | 0.11 | 0.0 | 3.42 | 28.90 | 0.0 | 52.38 | 0.11 | 0.07 | 0.11 | 0.11 | 0.12 | 0.0 | 0.12 | 0.0 | 0.41 | 82.53 | 17.47 |
| 44 | 0.13 | 0.25 | 0.08 | 17.88 | 1.40 | 0.13 | 1.33 | 4.62 | 31.15 | 0.25 | 39.53 | 0.12 | 0.22 | 0.09 | 0.13 | 0.97 | 0.21 | 0.19 | 1.09 | 0.23 | 75.5 | 24.44 |
| 45 | 0.10 | 0.03 | 0.0 | 12.55 | 0.03 | 0.26 | 0.0 | 3.36 | 27.26 | 0.0 | 55.56 | 0.0 | 0.10 | 0.09 | 0.10 | 0.0 | 0.0 | 0.10 | 0.0 | 0.47 | 83.61 | 16.39 |
| 46 | 0.0 | 0.0 | 0.0 | 20.77 | 0.85 | 1.53 | 0.0 | 4.84 | 36.33 | 0.06 | 34.20 | 0.0 | 0.06 | 0.0 | 0.13 | 1.01 | 0.22 | 0.0 | 0.0 | 0.0 | 71.50 | 28.50 |
| n-hexane extracted | 0.08 | 0.0 | 0.0 | 11.97 | 0.0 | 0.0 | 0.0 | 2.99 | 25.70 | 0.0 | 58.31 | 0.26 | 0.0 | 0.10 | 0.0 | 0.0 | 0.05 | 0.18 | 0.46 | 0.003 | 84.65 | 15.35 |
| Range | 0.0 - 0.15 | 0.0 - 0.25 | 0.0 - 0.83 | 11.40 - 23.58 | 0.0 – 2.48 | 0.0 – 1.81 | 0.0 – 1.33 | 2.96 – 5.92 | 25.29 – 41.46 | 0.0 – 0.79 | 22.54 – 59.07 | 0.0 – 0.46 | 0.0 – 0.69 | 0.0 – 0.19 | 0.0 – 0.19 | 0.0 - 1.88 | 0.0 – 0.38 | 0.0 – 0.45 | 0.0 – 1.09 | 0.0 – 1.41 | 66.53 - 85.10 | 14.90 – 33.47 |

RT : Retention time
USFA : Unsaturated fatty acids
SFA : Saturated fatty acids

5.8.2 Characterization of PP seed and seed oil

A PP seed having 10-20 mm long and light brown in color is obtained from a fruit of the Pongamia pinnata (L.) tree which is ovoid in shape with dimensions 3–6 cm long and 2–3 cm wide thick walled (Sangwan et al., 2010). A red-brown, bitter, thick, non-edible, non-drying oil (27-39% of seed) has been reported from the PP seeds in literature, which is also called Pongamia oil or Karanja oil, used -in tanning leather, -in soap, -as a liniment to treat scabies, herpes, and rheumatism and -as an illuminating oil (Bala et al., 2011; Rao et al., 2011). Seed oil has also been used for treating various inflammatory and infectious diseases such as leukoderma, leprosy, lumbago, and rheumatism (Bala et al., 2011; Prabha et al., 2009). Various percentage of fatty acids (e.g. palmitic acid (7.2-14.1 %), stearic acid (3.3-10.9%), oleic acid (44-71.3%), linoleic acid (10.8-27.1%), eicosenoic acid (0.78% -1.5%), arachidic acid (0.8 – 4.7) and behenic acid (2.5% -5.3%) have been reported in literature. These fatty acids play an important role in the regulation of a variety of physiological and biological functions in living organisms and for the development of new source for bio-fuel (Kumar et al., 2011; Dwivedi and Sharma, 2014).

Some researchers (e.g. Vismaya et al., 2010; Prabhu et al., 2002; Pradhan et al., 2008) have also reported non-fatty components of the oil which includes karanjin, furanoflavonoid, furanoflavones, furanoflavonols, chromenoflavones, flavones and furanodiketones which make the oil non-edible and hence further encourages its application for bio-fuel production. PP seed oil is eco-friendly, biodegradable and it has been identified as one of the best alternatives to petrochemicals.

All parts of the plant have also been used as a crude drug for the treatment of tumours, piles, skin diseases, itches, abscess, painful rheumatic joints wounds, ulcers, diarrhea etc. (Dwivedi and Sharma, 2014). Traditionally, its root and bark is used in piles (Arote et al., 2009), leaves are used for anthemintic, digestive and laxative for inflammations piles and wounds and its juice has been used for cold, coughs, diarrhea (Bobade and Khyade, 2012). The flowers are used for diabetes while its fruit and seed have been used for keratitis, piles, urinary discharge and diseases of the brain, eye, head and skin (Arote et al., 2009; Meher et al., 2004). TG and FTIR analysis were performed for the qualitative analysis of the PP seeds while the quantitative analysis of the extracted oil is done by gas chromatography.

5.8.2.1 Thermo-gravimetric (TG) analysis of PP seeds

The thermogram obtained from thermo-gravimetric (TG) analysis of PP seed samples is shown in Fig. 5.51, which provides an approximate estimation of moisture content, total organic components and ash content.

Thermo-gravimetric (TG) analysis of PP seed particle samples, was carried out with the help of EXSTAR TG/DTA 6300 instrument. The TG analysis was conducted to analyze the thermal degradation of the material. The TG curve (Fig. 5.51) is divided into three sections, which correspond to moisture removal (31 - 140 ℃), decomposition of organic substance (140 - 491 °C) and decomposition of carbonaceous matter (491 - 1200 °C). The TG analysis confirms the presence of moisture (5.9%), organic substance (73.6%), remaining carbonaceous substance (18.7%) and finally inorganic ash content (1.8%).

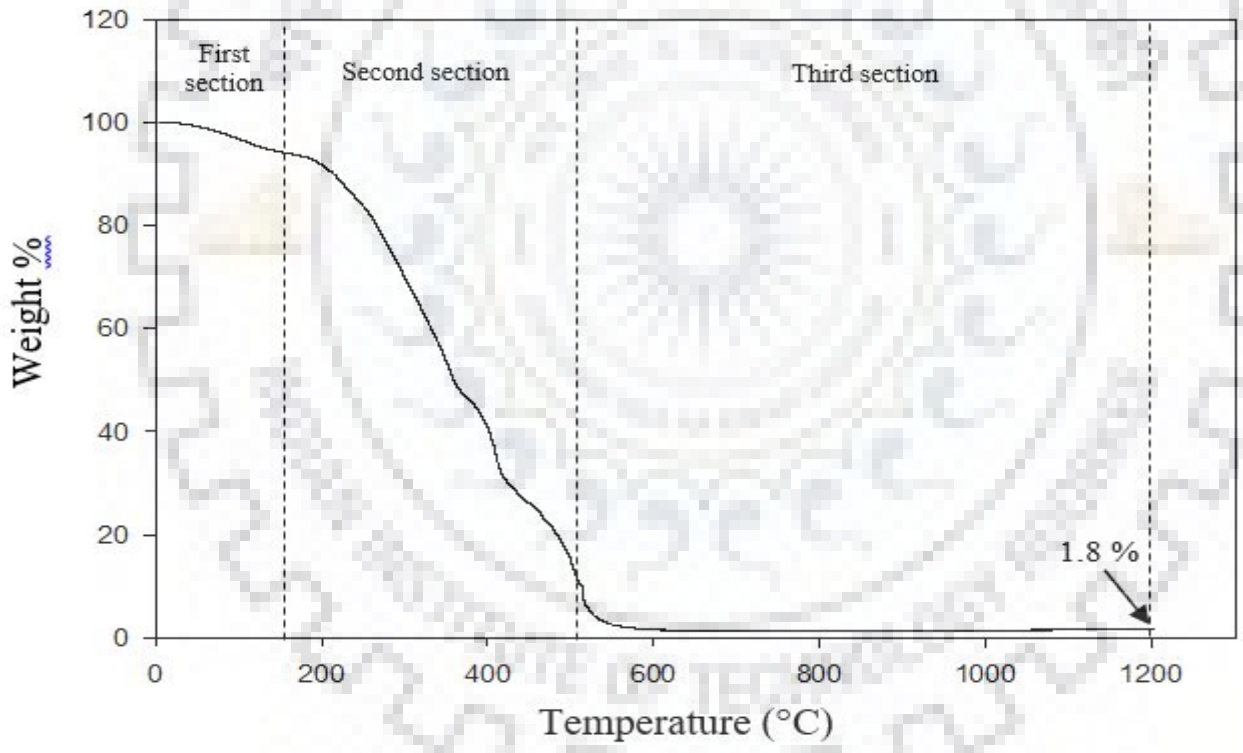


Fig. 5.51: TG thermogram of PP seed particles.

5.8.2.2 Fourier transform infrared spectroscopy (FTIR) analysis of PP seeds

Fourier transform infrared (FTIR) spectroscopy technique was used for the identification of the various functional groups (bonds) present in the PP seeds. The sample of PP seed particles was dried and powdered for the FTIR analysis. FTIR spectrum, which was recorded in the frequency range of 500 – 4000 $cm^{-1}$ using FTIR instrument (Thermo Scientific -6700), as shown in Fig 5.52. The band around 3600–3000 $cm^{-1}$ assigned to stretching vibrations of O–H and C–H is observed in PP seeds which indicates the presence of cellulose-related functional groups (Qiao et al., 2016). The bandwidth appeared at wave number (~ 3436 $cm^{-1}$) may be attributed to the stretching of O-H bonds which are present in carbohydrates, fatty acids and proteins while the bandwidth at wavenumbers (~ 2924 $cm^{-1}$ & ~ 2856 $cm^{-1}$) may be attributed to the presence of C-H bonds which is the functional group of 'Karanjin' (Pandey et al., 2014). The bandwidth at wavenumbers (1744 $cm^{-1}$ & 1646 $cm^{-1}$) corresponds to the presence of lipids or esters and amides respectively (Stuart, 2005). The peaks at 1456 $cm^{-1}$ and 1180 $cm^{-1}$correspond to the asymmetric stretching of $–CH_3$ and $O–CH_3$ respectively, which are present in the biodiesel spectrum (Rabelo et al., 2015). Several peaks were attributed at 1455.25 $cm^{-1}$, 1237.44 $cm^{-1}$, 1160.55 $cm^{-1}$ and 721.39 $cm^{-1}$ which confirm the presence of nitrogen-containing compounds like alkaloids (e.g. karanjin) (Baranska and Schulz, 2009).

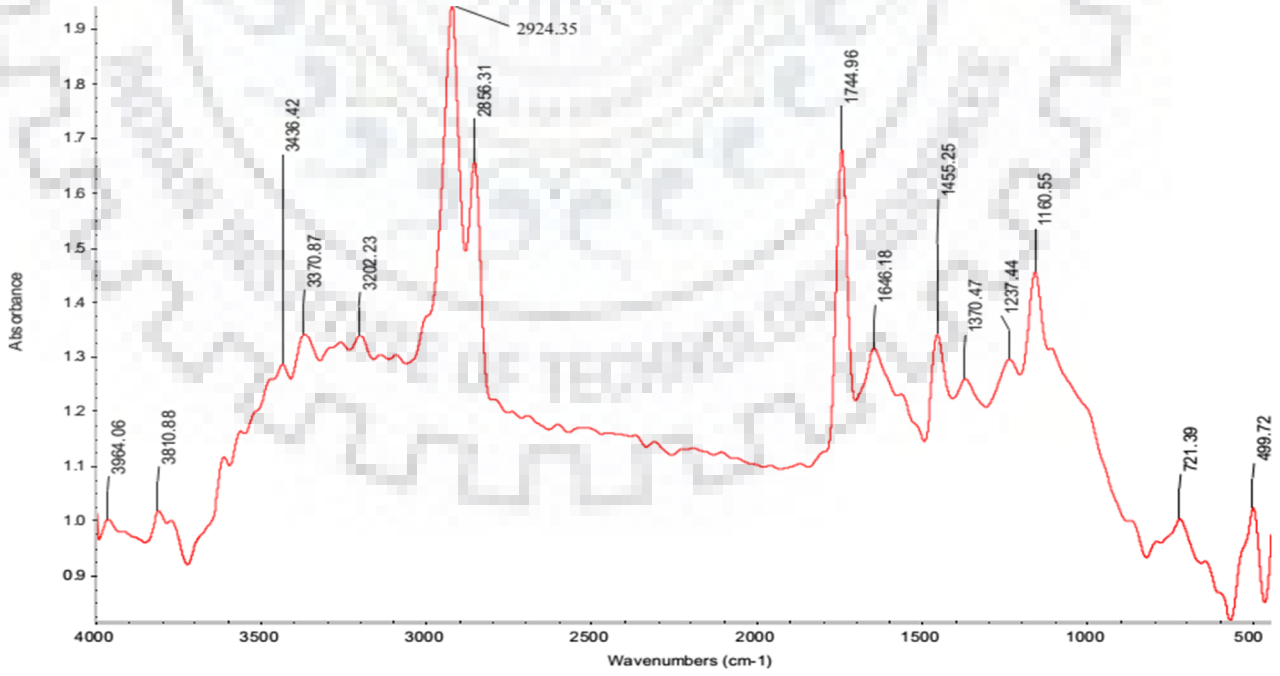


Fig. 5.52: FTIR spectrum of PP seed particles.

5.8.2.3 Physico-chemical properties of extracted PP seed oil

The essential fuel properties are compared and presented in Table 5.29. The measured properties of PP seed oil are found to be in a good agreement with the prescribed fuel properties reported in the literature. The acid value (5.40 mg KOH/g) of the PP seed oil was determined as the number of milligrams (mg) of potassium hydroxide required to neutralize the free fatty acid in 1 g of fatty oil in the presence of phenolphthalein indicator. The peroxide value (6.90 mew/kg sample) was determined by titrating against sodium thiosulphate in presence of potassium iodide with starch as an indicator. The calculated acid and peroxide values suggest that PP seed oil can be stored for a longer duration. This is a desirable property especially when it is proposed to be used for bio-diesel production. The saponification value (192 mg KOH/g) of PP seed oil was determined as the number of milligrams of potassium hydroxide required to neutralize the fatty acids resulting from the complete hydrolysis of 1 g of PP seed oil. This value shows the bounded and unbounded free fatty acids present in the oil.

Table 5.29. Physico-chemical properties of PP seed oil.

| Properties | Reported in literature (Sangwan et al., 2010; Kesari et al., 2010; Meher et al., 2004; Bobade and Khyade, 2012; Khayoon et al., 2012; Goembira and Saka, 2015; Das et al., 2009; De and Patel, 2009; Sarin et al., 2010; Obadiah et al., 2012) | Present study |
|---|---|---|
| Acid value (mg KOH/g) | 1.0 – 38.2 | 5.40 |
| Peroxide value (meq/kg sample) | 5.07 - 46.3 | 6.90 |
| Soponification value (mg KOH /g) | 184 - 198 | 192 |
| Calorific value (MJ/kg) | 30 – 35.4 | 32 |
| Flash point (°C) | 110 - 232 | 216 |
| Cloud point (°C) | 3.5 - 22 | 13 |
| Fire point (°C) | 230 | 231 |
| Pour point (°C) | 3 – 15.8 | 3 |

On the other hand, some fuel properties such as Heating value/Calorific value (determined by bomb calorimeter), Flash point (determined by 'Pensky marten' closed type), Fire point (determined by 'Pensky marten'), Cloud point and Pour point (determined by NOVA apparatus) were also determined following the methods as described in section 3.14 of Chapter 3.. These properties confirm its suitability for fuel purposes.

5.8.2.4 Fatty acids composition of PP seed oil using gas chromatography

The fatty acid analysis (chromatogram of all 46 runs) by gas chromatography (GC) of the PP seed oil extracted by SFE (without co-solvent), SFE (with co-solvent) is shown in Appendix C. In addition, chromatogram of sample obtained from soxhlet extraction using n-hexane is shown in Fig. A.3. Table 5.30 shows the fatty acids composition in each run (1-46). From the Table 5.30, it cloud be clearly understood that PP seed oil comprises unsaturated fatty acids ranging from '73.31 to 77.08%' and saturated fatty acids ranging from '22.92 to 26.69%'. The average values of unsaturated and saturated fatty acids present in PP seed oil are 76.24 and 23.76% respectively. From the Table 5.30, it also is clear that, oleic acid (C18:1n9c), arachidic acid (C20:0), cis-10-pentadecanoic acid (C15:1), stearic acid (C18:0), cis-8,11,14-Eicosatrienoic acid (C20:3n6), linolenic acid (C18:3n3), gamma(ϒ)-linolenic acid (C18:3n6) and cis-11-Eicosenoic acid (C20:1) are the main fatty acids present in PP seed oil ranging (45.42 - 58.62%), (15.34 – 18.02%), (8.64 - 11.95%), (5.74 - 7.04%), (2.62 - 4.45%), (1.24 - 4.01%), (0.34 - 1.53%) and (0.0 - 3.93%) respectively, which have also been confirmed by Arote et al., 2009; Pavithra et al., 2012 and Bala et al., 2011. Apart from these main compositions, PP seed oil also contains some fatty acids (listed in Table 5.30) in traces amount. Various studies have shown that oleic, cis-10-pentadecenoic, linolenic, and cis-11-Eicosenoic acid which are important constituents of PP seed oil have potential antibacterial and antifungal properties (Henry et al., 2002; Sun et al., 2004; Zheng et al., 2005). In addition to this, the higher percentage of unsaturated fatty acids (73.31 - 77.08%) in PP seed oil reveals that this oil can be used as raw material for the production of biodiesel.

5.8.3 A final comparison of outcomes from the characterization of PP and AM seed oils

A final comparison of characteristics of PP and AM seed oils has been reported in Table 5.31. From the Table 5.31, it is clear that the both oils (AM and PP seed oils) are found liable to be used for medicinal purposes as well as biofuel production.

Table 5.30. A comparison between fatty acid compositions (%w/w) of PP seed oil extracted by SFE with co-solvent (runs without '*' superscript notation), SFE without co-solvent (runs with '*' superscript notation) and Soxhlet extraction (named as 'n-hexane extracted').

| Run | Fatty acid composition (%) | | | | | | | | | | | | | | | | | |
|---|---|---|---|---|---|---|---|---|---|---|---|---|---|---|---|---|---|---|
| | C8:0 | C10:0 | C15:1 | C16:1 | C18:0 | C18:1n9c | C20:0 | C18:3n6 | C18:3n3 | C20:1 | C21:0 | C20:3n6 | C23:0 | C20:5n3 | C24:1n9 | C22:6n3 | SFA | USFA |
| RT | 8.25 | 9.17 | 17.42 | 20.08 | 22.75 | 24.08 | 26.33 | 27.92 | 28.58 | 29 | 29.83 | 33.67 | 37.08 | 39.92 | 42.42 | 44.33 | | |
| 1 | 0.00 | 0.18 | 10.96 | 0.00 | 6.57 | 55.16 | 16.29 | 1.20 | 1.27 | 3.40 | 0.98 | 3.55 | 0.00 | 0.45 | 0.00 | 0.00 | 24.02 | 75.98 |
| 2 | 0.00 | 0.00 | 11.43 | 0.00 | 6.60 | 55.11 | 16.86 | 1.10 | 3.94 | 0.95 | 0.00 | 3.08 | 0.00 | 0.63 | 0.31 | 0.00 | 23.47 | 76.53 |
| 3 | 0.00 | 0.00 | 10.31 | 0.02 | 6.77 | 53.25 | 16.28 | 1.22 | 3.72 | 2.90 | 1.13 | 3.46 | 0.00 | 0.86 | 0.08 | 0.00 | 24.17 | 75.83 |
| 4* | 0.00 | 0.15 | 10.73 | 0.07 | 6.54 | 54.91 | 16.50 | 0.34 | 1.45 | 3.50 | 1.10 | 3.55 | 0.22 | 0.93 | 0.00 | 0.00 | 24.51 | 75.49 |
| 5 | 0.00 | 0.05 | 10.11 | 0.00 | 6.64 | 53.08 | 16.04 | 1.37 | 3.60 | 3.87 | 1.09 | 3.32 | 0.00 | 0.83 | 0.00 | 0.00 | 23.82 | 76.18 |
| 6 | 0.00 | 0.04 | 11.07 | 0.07 | 6.74 | 54.90 | 16.27 | 1.69 | 3.50 | 1.06 | 0.00 | 3.58 | 0.00 | 0.95 | 0.13 | 0.00 | 23.04 | 76.96 |
| 7 | 0.00 | 0.08 | 10.35 | 0.04 | 6.92 | 54.89 | 16.35 | 1.40 | 3.56 | 1.15 | 0.00 | 3.93 | 0.08 | 1.15 | 0.082 | 0.022 | 23.43 | 76.57 |
| 8 | 0.00 | 1.04 | 11.13 | 0.00 | 6.71 | 55.59 | 15.82 | 1.34 | 1.63 | 3.68 | 1.07 | 3.47 | 0.07 | 0.07 | 0.00 | 0.00 | 24.71 | 75.29 |
| 9 | 0.00 | 0.00 | 10.77 | 0.00 | 6.78 | 55.54 | 16.07 | 1.25 | 3.65 | 1.11 | 0.00 | 3.81 | 0.06 | 0.82 | 0.13 | 0.00 | 22.92 | 77.08 |
| 10 | 0.00 | 0.00 | 11.07 | 0.00 | 6.72 | 54.80 | 16.52 | 1.27 | 3.64 | 1.12 | 0.00 | 3.49 | 0.00 | 0.97 | 0.39 | 0.00 | 23.24 | 76.76 |
| 11 | 0.00 | 0.03 | 10.59 | 0.04 | 6.82 | 54.77 | 16.51 | 0.38 | 1.53 | 3.51 | 1.12 | 3.65 | 0.00 | 0.96 | 0.09 | 0.00 | 24.47 | 75.53 |
| 12 | 0.00 | 0.00 | 11.43 | 0.00 | 6.60 | 55.11 | 16.86 | 1.10 | 3.94 | 0.95 | 0.00 | 3.08 | 0.00 | 0.63 | 0.31 | 0.00 | 23.47 | 76.53 |
| 13 | 0.00 | 0.00 | 11.69 | 0.00 | 6.40 | 55.70 | 16.56 | 1.44 | 3.61 | 0.84 | 0.00 | 2.88 | 0.00 | 0.69 | 0.20 | 0.00 | 22.95 | 77.05 |
| 14 | 0.14 | 0.00 | 11.95 | 0.08 | 6.73 | 55.86 | 15.87 | 0.25 | 1.49 | 3.24 | 1.01 | 2.69 | 0.06 | 0.64 | 0.00 | 0.00 | 23.81 | 76.19 |
| 15 | 0.00 | 0.05 | 10.52 | 0.00 | 6.91 | 55.21 | 16.69 | 1.43 | 3.74 | 1.14 | 0.00 | 3.45 | 0.00 | 0.86 | 0.00 | 0.00 | 23.65 | 76.35 |
| 16 | 0.00 | 0.00 | 10.72 | 0.00 | 6.76 | 54.83 | 16.70 | 1.41 | 3.75 | 1.11 | 0.00 | 3.74 | 0.00 | 0.96 | 0.03 | 0.00 | 23.45 | 76.55 |
| 17 | 0.00 | 0.00 | 10.17 | 0.02 | 6.86 | 55.09 | 16.66 | 1.46 | 3.60 | 1.18 | 0.00 | 3.81 | 0.08 | 1.01 | 0.00 | 0.07 | 23.60 | 76.40 |
| 18* | 0.22 | 0.59 | 10.34 | 0.00 | 6.24 | 52.60 | 15.34 | 1.38 | 3.30 | 3.61 | 1.02 | 3.72 | 0.68 | 0.83 | 0.12 | 0.00 | 24.10 | 75.90 |
| 19* | 0.00 | 0.07 | 11.27 | 0.00 | 6.34 | 55.86 | 16.36 | 1.09 | 3.85 | 0.99 | 0.00 | 3.04 | 0.38 | 0.75 | 0.00 | 0.00 | 23.16 | 76.84 |
| 20 | 0.00 | 0.00 | 11.48 | 0.00 | 6.87 | 55.07 | 16.66 | 1.25 | 3.73 | 1.08 | 0.00 | 3.03 | 0.00 | 0.83 | 0.00 | 0.00 | 23.53 | 76.47 |
| 21 | 0.00 | 0.00 | 11.43 | 0.00 | 6.60 | 55.11 | 16.86 | 1.10 | 3.94 | 0.95 | 0.00 | 3.08 | 0.00 | 0.63 | 0.31 | 0.00 | 23.47 | 76.53 |
| 22 | 0.00 | 0.00 | 10.17 | 0.02 | 6.86 | 55.09 | 16.66 | 1.46 | 3.60 | 1.18 | 0.00 | 3.81 | 0.08 | 1.01 | 0.00 | 0.07 | 23.59 | 76.41 |
| 23* | 0.00 | 0.00 | 11.64 | 0.00 | 6.74 | 54.79 | 16.50 | 0.91 | 1.24 | 3.64 | 1.08 | 2.88 | 0.00 | 0.58 | 0.00 | 0.00 | 24.32 | 75.68 |

Cont…

| | Fatty acid composition (%) | | | | | | | | | | | | | | | | | |
|---|---|---|---|---|---|---|---|---|---|---|---|---|---|---|---|---|---|---|
| | C8:0 | C10:0 | C15:1 | C16:1 | C18:0 | C18:1n9c | C20:0 | C18:3n6 | C18:3n3 | C20:1 | C21:0 | C20:3n6 | C23:0 | C20:5n3 | C24:1n9 | C22:6n3 | SFA | USFA |
| 24 | 0.00 | 0.06 | 11.23 | 0.00 | 6.78 | 58.62 | 18.02 | 0.36 | 1.54 | 3.93 | 1.23 | 3.92 | 0.00 | 1.02 | 0.00 | 0.06 | 26.09 | 73.91 |
| 25 | 0.00 | 0.00 | 10.62 | 0.07 | 6.56 | 55.06 | 16.18 | 0.54 | 1.43 | 3.80 | 1.11 | 3.63 | 0.00 | 1.00 | 0.00 | 0.00 | 23.85 | 76.15 |
| 26 | 0.00 | 0.00 | 10.52 | 0.00 | 6.67 | 52.91 | 16.16 | 1.31 | 3.66 | 3.38 | 1.08 | 3.37 | 0.00 | 0.86 | 0.08 | 0.00 | 23.91 | 76.09 |
| 27 | 0.00 | 0.05 | 10.69 | 0.07 | 6.73 | 54.95 | 16.50 | 1.40 | 3.53 | 1.12 | 0.00 | 3.82 | 0.03 | 1.01 | 0.10 | 0.00 | 23.31 | 76.69 |
| 28 | 0.00 | 0.00 | 11.43 | 0.00 | 6.60 | 55.11 | 16.86 | 1.10 | 3.94 | 0.95 | 0.00 | 3.08 | 0.00 | 0.63 | 0.31 | 0.00 | 23.47 | 76.53 |
| 29 | 0.00 | 0.00 | 10.54 | 0.00 | 6.79 | 55.47 | 16.65 | 1.36 | 3.63 | 1.02 | 0.00 | 3.57 | 0.00 | 0.80 | 0.16 | 0.00 | 23.45 | 76.55 |
| 30* | 0.00 | 0.00 | 11.36 | 0.00 | 6.31 | 55.50 | 16.93 | 1.30 | 3.87 | 0.84 | 0.00 | 3.20 | 0.00 | 0.70 | 0.00 | 0.00 | 23.23 | 76.77 |
| 31 | 0.00 | 0.00 | 11.58 | 0.00 | 6.69 | 56.01 | 16.36 | 1.21 | 3.48 | 1.04 | 0.00 | 2.96 | 0.10 | 0.52 | 0.05 | 0.00 | 23.15 | 76.85 |
| 32* | 0.00 | 0.00 | 11.45 | 0.00 | 6.17 | 56.05 | 17.07 | 0.91 | 4.01 | 0.94 | 0.00 | 2.67 | 0.11 | 0.61 | 0.00 | 0.00 | 23.35 | 76.65 |
| 33 | 0.00 | 0.00 | 11.43 | 0.00 | 6.60 | 55.11 | 16.86 | 1.10 | 3.94 | 0.95 | 0.00 | 3.08 | 0.00 | 0.63 | 0.31 | 0.00 | 23.47 | 76.53 |
| 34 | 0.00 | 0.00 | 10.75 | 0.07 | 6.78 | 54.70 | 16.59 | 1.37 | 3.71 | 1.14 | 0.00 | 3.77 | 0.00 | 1.01 | 0.12 | 0.00 | 23.37 | 76.63 |
| 35 | 0.00 | 0.00 | 11.56 | 0.00 | 7.03 | 55.31 | 15.81 | 1.48 | 3.42 | 1.15 | 0.00 | 3.23 | 0.19 | 0.82 | 0.00 | 0.00 | 23.03 | 76.97 |
| 36 | 0.00 | 0.00 | 11.43 | 0.00 | 6.60 | 55.11 | 16.86 | 1.10 | 3.94 | 0.95 | 0.00 | 3.08 | 0.00 | 0.63 | 0.31 | 0.00 | 23.47 | 76.53 |
| 37 | 0.00 | 0.00 | 9.86 | 0.08 | 6.86 | 54.44 | 16.39 | 1.53 | 3.63 | 1.21 | 0.00 | 4.45 | 0.07 | 1.38 | 0.03 | 0.07 | 23.32 | 76.68 |
| 38 | 0.00 | 0.09 | 10.26 | 0.04 | 6.84 | 54.80 | 16.58 | 1.47 | 3.70 | 1.09 | 0.00 | 3.84 | 0.15 | 1.00 | 0.08 | 0.06 | 23.66 | 76.34 |
| 39 | 0.00 | 0.00 | 11.36 | 0.00 | 6.31 | 55.50 | 16.93 | 1.30 | 3.87 | 0.84 | 0.00 | 3.20 | 0.00 | 0.70 | 0.00 | 0.00 | 23.24 | 76.76 |
| 40* | 0.00 | 0.00 | 11.24 | 0.00 | 6.84 | 55.47 | 16.21 | 1.38 | 3.66 | 1.07 | 0.00 | 3.31 | 0.00 | 0.83 | 0.00 | 0.00 | 23.04 | 76.96 |
| 41 | 0.00 | 0.00 | 10.93 | 0.00 | 6.84 | 54.62 | 16.98 | 1.31 | 3.98 | 1.11 | 0.00 | 3.42 | 0.00 | 0.80 | 0.00 | 0.00 | 23.82 | 76.18 |
| 42* | 0.11 | 0.30 | 10.64 | 0.01 | 6.67 | 55.00 | 16.12 | 1.48 | 3.38 | 1.08 | 0.00 | 3.78 | 0.39 | 0.93 | 0.09 | 0.00 | 23.60 | 76.40 |
| 43 | 0.00 | 0.00 | 10.30 | 0.05 | 7.04 | 53.91 | 16.48 | 0.36 | 1.48 | 3.68 | 1.19 | 4.20 | 0.05 | 1.11 | 0.07 | 0.06 | 24.76 | 75.24 |
| 44 | 0.00 | 0.00 | 11.26 | 0.00 | 6.74 | 54.83 | 16.80 | 1.21 | 3.77 | 0.98 | 0.00 | 3.34 | 0.00 | 0.92 | 0.16 | 0.00 | 23.53 | 76.47 |
| 45 | 0.00 | 0.00 | 11.03 | 0.00 | 6.73 | 54.98 | 16.93 | 1.31 | 3.99 | 1.09 | 0.00 | 3.09 | 0.00 | 0.77 | 0.07 | 0.00 | 23.66 | 76.34 |
| 46 | 0.00 | 0.00 | 10.67 | 0.07 | 6.60 | 55.36 | 16.27 | 1.15 | 1.44 | 3.82 | 1.11 | 3.65 | 0.00 | 1.01 | 0.00 | 0.00 | 23.98 | 76.02 |
| n-hexane extracted | 0.00 | 0.00 | 8.64 | 0.07 | 5.74 | 45.42 | 15.85 | 1.06 | 3.69 | 0.00 | 0.88 | 2.62 | 0.21 | 0.70 | 0.00 | 0.07 | 26.69 | 73.31 |
| Range (%) | 0.0 – 0.22 | 0.0 – 1.04 | 8.64 – 11.95 | 0 – 0.07 | 5.74 – 7.04 | 45.42 – 58.62 | 15.81 – 17.07 | 0.25 – 1.69 | 1.24 – 4.01 | 0 – 3.82 | 0 – 1.23 | 2.62 – 4.45 | 0 – 0.39 | 0.45 – 1.38 | 0 – 0.31 | 0 – 0.07 | 23.04 – 26.69 | 73.31 – 77.08 |

RT: Retention time
SFA: Saturated fatty acids
USFA: Unsaturated fatty acids

Table 5.31. A final comparison of PP and AM seed oil.

| Analysis of the structure | | | |
|---|---|---|---|
| **Parameters** | **AM seed/oil** | **PP seed/oil** | **Remark** |
| Surface appearance (before SFE) | Cloudy and smooth layer appearance | Cloudy and smooth layer appearance | Confirm the presence of oil |
| Surface appearance (after SFE) | Broken cells/cavities and empty black spots | Broken cells/cavities and empty black spots | Confirm the absence of oil |
| **Oil content and its uses** | | | |
| Oil content (%) | 22 – 43 % | 27 – 39 % | Due to different geographical location of seeds |
| Color, test and state | Pale-yellow, bitter and thick | Red-brown, bitter and thick | Natural characteristics |
| Chemical components (to make the oil for medicinal uses) | Fatty acids: C16:0, C18:0, C18:1n9c, C18:2n6c etc. Alkaloids: Sanguinarine, dihydro-sanguinarine, berberine, protopine) | Fatty acids: C20:0, C15:1, C20:3n6, C18:3n3, C18:3n6 etc. Alkaloids: karanjin, furano-(flavonoid, flavones, flavonols, diketones) | Best suitable for medicinal purposes |
| Medicinal uses (to cure various diseases such as) | Ulcers, Dysentery, Asthma, Intestinal infection, diabetes, cancer, allergy | Leukoderma, leprosy, lumbago, rheumatism, | Based on literature |
| **Fatty acids content** | | | |
| SFA (%) | 14.90 – 33.47 % | 22.95 – 26.69 % | |
| USFA (%) | 66.53 – 85.10 % | 73.31 – 77.08 % | Suitable for bio-diesel |
| Highest % of FA component found | C18:2n6c (22.54 – 59.07 %) | C18:1n9c (45.42 – 58.62 %) | Suitable for bio-diesel, oil paints and varnishes |
| **Thermo-gravimetric analysis** | | | |
| Moisture (%) | 10 % | 5.9 % | |
| Total organic (%) | 76 % | 73.6 % | |
| Ash (%) | 3.6 % | 1.8 % | |
| **Physico-chemical properties of seed oils** | | | |
| Heating value | 37.2 MJ/kg | 32 MJ/kg | Found within the range as reported in literature. |
| Flash point | 236 °C | 216 °C | |
| Fire point | 263 °C | 231 °C | |
| Cloud point | 13 °C | 13 °C | |
| Pour point | 1 °C | 3 °C | |
| Saponification value | 198.5 mg KOH/g | 192 mg KOH/g | |
| Peroxide value | 148 meq/kg sample | 6.90 meq/kg sample | |
| Acid value | 62.7 mg KOH/g | 5.40 mg KOH/g | |
| **Suitability for bio-diesel production** | | | |
| As raw material for further processing | Suitable | Suitable | Due to the favorable physico-chemical properties of raw seed oils. |
| **Suitability for direct consumption by human and animals** | | | |
| As raw seed oil | Non-edible | Non-edible | Due to the presence of alkaloids |
| As refined alkaloid free oil | Edible (Pramanik et al., 2012) | Edibility is under research | Based on the reported literature |

5.9 Economic analysis of SFE process to extract the seed oil from AM and PP seeds

The economic analysis of the SFE process for the AM and PP seed oils is presented in Table 5.32 and Table 5.33 respectively. This economic analysis (EA) consists the values of the fixed cost (FC), cost of the raw materials (CRM), operating cost (OC), annual cost of capital recovery (ACCR), total annual cost (TAC), manufacturing cost (MC), selling cost (SC) and payback period of the process for both seeds oils.

The annual feed rate (kg/year) of raw materials and the production rate (kg/year) of seed oils from the SFE process of AM and PP seeds were calculated on the basis of 800 kg batch size with 1000 liter capacity of extraction vessel. The optimum operating parameters, observed in present study from the RSM (as shown in sections 5.1.1 and 5.1.2) were used to calculate the required flow rate of SC-$CO_2$ and co-solvent (Ethanol). The Waters India Limited provided the equipment cost with installation for a plant with extractor capacity of 1000 liters and this cost is considered as fixed cost (FC). The preliminary computations are given below:

***Basis:*** 800 kg of raw seed particles of AM and PP seeds is used per batch.

Each batch/experimental run proceeds for 285 min, which includes 250 min for the SFE plus 35 min for the cleaning and batch charging. Therefore, only five batches per day are designed for the operation of any one seed. In fact, only one seed will be processed at one time.

Five batches in a day require = $5 \times 800 = 4000$ kg of seeds/day.

Assuming 300 days in a year of operation:

Therefore, the annual consumption of raw seed (e.g. AM and PP seeds) would be as given below:

$$4000 \times 300 = 1200000 \text{ kg/year.}$$

As the optimum extraction yields achieved for the AM and PP seeds are 0.4286 and 0.36 kg oil/kg seeds respectively. Therefore, the annual production rate of AM and PP seeds oil would be as follows:

For AM seed oil: $1200000 \times 0.4286 = 514320$ kg/year.

For PP seed oil: $1200000 \times 0.36 = 432000$ kg/year.

Further, computations (as shown in Appendix D) for the total $CO_2$ used and the total co-solvent (Ethanol) used are based on the optimum conditions of these two seeds during the SFE process. For example, the optimum values of $CO_2$ flow rate (kg/min) and the % of co-solvent (% of $CO_2$ flow rate) of AM seed oil are 0.011 kg/min and 9 % of $CO_2$ flow rate while the optimum values of flow rate-$CO_2$ (kg/min) and the % of co-solvent (% of flow rate-$CO_2$) of PP seed oil are 0.009 kg/min and 7 % of flow rate-$CO_2$. In addition to above, the computations such as the total labor used, total electricity consumed were also given in Appendix D.

The fixed cost (FC) Rs. 277210000 is same for both seeds (as the same plant will be used for processing the seeds) but a significant variation is found in CRM, OC, MC, TAC and SC of each seed oil, which results in a significant difference in gross profit as shown in Table 5.32 and Table 5.33. After applying the income tax (30 %) on the gross profit and then the depreciation (by assuming the salvage value to be Rs 0), the actual net profits from the SFE of AM and PP seed oils are Rs. 492067624 and Rs. 350798159 respectively. The respective payback periods are 1.63 year and 1.84 year, for the envisaged plant of SFE process, when AM and PP seeds are taken into consideration.

The cost of raw materials (CRM) (for the SFE of AM seeds) is computed as Rs. 299243274 per year, which includes costs of seeds, $CO_2$ and ethanol as provided in Table 5.32. The OC is the sum of CRM, cost of labor (CL), cost of electricity (CE), and $CO_2$ liquefaction cost (CLC) which is found to be Rs. 524698274 per year. The total annual cost (TAC) of the process, calculated using Eq. D.3 is Rs. 568985752 per year by considering 15% of interest rate for the period of 20 years on the loan amount. The manufacturing cost (MC) of the product is found to be Rs. 1106 per kg, obtained by dividing the TAC by the annual production rate of AM seed oil, which is 514320 kg/year. The selling cost (SC) of product (AM seed oil) is estimated to be Rs. 1285800000 per year considering the market price as Rs. 2500 per kg. This offered 'SC' is lower than the other suppliers of AM seed oil of therapeutic grade as shown in Table 5.34. On the basis, of outcomes discussed above, the payback period '1.63' year is found to be lower than the 2 years. Hence, SFE process of AM seed oil production can be considered as profitable method for extraction.

On the other hand, the CRM (for the SFE of PP seeds) has been obtained as Rs. 213176796 per year which is the result of adding costs of raw material (PP seeds), Solvent (e.g. $CO_2$) and co-solvent (e.g. Ethanol) as given in Table 5.33. The OC is found to be as Rs. 369511796 per year while

the TAC of the SFE process (for PP seed oil), calculated using Eq, D.3 is Rs. 413799273 per year. The manufacturing cost (MC) of the PP seed oil is found as Rs. 958 per kg, obtained in a similar way as described above. The SC of product (PP seed oil) is estimated to be Rs. 928800000 per year considering the market price as Rs. 2150 per kg. This offered 'SC' of the PP seed oil is lower than the SC offered by other suppliers for the therapeutic grade, as shown in Table 5.34. Therefore, a similar, conclusion can also be made from the economic analysis of the SFE of PP seed oil. From the Table 5.32 and 5.33, the SFE process has been found economic feasible based on OC, MC, SC, and the PP for both seeds (AM and PP seeds). Finally, a comparison of prices offered by different suppliers of AM and PP seed oils extracted using different methods is given in Table 5.34 which reveals that the present envisaged SFE plant produces PP seed oil at comparatively lower price. On the other hand, none of the suppliers is available for AM seed oil.

Table 5.32. Economic analysis (FC, CRM, OC, MC and SC) of the SFE process for AM seed oil.

| Particulars | Unit | Cost per unit | Amount consumed (kg/year) | Annual cost (Rs/year) |
|---|---|---|---|---|
| SFE equipment cost with installation | Rs | | | 277210000 |
| **Fixed Cost (FC)** | **Rs** | | | **277210000** |
| Feedstock (AM seeds) flow rate | kg/year | | 1200000 | 36000000 |
| Cost of $CO_2$ | Rs/kg | 18 | 10800000 | 237600000 |
| Cost of Ethanol | Rs/L | 21 | 718635 | 25643274 |
| **Cost of Raw Materials (CRM)** | | | | **299243274** |
| Cost of Labor (CL) | Rs/labor | 550 | | 990000 |
| Cost of Electricity (CE) | Rs/kWh | 5.29 | 6500000 | 34385000 |
| $CO_2$ Liquefaction cost (80 % of $CO_2$ cost/kg) | Rs/kg | 14.4 | | 190080000 |
| **Operating Cost (OC)** | | | | **524698274** |
| **Annual Cost of Capital Recovery (ACCR) using 15% rate of interest** | **Rs/year** | | | **44287477** |
| **Total Annual Cost (TAC)** | | | | **568985752** |
| **Manufacturing Cost (MC)** | **Rs/kg** | **1106** | | **568985752** |
| **Selling Cost (AM seed oil)** | **Rs/kg** | **2500** | | **1285800000** |
| Gross profit before depreciation (GPBD) | | | | 716814248 |
| Gross profit after depreciation (GPAD) | | | | 702953748 |
| Income tax (30 %) on GPAD | | | | 210886125 |
| Net profit after tax | Rs | | | 492067624 |
| Salvage value | Rs | | | 0 |
| Depreciation using straight line method | Rs | | | 13860500 |
| **Payback Period** | **year** | | | **1.63** |

Table 5.33. Economic analysis (FC, CRM, OC, MC, and SC) of the SFE process for PP seed oil.

| **Particulars** | **Unit** | **Cost per unit** | **Amount consumed (kg/year)** | **Annual cost (Rs/year)** |
|---|---|---|---|---|
| SFE equipment cost with installation | Rs | | | 277210000 |
| **Fixed Cost (FC)** | Rs | | | **277210000** |
| Feedstock (PP seeds) flow rate | kg/year | | 1200000 | 48000000 |
| Cost of $CO_2$ | Rs/kg | 18 | 10800000 | 151200000 |
| Cost of Ethanol | Rs/L | 21 | 718635 | 13976796 |
| **Cost of Raw Materials (CRM)** | | | | **213176796** |
| Cost of Labor (CL) | Rs/labor | 550 | | 990000 |
| Cost of Electricity (CE) | Rs/kWh | 5.29 | 6500000 | 34385000 |
| $CO_2$ Liquefaction cost (80 % of $CO_2$ cost/kg) | Rs/kg | 37.36 | | 120960000 |
| **Operating Cost (OC)** | | | | **369511796** |
| **Annual Cost of Capital Recovery (ACCR) using 15% rate of interest** | **Rs/year** | | | **44287477** |
| **Total Annual Cost (TAC)** | | | | **413799273** |
| **Manufacturing Cost (MC)** | **Rs/kg** | **958** | | **413799273** |
| **Selling Cost (PP seed oil)** | **Rs/kg** | **2150** | | **928800000** |
| Gross Profit before depreciation (GPBD) | | | | 515000727 |
| Gross profit after depreciation (GPAD) | | | | 501140227 |
| Income tax (30 %) on GPAD | | | | 150342068 |
| Net profit after tax | | | | 350798159 |
| Salvage value | Rs | | | 0 |
| Depreciation using straight line method | Rs | | | 13860500 |
| **Payback Period** | **year** | | | **1.84** |

Table 5.34. A comparison of prices offered by different suppliers of AM and PP seed oil of therapeutic grades.

| Product name | Supplier name | Method of extraction | Purity (Claimed) | Price (Rs/kg) |
|---|---|---|---|---|
| **AM seed oil** | | | | |
| AM seed oil | NA | NA | NA | NA |
| **PP seed oil** | | | | |
| PP seed oil | Kazima Perfumers, New Delhi, India | Cold Pressing | 100 % | 7646 |
| PP seed oil | Devinez Nature Science, India | Cold Pressing | 100 % | 2685 |
| PP seed oil | Crysalis, Utah, USA | Cold Pressing | 100 % | 10063 |

NA: Not Available

# CONCLUSIONS AND RECOMMENDATIONS

This chapter summarizes salient conclusions drawn from the present investigations along with recommendations for future work.

## 6.1 Conclusions

Based on the result and discussions presented in Chapter 5, several significant conclusions can be drawn. The salient conclusions are listed below point wise for the six different types of investigations that had been carried out in the present work.

### 6.1.1 Based on RSM analysis

- From statistical analysis, it is evident that, the extraction pressure, particle size, flow rate-$CO_2$, and % of co-solvent have significant ($p<0.05$) effects on extraction yield of AM seed oil. On the other hand, all the five parameters (including temperature also) have significant ($p<0.05$) effects on extraction yield of PP seed oil also.
- Regression analysis of the CEY (g oil/g seeds) data with input parameters of SFE process shows that, the quadratic model is the best for both seeds (e.g. AM and PP).
- The regression coefficients of the developed second order polynomial model shows that developed model fitted well to the experimental data of SFE of AM seed oil, within error limits of +14.4% and -11.28%. On the other hand, the developed second order polynomial model fitted well to experimental data of SFE of PP seed oil, within error limits of +12.98% and -4.34%.
- The % of co-solvent followed by pressure have been observed as the most influencing parameters during the SFE of AM seed oil. Similarly, the pressure followed by the % of co-solvent have been observed as the most influencing parameters during the SFE of PP seed oil.
- The interaction between all five parameters (excluding the 'particle size - flow rate-$CO_2$') exists during the SFE of AM seed oil, while, the interaction between all five parameters (excluding the 'temperature-pressure', 'temperature-particle size', and 'pressure-particle

size') exists during the SFE of PP seed oil.

- The interactive terms 'temperature - % of co-solvent' and 'pressure-% of co-solvent' have been observed as the most influencing terms during the SFE of AM and PP seed oils respectively. Similarly, the interactive terms 'particle size-flow rate-$CO_2$' and 'temperature-pressure' have been observed as the least influencing terms during the SFE of AM and PP seed oils.
- The maximum oil yield (42.86%) of AM seed oil during the SFE process was obtained at the optimal conditions of parameters as follows: temperature (85 °C), pressure (305 bar), flow rate-$CO_2$ (11 g/min), particle size (0.75 mm) and % of co-solvent (9.0 %). On the other hand, the maximum oil yield (36%) of PP seed oil was achieved at the optimal conditions of parameters as follows: temperature (60 °C), pressure (333 bar), particle size (1.0 mm), flow rate-$CO_2$ (7 g/min), and % of co-solvent (9 %).

6.1.2 Based on ANN analysis

- The developed FFBP-ANN [5-6-1] model with five numbers of input neurons, six numbers of hidden neurons in a single hidden layer and one number of output neuron was found to be suitable for the SFE process of both AM and PP seed oils.
- From the finding of optimized FFBP-ANN [5-6-1] model, it can be seen that all five-extraction parameters have significant effect, in the following order: % of co-solvent > pressure > particle size > flow rate-$CO_2$ > temperature, on the extraction yield of AM seed oil. Similarly, during the SFE of PP seed oil, the order of influencing parameters is pressure > % of co-solvent > temperature > flow rate-$CO_2$ > particle size.

6.1.3 Based on Sovova model

The Sovova model has been used to fit the experimental data with, $Z, W$, and $x_k$ as tuning parameter which, were optimized using GA approach. The following silent conclusions have been drawn from the model fitting:

- It has been observed in the present study that the mass transfer coefficient in the solvent phase ($k_{ya}$) is several order of magnitude greater than that in the solid phase ($k_{xa}$) for all pressure values investigated during the SFE of both seeds.

- The maximum percentage of AM and PP seed oil has been extracted during the transition period (constant extraction period + falling extraction period). In the first extraction period, the mass transfer is governed by convection and in the second extraction period, it is governed by convection as well as diffusion.
- It is clear that the Sovova model fits the experimental CEY data of AM seed oil with an AARD % range of '1.436 – 14.198 %', and an average AARD % of '5.224 %', while the experimental CEY data of PP seed oil with an AARD % range of '0.7706 – 14.17 %', and an average AARD % of '4.254 %'.
- Sovova model has offered better fitting of experimental data with an AARD % as '4.67%' and '3.59%' for '93.5%' of total number of runs (e.g. 43 runs out of 46 runs) during the SFE of AM and PP seed oils respectively.

5.1.4 Based on Reverchon model

- Reverchon model has fitted well the linear behavior of CEY of both seeds.
- It is clear that the Reverchon model fits the experimental CEY data of AM seed oil with an AARD % range of '5.52 - 96.3%', and an average AARD % of '37.76 %', while the experimental CEY data of PP seed oil with an AARD % range of '2.64 - 19.74%', and an average AARD % of '17.93%'. Thus, it can be concluded that the Reverchon model does not fit well with the experimental CEY data of AM seed oil. However, it has shown better fitting in some parts of extraction curves of PP seed oil.
- Reverchon model moderately fitted experimental CEY data of AM seed oil with an AARD % as '12.36%' only of total number of runs (e.g. 13 runs out of 46 runs). On the other hand, it has shown a better fitting with experimental CEY data of PP seed oil with an AARD % as '10.31%' for 74% of total runs (e.g. 34 runs out of 46 runs).
- Though, Reverchon model does not fit CEY vs. time data of extraction curve well, it predicts the final CEY value correctly at the end of the extraction period and thus can be used to predict the CEY value at the end of extraction period.

6.1.5 Based on characterization of feeds and products

- The SEM analysis of AM and PP seed samples at before and after the SFE revealed that the initially the oil was contained by some cells/cavities which were broken up due to the influence of extraction parameters (e.g. temperature, pressure, particle size, flow rate-$CO_2$

and % of co-solvent). The oil was extracted out as evident from the broken and empty portions of cell that had appeared in after SFE samples of both seed particles.

- The TG analysis of AM seed particles shows the vaporization of 10% moisture and 76.4% organic matter, 10% decomposition of remaining component of seed particles and 3.6% ash. Similarly, the TG analysis of PP seed particles shows the vaporization of 5.9% moisture and 73.6% organic matter, 18.7% decomposition of remaining component of seed particles and 1.8% ash.
- The FTIR analysis of seed particles has confirmed the presence of the fatty acids, protein and carbohydrates in AM and PP seeds. In addition to these, FTIR has also confirmed the presence of alkaloids (e.g. sanguinarine) and flavonoids (e.g. karanjin) in AM and PP seed respectively.
- The determined physico-chemical properties of AM and PP seed oil such as acid value, peroxide value, soponification value, calorific value, flash point, cloud point, fire point, and pour point confirm its suitability for fuel purposes.
- Based on the fatty acid components found in the oils of these two seeds (AM and PP seeds), it can be concluded that these oils can be used in the field of medicine to cure various chronic diseases such as the coronary heart disease, blood cholesterol, diabetes, cancer, paracoccidioidomycosis (PCM), atherosclerosis, obesity, allergy etc.. In addition to this, analysis also shows that, AM and PP seed oils have a higher concentration range of unsaturated fatty acids (USFAs = 66.53 - 85.1%) and (USFAs = 73.31 - 77.08%) respectively, which is responsible for the lower viscosity of trans-esterified oil - one of the most desirable qualities for biofuel production.

6.1.6 Based on the economic analysis of the envisaged plant of SFE process

- Finally, the economic analysis of the SFE process at industrial scale (for 1000 liters capacity of extraction vessel) has confirmed the economic feasibility, based on the obtained payback periods as ‘1.63’ and ‘1.84’ years for the envisaged plant of SFE process of AM and PP seed oils respectively.

## 6.2 **Recommendations**

For the advancement of knowledge in the area of SFE of natural products and its modeling, following recommendations for future work are made:

- The Reverchon model proposed by Reverchon, 1996 does not fits the experimental data well at low pressure for AM and PP seed oil extraction hence it is recommended that this model should be improved based on the physics of extraction.
- The quantification and isolation of alkaloids and flavonoids present in AM and PP seed oils (as reported in literature) should be done to explore their further applications as medicines.
- Some other available organic solvents (e.g. ethanol, methanol, propanol etc.) can be tested for the SFE process.

## REFERENCES


1. Abaroudi, K., Trabelsi, F., Calloud-Gabriel, B., Recasens, F., 1999. Mass transport ehancement in modified supercritical fluid. Ind. Eng. Chem. Res. 38, 3505–3518.

2. Adeoti, I.A., Hawboldt, K., 2015. Experimental and mass transfer modelling of oil extraction from salmon processing waste using SC-$CO_2$. J. Supercrit. Fluids 104, 160–170.

3. Ahmed, Z., Abdeslam-Hassan, M., Ouassila, L., Danielle, B., 2012. Extraction and modeling of Algerian Rosemary essential oil using supercritical $CO_2$: Effect of pressure and temperature. Energy Procedia 18, 1038–1046.

4. Al-Darmaki, N., Lu, T., Al-Duri, B., Harris, J.B., Favre, T.L.F., Bhaggan, K., Santos, R.C.D., 2011. Solubility measurements and analysis of binary, ternary and quaternary systems of palm olein, squalene and oleic acid in supercritical carbon dioxide. Sep. Purif. Technol. 83, 189–195.

5. Aladic, K., Jokic, S., Moslavac, T., Tomas, S., Vidovic, S., Vladic, J., Subaric, D., 2014. Cold pressing and supercritical $CO_2$ extraction of Hemp (Cannabis sativa) seed oil. Chem. Biochem. Eng. 28, 481–490.

6. Aleksovski, S., Sovová, H., Urapova, B., Poposka, F., 1998. Supercritical $CO_2$ extraction and soxhlet extraction of grape seed oil. Bull. Chem. Technol. Maced. 17, 129–134.

7. Aliada, S.R., 1984. Solubility parameters of supercritical fluids. Ind. Eng. Chem. Process Des. Dev. 23, 344–348.

8. Alzate, L.M., Gonzalez, D., Londono Londono, J., 2013. Recovery of carotenoids from agroindustrial byproducts using clean extraction techniques: Supercrital fluid extraction and ultrasound assisted extraction, in: III Iberoamerican Conference on Supercritical Fluids. pp. 1–7.

9. Ambasta, S., 1986. The useful plants of India. CSIR, New Delhi, India.

10. Araus, K., Uquiche, E., del Valle, J.M., 2009. Matrix effects in supercritical $CO_2$ extraction of essential oils from plant material. J. Food Eng. 92, 438–447.

11. Arote, S.R., Dahikar, S.B., Yeole, P.G., 2009. Phytochemical screening and antibacterial properties of leaves of Pongamia pinnata Linn. (Fabaceae) from India. African J. Biotechnol. 8, 6393–6396.

12. Asep, E.K., Jinap, S., Jahurul, M.H.A., Zaidul, I.S.M., Singh, H., 2013. Effects of polar cosolvents on cocoa butter extraction using supercritical carbon dioxide. Innov. Food Sci. Emerg. Technol. 20, 152–160.

13. Ayas, N., Yilmaz, O., 2014. A shrinking core model and empirical kinetic approaches in supercritical $CO_2$ extraction of safflower seed oil. J. Supercrit. Fluids 94, 81–90.

14. Azam, M.M., Waris, A., Nahar, N.M., 2005. Prospects and potential of fatty acid methyl esters of some non-traditional seed oils for use as biodiesel in India. Biomass and Bioenergy 29, 293–302.

15. Back, T., Fogel, D.B., Michalewicz, Z., 2000. Evolutionary Computation- Basic Algorithms and Operators, 1st ed. CRC Press, Taylor and Francis Group.

16. Bakhbakhi, Y., 2011. Phase equilibria prediction of solid solute in supercritical carbon dioxide with and without a cosolvent: The use of artificial neural network. Expert Syst. Appl. 38, 11355–11362.

17. Bala, M., Nag, T.N., Kumar, S., Vyas, M., Kumar, A., Bhogal, N.S., 2011. Proximate composition and fatty acid profile of Pongamia pinnata, a potential biodiesel crop. J. Am. Oil Chem. Soc. 88, 559–562.

18. Balasubramanian, R.K., Yen Doan, T.T., Obbard, J.P., 2013. Factors affecting cellular lipid extraction from marine microalgae. Chem. Eng. J. 215–216, 929–936.

19. Bankovi-Ilic, I.B., Stamenkovi, O.S., Veljkovi, V.B., 2012. Biodiesel production from non-edible plant oils. Renew. Sustain. Energy Rev. 16, 3621–3647.

20. Baranska, M., Schulz, H., 2009. Determination of Alkaloids through Infrared and Raman Spectroscopy, in: The Alkaloids. Elsevier, pp. 217–255.

21. Barrales, F.M., Rezende, C.A., Martínez, J., 2015. Supercritical $CO_2$ extraction of passion fruit (Passiflora edulis sp.) seed oil assisted by ultrasound. J. Supercrit. Fluids 104, 183–192.

22. Bartle, K.D., Clifford, A.A., Hawthorne, S.B., Langenfeld, J.J., Miller, D.J., Robinsona, R., 1990. A model for dynamic extraction using a supercritical fluid. J. Supercrit. Fluids 3, 143–149.

23. Bartle, K.D., Clifford, A.A., Jafar, S.A., Shilstone, G.F., 1991. Solubilities of solids and liquids of low volatility in supercritical $CO_2$. J. Phys. Chem. Ref. Data 20, 713–755.

24. Basaar, O., Fatema, S., Alrabie, A., Mohsin, M., Farooqui, M., 2017. Supercritical carbon dioxide extraction of Triognella foenum graecum Linn seeds: Determination of bioactive compounds and pharmacological analysis. Asian Pac. J. Trop. Biomed. 7, 1085–1091.

25. Beckman, E.J., 2004. Supercritical and near-critical $CO_2$ in green chemical synthesis and processing. J. Supercrit. Fluids 28, 121–191.

26. Belayneh, H.D., Wehling, R.L., Cahoon, E., Ciftci, O.N., 2015. Extraction of omega-3-rich oil from Camelina sativa seed using supercritical carbon dioxide. J. Supercrit. Fluids 104, 153–159.

27. Belbaki, A., Louaer, W., Meniai, A.H., 2017. Supercritical $CO_2$ extraction of oil from Crushed Algerian olives. J. Supercrit. Fluids 130, 165–171.

28. Bensebia, O., Barth, D., Bensebia, B., Dahmani, A., 2009. Supercritical $CO_2$ extraction of rosemary: Effect of extraction parameters and modelling. J. Supercrit. Fluids 49, 161–166.

29. Berna, A., Tárrega, A., Blasco, M., Subirats, S., 2000. Supercritical $CO_2$ extraction of essential oil from orange peel; effect of the height of the bed. J. Supercrit. Fluids 18, 227–237.

30. Bernardo-Gil, M.G., Casquilho, M., Esquível, M.M., Ribeiro, M.A., 2009. Supercritical fluid extraction of fig leaf gourd seeds oil: Fatty acids composition and extraction kinetics. J. Supercrit. Fluids 49, 32–36.

31. Bernardo-Gill, M.G., Casquilho, M., 2007. Modeling the supercritical fluid extraction of Hazelnut and Walnut oils. AIChE J. 56, 2980–2985.

32. Bhalke, Gosavi, S.A., 2009. Anti-stress and antiallergic effect of Argemone mexicana stems in asthma. Arch. Pharm. 1, 127–129.

33. Bimakr, M., Rahman, R.A., Taip, F.S., Adzahan, N.M., Sarker, M. zaidul I., Ganjloo, A., 2013. Supercritical carbon dioxide extraction of seed oil from winter melon (Benincasa hispida) and its antioxidant activity and fatty acid composition. Molecules 18, 997–1014.

34. Bobade, S.N., Khyade, V.B., 2012. Detail study on the properties of Pongamia Pinnata (Karanja ) for the production of biofuel. Res. J. Chem. Sci. Chem. Sci. 2, 16–20.

35. Borugadda, V.B., Goud, V. V., 2012. Biodiesel production from renewable feedstocks: Status and opportunities. Renew. Sustain. Energy Rev. 16, 4763–4784.

36. Box, G.E.P., Behnken, D.W., 1960. Simplex-Sum design: A class of second order rotatable designs derivable from those of first order. Ann. Math. Stat. 32, 12–40.

37. Brahmachari, G., Gorai, D., Roy, R., 2013. Argemone mexicana: chemical and pharmacological aspects. Brazilian J. Pharmacogn. 23, 559–575.

38. Brest, J., Greiner, S., Boskovic, B., Mernik, M., Zumer, V., 2006. Self-adapting control parameters in differential evolution: A comparative study on numerical benchmark problems. IEEE Trans. Evol. Comput. 10, 646–657.

39. Brondz, I., Sedunov, B., Sivaraman, N., 2017. Influence of modifiers on supercritical fluid chromatography (SFC) and supercritical fluid extraction (SFE), Part I. Int. J. Anal. Mass Spectrom. Chromatogr. 5, 17–39.

40. Bruno, T.J., Castro, C., Hamel, J.P., Palavra, A.M.F., 1993. Supercritical fluid extraction of biological products, in: John Wiley and Sons (Ed.), Recovery Process for Biological Materials. New York, pp. 303–354.

41. Bulley, N.R., Fattori, M., Meisen, A., Moyls, L., 1984. Supercritical fluid extraction of vegetable oil seeds. J. Am. Oil Chem. Soc. 61, 1362–1365.

42. Campos, L.M.A.S., Michielin, E.M.Z., Danielski, L., Ferreira, S.R.S., 2005. Experimental data and modeling the supercritical fluid extraction of marigold (Calendula officinalis) oleoresin. J. Supercrit. Fluids 34, 163–170.

43. Celik, H.T., Guru, M., 2015. Extraction of oil and silybin compounds from milk thistle seeds using supercritical carbon dioxide. J. Supercrit. Fluids 100, 105–109.

44. Chassagnez-mendez, A.L., Machado, N.T., Araujo, M.E., Maia, J.G., Meireles, M.A.A., 2000. Supercritical $CO_2$ extraction of Curcumins and essential oil from the Rhizomes of Turmeric (Curcuma longa L.). Ind. Eng. Chem. Res. 39, 4729–4733.

45. Cheng, S.H., Yang, F.C., Yang, Y.H., Hu, C.C., Chang, W.T., 2013. Measurements and modeling of the solubility of ergosterol in supercritical carbon dioxide. J. Taiwan Inst. Chem. Eng. 44, 19–26.

46. Chopra, R.N., Nayar, S.L., Chopra, I.C., 1956. Glossary of Indian medicinal plants. CSIR.

47. Christie, W.W., 1990. Gas chromatography and lipids: A practical guide, 3rd ed. The Oily Press, Bridgwater, Somerset.

48. Clifford, A.A., 1993. Introduction to supercritical fluid extraction in analytical science, in: Supercritical Fluid Extraction and Its Use in Chromatographic Sample Preparation. Springer, Dordrecht.

49. Cocero, M.., Garcia, J., 2001. Mathematical model of supercritical extraction applied to oil seed extraction by $CO_2$+saturated alcohol - I. Desorption model. J. Supercrit. Fluids 20, 229–243.

50. Cocero, M.J., Calvo, L., 1996. Supercritical fluid extraction of sunflower seed oil with $CO_2$ - ethanol mixtures. J. Am. Oil Chem. Soc. 73, 1573–1578.

51. Cunha, V.M.B., Silva, M.P. da, Sousa, S.H.B. de, Bezerra, P. do N., Menezes, E.G.O., Silva, N.J.N. da, Banna, D.A.D. da S., Araújo, M.E., Carvalho Junior, R.N. de, 2019. Bacaba-de-leque (Oenocarpus distichus Mart.) oil extraction using supercritical $CO_2$ and bioactive compounds determination in the residual pulp. J. Supercrit. Fluids 144, 81–90.

52. Cybenko, G., 1989. Approximation by superpositions of a sigmoidal function. Math. Control Signals Syst. 2, 303–314.

53. Cygnarowicz-Provost, M., O'Brien, D.J., Maxwell, R.J., Hampson, J.W., 1992. Supercritical-Fluid Extraction of Fungal Lipids Using Mixed Solvents : Experiment and Modeling. J. Supercrit. Fluids 5, 24–30.

54. Da Porto, C., Decorti, D., Natolino, A., 2016. Microwave pretreatment of Moringa oleifera seed: effect on oil obtained by pilot-scale supercritical carbon dioxide extraction and soxhlet apparatus. J. Supercrit. Fluids 107, 38–43.

55. Da Porto, C., Natolino, A., 2017. Supercritical fluid extraction of polyphenols from grape seed (Vitis vinifera): study on process variables and kinetics. J. Supercrit. Fluids 130, 239–245.

56. Dalvi, S. V., Mukhopadhyay, M., 2009a. A novel process for precipitation of ultra-fine particles using sub-critical $CO_2$. Powder Technol. 195, 190–195.

57. Dalvi, S. V., Mukhopadhyay, M., 2009b. Use of subcritical $CO_2$ for production of ultrafine particles by pressure reduction of gas-expanded organic liquids. Ind. Eng. Chem. Res. 48, 5696–5707.

58. Das, L.M., Bora, D.K., Pradhan, S., Naik, M.K., Naik, S.N., 2009. Long-term storage stability of biodiesel produced from Karanja oil. Fuel 88, 2315–2318.

59. Davoodbasha, M., Edachery, B., Nooruddin, T., Lee, S., 2018. An evidence of C16 fatty acid methyl esters extracted from microalga for effective antimicrobial and antioxidant property. Microb. Pthogenes. 115, 233–238.

60. de Albuquerque, U.P., Monteiro, J.M., Ramos, M.A., de Amorim, E.L.C., 2007. Medicinal and magic plants from a public market in northeastern Brazil. J. Ethnopharmacol. 110, 76–91.

61. De, B.K., Patel, J.D., 2009. Optimization of solvent requirement for refining of karanja (Pongamia glabra) oil by liquid- liquid extraction. J. Sci. Ind. Res. (India). 68, 319–324.

62. de França, L.F., Reber, G., A, M.M.A., Machado, N.T., Brunner, G., 1999. Supercritical extraction of carotenoids and lipids from buriti (Mauritia flexuosa), a fruit from the Amazon region. J. Supercrit. Fluids 14, 247–256.

63. de Lorgeril, M., Salen, P., Laporte, F., Leiris, J. De, 2001. Alpha-linolenic acid in the prevention and treatment of coronary heart disease. Eur. Hear. J. Suppl. 3, 26–32.

64. de Melo, A.R., Pereira Garcia, I.J., Serrão, J.E., Alves, S.N., Santos, H.L., de Melo, A.R., Rodrigues dos Santos Lima, L.A., 2018. Toxicity of different fatty acids and methyl esters on Culex quinquefasciatus larvae. Ecotoxicol. Environ. Saf. 154, 1–5.

65. de Melo, M.M.R., Silvestre, A.J.D., Silva, C.M., 2014. Supercritical fluid extraction of vegetable matrices: applications, trends and future perspectives of a convincing green technology. J. Supercrit. Fluids 92, 115–176.

66. del Valle, J.M., Aguilera, J.M., 1999. Review: High pressure $CO_2$ extraction. Fundamentals and applications in the food industry. Food Sci Tech Int 5, 1–24.

67. del Valle, J.M., Mena, C., Budinich, M., 2008. Extraction of garlic with supercritical $CO_2$ and conventional organic solvents. Brazilian J. Chem. Eng. 25, 535–542.

68. Demirbas, A., 2000. Liquefaction of olive husk by supercritical fluid extraction. Energy Convers. Manag. 41, 1875–1883.

69. Dey, N.R., Das, K.C., Rai, Y., 2008. Argemone mexicana: a multicentric double blind homoeopathic pathogenetic trial (drug proving) carried out by CCRH. Indian J. Res. Homoeopath. 2, 13–18.

70. Doker, O., Salgin, U., Sanal, I., Mehmetoglu, U., Calimli, A., 2004. Modeling of extraction of β-carotene from apricot bagasse using supercritical CO2 in packed bed extractor. J. Supercrit. Fluids 28, 11–19.

71. Duba, K.S., Fiori, L., 2015. Supercritical $CO_2$ extraction of grape seed oil: effect of process parameters on the extraction kinetics. J. Supercrit. Fluids 98, 33–43.

72. Dwivedi, G., Sharma, M.P., 2014. Prospects of biodiesel from Pongamia in India. Renew. Sustain. Energy Rev. 32, 114–122.

73. Erkucuk, A., Akgun, I.H., Yesil-Celiktas, O., 2009. Supercritical $CO_2$ extraction of glycosides from Stevia rebaudiana leaves: Identification and optimization. J. Supercrit. Fluids 51, 29–35.

74. Esquivel, M.M., Bernardo-gil, M.G., King, M.B., 1999. Mathematical models for supercritical extraction of olive husk oil. J. Supercrit. Fluids 16, 43–58.

75. Fernandez, I., Dachs, J., Bayona, J.M., 1996. Application of experimental design approach to the optimization of supercritical fluid extraction of polychlorinated biphenyls and polycyclic aromatic hydrocarbons. J. Chromatogr. A 719, 77–85.

76. Ferreira, S.L.C., Bruns, R.E., Ferreira, H.S., Matos, G.D., David, J.M., Brandao, G.C., da Silva, E.G.P., Portugal, L.A., dos Reis, P.S., Souza, A.S., dos Santos, W.N.L., 2007. Box-Behnken design: an alternative for the optimization of analytical methods. Anal. Chim. Acta 597, 179–186.

77. Ferreira, S.R.S., Angela, M., Meireles, A., 2002. Modeling the supercritical fluid extraction of black pepper (Piper nigrum L.) essential oil. J. Food Eng. 54, 263–269.

78. Fetzer, D.L., Cruz, P.N., Hamerski, F., Corazza, M.L., 2018. Extraction of baru (Dipteryx alata vogel) seed oil using compressed solvents technology. J. Supercrit. Fluids 137, 23–33.

79. Fiori, L., Lavelli, V., Duba, K.S., Sri Harsha, P.S.C., Mohamed, H. Ben, Guella, G., 2014. Supercritical $CO_2$ extraction of oil from seeds of six grape cultivars: Modeling of mass transfer kinetics and evaluation of lipid profiles and tocol contents. J. Supercrit. Fluids 94, 71–80.

80. Ghoreishi, S.M., Heidari, E., 2013. Extraction of Epigallocatechin-3-gallate from green tea via supercritical fluid technology: Neural network modeling and response surface optimization. J. Supercrit. Fluids 74, 128–136.

81. Ghoreishi, S.M., Shahrestani, G.R., Ghaziaskar, H.S., 2009. Experimental and modeling investigation of supercritical extraction of mannitol from Olive leaves. Chem. Eng. Technol. 32, 45–54.

82. Goembira, F., Saka, S., 2015. Advanced supercritical methyl acetate method for biodiesel production from Pongamia pinnata oil. Renew. Energy 83, 1245–1249.

83. Goldberg, D.E., 1989. Genetic Algorithms in Search Optimization and Machine Learning. Addison-Wesely Publishing Company, INC.

84. Goleroudbary, M.G., Ghoreishi, S.M., 2016. Response surface optimization of Safranal and Crocin extraction from Crocus sativus L. via supercritical fluid technology. J. Supercrit. Fluids 108, 136–144.

85. Goodarznia, I., Eikani, M.H., 1998. Supercritical carbon dioxide extraction of essential oils: modeling and simulation. Chem. Eng. Sci. 53, 1387–1395.

86. Gooding, O.W., 2004. Process optimization using combinatorial design principles: parallel synthesis and design of experiment methods. Curr. Opin. Chem. Biol. 8, 297–304.

87. Gosh, A., 2003. Herbal folk remedies of Bantura & Medinipur districts, West Bengal (India). Indian J. Tradit. Knowl. 2, 393–396.

88. Goto, M., Roy, B.C., Hirose, T., 1996. Shrinking core leaching model for supercritical fluid extraction. J. Supercrit. Fluids 9, 128–133.

89. Goto, M., Sato, M., Hirose, T., 1993. Extraction of Peppermint oil by supercritical carbon dioxide. J. Chem. Eng. Japan 26, 401–407.

90. Grijo, D.R., Vieitez Osorio, I.A., Cardozo-Filho, L., 2018. Supercritical extraction strategies using CO2 and ethanol to obtain cannabinoid compounds from Cannabis hybrid flowers. J. $CO_2$ Util. 28, 174–180.

91. Guoliang, L., Junyou, S., Yourui, S., Zhiwei, S., Lian, X., Jie, Z., Jinmao, Y., Yongjun, L., 2011. Supercritical $CO_2$ cell breaking extraction of Lycium barbarum seed oil and determination of its chemical composition by HPLC/APCI/MS and antioxidant activity. LWT - Food Sci. Technol. 44, 1172–1178.

92. Ha, H.K.P., Maridable, J., Gaspillo, P., Hasika, M., Malaluan, R., Kawasaki, J., 2007. Modeling and optimization of supercritical carbon dioxide extraction on essential oil from Lemongrass using response surface methodology. J. Res. Sci. Comput. Eng. 3, 1–10.

93. Haloui, I., Meniai, A.H., 2017. Supercritical $CO_2$ extraction of essential oil from Algerian argan (Argania spinosa L.) seeds and yield optimization. Int. J. Hydrogen Energy 42, 12912–12919.

94. Han, X., Cheng, L., Zhang, R., Bi, J., 2009. Extraction of safflower seed oil by supercritical $CO_2$. J. Food Eng. 92, 370–376.

95. Hannay, J.B., Hogarth, J., 1879. On the solubility of solids in gases. Nat. Publ. Gr. 82.

96. Hawthorne, S.B., Grabanski, C.B., Martin, E., Miller, D.J., 2000. Comparisons of Soxhlet extraction, pressurized liquid extraction, supercritical fluid extraction and subcritical water extraction for environmental solids: recovery, selectivity and effects on sample matrix. J. Chromatogr. A 892, 421–433.

97. Hegel, P.E., Camy, S., Destrac, P., Condoret, J.S., 2011. Influence of pretreatments for extraction of lipids from yeast by using supercritical carbon dioxide and ethanol as cosolvent. J. Supercrit. Fluids 58, 68–78.

98. Henry, G.E., Momin, R.A., Nair, M.G., Dewitt, D.L., 2002. Antioxidant and Cyclooxygenase Activities of Fatty Acids Found in Food. J. Agric. Food Chem. 50, 2231–2234.

99. Hilditch, T.P., 1949. The industrial chemistry of fats and waxes, 3rd ed. Chapman and Hall.

100. Holland, J.H., 1992. Adaptation in Natural and Artificial Systems, 2nd ed. MIT Press Campbridge.

101. Honarvar, B., Sajadian, S.A., Khorram, M., Samimi, A., 2013. Mathematical modeling of supercritical fluid extraction of oil from canola and sesame seeds. Brazilian J. Chem. Eng. 30, 159–166.

102. Hong, I.K., Rho, S.W., Lee, K.S., Lee, W.H., Yoo, K.P., 1990. Modeling of soybean oil bed extraction with supercritical carbon dioxide. Korean J. Chem. Eng. 7, 40–46.

103. Hong, S.I., Pyun, Y.R., 2001. Membrane damage and enzyme inactivation of Lactobacillus plantarum by high pressure $CO_2$ treatment. Int. J. Food Microbiol. 63, 19–28.

104. Hortacsu, G., 2000. Modeling of natural materials extraction, in: Supercritical Fluids - Fundamental and Applications. lOS Press and Kluwer Academic, Turkey, pp. 499.

105. Hrncic, D., Mernik, M., Hrncic, M.K., 2010. Use of genetic algorithm for fitting Sovova's mass transfer model. Acta Chim. Slov. 57, 788–797.

106. Hrncic, M.K., Cor, D., Verboten, M.T., Knez, Z., 2018. Application of supercritical and subcritical fluids in food processing. Food Qual. Saf. 2, 59–67.

107. Hu, Y.H., Hwang, J.N., 2002. Handbook of Neural Network Signal Processing, CRC Press. CRC Press, Washington D.C.

108. Huang, Z., Xu, L., Li, J.H., 2011a. Amine extraction from hexagonal mesoporous silica materials by means of methanol-enhanced supercritical $CO_2$: experimental and modeling. Chem. Eng. J. 166, 461–467.

109. Huang, Z., Yang, M.-J., Liu, S.-F., Ma, Q., 2011b. Supercritical carbon dioxide extraction of Baizhu: experiments and modeling. J. Supercrit. Fluids 58, 31–39.

110. Ibrahim, M., Alaam, M., El-haes, H., Jalbout, A.F., Leon, A. De, 2006. Analysis of the structure and vibrational spectra of glucose and fructose. Eclet. Quim. 31, 15–22.

111. Illes, V., Szalai, O., Then, M., Daood, H., Perneczki, S., 1997. Extraction of hiprose fruit by supercritical $CO_2$ and propane. J. Supercrit. Fluids 10, 209–218.

112. Ivanovic, J., Meyer, F., Stamenic, M., Jaeger, P., Zizovic, I., Eggers, R., 2014. Pretreatment of natural materials used for supercritical fluid extraction of commercial phytopharmaceuticals. Chem. Eng. Technol. 37, 1–7.

113. Ivanovic, J., Ristic, M., Skala, D., 2011. Supercritical $CO_2$ extraction of Helichrysum italicum: Influence of $CO_2$ density and moisture content of plant material. J. Supercrit. Fluids 57, 129–136.

114. Ixtaina, V.Y., Vega, A., Nolasco, S.M., Tomás, M.C., Gimeno, M., Bárzana, E., Tecante, A., 2010. Supercritical carbon dioxide extraction of oil from Mexican chia seed (Salvia hispanica L.): characterization and process optimization. J. Supercrit. Fluids 55, 192–199.

115. Jacob, M.B., 1958. The chemical analysis of food and food products, 3rd ed. D. Van Nostrand Company Ltd., New York.

116. Jaglan, N., Kumar, S., Choudhury, P.K., Tyagi, B., Tyagi, A.K., 2019. Isolation, characterization and conjugated linoleic acid production potential of bifidobacterial isolates from ruminal fluid samples of Murrah buffaloes. Anaerobe 56, 40–45.

117. Jain, S., Sharma, M.P., 2012. Application of thermogravimetric analysis for thermal stability of Jatropha curcas biodiesel. Fuel 93, 252–257.

118. Jandacek, R.J., 2017. Linoleic Acid : A Nutritional Quandary. Healthcare 5, 1–8.

119. Jia, D., Li, S., Xiao, L., 2009. Supercritical $CO_2$ extraction of Plumula nelumbinis oil: Experiments and modeling. J. Supercrit. Fluids 50, 229–234.

120. Jokic, S., Nagy, B., Zeković, Z., Vidović, S., Bilić, M., Velić, D., Simándi, B., 2012. Effects of supercritical $CO_2$ extraction parameters on soybean oil yield. Food Bioprod. Process. 90, 693–699.

121. Kagliwal, L.D., Patil, S.C., Pol, A.S., Singhal, R.S., Patravale, V.B., 2011. Separation of bioactives from seabuckthorn seeds by supercritical carbon dioxide extraction methodology through solubility parameter approach. Sep. Purif. Technol. 80, 533–540.

122. Kane, M., Dean, J.R., Hitchen, S.M., Dowle, C.J., Tranter, R.L., 1993. Experimental design approach for supercritical fluid extraction. Anal. Chim. Acta 271, 83–90.

123. Kawamura, H., Mishima, K., Sharmin, T., Ito, S., Kawakami, R., Kato, T., Misumi, M., Suetsugu, T., Orii, H., Kawano, H., Irie, K., Sano, K., Mishima, K., Harada, T., Mustofa, S., Hasanah, F., Siregar, Y.D.I., Zahroh, H., Putri, L.S.E., Salim, A., 2016. Ultrasonically enhanced extraction of luteolin and apigenin from the leaves of Perilla frutescens (L.) Britt. using liquid carbon dioxide and ethanol. Ultrason. Sonochem. 29, 19–26.

124. Kenneth Helrich, 1990. AOAC: Official Methods of Analysis.

125. Kerrola, K., Kallio, H., 1993. Volatile compounds and odor characteristics of carbon dioxide extracts of coriander (Coriandrum sativum L.) fruits. J. Agric. Food Chem. 41, 785–790.

126. Kesari, V., Das, A., Rangan, L., 2010. Physico-chemical characterization and antimicrobial activity from seed oil of Pongamia pinnata, a potential biofuel crop. Biomass and Bioenergy 34, 108–115.

127. Khajeh, M., Yamini, Y., Shariati, S., 2010. Comparison of essential oils compositions of Nepeta persica obtained by supercritical carbon dioxide extraction and steam distillation methods. Food Bioprod. Process. 88, 227–232.

128. Khanpour, R., Sheikhi-Kouhsar, M.R., Esmaeilzadeh, F., Mowla, D., 2014. Removal of contaminants from polluted drilling mud using supercritical carbon dioxide extraction. J. Supercrit. Fluids 88, 1–7.

129. Khaw, K.Y., Parat, M.O., Shaw, P.N., Falconer, J.R., 2017. Solvent supercritical fluid technologies to extract bioactive compounds from natural sources: a review. Molecules 22, 1–24.

130. Khayoon, M.S., Olutoye, M.A., Hameed, B.H., 2012. Utilization of crude karanj (Pongamia pinnata) oil as a potential feedstock for the synthesis of fatty acid methyl esters. Bioresour. Technol. 111, 175–179.

131. Khosravi-Darani, K., Vasheghani-Farahani, E., 2005. Application of supercritical fluid extraction in biotechnology. Crit. Rev. Biotechnol. 25, 231–242.

132. Khraisha, Y.H., Shabib, I.M., 2002. Thermal analysis of shale oil using thermogravimetry and differential scanning calorimetry. Energy Convers. Manag. 43, 229–239.

133. King, J.W., 1989. Fundamentals and applications of supercritical fluid extraction in chromatographic science. J. Chromatogr. Sci. 27, 355–364.

134. Kiran, E., Debenedetti, P.G., Peters, C.J., 2012. Supercritical Fluids: Fundamentals and Applications. Springer Science.

135. Kiriamiti, H.K., Rascol, E., Marty, A., Condoret, J.S., 2001. Extraction rates of oil from high oleic sunflower seeds with supercritical carbon dioxide. Chem. Eng. Process. 41, 711–718.

136. Kitzberger, C.S.G., Lomonaco, R.H., Michielin, E.M.Z., Danielski, L., Correia, J., Ferreira, S.R.S., 2009. Supercritical fluid extraction of shiitake oil: Curve modeling and extract composition. J. Food Eng. 90, 35–43.

137. Koenhen, D.M., Smolders, C.A., 1975. The determination of solubility parameters of solvents and polymers by means of correlations with other physical quantities. J. Appl. Polym. Sci. 19, 1163–1179.

138. Koubaa, M., Mhemdi, H., Vorobiev, E., 2016. Influence of canola seed dehulling on the oil recovery by cold pressing and supercritical $CO_2$ extraction. J. Food Eng. 182, 18–25.

139. Kueh, B.W. Bin, Yusup, S., Osman, N., 2018. Supercritical carbon dioxide extraction of Melaleuca cajuputi leaves for herbicides allelopathy: optimization and kinetics modelling. J. $CO_2$ Util. 24, 220–227.

140. Kumar, K.A., Chattaraj, R., Dhumal, U., Mukhopadhyay, M., Vinjamur, M., Dalvi, S. V., 2013. Modeling of precipitation of ultra-fine particles by pressure reduction over $CO_2$-expanded liquids. J. Supercrit. Fluids 79, 227–235.

141. Kumar, R., Kumar, G.R., Chandrashekar, N., 2011. Microwave assisted alkali-catalyzed transesterification of Pongamia pinnata seed oil for biodiesel production. Bioresour. Technol. 102, 6617–6620.

142. Kumar, R., Madras, G., Modak, J., 2004. Enzymatic Synthesis of Ethyl Palmitate in Supercritical Carbon Dioxide. Ind. Eng. Chem. Res. 43, 1568–1573.

143. Kumar, R., Modak, J., Madras, G., 2005. Effect of the chain length of the acid on the enzymatic synthesis of flavors in supercritical carbon dioxide. Ind. Eng. Chem. Res. 41, 199–202.

144. Kumhom, T., Elkamel, A., Douglas, P.L., Douglas, S., Pongamphai, S., Teppaitoon, W., 2011. Prediction of isoflavone extraction from soybean meal using supercritical carbon dioxide with cosolvents. Chem. Eng. J. 172, 1023–1032.

145. Kumoro, A.C., Hasan, M., 2006. Modelling of supercritical carbon dioxide extraction of Andrograpgolide from Andrographis paniculata leaves by employing integral desorption concept. Int. J. Eng. Technol. 3, 13–20.

146. Kumoro, A.C., Singh, H., Hasan, M., 2009. Solubility of Piperine in Supercritical and near critical carbon dioxide. Chinese J. Chem. Eng. 17, 1014–1020.

147. Kwaambwa, H.M., Maikokera, R., 2008. Infrared and circular dichroism spectroscopic characterisation of secondary structure components of a water treatment coagulant protein extracted from Moringa oleifera seeds. Colloids Surfaces B Biointerfaces 64, 118–125.

148. Lack, E.A., 1985. Criteria for the design of installations for the high pressure extraction of natural substances. Graz University of Technology.

149. Lang, Q., Hunt, F., Wai, C.M., 2000. Supercritical fluid extraction of polycyclic aromatic hydrocarbons from white pine (Pinus strobus) needles and its implications. J. Environ. Monit. 2, 639–644.

150. Lang, Q., Wai, C.M., 2001. Supercritical fluid extraction in herbal and natural product studies: a practical review. Talanta 53, 771–782.

151. Lashkarbolooki, M., Shafipour, Z.S., Hezave, A.Z., 2013. Trainable cascade-forward back-propagation network modeling of spearmint oil extraction in a packed bed using SC-$CO_2$. J. Supercrit. Fluids 73, 108–115.

152. Lee, A.K.K., Bulley, N.R., Fattori, M., Meisen, A., 1986. Modelling of supercritical carbon dioxide extraction of canola oilseed in fixed beds. J. Am. Oil Chem. Soc. 63, 921–925.

153. Lenucci, M.S., De Caroli, M., Marrese, P.P., Iurlaro, A., Rescio, L., Böhm, V., Dalessandro, G., Piro, G., 2015. Enzyme-aided extraction of lycopene from high-pigment tomato cultivars by supercritical carbon dioxide. Food Chem. 170, 193–202.

154. Li, J. lin, Jin, J. su, Zhang, Z. ting, Wang, Y. bo, 2011. Measurement and correlation of solubility of benzamide in supercritical carbon dioxide with and without cosolvent. Fluid Phase Equilib. 307, 11–15.

155. Librando, V., Hutzinger, O., Tringali, G., Aresta, M., 2004. Supercritical fluid extraction of polycyclic aromatic hydrocarbons from marine sediments and soil samples. Chemosphere 54, 1189–1197.

156. Lin, M., Tsai, M., Wen, K., 1999. Supercritical fluid extraction of flavonoids from Scutellariae Radix.PDF. J. Chromatogr. A 830, 387–395.

157. Ling, Y.C., Liao, J.H., 1996. Matrix effect on supercritical fluid extraction of organochlorine pesticides from sulfur containing soils. J. Chromatogr. A 754, 285–294.

158. Liu, J., Chen, P., He, J., Deng, L., Wang, L., Lei, J., Rong, L., 2014. Extraction of oil from Jatropha curcas seeds by subcritical fluid extraction. Ind. Crops Prod. 62, 235–241.

159. Liu, Z., Mei, L., Wang, Q., Shao, Y., Tao, Y., 2014. Optimization of subcritical fluid extraction of seed oil from Nitraria tangutorum using response surface methodology. LWT - Food Sci. Technol. 56, 168–174.

160. Lu, T., Gaspar, F., Marriott, R., Mellor, S., Watkinson, C., Al-Duri, B., Seville, J., Santos, R., 2007. Extraction of borage seed oil by compressed $CO_2$: Effect of extraction parameters and modelling. J. Supercrit. Fluids 41, 68–73.

161. Lundstedt, T., Seifert, E., Abramo, L., Thelin, B., Nystrom, A., Pettersen, J., Bergman, R., 1998. Experimental design and optimization. Chemom. Intell. Lab. Syst. 42, 3–40.

162. Luo, H., Rui, W., 2015. Calculation of solubility parameter of supercritical $CO_2$ by molecular dynamics simulation. Acta Pet. Sin. 31, 78–83.

163. Madras, G., Kumar, R., Modak, J., 2004. Synthesis of Octyl Palmitate in various supercritical fluids. Ind. Eng. Chem. Res. 43, 7697–7701.

164. Maksimovic, S., Ivanovic, J., Skala, D., 2012. Supercritical extraction of essential oil from Mentha and mathematical modelling- the influence of plant particle size. Procedia Eng. 42, 1767–1777.

165. Maran, J.P., Priya, B., 2015. Supercritical fluid extraction of oil from muskmelon (Cucumis melo) seeds. J. Taiwan Inst. Chem. Eng. 47, 71–78.

166. Marr, R., Gamse, T., 2000. Use of supercritical fluids for different processes including new developments — a review. Chem. Eng. Process. 39, 19–28.

167. Marrone, C., Poletto, M., Reverchon, E., Stassi, A., 1998. Almond oil extraction by supercritical CO2: Experiments and modelling. Chem. Eng. Sci. 53, 3711–3718.

168. Martin, L., Gonzalez-Coloma, A., Diaz, C.E., Mainar, A.M., Urieta, J.S., 2011. Supercritical CO2 extraction of Persea indica: Effect of extraction parameters, modelling and bioactivity of its extracts. J. Supercrit. Fluids 57, 120–128.

169. Martinez, J., Martinez, J.M., 2008. Fitting the Sovova's supercritical fluid extraction model by means of a global optimization tool. Comput. Chem. Eng. 32, 1735–1745.

170. Martínez, J., Monteiro, A.R., Rosa, P.T. V, Rcia, M., Marques, O.M., Angela, M., Meireles, A., 2003. Multicomponent model to describe extraction of Ginger Oleoresin with supercritical carbon dioxide. ind. Eng. Chem. Res. 42, 1057–1063.

171. Martinez, J., Rosa, P.T.V., Meireles, M.A.A., 2007. Extraction of Clove and Vetiver oils with supercritical carbon dioxide: Modeling and Simulation. Open Chem. Eng. Journal,11 1-7 1, 1–7.

172. Meher, L.C., Dharmagadda, V.S.S., Naik, S.N., 2006. Optimization of alkali-catalyzed transesterification of Pongamia pinnata oil for production of biodiesel. Bioresour. Technol. 97, 1392–1397.

173. Meher, L.C., Naik, S.N., Das, L.M., 2004. Methanolysis of Pongamia pinnata ( karanja ) oil for production of biodiesel. J. od Sci. Ind. Res. 63, 913–918.

174. Melanie, M., 1999. An Introduction to Genetic Algorithms, 5th ed. London, England.

175. Mezzomo, N., Martínez, J., Ferreira, S.R.S., 2009. Supercritical fluid extraction of peach (Prunus persica) almond oil: Kinetics, mathematical modeling and scale-up. J. Supercrit. Fluids 51, 10–16.

176. Michalewicz, Z., 1992. Genetic Algorithms + Data Structures = Evolution Programs, First edit. ed. Springer-Verlag Berlin Heidelberg, New York.

177. Micic, V., Novakovic, D., Lepojevic, Ž., Jotanovic, M., Pejovic, B., Dugic, P., Petrovic, Z., 2011. Supercritical fluid extraction with carbon dioxide at different pressures. Contemp. Mater. 2, 84–87.

178. Minu, V., Harsh, V., Ravikant, T., Paridhi, J., Noopur, S., 2012. Medicinal plants of chhattisgarh with anti-snake venom property. Int. J. Curr. Pharm. Rev. Res. 3, 1–10.

179. Mira, B., Blasco, M., Berna, A., Subirats, S., 1999. Supercritical $CO_2$ extraction of essential oil from orange peel. Effect of operation conditions on the extract composition. J. Supercrit. Fluids 14, 95–104.

180. Mira, B., Blasco, M., Subirats, S., Berna, A., 1996. Supercritical $CO_2$ extraction of essential oils from Orange Peel. J. Supercrit. Fluids 9, 238–243.

181. Mishra, V., Saxena, D.K., Das, M., 2009. Effect of argemone oil and argemone alkaloid, sanguinarine on sertoli-germ cell coculture. Toxicol. Lett. 186, 104–110.

182. Mongkholkhajornsilp, D., Douglas, S., Douglas, P.L., Elkamel, A., Teppaitoon, W., Pongamphai, S., 2005. Supercritical $CO_2$ extraction of nimbin from neem seeds - A modelling study. J. Food Eng. 71, 331–340.

183. Montanes, F., Catchpole, O.J., Tallon, S., Mitchell, K.A., Scott, D., Webby, R.F., 2018. Extraction of apple seed oil by supercritical carbon dioxide at pressures up to 1300 bar. J. Supercrit. Fluids 141, 128–136.

184. Montgomery, D.C., 2004. Design and analysis of Experiments, 5th ed.

185. Moyler, D.A., 1993. Extraction of essential oils with carbon dioxide. Flavour Fragr. J. 8, 235–247.

186. Mukhopadhyay, M., 2000. Natural Extracts Using Supercritical Carbon Dioxide. CRC Press, Washington D.C.

187. Mukta, N., Sreevalli, Y., 2010. Propagation techniques, evaluation and improvement of the biodiesel plant, Pongamia pinnata (L.) Pierre - A review. Ind. Crop. Prod. Prod. 31, 1–12.

188. Nagy, B., Simandi, B., 2008. Effects of particle size distribution, moisture content, and initial oil content on the supercritical fluid extraction of paprika. J. Supercrit. Fluids 46, 293–298.

189. Naik, S., Goud, V. V., Rout, P.K., Dalai, A.K., 2010a. Supercritical $CO_2$ fractionation of bio-oil produced from wheat-hemlock biomass. Bioresour. Technol. 101, 7605–7613.

190. Naik, S.N., Lentz, H., Maheshwari, R.C., 1989. Extraction of perfumes and flavours from plant materials with liquidcarbon dioxide under liquid-vapor equilibrium conditions. Fluid Phase Equilib. 49, 115–126.

191. Nei, H.Z.N., Fatemi, S., Mehrnia, M.R., Salimi, A., 2008. Mathematical modeling and study of mass transfer parameters in supercritical fluid extraction of fatty acids from Trout powder. Biochem. Eng. J. 40, 72–78.

192. Nguyen, H.N., Gaspillo, P.D., Maridable, J.B., Malaluan, R.M., Hinode, H., Salim, C., Huynh, H.K.P., 2011. Extraction of oil from Moringa oleifera kernels using supercritical carbon dioxide with ethanol for pretreatment: optimization of the extraction process. Chem. Eng. Process. Process Intensif. 50, 1207–1213.

193. Ni, Q., Gao, Q., Yu, W., Liu, X., Xu, G., Zhang, Y., 2015. Supercritical carbon dioxide extraction of oils from two Torreya grandis varieties seeds and their physicochemical and antioxidant properties. LWT - Food Sci. Technol. 60, 1226–1234.

194. Nimet, G., da Silva, E.A., Palu, F., Dariva, C., Freitas, L. dos S., Neto, A.M., Filho, L.C., 2011. Extraction of sunflower (Heliantus annuus L.) oil with supercritical CO2 and subcritical propane: experimental and modeling. Chem. Eng. J. 168, 262–268.

195. Notar, M., Leskovsek, H., 1997. Optimisation of supercritical fluid extraction of polynuclear aromatic hydrocarbons from spiked soil and marine sediment standard reference material. Fresenius J. Anal. Chem. 358, 623–629.

196. Obadiah, A., Kannan, R., Ramasubbu, A., Kumar, S.V., 2012. Studies on the effect of antioxidants on the long-term storage and oxidation stability of Pongamia pinnata (L.) Pierre biodiesel. Fuel Process. Technol. 99, 56–63.

197. Ozkal, S.G., Yener, M.E., 2016. Supercritical carbon dioxide extraction of flaxseed oil: effect of extraction parameters and mass transfer modeling. J. Supercrit. Fluids 112, 76–80.

198. Panayiotou, C., 1997. Solubility parameter revisited: an equation-of-state approache for its estimation. Fluid Phase Equilib. 131, 21–35.

199. Pandey, A. kumar, Bajpai, A.K., Kumar, A., Pal, M., Baboo, V., Dwivedi, A., 2014. Isolation, identification, molecular and electronic structure, vibrational spectroscopic investigation, and anti-HIV-1 activity of Karanjin using density functional theory. J. Theor. Chem. 14, 1–13.

200. Papamichail, I., Louli, V., Magoulas, K., 2000. Supercritical fluid extraction of celery seed oil. J. Supercrit. Fluids 18, 213–226.

201. Patel, R.N., Bandyopadhyay, S., Ganesh, A., 2011. A simple model for super critical fluid extraction of bio oils from biomass. Energy Convers. Manag. 52, 652–657.

202. Patil, P.D., Dandamudi, K.P.R., Wang, J., Deng, Q., Deng, S., 2018. Extraction of bio-oils from algae with supercritical carbon dioxide and co-solvents. J. Supercrit. Fluids 135, 60–68.

203. Pavithra, H.R., Gowda, B., Kumar, K.R., Prasanna, K.T., Shivanna, M.B., 2012. Oil, fatty acid profile and karanjin content in developing pongamia pinnata (L.) pierre seeds. J. Am. Oil Chem. Soc. 89, 2237–2244.

204. Pederssetti, M.M., Palu, F., Da Silva, E.A., Rohling, J.H., Cardozo-Filho, L., Dariva, C., 2011. Extraction of canola seed (Brassica napus) oil using compressed propane and supercritical carbon dioxide. J. Food Eng. 102, 189–196.

205. Perakis, C., Louli, V., Magoulas, K., 2005. Supercritical fluid extraction of black pepper oil. J. Food Eng. 71, 386–393.

206. Perakis, C., Louli, V., Voutsas, E., Magoulas, K., 2010. Supercritical $CO_2$ extraction of dittany oil: Experiments and modelling. J. Supercrit. Fluids 55, 573–578.

207. Perrut, M., 2012. Sterilization and virus inactivation by supercritical fluids (a review). J. Supercrit. Fluids 66, 359–371.

208. Perrut, M., Clavier, J.Y., Poletto, M., Reverchon, E., 1997. Mathematical Modeling of Sunflower Seed Extraction by Supercritical $CO_2$. Ind. Eng. Chem. Res. 36, 430–435.

209. Pfaf-Sovljanski, I.I., Grujic, O.S., Perunicic, M.B., Cvetkovic, I.M., Zekovic, Z.P., 2005. Supercritical carbon dioxide hop extraction. Acta Period. Technol. 36, 111–121.

210. Phelps, C.L., Smart, N.G., Wai, C.M., 1996. Past, present, and possible future applications of supercritical fluid extraction technology. J. Chem. Educ. 73, 1163–1168.

211. Pilavtepe, M., Yucel, M., Helvaci, S.S., Demircioglu, M., Yesil-Celiktas, O., 2012. Optimization and mathematical modeling of mass transfer between Zostera marina residues and supercritical $CO_2$ modified with ethanol. J. Supercrit. Fluids 68, 87–93.

212. Pilkington, J.L., Preston, C., Gomes, R.L., 2014. Comparison of response surface methodology (RSM) and artificial neural networks (ANN) towards efficient extraction of artemisinin from Artemisia annua. Ind. Crops Prod. 58, 15–24.

213. Pinto, M.E.A., Araújo, S.G., Morais, M.I., Sá, N.P., Caroline, M., 2017. Antifungal and antioxidant activity of fatty acid methyl esters from vegetable oils. Ann. Brazilian Acad. Sci. 89, 1671–1681.

214. Poling, B.E., Prausnitz, M., O'Connell, J.P., 2001. The Properties of Gases and Liquids, 5th ed, Library. McGRAW HILL, New York.

215. Pourmortazavi, S.M., Hajimirsadeghi, S.S., 2007. Supercritical fluid extraction in plant essential and volatile oil analysis. J. Chromatogr. A 1163, 2–24.

216. Povh, N.P., Marques, M.O.M., Meireles, M.A.A., 2001. Supercritical $CO_2$ extraction of essential oil and oleoresin from chamomile (Chamomilla recutita [L.] Rauschert). J. Supercrit. Fluids 21, 245–256.

217. Prabha, T., Dorababu, M., Goel, S., Agarwal, P.K., Singh, A., Joshi, A., Goel, A.K., 2009. Effect of methanol extract of Pongamia pinnata Linn seed on gastro-duodenal ulceration and mucosal offensive and defensive factors in rats. Indian J. Exp. Biiology 47, 649–659.

218. Prabhu, T.M., Devakumar, C., Sastry, V.R.B., Agrawal, D.K., 2002. Quantification of Karanjin using high performance liquid chromatography in raw and detoxified Karanj (Pongamia glabra vent) seed cake. Asian-Australasian J. Anim. Sci. 15, 416–420.

219. Pradhan, R.C., Naik, S.N., Bhatnagar, N., Swain, S.K., 2008. Moisture-dependent physical properties of Karanja (Pongamia pinnata) kernel. Ind. Crops Prod. 28, 155–161.

220. Prajapati, N., Purohit, S., Sharma, A., 2003. A handbook of medicinal plants, 2nd ed. Agrobios, Jodhpur, India.

221. Pramanik, P., Das, P., Kim, P.J., 2012. Preparation of biofuel from argemone seed oil by an alternative cost-effective technique. Fuel 91, 81–86.

222. Przygoda, K., Wejnerowska, G., 2015. Extraction of tocopherol-enriched oils from Quinoa seeds by supercritical fluid extraction. Ind. Crops Prod. 63, 41–47.

223. Qiao, C., Chen, G., Zhang, J., Yao, J., 2016. Structure and rheological properties of cellulose nanocrystals suspension. Food Hydrocoll. 55, 19–25.

224. Rabelo, S.N., Ferraz, V.P., Oliveira, L.S., Franca, A.S., 2015. FTIR analysis for quantification of fatty acid methyl esters in biodiesel produced by microwave-assisted transesterification. Int. J. Environ. Sci. Dev. 6, 964–969.

225. Radzali, S.A., Baharin, B.S., Othman, R., Markom, M., Rahman, R.A., 2014. Co-solvent selection for supercritical fluid extraction of astaxanthin and other carotenoids from penaeus monodon waste. J. Oleo Sci. 63, 1–9.

226. Rahman, M.S., Seo, J.K., Choi, S.G., Gul, K., Yang, H.S., 2018. Physicochemical characteristics and microbial safety of defatted bovine heart and its lipid extracted with supercritical-CO2 and solvent extraction. LWT-Food Sci. Technol. 97, 355–361.

227. Rahman, W., Ilyas, M., 1962. Flavonoids from Argemone mexicana linn. (Papaveraceae). Flower Pigment. 27, 153–155.

228. Rai, A., Mohanty, B., Bhargava, R., 2016a. Supercritical extraction of sunflower oil: a central composite design for extraction variables. Food Chem. 192, 647–659.

229. Rai, A., Mohanty, B., Bhargava, R., 2016b. Fitting of broken and intact cell model to supercritical fluid extraction (SFE) of sunflower oil. Innov. Food Sci. Emerg. Technol. 38, 32–40.

230. Rai, A., Mohanty, B., Bhargava, R., 2015. Modeling and response surface analysis of supercritical extraction of watermelon seed oil using carbon dioxide. Sep. Purif. Technol. 141,

354–365.

231. Rai, A., Punase, K.D., Mohanty, B., Bhargava, R., 2014. Evaluation of models for supercritical fluid extraction. Int. J. Heat Mass Transf. 72, 274–287.

232. Rajvaidhya, S., Nagori, B.P., Singh, G.K., Dubey, B.K., Desai, P., Jain, S., 2012. A review on Argemone mexicana Linn. - an Indian medicinal plant. Int. J. Pharm. Sci. Res. 3, 2494–2501.

233. Rao, G.R., Shanker, A.K., Srinivas, I., Korwar, G.R., Venkateswarlu, B., 2011. Diversity and variability in seed characters and growth of Pongamia pinnata ( L .) Pierre accessions. Trees - Struct. Funct. 25, 725–734.

234. Rao, R.Y., Zubaidha, P. k, Kondhare, D. d, Reddy, N.J., Deshmukh, S.S., 2012. Biodiesel production from Argemone mexicana seed oil using crystalline manganese carbonate. Polish J. Chem. Technol. 14, 65–70.

235. Razal, R.A., Daracan, V.C., Calapis, R.M., Angon, C.M.M., Demafelis, R.B., 2012. Solvent extraction of oil from Bani (Pongamia pinnata (L.) Pierre) seeds. Philipp. J. Crop Sci. 37, 1–7.

236. Rebolleda, S., Rubio, N., Beltrán, S., Sanz, M.T., González-Sanjosé, M.L., 2012. Supercritical fluid extraction of corn germ oil: Study of the influence of process parameters on the extraction yield and oil quality. J. Supercrit. Fluids 72, 270–277.

237. Reis-Vasco, E.M.C., Coelho, J.A.P., Palavra, A.M.F., Marrone, C., Reverchon, E., 2000. Mathematical modelling and simulation of pennyroyal essential oil supercritical extraction. Chem. Eng. Sci. 55, 2917–2922.

238. Reverchon, E., 1996. Mathematical modeling of supercritical extraction of Sage oil. AIChE J. 42, 1765–1771.

239. Reverchon, E., Donsi, G., Osseo, L.S., 1993. Modeling of supercritical fluid extraction from herbaceous matrices. Ind. Eng. Chem. Res. 32, 2721–2726.

240. Reverchon, E., Kaziunas, A., Marrone, C., 2000. Supercritical $CO_2$ extraction of hiprose seed oil: experiments and mathematical modelling. Chem. Eng. Sci. 55, 2195–2201.

241. Reverchon, E., Osseo, L.S., Gorgoglione, D., 1994. Supercritical $CO_2$ extraction of basil oil: Characterization of products and process modeling. J. Supercrit. Fluids 7, 185–190.

242. Reverchon, E., Poletto, M., 1996. Mathematical modelling of supercritical $CO_2$ fractionation of flower concretes. Chem. Eng. Sci. 51, 3741–3753.

243. Reverchon, E., Senatore, F., 1992. Isolation of rosemary oil: comparison between hydrodistillation and supercritical $CO_2$ extraction. Flavour Fragr. J. 7, 227–230.

244. Rochova, K., Sovova, H., Sobolík, V., Allaf, K., 2008. Impact of seed structure modification on the rate of supercritical $CO_2$ extraction. J. Supercrit. Fluids 44, 211–218.

245. Rodrigues, V.H., de Melo, M.M.R., Portugal, I., Silva, C.M., 2018. Extraction of Eucalyptus leaves using solvents of distinct polarity. Cluster analysis and extracts characterization. J. Supercrit. Fluids 135, 263–274.

246. Roy, B.C., Goto, M., Hirose, T., 1996. Extraction of Ginger oil with Supercritical carbon dioxide: Experiments and modeling. Ind. Eng. Chem. Res. 35, 607–612.

247. Roy, B.C., Goto, M., Hirose, T., Navaro, O., Hortacsu, O., 1994. Extraction rate of oil from tomato seed with supercriticle carbon dioxide. J. Chem. Eng. 27, 768–772.

248. Roy, B.C., Sasaki, M., Goto, M., 2006. Effect of temperature and pressure on the extraction yield of oil from sunflower seed with supercritical carbon dioxide. J. Appl. Sci. 6, 71–75.

249. Ruetsch, L., Daghero, J., Mattea, M., 2003. Supercritical extraction of solid matrices. Model formulation and experiments. Lat. Am. Appl. Res. 33, 103–107.

250. Sabet, J.K., Ghotbi, C., Dorkoosh, F., Striolo, A., 2012. Solubilities of acetaminophen in supercritical carbon dioxide with and without menthol cosolvent: measurement and correlation. Sci. Iran. 19, 619–625.

251. Sahu, A., Bala, S.N., Mohanty, S., 2015. A study on optimization through genetic algorithm. Int. J. Appl. Sci. Math. 2, 62–64.

252. Saikaew, C., Kajorncheappunngam, S., 2008. An application of design of experiments and response surface methodology to optimize proanthocyanidins yield extracted from Grape seeds, in: Technology and Innovation for Sustainable Development Conference. Thailand, pp. 725–733.

253. Salea, R., Veriansyah, B., Tjandrawinata, R.R., 2017. Optimization and scale-up process for supercritical fluids extraction of ginger oil from Zingiber officinale var . Amarum. J. Supercrit. Fluids 120, 285–294.

254. Salgin, U., Doker, O., Calimli, A., 2006. Extraction of sunflower oil with supercritical $CO_2$: experiments and modeling. J. Supercrit. Fluids 38, 326–331.

255. Salgin, U., Korkmaz, H., 2011. A green separation process for recovery of healthy oil from pumpkin seed. J. Supercrit. Fluids 58, 239–248.

256. Salgın, U., Salgın, S., Ekici, D.D., Uludağ, G., 2016. Oil recovery in rosehip seeds from food plant waste products using supercritical $CO_2$ extraction. J. Supercrit. Fluids 118, 194–202.

257. Sangwan, S., Rao, D. V, Sharma, R.A., 2010. A review on Pongamia Pinnata ( L .) Pierre : a great versatile leguminous plant. Nat. Sci. 8, 130–139.

258. Santos, F.J., Jauregui, O., Pinto, F.J., Galceran, M.T., 1998. Experimental design approach for the optimization of supercritical fluid extraction of chlorophenols from polluted soils. J. Chromatogr. A 823, 249–258.

259. Sarin, A., Arora, R., Singh, N.P., Sarin, R., Sharma, M., Malhotra, R.K., 2010. Effect of metal contaminants and antioxidants on the oxidation stability of the methyl ester of pongamia. J. Am. Oil Chem. Soc. 87, 567–572.

260. Sarkari, M., Knutson, B.L., Chen, C.S., 1999. Enzymatic catalysis in cosolvent modified pressurized organic solvents. Biotechnol. Bioeng. 65, 258–264.

261. Sasmal, S., Goud, V. V., Mohanty, K., 2012. Characterization of biomasses available in the region of North-East India for production of biofuels. Biomass and Bioenergy 45, 212–220.

262. Savage, P.E., Gopalan, S., Mizan, T.I., Martino, C.J., Brock, E.E., 1995. Reactions at supercritical conditions: applications and fundamentals. AIChE J. 41, 1723–1778.

263. Savithramma, N., Sulochana, C., Rao, K.N., 2007. Ethnobotanical survey of plants used to treat asthma in Andhra Pradesh, India. J. Ethnopharmacol. 113, 54–61.

264. Schaeffer, S.T., Zalkow, L.H., Teja, A.S., 1989. Modelling of the supercritical fluid extraction of monocrotaline from Crotalaria Spectabilis. J. Supercrit. Fluids 2, 15–21.

265. Schmitt, W.J., Reid, R.C., 1986. The use of entrainers in modifying the solubility of phenanthrene and benzoic acid in supercritical carbon dioxide and ethane. Fluid Phase Equilib. 32, 77–99.

266. Scopel, R., Neto, R.G., Falcão, M.A., Cassel, E., Vargas, R.M.F., 2013. Supercritical $CO_2$ extraction of Schinus molle L with co-solvents: Mathematical modeling and antimicrobial applications. Brazilian Arch. Biol. Technol. 56, 513–519.

267. Senyay-Oncel, D., Ertas, H., Yesil-Celiktas, O., 2011. Effects of supercritical fluid extraction parameters on unsaturated fatty acid yields of pistacia terebinthus berries. J. Am. Oil Chem. Soc. 88, 1061–1069.

268. Shadangi, K.P., Mohanty, K., 2014. Kinetic study and thermal analysis of the pyrolysis of non-edible oilseed powders by thermogravimetric and differential scanning calorimetric analysis. Renew. Energy 63, 337–344.

269. Shadangi, K.P., Mohanty, K., 2013. Characterization of nonconventional oil containing seeds towards the production of bio-fuel. J. Renew. Sustain. Energy 5, 1–13.

270. Shahidi, F., 2005. Bailey's Industrial Oil and fat oil and Fat Products, 6th ed. A John Wiley & Sons, Inc.,.

271. Shameel, S., Usmanghani, K., Ali, M.S., Ahmad, V.U., 1996. Chemical constituents from the seeds of Pongamia pinnata (L.) Pierre. Pak. J. Pharm. Sci. 9, 11–20.

272. Sharif, K.M., Rahman, M.M., Azmir, J., Mohamed, A., Jahurul, M.H.A., Sahena, F., Zaidul, I.S.M., 2014. Experimental design of supercritical fluid extraction - a review. J. Food Eng. 124, 105–116.

273. Sharma, J., Gairola, S., Gaur, R.D., Painuli, R.M., 2012. The treatment of jaundice with medicinal plants in indigenous communities of the sub-Himalayan region of Uttarakhand, India. J. Ethnopharmacol. 143, 262–291.

274. Sheibani, A., Ghaziaskar, H.S., 2008. Pressurized fluid extraction of pistachio oil using a modified supercritical fluid extractor and factorial design for optimization. LWT - Food Sci. Technol. 41, 1472–1477.

275. Silva, C.F., Huang, Z., Yang, M.J., Liu, S.F., Ma, Q., 2008. Supercritical carbon dioxide extraction of Baizhu: experiments and modeling. J. Supercrit. Fluids 58, 31–39.

276. Silva, D.C.M.N., Bresciani, L.F. V, Dalagnol, R.L., Danielski, L., Yunes, R.A., Ferreira, S.R.S., 2009. Supercritical fluid extraction of carqueja (Baccharis trimera) oil: Process parameters and composition profiles. Food Bioprod. Process. 87, 317–326.

277. Singh, D., Singh, S.P., 2010. Low cost production of ester from non edible oil of Argemone mexicana. Biomass and Bioenergy 34, 545–549.

278. Singh, D., Singh, S.P., Prerna, P., 2010. Production of both esters and biogas from Mexican poppy. African J. Environ. Sci. Technol. 4, 866–871.

279. Skerget, M., Knez, E., 2001. Modelling high pressure extraction processes. Comput. Aided Chem. Eng. 25, 879–886.

280. Sodeifian, G., Ardestani, N.S., Sajadian, S.A., Moghadamian, K., 2018. Properties of portulaca oleracea seed oil via supercritical fluid extraction: experimental and optimization. J. Supercrit. Fluids 135, 34–44.

281. Sodeifian, G., Ghorbandoost, S., Sajadian, S.A., Saadati Ardestani, N., 2016b. Extraction of oil from Pistacia khinjuk using supercritical carbon dioxide: Experimental and modeling. J. Supercrit. Fluids 110, 265–274.

282. Sodeifian, G., Sajadian, S.A., Saadati Ardestani, N., 2017. Supercritical fluid extraction of omega-3 from Dracocephalum kotschyi seed oil: process optimization and oil properties. J. Supercrit. Fluids 119, 139–149.

283. Sodeifian, G., Sajadian, S.A., Saadati Ardestani, N., 2016c. Extraction of Dracocephalum kotschyi Boiss using supercritical carbon dioxide: Experimental and optimization. J. Supercrit. Fluids 107, 137–144.

284. Solati, Z., Baharin, B.S., Bagheri, H., 2012. Supercritical carbon dioxide (SC-$CO_2$) extraction of Nigella sativa L . oil using full factorial design. Ind. Crops Prod. 36, 519–523.

285. Sovova, H., 1994. Rate of the vegetable oil extraction with supercritical $CO_2$-I. modelling of extraction curves. Chem. Eng. Sci. 49, 409–414.

286. Sovova, H., Kucera, J., J Jez, 1994. Rate of the vegetable oil extraction with extraction of Grape Oil. Chem. Eng. Sci. 49, 415–420.

287. Stahl, E., Schutz, E., Mangold, H.K., 1980. Extraction of seed oils with liquid and supercritical carbon dioxide. J. Agric. Food Chem. 28, 1153–1157.

288. Stuart, B., 2005. Infrared Spectroscopy: fundamentals and applications. John Wiley & Sons, Ltd.

289. Sun, J.X., Sun, X.F., Sun, R.C., Su, Y.Q., 2004. Fractional extraction and structural characterization of sugarcane bagasse hemicelluloses. Carbohydr. Polym. 56, 195–204.

290. Sun, Y.C., Chung, Y.T., Mierzwa, J., 2001. Study of matrix influence on supercritical fluid extraction of polar mercury species from solid samples. Analyst 126, 1694–1699.

291. Suryawanshi, Mohanty, 2018a. Modeling and optimization: Supercritical $CO_2$ extraction of Pongamia pinnata (L.) seed oil. J. Environ. Chem. Eng. 6, 2660–2673.

292. Suryawanshi, Mohanty, 2018b. Modeling and optimization of process parameters for supercritical $CO_2$ extraction of Argemone mexicana (L.) seed oil. Chem. Eng. Commun. 1–20.

293. Suryawanshi, Mohanty, 2018c. Application of an artificial neural network model for the supercritical fluid extraction of seed oil from Argemone mexicana (L.) seeds. Ind. Crops Prod. 123, 64–74.

294. Taher, H., Al-Zuhair, S., Al-Marzouqi, A.H., Haik, Y., Farid, M., 2014. Mass transfer modeling of Scenedesmus sp. lipids extracted by supercritical $CO_2$. Biomass and Bioenergy 70, 530–541.

295. Tan, T.J., Jinap, S., Kusnadi, A.E., Hamid, N.S.A., 2008. Extraction of cocoa butter by supercritical carbon dioxide: Optimization of operating conditions and effect of particle size. J. Food Lipids 15, 263–276.

296. Tomita, K., Machmudah, S., Wahyudiono, Fukuzato, R., Kanda, H., Quitain, A.T., Sasaki, M., Goto, M., 2014. Extraction of rice bran oil by supercritical carbon dioxide and solubility consideration. Sep. Purif. Technol. 125, 319–325.

297. Tong, P., Imagawa, T., 1995. Optimization of supercritical fluid extraction for polychlorinated biphenyls from sediments. Anal. Chim. Acta 310, 93–100.

298. Ushiki, I., Kikuchi, K., Takahashi, N., Sato, Y., Ito, Y., Inomata, H., 2017. Desorption behavior of various volatile organic compounds from activated carbon in supercritical carbon dioxide: measurement and kinetic modeling. J. Supercrit. Fluids 121, 41–51.

299. Vargas, R.M.F., Cassel, E., Gomes, G.M.F., Longhi, L.G.S., Atti-Serafini, L., Atti-Santos, A.C., 2006. Supercritical extraction of carqueja essential oil: Experiments and modeling.

Brazilian J. Chem. Eng. 23, 375–382.

300. Viguera, M., Prieto, C., Casas, J., Casas, E., Cabañas, A., Calvo, L., 2018. The parameters that affect the supercritical extraction of 2,4,6-trichloroanisol from cork. J. Supercrit. Fluids 141, 137–142.

301. Vilegas, J.H.Y., Lanças, F.M., Vilegas, W., 1994. Application of a home-made supercritical fluid extraction system to the study of essential oils. Flavour Fragr. J. 9, 39–43.

302. Vismaya, Eipeson, W.S., Manjunatha, J.R., Srinivas, P., Kanya, T.C.S., 2010. Extraction and recovery of karanjin: a value addition to karanja ( Pongamia pinnata ) seed oil. Ind. Crop. Prod. 32, 118–122.

303. Wagner, M.E., French, J., Rizvi, S.S.H., 2013. Supercritical fluid extraction of oil from potato chips: Two scale comparison and mathematical modeling. J. Food Eng. 118, 100–107.

304. Wang, L., Wang, X., Wang, P., Xiao, Y., Liu, Q., 2016. Optimization of supercritical carbon dioxide extraction, physicochemical and cytotoxicity properties of Gynostemma pentaphyllum seed oil: a potential source of conjugated linolenic acids. Sep. Purif. Technol. 159, 147–156.

305. Wen, D., Jiang, H., Zhang, K., 2009. Supercritical fluids technology for clean biofuel production. Prog. Nat. Sci. 19, 273–284.

306. Westerman, D., Santos, R.C.D., Bosley, J.A., Rogers, J.S., Al-Duri, B., 2006. Extraction of Amaranth seed oil by supercritical carbon dioxide. J. Supercrit. Fluids 37, 38–52.

307. Williams, K.A., 1966. Oils, fats and fatty foods, 4th ed. J and A Churchill Ltd.

308. Wypych, G., 2001. Handbook of Solvents, 2nd ed, Chem Tech Publishing. Toronto.

309. Zachova, Z., Triska, J., Vrchotova, N., Balik, J., Sajfrtova, M., Sovova, H., 2018. Combining high-pressure methods for extraction of stilbenes from grape cane. J. Supercrit. Fluids 142, 38–44.

310. Zaragoza, R., Barna, L., Blanchard, J.M., 1998. Experimental design approach for the optimization of supercritical fluid extraction of pyralene and aldrin in soil matrix. Waste Manag. 18, 117–123.

311. Zekovic, Z., Bera, O., Durovic, S., Pavlic, B., 2017. Supercritical fluid extraction of coriander seeds: kinetics modelling and ANN optimization. J. Supercrit. Fluids 125, 88–95.

312. Zhang, M., Dou, M., Wang, M., Yu, Y., 2017. Study on the solubility parameter of supercritical carbon dioxide system by molecular dynamics simulation. J. Mol. Liq. 248, 322–329.

313. Zhang, S., Liu, W., Granata, G., 2018. Effects of grain size gradation on the porosity of packed heap leach beds. Hydrometallurgy 179, 238–244.

314. Zhao, S., Zhang, D., 2014. An experimental investigation into the solubility of Moringa oleifera oil in supercritical carbon dioxide. J. Food Eng. 138, 1–10.

315. Zhao, Y., Jung, K., Shimoyama, Y., Shimogaki, Y., Momose, T., 2018. Kinetic effects of methanol addition on supercritical fluid deposition of $TiO_2$. J. Supercrit. Fluids 138, 63–72.

316. Zheng, C. ji, Yoo, J., Lee, T., Cho, H., Kim, Y., Kim, W., 2005. Fatty acid synthesis is a target for antibacterial activity of unsaturated fatty acids. FEBS Lett. 579, 5157–5162.

317. Zosel, K., 1978. Separation with supercritical gases: practical applications. Angew. Chemie Int. Ed. English 17, 702–709.

A.1. GC chromatograms of a Std FAME mixture of 37 fatty acids components and of the oil samples obtained through the Soxhlet extraction method.

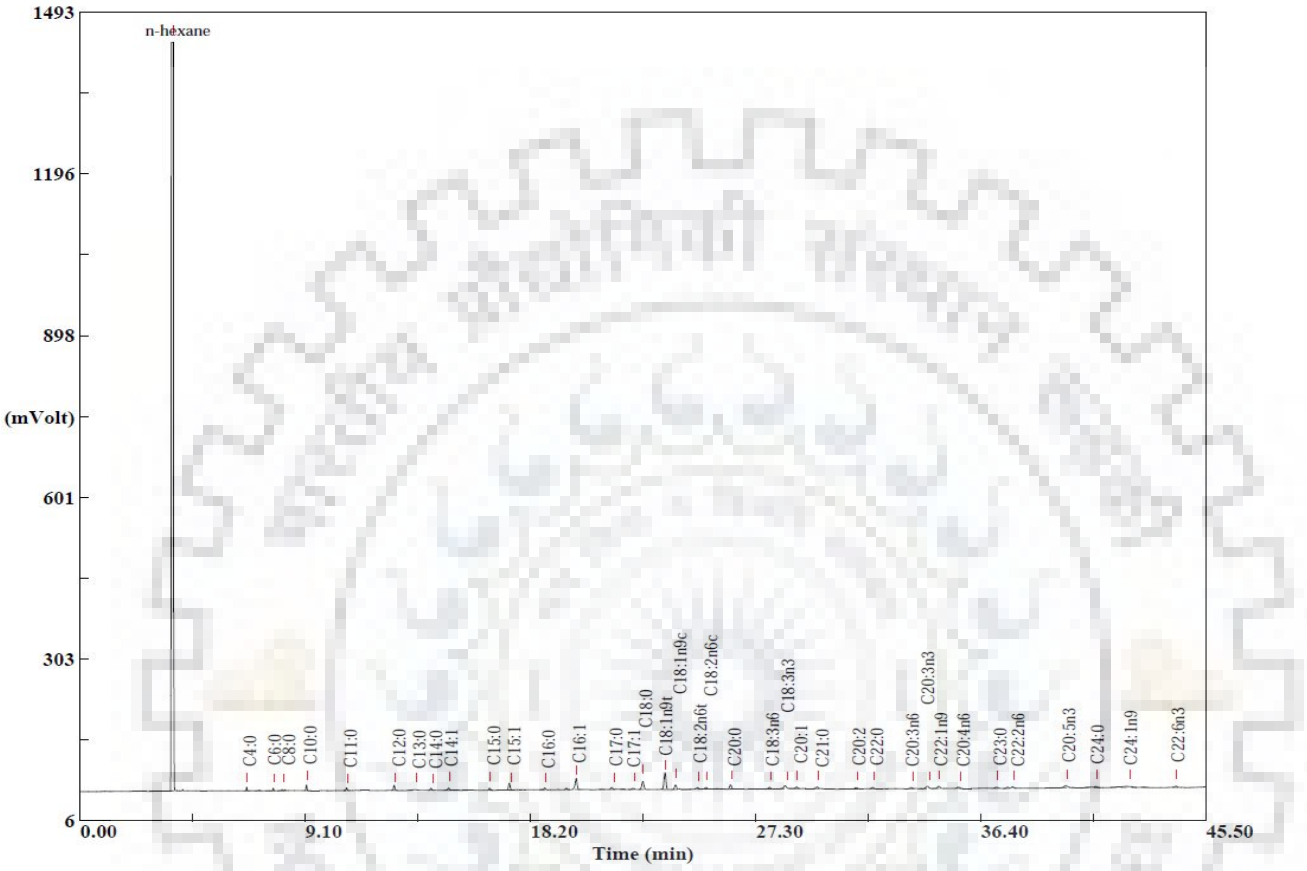


Fig. A.1: Calibration chromatogram with Std FAME mix of 37 FA components.

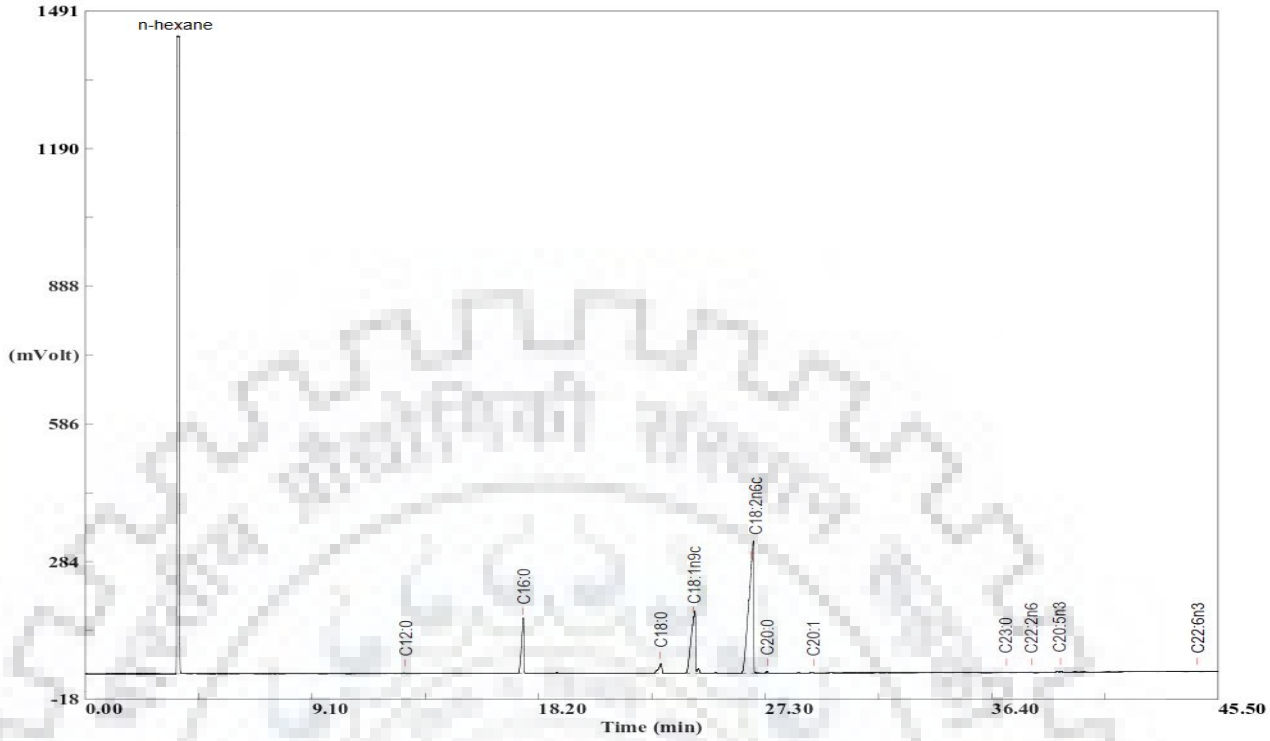


Fig. A.2: GC chromatogram of AM seed oil extracted by Soxhlet extraction method.

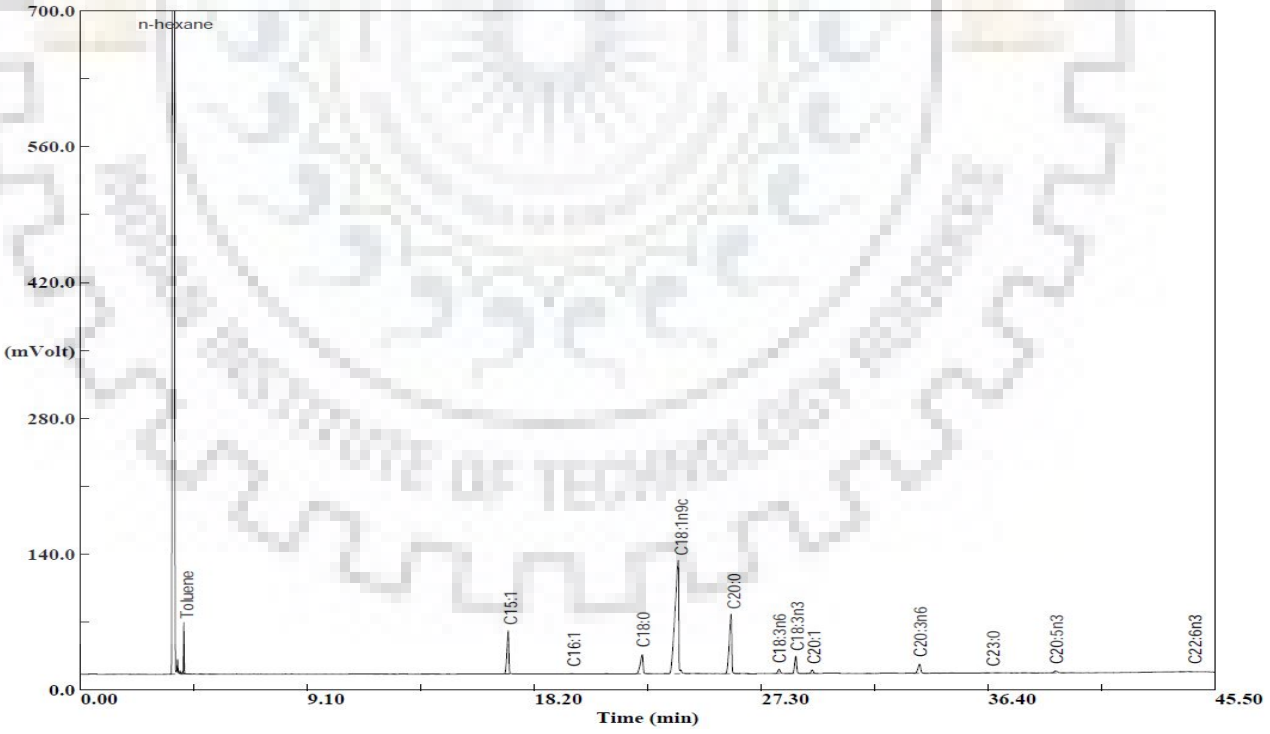


Fig. A.3: GC chromatogram of PP seed oil extracted by Soxhlet extraction method.

B.1. GC chromatograms of AM seed oil samples extracted in all 46 runs

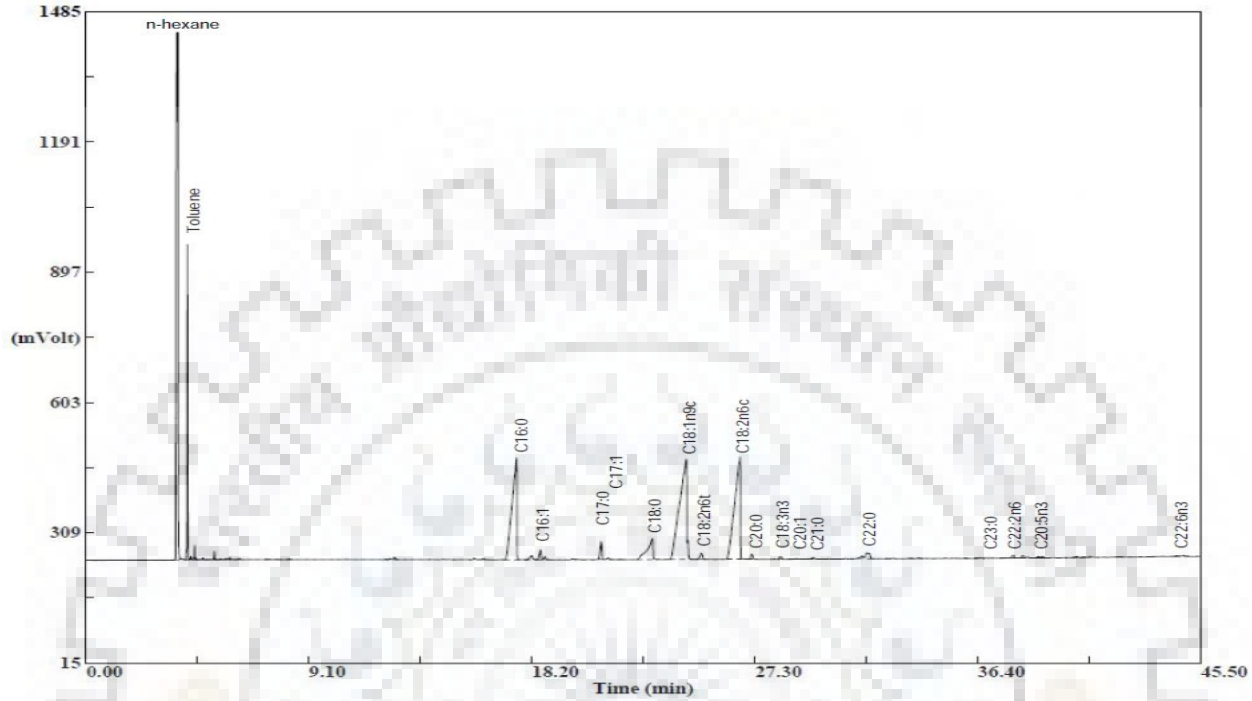


Fig. B.1: GC chromatogram of AM seed oil extracted by SFE in Run 01.

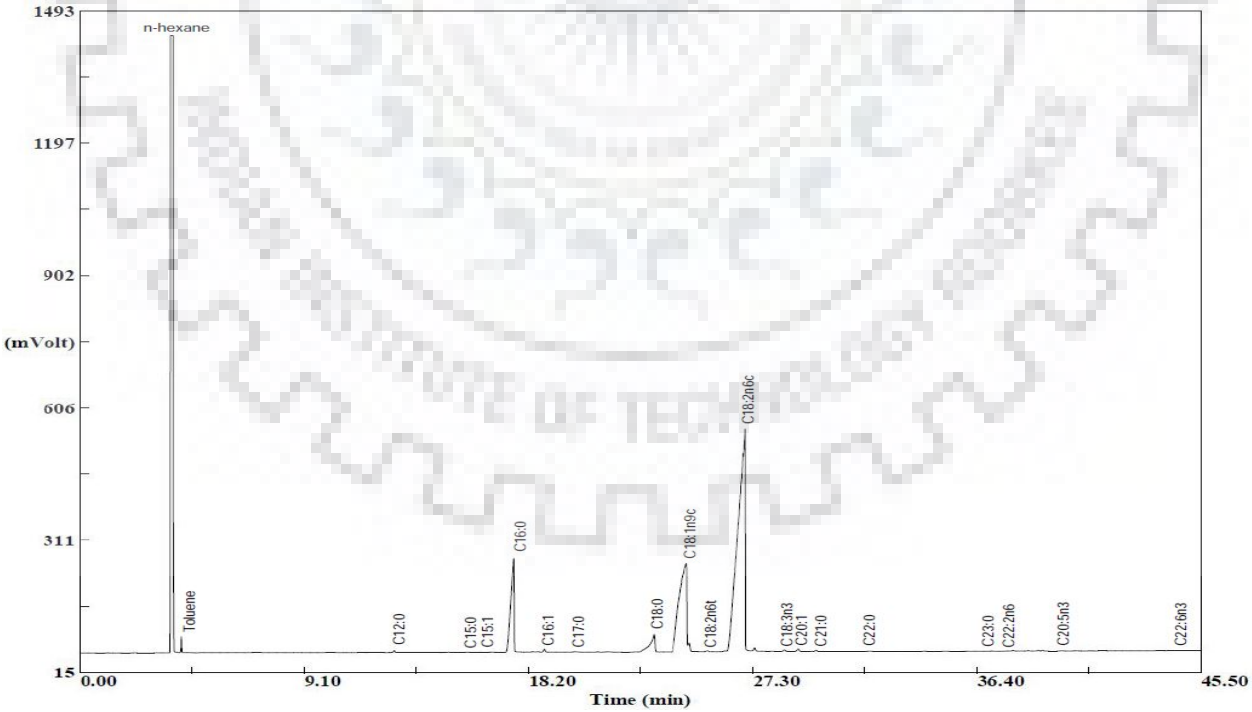


Fig. B.2: GC chromatogram of AM seed oil extracted by SFE in Run 02.

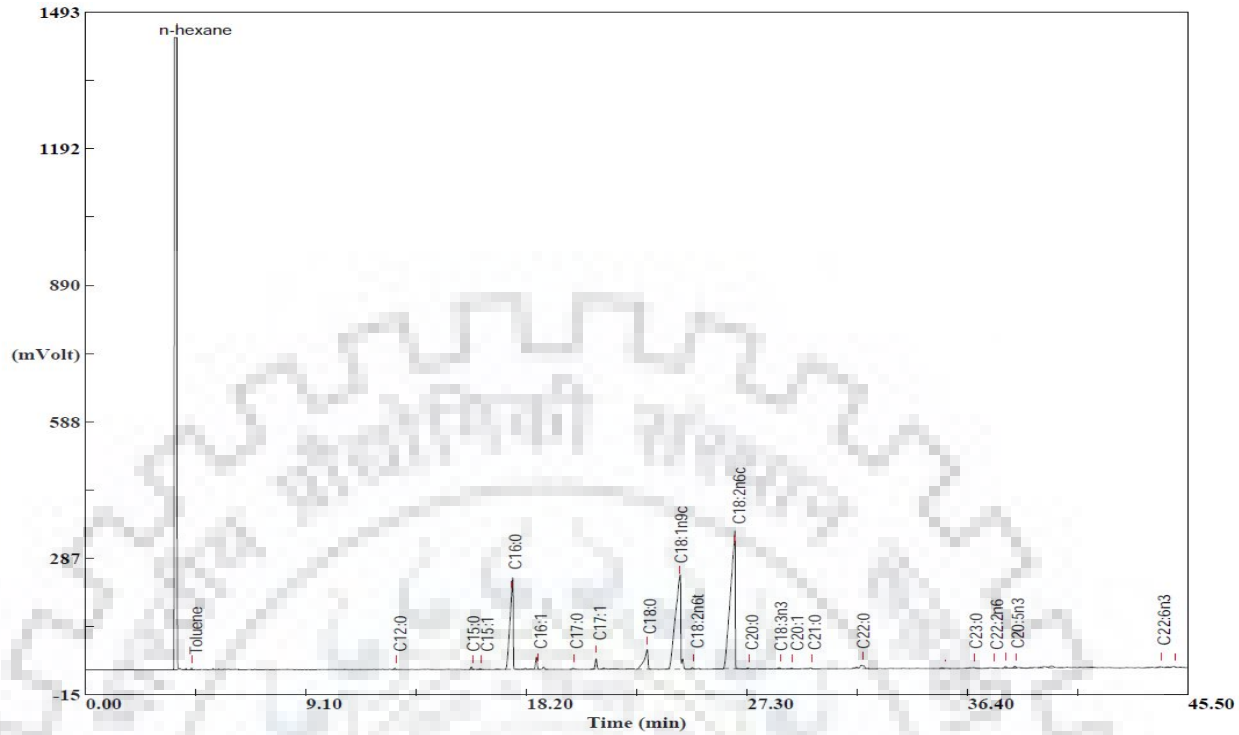


Fig. B.3: GC chromatogram of AM seed oil extracted by SFE in Run 03.

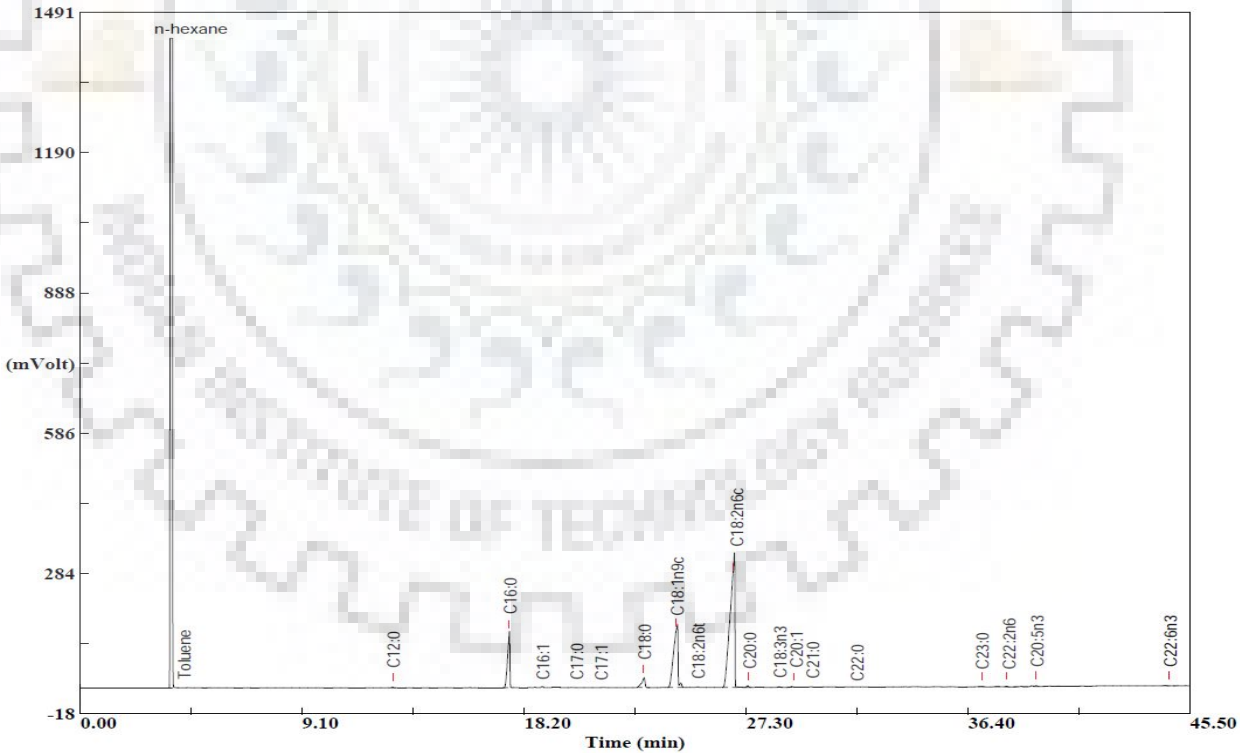


Fig. B.4: GC chromatogram of AM seed oil extracted by SFE in Run 04.

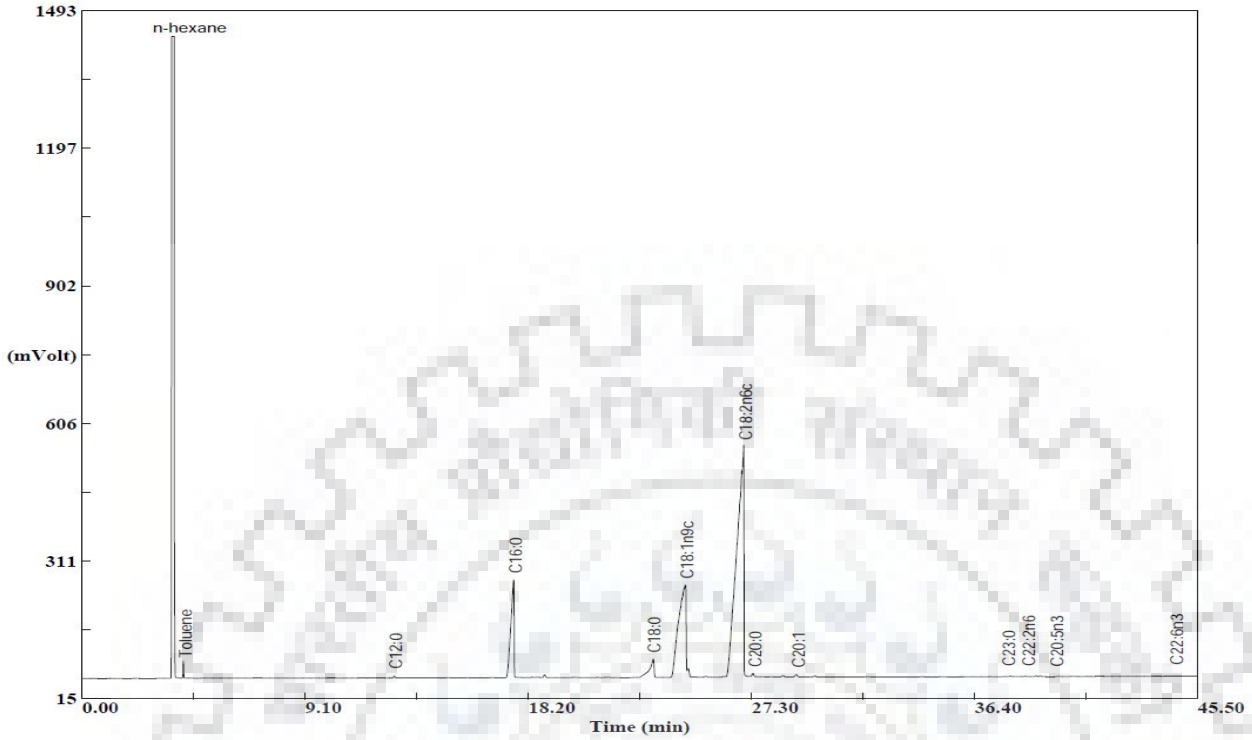


Fig. B.5: GC chromatogram of AM seed oil extracted by SFE in Run 05.

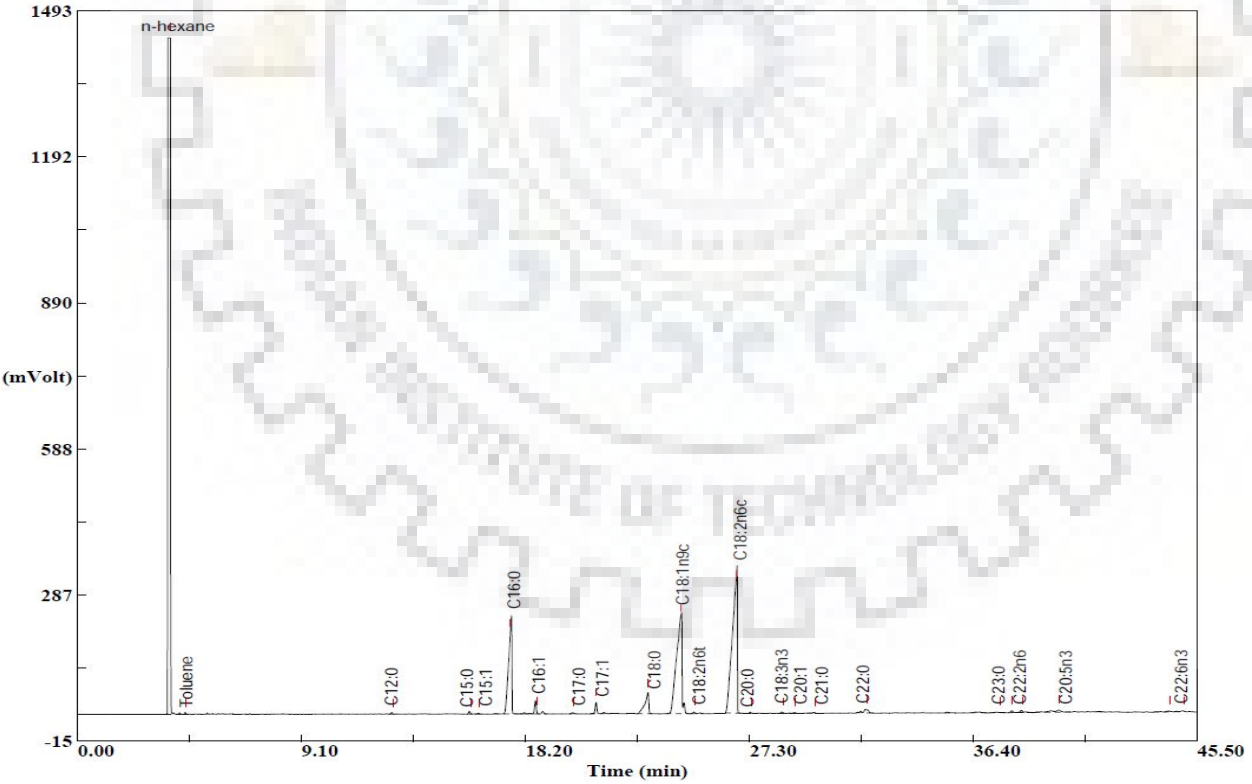


Fig. B.6: GC chromatogram of AM seed oil extracted by SFE in Run 06.

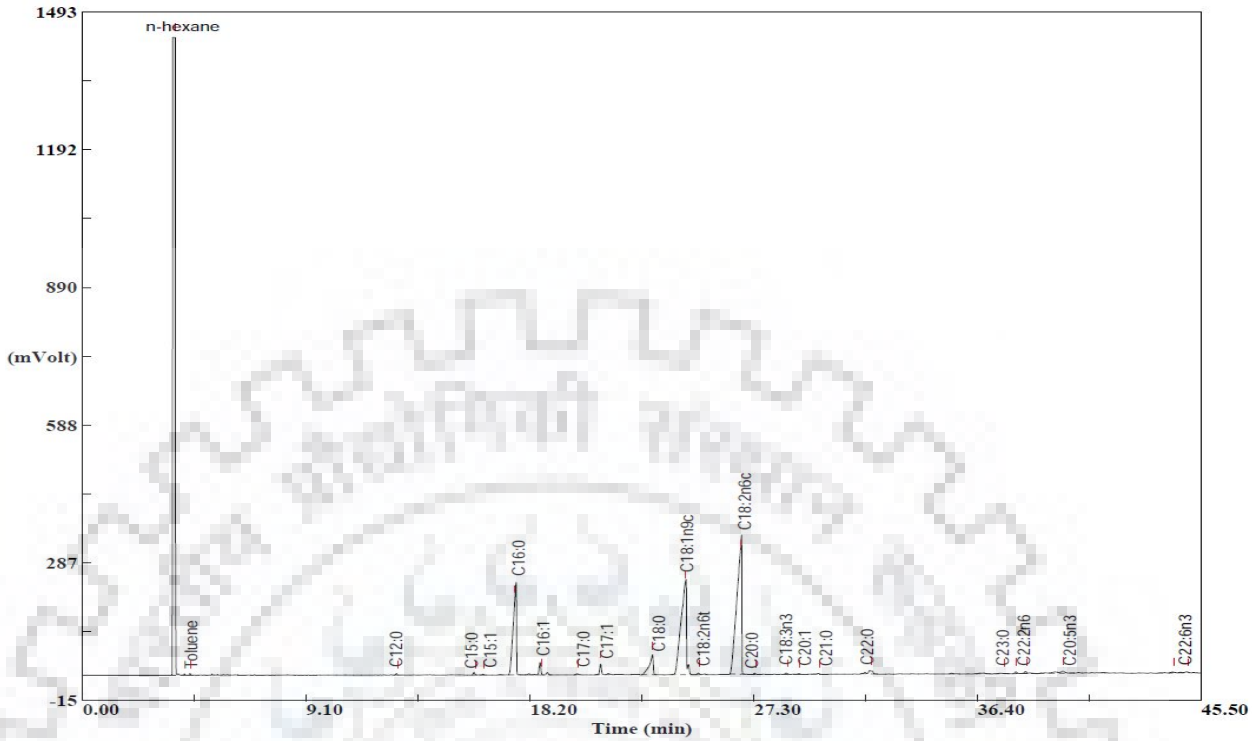


Fig. B.7: GC chromatogram of AM seed oil extracted by SFE in Run 07.

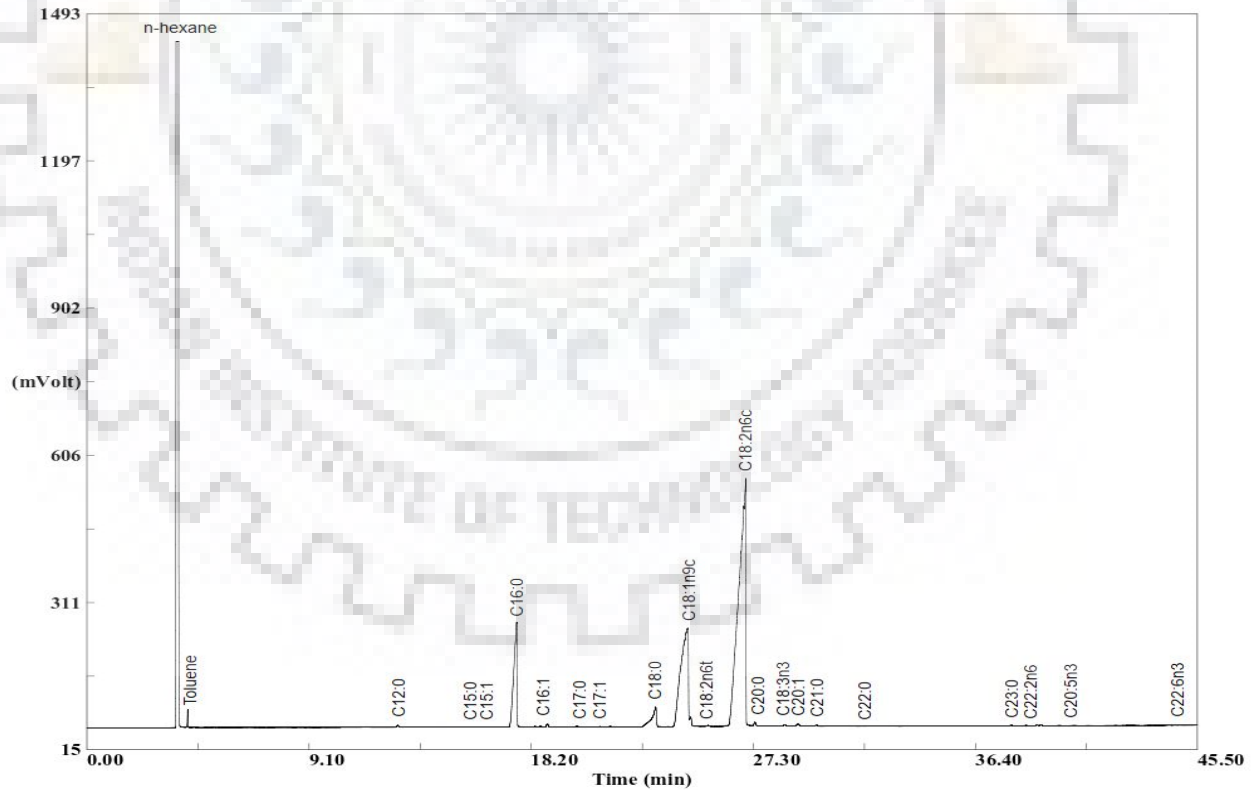


Fig. B.8: GC chromatogram of AM seed oil extracted by SFE in Run 08.

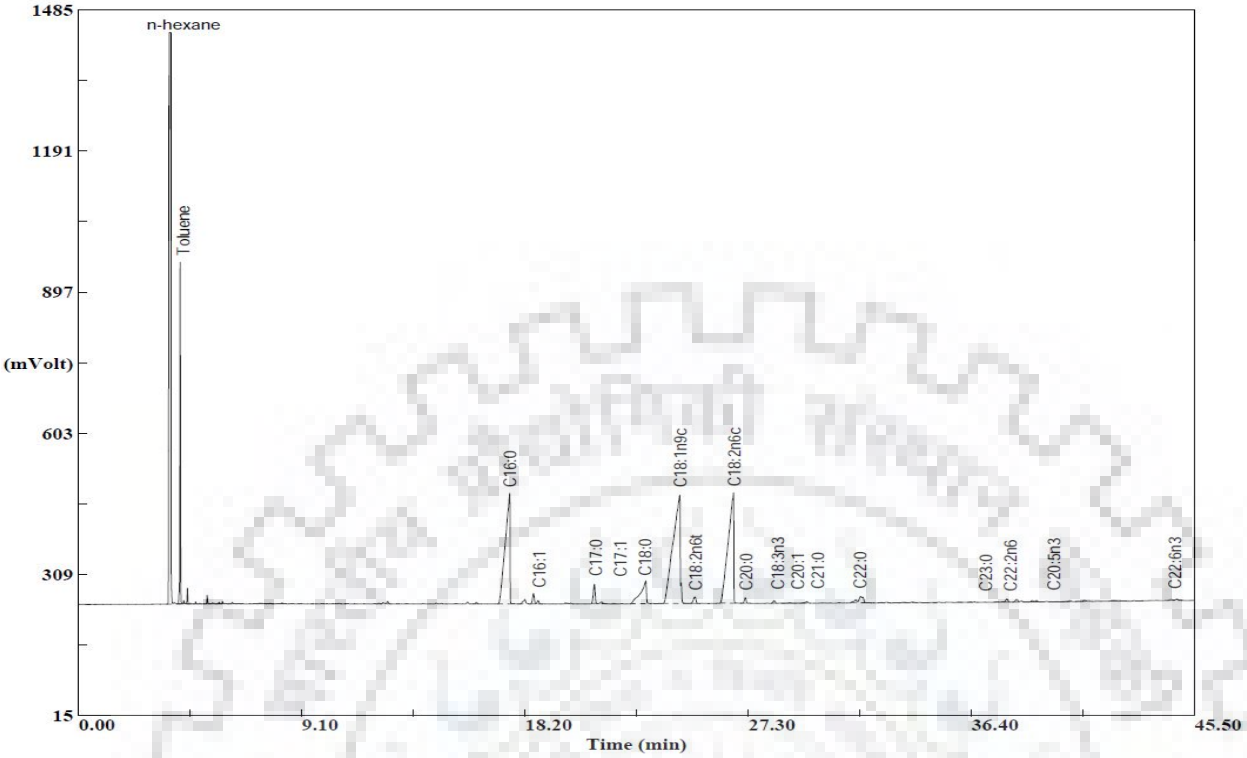


Fig. B.9: GC chromatogram of AM seed oil extracted by SFE in Run 09.

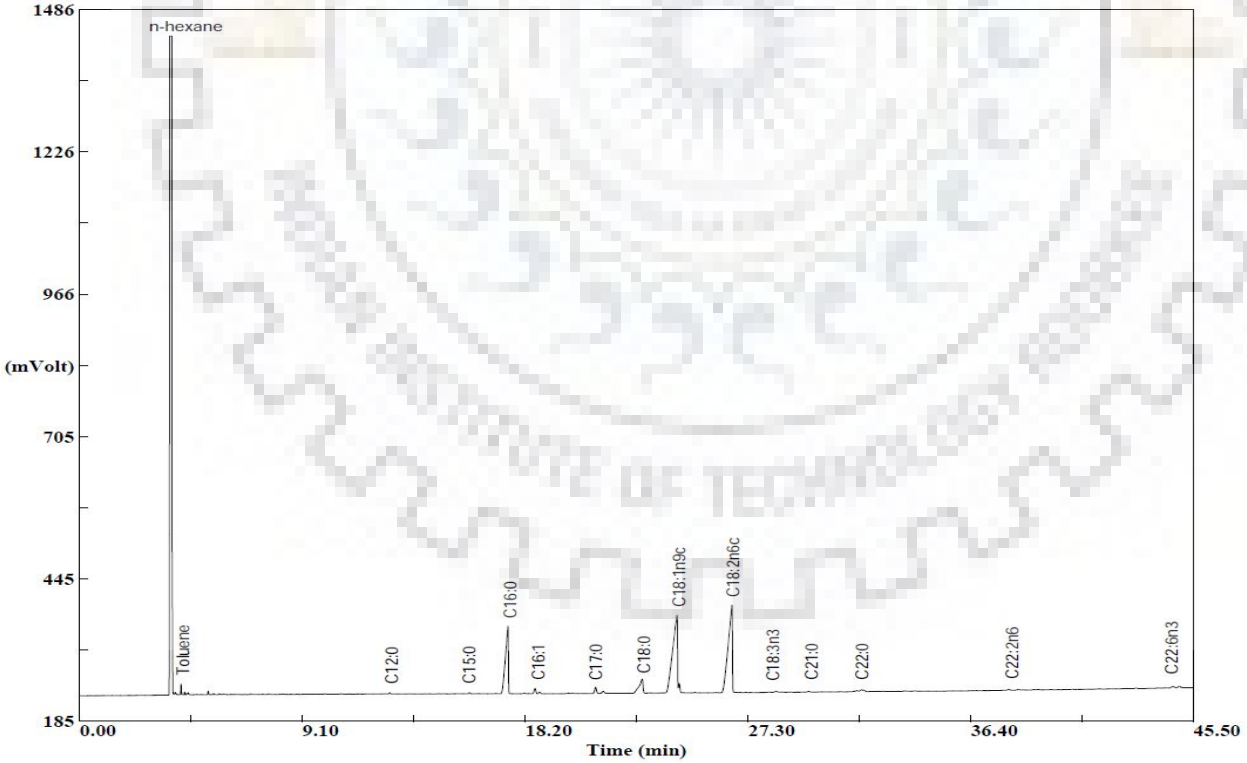


Fig. B.10: GC chromatogram of AM seed oil extracted by SFE in Run 10.

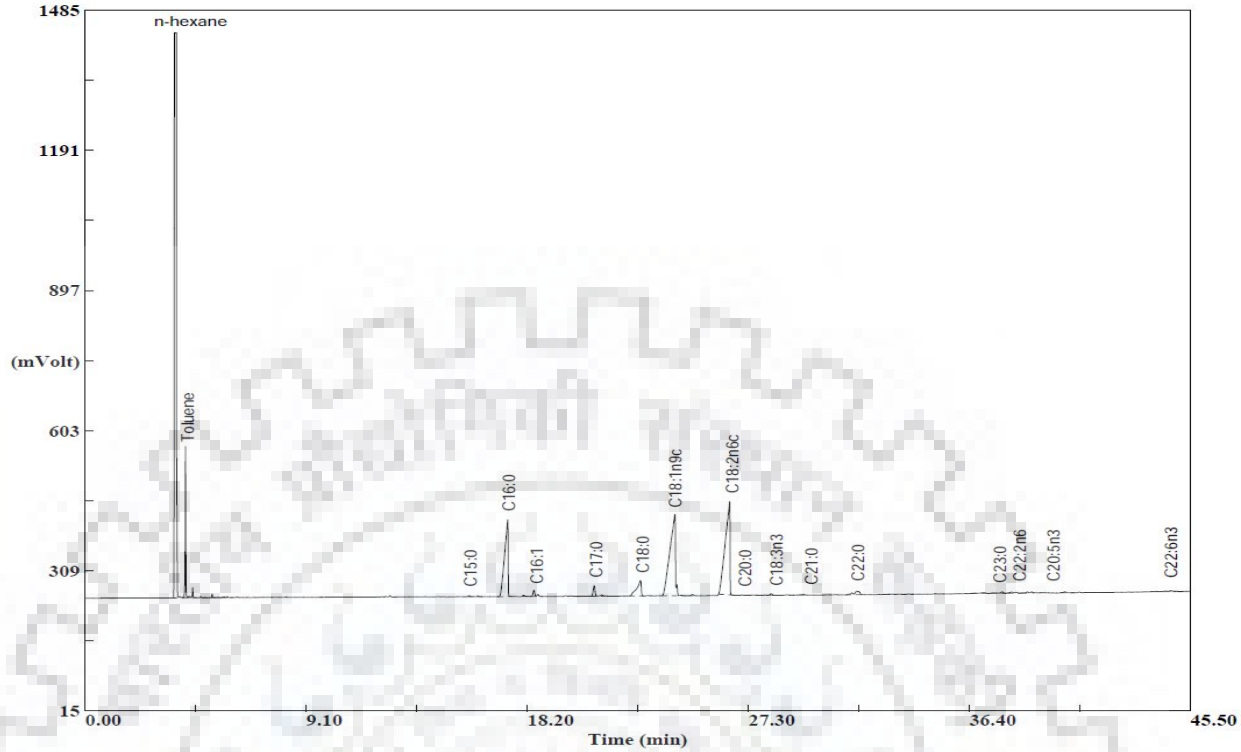


Fig. B.11: GC chromatogram of AM seed oil extracted by SFE in Run 11.

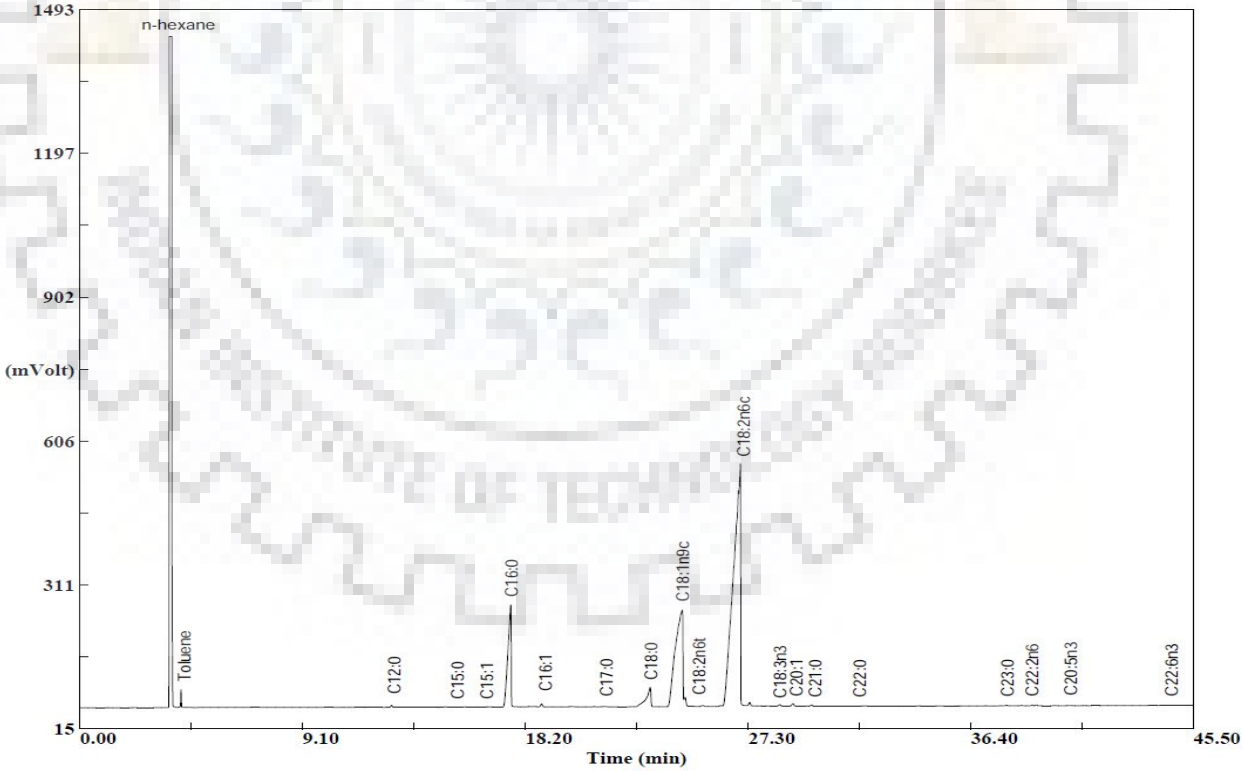


Fig. B.12: GC chromatogram of AM seed oil extracted by SFE in Run 12.

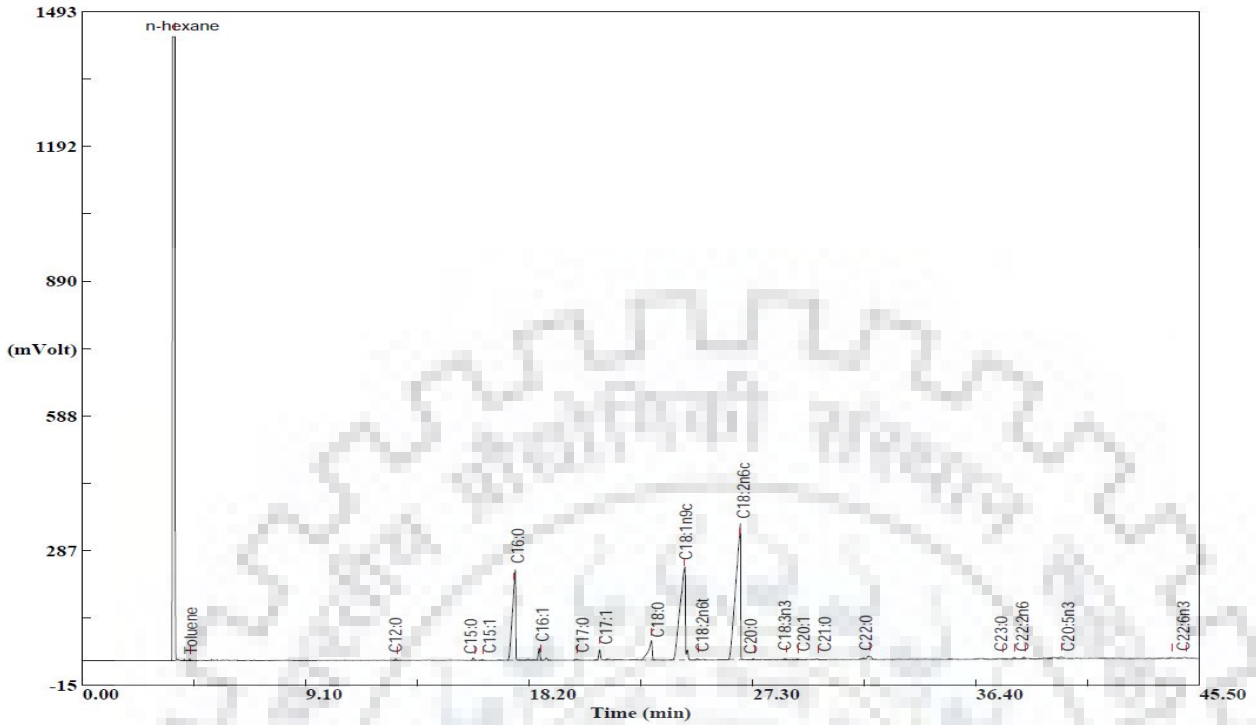


Fig. B.13: GC chromatogram of AM seed oil extracted by SFE in Run 13.

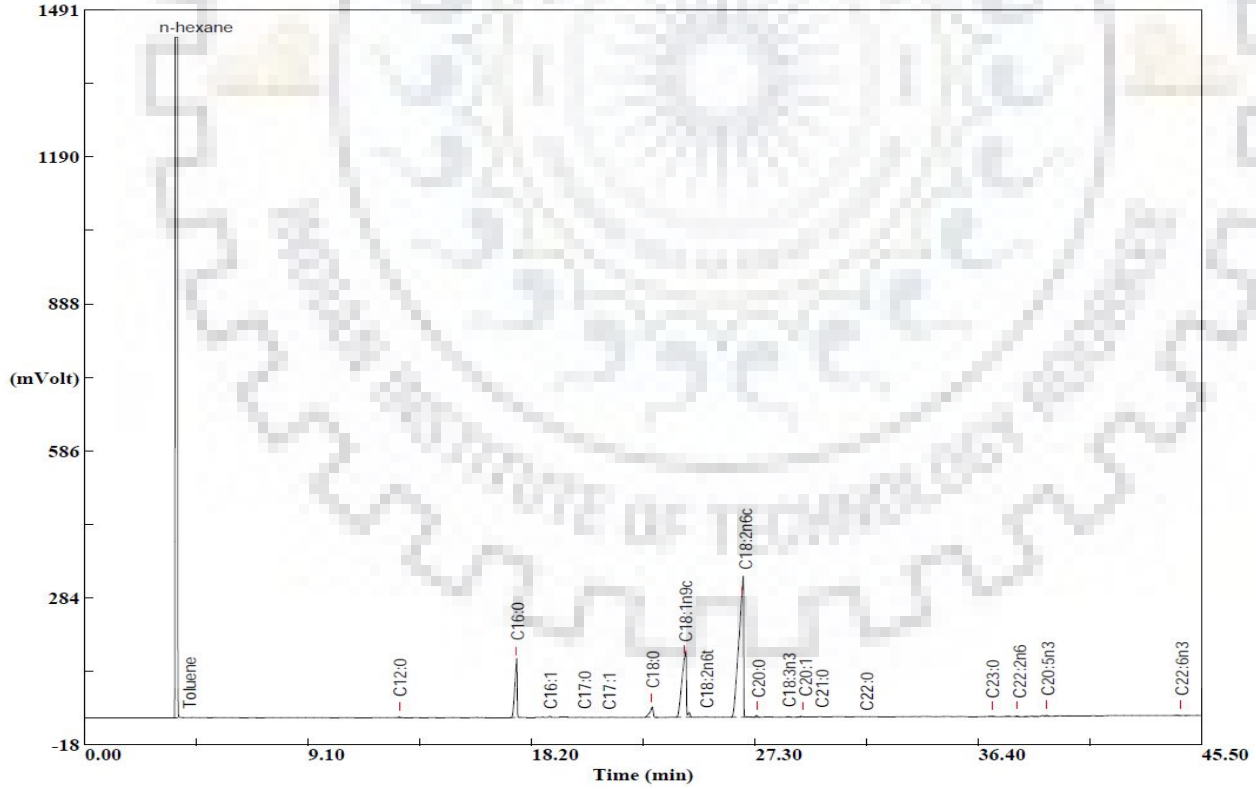


Fig. B.14: GC chromatogram of AM seed oil extracted by SFE in Run 14.

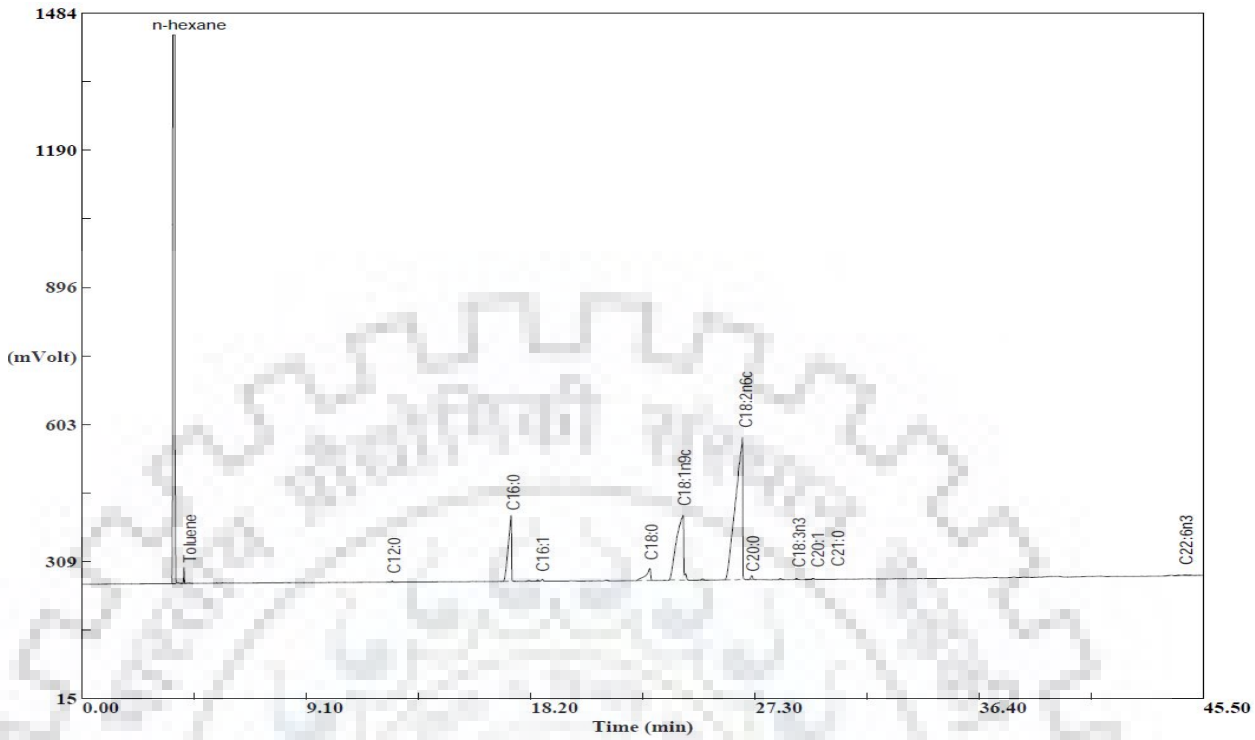


Fig. B.15: GC chromatogram of AM seed oil extracted by SFE in Run 15.

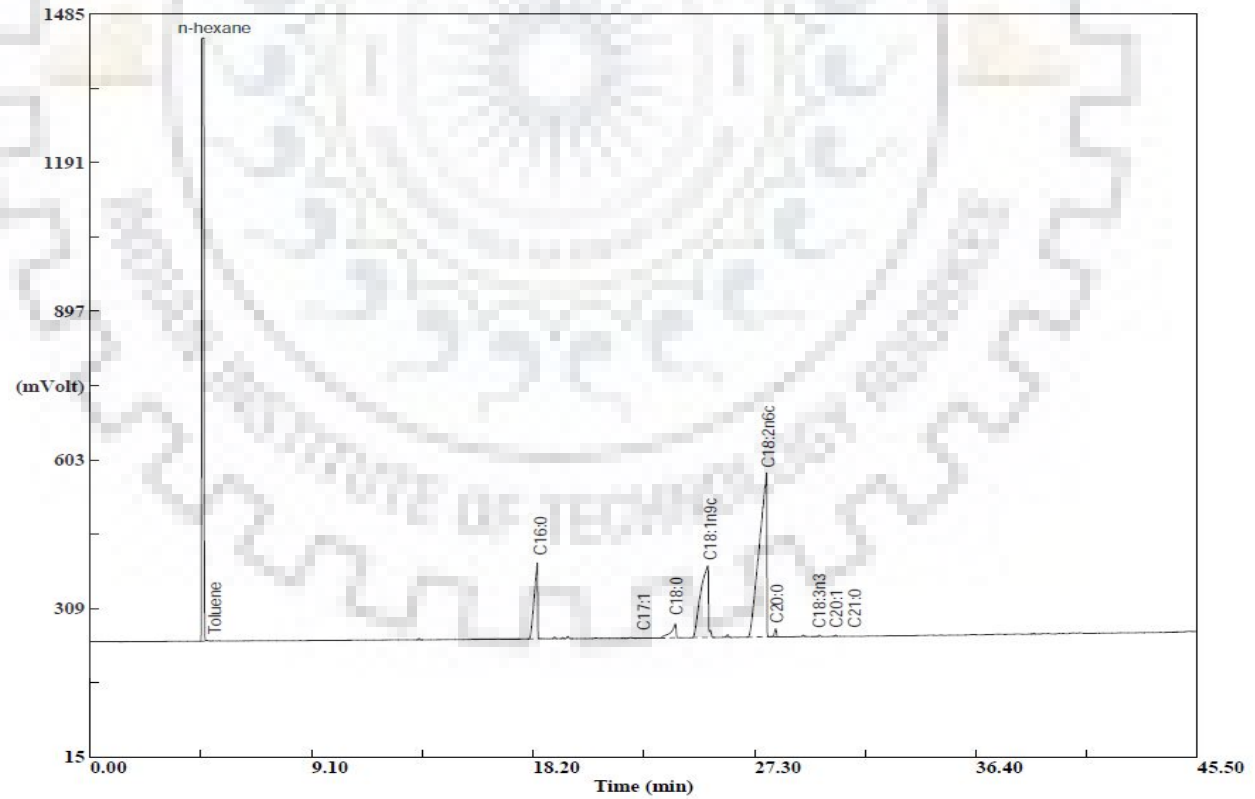


Fig. B.16: GC chromatogram of AM seed oil extracted by SFE in Run 16.

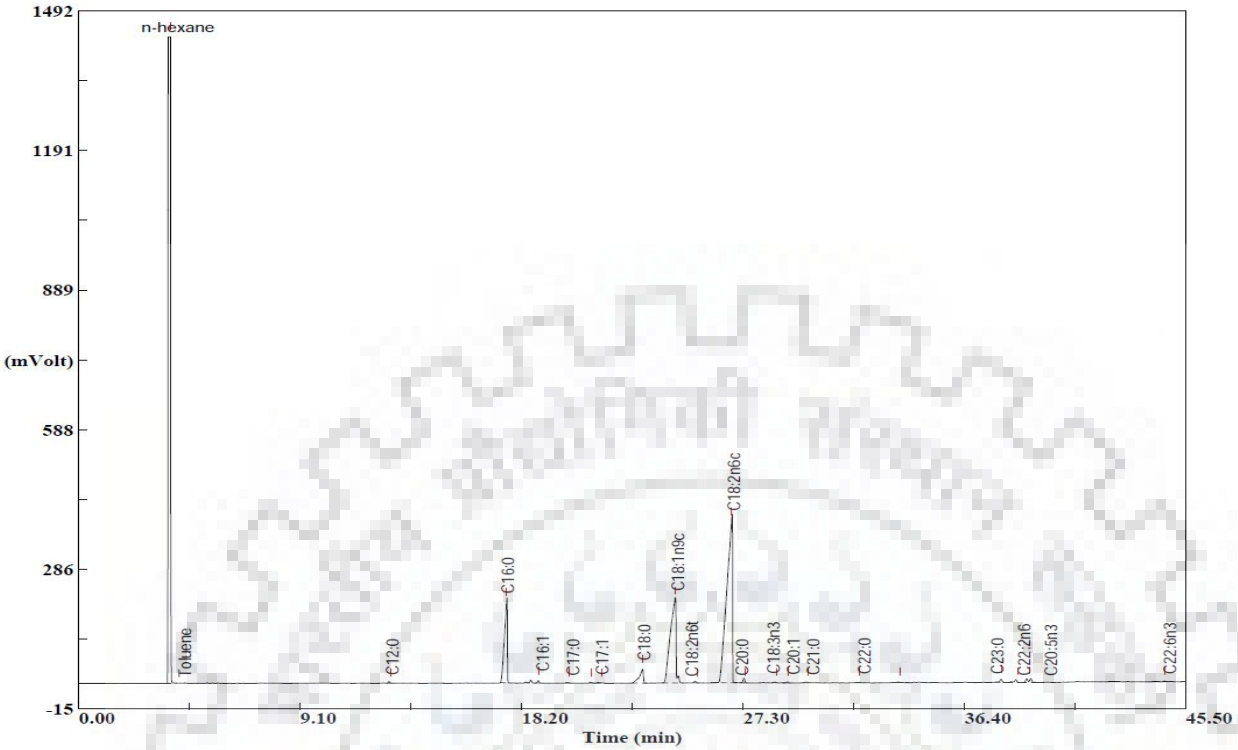


Fig. B.17: GC chromatogram of AM seed oil extracted by SFE in Run 17.

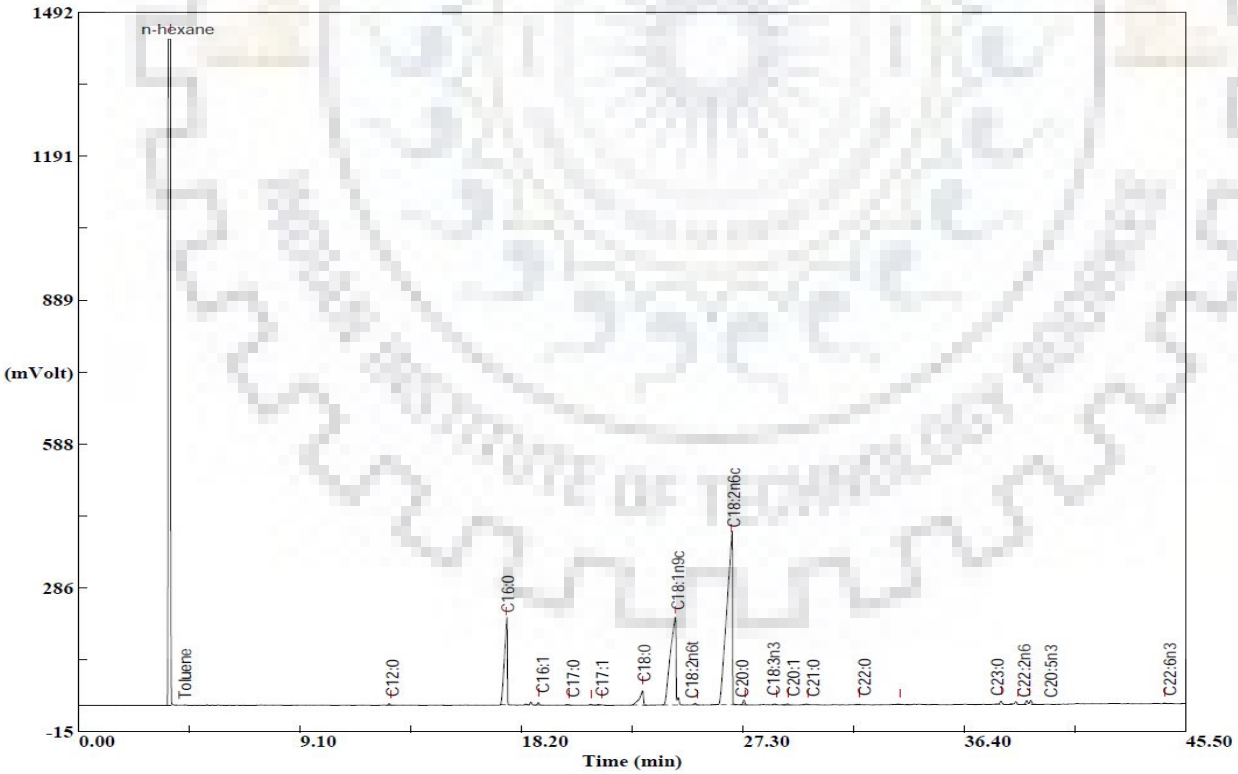


Fig. B.18: GC chromatogram of AM seed oil extracted by SFE in Run 18.

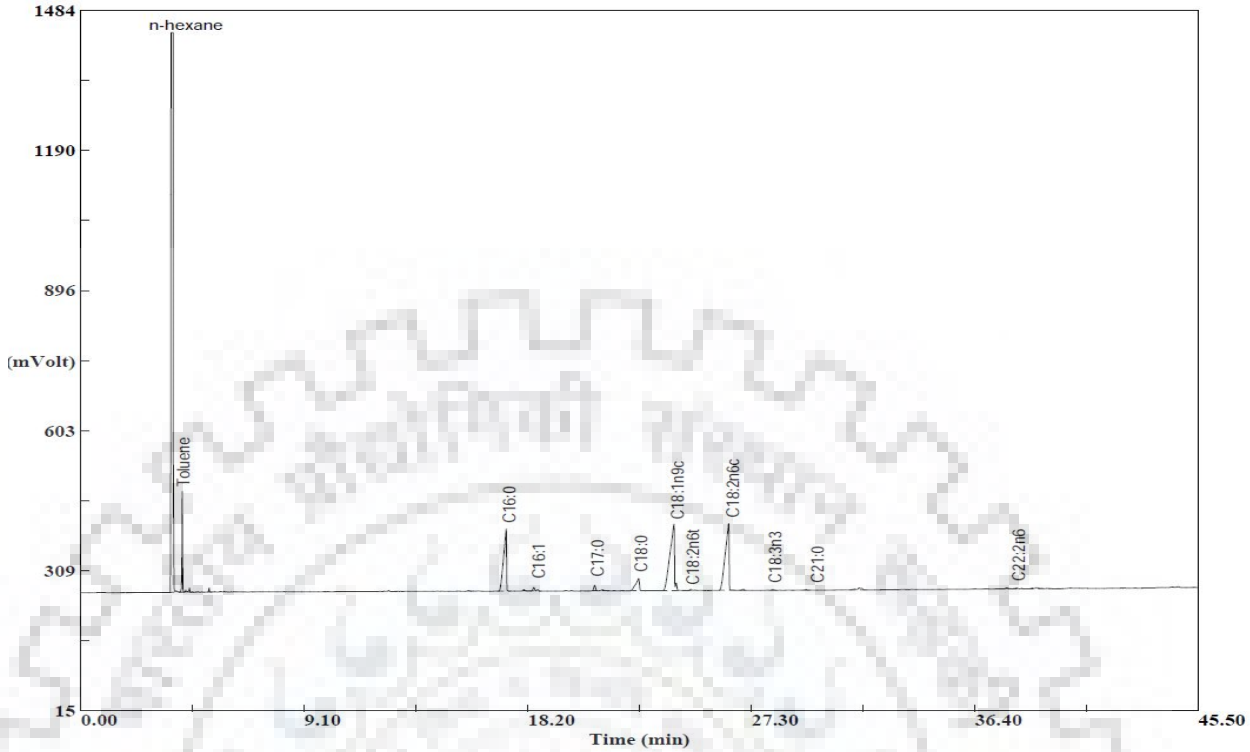


Fig. B.19: GC chromatogram of AM seed oil extracted by SFE in Run 19.

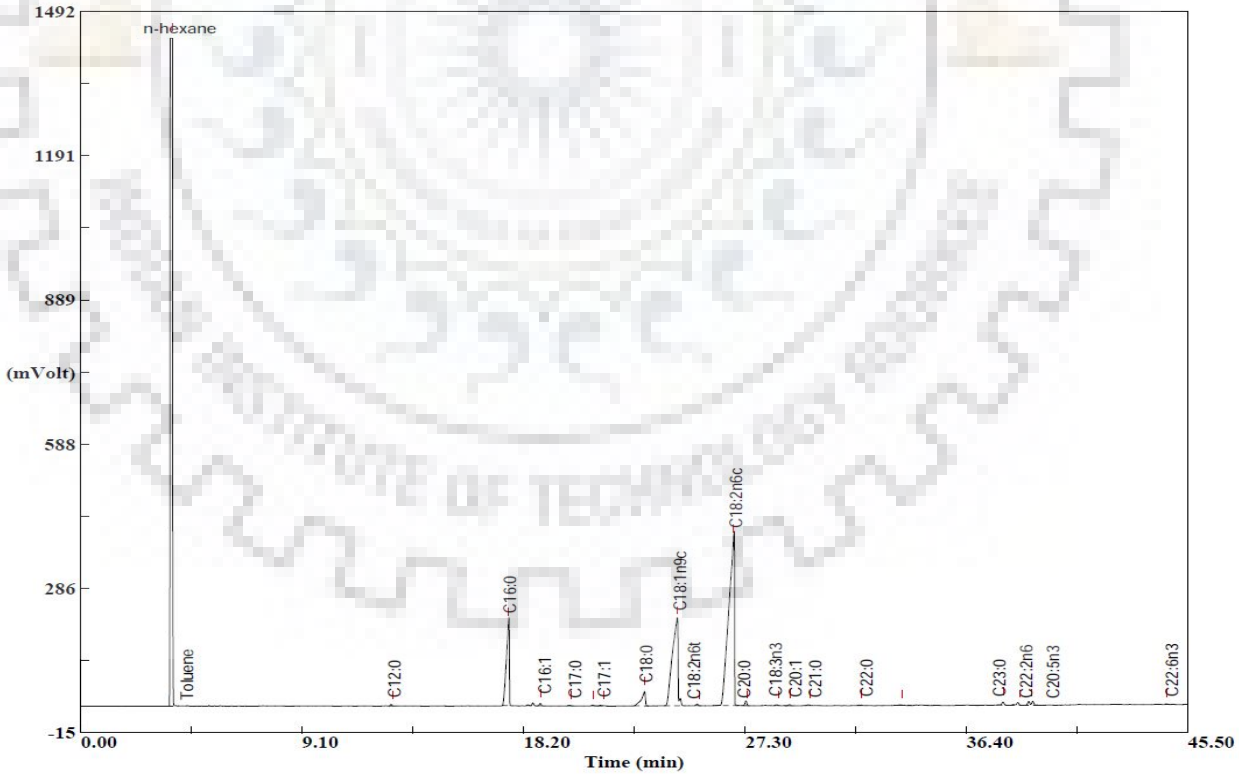


Fig. B.20: GC chromatogram of AM seed oil extracted by SFE in Run 20.

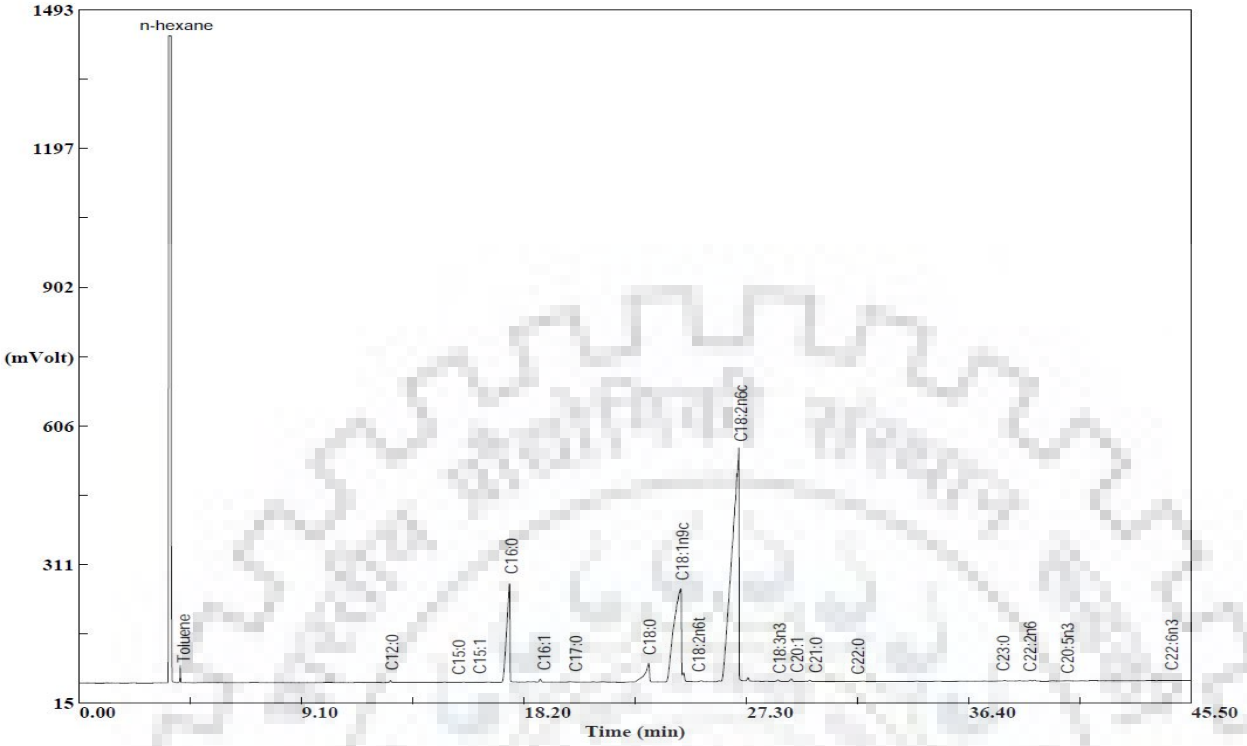


Fig. B.21: GC chromatogram of AM seed oil extracted by SFE in Run 21.

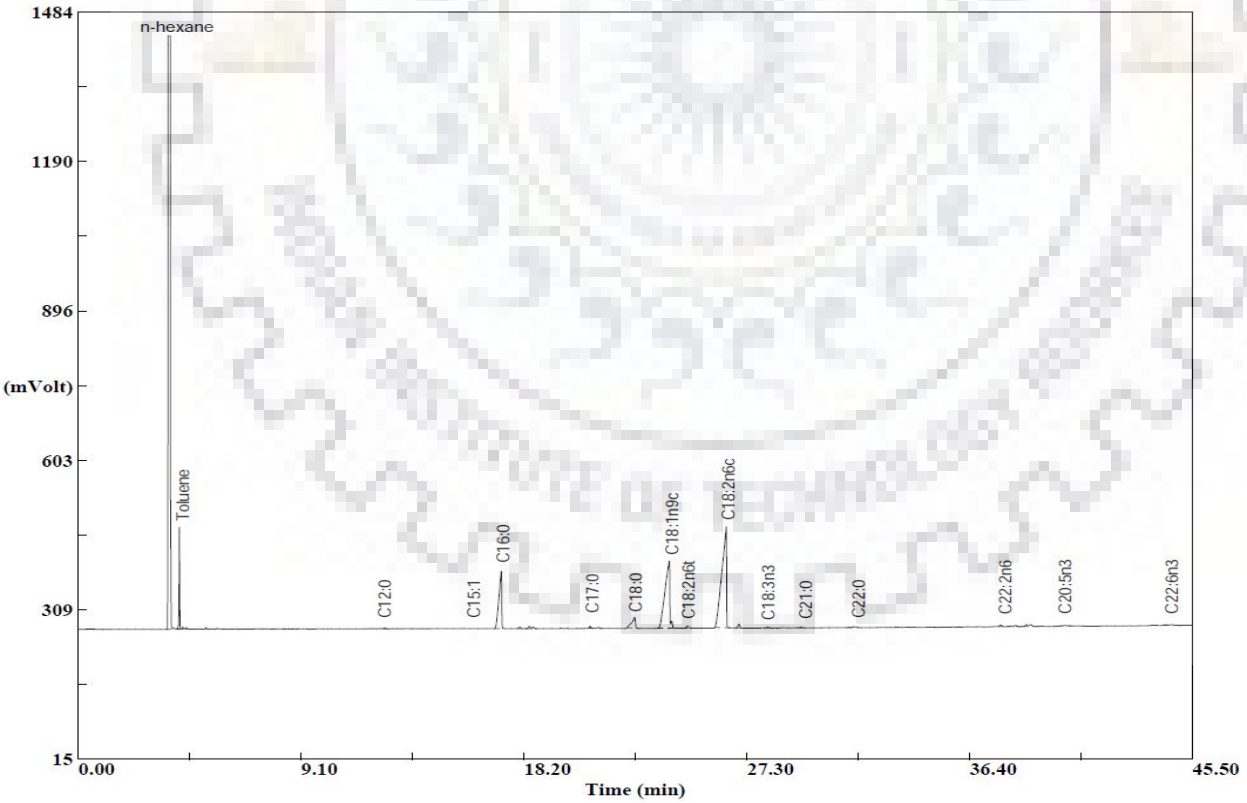


Fig. B.22: GC chromatogram of AM seed oil extracted by SFE in Run 22.

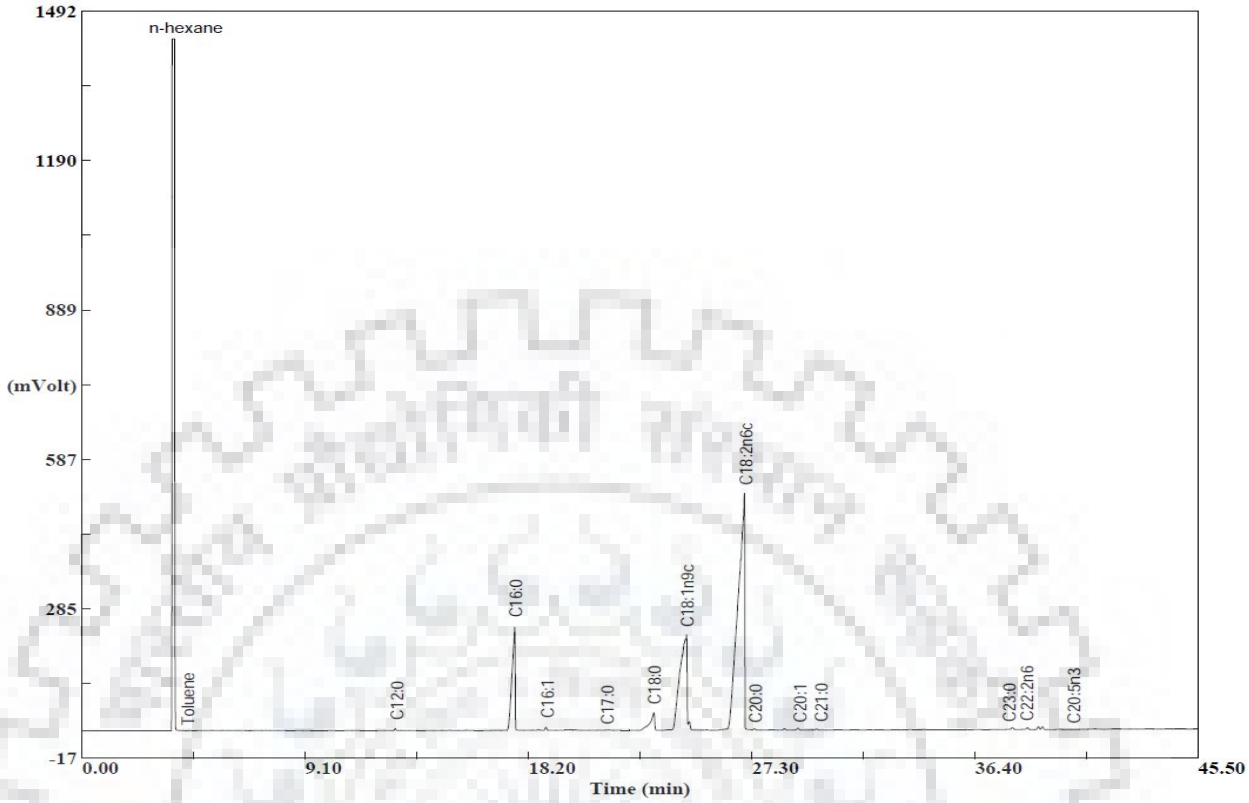


Fig. B.23: GC chromatogram of AM seed oil extracted by SFE in Run 23.

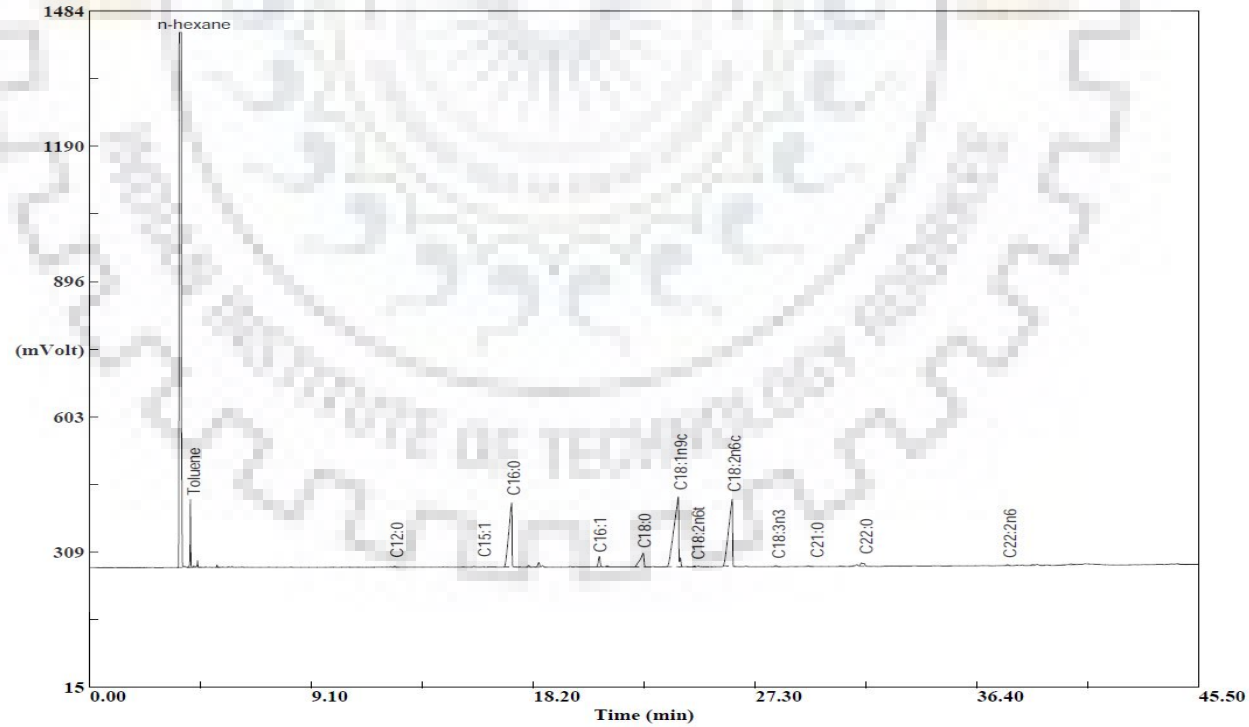


Fig. B.24: GC chromatogram of AM seed oil extracted by SFE in Run 24.

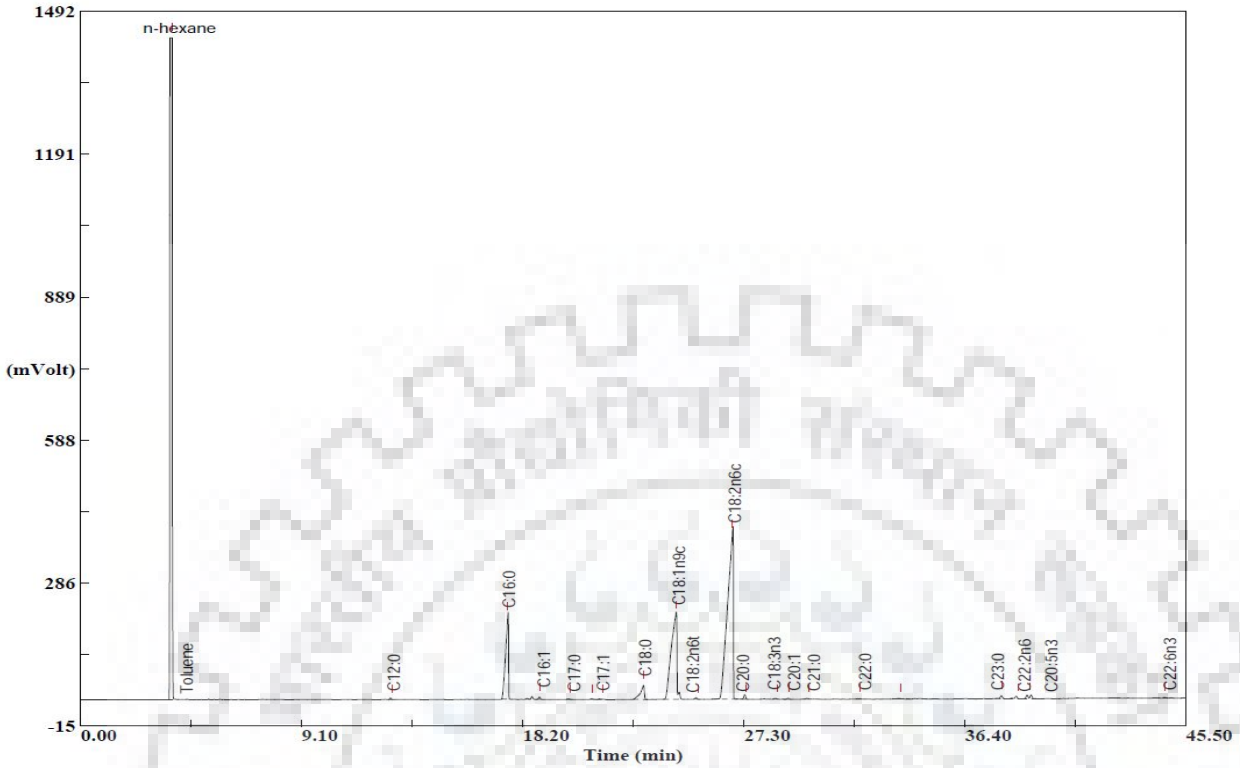


Fig. B.25: GC chromatogram of AM seed oil extracted by SFE in Run 25.

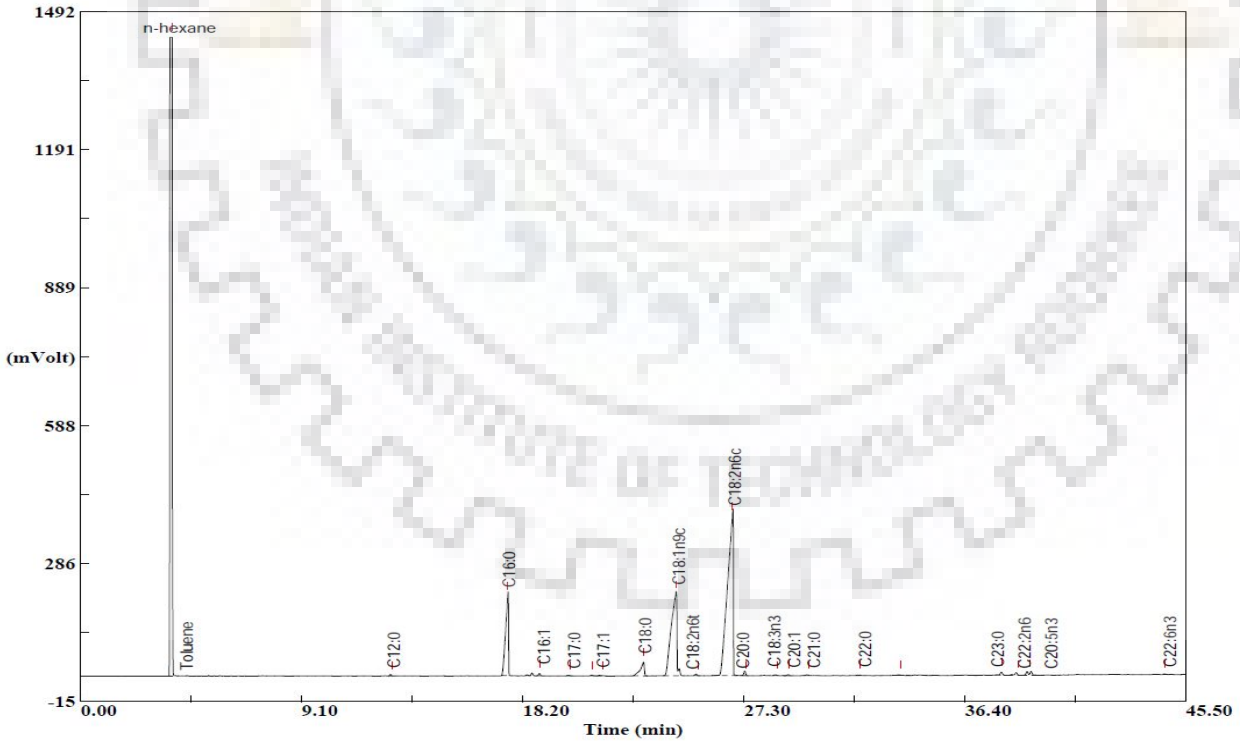


Fig. B.26: GC chromatogram of AM seed oil extracted by SFE in Run 26.

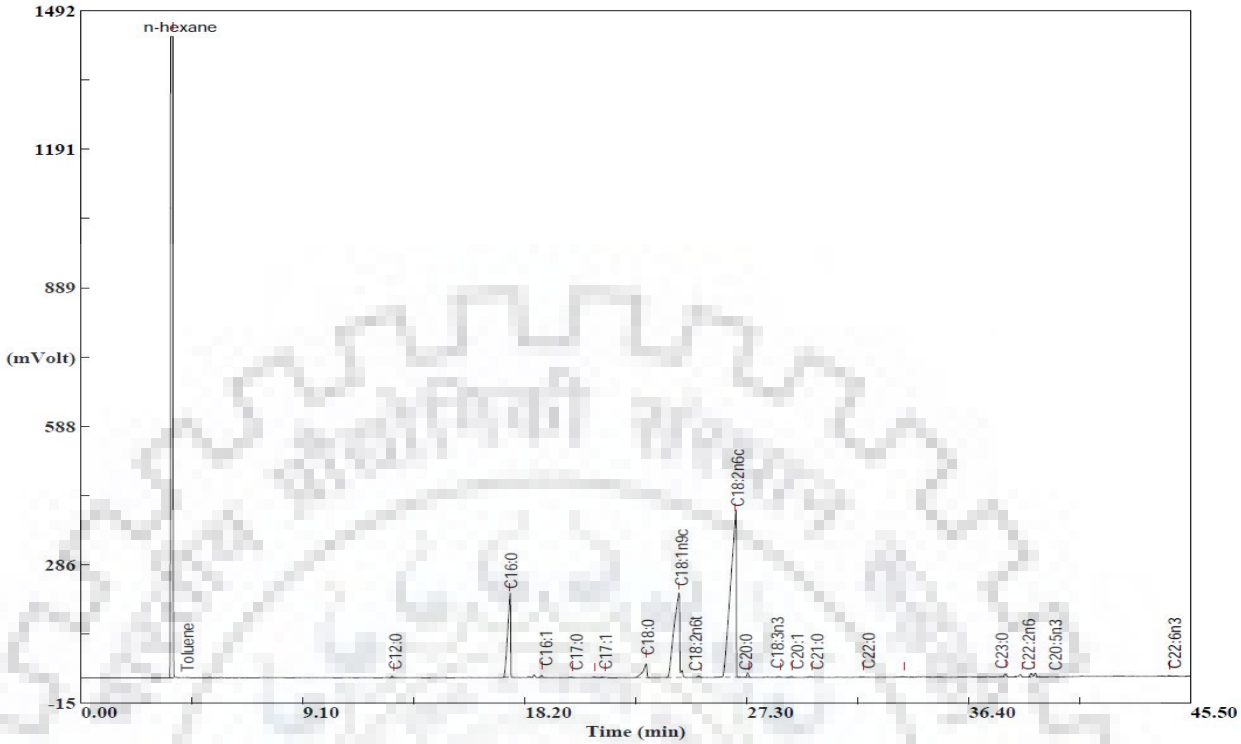


Fig. B.27: GC chromatogram of AM seed oil extracted by SFE in Run 27.

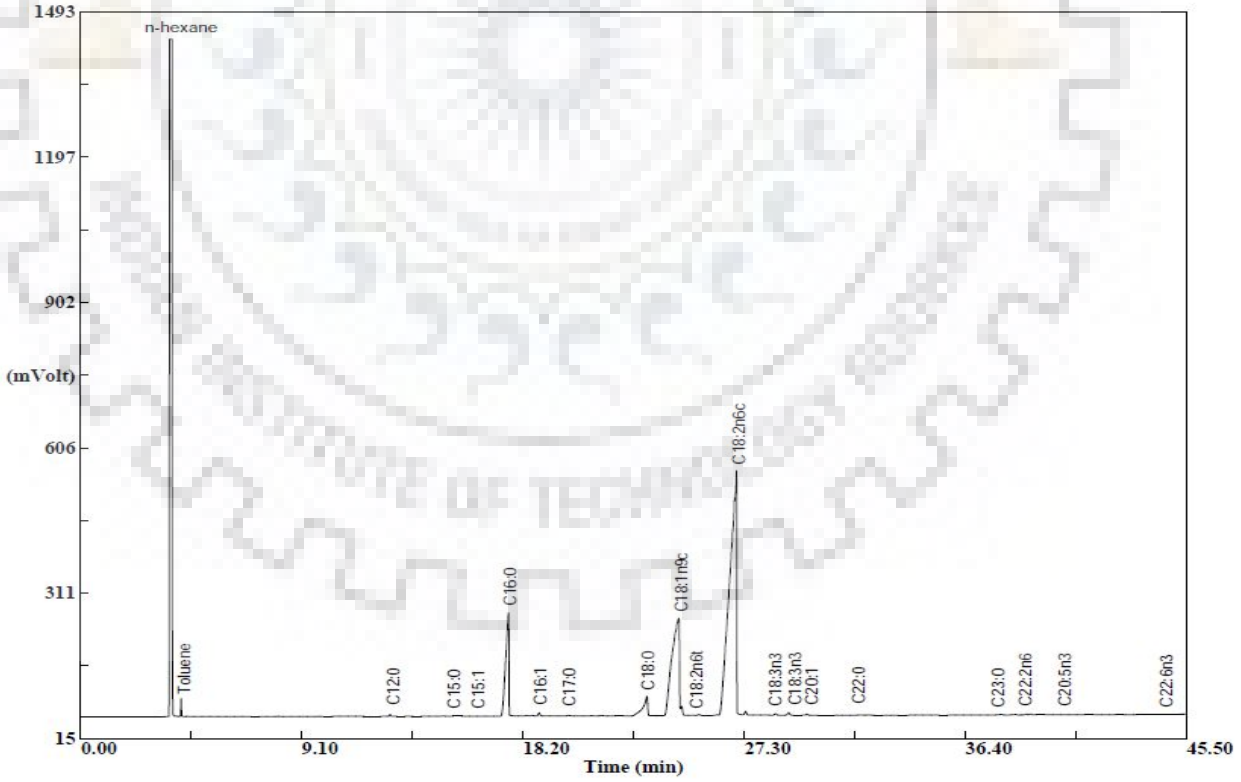


Fig. B.28: GC chromatogram of AM seed oil extracted by SFE in Run 28.

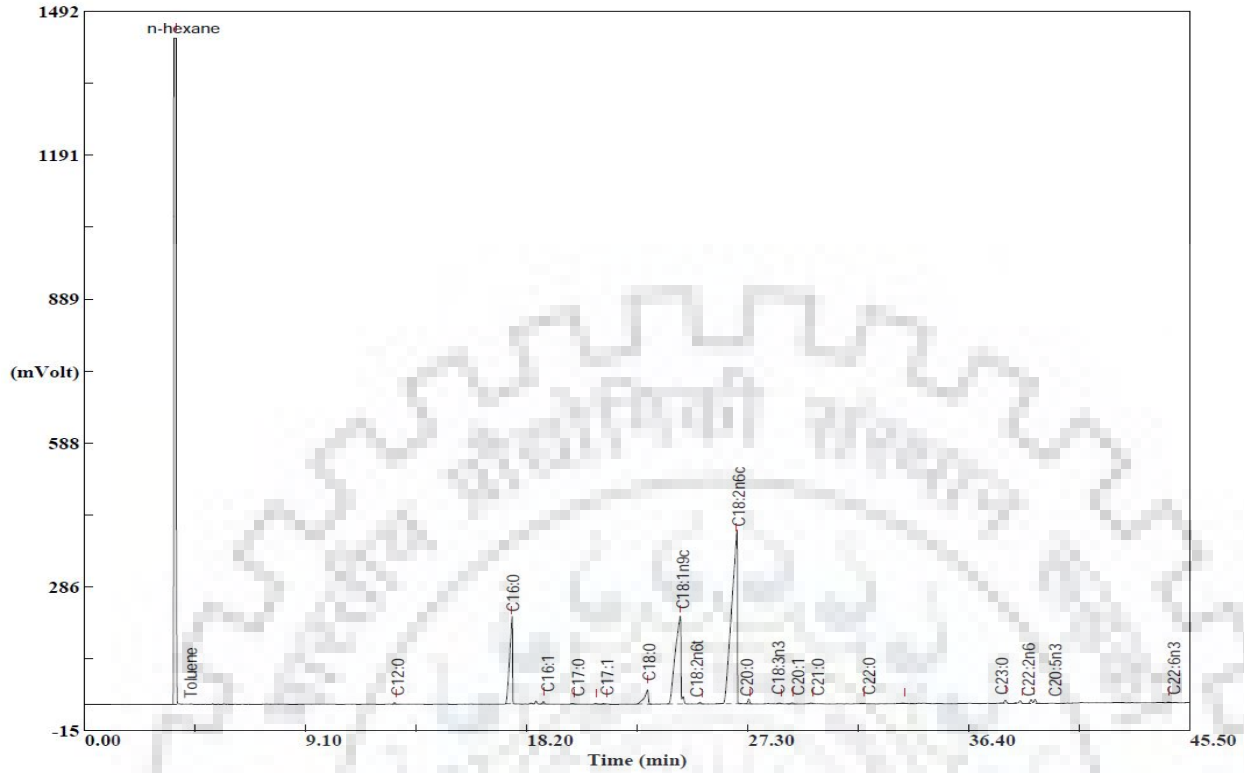


Fig. B.29: GC chromatogram of AM seed oil extracted by SFE in Run 29.

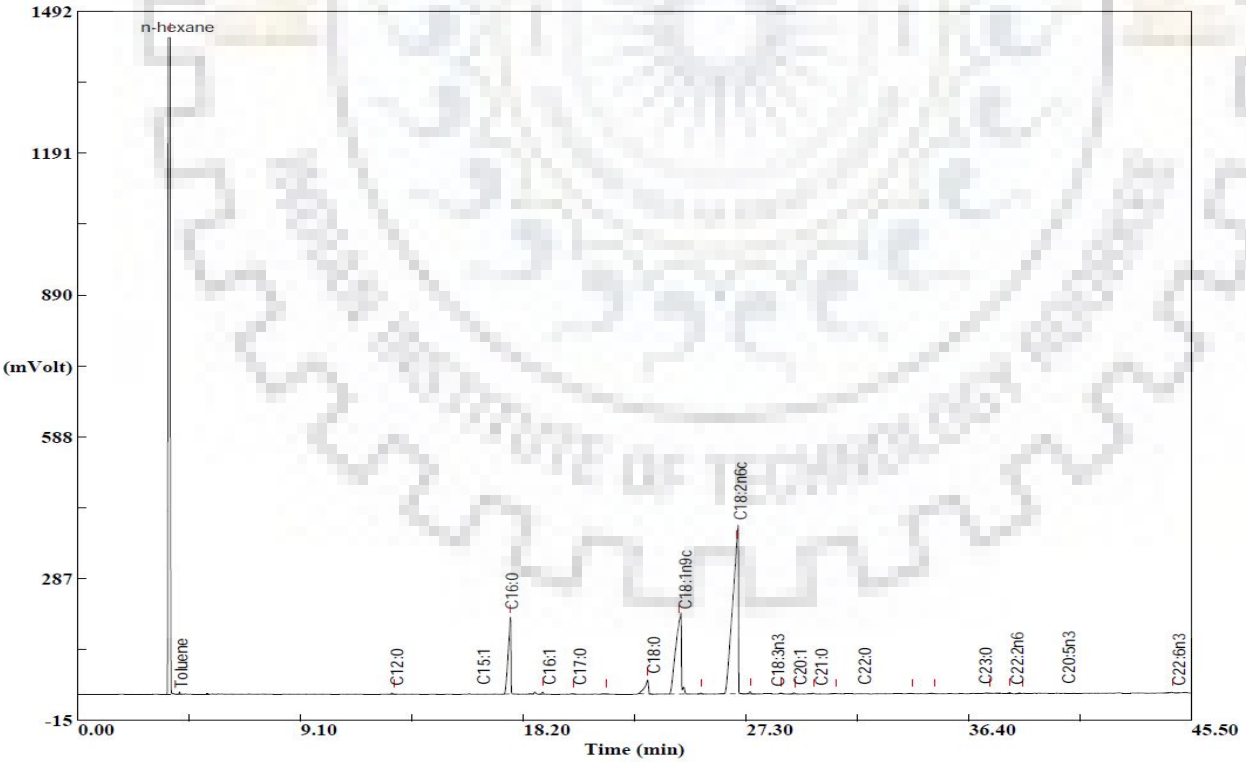


Fig. B.30: GC chromatogram of AM seed oil extracted by SFE in Run 30.

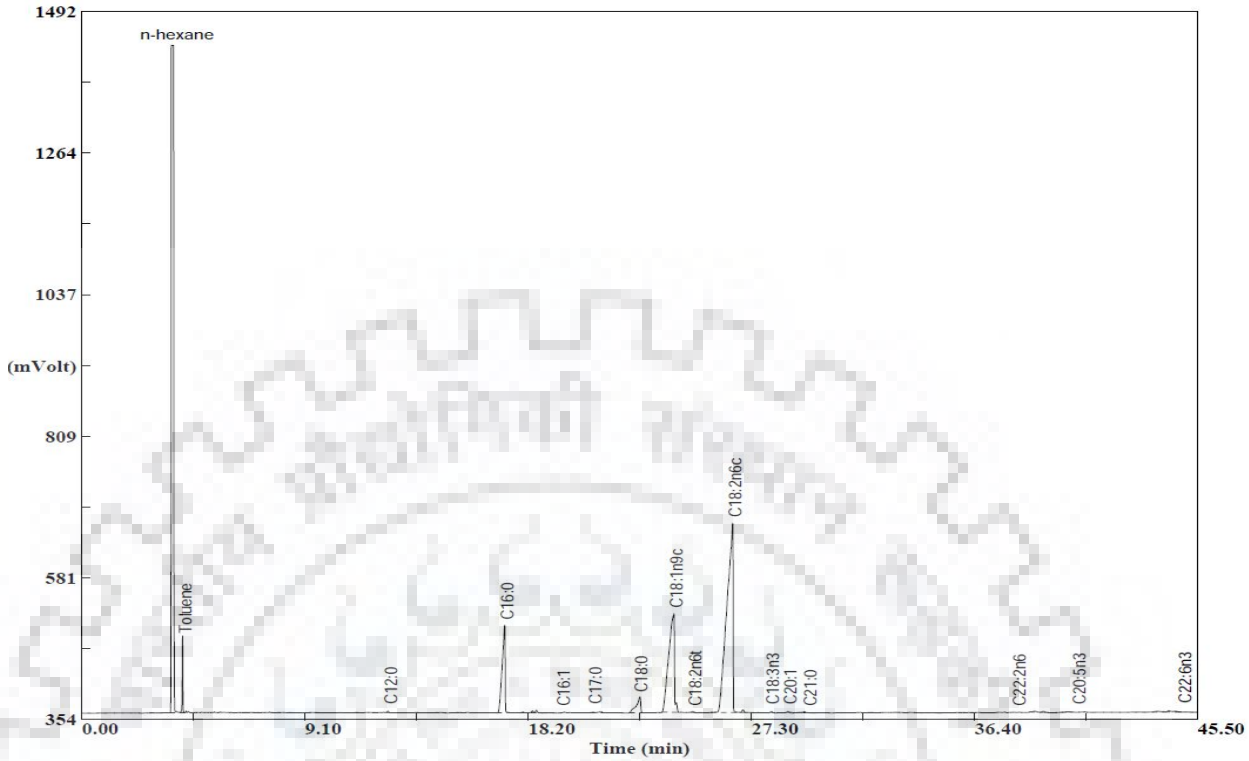


Fig. B.31: GC chromatogram of AM seed oil extracted by SFE in Run 31.

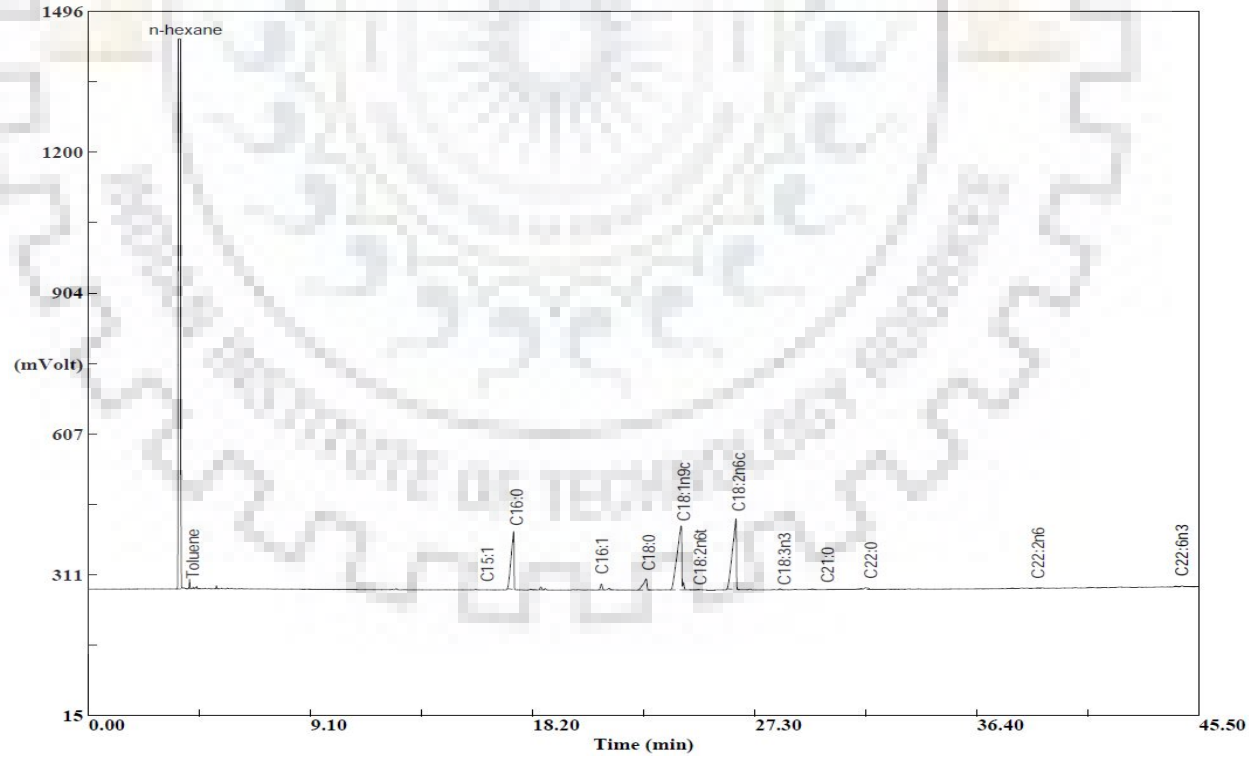


Fig. B.32: GC chromatogram of AM seed oil extracted by SFE in Run 32.

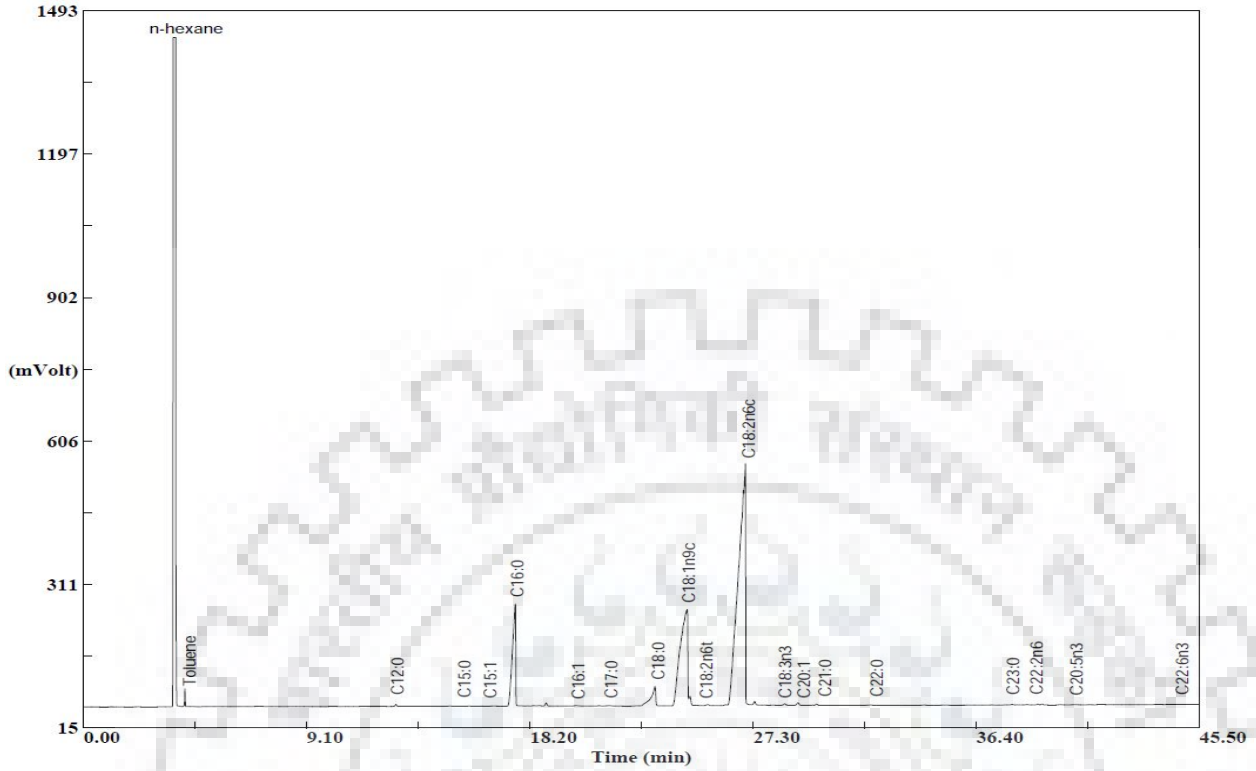


Fig. B.33: GC chromatogram of AM seed oil extracted by SFE in Run 33.


Fig. B.34: GC chromatogram of AM seed oil extracted by SFE in Run 34.

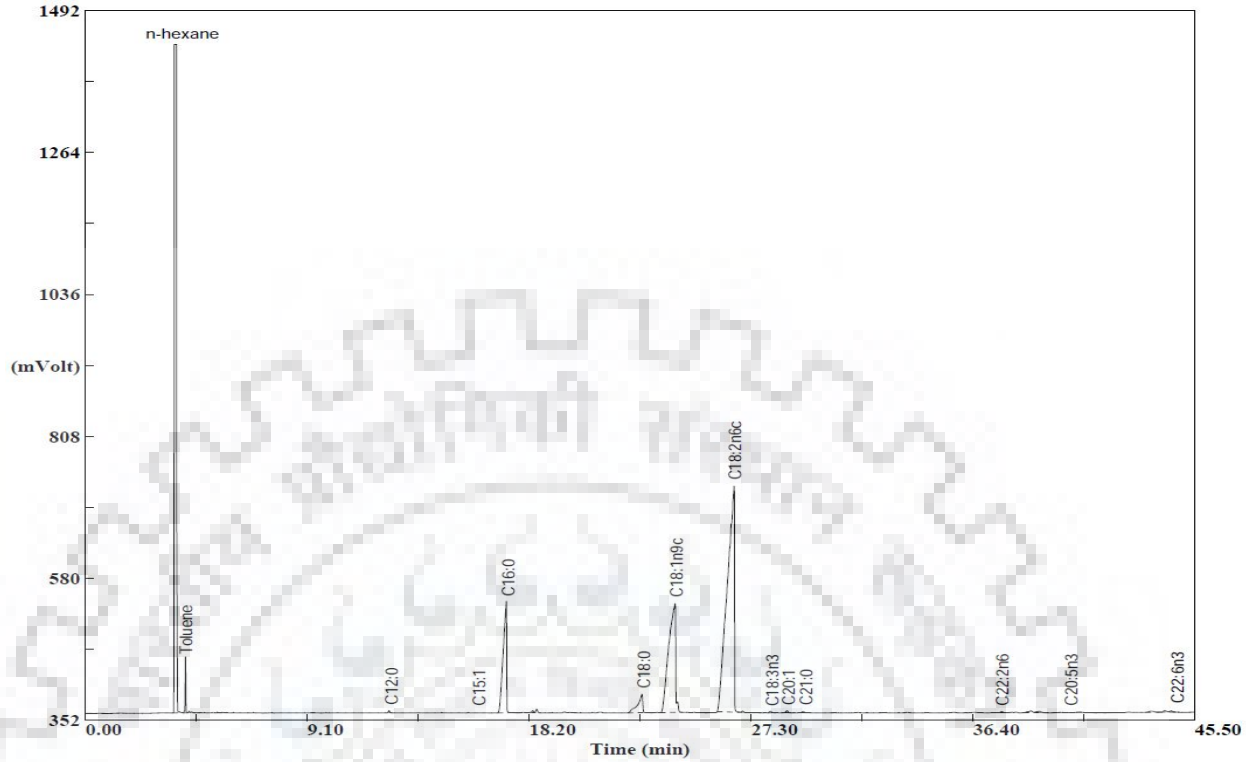


Fig. B.35: GC chromatogram of AM seed oil extracted by SFE in Run 35.

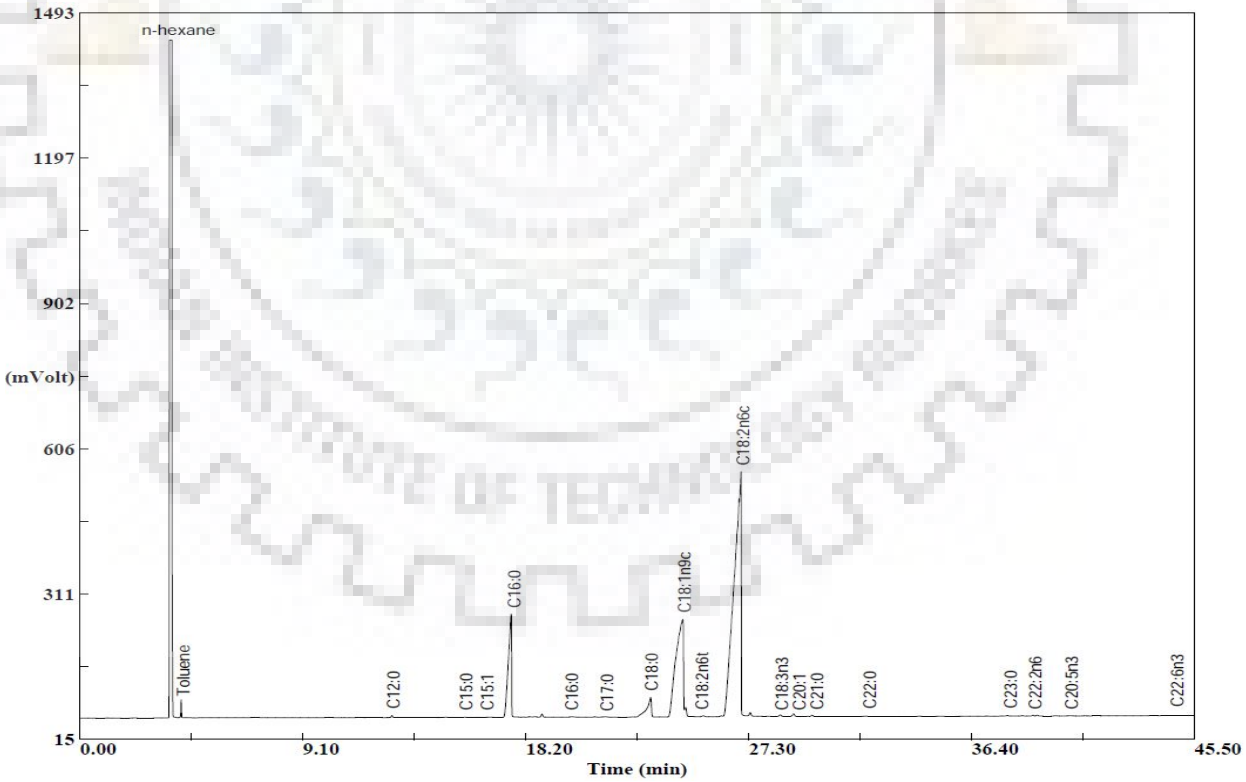


Fig. B.36: GC chromatogram of AM seed oil extracted by SFE in Run 36.

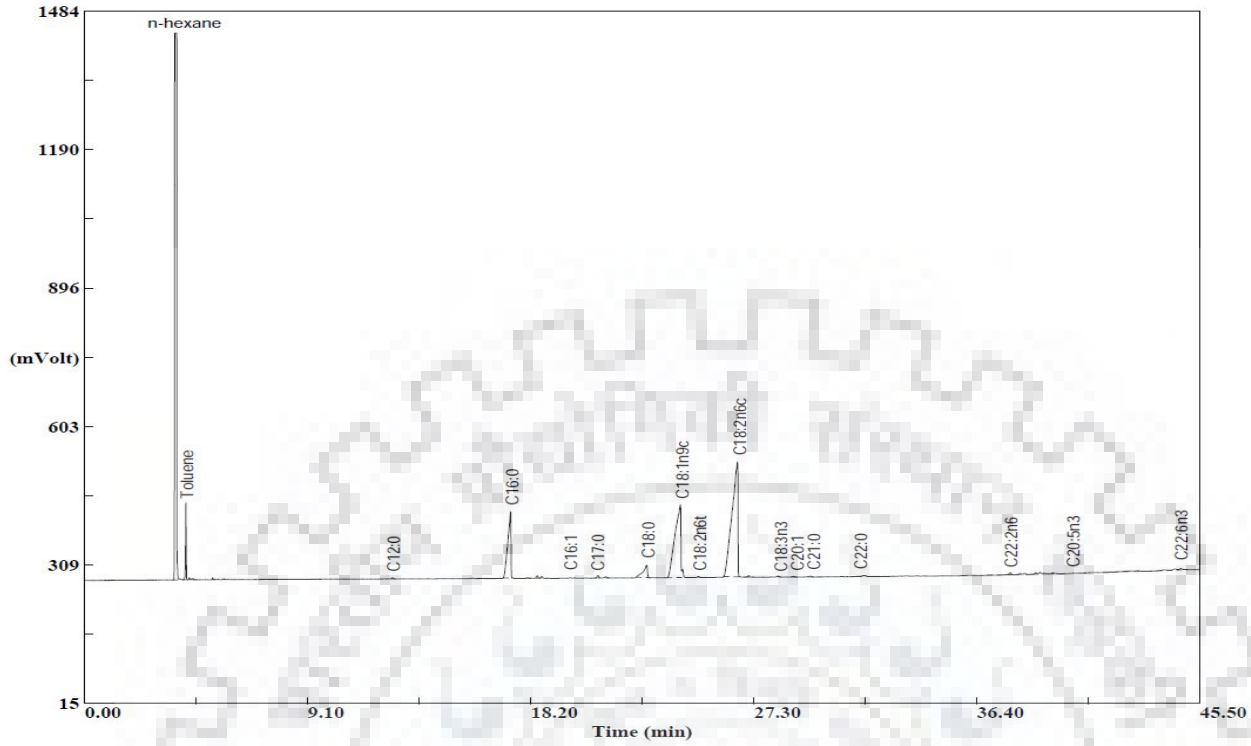


Fig. B.37: GC chromatogram of AM seed oil extracted by SFE in Run 37.

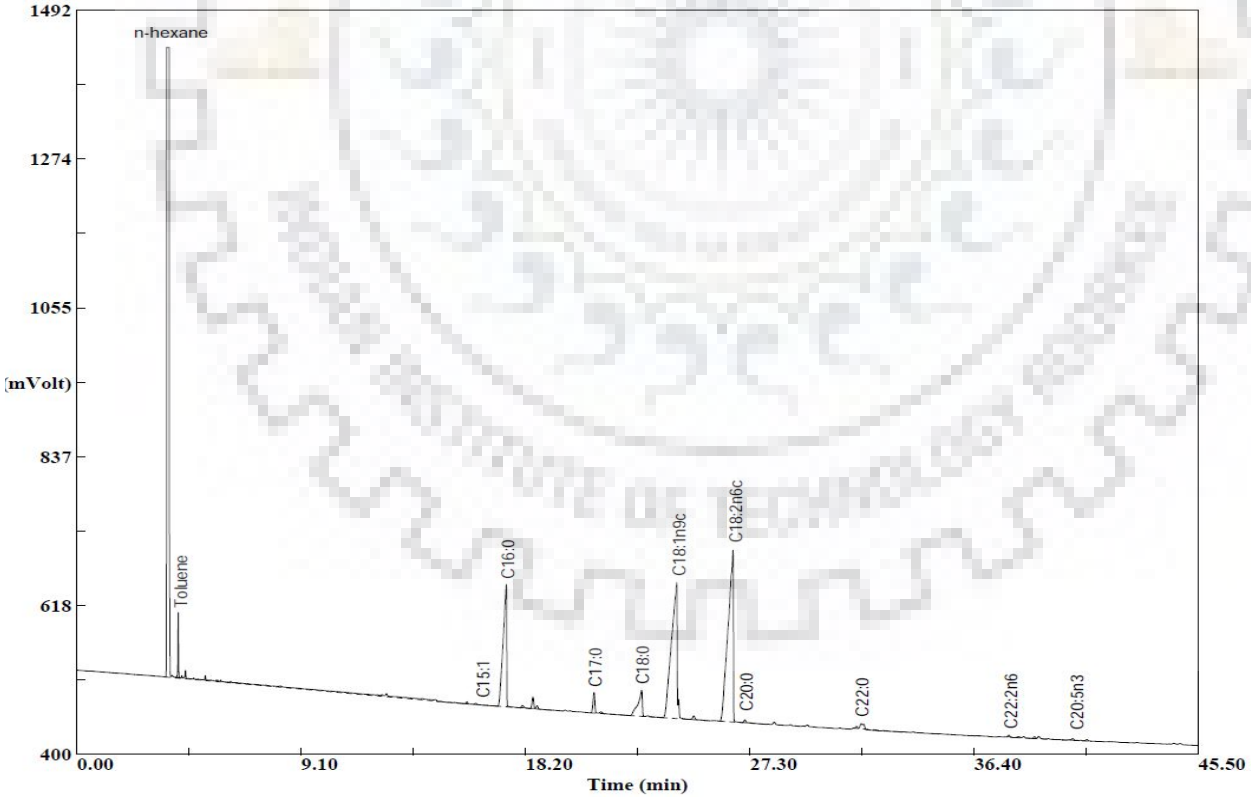


Fig. B.38: GC chromatogram of AM seed oil extracted by SFE in Run 38.

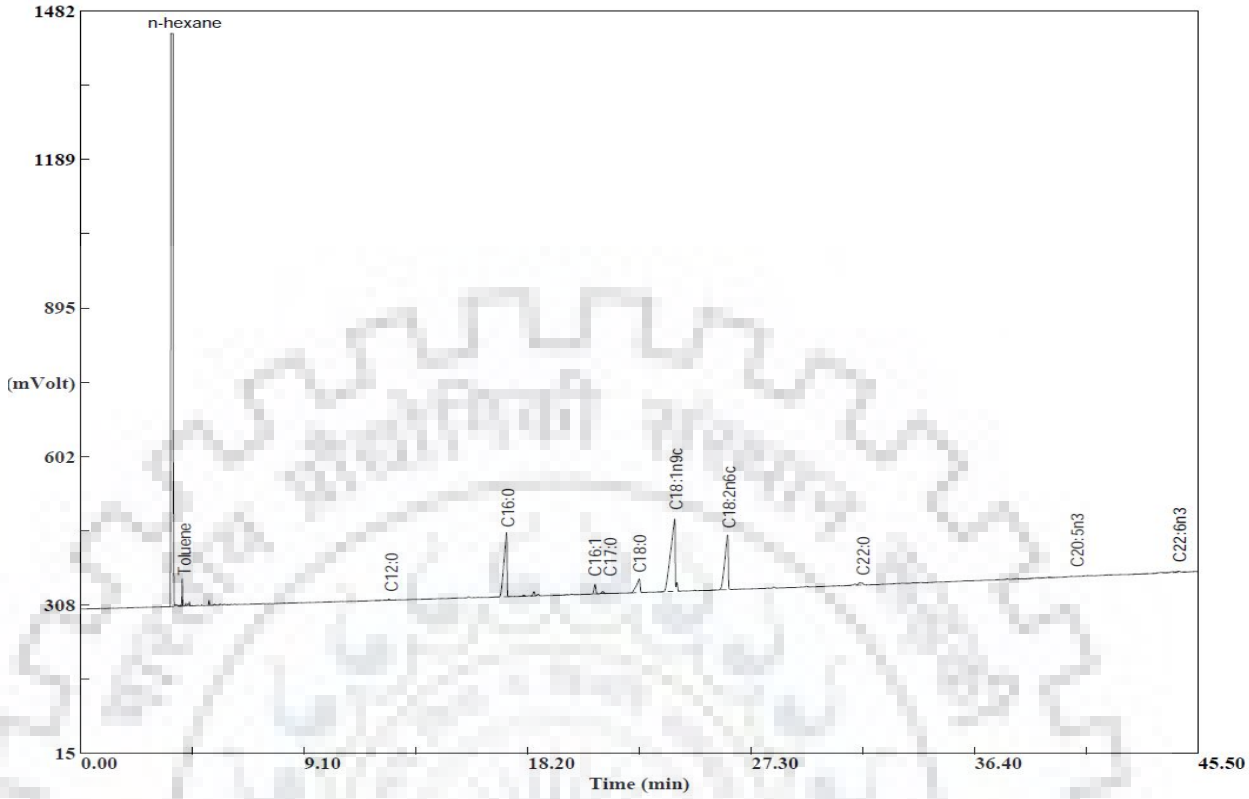


Fig. B.39: GC chromatogram of AM seed oil extracted by SFE in Run 39.

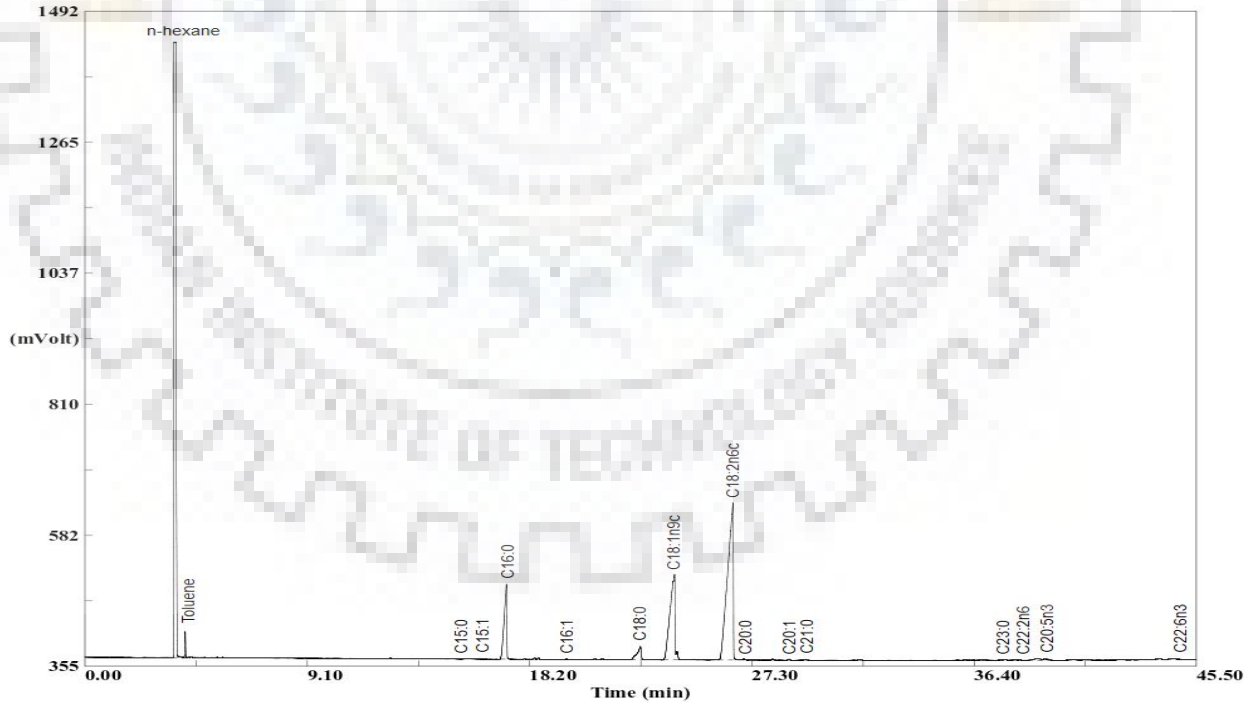


Fig. B.40: GC chromatogram of AM seed oil extracted by SFE in Run 40.

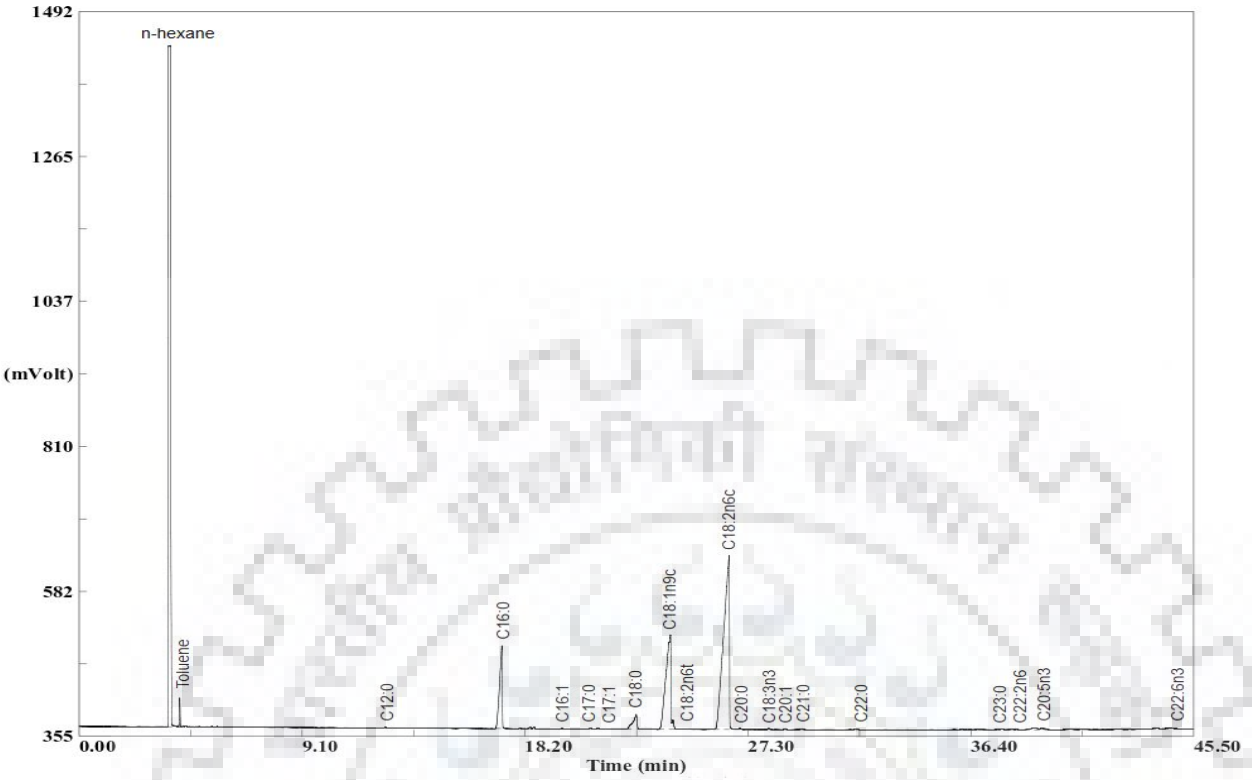


Fig. B.41: GC chromatogram of AM seed oil extracted by SFE in Run 41.

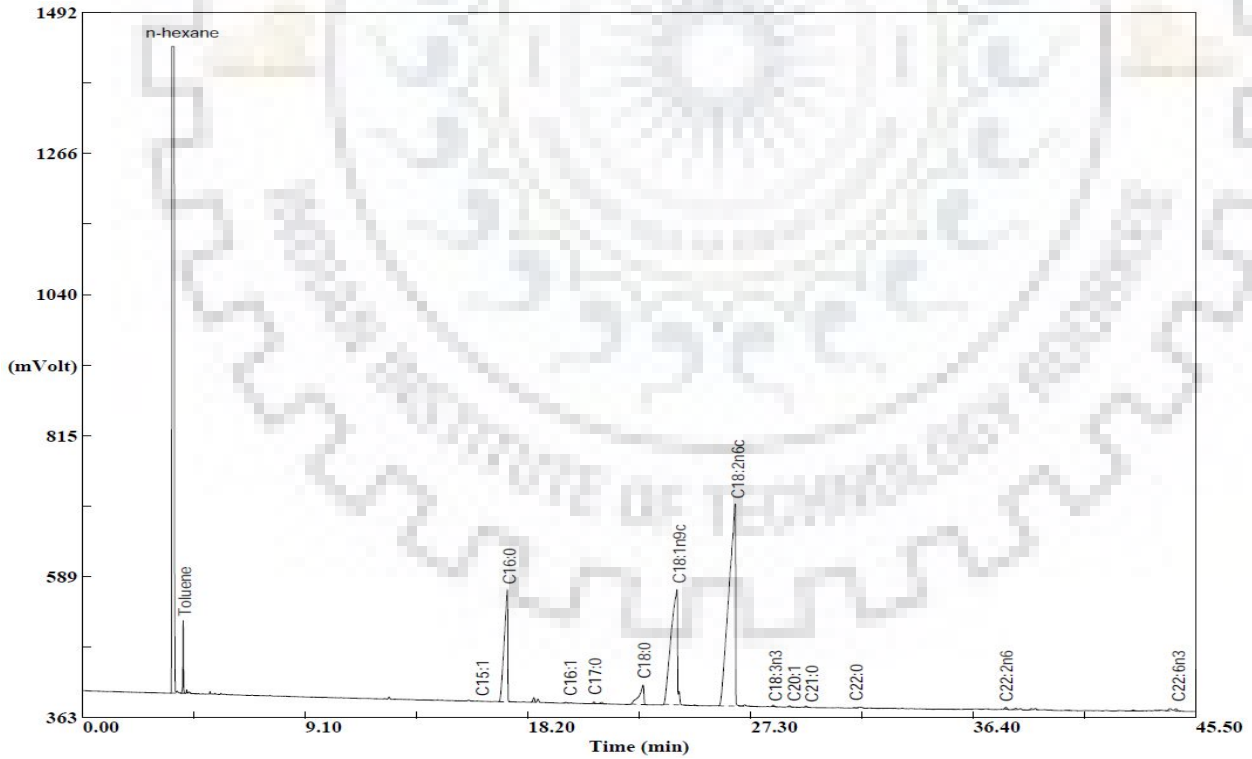


Fig. B.42: GC chromatogram of AM seed oil extracted by SFE in Run 42.

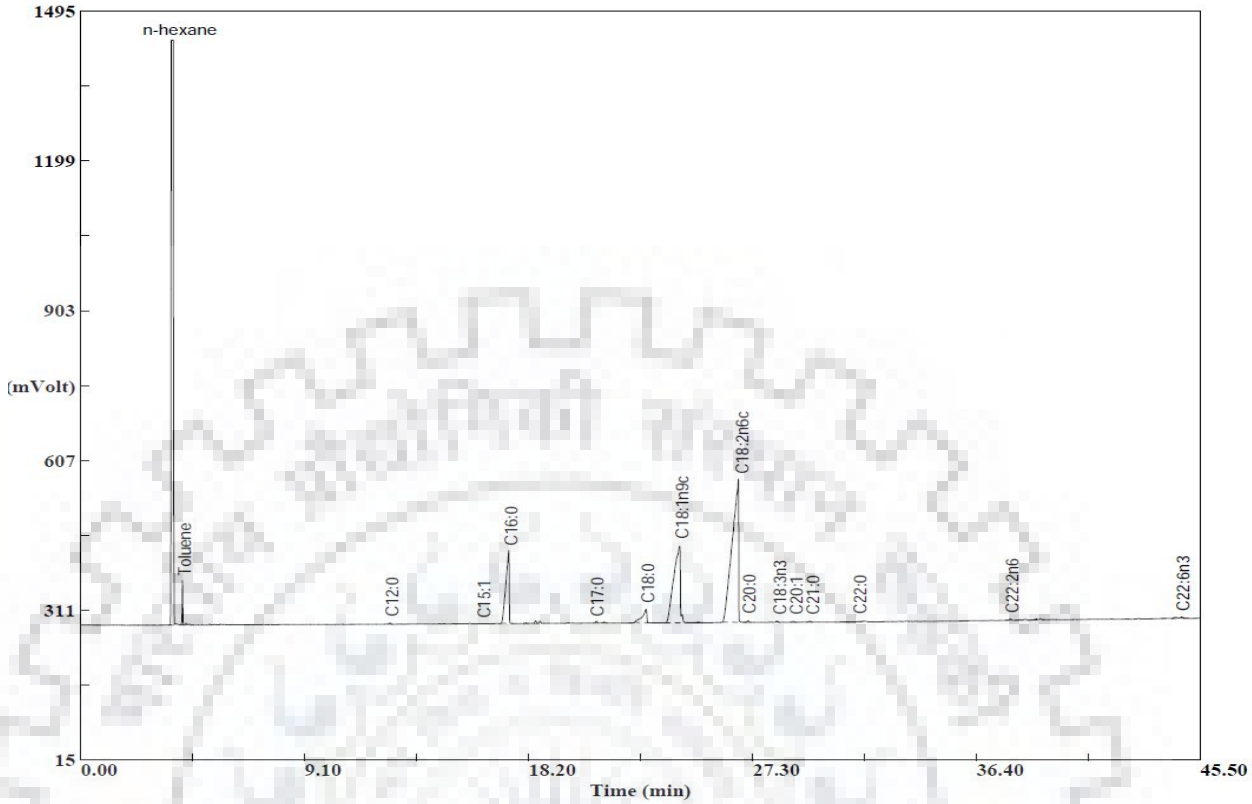


Fig. B.43: GC chromatogram of AM seed oil extracted by SFE in Run 43.

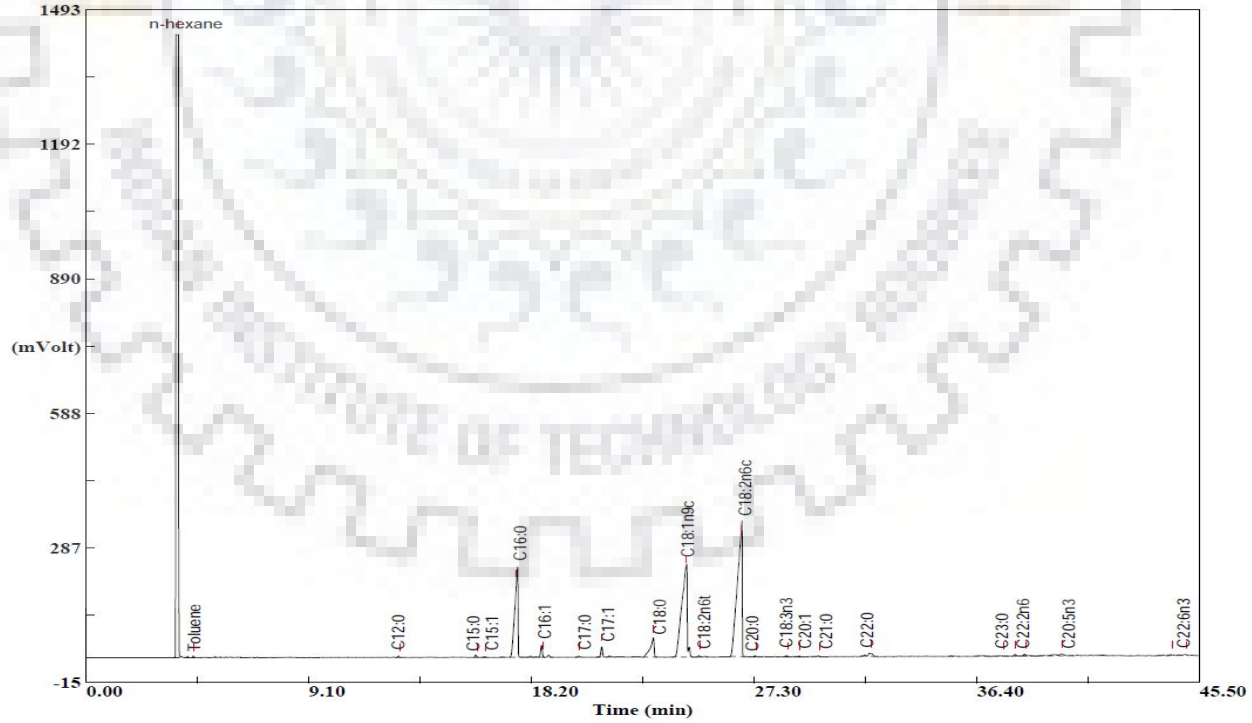


Fig. B.44: GC chromatogram of AM seed oil extracted by SFE in Run 44.

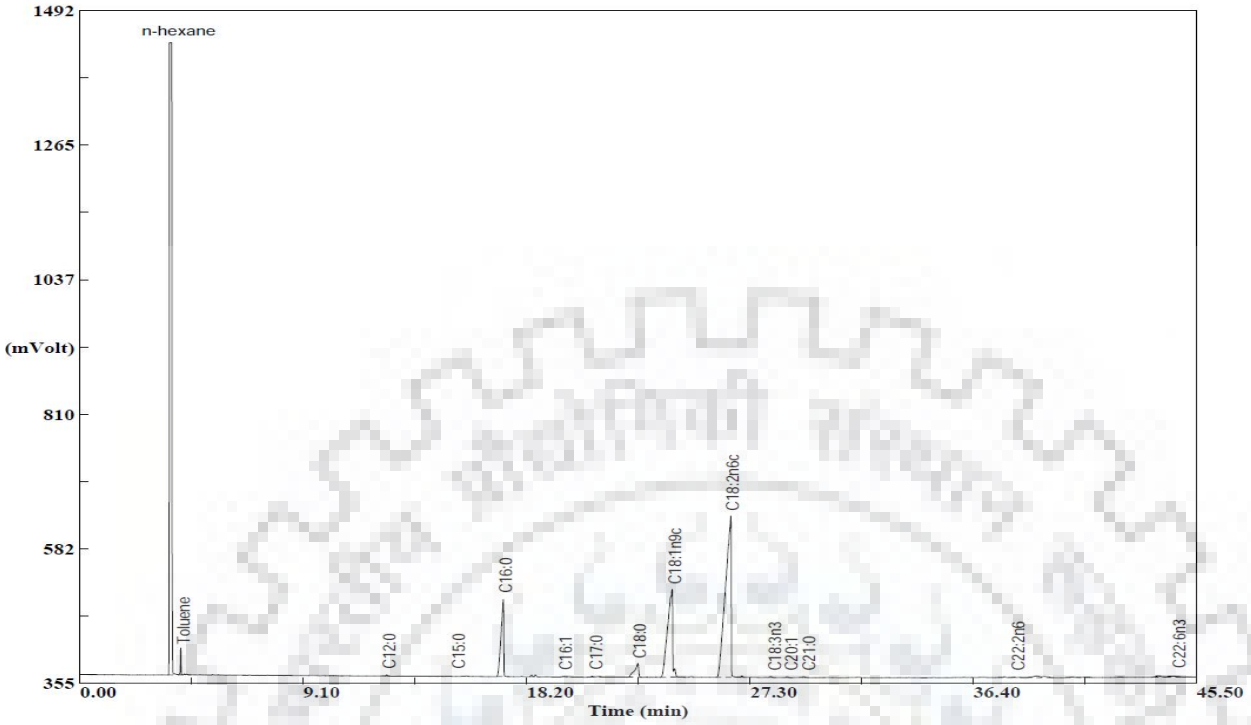


Fig. B.45: GC chromatogram of AM seed oil extracted by SFE in Run 45.

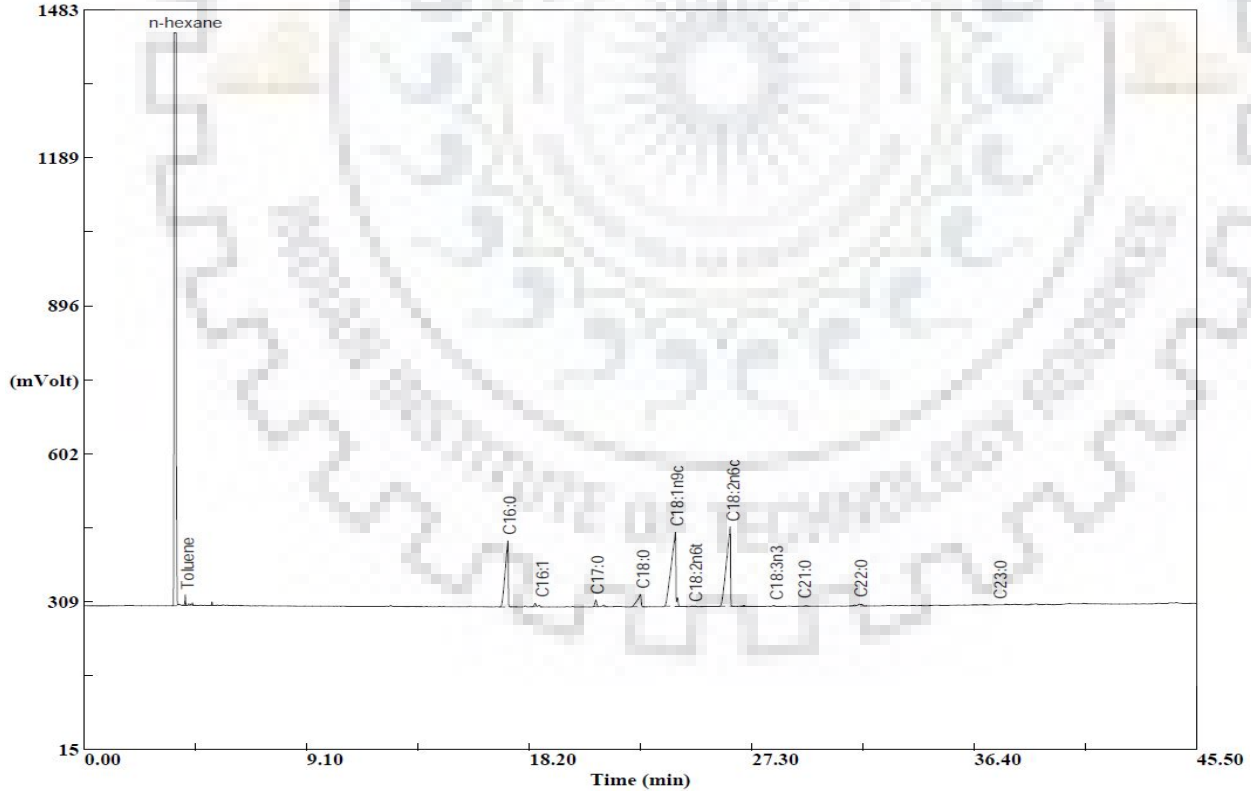


Fig. B.46: GC chromatogram of AM seed oil extracted by SFE in Run 46.

C.1. GC chromatograms of PP seed oil samples extracted in all 46 runs

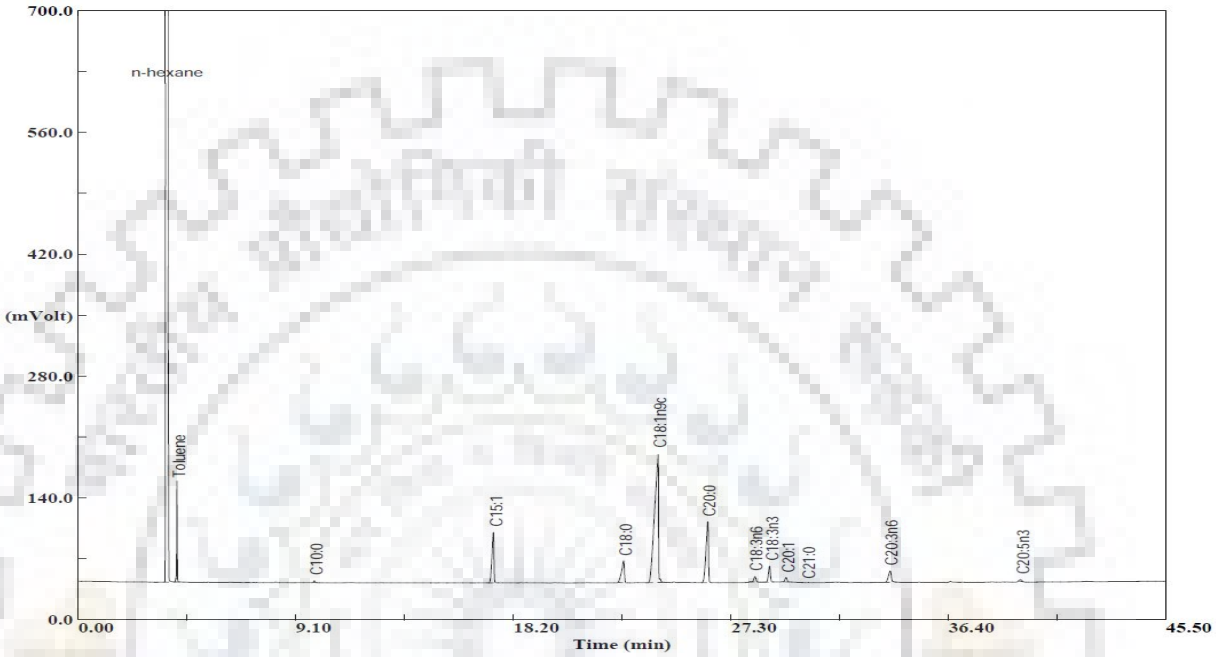


Fig. C.1: GC chromatogram of PP seed oil extracted by SFE in Run 01.

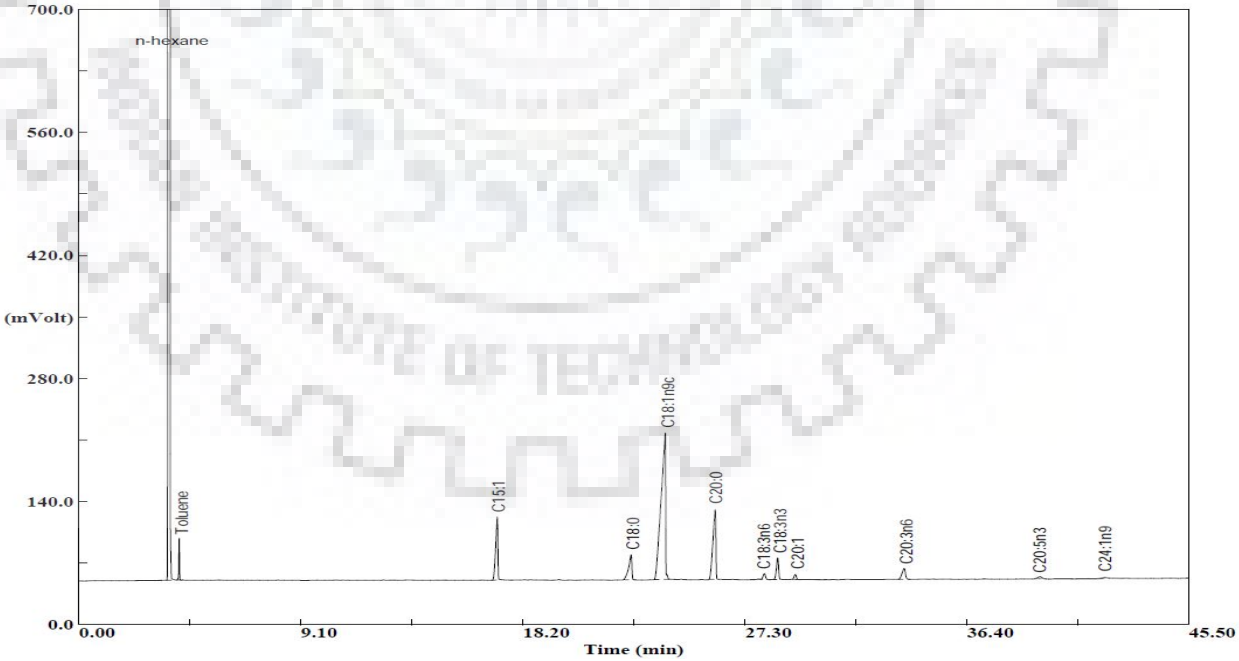


Fig. C.2: GC chromatogram of PP seed oil extracted by SFE in Run 02.

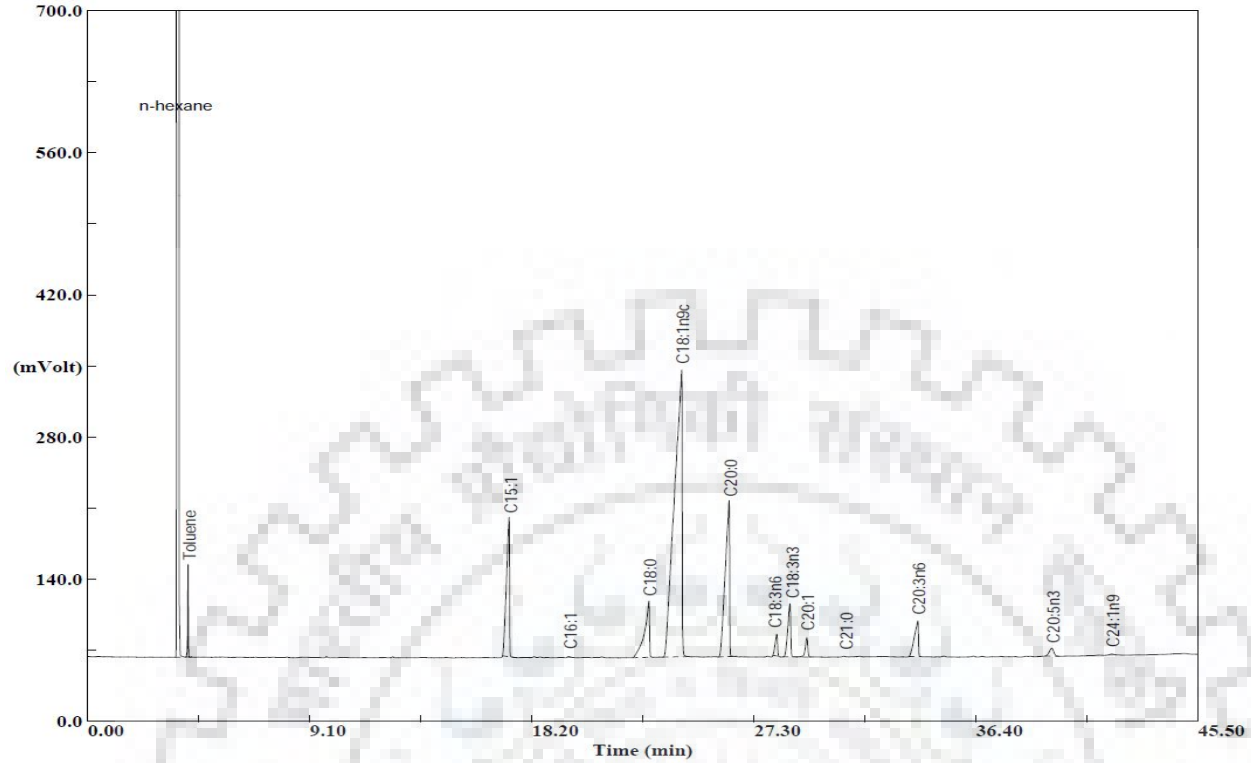


Fig. C.3: GC chromatogram of PP seed oil extracted by SFE in Run 03.

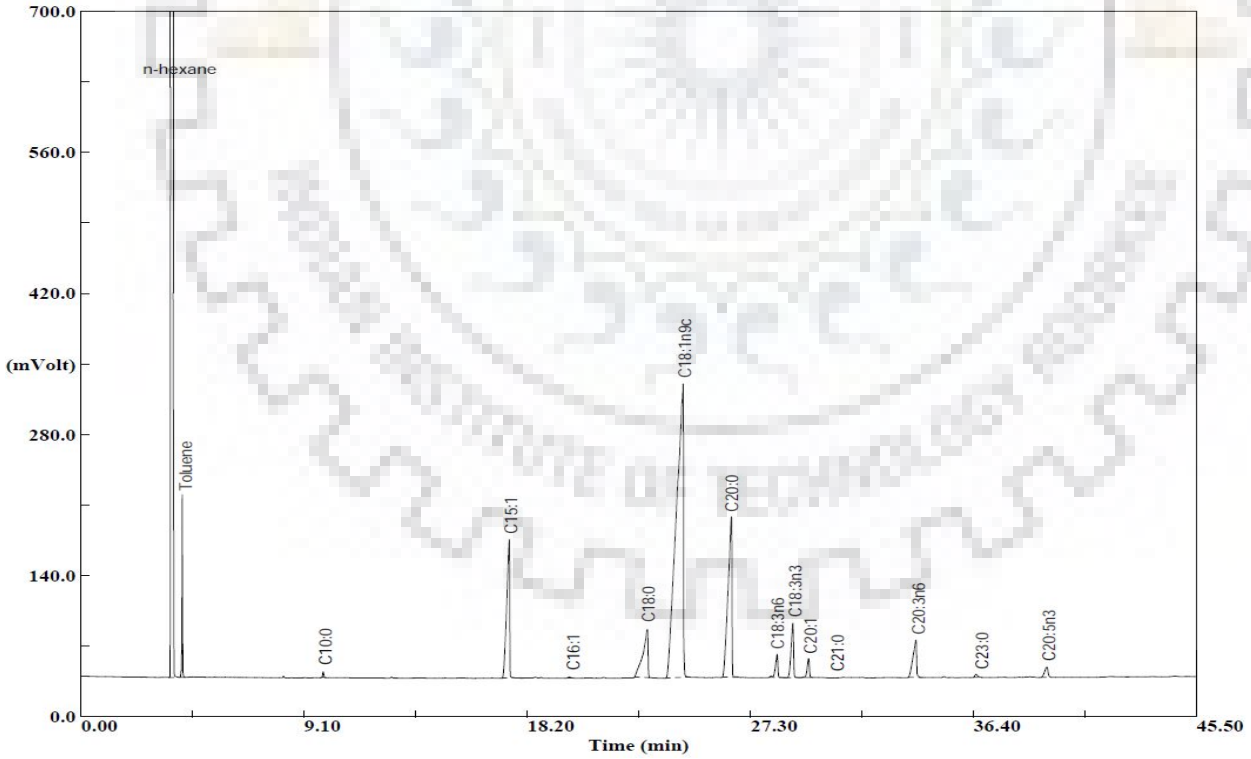


Fig. C.4: GC chromatogram of PP seed oil extracted by SFE in Run 04.

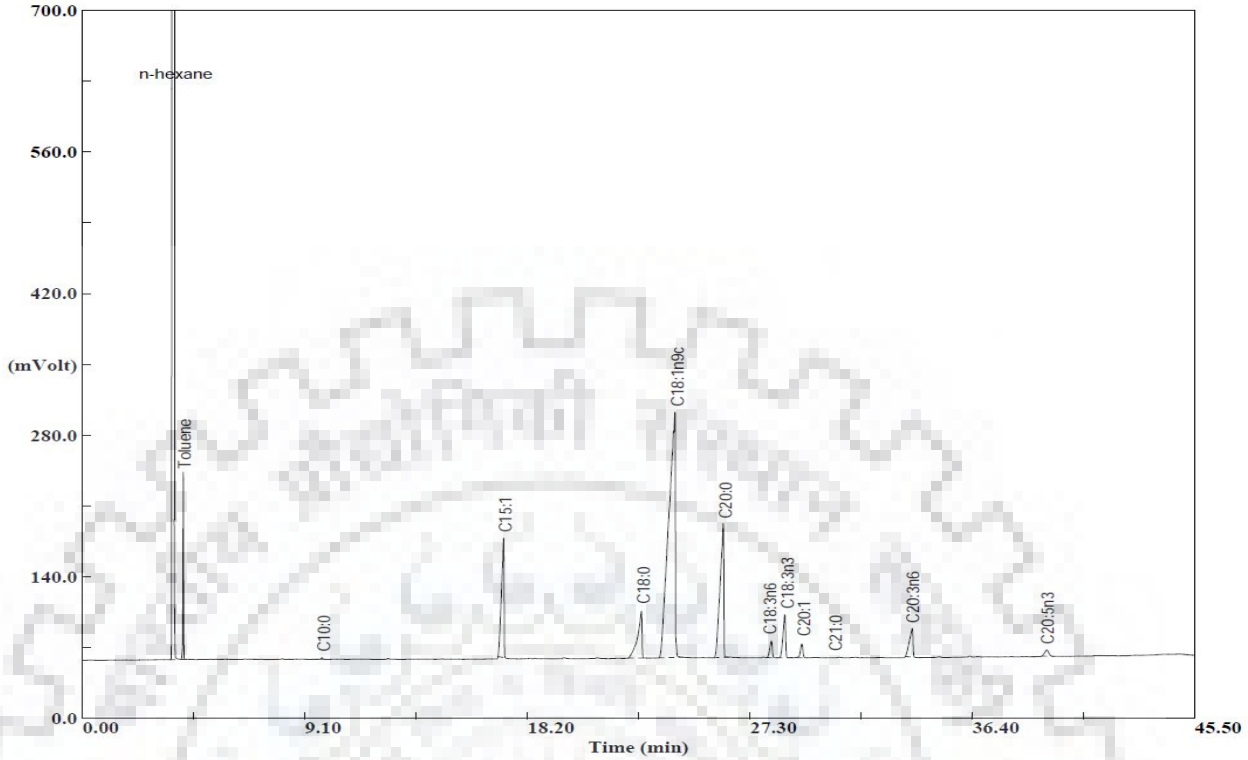


Fig. C.5: GC chromatogram of PP seed oil extracted by SFE in Run 05.

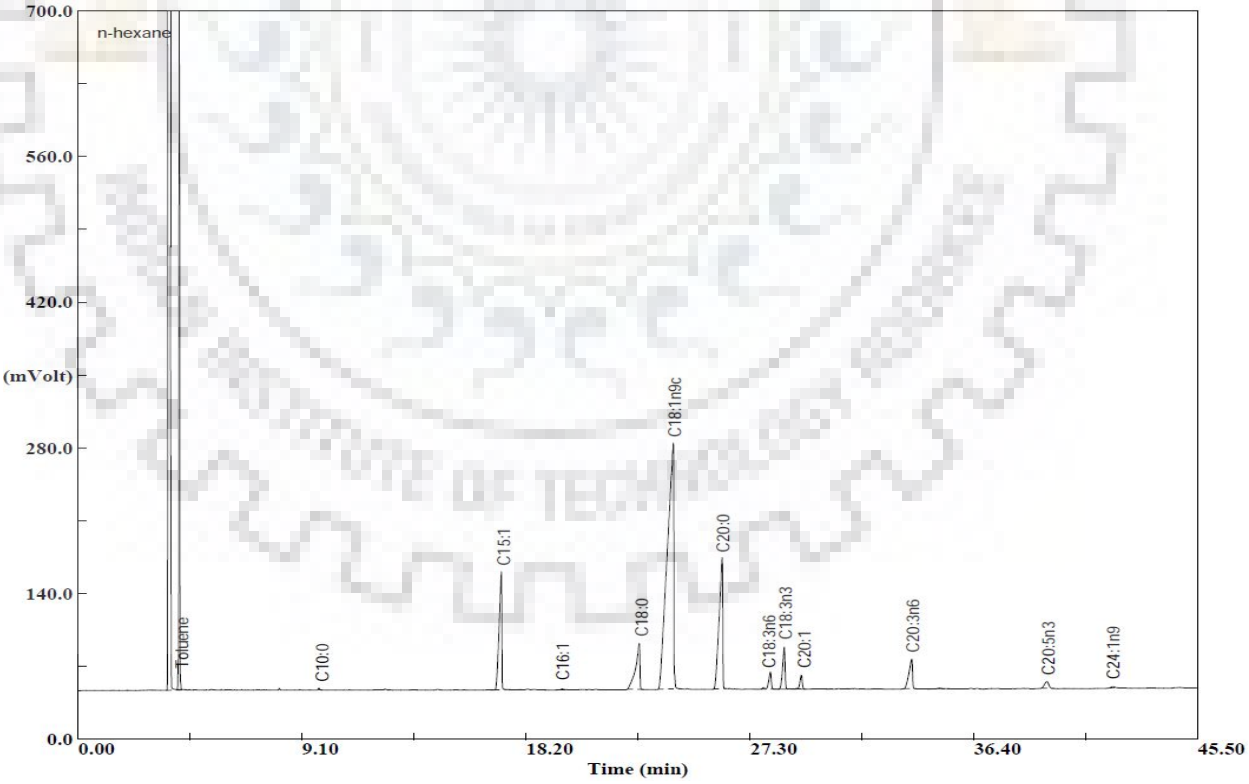


Fig. C.6: GC chromatogram of PP seed oil extracted by SFE in Run 06.

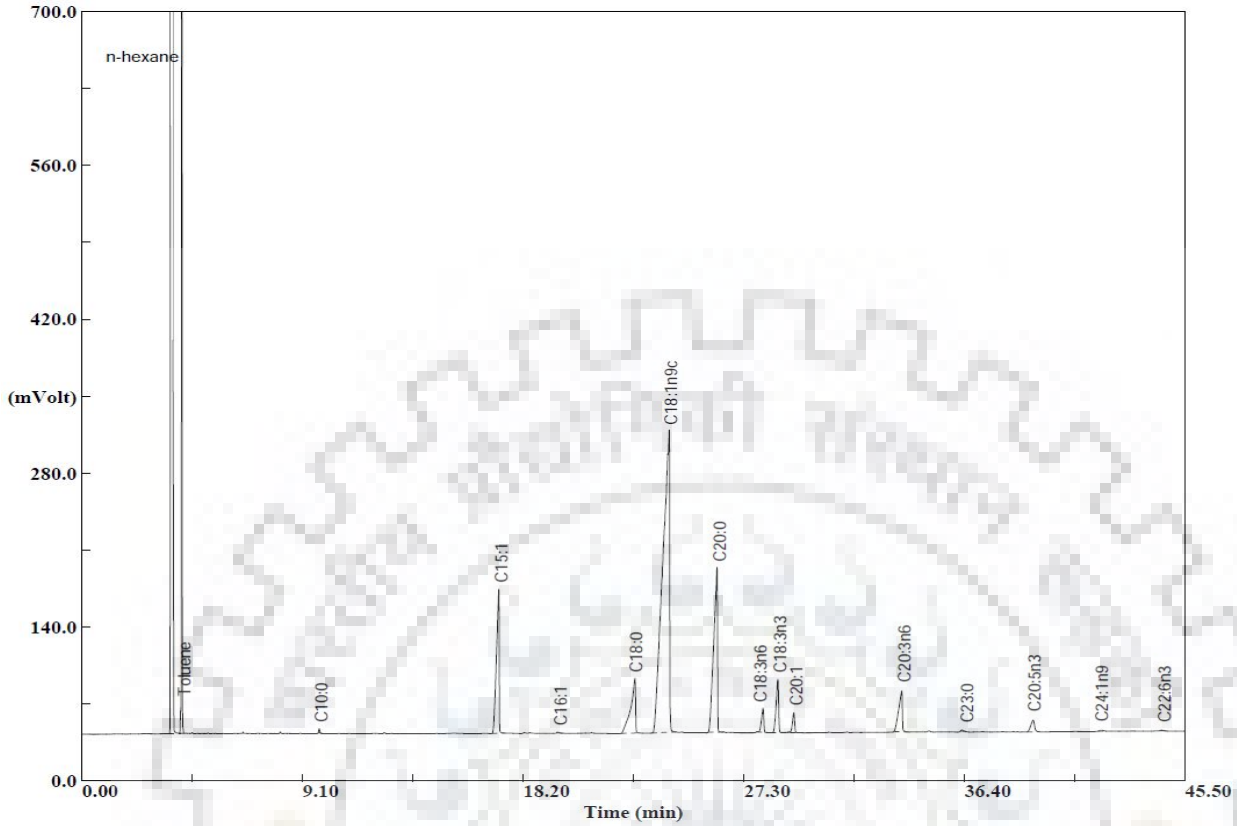


Fig. C.7: GC chromatogram of PP seed oil extracted by SFE in Run 07.

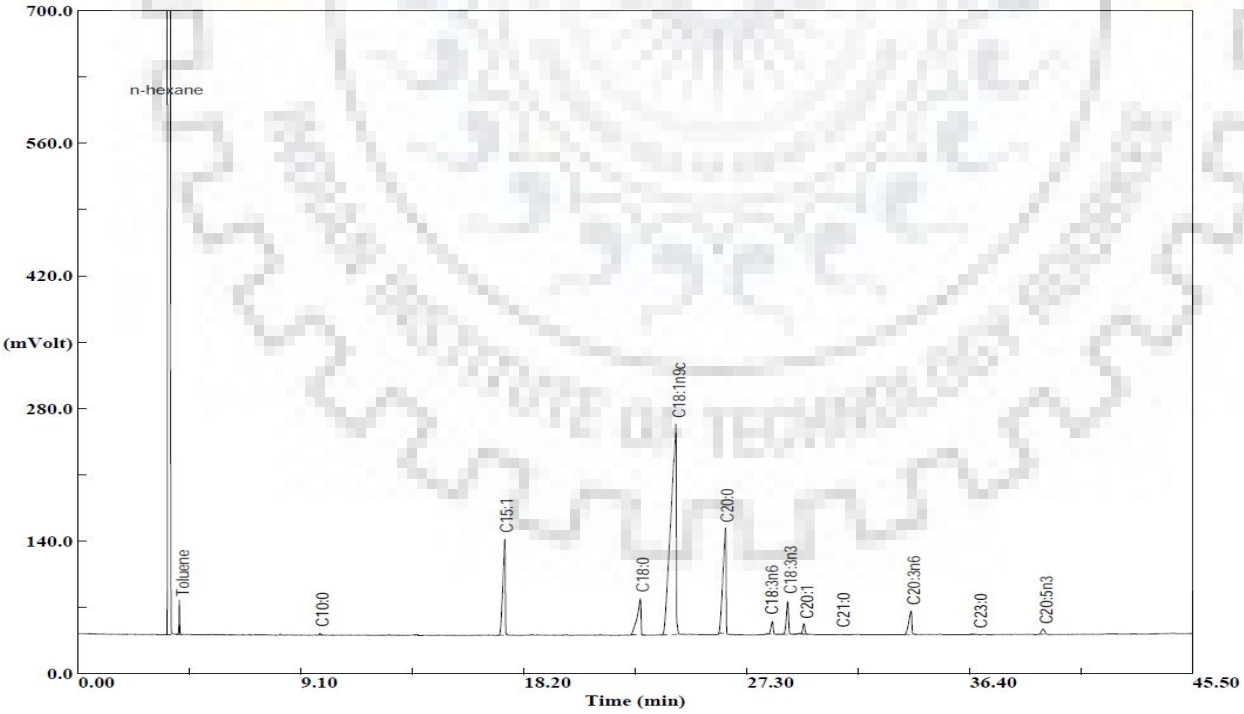


Fig. C.8: GC chromatogram of PP seed oil extracted by SFE in Run 08.

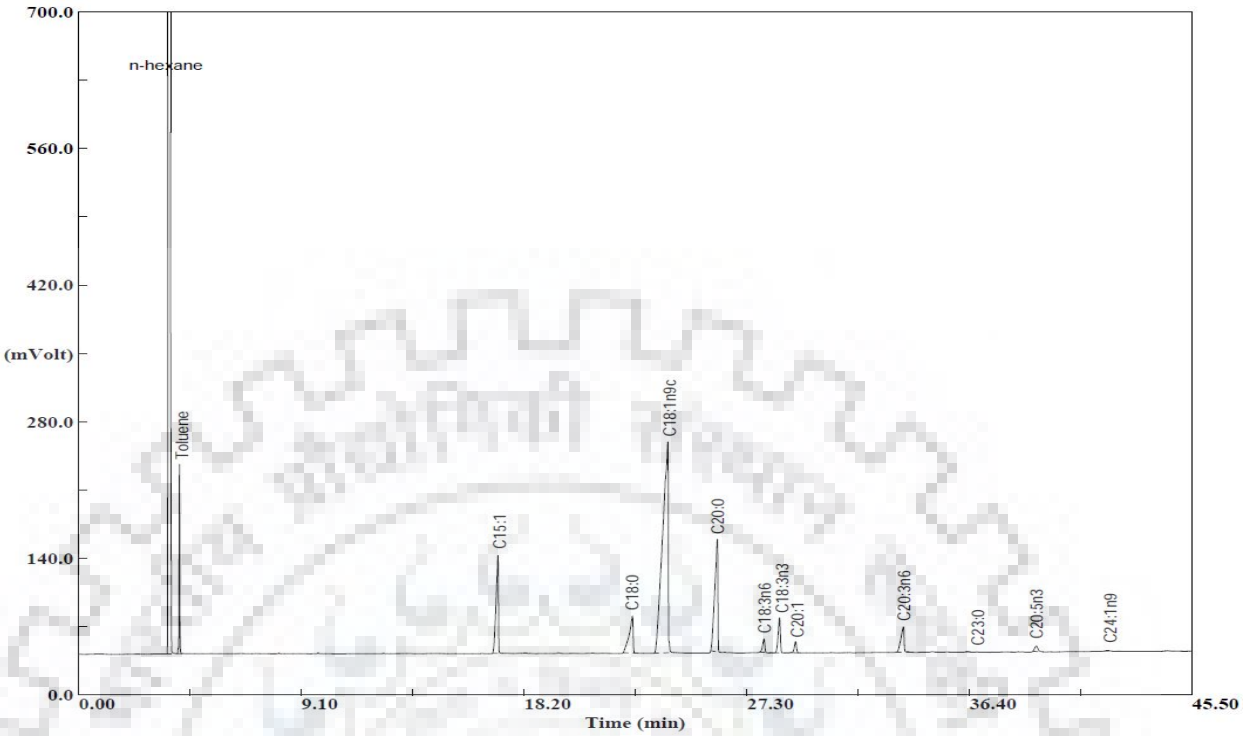


Fig. C.9: GC chromatogram of PP seed oil extracted by SFE in Run 09.

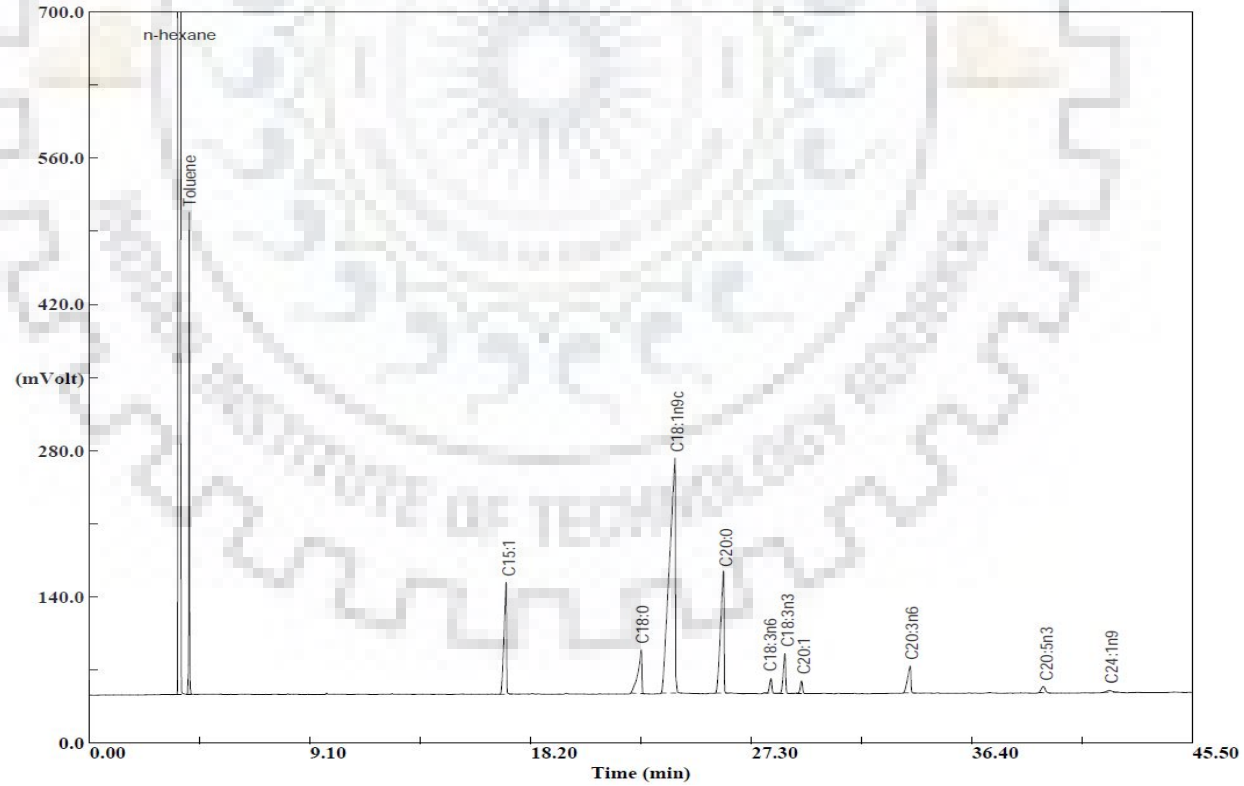


Fig. C.10: GC chromatogram of PP seed oil extracted by SFE in Run 10.

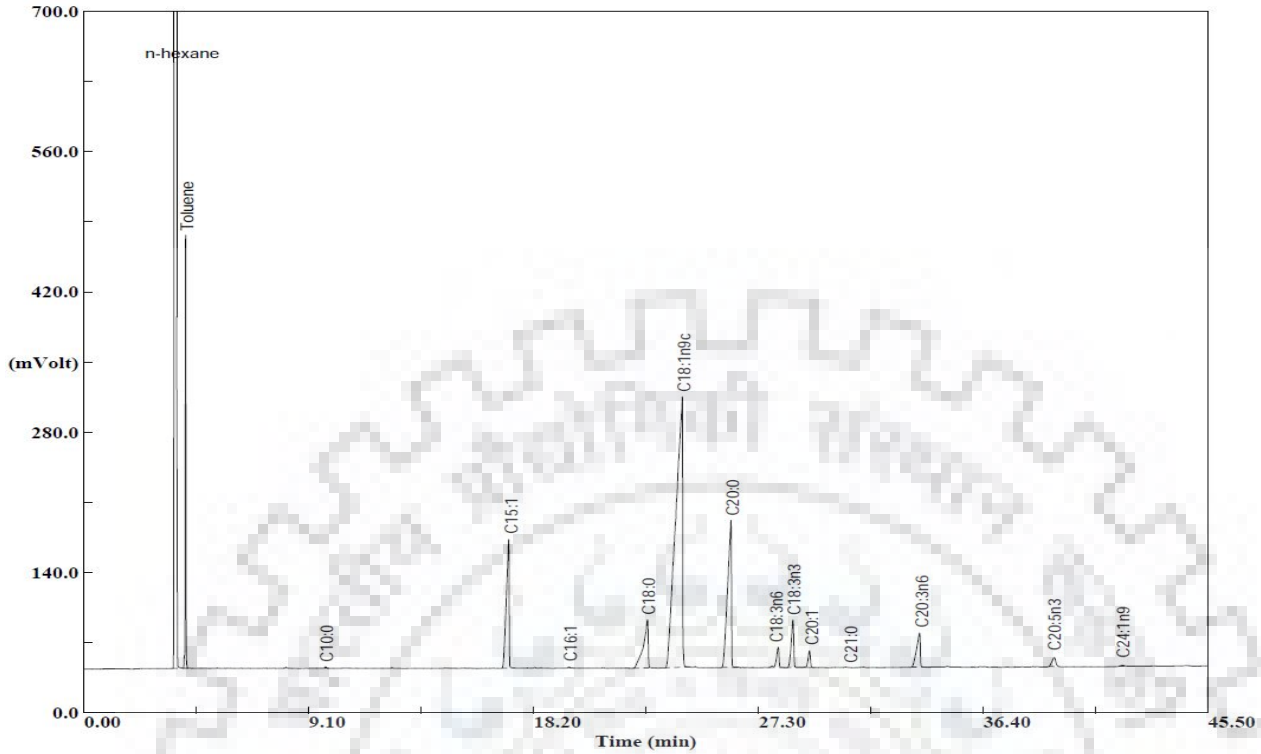


Fig. C.11: GC chromatogram of PP seed oil extracted by SFE in Run 11.

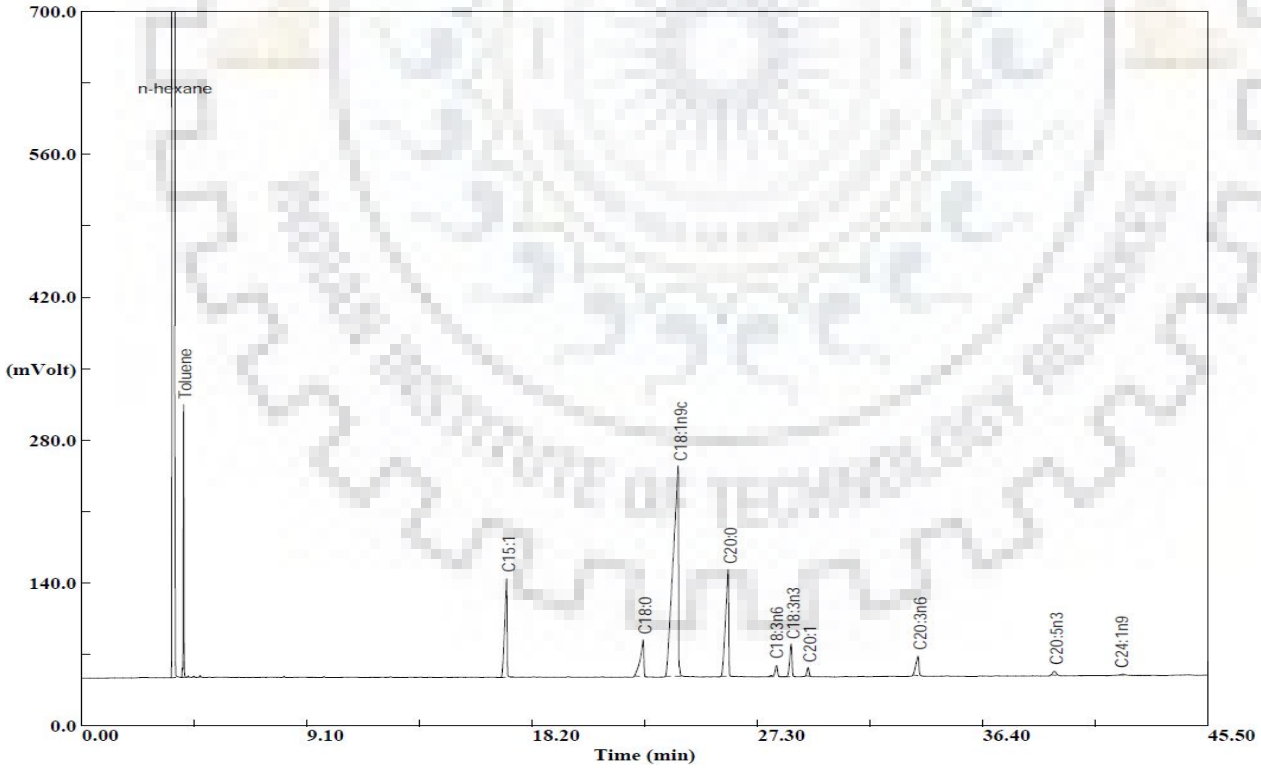


Fig. C.12: GC chromatogram of PP seed oil extracted by SFE in Run 12.

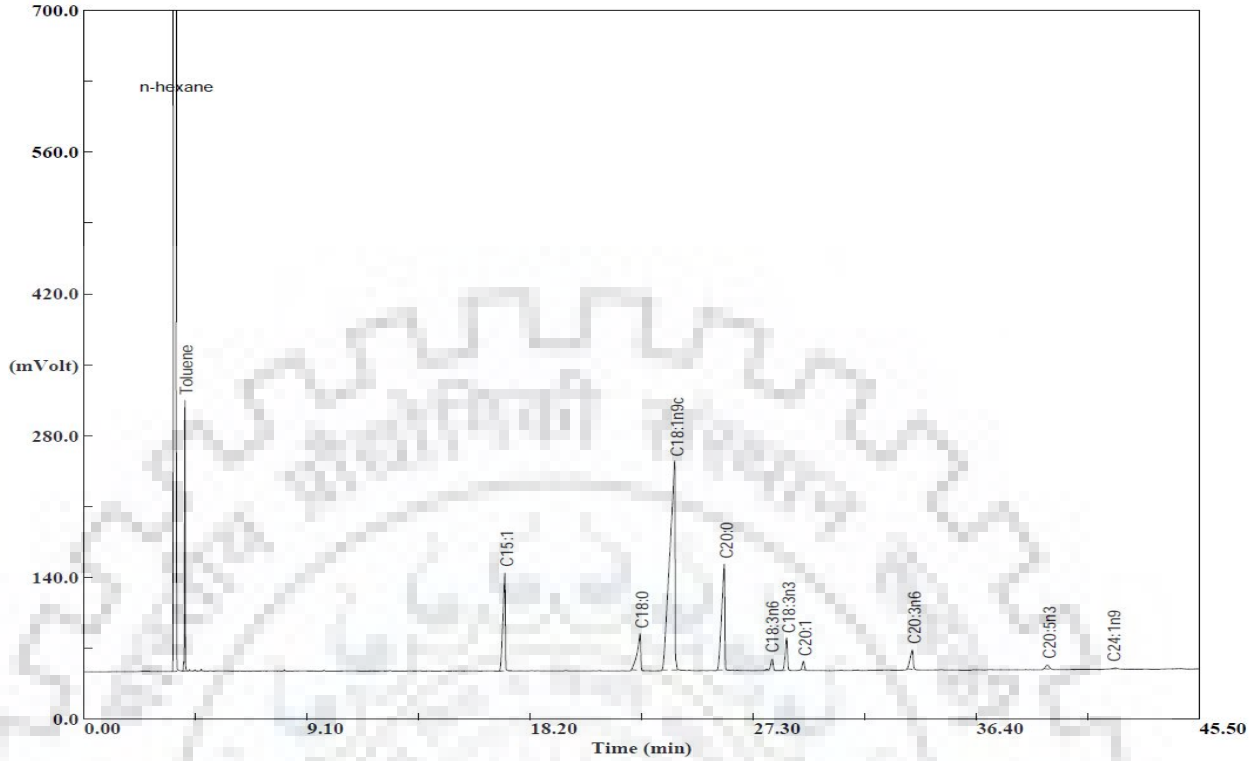


Fig. C.13: GC chromatogram of PP seed oil extracted by SFE in Run 13.

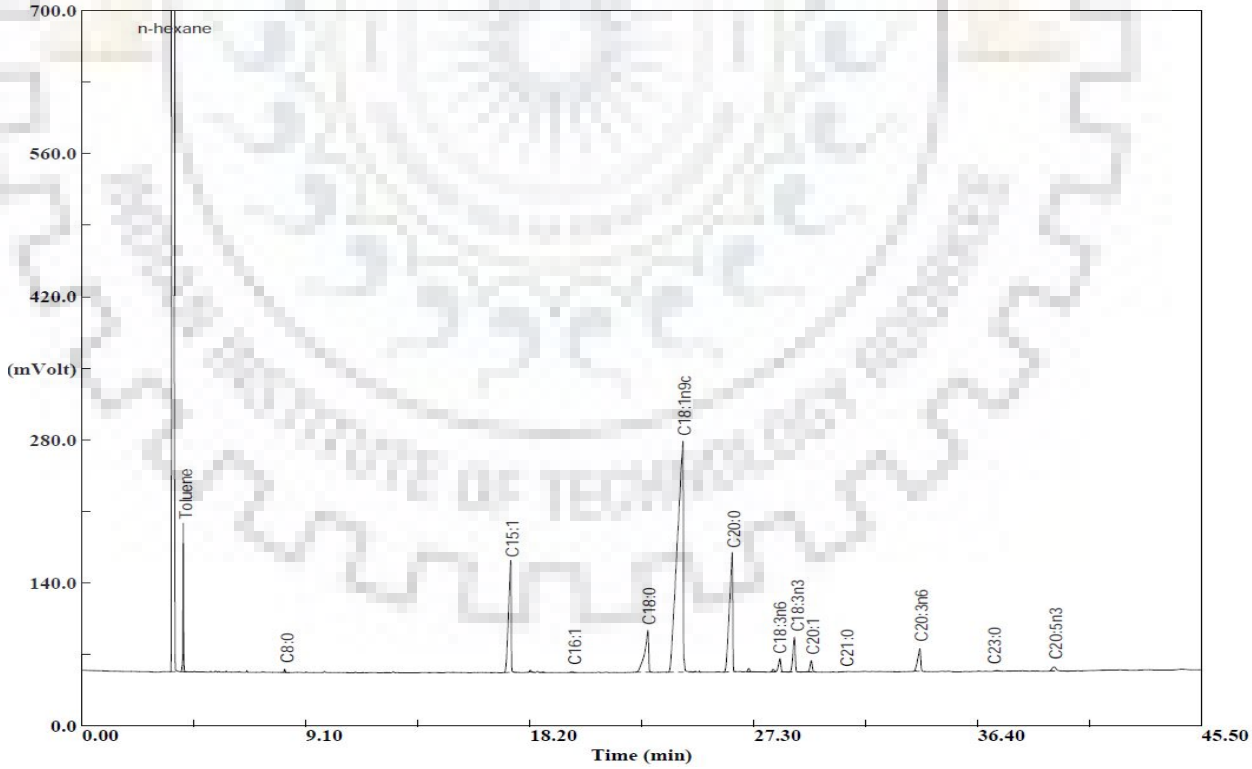


Fig. C.14: GC chromatogram of PP seed oil extracted by SFE in Run 14.

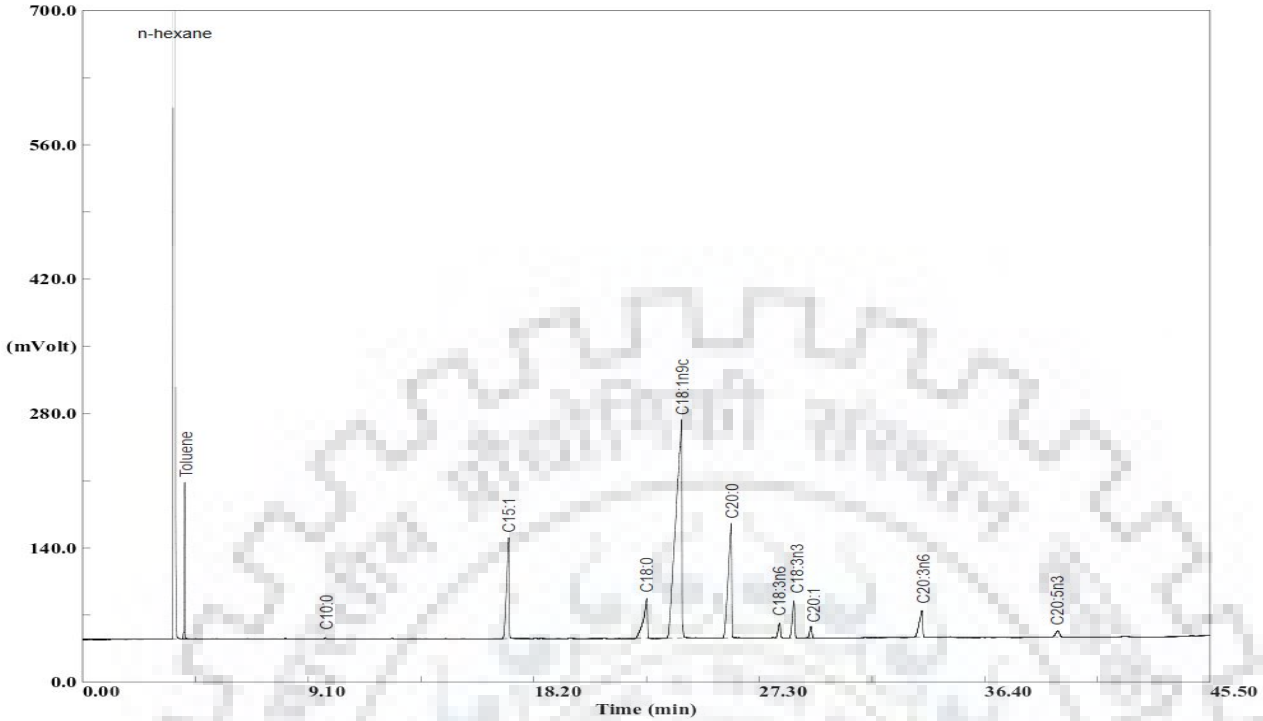


Fig. C.15: GC chromatogram of PP seed oil extracted by SFE in Run 15.

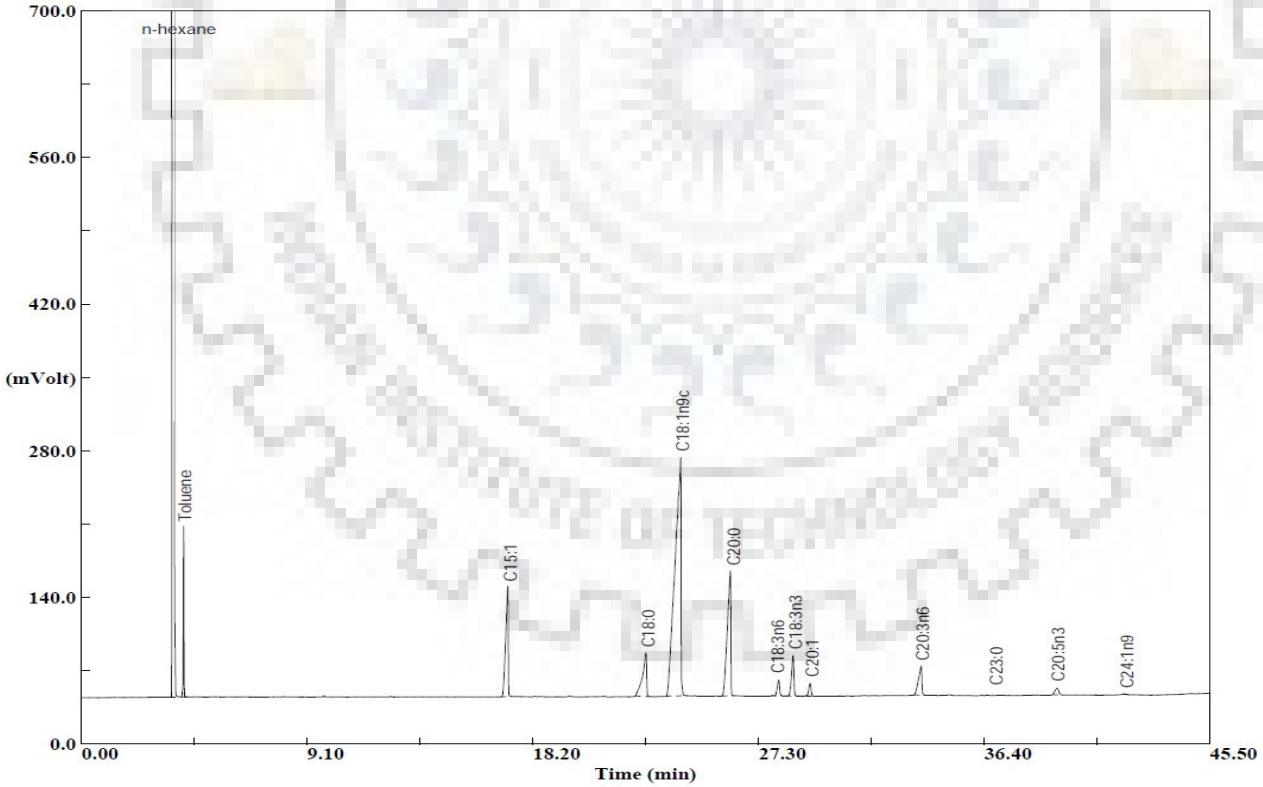


Fig. C.16: GC chromatogram of PP seed oil extracted by SFE in Run 16.

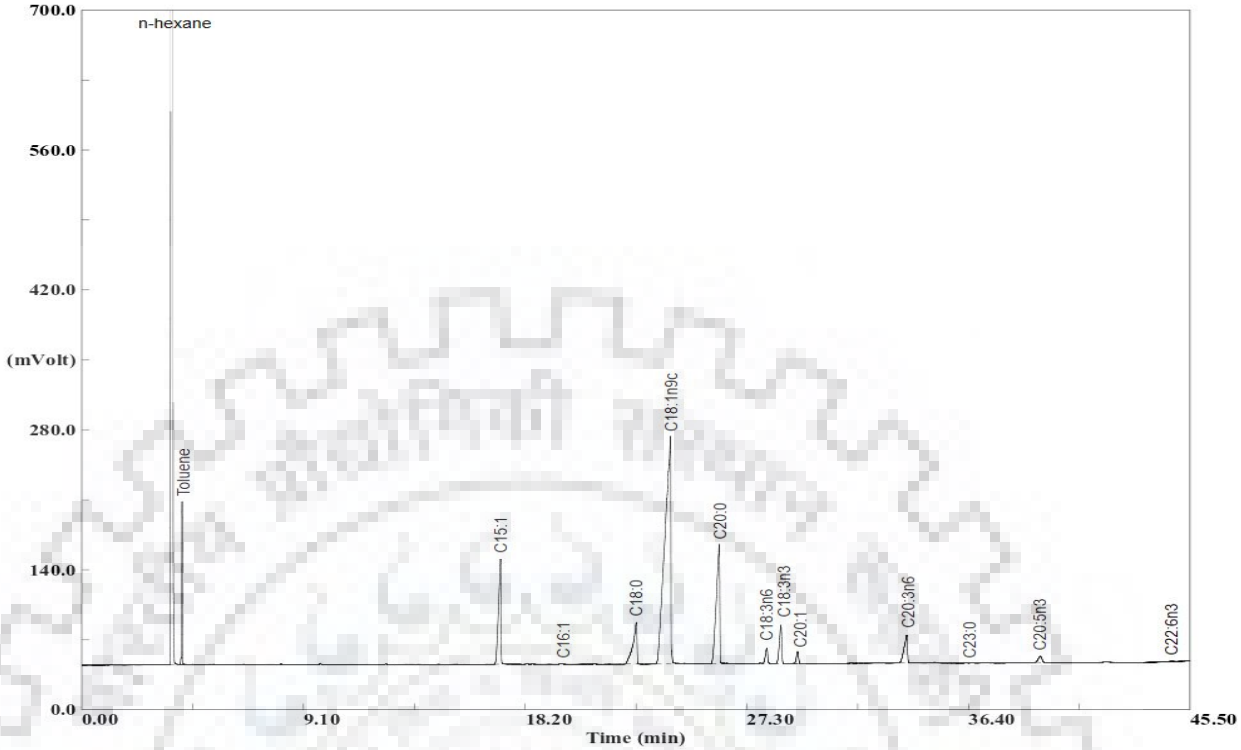


Fig. C.17: GC chromatogram of PP seed oil extracted by SFE in Run 17.

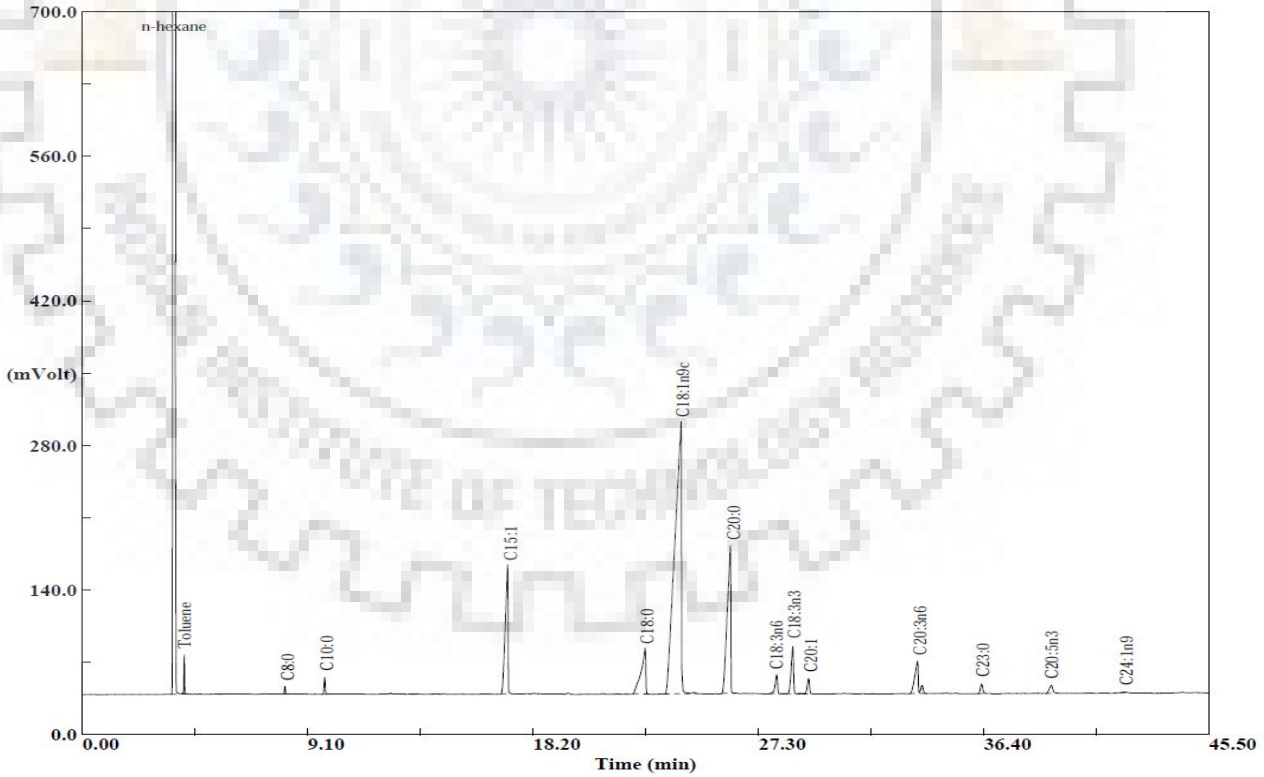


Fig. C.18: GC chromatogram of PP seed oil extracted by SFE in Run 18.

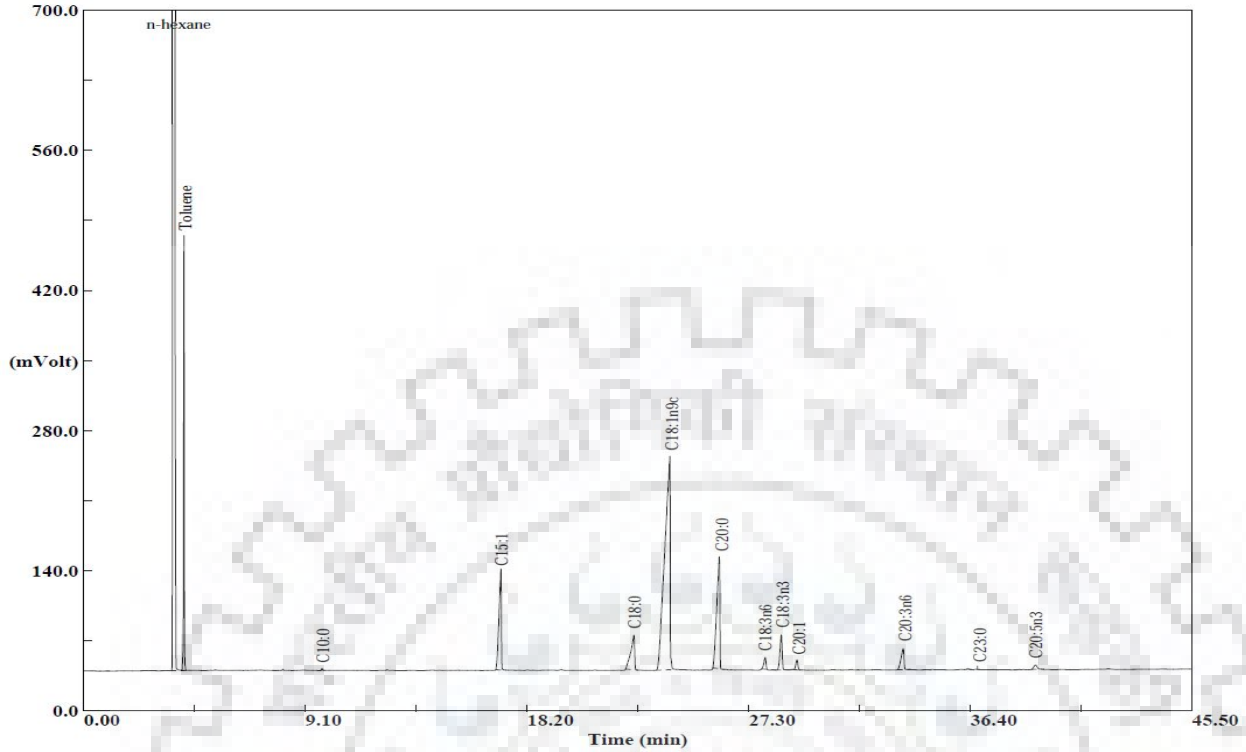


Fig. C.19: GC chromatogram of PP seed oil extracted by SFE in Run 19.

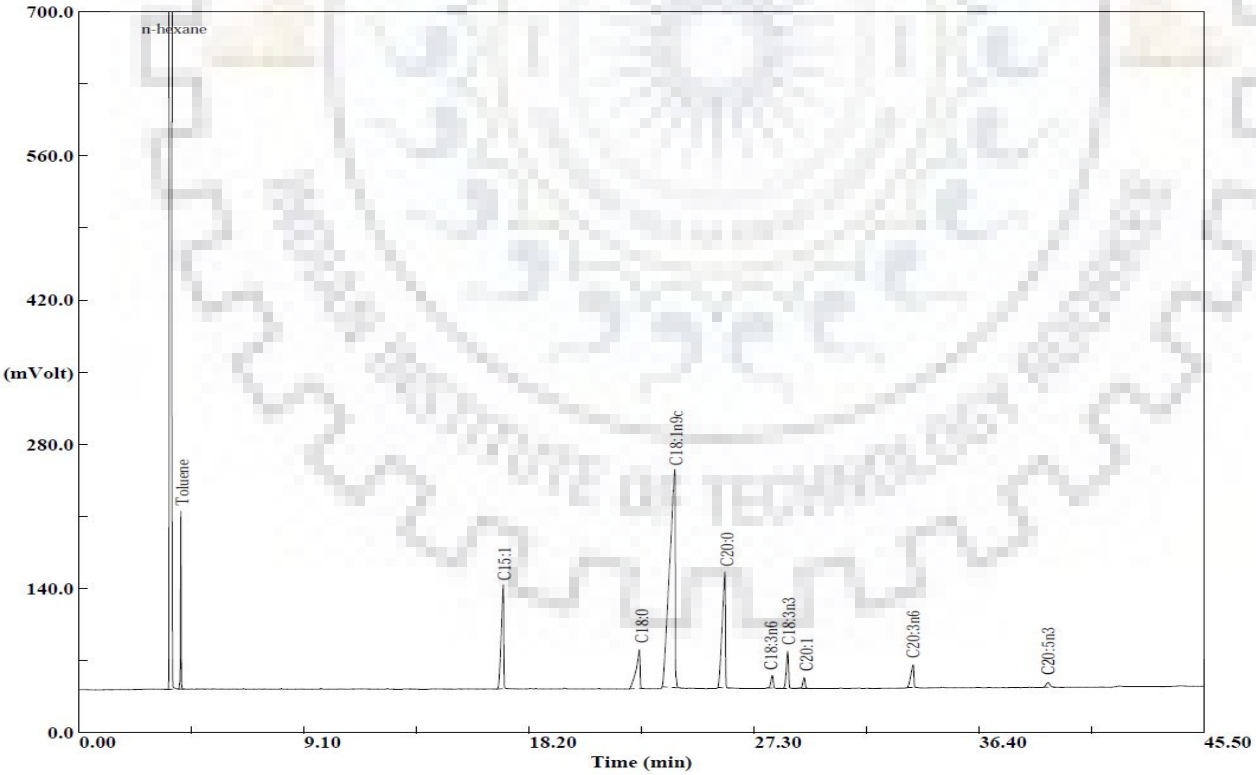


Fig. C.20: GC chromatogram of PP seed oil extracted by SFE in Run 20.

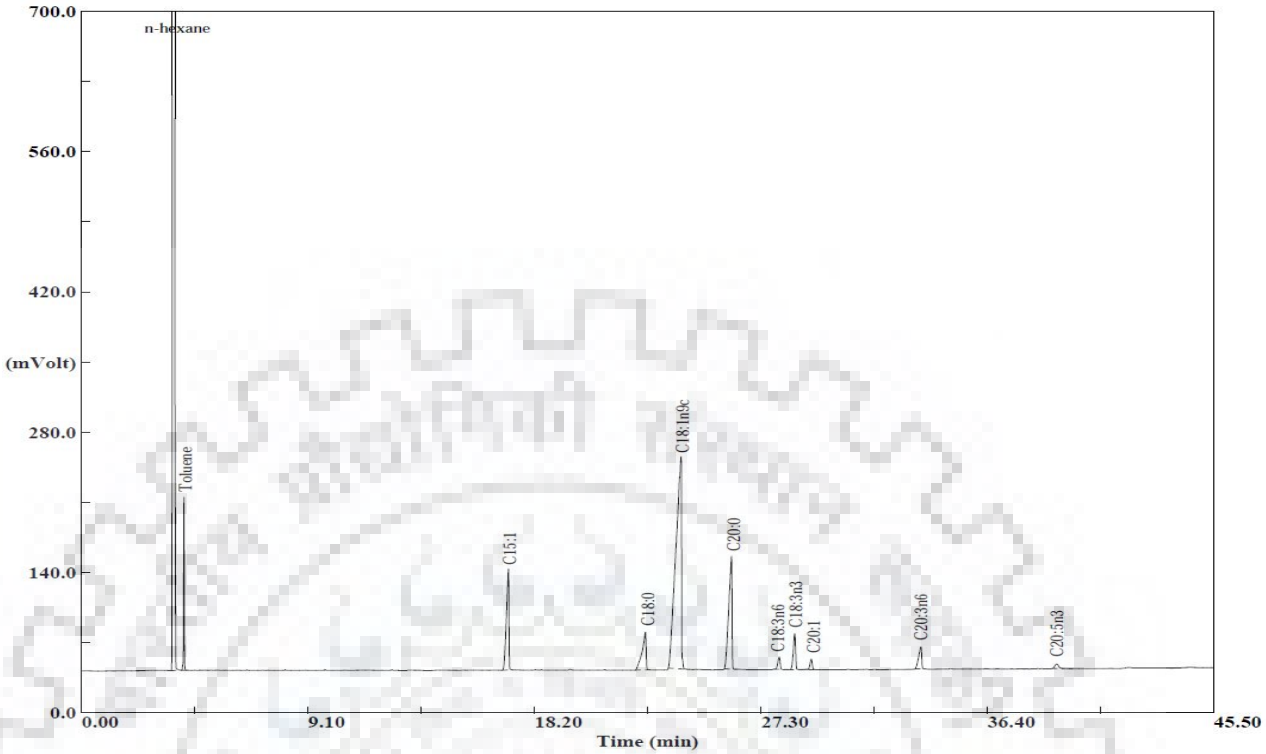


Fig. C.21: GC chromatogram of PP seed oil extracted by SFE in Run 21.

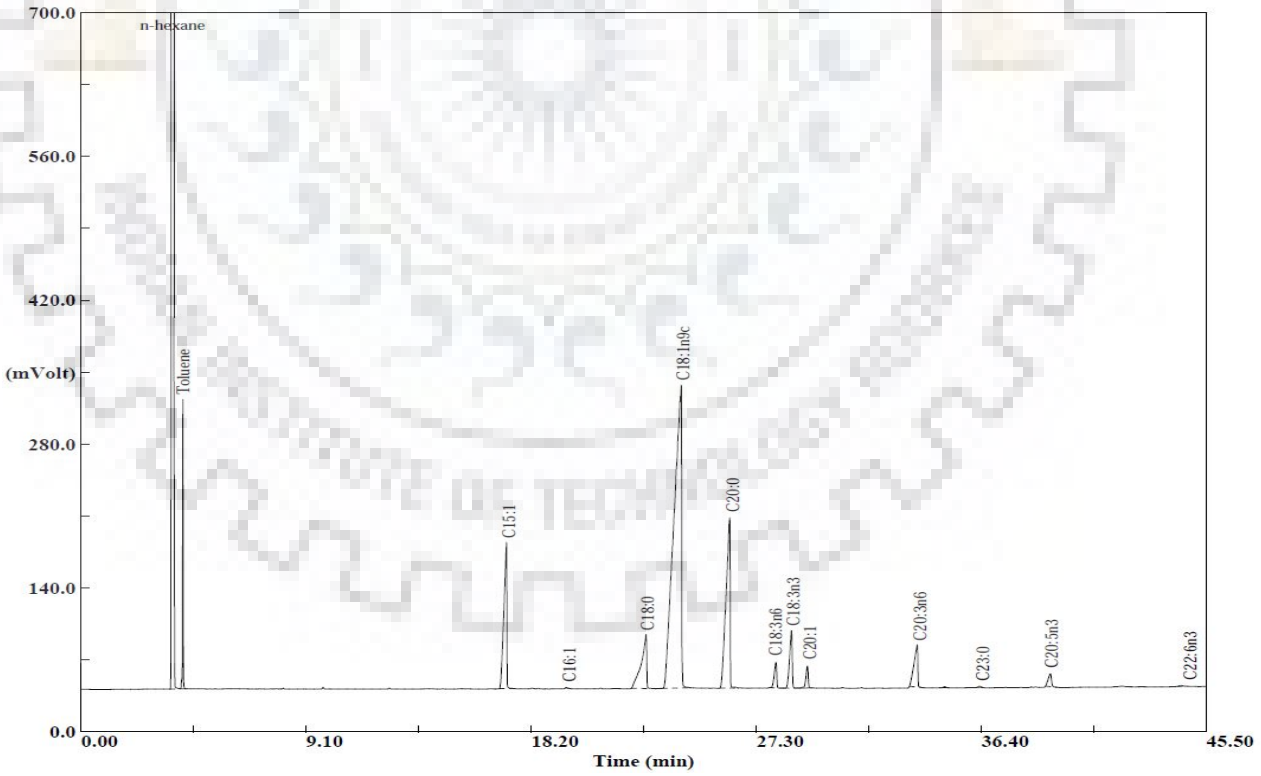


Fig. C.22: GC chromatogram of PP seed oil extracted by SFE in Run 22.

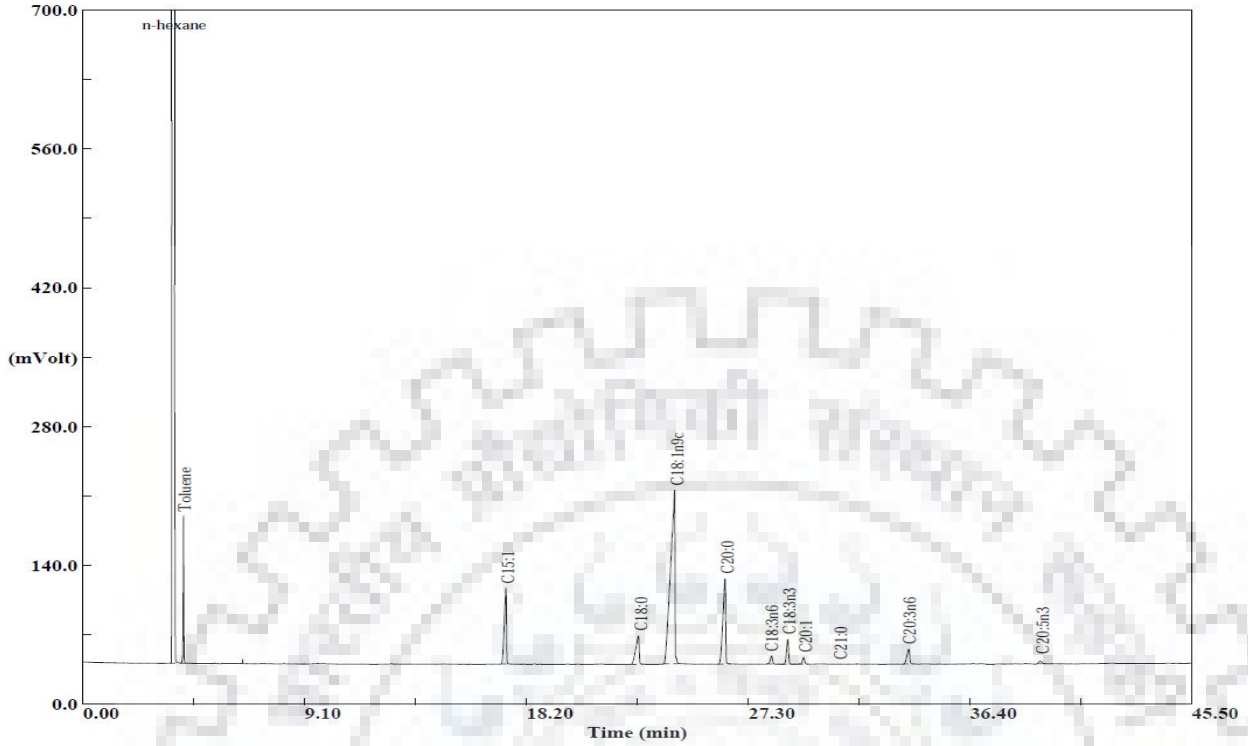


Fig. C.23: GC chromatogram of PP seed oil extracted by SFE in Run 23.

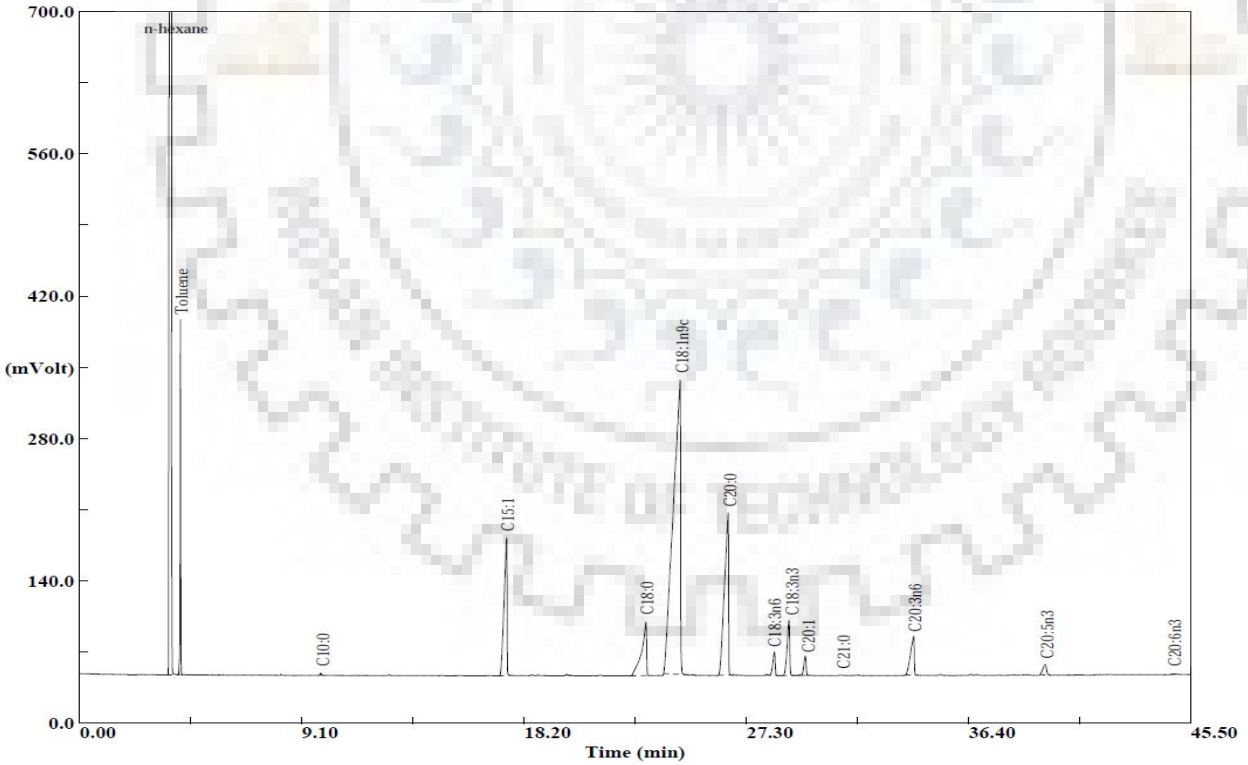


Fig. C.24: GC chromatogram of PP seed oil extracted by SFE in Run 24.

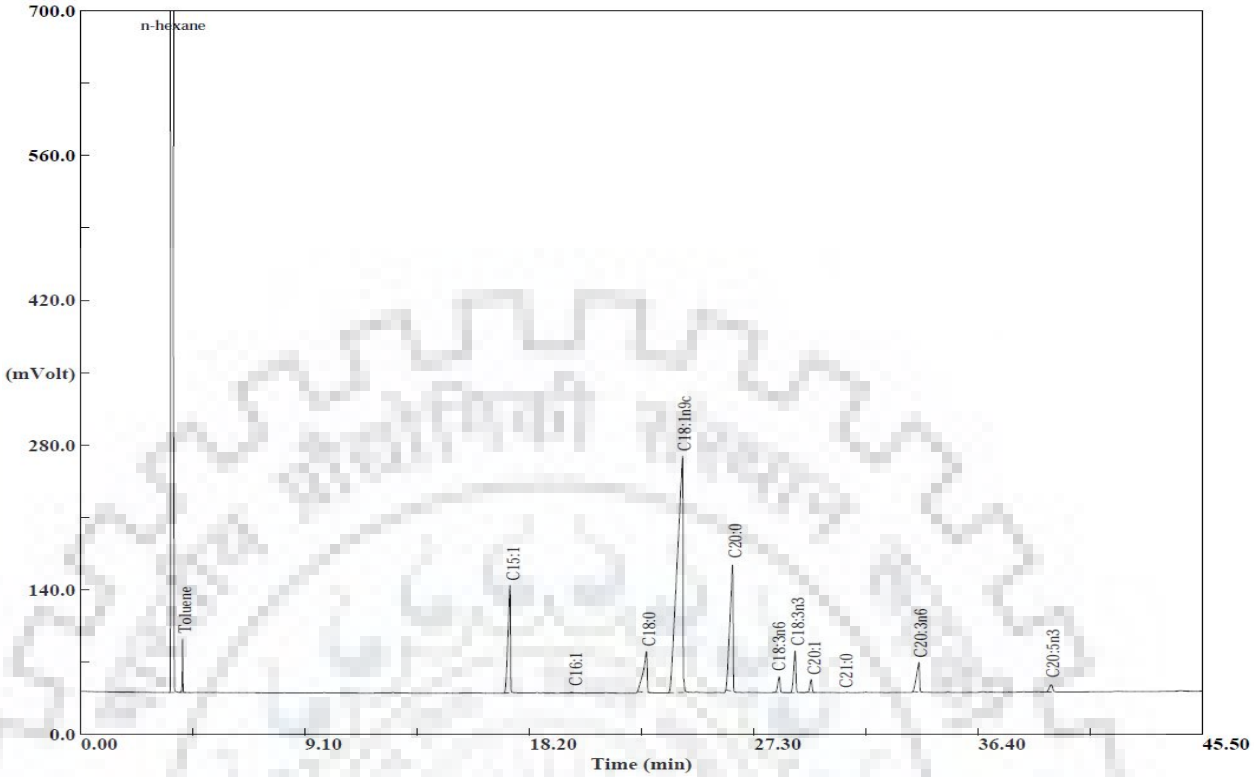


Fig. C.25: GC chromatogram of PP seed oil extracted by SFE in Run 25.

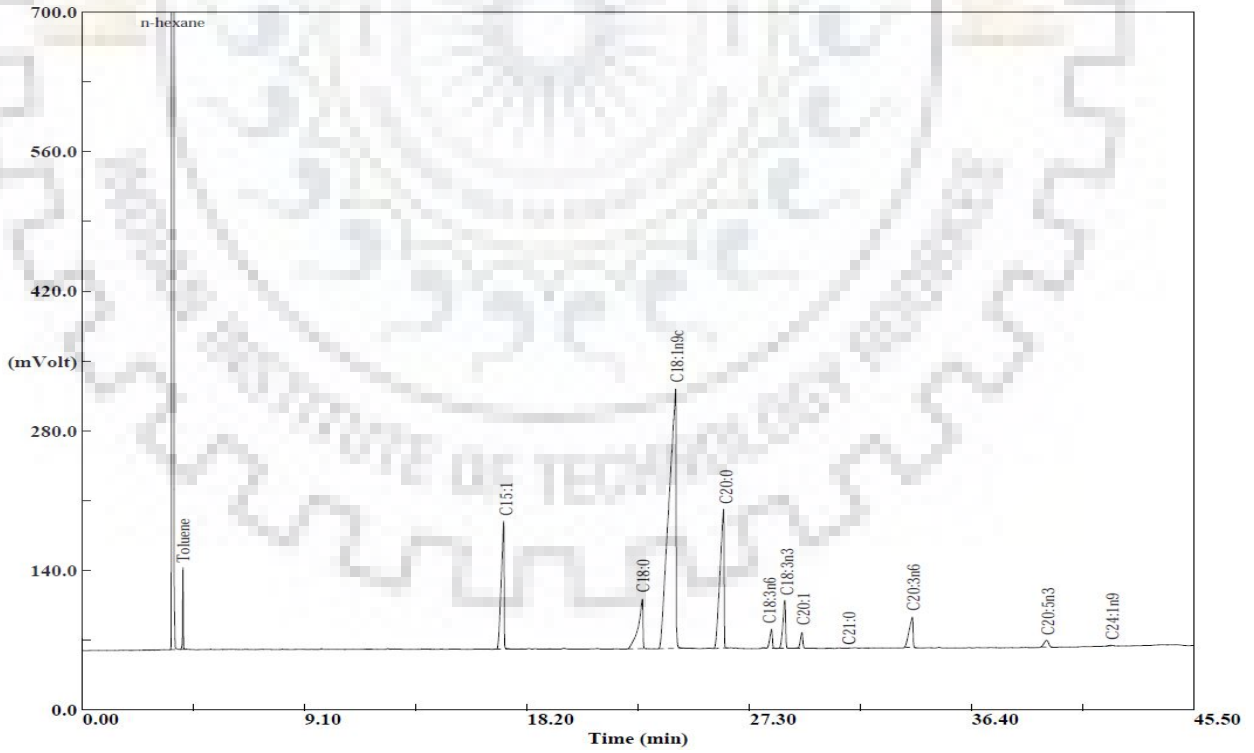


Fig. C.26: GC chromatogram of PP seed oil extracted by SFE in Run 26.

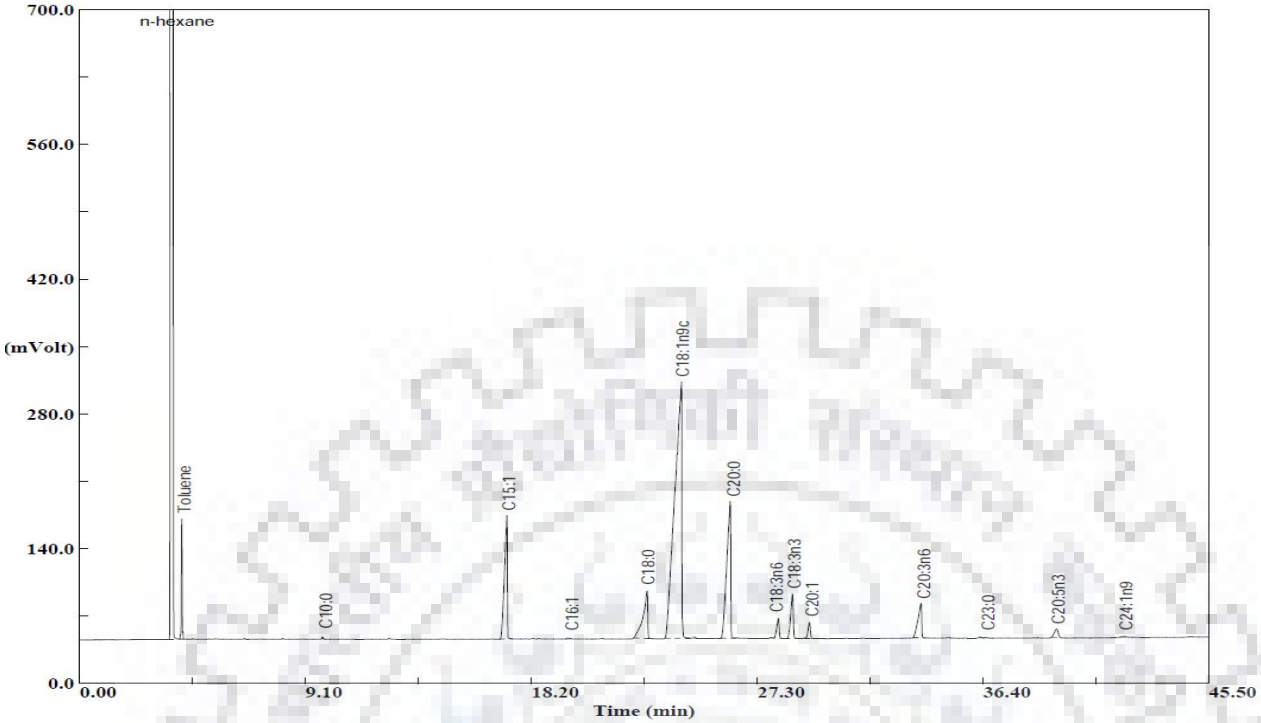


Fig. C.27: GC chromatogram of PP seed oil extracted by SFE in Run 27.

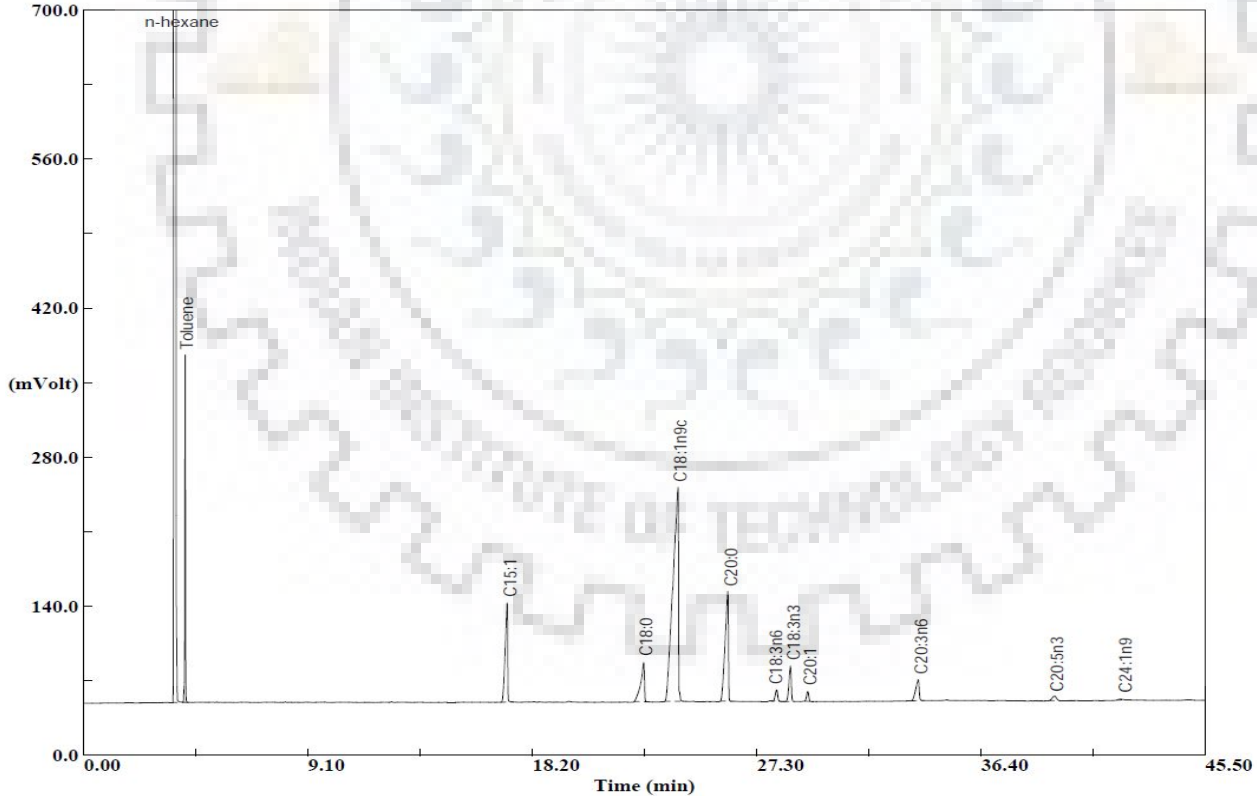


Fig. C.28: GC chromatogram of PP seed oil extracted by SFE in Run 28.

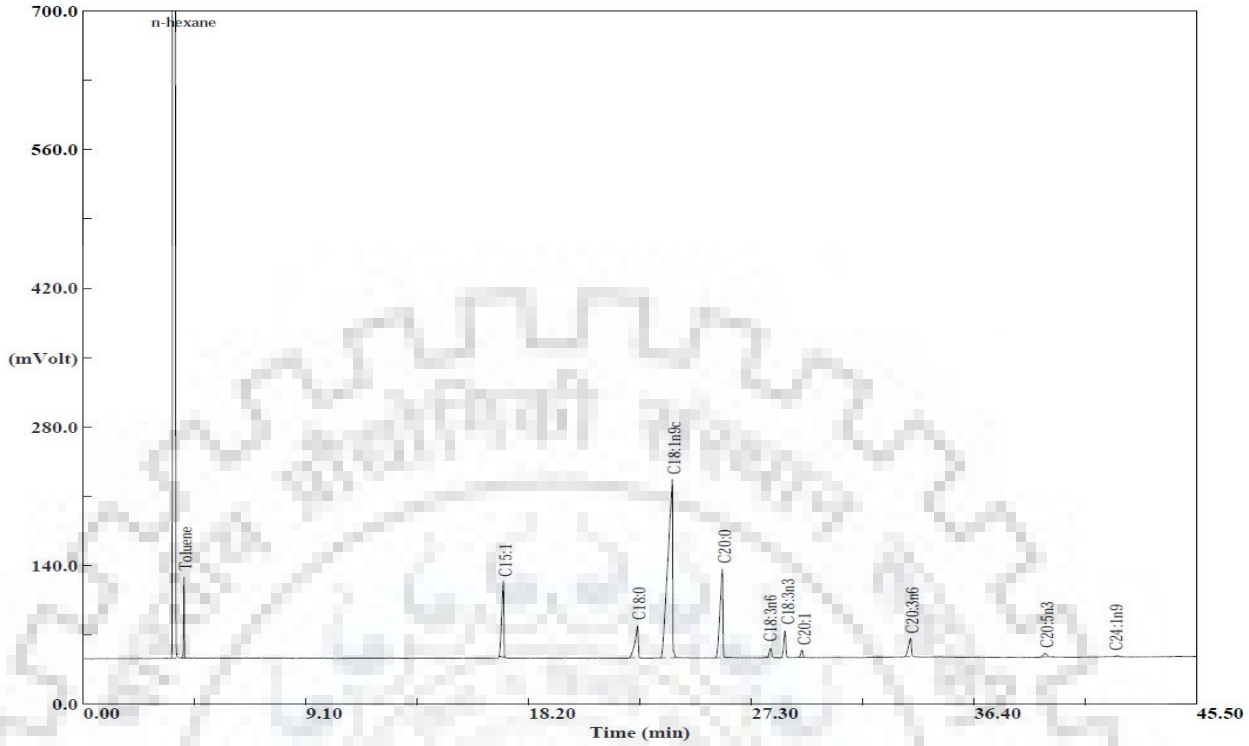


Fig. C.29: GC chromatogram of PP seed oil extracted by SFE in Run 29.

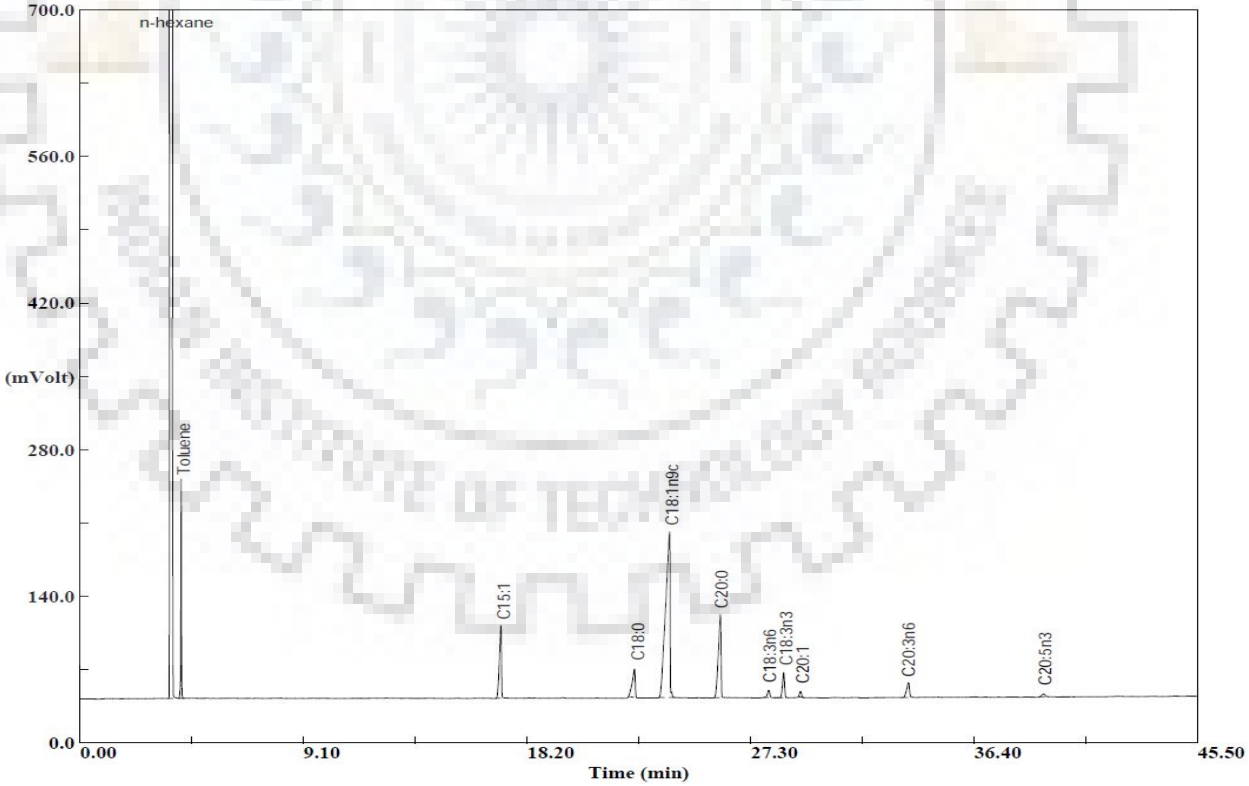


Fig. C.30: GC chromatogram of PP seed oil extracted by SFE in Run 30.

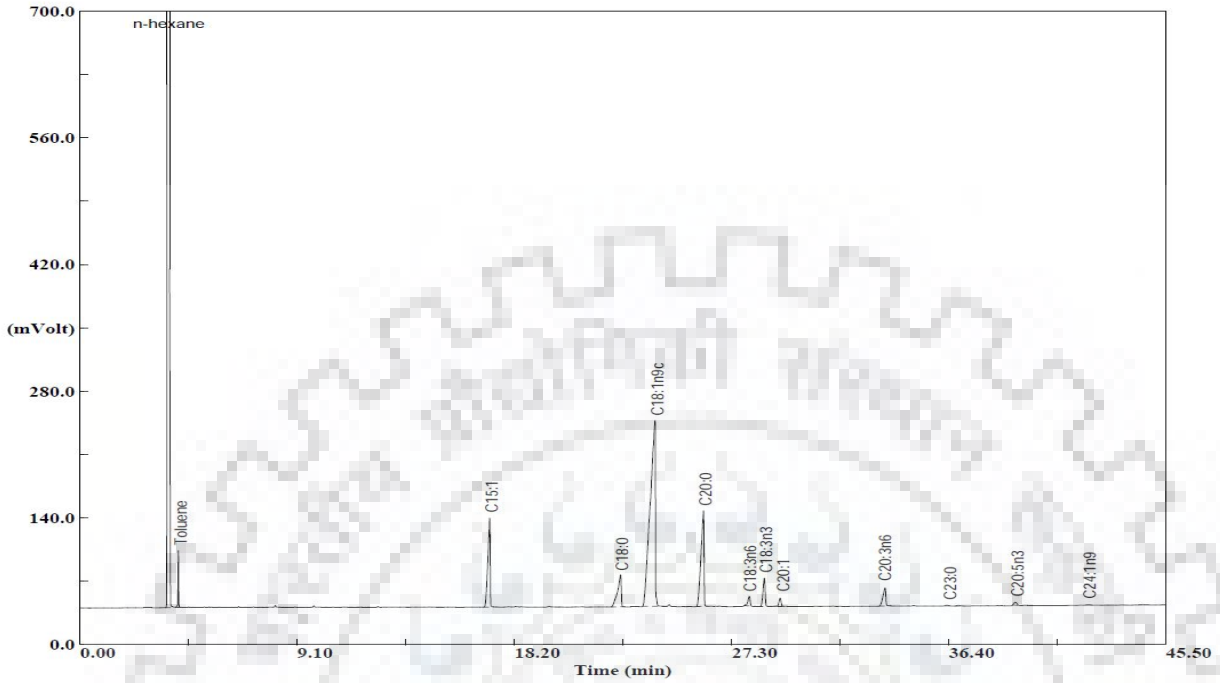


Fig. C.31: GC chromatogram of PP seed oil extracted by SFE in Run 31.

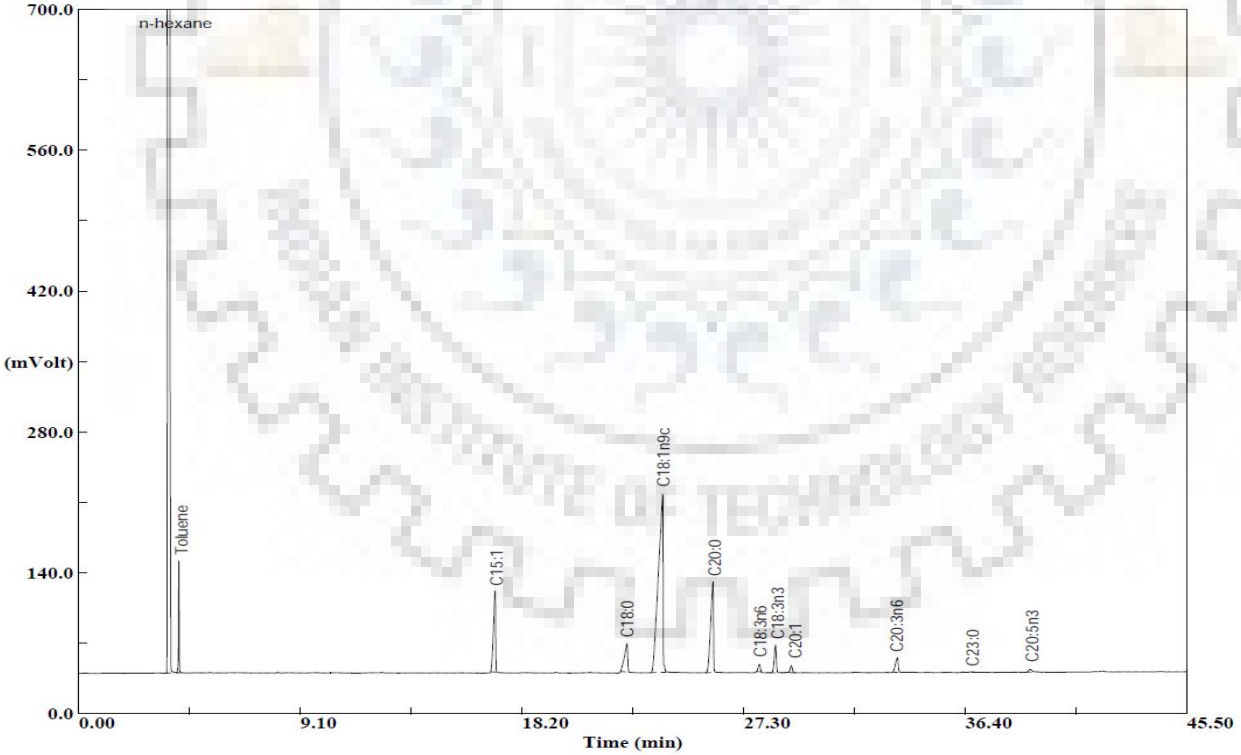


Fig. C.32: GC chromatogram of PP seed oil extracted by SFE in Run 32.

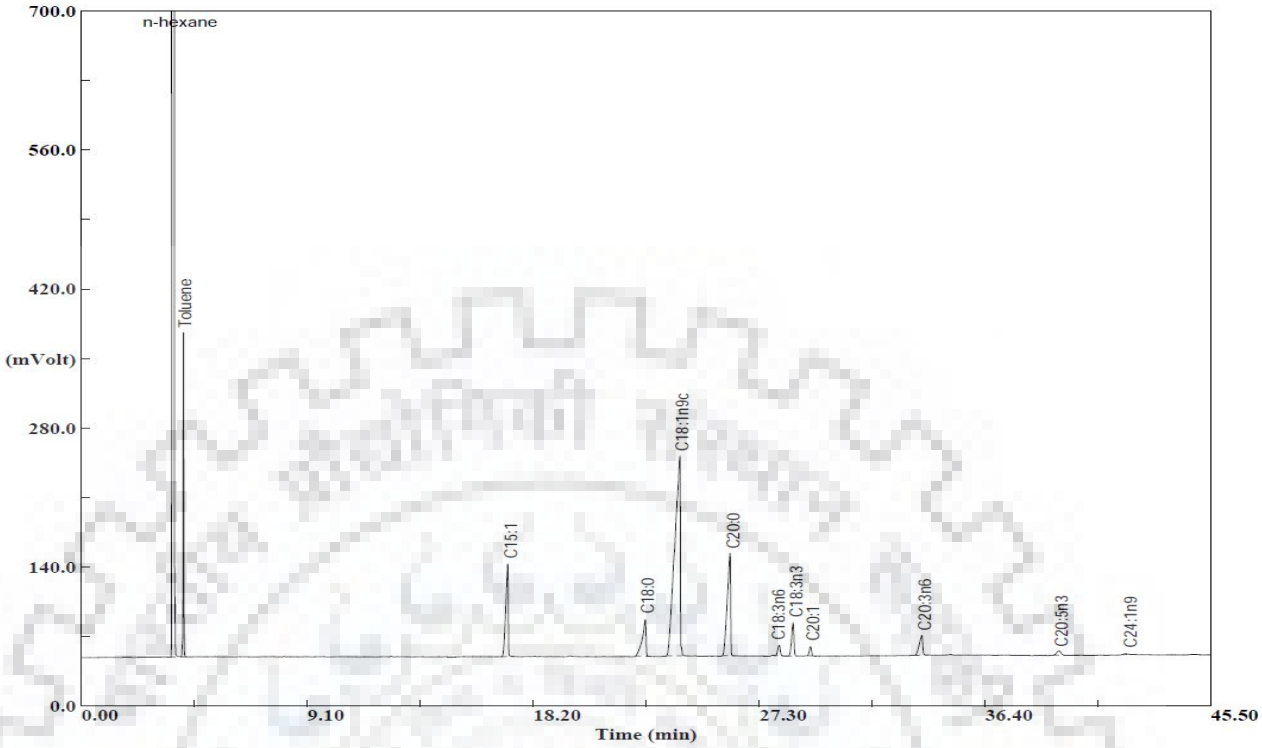


Fig. C.33: GC chromatogram of PP seed oil extracted by SFE in Run 33.

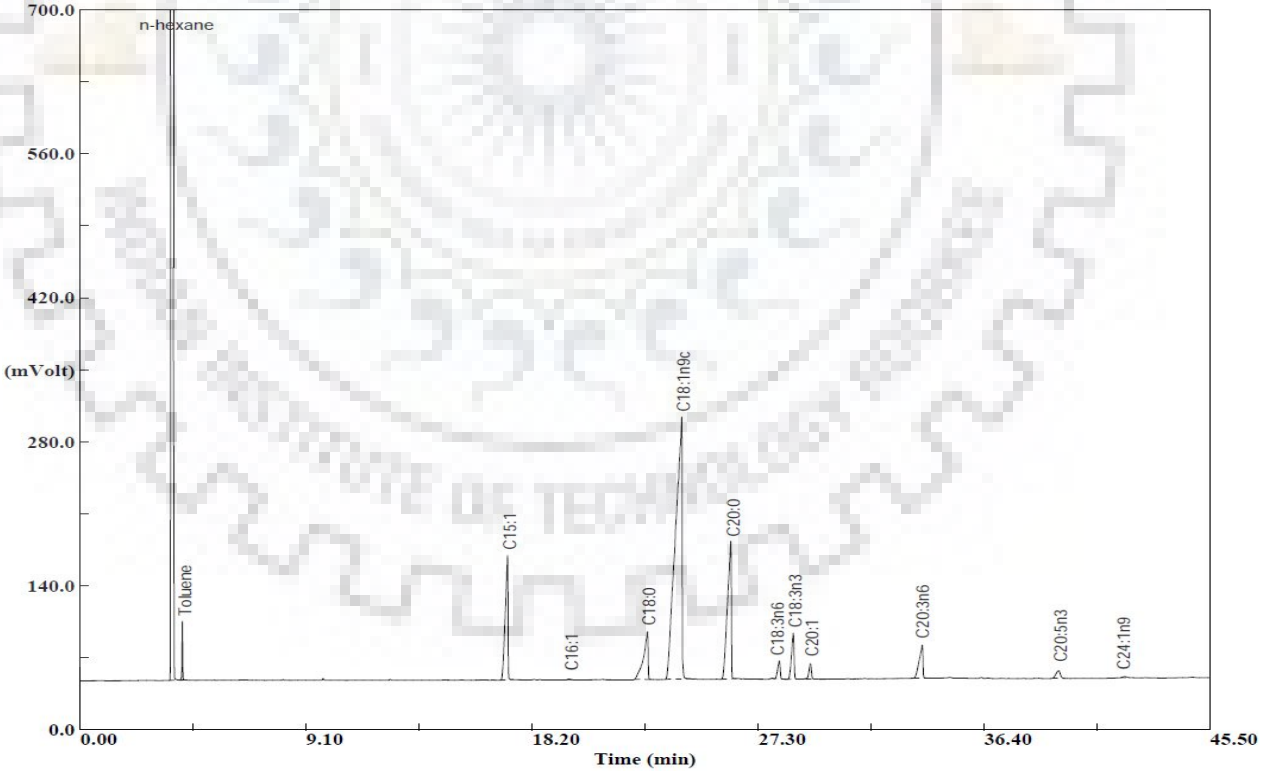


Fig. C.34: GC chromatogram of PP seed oil extracted by SFE in Run 34.

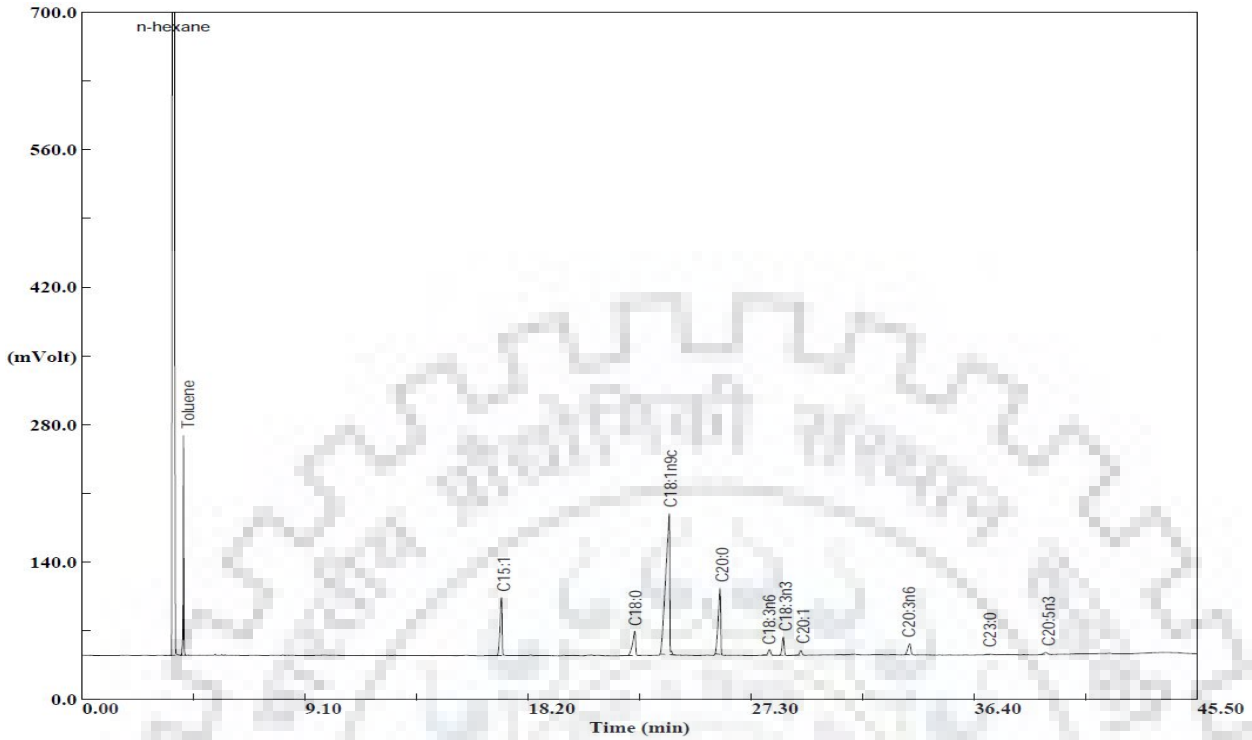


Fig. C.35: GC chromatogram of PP seed oil extracted by SFE in Run 35.

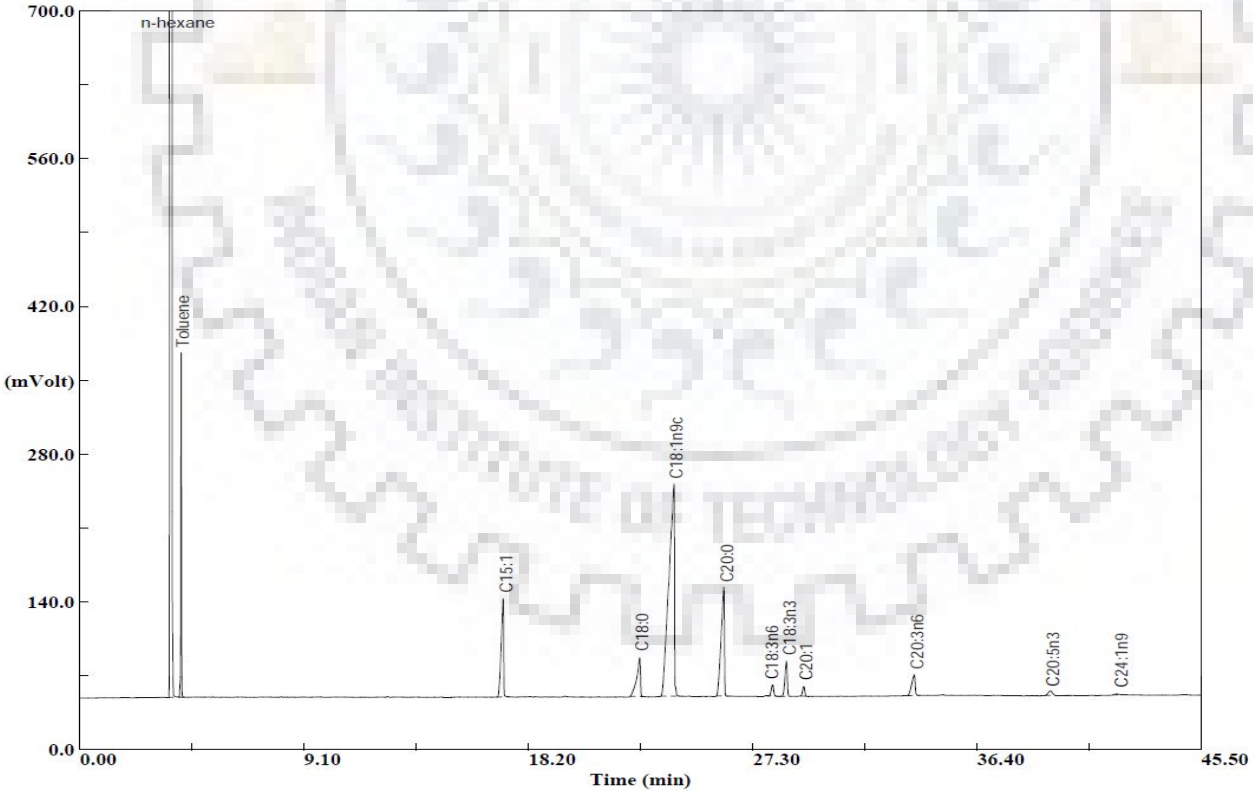


Fig. C.36: GC chromatogram of PP seed oil extracted by SFE in Run 36.

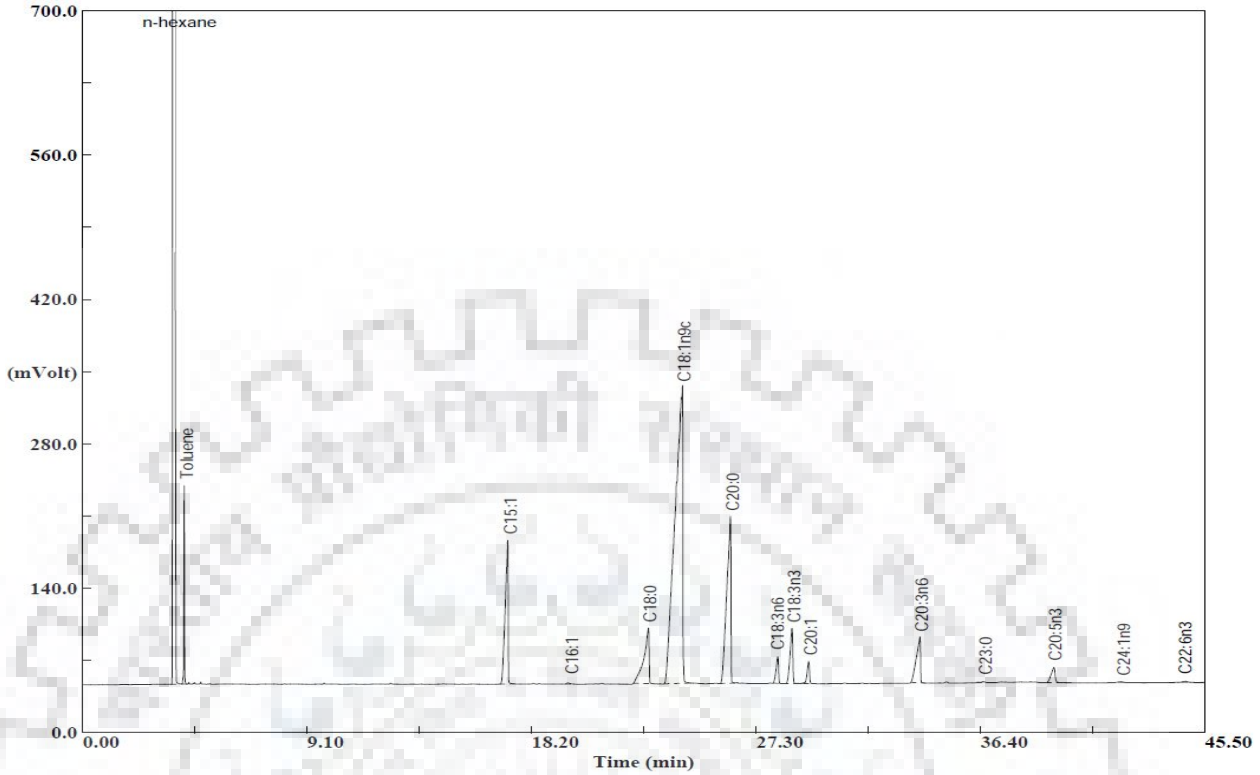


Fig. C.37: GC chromatogram of PP seed oil extracted by SFE in Run 37.

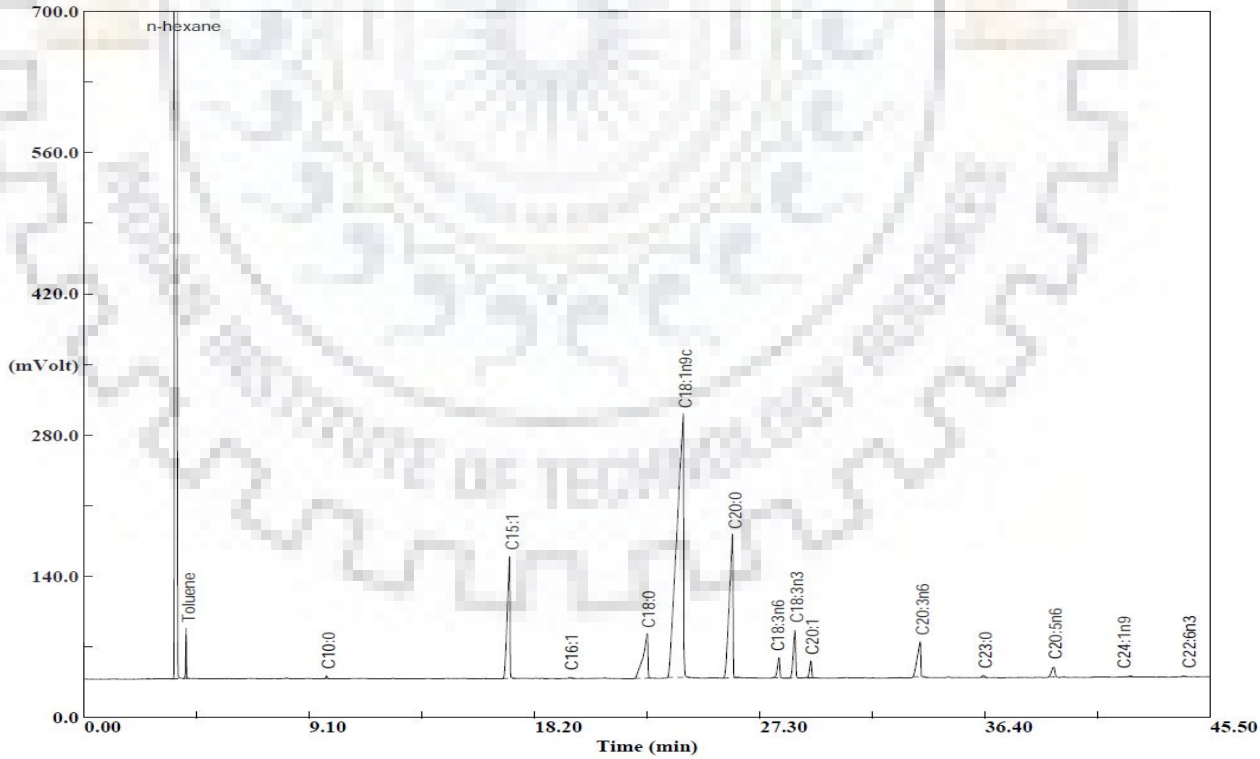


Fig. C.38: GC chromatogram of PP seed oil extracted by SFE in Run 38.

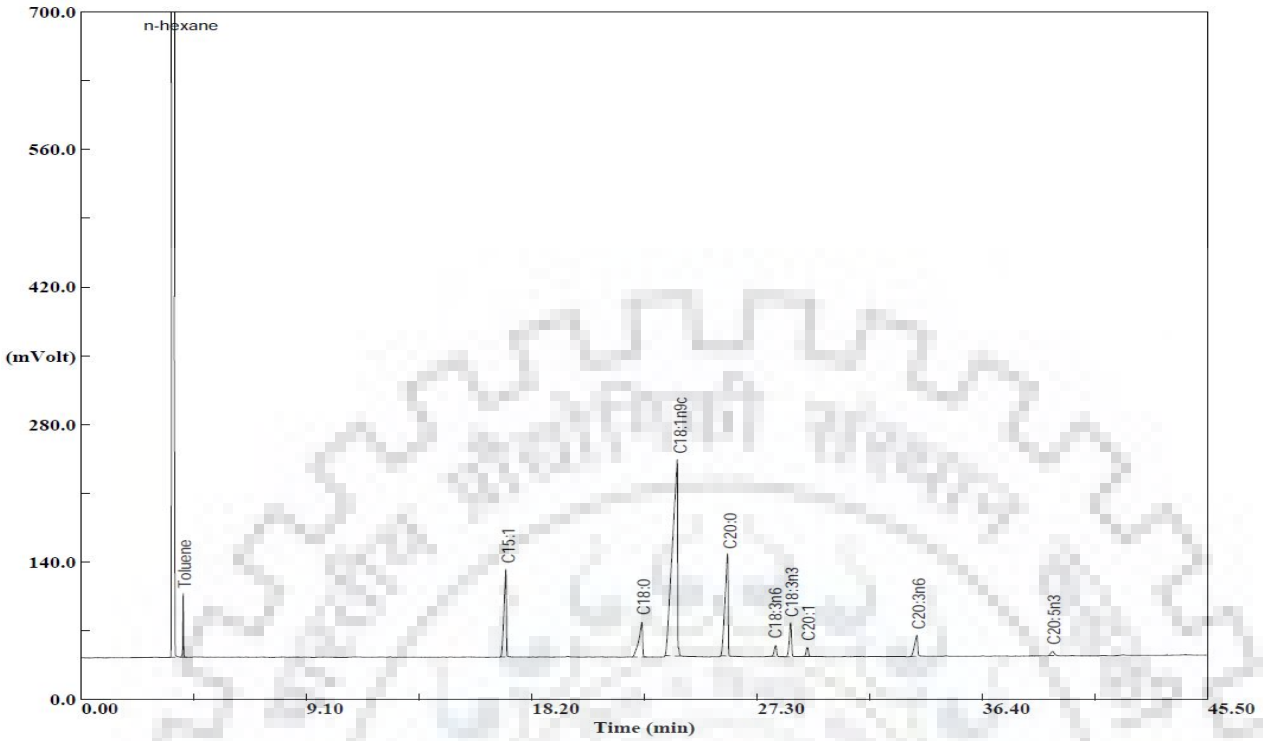


Fig. C.39: GC chromatogram of PP seed oil extracted by SFE in Run 39.

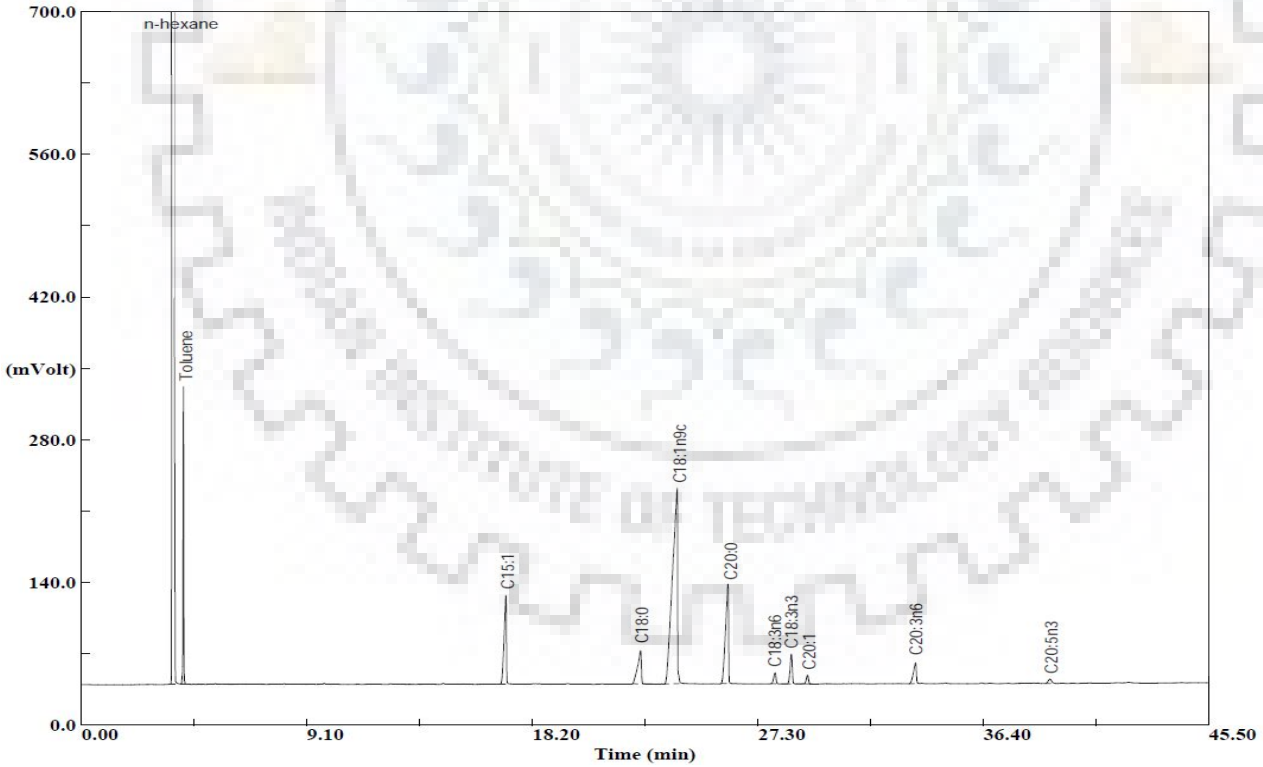


Fig. C.40: GC chromatogram of PP seed oil extracted by SFE in Run 40.

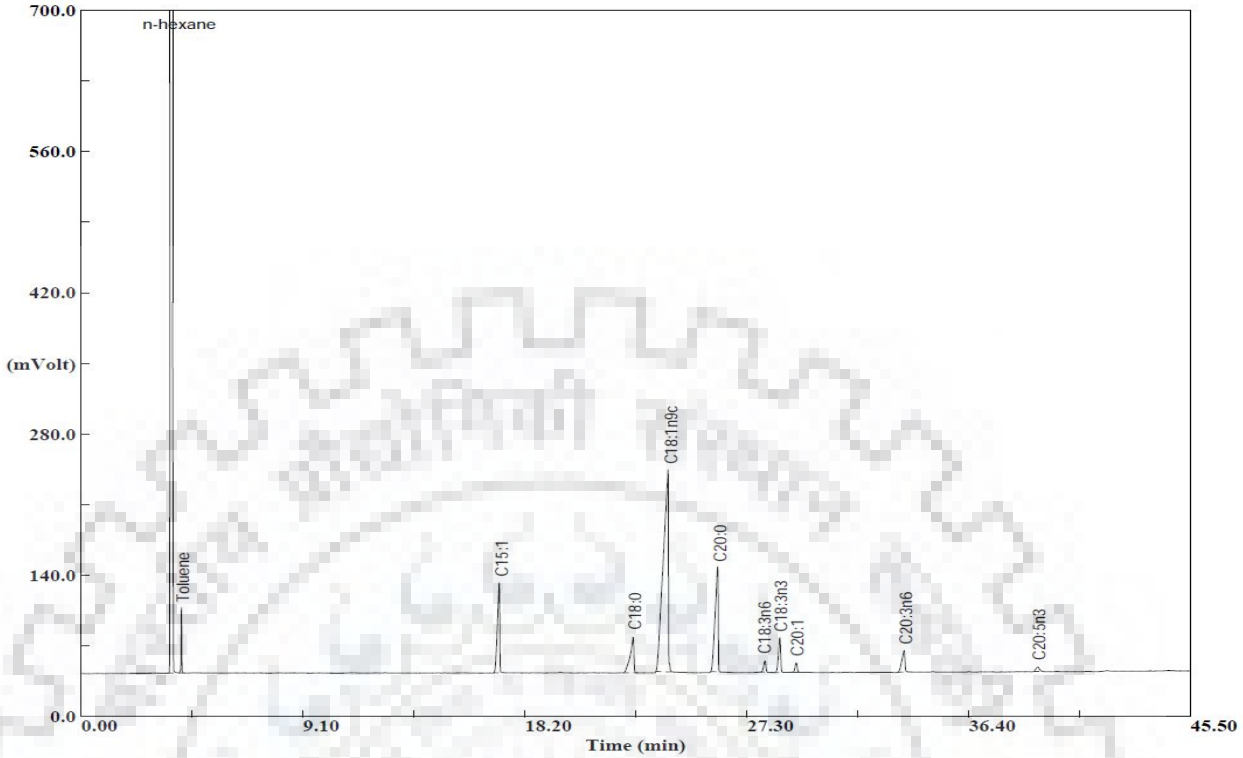


Fig. C.41: GC chromatogram of PP seed oil extracted by SFE in Run 41.

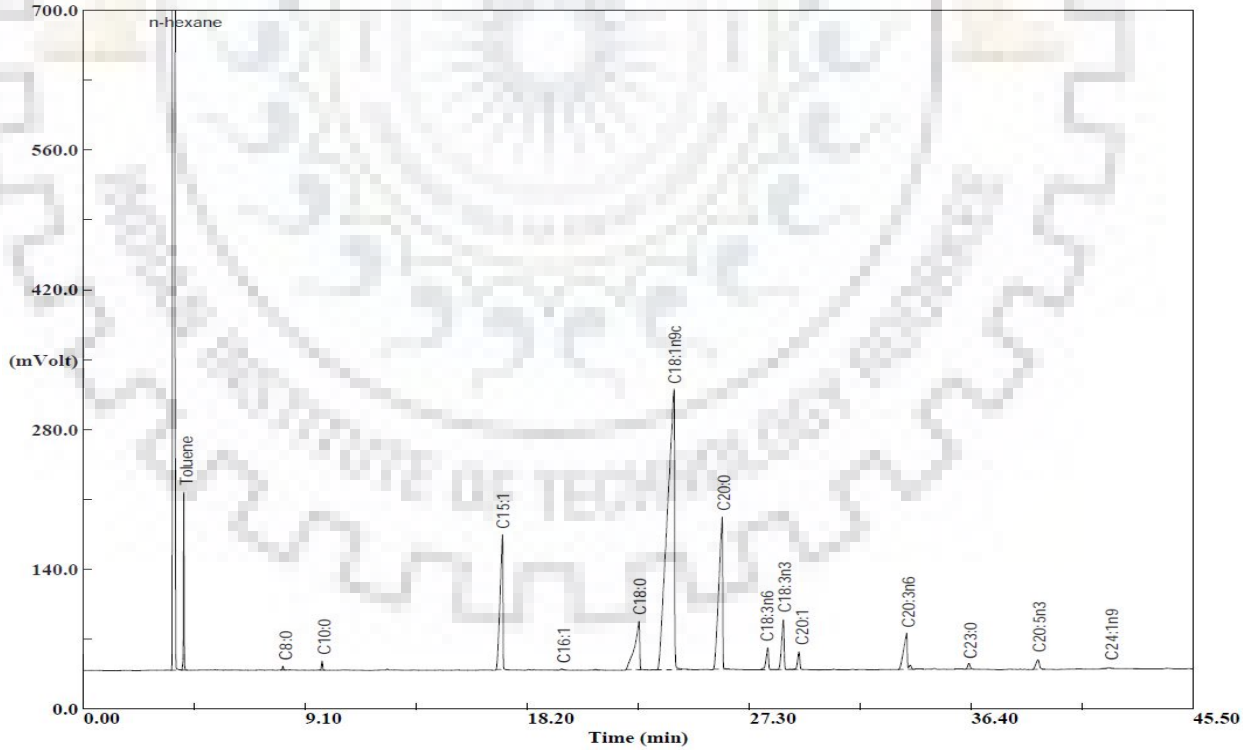


Fig. C.42: GC chromatogram of PP seed oil extracted by SFE in Run 42.

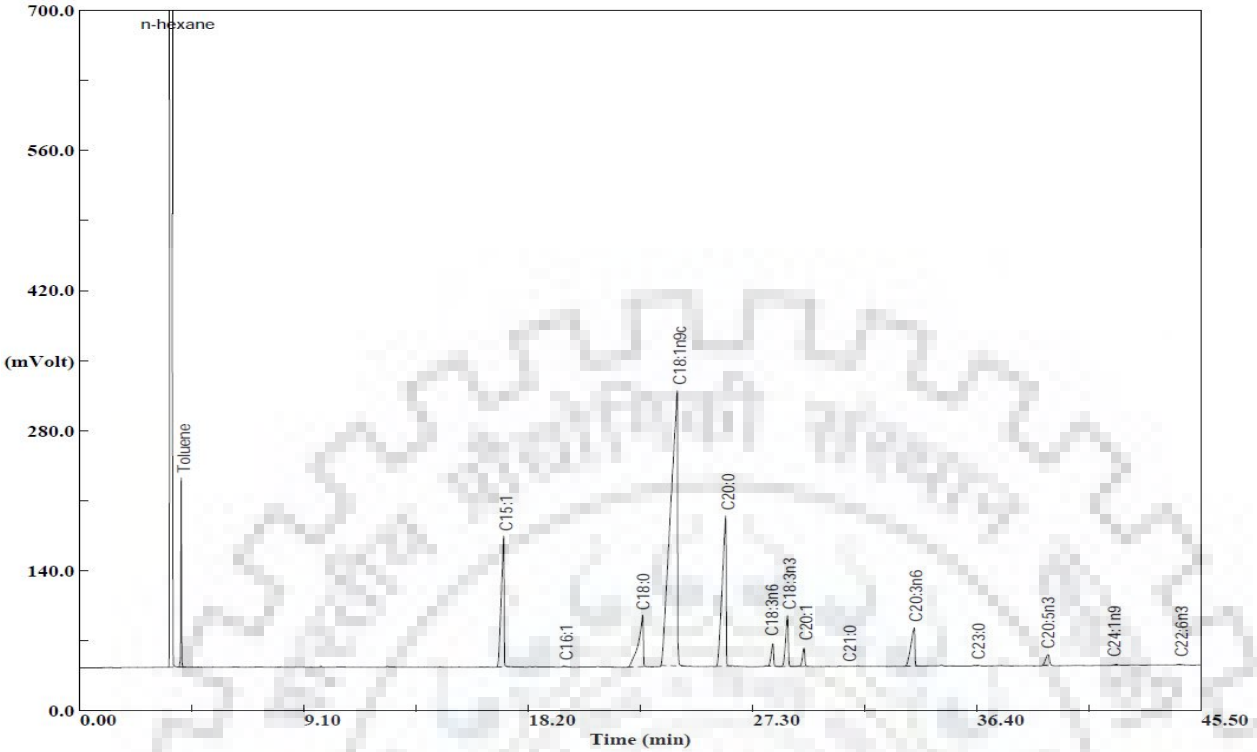


Fig. C.43: GC chromatogram of PP seed oil extracted by SFE in Run 43.

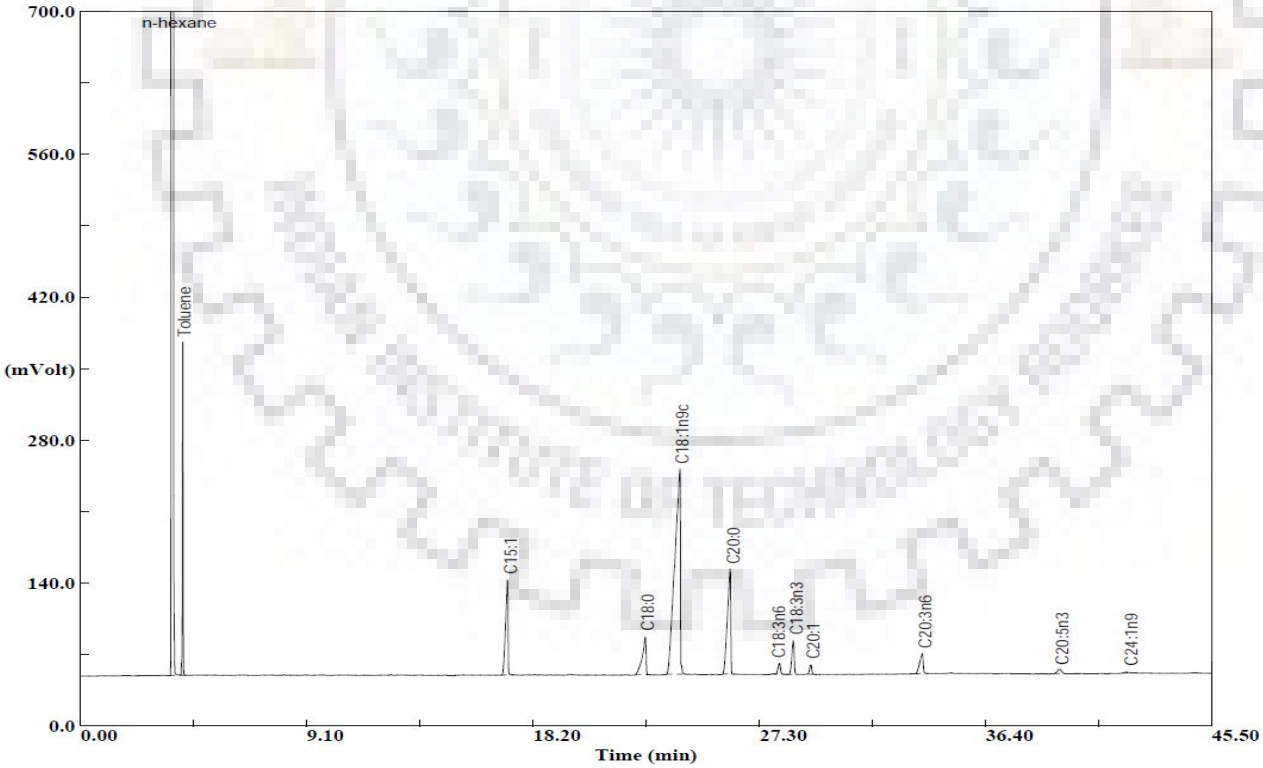


Fig. C.44: GC chromatogram of PP seed oil extracted by SFE in Run 44.

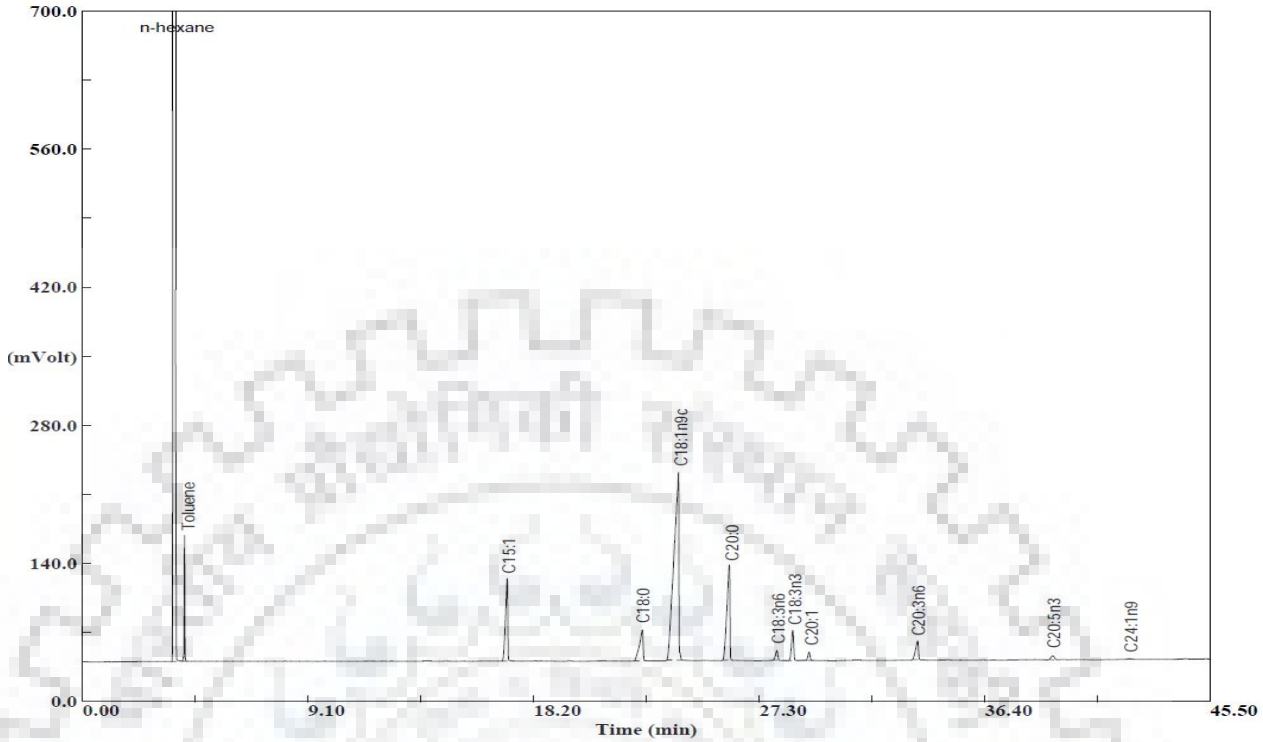


Fig. C.45: GC chromatogram of PP seed oil extracted by SFE in Run 45.

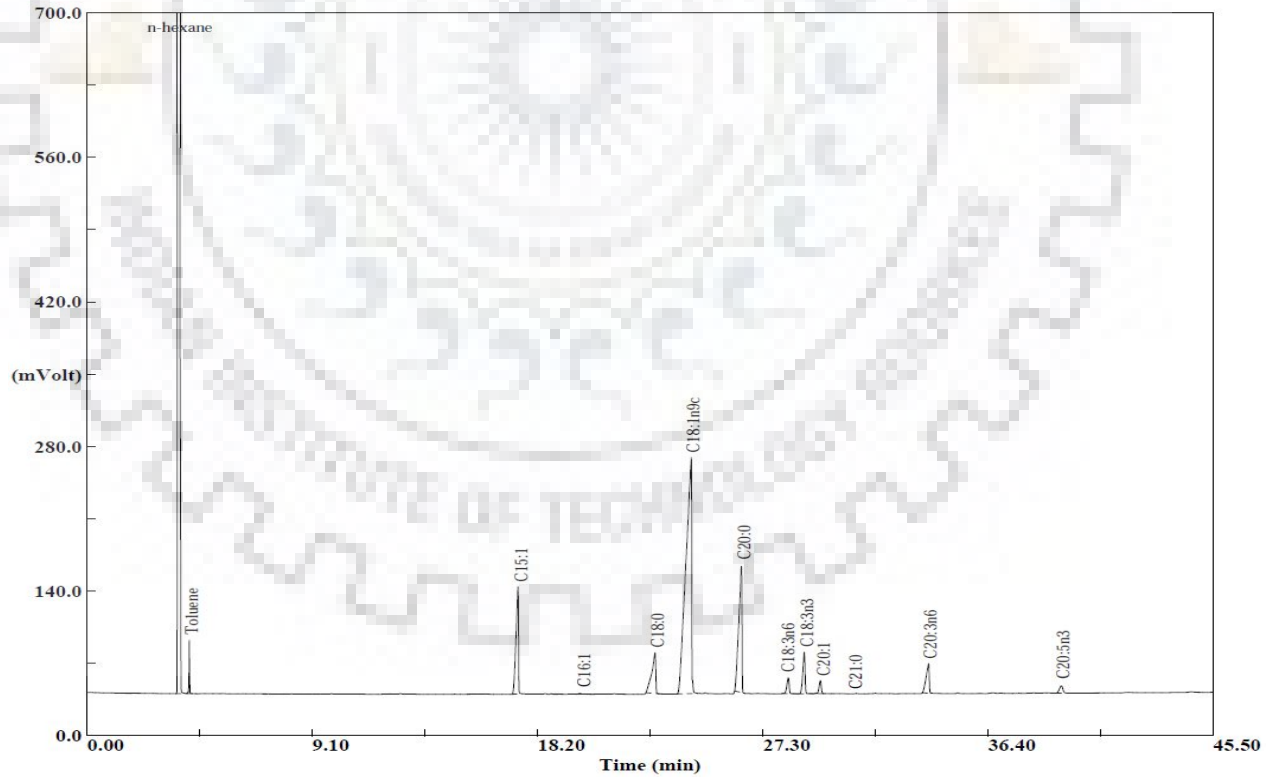


Fig. C.46: GC chromatogram of PP seed oil extracted by SFE in Run 46.

D.1. Computations performed during the economic analysis of envisaged SFE plant.

Capacity of extraction vessel (cell) during the SFE of AM and PP seed oil = 1000 liters.

Batch size = 800 kg of raw seed particles of AM and PP seeds is used per batch.

***Calculation of batch time:*** (for the SFE of both seeds)

Time duration for one SFE run = 250 min. (This time duration is based on the maximum extraction yield achieved at particular optimum conditions of operating parameters. However, this duration (e.g. 250 min.) could be lower than this).

Discharging plus cleaning plus charging time for new batch/run = 35 min.

Therefore, One batch/experimental run time = 285 min

Therefore, only five batches per day are designed for the operation of any one seed. In fact, only one seed will be processed at one time.

***Calculation of annual production rate (APR) of seed oils by the envisaged plant:*** (for the SFE of both seeds)

5 batches in a day require = $5 \times 800 = 4000$ kg of seeds/day

Assuming 300 days of operation in a year.

Therefore, the annual consumption of raw seed (e.g. AM and PP seeds) would be as given below:

$$4000 \times 300 = 1200000 \text{ kg/year.}$$

The achieved optimum extraction conditions as given below in Table D.1.

Table D.1. Optimum extraction conditions of AM and PP seed oils.

| ***SFE of AM seed oil for the Y = 0.4286 kg oil/kg seeds*** |
|---|
| Temperature = 85 °C, Pressure = 305 bar, Particle size = 0.75 mm, Flow rate-$CO_2$ = 0.011 kg/min and the % of co-solvent = 9 % |
| ***SFE of PP seed oil for the Y = 0.36 kg oil/kg seeds*** |
| Temperature = 60 °C, Pressure = 333 bar, Particle size = 1.0 mm, Flow rate-$CO_2$ = 0.007 kg/min and the % of co-solvent = 9 % |

As the optimum extraction yields achieved for the AM and PP seeds are 0.4286 and 0.36 kg oil/kg seeds respectively. Therefore, the annual production rate (APR) of AM and PP seeds oil would be as follows:

APR of AM seed oil = $1200000 \times 0.4286 = 514320$ kg/year.

APR of PP seed oil = $1200000 \times 0.36 = 432000$ kg/year.

***Calculation of total $CO_2$ used and the total co-solvent used:*** (for the SFE of both seeds)

The optimum conditions (as shown in Table C1) were achieved during the SFE of 0.05 kg of seed particles per batch. Therefore, for the 800 kg of seed particles per batch (e.g. AM and PP seeds), the further calculations can be done as follows:

***For AM seeds:*** (at optimum flow rate of $CO_2$ = 0.011 kg/min)

800 kg per batch of AM seeds requires = $\frac{0.011\left(\frac{kg}{min}\right) \times 800\ kg \times 250\ min}{0.05\ kg}$ = 44000 kg $CO_2$ per batch.

For five batches per day = $5 \times 44000$ = 220000 kg/day.

For 1500 batches per year = $1500 \times 44000$ = 66000000 kg/year.

According to the present envisaged plant, 80 % recovery of $CO_2$ is possible; therefore, the total $CO_2$ used per year is calculated as given below:

$$Total\ CO_2\ used\ =\ Total\ CO_2\ used\ (estimated) - Total\ CO_2\ recovered$$

Total $CO_2$ used = $66000000 - 66000000 \times 0.8\ = 13200000\ kg/year$

***For PP seeds:*** (at optimum flow rate of $CO_2$ = 0.007 kg/min)

800 kg per batch of PP seeds requires = $\frac{0.007\ \left(\frac{kg}{min}\right) \times 800\ kg\ \times 250\ min}{0.05\ kg}$ = 28000 kg $CO_2$ per batch.

For five batches per day = $5 \times 28000$ = 140000 kg/day.

For 1500 batches per year = $1500 \times 28000$ = 42000000 kg/year. (amount to be charged only)

According to the present envisaged plant, 80 % recovery of $CO_2$ is possible; therefore, the total $CO_2$ used per year is calculated as given below:

$$Total\ CO_2\ used\ =\ Total\ CO_2\ used\ (estimated) - Total\ CO_2\ recovered$$

Total $CO_2$ used = $42000000 - 42000000 \times 0.8\ = 8400000\ kg/year$ (amount to be charged only)

***Calculation of total co-solvent (Ethanol) used:*** (for the SFE of both seeds)

According to the optimum conditions of co-solvent (as mentioned in Table C1) used during the both seeds (e.g. AM and PP seeds), the amount of co-solvent (ethanol) used is calculated as given below:

***For AM seeds:*** (at optimum % of co-solvent = 9 % of flow rate of $CO_2$)

Density of $CO_2$ at 85 °C and 305 bar is found to be as = 729.665 kg/$m^3$.

The flow rate of co-solvent (ethanol) = 9 % of 66000000 kg/year of $CO_2$ = 5940000 kg/year.

After conversion (kg/year to lit/year), the total co-solvent used is = 8140722 lit/year.

According to the present envisaged plant, 85 % recovery of co-solvent (Ethanol) is possible; therefore, the total co-solvent used per year is calculated as given below:

$$Total\ cosolvent\ used$$
$$=\ Total\ co - solvent\ used\ (estimated) - Total\ cosolvent\ recovered$$

Total co-solvent used = 8140722 – 0.85×8140722 = 1221108 lit/year. (This amount is to be charged only).

***For PP seeds:*** (at optimum % of co-solvent = 9 % of flow rate of $CO_2$)

Density of $CO_2$ at 60 °C and 333 bar is found to be as = 851.912 kg/$m^3$.

After performing the similar computations as done for AM seeds.

Total co-solvent used = 4437078 – 0.85×4437078 = 665562 lit/year. (This amount is to be charged only).

In addition to the above quantities, the total number of labors and the total electricity consumed were also calculated and found to be 1800 nos/year and 6500000 kWh.

Further, the computed values of cost of all the used quantities during the SFE process for AM and PP seeds are reported in Table D.2.

Table D.2. Calculated values of all primary quantities, used for the calculation of other costs.

| | SFE of AM seed oil | | SFE of PP seed oil | |
|---|---|---|---|---|
| **Parameters** | **Amount used (kg/year)** | **Cost/Year (Rs./year)** | **Amount used** | **Cost/Year** |
| Cost of raw material | 1200000 | 36000000 | 1200000 | 48000000 |
| Cost of $CO_2$ | 13200000 | 237600000 | 8400000 | 151200000 |
| Cost of Ethanol | 1221108 lit/year | 25643274 | 665562 | 13976796 |
| Cost of Labor | 1800 nos/year | 990000 | 1800 nos/year | 990000 |
| Cost of Electricity | 6500000 kWh/year | 34385000 | 6500000 kWh/year | 34385000 |
| Cost of Product | 514320 kg/year | 1285800000 | 432000 kg/year | 928800000 |

| **Cost per unit used during the calculation of above quantities for the SFE of both seeds** | | |
|---|---|---|
| | SFE of AM seed oil | SFE of PP seed oil |
| Cost of raw material | 30 Rs/kg | 40 Rs/kg |
| Cost of $CO_2$ | 18 Rs/kg | 18 Rs/kg |
| Cost of Ethanol | 21 Rs/lit | 21 Rs/lit |
| Wage of one labor | 550 Rs/day | 550 Rs/day |
| Cost of electricity | 5.29 Rs/kWh | 5.29 Rs/kWh |
| Cost of product | 2500 Rs/kg | 2150 Rs/kg |
| Cost of $CO_2$ liquefaction | 80 % of the cost of $CO_2$ | 80 % of the cost of $CO_2$ |

***Calculation of annual cost of capital recovery (ACCR):*** (for the SFE of both seeds)

The ACCR with 15 % rate of interest is calculated from the fixed cost (SFE equipment cost with installation) of the envisaged plant as given below:

$$ACCR = Fixed\ Cost \times \left\{\frac{i\,(1+i)^n}{(1+i)^n-1}\right\} \quad \text{… Eq. D.1}$$

Where, i is the rate of interest imposed by the bank. n is the service life of the plant.

***For the SFE of both seeds:***

The Fixed cost (FC) of the equipment with installation is = Rs. 277210000

$$ACCR = 277210000 \times \left\{\frac{0.15\,(1+0.15)^{20}}{(1+0.15)^{20}-1}\right\}$$

ACCR (for both seeds) = 44287477 Rs/year.

***Calculation of operating cost (OC):*** (for the SFE of both seeds)

$$Operating\ Cost\ (OC) = Cost\ of\ raw\ material\ (CRM) + Cost\ of\ labor\ (CL) + Cost\ of\ electricity\ (CE) + cost\ of\ CO_2\ liquefaction\ (CCL) \quad \text{… Eq. D.2}$$

Where, $CRM = Cost\ of\ feedstock\ (AM\ or\ PP\ seeds) + Cost\ of\ CO_2 + Cost\ of\ Ethanol$

***For AM seed oil:***

$OC\ (Rs/year)$ = [(36000000 + 237600000 + 25643274) + 990000 + 34385000 + 190080000

= 524698274 Rs/year.

***For PP seed oil:***

$OC\ (Rs/year)$ = [(48000000 + 151200000 + 13976796) + 990000 + 34385000 + 120960000

= 369511796 Rs/year.

***Calculation of total annual cost (TAC):*** (for the SFE of both seeds)

$$TAC\ (Rs/year) = ACCR + OC \quad \text{… Eq. D.3}$$

***For AM seed oil:*** TAC = 568985752 Rs/year

***For PP seed oil***: TAC = 413799273 Rs/year

***Calculation of manufacturing cost (MC):*** (for the SFE of both seeds)

$$MC(Rs/kg) = \frac{TAC\ (Rs/year)}{APR\ (kg/year)}\ (or) = TAC\ (Rs/year) \quad \text{… Eq. D.4}$$

***For AM seed oil***: 1106 Rs/kg (or) 568985752 Rs/year

***For PP seed oil:*** 958 Rs/kg (or) 413799273 Rs/year

***Calculation of depreciation (D) using straight-line method:*** (for the SFE of both seeds)

$$Depreciation\ (D) = \frac{(Fixed\ cost\ (Rs) - salvage\ value\ (Rs))}{Service\ life\ of\ plant\ (year)} \quad \text{… Eq. D.5}$$

D (for both seed oils) = 13860500 Rs/year

***Calculation of Gross profit before depreciation (GPBD):*** (for the SFE of both seeds)

$$GPBD\ (Rs/year) = (Cost\ of\ product\ (Rs/kg) - MC\ (Rs/kg)) \times APR\ (kg/year)$$

… Eq. D.6

***For AM seed oil:*** GPBD (Rs/year) = 716814248 Rs/year

***For PP seed oil:*** GPBD (Rs/year) = 515000727 Rs/year

***Calculation of Gross profit after depreciation (GPAD):*** (for the SFE of both seeds)

$$GPAD\ (Rs/year) = (GPBD(Rs/year) - D(Rs/year)) \quad \text{… Eq. D.7}$$

***For AM seed oil:*** GPAD (Rs/year) = 702953748 Rs/year

***For PP seed oil:*** GPAD (Rs/year) = 501140227 Rs/year

Calculation ***of Actual (net) profit (AP):*** (for the SFE of both seeds)

$$Actual\ (net) profit\ (AP) = GPAD\ (Rs/year) - Income\ tax\ (30\ \%) on\ GPAD \quad \ldots \text{Eq. D.8}$$

***For AM seed oil:*** *492067624* Rs/year.

***For PP seed oil:*** ***350798159*** Rs/year.

***Calculation of Payback period (PP) (PP):*** (for the SFE of both seeds)

$$PP\ (year) = \frac{(Fixed\ cost + OC)}{AP} \quad \ldots \text{Eq. D.9}$$

***For AM seed oil:*** 1.63 years

***For PP seed oil:*** 1.84 years

E.1. Photographic view experimental setup of the SFE unit

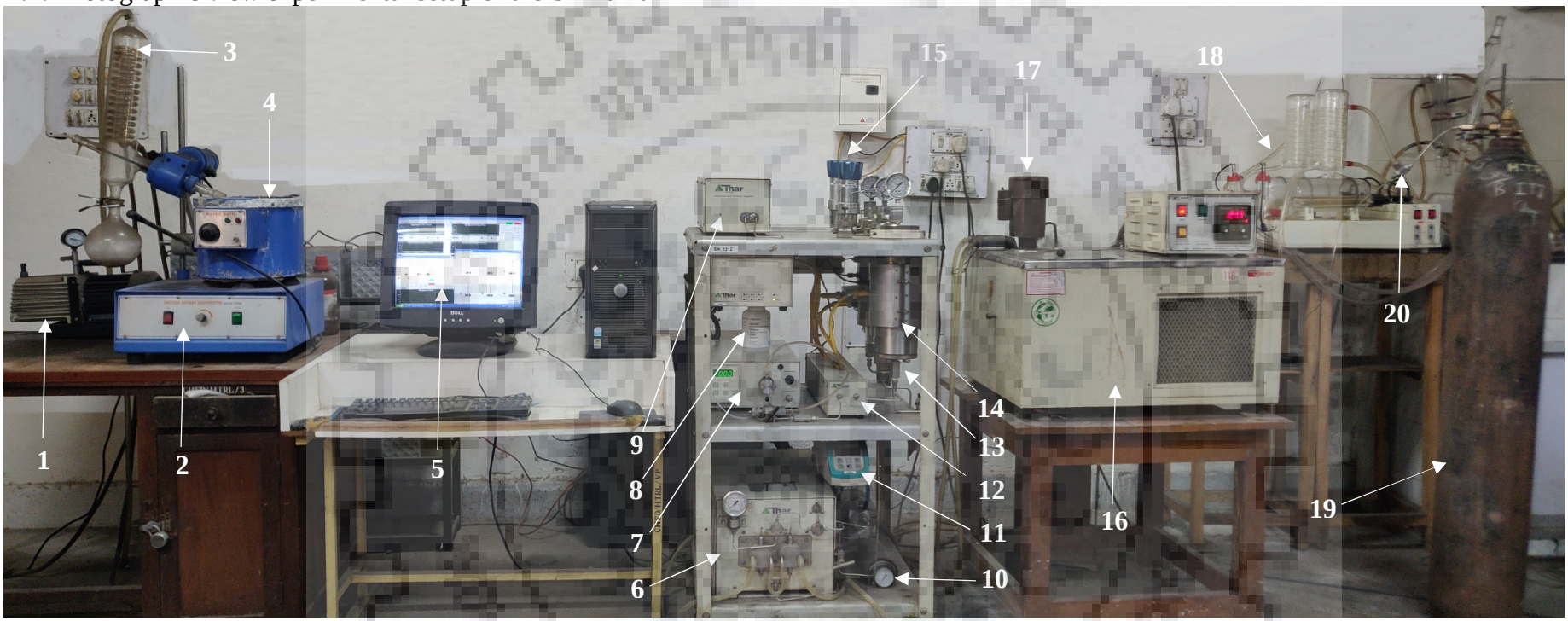


Fig. E.1: Photographic view experimental setup of the SFE unit.

1. Vaccum pump
2. Vacuum effect-rotary evaporator
3. Condenser
4. Water bath
5. Software 'Process Suit'
6. High pressure pump
7. Co-solvent pump
8. Co-solvent container
9. Automated back pressure regulator (ABPR)
10. Heat exchanger-1 (HE1)
11. Flow meter
12. Heat exchanger-2 (HE2)
13. Sample point
14. Extractor/cell
15. Manual back pressure regulator (MBPR)
16. Chiller
17. Stirrer
18. Water distillation unit
19. $CO_2$ cylinder
20. Micro filter

F.1. ANOVA analysis for the SFE of AM and PP seed oils

Table F.1. ANOVA analysis and regression coefficients of predicted second-order polynomial model (Eq. 5.2) for AM seed oil yield.

| Source | Df | Effect | Coefficient | SE coefficient | Adj SS | Adj MS | t-value | F-value | p-value | |
|---|---|---|---|---|---|---|---|---|---|---|
| **Model** | 20 | | -1.77995 | 0.0079 | 0.3488 | 0.0174 | 46.613 | 47.14 | < 0.0001 | Significant |
| **Linear Terms** | 5 | | | | | | | | | |
| Temperature: $X_1$ | 1 | 0.01015 | 0.005075 | 0.0048 | 0.0004 | 0.0004 | -1.0787 | 1.16 | 0.2910 | Less significant |
| Pressure: $X_2$ | 1 | 0.00904 | 0.004520 | 0.0048 | 0.0886 | 0.0886 | 15.476 | 239.52 | <0.0001 | Significant |
| Particle size: $X_3$ | 1 | 4.3145 | 2.157250 | 0.0048 | 0.0455 | 0.0455 | 11.091 | 123.02 | <0.0001 | Significant |
| Flow rate - $CO_2$: $X_4$ | 1 | 0.07912 | 0.039559 | 0.0048 | 0.0027 | 0.0027 | 2.7072 | 7.33 | 0.0121 | Significant |
| % of co-solvent: $X_5$ | 1 | 0.04356 | 0.021779 | 0.0048 | 0.1087 | 0.1087 | 17.139 | 293.73 | <0.0001 | Significant |
| **2- way interactions** | 10 | | | | | | | | | |
| $X_1X_2$ | 1 | 0.00005 | 0.000027 | 0.0096 | 0.0064 | 0.0064 | 4.1485 | 17.21 | 0.0003 | Significant |
| $X_1X_3$ | 1 | -0.01631 | -0.008155 | 0.0096 | 0.0067 | 0.0067 | -4.2395 | 17.97 | 0.0003 | Significant |
| $X_1X_4$ | 1 | 0.00035 | 0.000175 | 0.0096 | 0.0012 | 0.0012 | 1.8195 | 3.31 | 0.0808 | Significant |
| $X_1X_5$ | 1 | 0.00087 | 0.000434 | 0.0096 | 0.0075 | 0.0075 | 4.5098 | 20.34 | 0.0001 | Significant |
| $X_2X_3$ | 1 | 0.00274 | 0.001372 | 0.0096 | 0.0026 | 0.0026 | 2.6747 | 7.15 | 0.0130 | Significant |
| $X_2X_4$ | 1 | -0.00016 | -0.000081 | 0.0096 | 0.0037 | 0.0037 | -3.1452 | 9.89 | 0.0042 | Significant |
| $X_2X_5$ | 1 | -0.00016 | -0.000079 | 0.0096 | 0.0035 | 0.0035 | -3.0646 | 9.39 | 0.0052 | Significant |
| $X_3X_4$ | 1 | 0.01036 | 0.005180 | 0.0096 | 0.0002 | 0.0002 | 0.6732 | 0.45 | 0.5070 | Insignificant |
| $X_3X_5$ | 1 | 0.03492 | 0.017460 | 0.0096 | 0.0019 | 0.0019 | 2.2692 | 5.15 | 0.0321 | Significant |
| $X_4X_5$ | 1 | -0.00258 | -0.001288 | 0.0096 | 0.0041 | 0.0041 | -3.3479 | 11.21 | 0.0026 | Significant |
| **Square** | 5 | | | | | | | | | |
| $X_1^2$ | 1 | -0.00013 | -0.000065 | 0.0065 | 0.0060 | 0.006 | -4.0129 | 16.10 | 0.0005 | Significant |
| $X_2^2$ | 1 | -0.00002 | -0.000010 | 0.0065 | 0.0275 | 0.0275 | -8.6151 | 74.22 | <0.0001 | Significant |
| $X_3^2$ | 1 | -2.41054 | -1.205270 | 0.0065 | 0.0495 | 0.0495 | -11.569 | 133.84 | <0.0001 | Significant |
| $X_4^2$ | 1 | -0.00262 | -0.001311 | 0.0065 | 0.0094 | 0.0094 | -5.0329 | 25.33 | 0.0001 | Significant |
| $X_5^2$ | 1 | -0.00372 | -0.001860 | 0.0065 | 0.0189 | 0.0189 | -7.1394 | 50.97 | <0.0001 | Significant |
| Residual | 25 | | | | 0.3488 | 0.0174 | | | | |
| Lack of Fit | 20 | | | | 0.0093 | 0.0004 | | 3.72 | 0.0753 | Insignificant |
| Pure Error | 5 | | | | 0.0006 | 0.0001 | | | | |
| Cor Total | 45 | | | | 0.0087 | 0.0004 | | | | |

| | | | |
|---|---|---|---|
| Std. Deviation | 0.019 | $R^2$ | 0.9742 |
| Mean | 0.28 | Adj $R^2$ | 0.9535 |
| C.V. % | 6.78 | Pred $R^2$ | 0.9008 |
| PRESS | 0.036 | Adeq Precision | 25.921 |

Table F.2. ANOVA analysis and regression coefficients of predicted second-order polynomial model (Eq. 5.5) for PP seed oil yield.

| Source | Df | Effect | Coefficient | SE coefficient | Adj SS | Adj MS | t-value | F-value | p-value | |
|---|---|---|---|---|---|---|---|---|---|---|
| **Model** | 20 | | 0.1886 | 0.0031 | 0.3100 | 0.0150 | 60.79 | 267.64 | < 0.0001 | Significant |
| **Linear Terms** | 5 | | | | | | | | | |
| Temperature: $X_1$ | 1 | -0.0940 | -0.0470 | 0.0019 | 0.0354 | 0.0354 | -24.76 | 613.05 | <0.0001 | Significant |
| Pressure: $X_2$ | 1 | 0.1878 | 0.0939 | 0.0019 | 0.1410 | 0.1410 | 49.42 | 2,442.71 | <0.0001 | Significant |
| Particle size: $X_3$ | 1 | 0.0260 | 0.0130 | 0.0019 | 0.0026 | 0.0026 | 6.73 | 45.23 | 0.0030 | Significant |
| Flow rate - $CO_2$: $X_4$ | 1 | 0.0500 | 0.0250 | 0.0019 | 0.0104 | 0.0104 | 13.41 | 179.715 | <0.0001 | Significant |
| Co-solvent %: $X_5$ | 1 | 0.1520 | 0.0760 | 0.0019 | 0.0914 | 0.0914 | 39.80 | 1,584.07 | <0.0001 | Significant |
| **2- way interactions** | 10 | | | | | | | | | |
| $X_1X_2$ | 1 | 0.0012 | 0.0006 | 0.0038 | 0.0000 | 0.0000 | 0.15 | 0.023 | 0.8819 | Insignificant |
| $X_1X_3$ | 1 | -0.0016 | -0.0008 | 0.0038 | 0.0000 | 0.0000 | -0.20 | 0.04 | 0.8425 | Insignificant |
| $X_1X_4$ | 1 | -0.0276 | -0.0138 | 0.0038 | 0.0008 | 0.0008 | -3.64 | 13.24 | 0.0012 | Significant |
| $X_1X_5$ | 1 | -0.0412 | -0.0206 | 0.0038 | 0.0017 | 0.0017 | -5.42 | 29.38 | <0.0001 | Significant |
| $X_2X_3$ | 1 | -0.0128 | -0.0064 | 0.0038 | 0.0002 | 0.0002 | -1.69 | 2.87 | 0.1024 | Insignificant |
| $X_2X_4$ | 1 | 0.0420 | 0.0210 | 0.0038 | 0.0017 | 0.0017 | 5.40 | 29.16 | <0.0001 | Significant |
| $X_2X_5$ | 1 | 0.0592 | 0.0296 | 0.0038 | 0.0035 | 0.0035 | 7.79 | 60.69 | <0.0001 | Significant |
| $X_3X_4$ | 1 | 0.0252 | 0.0126 | 0.0038 | 0.0006 | 0.0006 | 3.33 | 11.08 | 0.0027 | Significant |
| $X_3X_5$ | 1 | 0.0394 | 0.0197 | 0.0038 | 0.0016 | 0.0016 | 5.19 | 26.92 | <0.0001 | Significant |
| $X_4X_5$ | 1 | 0.0466 | 0.0233 | 0.0038 | 0.0022 | 0.0022 | 6.13 | 37.54 | <0.0001 | Significant |
| **Square** | 5 | | | | | | | | | |
| $X_1^2$ | 1 | -0.0282 | -0.0141 | 0.0026 | 0.0017 | 0.0017 | -5.48 | 30.04 | <0.0001 | Significant |
| $X_2^2$ | 1 | -0.0076 | -0.0038 | 0.0026 | 0.0001 | 0.0001 | -1.46 | 2.13 | 0.1567 | Insignificant |
| $X_3^2$ | 1 | 0.0144 | 0.0072 | 0.0026 | 0.0005 | 0.0005 | 2.79 | 7.80 | 0.0099 | Significant |
| $X_4^2$ | 1 | -0.0714 | -0.0357 | 0.0026 | 0.0111 | 0.0111 | -13.90 | 193.13 | <0.0001 | Significant |
| $X_5^2$ | 1 | -0.0368 | -0.0184 | 0.0026 | 0.0030 | 0.0030 | -7.16 | 51.23 | <0.0001 | Significant |
| Residual | 25 | | | | 0.0014 | 0.00006 | | | | |
| Lack of Fit | 20 | | | | 0.0014 | 0.00007 | | 4.4 | 0.0539 | Insignificant |
| Pure Error | 5 | | | | 0.00008 | 0.00002 | | | | |
| Cor Total | 45 | | | | 0.361 | | | | | |

| | | | | | |
|---|---|---|---|---|---|
| Std. Deviation | : 0.00759 | $R^2$ | : 0.9954 | | |
| Mean | : 0.17 | Adj $R^2$ | : 0.9916 | | |
| C.V. % | : 4.58 | Pred $R^2$ | : 0.9820 | | |
| PRESS | : 0.005574 | Adeq Precision | : 66.0270 | | |